Harry G. Kwatny* Gilmer L. Blankenship†

Nonlinear Control & Analytical Mechanics: a Computational Approach

June 1, 2017

Springer

Berlin Heidelberg New York
Hong Kong London
Milan Paris Tokyo

*Department of Mechanical Engineering & Mechanics, Drexel University, Philadelphia, PA 19104; hkwatny@coe.drexel.edu

†Department of Electrical & Computer Engineering, University of MaryLand, College Park, MD 20742; gilmer@eng.umd.edu

Dedication

Preface

During the past decade we have had to confront a series of control design problems – involving, primarily, multibody electro-mechanical systems – in which nonlinearity plays an essential role. Fortunately, the geometric theory of nonlinear control system analysis progressed substantially during the 1980s and 90s, providing crucial conceptual tools that addressed many of our needs. However, as any control systems engineer can attest, issues of modeling, computation, and implementation quickly become the dominant concerns in practice. The problems of interest to us present unique challenges because of the need to build and manipulate complex mathematical models for both the plant and controller. As a result, along with colleagues and students, we set out to develop computer algebra tools to facilitate model building, nonlinear control system design, and code generation, the latter for both numerical simulation and real time control implementation. This book is an outgrowth of that continuing effort. As a result, the unique features of the book includes an integrated treatment of nonlinear control and analytical mechanics and a set of symbolic computing software tools for modeling and control system design.

By simultaneously considering both mechanics and control we achieve a fuller appreciation of the underlying geometric ideas and constructions that are common to both. Control theory has had a fruitful association with analytical mechanics from its birth in the late 19th century. That historical relationship has been reaffirmed during the past two decades with the emergence of a geometric theory for nonlinear control systems closely linked to the modern geometric formulation of analytical mechanics. Not surprisingly, the shared evolution of these fields has paralleled the needs of technology. Today, mechanicians and control engineers are brought together in fields like space systems engineering, robotics, ground and sea vehicle design, and biomechanics. Consequently, our integrated approach provides a rich set of models and control design examples that are of contemporary and practical interest.

Control theory would be quite sterile without concrete connections to the natural world. The process of modeling is just as central to control engineering as is control theory itself. A control system design project does not begin when a control engineer is handed a model; it begins at the onset of model formulation.

Our main thesis is that a full appreciation of the meaning and significance of either theory benefits by developing their connection and by applying them to meaningful examples. The capability to do the latter requires supporting computational tools. In this book, we highlight and exploit the computational infrastructure common to both modern analytical mechanics and nonlinear control. To achieve the full benefits of the concepts now available, we need to exploit symbolic as well as numerical computing techniques. However fortuitous it may be, it is only during the past decade that symbolic computing technology (or computer algebra) has matured to the level of serious engineering application.

We emphasize symbolic computing because it is essential for working with nonlinear, parameter-dependent systems and it is a relatively new tool for engineers. Symbolic computing does not replace numerical computing. It supplements and enhances it. Recognizing the distinctions between symbolic and numerical computing and how best to integrate them is a significant challenge. We will use symbolic computing for several purposes:

1. to perform basic mathematical operations (like implement a coordinate transformation or compute a Lie bracket),
2. to build explicit mathematical models,
3. to simplify models (e.g., via Taylor linearization or symmetry reduction),
4. to generate numerical simulation code,
5. to implement nonlinear control constructions (such as compute an inverse system or perform feedback linearization),
6. to generate numerical code for implementing controllers.

In this work we employ examples of various levels of complexity from simple examples that illustrate a theoretical point in a transparent way to examples with detailed models for which results are too complex to exhibit in print, but can nevertheless be manipulated using a computer. We will provide examples of the latter type using electronic media, specifically, *Mathematica* notebooks. The point is that when working with engineering grade models it is not reasonable to visually examine or manually manipulate symbolic expressions by hand. However, it is possible to work effectively with such expressions using a computer.

Many of us were attracted to control systems engineering because it enables a broad exposure to numerous areas from traditional engineering disciplines to computer and information sciences and mathematics, to economics, biology, and even social sciences. Indeed, it would be quite a challenge to find an engineer in the field for more than a few years without cross-disciplinary experience. While, in recent years, the need for a multidisciplinary approach has been touted as generally necessary for technological progress, it has always been that way in the control field. Because of the extraordinary scope of control applications, control engineers have traditionally sought out the unifying principles that make it possible to function creatively in a varied and complicated environment.

From its emergence as a coherent discipline, control engineering has involved a high level of abstraction. Mathematics, perhaps the ultimate unifying principle, and certainly the most successful language invented by man to clarify and communicate complex ideas without ambiguity, has been a cornerstone of its development. In writing this book, we had to make choices to balance competing objectives. One of the most difficult was to establish a correct level of mathematical abstraction and rigor. We view ourselves as engineers, not mathematicians, and it is from that point of view that we came to a judgment. Mathematicians may decide that our arguments lack rigor and some engineers may find our discussion too formal. However, we can judiciously sacrifice rigor for accessibility, but we often need precise statements to clearly identify the range of applicability of a technique or to establish reliable machinery for computing.

We are indebted to many students and colleagues whose collaborations with us on various research and engineering projects contributed in countless ways to the writing of this book. In particular, we would like to acknowledge Dr.Reza Ghanadan of Bell Laboratories, Mr. Chris LaVigna, Dr. Carole Teolis, and Mr. Eric Salter, all of Techno-Sciences, Inc., for their contributions to the development and application of the *ProPac* software package, and to Mr. Gaurav Bajpai of Drexel University for his careful reading of the manuscript.

Philadelphia, Pennsylvania — Harry G. Kwatny
College Park, Maryland — Gilmer L. Blankenship

Contents

Part IV Optimal and Switched Systems

Part I

Preliminaries

1

Introduction

As inexpensive processors have become increasingly ubiquitous in all manner of physical devices, the opportunities and demand for using them to improve functionality and performance has pushed control design technology to new limits. While 'emergent' application areas like robotics, biomedical and micro-electromechanical systems bring with them their special requirements, traditional fields like the aerospace, automotive, marine and process industries have also expanded the role of automation. In many of the new control problems a direct confrontation with nonlinearity is unavoidable.

Notwithstanding the advances in our understanding of nonlinear dynamical behavior and in nonlinear control theory itself, the state of control design for nonlinear systems must be considered embryonic as compared to that of linear systems. This is in part because the possibilities of nonlinear behavior are so vast and varied, but also because of the lack of tools for working efficiently with nonlinear problems of even modest engineering scale.

The control design process, while not rigidly structured, always includes three crucial elements:

1. model building
2. control design
3. control implementation

A typical control design project might follow the process in the flow chart of Figure (1.1). Modeling is central to formulating the control design problem as well as solving it. In our view it is an integral part of control system design. The diagram also accurately suggests that model building, control design and control implementation may be repeated several times during the course of a project. Clearly, tools that facilitate and automate these processes are necessary.

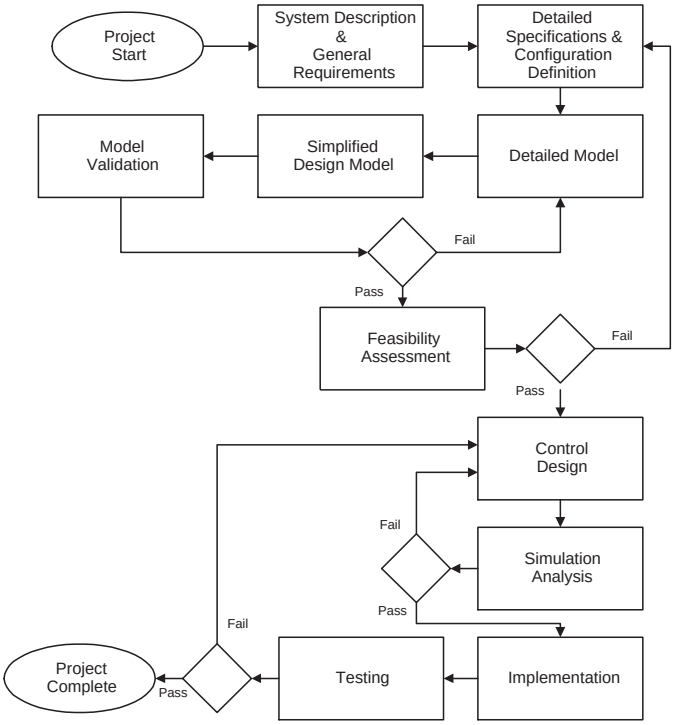

Fig. 1.1: A typical design project flow chart.

Primarily for these reasons this book addresses both modeling and control and exploits symbolic computing as a means for minimizing the painful calculations, expression manipulaton and coding that would otherwise be required. A software toolbox, *ProPac* , is included with the book. It is a package to be used with the *Mathematica* [1] computer algebra system. More will be said about the software later.

1.1 Scope and Organization

This book provides an integrated treatment of geometric nonlinear control and analytical mechanics. Their common geometric foundation and the recurrent cross fertilization between the two fields is certainly justification enough for doing so. In fact, the two subjects are so well matched that in describing one it is impossible to resist drawing examples from the other. However, not the least important factors motivating us to unify this material derive from the practical considerations described above. Control system design simply can not be divorced from modeling.

[1] For information about *Mathematica* visit the web site www.wolfram.com

Chapters 2 and 3 deal with important preliminary material. A short summary of ordinary differential equations including basic Lyapunov stability concepts is given in Chapter 2. Our treatment of these topics is brief and focuses on those items of immediate use. There are many excellent texts for the interested reader to gather additional information. A somewhat more detailed introduction to differential geometry is provided in Chapter 3. Yet, we are still selective in our choice of material from a vast literature, including only what we think is essential background. Basic calculations using *Mathematica* and *ProPac* are introduced.

Our treatment of analytical mechanics is based on the Hamilton-Lagrange formulation. It begins with a general construction for the kinematic parameters of multibody tree structures in Chapter 4. System configuration coordinates are defined in terms of a natural and general parameterization of the individual joints. Formulas that define node inertial positions and velocities in terms of configuration coordinates and generalized quasi-velocities are derived. These calculations are implemented in the accompanying software. The dynamics of tree structures as well as systems with closed loops are developed in terms of Poincaré's form of Lagrange's equations in Chapter 5. Closed loops are treated by adding constraints to an underlying tree. Constraints may be algebraic relations among the configuraton variables and/or holonomic or nonholonomic differential constraints. Constructive procedures for deriving the equations are presented and, again, implemented in the accompanying software. Examples illustrate the assembly of models of undersea vehicles, robotic systems, ground vehicles and other systems.

Nonlinear control is the subject of Chapter 6. Here, we discuss smooth affine control systems. Basic concepts of nonlinear controllability and observabilty and local decompositions via coordinate transformation are discussed first. In terms of control system design the focus of this book is on feedback linearization and dynamic inversion. Exact (state) linearization as well as partial (input-output) linearization are fully described. The chapter closes with a discussion of nonlinear observers. Of course, computation is a key issue. *ProPac* functions that implement the required calculations are introduced and illustrated.

Feedback linearization methods are strongly model based, relying, in fact, on direct cancellation. Consequently, robustness is a major concern and we devote the next two chapters to robust control. Chapter 7 addresses smooth robustification of feedback linearizing controllers. It begins with a discussion of how uncertainty propagates through the reduction to normal form of a nominal system. The notion of matched and nonmatched uncertainty is developed. Then Lyapunov redesign for matched uncertainty and robust stabilization via backstepping for strict triangular nonmatched uncertainty are described. Adaptive control methods for systems with uncertainty that can be parameterized are then presented. Once again, software tools that implement the required calculations are described and illustrated.

Chapter 8 deals with variable structure control system design. The view of variable structure control as a nonsmooth, robust variant of input-output linearization is emphasized. The chapter begins with a general discussion of discontinuous dynamics

including a formulation of Lyapunov stability analysis in that context. Methods for sliding mode and reaching control design are presented. Chattering reduction via regularizaton and other methods are described. The inherent robustness of variable structure controls with respect to matched uncertainty is established and a backstepping method is described for strict triangular nonmatched uncertainty. Supporting software is illustrated. The method also applies to a class of nonsmooth plants that includes a variety of discontinuous friction models and other so-called 'hard' nonlinearities. Examples are given.

1.2 Theme Problems

A new feature in the second edition is the inclusion of theme problems. We have chosen three areas in which the methods and tools described here have been applied.

1.2.1 Wheeled Vehicles

We examine vehicles with a variety of configurations and assumptions. The simplest is a vehicle with two active drive wheels and a third idler wheel which stabilizes the platform. A more complex two wheel vehicle does not have an idler wheel so requires balancing. In both of these examples the drive wheels model assumes perfect rolling without sideslip. Variations of a four wheel vehicle are also considered. Two and four wheel drive with front wheel steering and both front and real steering are considered. Both perfect rolling and pneumatic tire models are employed. Finally, a four wheel tractor with trailer and pneumatic tires is examined.

The treatment includes model development, dynamical studies including stability and bifurcation analysis, and control analysis.

Two Wheel Vehicles

Four Wheel Vehicles

Vehicles With Trailers

1.2.2 Aircraft

1.2.3 Electric Power Networks

1.3 Software

Most of the examples in this book have been developed using the software package *ProPac* developed by Techno-Sciences, Inc., Lanham, MD. *ProPac* 2.0 is included

with this book. It is a *Mathematica* package that provides a set of symbolic computing tools for modeling multibody mechanical systems as well as for linear and nonlinear control system design and analysis. There are excellent introductory books and tutorials available for *Mathematica*. Many of these are identified on the Wolfram web site.

The *ProPac* CD contains a set of tutorial and application notebooks. These include Dynamics.nb and Controls.nb which introduce the basic modeling and control tools available in *ProPac*. On-line help is available through *Mathematica's* Help Browser. For more information, notebooks and other documents visit the web site: www.technosci.com.

Using *ProPac* requires version 3 or later of *Mathematica*. That is all that is required to develop the equations of motion, for conducting numerical simulations within *Mathematica*, and building the C source code required for simulations in SIMULINK [2]. Use of the latter requires MATLAB/SIMULINK and a C compiler as recommended by the MathWorks for compiling MEX-files on the user's platform. Functions in *ProPac* generate C-code that compiles as SIMULINK S-functions. In this way modules for the plant and controller are easily generated for inclusion in SIMULINK simulations. Controllers, with embellishments like filters, etc., can be downloaded into DSP boards via MATLAB's Real Time Workshop. The setup is illustrated in Figure (**??**).

1.3.1 Installing *ProPac*

To install *ProPac*, follow the two step procedure:

Step 1: Put the entire ProPac directory in Mathematica's Applications directory. For the PC the full path is ordinarily

```
C:\Program Files\Wolfram Research
                          \Mathematica\7.0
                                  \AddOns\Applications\
```

Step 2: Start Mathematica and rebuild the Help index. The latter is accomplished with the following simple procedure. From the main menu choose: Help ⇒ Rebuild Help Index

Once this is done, on-line help is available. In the Help Browser select Add-ons and then TSi ProPac.

The Mex folder contains 3 C-source files that need to be included when compiling MATLAB/SIMULINK MEX files. These may stored in any convenient location, but must be available at the time of compilation.

[2] for information about MATLAB/SIMULINK visit the web site www.MathWorks.com

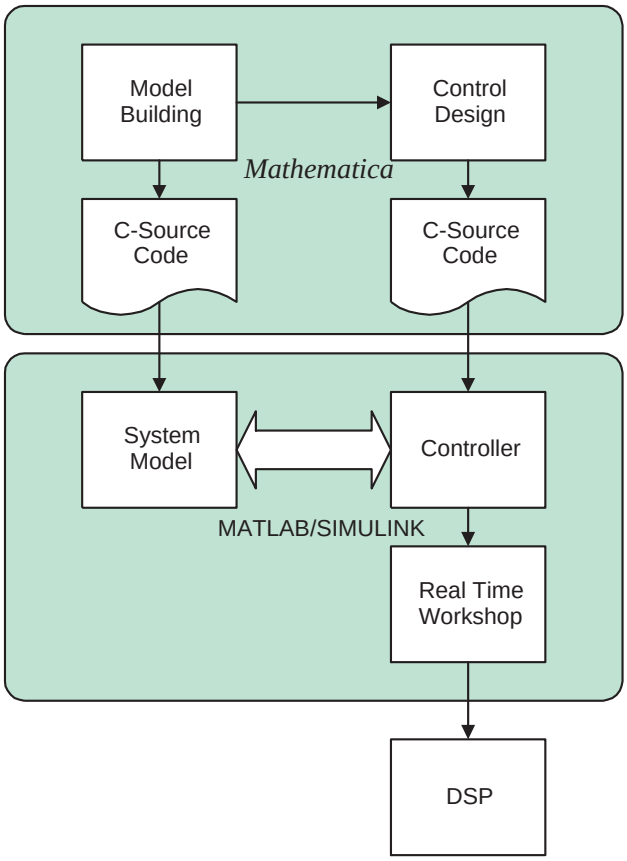

Fig. 1.2: *ProPac* is a *Mathematica* package with links to MATLAB/SIMULINK.

1.3.2 Package Content

ProPac consists of seven packages: Dynamics, ControlL, ControlN, GeoTools, MEXTools, NDTools, and VSCTools. Once *ProPac* is loaded all of the functions in these packages are available for use and the appropriate packages will be automatically loaded as required. In general, a user does not have to be concerned about loading any particular package. To load *ProPac* simply enter `<<ProPac`` (most of the package functionality is available in Mathematica 2.2, enter `<<ProPac` Master``).

Dynamics contains the model building functions and ControlL and ControlN the linear and nonlinear control analysis functions, respectively. GeoTools includes basic functions used in differential geometry calculations. NDTools contains supporting functions for working with nondifferentiable nonlinearities and VSCTools contains functions for variable structure control. MEXTools includes functions for creating

C-code files for both models and controllers that compile as S-functions for use with MATLAB/SIMULINK.

The Tables in the Appendix contain a brief summary of many of the available functions. More details and numerous examples can be found in the help browser and in the notebooks.

2

Introduction to Dynamical Systems

2.1 Introduction

In this chapter we briefly review some basic material about nonlinear ordinary differential equations that is important background for later chapters. After a preliminary discussion of the basic properties of differential equations including the existence and uniqueness of solutions, we turn to a short discussion of stability in the sense of Lyapunov. In addition to stating the most important theorems on stability and instability we provide a number of illustrative examples. As part of this discussion we introduce Lagrangian systems – a topic to be treated at great length later. This chapter is concerned exclusively with dynamical systems (as opposed to control systems) and with smooth systems (as opposed to systems that contain nondifferentiable nonlinearities). Those topics will be treated in later chapters. It is presumed that the material discussed is not new to the reader and we provide only a short summary of those elements considered immediately relevant. For a more complete discussion many excellent text books are available. We reference a number of them in the sequel.

2.2 Preliminaries

A *linear vector space* , $\mathscr{V}$- over the field R is a set of elements called vectors such that:

1. for each pair $x, y \in \mathscr{V}$, the sum $x+y$ is defined, $x+y \in \mathscr{V}$ and $x+y = y+x$.
2. there is an element '0' in $\mathscr{V}$ such that for every $x \in \mathscr{V}$, $x+0 = x$.
3. for any number $a \in R$ and vector $x \in \mathscr{V}$ scalar multiplication is defined and $ax \in \mathscr{V}$.
4. for any pair of numbers $a, b \in R$ and vectors $x, y \in \mathscr{V}$: $1 \cdot x = x$, $(ab)x = a(bx)$, $(a+b)x = ax+bx$.

A linear vector space is a *normed linear space* if for each vector $x \in \mathscr{V}$ - there corresponds a real number $\|x\|$ called the *norm* of x which satisfies:

1. $\|x\| > 0,\ x \neq 0,\ \|0\| = 0$
2. $\|x+y\| \leq \|x\| + \|y\|$ (triangle inequality)
3. $\|ax\| = |a|\ \|x\|\ \forall a \in R,\ x \in \mathscr{V}$

When confusion can arise as to which space a norm is defined in we replace $\|\bullet\|$ by $\|\bullet\|_{\mathscr{V}}$.

A sequence $\{x_k\} \subset \mathscr{V}$, $\mathscr{V}$ a normed linear space, *converges* to $x \in \mathscr{V}$ if

$$\lim_{k\to\infty} \|x_k - x\| = 0$$

. A sequence $\{x_k\} \subset \mathscr{V}$-is a *Cauchy sequence* if for every $\varepsilon > 0$ there is an integer, $N(\varepsilon) > 0$ such that $\|x_n - x_m\| < \varepsilon$ if $n,m > N(\varepsilon)$. Every convergent sequence is a Cauchy sequence but not vice versa. The space - is *complete* if every Cauchy sequence is a convergent sequence. A complete normed linear space is called a *Banach* space .

The most basic Banach space of interest herein is n-dimensional *Euclidean* space, the set of all n-tuples of real numbers, denoted R^n. The most common types of norms applied to R^n are the p-norms, defined by

$$\|x\|_p = (|x_1|^p + \cdots + |x_n|^p)^{1/p}, \quad 1 \leq p < \infty$$

and

$$\|x\|_\infty = \max_{i\in\{1,\ldots,n\}} |x_i|$$

An ε-*neighborhood* of an element x of the normed linear space $\mathscr{V}$ is the set $S(x,\varepsilon) = \{y \in V |\ \|y-x\| < \varepsilon\}$. A set A in $\mathscr{V}$ is *open* if for every $x \in A$ there exists an ε-neighborhood of x also contained in A. An element x is a *limit point* of a set $A \subset \mathscr{V}$ if each ε-neighborhood of x contains points in A. A set A is *closed* if it contains all of its limit points. The *closure* of a set A, denoted $\bar{A}$, is the union of A and its limit points. A set A is *dense* in $\mathscr{V}$ if the closure of A is $\mathscr{V}$.

If B is a subset of $\mathscr{V}$, A is a subset of R, and $\{V_a, a \in A\}$ is a collection of open subsets of $\mathscr{V}$ such that $\cup_{a\in A} V_a \supset B$, then the collection V_a is called an *open covering* of B. A set B is *compact* if every open covering of B contains a finite number of subsets which is also an open covering of B. For a Banach space this is equivalent to the property that every sequence $\{x_n\}, x_n \in B$, contains a subsequence which converges to an element of B. A set B is *bounded* if there exists a number $r > 0$ such that $B \subset \{x \in \mathscr{V} |\ \|x\| < r\}$. A set B in R^n is compact if and only if it is closed and bounded.

A function f taking a set A of a space $\mathscr{X}$ into a set B of a space $\mathscr{Y}$ is called a *mapping* of A into B and we write $f : A \to B$. A is the *domain* of the mapping and

B is the *range* or *image*. The image of f is denoted $f(A)$. f is *continuous* if, given $\varepsilon > 0$, there exists $\delta > 0$ such that

$$\|x-y\| < \delta \Rightarrow \|f(x)-f(y)\| < \varepsilon$$

A function f defined on a set A is said to be *one-to-one* on A if and only if for every $x,y \in A$, $f(x) = f(y) \Rightarrow x = y$. If f is one-to-one it has an inverse denoted f^{-1}. If the one-to-one mapping f and its inverse f^{-1} are continuous, f is called a *homeomorphism* of A onto B.

Suppose $\mathscr{X}$ and $\mathscr{Y}$ are Banach spaces and $f : \mathscr{X} \to \mathscr{Y}$. f is a *linear map* if $f(a_1x_1 + a_2x_2) = a_1f(x_1) + a_2f(x_2)$ for all $x_1, x_2 \in \mathscr{X}$ and $a_1, a_2 \in R$ (or C). In general, we can write a linear mapping in the form $y = Lx$, where L is an appropriately defined 'linear operator.' A linear map f is said to be *bounded* if there is a constant K such that $\|f(x)\|_{\mathscr{Y}} \leq K\|x\|_{\mathscr{X}}$ for all $x \in \mathscr{X}$. A linear map $f : \mathscr{X} \to \mathscr{Y}$ is bounded if and only if it is continuous. A linear map from $R^n \to R^m$ is characterized by an $m \times n$ matrix of real elements, e.g., $y = Ax$. The 'size' of the matrix A can be measured by the *induced p-norm* (or gain) of A

$$\|A\|_p = \sup_{x \neq 0} \frac{\|Ax\|_p}{\|x\|_p}$$

for which we write the following special cases

$$\|A\|_1 = \max_{1 \leq j \leq n} \sum_{i=1}^{m} |a_{ij}|$$

$$\|A\|_2 = \sqrt{\lambda_{\max}(A^TA)}$$

$$\|A\|_\infty = \max_{1 \leq i \leq m} \sum_{j=1}^{n} |a_{ij}|$$

Here, $\lambda_{\max}(A^TA)$ denotes the largest eigenvalue of the nonnegative matrix A^TA.

f is said to be (*Frechet*) *differentiable* at a point $x \in A$ if there exists a bounded linear operator $L(x)$ mapping $\mathscr{X} \to \mathscr{Y}$ such that for every $h \in \mathscr{X}$ with $x + h \in A$

$$\|f(x+h) - f(x) - L(x)h\| / \|h\| \to 0$$

as $\|h\| \to 0$. $L(x)$ is called the derivative of f at x. If $f : R^n \to R^m$ is differentiable at x then $L(x) = \partial f(x)/\partial x$, the Jacobian of f with respect to x. If f and f^{-1} have continuous first derivatives, f is a *diffeomorphism*.

A function $f : A \to B$ is said to belong to the class C^k of functions if it has continuous derivatives up to order k. It belongs to the class C^∞ if it has continuous derivatives of any order. C^∞ functions are sometimes called *smooth*. A function f is said to be *analytic* if for each $x_0 \in A$ there is a neighborhood U of x_0 such that the Taylor series expansion of f at x_0 converges to $f(x)$ for all $x \in U$.

Consider a transformation $T : \mathscr{X} \to \mathscr{X}$, where $\mathscr{X}$ is a Banach space. $x \in \mathscr{X}$ is a *fixed point* of T if $x = T(x)$. Suppose A is a subset of Banach space $\mathscr{X}$ and T is a mapping of A into a Banach space $\mathscr{B}$. The transformation T is a *contraction* on A if there exists a number $0 \leq \lambda < 1$ such that

$$\|T(x) - T(y)\| \leq \lambda \|x - y\|, \quad \forall x, y \in A$$

Proposition 2.1 (Contraction Mapping Theorem). *Suppose A is a closed subset of a Banach space $\mathscr{X}$ and $T : A \to A$ is a contraction on A. Then*

1. *T has a unique fixed point $\bar{x} \in A$*
2. *If $x_0 \in A$ is arbitrary, then the sequence $\{x_{n+1} = T(x_n),\ n = 0, 1, \ldots\}$ converges to $\bar{x}$.*
3. *$\|x_n - \bar{x}\| \leq \lambda^n \|x_1 - x_0\| / (1 - \lambda)$, where $\lambda < 1$ is the contraction constant for T on A.*

Proof: [33], page 5.

We will make use of the following important theorem.

Proposition 2.2 (Implicit Function Theorem). *Suppose $F : R^n \times R^m \to R^n$ has continuous first partial derivatives and $F(0,0) = 0$. If the Jacobian matrix $\partial F(x,y)/\partial x$ is nonsingular, then there exists neigborhoods U, V of the origin in R^n, R^m, respectively, such that for each $y \in V$ the equation $F(x,y) = 0$ has a unique solution $x \in U$. Furthermore, this solution can be given as $x = g(y)$, i.e., $F(g(y), y) = 0$ on V, where g has continuous first derivatives and $g(0) = 0$.*

Proof: [33], page 8.

2.3 Ordinary Differential Equations

Existence and Uniqueness

Let $t \in R$, $x \in R^n$, D an open subset of R^{n+1}, $f : D \to R^n$ a map and let $\dot{x} = dx/dt$. We will consider differential equations of the type

$$\dot{x} = f(x,t), \quad x \in R^n,\ t \in R \tag{2.1}$$

When t is explicitly present in the right hand side of (2.1), then the system is said to be *nonautonomous*. Otherwise it is *autonomous*. A solution of (2.1) on a time

interval $t \in [t_0, t_1]$ is a function $x(t) : [t_0, t_1] \to R^n$, such that $dx(t)/dt = f(x, t(t))$ for each $t \in [t_0, t_1]$. We can visualize an individual solution as a graph $x(t) : t \to R^n$. For autonomous systems it is convenient to think of $f(x)$ as a 'vector field' on the space R^n. $f(x)$ assigns a vector to each point $x \in R^n$. As t varies, a solution $x(t)$ traces a path through R^n. These curves are often called *trajectories* or *orbits*. At each point $x \in R^n$ the trajectory $x(t)$ is tangent to the vector $f(x)$. The collection of all trajectories in R^n is called the *flow* of the vector field $f(x)$. This point of view can be extended to nonautonomous differential equations in which case the vector field $f(x,t)$ and its flow vary with time.

Example 2.3 (Phase portraits). For two dimensional systems the trajectories can be plotted in a plane. We will consider two systems, the Van der Pol system

$$\begin{bmatrix} \dot{x}_1 \\ \dot{x}_2 \end{bmatrix} = \begin{bmatrix} x_2 \\ -0.8(1 - x_1^2)x_2 - x_1 \end{bmatrix}$$

and the damped pendulum

$$\begin{bmatrix} \dot{x}_1 \\ \dot{x}_2 \end{bmatrix} = \begin{bmatrix} x_2 \\ -x_2/2 - \sin x_1 \end{bmatrix}$$

Both of these systems are in so-called phase variable form (the first equation, $\dot{x}_1 = x_2$, defines velocity) so the trajectory plots are called phase portraits.

Van der Pol

```
In[1]:= f = {x2, -x1 + 0.8  (1 - x1^2)x2}; x = {x1, x2};

In[2]:= graphs3 = PhasePortrait[f, x, 15, {{-6, 6, 0.5}, {-5, 5, 5}}];

In[3]:= Show[graphs3, AxesLabel → {x1, x2}, PlotRange → {{-4, 4}, {-4, 4}},
          DisplayFunction → $DisplayFunction]
```

$$f = \left\{x_2, -x_1 + .8\left(1 - {x_1}^2\right)x_2\right\}; x = \{x_1, x_2\};$$
graphs3 = Flatten[Table[PhaseTrajectory($f, x, 15, s_1, s_2$), {s$_1$, −6, 6, 0.5}, {s_2, −5, 5, 5}]];

Damped Pendulum

```
In[4]:= f = {x2, -Sin[x1] - x2/2}; x = {x1, x2};

In[5]:= graphs2 = PhasePortrait[f, x, 15, {{-20, 20, 0.5}, {-3, 3, 3}}];

In[6]:= Show[graphs2, AxesLabel → {x1, x2}, PlotRange → {{-10, 10}, {-3, 3}},
          DisplayFunction → $DisplayFunction]
```

The above examples illustrate several important properties of nonlinear dynamical systems. In both cases the flow directions are to the right in the upper half plane and to the left in the lower half plane (recall $\dot{x}_1 = x_2$). Thus, it is easily seen that

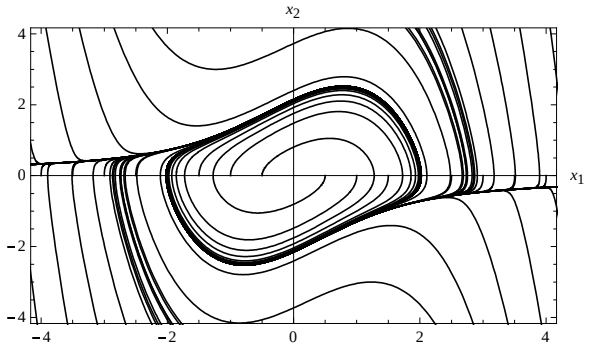

Fig. 2.1: Phase portrait for the Van der Pol equation.

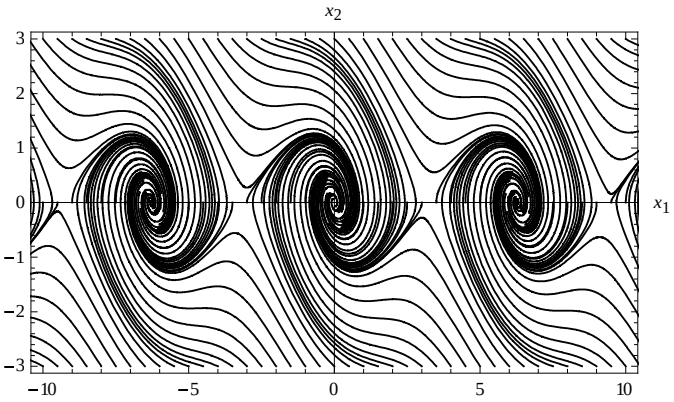

Fig. 2.2: Phase portrait for the damped pendulum.

trajectories of the pendulum ultimately converge to rest points corresponding to the pendulum hanging straight down. These have the property that $f(x) = 0$. Any point $x \in R^n$ satisfying the condition $f(x) = 0$ is called an *equilibrium point*. The pendulum has an infinite number of equilibria spaced π radians apart. Some of these are attracting (the pendulum points straight down) and some repelling (straight up).

In contrast, all trajectories of the Van der Pol equation approach a periodic trajectory. Such an isolated periodic trajectory is called a *limit cycle*. Some systems can exhibit multiple limit cycles and they can be repelling as well as attracting. Equilibria and limit cycles are two types of 'limit sets' that are associated with differential equations. We will define limit sets precisely below. As a matter of fact, these are the only type of limit sets exhibited by two-dimensional systems. More exotic ones, like 'strange attractors' require at least three dimensional state spaces.

The existence and uniqueness of solutions to (2.1) depend on properties of the function f. In many applications $f(x,t)$ is continuous in the variables t and x. We will impose a somewhat less restrictive characterization of f. We say that a function $f : R^n \to R^n$ is *locally Lipschitz* on an open and connected subset $D \subset R^n$, if each point $x_0 \in D$ has a neighborhood U_0 such that

$$\| f(x) - f(x_0) \| \leq L \| x - x_0 \| \tag{2.2}$$

for some constant L and all $x \in U_0$. The function $f(x)$ is said to be *Lipschitz* on the set D if it satisfies the (local) Lipschitz condition uniformly (with the same constant L) at all points $x_0 \in D$. It is *globally Lipschitz* if it is Lipschitz on $D = R^n$. We apply the terminology 'Lipschitz in x' to functions $f(x,t)$ provided the Lipschitz condition holds uniformly for each t in a given interval of R.

Note that C^0 functions need not be Lipschitz but C^1 functions always are. The following theorems relate the notion of Lipshitz with the property of continuity.

Lemma 2.4. *Let $f(x,t)$ be continuous on $D \times [a,b]$, for some domain $D \subset R^n$. If $\partial f / \partial x$ exists and is continuous on $D \times [a,b]$, then f is locally Lipschitz in x on $D \times [a,b]$.*

Proof: (following Khalil [52], p. 77) For $x_0 \in D$ there is an r sufficiently small that

$$D_0 = \{ x \in R^n \, | \| x - x_0 \| < r \} \subset D$$

The set D_0 is convex and compact. Since f is C^1, $\partial f / \partial x$ is bounded on $[a,b] \times D_0$. Let L_0 denote such a bound. If $x, y \in D_0$, then by the mean value theorem there is a point z on the line segment joining x, y such that

$$\| f(x,t) - f(t,y) \| = \left\| \frac{\partial f(t,z)}{\partial x} (x - y) \right\| \leq L_0 \| x - y \|$$

■

The proof of this Lemma is easily adapted to prove the following.

Proposition 2.5. *Let $f(x,t)$ be continuous on $[a,b] \times R^n$. If f is C^1 in $x \in R^n$ for all $t \in [a,b]$ then f is globally Lipschitz in x if and only if $\partial f / \partial x$ is uniformly bounded on $[a,b] \times R^n$.*

Let us state the key existence result.

Proposition 2.6 (Local Existence and Uniqueness). *Let $f(x,t)$ be piecewise continuous in t and satisfy the Lipschitz condition*

$$\| f(x,t) - f(t,y) \| \leq L \| x - y \|$$

for all $x,y \in B_r = \{x \in R^n \,|\, \|x-x_0\| < r\}$ and all $t \in [t_0,t_1]$. Then there exists a $\delta > 0$ such that the differential equation with initial condition

$$\dot{x} = f(x,t), \quad x(t_0) = x_0 \in B_r$$

has a unique solution over $[t_0, t_0+\delta]$.

Proof: ([52], p. 74)

A continuation argument leads to the following global extension.

Proposition 2.7 (Global Existence and Uniqueness). *Suppose $f(x,t)$ is piecewise continuous in t and satisfies*

$$\|f(x,t) - f(t,y)\| \le L\|x-y\|$$

$$\|f(x,t_0)\| < h$$

for all $x,y \in R^n$ and all $t \in [t_0,t_1]$. Then the equation

$$\dot{x} = f(x,t), \quad x(t_0) = x_0$$

has a unique solution over $[t_0,t_1]$.

Continuous Dependence on Parameters and Initial Data

Let $\mu \in R^k$ and consider the parameter dependent differential equation

$$\dot{x} = f(x,t,\mu), \quad x(t_0) = x_0 \tag{2.3}$$

We will show that a solution $x(t;t_0,x_0,\mu)$ defined on a finite time interval $[t_0,t_1]$ is continuously dependent on the parameter μ and the initial data t_0, x_0.

Definition 2.8. *Let $x(t;t_0,\xi_0,\mu_0)$ denote a solution of (2.3) defined on the finite interval $t \in [t_0,t_1]$ with $\mu = \mu_0$ and $x(t_0;t_0,\xi_0,\mu_0) = \xi_0$. The solution is said to* depend continuously on μ at μ_0 *if for any $\varepsilon > 0$ there is a $\delta > 0$ such that such that for all μ in the neighborhood $U = \{\mu \in R^k \,|\, \|\mu - \mu_0\| < \delta\}$, (2.3) has a solution $x(t;t_0,\xi_0,\mu)$ such that*

$$\|x(t;t_0,\xi_0,\mu) - x(t;t_0,\xi_0,\mu_0)\| < \varepsilon$$

for all $t \in [t_0,t_1]$. Similarly, the solution is said to depend continously on ξ at ξ_0 *if for any $\varepsilon > 0$ there is a $\delta > 0$ such that such that for all ξ in the neighborhood $X = \{\xi \in R^k \,|\, \|\xi - \xi_0\| < \delta\}$, (2.3) has a solution $x(t;t_0,\xi,\mu_0)$ such that*

$$\|x(t;t_0,\xi,\mu_0) - x(t;t_0,\xi_0,\mu_0)\| < \varepsilon$$

for all $t \in [t_0,t_1]$.

The following result establishes the basic continuity properties of (2.3) on finite time intervals.

Proposition 2.9. *Suppose $f(x,t,\mu)$ is continuous in (x,t,μ) and locally Lipschitz in x (uniformly in t and μ) on $[t_0,t_1]\times D\times\{\|\mu-\mu_0\|<c\}$ where $D\subset R^n$ is an open connected set. Let $x(t;t_0,\xi_0,\mu_0)$ denote a solution of (2.3) that belongs to D for all $[t_0,t_1]$. Then given $\varepsilon>0$ there is $\delta>0$ such that*

$$\|\xi-\xi_0\|<\delta,\ \|\mu-\mu_0\|<\delta$$

implies that there is a unique solution $x(t;t_0,\xi,\mu)$ of (2.3) defined on $t\in[t_0,t_1]$ and such that

$$\|x(t;t_0,\xi,\mu)-x(t;t_0,\xi_0,\mu_0)\|<\varepsilon,\ \forall t\in[t_0,t_1]$$

Proof: ([52], p. 86)

We emphasize that the results on existence and continuity of solutions hold on finite time intervals $[t_0,t_1]$. Stability, as we shall see below, requires us to consider solutions defined on infinite intervals. We will often tacitly assume that they are so defined. Continuity issues with respect to both initial conditions and parameters for solutions on infinite time intervals are quite subtle.

Invariant Sets

In the following paragraphs we shall restrict attention to autonomous systems

$$\dot{x}=f(x),\quad x(t_0)=x_0 \tag{2.4}$$

In many instances the results can be extended to nonautonomous systems by extending the nonautonomous differential equation with the addition of a new state $\dot{x}_{n+1}=1$ to replace t in the right side of the differential equation.

Let us denote by $\Psi(x,t)$ the flow of the vector field f on R^n defined by (2.4) i.e. $\Psi(x,t)$ is the solution of (2.4) with $\Psi(0,x)=x$:

$$\frac{\partial\Psi(x,t)}{\partial t}=f\left(\Psi(x,t)\right),\quad \Psi(0,x)=x$$

Definition 2.10. *A set of points $S\subset R^n$ is* invariant *with respect to f if trajectories beginning in S remain in S both forward and backward in time, i.e., if $s\in S$, then $\Psi(t,s)\in S,\forall t\in R$.*

Obviously, any entire trajectory of (2.4) is an invariant set. Such an invariant set is minimal in the sense that it does not contain any proper subset which is itself an invariant set.

A set S is invariant if and only if $\Psi(t,S)\mapsto S$ for each $t\in R$.

Nonwandering Sets

Definition 2.11. *A point $p \in R^n$ is a* nonwandering point *with respect to the flow Ψ if for every neighborhood U of p and $T > 0$, there is a $t > T$ such that $\Psi(t,U) \cap U \neq \emptyset$. The set of nonwandering points is called the* nonwandering set, *and denoted Ω. Points that are not nonwandering are called* wandering points.

The nonwandering set is a closed, invariant set. For proofs and other details see, for example, Guckenheimer and Holmes [32], Arrowsmith and Place [3] or Sibirsky [94]. The detailed structure of the nonwandering set is an important aspect of the analysis of strange attractors.

Obviously, fixed points and periodic trajectories belong to Ω.

Limit Sets

Definition 2.12. *A point $q \in R^n$ is said to be an* ω-limit point *of the trajectory $\Psi(t,p)$ if there exists a sequence of time values $t_k \to +\infty$ such that*

$$\lim_{t_k \to \infty} \Psi(t_k, p) = q$$

q is said to be an α-limit point *of $\Psi(t,p)$ if there exists a sequence of time values $t_k \to -\infty$ such that*

$$\lim_{t_k \to -\infty} \Psi(t_k, p) = q$$

The set of all ω-limit points of the trajectory through p is the ω-limit set, *$\Lambda_\omega(p)$, and the set of all α-limit points of the trajectory through p is the* α-limit set, *$\Lambda_\alpha(p)$.*

Hirsch and Smale [41] remind us that α, ω are the first and last letters of the Greek alphabet and, hence, the terminology.

Proposition 2.13. *The α-, ω- limit sets of any trajectory are closed invariant sets and they are subsets of the nonwandering set Ω.*

Proof: Hirsch and Smale [41] or Sibirsky [94] for closed, invariant sets. That they are subsets of Ω is obvious.

We can make some simple observations

1. if $r \in \Psi(t,p)$, then $\Lambda_\omega(r) = \Lambda_\omega(p)$ and $\Lambda_\alpha(r) = \Lambda_\alpha(p)$, i.e., any two points on a given trajectory have the same limit points.
2. if p is an equilibrium point, i.e., $f(p) = 0$ or $p = \Psi(t,p)$, then $\Lambda_\omega(p) = \Lambda_\alpha(p) = p$.

3. If $\Psi(t,p)$ is a periodic trajectory $\Lambda_\omega(p) = \Lambda_\alpha(p) = \Psi(R,p)$, i.e., the α and ω limit sets are the entire trajectory.

Finally, let us state the following important result.

Proposition 2.14. *A homeomorphism of a dynamical system maps ω-, α- limit sets into ω-, α- limit sets.*

Proof: [94].

2.4 Lyapunov Stability

2.4.1 Autonomous Systems

In the following paragraphs we consider autonomous differential equations and assume that the origin is an equilibrium point:

$$\dot{x} = f(x), \quad f(0) = 0 \tag{2.5}$$

with $f : D \to R^n$, locally Lipschitz in the domain D.

Definition 2.15. *The origin of (2.5) is*

1. *a* stable equilibrium point *if for each $\varepsilon > 0$, there is a $\delta(\varepsilon) > 0$ such that*

$$\|x(0)\| < \delta \Rightarrow \|x(t)\| < \varepsilon \ \forall t > 0$$

2. unstable *if it is not stable, and*
3. asymptotically stable *if δ can be chosen such that*

$$\|x(0)\| < \delta \Rightarrow \lim_{t\to\infty} x(t) = 0$$

The concept of Lyapunov stability is depicted in Figure (2.3).

The next seemingly trivial observation is nontheless useful. Among other things, it highlights the distinction between stability and asymptotic stability.

Lemma 2.16 (Necessary condition for asymptotic stability). *Consider the dynamical system $\dot{x} = f(x)$ and suppose $x = 0$ is an equilibrim point, i.e., $f(0) = 0$. Then $x = 0$ is asymptotically stable only if it is an isolated equilibrium point.*

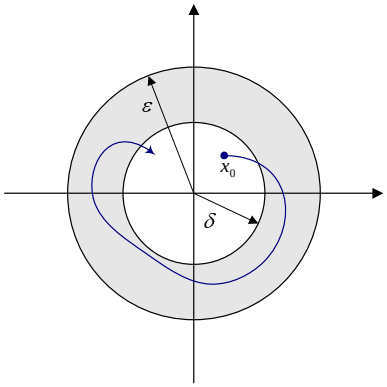

Fig. 2.3: Definition of Lyapunov stability.

Proof: If $x = 0$ is not an isolated equilibrium point, then in every neighborhood U of 0 there is at least one other equilibrium point. Thus, that not all trajectories beginning in U tend to 0 as $t \to \infty$. ■

For linear systems the following result is easily obtained.

Proposition 2.17. *The origin of the linear system $\dot{x} = Ax$ is a stable equilibrium point if and only if*

$$\left\|e^{At}\right\| \leq N < \infty \; \forall t > 0$$

It is asymptotically stable if and only if, in addition, $\left\|e^{At}\right\| \to 0$, $t \to \infty$

Proof: Exercise (choose $\delta = \varepsilon / N$)

Positive Definite Functions

Definition 2.18. *A function $V : R^n \to R^n$ is said to be*

1. positive definite *if $V(0) = 0$ and $V(x) > 0$, $x \neq 0$,*
2. positive semidefinite *if $V(0) = 0$ and $V(x) \geq 0$, $x \neq 0$,*
3. negative definite *(*negative semidefinite*) if $-V(x)$ is positive definite (positive semidefinite)*

For a quadratic form $V(x) = x^T Q x$, $Q = Q^T$, the following statements are equivalent

1. $V(x)$ is positive definite
2. the eigenvalues of Q are positive real numbers

3. all of the principal minors of Q are positive

$$|q_{11}| > 0, \begin{vmatrix} q_{11} & q_{12} \\ q_{21} & q_{22} \end{vmatrix} > 0, \ldots, |Q| > 0$$

Definition 2.19. *A C^1 function $V(x)$ defined on a neighborhood D of the origin is called a* Lyapunov function *relative to the flow defined by $\dot{x} = f(x)$ if it is positive definite and it is nonincreasing along trajectories of the flow, i.e.,*

$$V(0) = 0,\ V(x) > 0,\ x \in D - \{0\}$$

$$\dot{V} = \frac{\partial V(x)}{\partial x} f(x) \leq 0$$

2.4.2 Basic Stability Theorems

Stability of a dynamical system may determined directly from an examination of the trajectories of the system or from a study of Lyapunov functions. The basic idea of the Lyapunov method derives from the idea of energy exchange in physical systems. A general physical conception is that stable systems dissipate energy so that the stored energy of a stable system decreases or at least does not increase as time evolves. The notion of a Lyapunov function is thereby an attempt to formulate a precise, energy-like theory of stability.

Proposition 2.20 (Lyapunov Stability Theorem). *If there exists a Lyapunov function $V(x)$ on some neighborhood D of the origin, then the origin is stable. Furthermore, if $\dot{V}$ is negative definite on D then the origin is asymptotically stable.*

Proof: Given $\varepsilon > 0$ choose $r \in (0, \varepsilon]$ such that

$$B_r = \{x \in R^n \,|\, \|x\| < r\} \subset D$$

Now, we can find a level set $C_\alpha = \{x \in R^n \,|\, V(x) = \alpha\}$ which lies entirely within B_r. Refer to Figure (2.4). The existence of such a set follows from the fact that since V is positive and continuous on B_r, it has a positive minimum, α, on ∂B_r. The level set C_α defined by $V(x) = \alpha$ must lie entire in B_r.

Now, since V is continuous and vanishes at the origin, there exists a $\delta > 0$ such that B_δ lies entirely within the set bounded by C_α, i.e.,

$$\Omega_\alpha = \{x \in R^n \,|\, V(x) \leq \alpha\}$$

Since V is nonincreasing along trajectories, trajectories which begin in B_δ must remain in Ω_α, $\forall t > 0$. Hence they remain in B_ε. In the event that $\dot{V}$ is negative definite, V decreases steadily along trajectories. For any $0 < r_1 < r$ there is a $\beta < \alpha$ such that

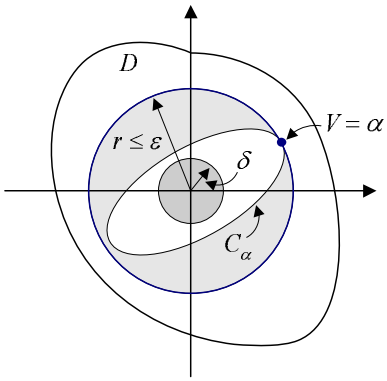

Fig. 2.4: Sets used in proof of the Lyapunov stability theorem, Proposition (2.20).

B_β lies entirely within B_{r_1}. Since $\dot{V}$ has a strictly negative maximum in the annular region $B_r - B_{r_1}$, any trajectory beginning in the annular region must eventually enter B_{r_1}. Thus, all trajectories must tend to the origin as $t \to \infty$. ■

Unlike linear systems, an asymptotically stable equilibrium point of a nonlinear system may not attract trajectories from all possible initial states. It is more likely that trajectories beginning at states in a restricted vicinity of the equilibrium point will actually tend to the equilibrium point as $t \to \infty$. The above theorem can be used to establish stability and also to provide estimates of the *domain of attraction* using level sets of the Lyapunove function $V(x)$.

The following theorem due to LaSalle allows us to more easily characterize the domain of attraction of a stable equilibrium point and is a more powerful result than the basic Lyapunov stability theorem because the conditions for asymptotic stability do not require $\dot{V}$ to be negative definite.

Proposition 2.21 (LaSalle Invariance Theorem). *Consider the system defined by equation (2.5). Suppose $V(x) : R^n \to R$ is C^1 and let Ω_c designate a component of the region $\{x \in R^n \,|V(x) < c\}$. Suppose Ω_c is bounded and that within Ω_c $\dot{V}(x) \leq 0$. Let E be the set of points within Ω_c where $\dot{V} = 0$, and let M be the largest invariant set of (2.5) contained in E. Then every solution $x(t)$ of (2.5) beginning in Ω_c tends to M as $t \to \infty$.*

Proof: (following [71]) $\dot{V}(x) \leq 0$ implies that $x(t)$ starting in Ω_c remains in Ω_c. $V(x(t))$ nonincreasing and bounded implies that $V(x(t))$ has a limit c_0 as $t \to \infty$ and $c_0 < c$. By continuity of $V(x)$, $V(x) = c_0$ on the positive limit set $\Lambda_\omega(x_0)$ of $x(t)$ beginning at $x_0 \in \Omega_c$. Thus, $\Lambda_\omega(x_0)$ is in Ω_c and $\dot{V}(x) = 0$ on $\Lambda_\omega(x_0)$. Consquently, $\Lambda_\omega(x_0)$ is in E, and since it is an invariant set, it is in M. ■

Note that the theorem does not specify that $V(x)$ should be positive definite, only that it have continuous first derivatives and that there exist a bounded region on which $V(x) < c$ for some constant c. A number of useful results follow directly from this one.

Corollary 2.22. *Let $x = 0$ be an equilibrium point of (2.5). Suppose D is a neighborhood of $x = 0$ and $V : D \to R$ is C^1 and positive definite on D such that $\dot{V}(x) \leq 0$ on D. Let $E = \left\{ x \in D \,\middle|\, \dot{V}(x) = 0 \right\}$ and suppose that the only entire solution contained in E is the trivial solution. Then the origin is asymptotically stable.*

Corollary 2.23. *Let $x = 0$ be an equilibrium point of (2.5). Suppose*

1. *$V(x)$ is C^1*
2. *$V(x)$ is radially unbounded (Barbashin-Krasovskii condition), i.e.,*
$$\|x\| \to \infty \Rightarrow V(x) \to \infty$$
3. *$\dot{V}(x) \leq 0$, $\forall x \in R^n$*
4. *the only entire trajectory contained in the set $E = \left\{ x \in D \,\middle|\, \dot{V}(x) = 0 \right\}$ is the trivial solution.*

Then the origin is globally asymptotically stable.

The stability theorems provide only sufficient conditions for stability and construction of a suitable Lyapunov function may require a fair amount of ingenuity. In the event that attempts to establish stability do not bear fruit it may be useful to try to confirm instabilty.

Proposition 2.24 (Chetaev Instability Theorem). *Consider equation (2.5) and suppose $x = 0$ is an equilibrium point. Let D be a neighborhood of the origin. Suppose there is a function $V(x) : D \to R$ and a set $D_1 \subset D$ such that*

1. *$V(x)$ is C^1 on D,*
2. *the origin belongs to the boundary of D_1, ∂D_1,*
3. *$V(x) > 0$ and $\dot{V}(x) > 0$ on D_1,*
4. *On the boundary of D_1 inside D, i.e. on $\partial D_1 \cap D$, $V(x) = 0$*

Then the origin is unstable

Proof: Choose an r such that $B_r = \{ x \in R^n \,|\, \|x\| \leq r \}$ is in D. Refer to Figure (2.5). For any trajectory beginning inside $U = D_1 \cap B_r$ at $x_0 \neq 0$, $V(x(t))$ increases indefinitely from $V(x_0) > 0$. But by continuity, $V(x)$ is bounded on U. Hence $x(t)$ must leave U. It cannot do so across its boundary interior to B_r so it must leave B_r. ■

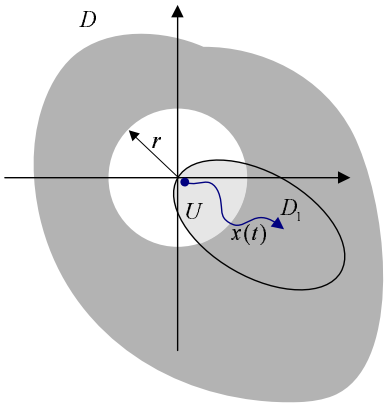

Fig. 2.5: Sets used in proof of the Chetaev instability theorem, Proposition (2.24).

Stability of Linear Systems

Consider the linear system

$$\dot{x} = Ax \tag{2.6}$$

Proposition 2.25. *Consider the Lyapunov equation*

$$A^T P + PA = -Q \tag{2.7}$$

(a) If there exists a positive definite pair of symmetric matrices P, Q satisfying the Lyapunov equation then the origin of the system (2.6) is asymptotically stable.

(b) If there exists a pair of symmetric matrices P, Q such that P has at least one negative eigenvalue and Q is positive definite, then the origin is unstable.

Proof: Consider (a) first. Choose $V(x) = x^T Px$ and compute $\dot{V} = x^T(A^T P + PA)x = -x^T Qx$. The assumptions and the LaSalle stability theorem lead to the conclusion that all trajectories tend to the orgin as $t \to \infty$. Case (b) requires application of Chetaev's instability theorem. In this case consider $V(x) = -x^T Px$. Recall that for symmetric P the eigenvalues of P are real, they may be positive, negative or zero. On the positive eigenspace, $V < 0$, on the negative eigenspace, $V > 0$, and on the zero eigenspace, $V = 0$. Since P has at least one negative eigenvalue, the negative eigenspace is nontrivial and there is a set of points, D, for which $V > 0$. Let B_ε be an open sphere of small radius ε centered at the origin. Since V is continuous, the boundary of D in B_ε, $\partial D \cap B_r$, consists of points of points at which $V = 0$. It includes the origin and is never nonempty (even if all eigenvalues of P are negative). For $V(x) = -x^T Px$, $\dot{V} = x^T Qx$ and it is always positive since Q is assumed positive definite. Thus, the conditions of Proposition (2.24) are satisfied. ■

Suppose $Q > 0$ and the P has a zero eigenvalue. If the matrix P has a zero eigenvalue then there are points $x \neq 0$ such that $V(x) = x^T Px = 0$. But at such points $\dot{V}(x) = -x^T Qx < 0$. Since V(x) is continuous this means that there must be points at which V assumes negative values. Thus, P must also have a negative eigenvalue. Thus, we have the following corollary to Proposition (2.25).

Corollary 2.26. *The linear system (2.6) is asymptotically stable if and only if for every positive definite symmetric Q there exists a positive definite symmetric P that satisfies the Lyapunov equation (2.7).*

Lagrangian Systems

The Lyapunov analysis of the stability of nonlinear dynamical systems evolved from a tradition of stability analysis via energy functions that goes back at least to Lagrange and Hamilton. We will consider a number of examples which are physically motivated and for which there are energy functions that serve as natural Lyapunov function candidates. Consider the class of Lagrangian systems characterized by the set of second order differential equations

$$\frac{d}{dt}\frac{\partial L(x,\dot{x})}{\partial \dot{x}} - \frac{\partial L(x,\dot{x})}{\partial x} = Q^T \tag{2.8}$$

where

1. $x \in R^n$ denotes a vector of *generalized coordinates* and $\dot{x} = dx/dt$ are the *generalized velocities*.
2. $L : R^{2n} \to R$ is the *Lagrangian*. It is constructed from the kinetic energy function $T(x,\dot{x})$ and the potential energy function $U(x)$, via $L(x,\dot{x}) = T(x,\dot{x}) - U(x)$.
3. The kinetic energy has the form

   $$T(x,\dot{x}) = \tfrac{1}{2}\dot{x}^T M(x)\dot{x}$$

   where for each fixed x, the matrix $M(x)$ is positive definite.
4. The potential energy is related to a force vector $f(x)$ via

   $$U(x) = \int f(x)dx$$

5. $Q(x,\dot{x},t)$ is a vector of generalized forces.

Occasionally it is convenient to write the second order equations in first order form by defining new variable $v = \dot{x}$ to obtain

$$\begin{bmatrix} \dot{x} \\ \dot{v} \end{bmatrix} = \begin{bmatrix} v \\ -M^{-1}(x)f(x) - \frac{1}{2}M^{-1}(x)\left[\partial M(x)/\partial x\right] + M^{-1}(x)Q \end{bmatrix} \tag{2.9}$$

Another useful first order form is Hamilton's equations obtained as follows. Define the *generalized momentum* as

$$p^T = \frac{\partial L}{\partial \dot{x}} = \dot{x}^T M(x) \Rightarrow \dot{x} = M^{-1}(x)p \tag{2.10}$$

Define the *Hamiltonian* $H : R^{2n} \to R$

$$H(x,p) = \left[p^T \dot{x} - L(x,\dot{x})\right]_{\dot{x}\to M^{-1}p} = \tfrac{1}{2} p^T M^{-1}(x)p + U(x) \tag{2.11}$$

The Hamiltonian is the total energy expressed in momentum rather than velocity coordinates. Notice that Lagrange's equation can be written

$$\dot{p}^T - \frac{\partial L}{\partial x} = Q^T \tag{2.12}$$

Now, using the definition of H, (2.11), write

$$dH = \frac{\partial H}{\partial x}dx + \frac{\partial H}{\partial p}dp = dp^T \dot{x} + p^T d\dot{x} - \frac{\partial L}{\partial x}dx - \frac{\partial L}{\partial \dot{x}}d\dot{x} = dp^T \dot{x} - \frac{\partial L}{\partial x}dx$$

Using (2.12) we have

$$\frac{\partial H}{\partial x}dx + \frac{\partial H}{\partial p}dp = \dot{x}^T dp - (\dot{p} - Q)^T dx$$

Comparing coefficients of dp and dx, we have Hamilton's equations.

$$\dot{x} = \frac{\partial H(x,p)}{\partial p^T}, \quad \dot{p} = -\frac{\partial H(x,p)}{\partial x^T} + Q \tag{2.13}$$

Example 2.27 (Soft Spring). Consider a system of with kinetic and potential energy functions

$$T = \frac{x_2^2}{2}, \quad U = \frac{x_1^2}{1+x_1^2}$$

Lagrange's equations in first order form ($\dot{x}_1 = x_2$) with viscous damping are

$$\begin{bmatrix} \dot{x}_1 \\ \dot{x}_2 \end{bmatrix} = \begin{bmatrix} x_1 \\ -2\frac{x_1}{(1+x_1^2)^2} - cx_2 \end{bmatrix}$$

If we take the total energy as a candidate Lyapunov function,

$$V(x_1,x_2) = \tfrac{1}{2}x_2^2 + \frac{x_1^2}{1+x_1^2}$$

an easy calculation shows that $\dot{V} = -cx_2 \leq 0$ for $c > 0$. Furthermore, the set $\dot{V} = 0$ consists of the x_1-axis and the only entire solution contained therein is the trivial solution. We conclude that the origin is asymptotically stable. We can not, however,

conclude global aymptotic stability because the Lyapunov function is not radially unbounded. Let us look at the level sets of V:

```
In[7]:= ContourPlot[V, {x1, -5, 5}, {x2, -2, 2}, PlotPoints → 50,
          Contours → 15, ColorFunction → (GrayLevel[((# + 0.1)/1.1)^(1/4)]&),
          FrameLabel → {x1, x2}]
```

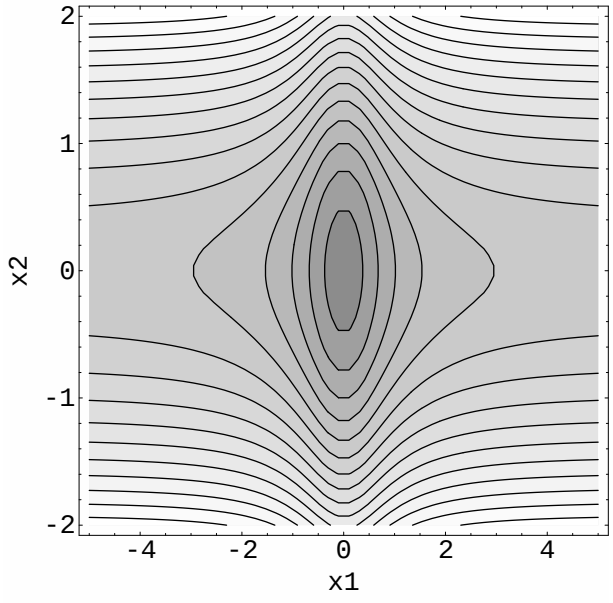

and, finally, at the trajectories:

```
In[8]:= Show[graphs2, AxesLabel → {x1, x2}, PlotRange → {{-5, 5}, {-2, 2}},
          DisplayFunction → $DisplayFunction]
```

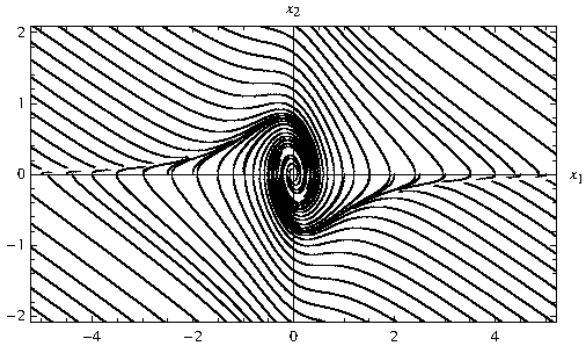

Example 2.28 (Variable Mass). Consider a system with variable inertia, typical of a crankhaft. The kinetic and potential energy functions are

$$T = (2-\cos 2x_1)\,x_2^2, \quad U = x_1^2 + \tfrac{1}{4}x_1^4$$

Systems with variable mass are much easier to analyze using Hamilton's equations, so we define the generalized momentum $p = (2-\cos 2x_1)\,x_2$ and the Hamiltonian

$$H(x_1, p) = \frac{p^2}{2(2-\cos 2x_1)} + x_1^2 + \tfrac{1}{4}x_1^4$$

Again with viscous damping, Hamilton's equations are

$$\begin{bmatrix} \dot{x}_1 \\ \dot{p} \end{bmatrix} = \begin{bmatrix} \frac{p}{2-\cos 2x_1} \\ -2x_1 - x_1^3 - \frac{p^2 \sin 2x_1}{(2-\cos 2x_1)^2} + \frac{2c\,p}{(2-\cos 2x_1)^2} \end{bmatrix}$$

It is not difficult to compute $\dot{H}$, indeed,

```
In[9]:= Simplify[Jacob[H, {p, x1}].{-D[H, x1] - D[R, p], D[H, p]}]
Out[9]= 2 c p^2 / (-2 + Cos[2 x1])^3
```

We conclude that $\dot{H} \leq 0$ for $c > 0$. Moreover, the only entire trajectory in the set $\dot{H} = 0$ is the trivial solution, and since H is radially unbounded, we can cnclude that the origin is globally asymptotically stable. Let is look at the level curves of H

```
In[10]:= ContourPlot[H, {x1, -6, 6}, {p, -12, 12}, PlotPoints → 100, Contours → 25,
           ColorFunction → (GrayLevel[(# + 0.1)/1.1)^(1/4)]&), FrameLabel → {x1, p}]
```

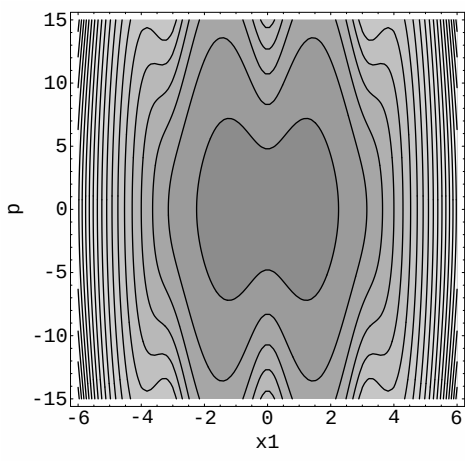

and at the state space trajectories

```
In[11]:= graphs3 = PhasePortrait[f, x, 15, {{-6, 6, 2}, {-5, 5, 5}}];
         Show[graphs3, AxesLabel → {x1, p}, PlotRange → {{-4, 4}, {-4, 4}},
           DisplayFunction → $DisplayFunction]
```

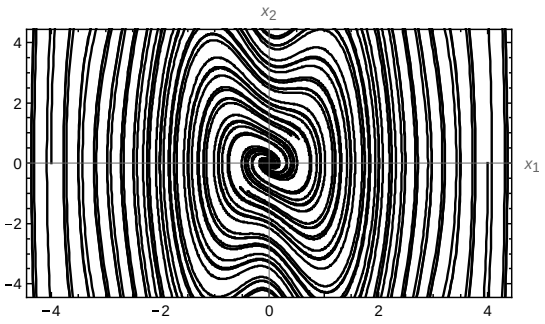

Example 2.29 (Multiple Equilibria). Consider the system

$$\ddot{x} + \left|x^2 - 1\right|\dot{x}^3 - x + \sin\left(\frac{\pi x}{2}\right) = 0$$

Notice that the system has three equilibria $(x, \dot{x}) = (0,0), (-1,0), (1,0)$. We can determine their stability by examining the system phase portraits or using a Lyapunov analysis based on total energy as the candidate Lyapunov function. First let us examine the phase portraits.

```
In[12]:= U = -2/π + x1^2/2 + 2 Cos[π x1/2]/π;
In[13]:= T = x2^2/2; V = T + U;
In[14]:= F = Simplify[D[U, x1]];
         f = {x2, - Abs[x1^2 - 1] x2^3 - F}; x = {x1, x2};
In[15]:= graphs3 = PhasePortrait[f, x, 2, {{-2, 2, 0.5}, {-1, 1, 1}}];
In[16]:= Show[graphs3, AxesLabel → {x1, x2}, PlotRange → {{-1.5, 1.5}, {-1, 1}},
           DisplayFunction → $DisplayFunction]
```

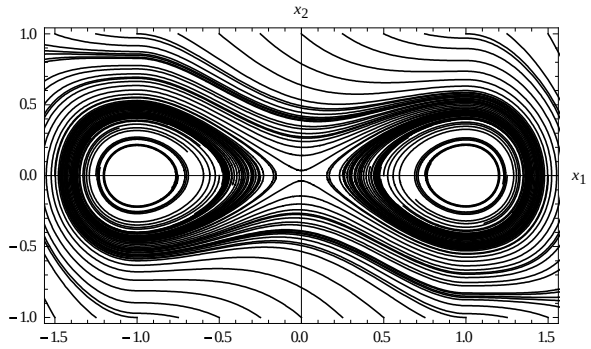

Thus, we see that the equilibrium point $(0,0)$ is unstable and that the other two, $(\pm 1,0)$, are asymptotically stable. Now, let us consider the Lyapunov viewpoint. The total energy is

$$V = \frac{\dot{x}^2}{2} + \frac{x^2}{2} - \frac{2}{\pi}\left(1 - \cos\left(\frac{\pi x}{2}\right)\right)$$

A straightforward calculation leads to

$$\dot{V} = -\left|x^2 - 1\right|\dot{x}^2$$

The LaSalle theorem (2.21) can now be applied. Let us view the level surfaces.

```
In[17]:= ContourPlot[V, {x1, -2, 2}, {x2, -1, 1}, PlotPoints → 50,
           Contours → 15, ColorFunction → (GrayLevel[((# + 0.1)/1.1)^(1/4)]&),
           FrameLabel → {x1, x2}]
```

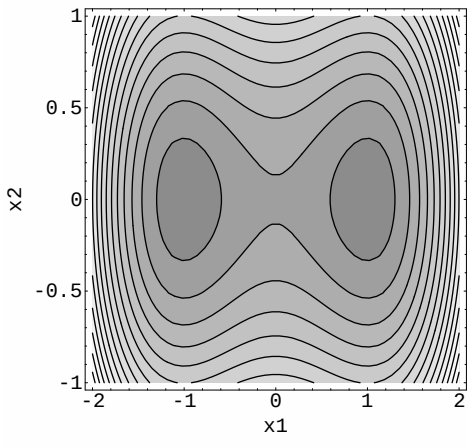

Notice that there are level surfaces that bound compact sets that include the equilibrium point $(1,0)$. Pick one and designate it Ω_{c_1}. Moreover, $\dot{V} \leq 0$ everywhere, hence specifically in Ω_{c_1}, and the maximum invariant set contained in Ω_{c_1} is the equilibrium point. Consequently, all trajectories beginning in Ω_{c_1} tend to $(1,0)$ so it is an asymptotically stable equilibrium point. A similar conclusion can be reached for the equilibrium point $(-1,0)$.

2.4.3 Stable, Unstable, and Center Manifolds

Consider the autonomous system (2.5) and suppose $x = 0$ is an equilibrium point so that $f(0) = 0$. Let $A := \partial f(0)/\partial x$. Define three subspaces of R^n:

1. the *stable subspace*, E^s: the eigenspace of eigenvalues with negative real parts
2. the *unstable subspace*, E^u: the eigenspace of eigenvalues with positive real parts
3. the *center subspace*, E^c: the eigenspace of eigenvalues with zero real parts

An equilibrium point is called *hyperbolic* if A has no eigenvalues with zero real part, i.e., there is no center subspace, E^c. In the absence of center subspace the linearization is a reliable predictor of important qualitative features of the nonlinear system. The basic result is given by the following theorem. First, some definitions.

Let f, g be C^r vector fields on R^n with $f(0) = 0, g(0) = 0$. M is an open subset of the origin in R^n.

Definition 2.30. *Two vector fields f and g are said to be C^k-*equivalent *on M if there exists a C^k diffeomorphism h on M, which takes orbits of the flow generated by f on M, $\Phi(x,t)$, into orbits of the flow generated by g on M, $\Psi(x,t)$, preserving orientation but not necessarily parameterization by time. C^0-equivalence is referred to as* topological equivalence. *If there is such an h which does preserve parameterization by time then f, g are said to be C^k -*conjugate. *C^0-conjugacy is referred to as* topological-conjugacy.

Proposition 2.31 (Hartman-Grobman Theorem). *Let $f(x)$ be a C^k vector field on R^n with $f(0) = 0$ and $A := \partial f(0)/\partial x$. If A is hyperbolic then there is a neighborhood U of the origin in R^n on which the nonlinear flow of $\dot{x} = f(x)$ and the linear flow of $\dot{x} = Ax$ are topologically conjugate.*

Proof: (Chow & Hale [21], p. 108)

Definition 2.32. *Let U be a neighborhood of the origin. We define the* local stable manifold *and* local unstable manifold *of the equilibrium point $x = 0$ as, respectively,*

$$W^s_{loc} = \{x \in U \,|\Psi(x,t) \to 0 \text{ as } t \to \infty \wedge \Psi(x,t) \in U \,\forall t \geq 0\}$$
$$W^u_{loc} = \{x \in U \,|\Psi(x,t) \to 0 \text{ as } t \to -\infty \wedge \Psi(x,t) \in U \,\forall t \leq 0\}$$

Proposition 2.33 (Center Manifold Theorem). *Let $f(x)$ be a C^r vector field on R^n with $f(0)=0$ and $A := \partial f(0)/\partial x$. Let the spectrum of A be divided into three sets $\sigma_s, \sigma_c, \sigma_u$ with*

$$\operatorname{Re}\lambda = \begin{cases} <0 & \lambda \in \sigma_s \\ =0 & \lambda \in \sigma_c \\ >0 & \lambda \in \sigma_u \end{cases}$$

Let the (generalized) eigenspaces of $\sigma_s, \sigma_c, \sigma_u$ be E^s, E^c, E^u, respectively. Then there exist C^r stable and unstable manifolds W^s and W^u tangent to E^s and E^u, respectively, at $x=0$ and a C^{r-1} center manifold W^c tangent to E^c at $x=0$. The manifolds W^s, W^c, W^u are all invariant with respect to the flow of $f(x)$. The stable and unstable manifolds are unique, but the center manifold need not be.

Proof: [82].

Example 2.34 (Center Manifold). Consider the system

$$\dot{x} = x^2, \quad \dot{y} = -y$$

from which it is a simple matter to compute

$$x(t) = x_0/(1-tx_0),\ y(t) = y_0 e^{-t} \Rightarrow y(x) = \left[y_0 e^{-1/x_0}\right] e^{1/x}$$

The phase portrait is shown below. Observe that $(0,0)$ is an equilibrium point with:

$$A = \begin{bmatrix} 0 & 0 \\ 0 & -1 \end{bmatrix} \Rightarrow E^s = span\left\{\begin{matrix} 0 \\ 1 \end{matrix}\right\}, \quad E^c = span\left\{\begin{matrix} 1 \\ 0 \end{matrix}\right\}$$

Notice that the center manifold can be defined using any trajectory beginning with $x<0$ and joining with it the positive x-axis. Also, the center manifold can be chosen to be the entire x-axis. This is the only choice which yields an analytic center manifold.

In[1]:=

```
f={x1^2,-x2};x={x1,x2};
graphs3=PhasePortrait[f,x,8,{{-0.2,0.1,.05},{-0.5,0.5,0.5}}];

Show[graphs3,AxesLabel->{"x,W^C","y,W^S"},
PlotRange->{{-0.2,0.2},{-0.25,0.25}},
DisplayFunction->$DisplayFunction,Frame->True,FrameStyle->Black,
ImageSize->{360,215},AspectRatio->Full,AxesOrigin->Automatic,
AxesStyle->Directive[Black,Thick]]
```

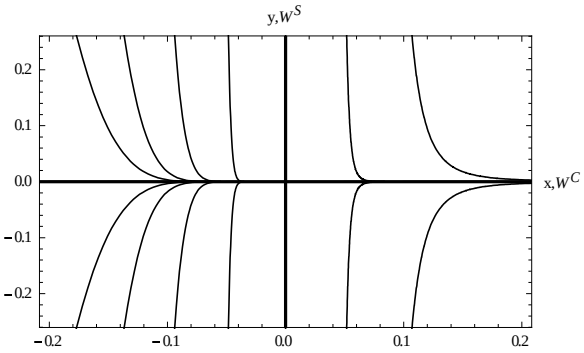

There are some important properties of these manifolds that will not be examined here. See, for example, [32] and [3]. Let us note, however, that existence and uniqueness of solutions insure that two stable (or unstable) manifolds cannot intersect or self-intersect. However, a stable and an unstable manifold can intersect. The global stable and unstable manifolds need not be simple submanifolds of R^n, since they may wind around in a complex manner, approaching themselves arbitrarily closely.

Motion on the Center Manifold

Consider the system of differential equations

$$\begin{aligned} \dot{x} &= Bx + f(x,y) \\ \dot{y} &= Cy + g(x,y) \end{aligned} \tag{2.14}$$

where $(x,y) \in R^{n+m}$, f,g and their gradients vanish at the origin, and the eigenvalues of B have zero real parts, those of C negative real parts. The center manifold is tangent to E^c:

$$E^c = \text{span} \begin{bmatrix} I_n \\ 0_{m\times n} \end{bmatrix}$$

It has a local graph

$$W^c = \left\{ (x,y) \in R^{n+m} \,|y = h(x) \right\}, \quad h(0) = 0, \; \frac{\partial h(0)}{\partial x} = 0$$

Once h is determined, the vector field on the center manifold W^c (i.e., the surface defined by $y = h(x)$) can be projected onto the Euclidean space E^c as

$$\dot{x} = Bx + f(x, h(x)) \tag{2.15}$$

These calculations lead to the following result (see [32]).

Proposition 2.35 (Center Manifold Stability Theorem). *If the origin of (2.15) is asymptotically stable (resp. unstable) then the origin of (2.14) is asymptotically stable (resp. ustable).*

To compute h, we use the fact that on W^c it is required that $y = h(x)$ so that

$$\dot{y} = \frac{\partial h(x)}{\partial x}\dot{x} = \frac{\partial h(x)}{\partial x}\left[Bx + f(x, h(x)\right]$$

But $\dot{y}$ is also governed by (2.14) so we have the partial differential equation

$$\frac{\partial h(x)}{\partial x}\left[Bx + f(x, h(x)\right] = Ch(x) + g(x, h(x) \tag{2.16}$$

that needs to be solved along with the boundary conditions $h(0) = 0,\ \frac{\partial h(0)}{\partial x} = 0$.

Example 2.36. Consider the following two dimensional system from Isidori [46].

$$\dot{x} = cyx - x^3$$

$$\dot{y} = -y + ayx + bx^2$$

where a, b, c are real numbers. It is easy to see that the origin is an equilibrium point and that it is in the form of (2.14) with $B = 0$ and $C = -1$. To compute h we need to solve the partial differential equation

$$\frac{\partial h}{\partial x}\left[cxh(x) - x^3\right] + h(x) - ah(x)x - bx^2 = 0 \tag{2.17}$$

with boundary conditions $h(0) = 0,\ \frac{\partial h(0)}{\partial x} = 0$.

Assume a polynominal solution of the form

$$h(x) = a_0 + a_1 x + a_2 x^2 + a_3 x^3 + O(x^4)$$

In view of the boundary conditions we must have $a_0 = 0$ and $a_1 = 0$. Substitute h into (2.17) as follows, using *Mathematica*,

```
In[18]:= h = a2 x^2 + a3 x^3 + O[x]^4;
         F = D[h, x](c x h - x^3) + h - a h x - b x^2
Out[18]= (a2 - b) x^2 + (-a a2 + a3) x^3 + O[x]^4
```

Thus, we have

```
In[19]:= a2 = b; a3 = a a2; h
Out[19]= b x^2 + a b x^3 + O[x]^4
```

Now, obtain the motion on the center manifold

```
In[20]:= dx = c h x - x^3
Out[20]= (-1 + b c) x^3 + a b c x^4 + O[x]^5
```

The last result can be rewritten as

$$\dot{x} = (-1 + bc)x^3 + abcx^4 + O(x^5)$$

Thus, we have the following results,

(a) if $bc < 1$, the motion on the center manifold is asymptotically stable,

(b) if $bc > 1$, it is unstable,

(c) if $bc = 1$, and $a \neq 0$, it is unstable

(d) if $bc = 1$, and $a = 0$, the above calculations are inconclusive. But in this special case it is easy to verify that $h(x) = x^2$ and the center manifold dynamics are $\dot{x} = 0$. So the motion is stable, but not asymptotically stable.

2.5 Differential-Algebraic Equations

2.6 Problems

Problem 2.37. Plot the level sets of the following norms on R^2:

(a) $\|x\| = \sqrt{x_1^2 + x_2^2}$

(b) $\|x\| = |x_1| + |x_2|$

(c) $\|x\| = \sup(|x_1|, |x_2|)$

Problem 2.38. Consider a system described by the differential equation:

$$\ddot{x} + g(x) = 0$$

that describes a unit point mass with spring force $g(x)$. Show that $(x, \dot{x}) = (0,0)$ is a stable equilibrium point if

(a) $xg(x) > 0$, $x \neq 0$

(b) $g(0) = 0$

Problem 2.39. Consider the dissipative system

$$\ddot{x} + a\dot{x} + 2bx + 3x^2 = 0, \quad a, b > 0$$

(a) Show that there are two equilibrium points $(x, \dot{x}) = (0,0)$ and $(x, \dot{x}) = (-2b/3, 0)$

(b) By linear approximation show that $(0,0)$ is asymptotically stable and that $(-2b/3, 0)$ is unstable.

(c) Use the total energy of the undamped system ($a = 0$) as a Lyapunov function and identify a largest region of attraction for $(0,0)$. Show that the boundary of this region passes through the point $(-2b/3, 0)$.

(d) Pick values for $a, b > 0$ and plot state trajectories and level surfaces for the energy.

Problem 2.40. Consider the system

$$\begin{aligned}\dot{x}_1 &= x_2\\ \dot{x}_2 &= -x_1 - x_2\text{sat}(x_2^2 - x_3^2)\\ \dot{x}_3 &= x_3\text{sat}(x_2^2 - x_3^2)\end{aligned}$$

(a) Show that the origin is the unique equilibrium point.

(b) Taylor linearize at the origin and show that it is asymptotically stable.

(c) Using $V(x) = x^T x$, show that the origin is globally asymptotically stable.

Problem 2.41. Investigate the stability of the origin, including estimates of the domain of attraction, of the following systems:

(a) $\ddot{x} = x - \text{sat}(2x + \dot{x})$, Hint: Use $V(x) = x\dot{x}$,

(b) $\ddot{x} + \dot{x}|\dot{x}| + x - x^3 = 0$, Hint: Use total energy for $V(x)$.

3

Introduction to Differential Geometry

3.1 Introduction

This chapter provides an overview of the differential geometry concepts necessary for a modern discussion of nonlinear control and analytical mechanics. We need to develop a basic understanding of manifolds, vector fields and flows, distributions and integral submanifolds along with tools that allow us to compute and manipulate these objects. The material described only very briefly here is deep and rich and a more thorough discussion can be found in many text books, e.g., [14, 41, 107, 89]. It has its roots in analytical mechanics but it has become a cornerstone of nonlinear control.

In essence this chapter develops the tools required to address the evolutionary behavior of systems whose state spaces are curved rather than flat surfaces. Examples of the importance of this generalization abound. We have already considered the flow of a dynamical system on a curved surface when evaluating stability on a center manifold in the last chapter. Sometimes it is convenient to consider the state space of a pendulum to be a cylinder rather than the flat Euclidean space R^2. Electric power systems are typically modeled by systems of differential-algebraic equations in the form

$$\begin{aligned} \dot{x} &= f(x,y) \\ 0 &= g(x,y) \end{aligned}$$

where $x \in R^n$, $y \in R^m$, and $f : R^{n+m} \to R^n$, $g : R^{n+m} \to R^m$ are smooth functions. Clearly the motion is constrained to the set of points in R^{n+m} that satisfy the algebraic equation. Under the right circumstances, this set is an n-dimensional smooth surface. In other applications from robotics to spacecraft models often have state spaces that are not flat. Control design itself imposes the need to consider flows on general surfaces. Unique aspects of the navigation of ships and aircraft between points on earth arise because the motion takes place on a sphere. Control theoretic examples include the generalization of the concept of zero dynamics to nonlinear systems and the study of sliding modes in variable structure control systems.

While the subject matter might seem abstract on first acquaintance, its underlying concepts are quite intuitive and appealing. The formalism provides a precise basis for working with geometric ideas and the reader new to this material will no doubt find justification and clarification for familiar calculations.

We begin with a discussion of manifolds in Section 2 and then proceed to tangent spaces, vector fields and covector fields in Section 3. Section 4 introduces distributions, codistributions and the Frobenius theorem. Distributions play a role in nonlinear system theory much like that of linear subspaces in linear system theory. The Frobenius theorem answers classical questions of integrability central to problems of mechanics and partial differential equations. It turns out to be equally important to nonlinear control. Important tranformations of state equations are derived, based on distributions possessing certain properties and tools for computing such distribution are described. Section 5 provides a brief introdution to Lie Groups and Lie Algebras with the addition of some algebraic structure to the geometric objects of Sections 2, 3 and 4.

3.2 Manifolds

Roughly speaking a manifold is a smooth surface embedded in a Euclidean space of some dimension. We will need a more precise definition in order to work effectively with manifolds, but before proceeding formally let us examine how we ordinarily characterize such surfaces. Consider the Euclidean space R^2 and suppose x,y are its coordinates. The set of points that comprise a surface in R^2, e.g., the unit circle, is generally modeled in one of three ways:

- *explicitly*, by a mapping $y = g(x)$ (or, $x = g(y)$),
- *implicitly*, by a relation $f(x,y) = 0$,
- *parametrically*, by a mapping $x = h_1(s),\ y = h_2(s),\ s \in U \subset R$.

The explicit model is typically inadequate. For example, the unit circle, does not admit a global explicit representation. We would have to represent two pieces of the circle by separate expressions. Representations of the unit circle are

- explicit, top half: $y = \sqrt{1-x^2}$ and bottom half: $y = -\sqrt{1-x^2}$,
- implicit, $x^2 + y^2 = 1$,
- parametric, $y = \sin s,\ x = \cos s,\ s \in [0, 2\pi)$

In practice, interesting manifolds require either an implicit or a parametric representation even for a local characterization. Explicit representations, however, can also be useful as we have already seen in the computation of center manifolds in the previous chapter.

Now, let us turn to the formalities. Recall that a *homeomorphism* between any two topological spaces is a one-to-one continuous mapping with a continuous inverse. A homeomorphism not only maps points in a one-to-one manner, but it maps open sets in a one-to-one manner. Thus, if $\varphi : M \to N$ is a homeomorphism, M and N are topologically the same.

A differentiable manifold N of dimension n is a set of points that is locally topologically equivalent to the Euclidean space R^n. This concept can be made precise by introducing a set of local coordinate systems called charts. Each chart consists of an open set $U \subset N$ and a mapping φ that maps U homeomorphically onto $\varphi(U)$. A general discussion of differential manifolds and their application can be found in many texts including [14, 41, 107]. The key elements of the following definition are depicted in Figure (3.1).

Definition 3.1. *An m-dimensional manifold is a set M together with a countable collection of subsets $U_i \subset M$ and one-to-one mappings $\varphi_i : U_i \to V_i$ onto open subsets V_i of R^m, each pair (U_i, φ_i) called a* coordinate chart, *with the following properties:*

1. *the coordinate charts cover M, $\bigcup_i U_i = M$*
2. *on the overlap of any pair of charts the composite map*
$$f = \varphi_j \circ \varphi_i^{-1} : \ \varphi_i(U_i \cap U_j) \to \varphi_j(U_i \cap U_j)$$
is a smooth function.
3. *if $p \in U_i$, $\bar{p} \in U_j$ are distinct points of M, then there are neighborhoods, W of $\varphi_i(p)$ in V_i and $\bar{W}$ of $\varphi_j(\bar{p})$ in V_j such that*
$$\varphi_i^{-1}(W) \cap \varphi_j^{-1}(\bar{W}) = \emptyset$$

The coordinate charts provide the set M with a topological structure so that the manifold is a topological space. Condition 3. of the definition is a form of the so-called Hausdorff separation axiom so that these manifolds are Hausdorff topological spaces. The coordinates in R^m of the image of a coordinate map $\varphi(p)$, $p \in M$ are called the coordinates of p. A chart (U, φ) is called a local coordinate system. If the overlap functions $f = \varphi_j \circ \varphi_i^{-1}$ are k-times continuously differentiable, then the manifold is called a C^k-manifold. If $k = \infty$, then the manifold is said to be smooth. It is analytic if the overlap functions are analytic. A local coordinate system is called a cubic coordinate system if $\varphi(U)$ is an open cube about the origin in R^m. If $p \in M$ and $\varphi(p) = 0$, the coordinate system is said to be centered at p.

Example 3.2 (Differentiable Manifolds). The following are simple examples of differentiable manifolds.

1. The Euclidean space R_m is an m-dimensional manifold. There is a single chart, $U = R_m$. The corresponding coordinate map is simply the identity map $I_d : R^m \to R^m$.

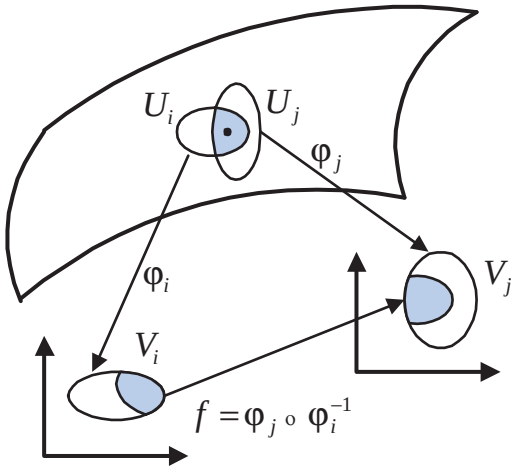

Fig. 3.1: This figure illustrates coordinate charts, local coordinate maps and compatibility (overlap) functions on manifold M.

2. Any open subset $U \subset R^m$ is an m-dimensional manifold with single chart U and coordinate map again the identity.

3. The unit circle $S_1 = \{(x,y)|x^2+y^2=1\}$ can be viewed as a one dimensional manifold with two coordinate charts. Define the charts $U_1 = S_1 - \{(-1,0)\}$ and $U_2 = S_1 - \{(1,0)\}$. Now we define the coordinate maps by isometric projection.

$$\varphi_1 = \frac{2y}{1-x} : S^1 - \{(-1,0)\} \to R^1 \cong \{(1,y)\}$$
$$\varphi_2 = \frac{2y}{1-x} : S^1 - \{(1,0)\} \to R^1 \cong \{(-1,y)\}$$

The overlap functions are given by

$$f_1 = \varphi_2 \circ \varphi_1^{-1} = \frac{1+x}{1-x} : R^1 - \{0\} \to R^1 - \{0\}$$
$$f_2 = \varphi_1 \circ \varphi_2^{-1} = \frac{1-x}{1+x} : R^1 - \{0\} \to R^1 - \{0\}$$

Another description is obtained if we identify a point on S^1 by its angular coordinate θ, where $(x,y) = (cos\theta, sin\theta$, with two angles equivalent if they differ by an integral multiple of 2π. Thus, we have a single chart $U = \{\,\theta\,|\,0 < \theta \leq 2\pi\}$.

4. The unit sphere $S^2 = \{(x,y,z)|x^2+y^2+z^2=1\}$ is another basic example of a manifold with two coordinate charts. We may choose

$$U_1 = S^2 - \{(0,0,1)\}$$
$$U_2 = S^2 - \{(0,0,-1)\}$$

obtained by deleting the north and south poles, respectively from the sphere. Local coordinate functions can be defined as stereographic projections (from, respectively, the north or south poles) onto the horizontal plane that passes through the origin:

$$\varphi_1(x,y,z) = \left\{ \frac{x}{1-z}, \frac{y}{1-z} \right\}$$
$$\varphi_2(x,y,z) = \left\{ \frac{x}{1+z}, \frac{y}{1+z} \right\}$$

The compatibility function is

$$f_{2,1} = \varphi_1 \circ \varphi_2^{-1} : R^2 - \{0\} \to R^2 - \{0\}$$
$$f_{2,1}(x,y) = \left\{ \frac{x}{x^2+y^2}, \frac{y}{x^2+y^2} \right\}$$

5. In general, if M and N are smooth manifolds of dimension m and n, then their Cartesian product $M \times N$ is a smooth manifold of dimension $m+n$. If their respective coordinate maps are $\varphi_i : U_i \to V_i \subset R^m$ and $\bar{\varphi}_j : \bar{U}_j \to \bar{V}_j \subset R^n$, then the induced coordinate charts on $M \times N$ are the Cartesian products

$$\varphi_i \times \bar{\varphi}_j : U_i \times \bar{U}_j \to V_i \times \bar{V}_j \subset R^{n+m}$$

For our purposes a differentiable manifold can always be conceived as a smooth surface embedded in a Euclidean space. The unit sphere S^2 and the torus T^2 are manifolds embedded in R^3. As noted, manifolds are ordinarily specified as submanifolds of Euclidean space in one of two ways, parametrically or implicitly. Before describing these repesentations formally we define the notion of maximal rank of maps.

Definition 3.3 (Maximal Rank Condition). *Let $F : R^m \to R^n$ be a smooth map. The rank of F at $x_0 \in R^m$ is the rank of the Jacobian $D_x F(x_0)$. F is of* maximal rank *on $S \subset R^m$ if the rank of F is maximal (the minimum of m and n) for each $x_0 \in S$.*

A submanifold can be defined parametrically as follows.

Definition 3.4. *A submanifold embedded in R^n is a set $M \subset R^n$, together with a smooth one-to-one map $\phi : \Pi \subset R^m \to M$, $m \leq n$, which satisfies the maximal rank condition everywhere, where Π is called the parameter space and $M = \phi(\Pi)$ is the image of ϕ. If the maximal rank condition holds but the map is not one-to-one, then the set M (or the function ϕ) is called an immersion.*

Example 3.5 (One Dimensional Submanifolds in R^2 and R^3). The following are some examples for parametrically defined one dimensional submanifolds. Notice that plots of parametrically defined submanifolds in R^2 and R^3 can easily be generated using the *Mathematica* functions `ParametricPlot` and `ParamtricPlot3D`.

Consider a submanifold N embedded in R^3 defined by mapping $f : R \to R^3$

$$f(t) = (\cos t, \sin t, t)$$

N is a helix which spirals up the z axis. It is one-to-one and $D_t f = (-sint, cost, 1)$ so that the maximal rank condition is satisfied.

```
In[21]:= ParametricPlot3D[{Cos[t], Sin[t], t}, {t, -3 π, 3 π},
           BoxRatios → {1, 1, 2}, Boxed → False, Ticks → None, Axes → False];
```

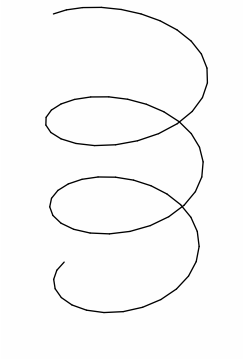

Now, consider a submanifold embedded in R^2 defined by the mapping

$$f(t) = ((1 + e^{-t/4})\cos t, (1 + e^{-t/4})\sin t)$$

Then as $t \to \infty$, N spirals in to the circle x2 + y2 = 1.

```
In[22]:= D[{(1 + Exp[-t/4]) Cos[ t], (1 + Exp[-t/4]) Sin[ t]}, t]
Out[22]= {-1/4 e^(-t/4) Cos[t] - (1 + e^(-t/4)) Sin[t], (1 + e^(-t/4)) Cos[t] - 1/4 e^(-t/4) Sin[t]}
In[23]:= ParametricPlot[{(1 + Exp[-t/4]) Cos[ t], (1 + Exp[-t/4]) Sin[ t]},
           {t, 0, 8 π}, AspectRatio → Automatic, Axes → False];
```

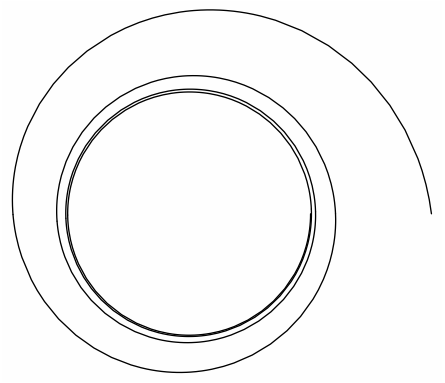

As another example, consider the mapping $f : R \to R^2$

$$f(t) = (\sin t, 2\sin 2t)$$

$N = f(R)$ is a figure eight which is self intersecting at the origin of R^2. Thus, f is not one-to-one although the maximum rank condition is satisfied since $D_t f = (-\cos t, -4\cos 2t)$ never vanishes.

```
In[24]:= ParametricPlot[{ Sin[ t], 2Sin[ 2 t]}, {t, 0, 2 π}, Axes → False];
```

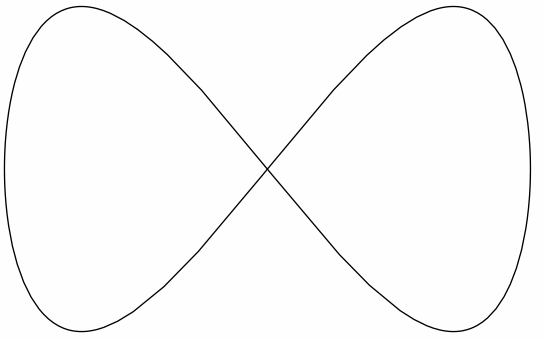

Let us modify the previous example by defining

$$f(t) = (\sin(2\arctan t), 2\sin(4\arctan t))$$

Now f is one-to-one and N passes through the origin only once. The maximal rank condition holds.

```
In[25]:= ParametricPlot[{ Sin[2 ArcTan[ t]], 2 Sin[ 4 ArcTan[ t]]},
           {t, 0, 100 π}, PlotPoints → 200, PlotRange → All, Axes → False];
```

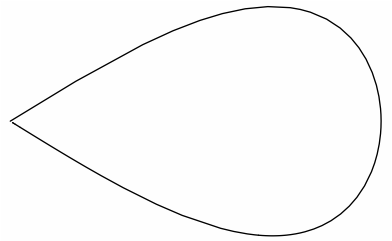

```
In[26]:= D[{ Sin[2 ArcTan[ t]], 2 Sin[ 4 ArcTan[ t]]}, t]
```

$$\text{Out[26]=}\ \left\{\frac{2\ \text{Cos}[2\ \text{ArcTan}[t]]}{1+t^2}, \frac{8\ \text{Cos}[4\ \text{ArcTan}[t]]}{1+t^2}\right\}$$

Example 3.6 (The sphere S^2). Now consider the sphere S^2. First, we generate a graph using a parametric specification of the sphere:

$$f(t,u) = \{\cos t \sin u, \sin t \sin u, \cos u\}$$

```
In[1]:= ParametricPlot3D[{Cos[t] Sin[u], Sin[t] Sin[u], Cos[u]},
          {t, 0, 2Pi}, {u, 0, Pi}]
```

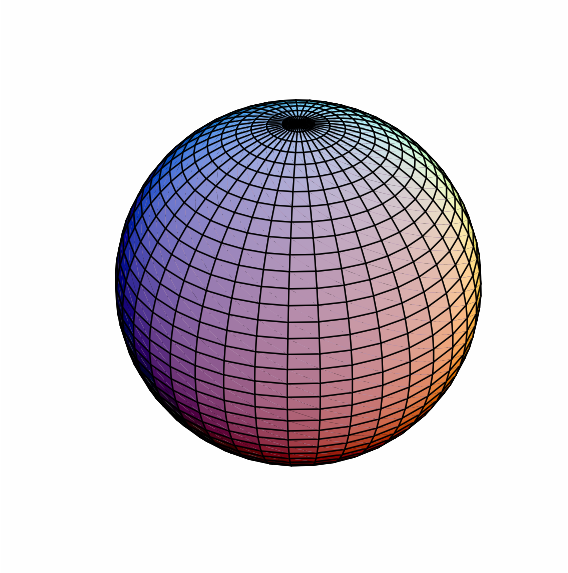

The maximal rank condition can be tested by computing the Jacobian using the *ProPac* function **Jacob** and then testing for its rank by examining the span of its columns using **Span**.

```
In[2]:= AA=Jacob[{Cos [t] Sin [u], Sin [t] Sin [u], Cos [u]},{t,u}]
Out[2]= {{-Sin[t]  Sin[u], Cos[t]  Cos[u]}, {Cos[t]  Sin[u], Cos[u]  Sin[t]},
          {0, -Sin[u]}}
```

```
In[3]:= Simplify[Cos [u] Span[Transpose[AA]]]
Out[3]= {{Cos[u], 0, -Cos[t]  Sin[u]}, {0, Cos[u], -Sin[t]  Sin[u]}}
```

We see that the rank condition is satisfied everywhere except at the poles. Thus, the given mapping defines a submanifold of R^3 that is the sphere with the poles removed.

Example 3.7 (The torus T^2).

Now consider the torus T^2. First, we generate a graph of the torus using the prametric representation:

$$f(t,u) = \{\cos t(3+\cos u), sint(3+\cos u), sinu\}$$

```
In[4]:= ParametricPlot3D[
        {Cos[t] (3 + Cos[u]), Sin[t] (3 + Cos[u]), Sin[u]},
        {t, 0, 2π}, {u, 0, 2π}, PlotPoints → 40, Axes → False,
          Boxed → False]
```

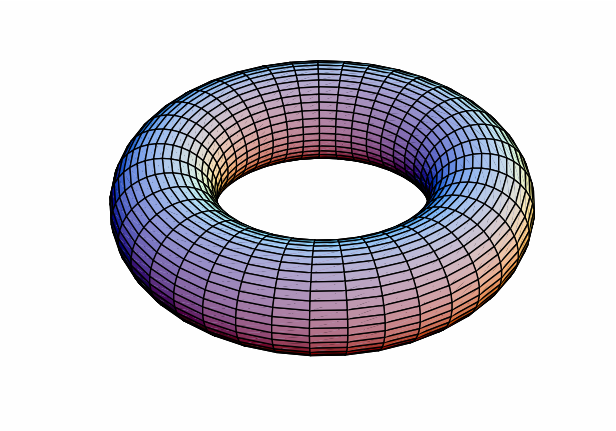

Now, let us exam the maximal rank condition.

```
In[5]:= AA = Jacob[{Cos[t] (3 + Cos[u]), Sin[t] (3 + Cos[u]), Sin[u]}, {t, u}]
Out[5]= {{-(3 + Cos[u])  Sin[t], -Cos[t]  Sin[u]},
           {Cos[t]  (3 + Cos[u]), -Sin[t]  Sin[u]}, {0, Cos[u]}}

In[6]:= Simplify[Span[Transpose[AA]]]
Out[6]= {{Sin[u], 0, -Cos[t]  Cos[u]}, {0, Sin[u], -Cos[u]  Sin[t]}}
```

The mapping fails to have have maximum rank when $u = 0$, i.e., on the outer edge (in the $x-y$ plane) of the torus. The torus with these points removed is a properly parametrically defined submanifold of R^3 as specified by the given mapping.

It is illustrative to consider generating one dimensional submanifolds of R^3 by drawing curves on the surface of the torus (these would be submanifolds of the torus as well). We will consider mappings $f : R \to R^3$ of the form:

$$f(t) = \{\cos t(3+\cos\alpha t), \sin t(3+\cos\alpha t), \sin t\}$$

where α is a parameter. These mappings produce curves on the torus surface. If α is a rational number they are closed curves. If α is irrational then, even though the mapping is one-to-one, its image is dense in the torus and its closure is the torus. The following computations illustrate these two cases.

```
In[7]:= ParametricPlot3D[
        {Cos[t] (3 + Cos[10 t]), Sin[t] (3 + Cos[10t]), Sin[10 t]},
        {t, 0, 2π}, PlotPoints → 200, Axes → False, Boxed → False];
```

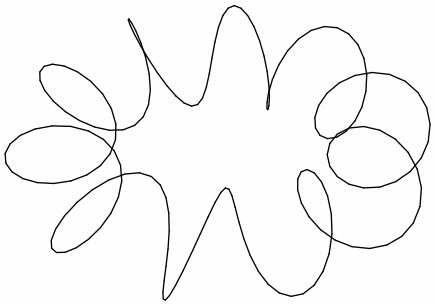

```
In[8]:= ParametricPlot3D[
        {Cos[t] (3 + Cos[π 10/3 t]), Sin[t] (3 + Cos[π 10/3t]), Sin[π 10/3 t]},
        {t, 0, 20π}, PlotPoints → 2000, Axes → False, Boxed → False];
```

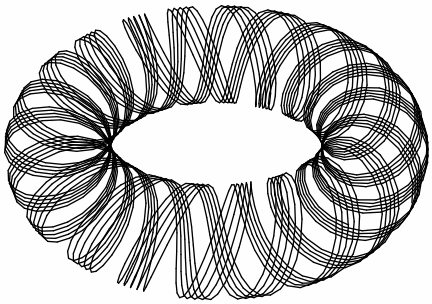

Among these examples two of them illustrate submanifolds that are somewhat pathological. Namely, the spiral in Example (3.5) and the irrational mapping onto the torus

in Example (3.7). In these cases, although the map f is one-to-one and satisfies the maximal rank condition, it is not a homeomorphism (see Figure (3.2). This is the source of the complex topology of these submanifolds. We define a class of submanifolds with a more congenial topological structure.

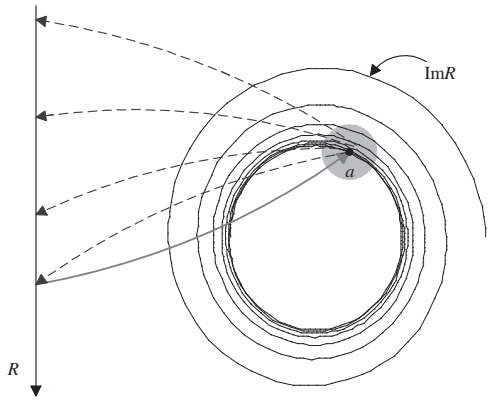

Fig. 3.2: The mapping is not a homeomorphism because the inverse is not continuous. Every neighborhood of points on the spiral arbitrarily close to the limiting circle contain points that map back into distinct points in the parameter space.

Definition 3.8. *A* regular manifold *M embedded in R^n is a manifold parameterized by a smooth mapping $\phi : \Pi \subset R^m \to M \subset R^n$, such that for each $x \in M$ there exists a neighborhood U of x in R^n such that $\phi^{-1}(U \cap M)$ is a connected open subset of Π (equivalently, ϕ maps homeomorphically onto its image).*

In applications, manifolds are sometimes specified by a parameterization, but it is equally common to define manifolds implicitly. The following theorem is a consequence of the implicit function theorem.

Proposition 3.9. *Consider a smooth mapping $F : R^n \to R^m$, $m \leq n$. If F satisfies the maximal rank condition on the set $S = \{ x \in R^n | \, F(x) = 0\}$, then S is a regular, $n-m$ dimensional manifold embedded in R^n.*

Let us make a few remarks and observations about Proposition (3.9).

1. Notice that it is only required that the maximal rank condition be satisfied on the set where F vanishes, i.e., on S itself. If the maximal rank condition is satisfied everywhere, then each level set of F, $\{x|F(x) = c\}$ is a regular submanifold of R^n of dimension $m-n$.
2. A manifold S so defined is called an *implicit* submanifold .

3. Suppose (U,φ) is a local coordinate system on M and that k is an integer $0 \leq k < m$. Let $a \in \varphi(U)$ and define

$$S = \{p \in U \,|\varphi_i(p) = \varphi_i(a), i = k+1,\ldots,m\} \tag{3.1}$$

The subset S of M together with the coordinate system $\{\varphi_j \backslash S,\ i = 1,\ldots,k\}$ forms a submanifold of M called a *slice* of the coordinate system (U,φ). The concept of a slice will be important in discusing controllability and observbility.

4. Any smooth manifold can be implicitly defined in a Euclidean space of suitable dimension.

Example 3.10. Consider the map $F : R^3 \to R$ defined by

$$F(x,y,z) = x^2 + y^2 + z^2 - 2\sqrt{2(x^2+y^2)}$$

F is of maximal rank everywhere except on the the circle $\{x^2+y^2 = 2, z = 0\}$ where the Jacobian vanishes and on the z-axis where it does not exist. The level sets $\{(x,y,z) \in R^3 \,|F(x,y,z) = c\}$ are tori for $-2 < c < 0$, and like spheres with indented poles for $c > 0$. For c=-2, the level set is the circle $\{x^2+y^2 = 2, z = 0\}$ on which the gradient of F vanishes.

Example 3.11. Consider the set of orthogonal matrices

$$O(2) = \{X \in R^{2\times 2} | X^T X = I\}$$

Such matrices form a subset of R^4. In fact, among the four coordinates x_1, x_2, x_3, x_4,

$$X = \begin{bmatrix} x_1 & x_2 \\ x_3 & x_4 \end{bmatrix}$$

there are three independent constraints

$$x_1^2 + x_3^2 = 1$$

$$x_1 x_2 + x_3 x_4 = 0$$

$$x_2^2 + x_4^2 = 1$$

It is easy to check that the Jacobian is of full rank on $O(2)$ so that $O(2)$ is an implicitly defined regular submanifold of dimension 1 in R^4. We can obtain a deeper insight into the structure of this manifold by seeking a (one-dimensional) parameterization. Let us attempt to identify

$$x_1 = \cos\theta, x_3 = \sin\theta$$

which clearly satisfies the first equation. The second equation is then satisfied by

$$x_2 = -\sin\theta, x_4 = \cos\theta$$

or

$$x_2 = \sin\theta, x_4 = -\cos\theta$$

either of which satisfies the fourth relation. It follows that the matrices can be either of the form

$$X_1 = \begin{bmatrix} \cos\theta & -\sin\theta \\ \sin\theta & \cos\theta \end{bmatrix}, \ 0 \leq \theta < 2\pi$$

or

$$X_2 = \begin{bmatrix} \cos\theta & \sin\theta \\ \sin\theta & -\cos\theta \end{bmatrix} = \begin{bmatrix} \cos\theta & -\sin\theta \\ \sin\theta & \cos\theta \end{bmatrix} \begin{bmatrix} 1 & 0 \\ 0 & -1 \end{bmatrix}, \ 0 \leq \theta < 2\pi$$

First, note that each family of matrices is in one-to-one correspondence with the points on a circle. They are disconnected because they have no common elements. Thus, we say that the manifold $O(2)$ has the structure of two disconnected copies of S^1. Second, note that the matrix X_1 (viewed as an operator on R^2) represents a rotation in the plane (through an angle θ) whereas, X_2 represents a relection in the x-axis followed by a rotation. Third, note that $\det\{X_1\} = 1$ and $\det\{X_2\} = -1$. The determinant distinguishes the two components of the manifold $O(2)$. Fourth, observe that the set of matrices $X_1(\theta)$ contains the identity element, in particular, $X_1(0) = I_2$. However, the set of matrices $X_2(\theta)$ does not.

3.3 Tangent Spaces and Vector Fields

3.3.1 The Tangent Space and Tangent Bundle

Consider a smooth two dimensional surface embedded in R^3. At each point on this surface it is easy to envision a tangent plane. Suppose a particle moves along a path in the surface. Then its velocity vector at a specified point on the path lies in the tangent plane to the surface at the prescribed particle location. The generalization of this concept to motion in more abstract manifolds is of central importance.

Definition 3.12. *Let $p : R \to M$ be a C^k, $k \geq 1$ map so that $p(t)$ is a curve in a manifold M. The tangent vector v to the curve $p(t)$ at the point $p_0 = p(t_0)$ is defined by*

$$v = \dot{p}(t_0) = \lim_{t \to t_0} \left\{ \frac{p(t) - p(t_0)}{t - t_0} \right\}$$

The set of tangent vectors to all curves in M passing through p_0 is the tangent space to M at p_0, denoted TM_{p_0}.

If M is an implicit submanifold of dimension m in R^{m+k}, i.e., $F : R^{m+k} \to R^k$, $M = \{x \in R^{m+k} | F(x) = 0\}$ and D_xF satisfies the maximum rank condition on M, Then TM_p is the $\ker D_xF(p)$ (translated, of course to the point p). That is TM_p is the tangent hyperplane to M at p. See Figure (3.3).

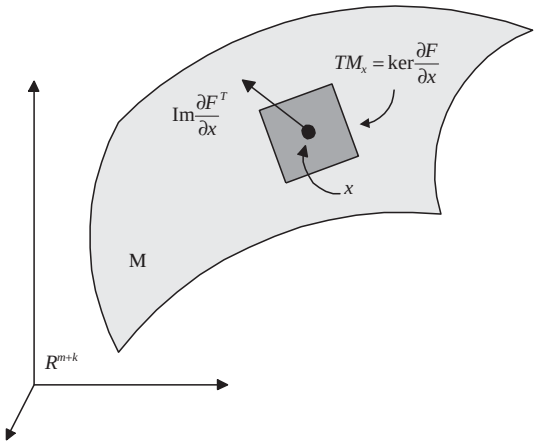

Fig. 3.3: The tangent space to the manifold M at the point x, TM_x.

Let (U,φ) be a local coordinate chart that contains the point $p_0 \in M$ and suppose $p(t)$, with $p(t_0) = p_0$, denotes a curve in M and $x(t) = \varphi(p(t) \cap U)$ its image in $V \subset \varphi(U) \subset R^m$, as depicted in Figure (3.4). The tangent vector to the curve $p(t)$ at p_0 in M is v and the corresponding tangent vector to $x(t)$ at x_0 in R^m is $\bar{v}$. Thus, we have the following definition.

Definition 3.13. *The components of the tangent vector v to the curve $p(t)$ in M in the local coordinates (U,φ) are the m numbers $v_1,\ldots,v_m$ where $v_i = d\varphi_i/dt$.*

Another interpretation of a tangent vector is as an operator on scalar valued smooth functions. Consider the C^k map $F : M \to R$. Let $y = f(x)$, $x \in \varphi(U) \subset R^m$ denote the realization of F in the local coordinates (U,φ). Again, suppose $p(t)$ denotes a curve in M with $x(t)$ its image in R^m. Then the rate of change of F at a point p on this curve is

$$\frac{df}{dt} = v_1\frac{\partial f}{\partial x_1} + \cdots + v_m\frac{\partial f}{\partial x_m} \tag{3.2}$$

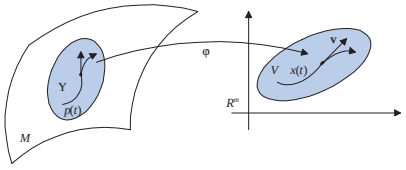

Fig. 3.4: Motion along a curve in the manifold M is quantified in a local coordinate system.

Let us remark on some alternative views of the tangent vector. Notice that there are many curves in M that pass through p and have the same tangent vector. We can define equivalence classes of curves by defining an equivalence relation among curves: two curves passing through p with the same tangent vector are equivalent. Each class is associated with a unique tangent vector. Thus, a tangent vector at p is sometimes defined as an equivalence class of curves through p. All curves belonging to the same class obviously produce the same value for dF/dt. Conversely, the tangent vector $(v_1,\ldots,v_m)$, is uniquely determined by the action of the directional derivative operator (called a *derivation*)

$$\mathbf{v} = v_1 \frac{\partial}{\partial x_1} + \cdots v_m \frac{\partial}{\partial x_m} \tag{3.3}$$

on such an equivalence class of curves. Thus, it is also possible to define the tangent vector as a map (the directional derivative) from the space of (equivalence classes of) differentiable functions passing through p to the real line. As a derivation, the tangent vector satisfies two important properties

1. linearity $\mathbf{v}(f+g) = \mathbf{v}(f) + \mathbf{v}(g)$
2. Liebniz' rule $\mathbf{v}(f \circ g) = \mathbf{v}(f) \circ g + f \circ \mathbf{v}(g)$

Both concepts of the tangent vector, 1) as a velocity vector - the curves approach, or 2) as a directional derivative - the derivation approach, are useful and may be used interchangeably. We can easily reconcile these viewpoints by noting that a tangent vector $(v_1,..,v_i,..,v_m) = (0,..,1,..,0)$ corresponds to the operator $\mathbf{v} = \partial/\partial x_i$.

Thus, we have the following definition.

Definition 3.14. *The set of partial derivative operators constitute a basis for the tangent space TM_p for all points $p \in U \subset M$ which is called the* natural basis.

The above definition makes sense when the tangent space is viewed as a space of differential operators. The formulation of the tangent vector as a directional derivative requires a local coordinate system, i.e., a chart (U,φ). We are free, however, to define a coordinate system for the tangent space TM_p. The 'natural' coordinate system on TM_p induced by (U,φ) has basis vectors which are tangent vectors to the coordinate lines on M passing through p. When taking the curves viewpoint, the tangent space TM_p is simply R^m and its elements may be thought of as column vectors and the symbols $\mathbf{v}_i = \partial/\partial x_i$ represent the (unit) basis vectors.

At each point $p \in M$, we have defined the tangent space. Taken together, these spaces form the tangent bundle.

Definition 3.15. *The union of all the tangent spaces to M is called the* tangent bundle *and is denoted TM,*

$$TM = \bigcup_{p \in M} TM_p$$

The tangent bundle is a manifold with $\dim\{TM\} = 2\dim\{M\}$. A point in TM is a pair (x,v) with $x \in M$, $v \in TM_x$. If $(x_1,..,x_m)$ are local coordinates on M and $(v_1,..,v_m)$ components of the tangent vector in the natural coordinate system on TM_x, then natural local coordinates on TM are $(x_1,\ldots,x_m,v_1,\ldots,v_m) = (x_1,\ldots,x_m,\dot{x}_1,\ldots,\dot{x}_m)$. Recall the natural 'unit vectors' on TM_x are $\mathbf{v}_1 = \partial/\partial x_1,...,\mathbf{v}_m = \partial/\partial x_m$.

The mapping $\pi : TM \to M$ which takes the point (x,v) in TM to x in M is called the *natural projection* on TM. The inverse image of x under π is the tangent space at x, $\pi^{-1}(x) = TM_x$. TM_x is called the *fiber* of the tangent bundle over the point x. A *section* of TM is a mapping $\sigma : M \to TM$ such that the composite mapping $\pi \circ \sigma : M \to M$ is the identity. The mapping $\iota : M \to TM$ such that $\iota(x)$ is the zero vector of TM_x is called the *null section*.

One of the most important applications of the idea of tangent bundle occurs in analytical mechanics where the tangent bundle generalizes the concept of a state space. A *mechanical system* is a collection of mass particles which interact through physical constraints or forces, such as the pendulum of Figure (3.5). A *configuration* is a specification of the position for each of its constituent particles. The *configuration space* is a set M of elements such that any configuration of the system corresponds to a unique point in the set M and each point in M corresponds to a unique configuration of the system. The configuration space of a mechanical system is a differentiable manifold called the *configuration manifold*. Any system of local coordinates q on the configuration manifold are called *generalized coordinates*. The *generalized velocities* $\dot{q}$ are elements of the tangent spaces to M, TM_q represented in the natural basis. The *state space* is the tangent bundle TM which has local coordinates $(q,\dot{q})$.

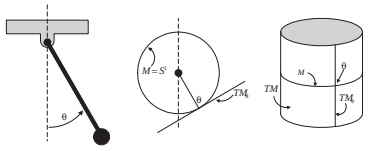

Fig. 3.5: The pendulum illustrates the relationships between the configuration manifold M, the tangent space TM_θ, and the state space TM.

3.3.2 The Differential Map

Let C be a curve in M parameterized by the mapping $\phi : R \to M$. Let $F : M \to N$ be a smooth mapping. The image of C under the mapping F is the curve $\bar{C}$ in N which has a parameterization $\bar{\phi} = F \circ \phi$. Refer to Figure (3.6). At any point p on C there is a tangent vector $v \in TM_p$ which maps to a tangent vector $\bar{v} \in TN_{F(p)}$. We wish to

determine the induced mapping $F_* : TM_p \to TN_{F(p)}$ which takes tangent vectors into tangent vectors.

In local coordinates, the chain rule provides

$$\frac{d\bar{\phi}}{dt} = \frac{\partial F}{\partial x}\frac{d\phi}{dt} \tag{3.4}$$

$$\bar{v} = \frac{\partial F}{\partial x} v \tag{3.5}$$

This relation defines the desired mapping, F_*, in local coordinates. We note that it is linear and that its matrix representation is simply the Jacobian of the mapping F. F_* is called the *differential map* of F and is sometimes denoted dF. Notice that

$$\bar{v_i} = v_1 \frac{\partial F_i}{\partial x_1} + \cdots + v_m \frac{\partial F_i}{\partial x_m} = \mathbf{v}(F_i), \quad i = 1, \ldots, n \tag{3.6}$$

So that

$$\bar{v}(y) = (\mathbf{v}(F_1(p)), \ldots, \mathbf{v}(F_n(p))), \quad y = F(p) \in N \tag{3.7}$$

From the derivational point of view, the mapping dF is realized in local coordinates by

$$\bar{\mathbf{v}} = \mathbf{v}(F_1(p))\frac{\partial}{\partial y_1} + \cdots + \mathbf{v}(F_n(p))\frac{\partial}{\partial y_n} = \sum_{i=1}^{n} \mathbf{v}(F_i(p))\frac{\partial}{\partial y_i} \tag{3.8}$$

where y are the local coordinates on N. Because the differential map takes tangent vectors in TM_p to $TN_{F(p)}$ it is defined at the point p. Thus, it would be appropriate to write $F_*|_p$ or $dF|_p$. However, the point of evaluation is typically not indicated and is normally clear from the context.

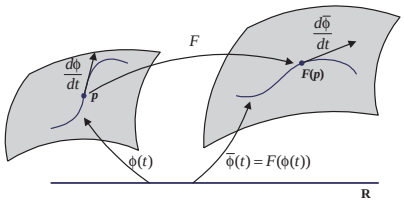

Fig. 3.6: Motion along a curve in the manifold M maps into a manifold N. The mapping induces a map between the tangent spaces TM_p and $TN_{F(p)}$.

The following is a useful result which provides for computing the differential map for composite functions

Lemma 3.16. *Suppose $F : M \to N$ and $H : N \to P$ are smooth maps between manifolds, then*

$$d(H \circ F) = dH \circ dF$$

where $dF : TM_x \to TN_{y=F(x)}$, $dH : TN_y \to TP_{z=H(y)}$ and $d(H \circ F) : TM_x \to TP_{z=H(F(x))}$.

Proof: Direct computation in local coordinates provides the matrix representation of $d(H \circ F)$. For any $v \in TM_x$

$$d(H \circ F)(v) = \frac{\partial H(F(x))}{\partial x}(v) = \frac{\partial H(y)}{\partial y}\frac{\partial F(x)}{\partial x}(v) = dH(dF(v)) = dH \circ dF(v)$$

■

3.3.3 Cotangent Spaces

The dual space to TM_p is denoted T^*M_p and it is called the *contagent space* to M at $p \in M$. The elements of T^*M_p are called *tangent covectors* . Recall that the dual space V^* of a linear vector space V is the space of linear functions from V to R. Thus, if we identify the elements of TM_p as column vectors of dimension m, the covectors may be thought of as row vectors of dimension m. There is a natural relationship between the differential mapping and the cotangent space. Let ϕ be a smooth mapping $\phi : M \to R$. Its differential at $p \in M$ is a linear map $\phi_* : TM_p \to TR_{\phi(p)} \cong R$. Since ϕ_* is a linear map from TM_p to the real line, it is an element of of the dual space to TM_p, that is, the cotangent space T^*M_p. In local coordinates ϕ_* is realized by

$$\tilde{v} = \left\lfloor \frac{\partial \phi}{\partial x_1}, \cdots, \frac{\partial \phi}{\partial x_m} \right\rfloor = \mathbf{v}(\phi)$$

Let $e^i, i = 1, , m$ denote the natural basis vectors of TM_p. The natural basis vectors e_i^* for T^*M_p are defined by the relations

$$e_i^* e_j = \delta_{ij}, i, j = 1, ..., m \tag{3.9}$$

Recall, that

$$e_1 \;=\; \begin{bmatrix} 1 \\ 0 \\ \vdots \\ \vdots \\ 0 \end{bmatrix},\; e_2 \;=\; \begin{bmatrix} 0 \\ 1 \\ 0 \\ \vdots \\ 0 \end{bmatrix},\; ...,\; e_m \;=\; \begin{bmatrix} 0 \\ \vdots \\ \vdots \\ \vdots \\ 0 \\ 1 \end{bmatrix} \tag{3.10}$$

so that the basis vectors for T^*M_p are the row vectors

$$e_1^* \;=\; [1, 0, .., 0],\; e_2^* \;=\; [0, 1, .., 0],\; ...,\; e_m^* \;=\; [0, 0, .., 1] \tag{3.11}$$

Correspondingly, in the derivations viewpoint, TM_p is a linear vector space of differential operators which act on scalar valued functions on M and the basis elements for TM_p are $\mathbf{e}_i = \partial / \partial x_i$, $i = 1, , m$. The differential map associated with the smooth mapping $\phi : M \to R$ is

$$\phi_*(\mathbf{v}) = \mathbf{v}(\phi)\frac{d}{dy} \tag{3.12}$$

Of course, there is a one to one correspondence between $\mathbf{v}(\phi)d/dy \in TR_{\phi(p)}$ and $\mathbf{v}(\phi) \in R$. Thus, it is convenient to write $d\phi(\mathbf{v}) = \mathbf{v}(\phi)$ and refer to $d\phi$ as the differential mapping. In this way we again identify the differential mappings of scalar valued functions as elements of T^*M_p, i.e., the differential mappings $d\phi(\mathbf{v})$ are cotangent vectors. We seek basis elements in T^*M_p, $\mathbf{e}_i^*$, such that

$$\mathbf{e}_i^*(\mathbf{e}_j) = \mathbf{e}_i^*\left(\frac{\partial}{\partial x_j}\right) = \delta_{ij}, i, j = 1, , m \tag{3.13}$$

Let $\phi = x_i$, the coordinate map, and notice that

$$dx_i \frac{\partial}{\partial x_j} = \frac{\partial x_i}{\partial x_j} = \delta_{ij} \tag{3.14}$$

Thus, the set of cotangent vectors $\{dx_1, .., dx_m\}$ constitute a basis for the cotangent space T^*M_p. Now, any smooth function $\phi : M \to R$ gives rise to a cotangent vector $d\phi$ which can be expressed

$$d\phi = \sum_{i=1}^m v_i^* dx_i \tag{3.15}$$

$$v_i^* = \frac{\partial \phi}{\partial x_i} \tag{3.16}$$

so that

$$d\phi = \sum_{i=1}^m \frac{\partial \phi}{\partial x_i} dx_i \tag{3.17}$$

Suppose $F : M \to N$ is a smooth map. Recall that its differential, F_* or $dF : TM_p \to TN_{F(p)}$, is a linear map that takes tangent vectors in M to tangent vectors in N. This map is realized in local coordinates by the Jacobian of F. Consequently, there is an induced map between cotangent spaces called the *codifferential* and denoted F^* or $\delta F : T^*N_{F(p)} \to T^*M_p$. This map, realized by the transpose of the Jacobian of F, is sometimes called the *pull-back* as it takes covectors on N back to covectors on M. To see this, consider a covector $\omega \in TM_p^*$. Then ω is a linear mapping that takes each $v \in TM_p$ to R. Let $F : M \to N$ be a smooth mapping. Then the induced differential map dF takes vectors in TM_p into $TN_{F(p)}$, in local coordinates

$$w = \frac{\partial F}{\partial x} v \tag{3.18}$$

We seek a covector $\mu \in TN_{F(p)}^*$ such that $\omega v = \mu w$ for all $v \in TM_p$, i.e.,

$$\omega v = \mu \frac{\partial F}{\partial x} v, \ \forall v \in TM_p \tag{3.19}$$

Clearly, in local coordinates, ω and μ are related by

$$\omega = \mu \frac{\partial F}{\partial x} \tag{3.20}$$

This is the pull-back mapping.

3.3.4 Vector Fields and Flows

A vector field $f(x)$ on a manifold M is a mapping that assigns a vector $f \in TM_x$, where TM_x is the tangent space to M at x, to each point $x \in M$. Formally, we define:

Definition 3.17. *A* vector field *v on M is a map which assigns to each point $p \in M$, a tangent vector $v(p) \in TM_p$. It is a C^k-*vector field *if for each $p \in M$ there exist local coordinates (U, φ) such that each component $v_i(x), i = 1, ..., m$ is a C^k function for each $x \in \varphi(U)$.*

A vector field can be viewed as a mapping $v : M \to TM$ with the property that the composite mapping $\pi \circ v : M \to M$ [1] is the identity mapping, i.e. $\pi \circ v(x) = x$. Thus, the vector field v is a section of the tangent bundle.

Definition 3.18. *An* integral curve *of a vector field v on M is a parameterized curve $p = \phi(t), t \in (t_1, t_2) \subset R$ whose tangent vector at any point coincides with v at that point.*

Consider local coordinates (U, φ) on M, and the induced natural coordinates on TM_p. Then if $\phi(t)$ is an integral curve, its image $x(t) = \varphi \circ \phi(t) \subset R^m$ must satisfy the differential equation $dx/dt = v(x)$.

If $v(x)$ is sufficiently smooth, standard existence and uniqueness theorems for systems of ordinary differential equations imply corresponding properties for integral curves on manifolds. First we define a maximal integral curve.

Definition 3.19. *Let I_p denote an open interval of R with $0 \in I_p$. Suppose $\phi : I_p \to M$ is an integral curve of the vector field v such that $\phi(0) = p$. The integral curve ϕ is maximal if for any other integral curve $\hat{\phi} : \hat{I}_p \to M$ with $\hat{\phi}(0) = p$, then $\hat{I}_p \subset I_p$ and $\hat{\phi}(t) = \phi(t)$ for $t \in \hat{I}_p$.*

Now, the existence and uniqueness theorem can be stated.

Proposition 3.20. *Suppose v is a smooth (C^k) vector field on M. Then there exists a unique maximal integral curve $\phi : I_p \to M$ passing through the point $p \in M$.*

Proof: The result follows from the standard results on differential equations. ■

Definition 3.21. *Let v be a smooth vector field on M and denote the parameterized maximal integral curve through $p \in M$ by $\Psi(t, p)$ so that $\Psi : I_p \times M \to M$ where I_p is a subinterval of R containing the origin and $\Psi(0, p) = p$. $\Psi(t, p)$ is called the* flow generated by *v.*

[1] recall that π is the natural projection.

The flow Ψ has the following basic property.

Proposition 3.22. *The flow Ψ of a smooth vector field v satisfies the differential equation on M*

$$\frac{d}{dt}\Psi(t,p) \;=\; v(\Psi(t,p)), \quad \Psi(0,p)=p$$

and has the semigroup property

$$\Psi(t_2,\Psi(t_1,p)) \;=\; \Psi(t_1+t_2,p)$$

for all values of $t_1,t_2 \in R$ and $p \in M$ such that both sides of the relation are defined.

Proof: The differential equation merely states that v is tangent to the curve $\Psi(t,p)$ for all fixed p. The initial condition is part of the definition of Ψ. The semigroup property follows from the uniqueness property of differential equations. Both sides of the equation satisfy the differential equation and have the same initial condition at $t_2 = 0$. ■

We will adopt the following notation

$$\exp(t\mathbf{v})p := \Psi(t,p) \tag{3.21}$$

The motivation for this is simply that the flow satisfies the three basic properties ordinarily associated with exponentiation. In particular, we have (from the properties of the flow function):

$$\exp(0\cdot\mathbf{v})p = p \tag{3.22}$$

$$\frac{d}{dt}[\exp(t\mathbf{v})p] \;=\; \mathbf{v}(\exp(t\mathbf{v})p) \tag{3.23}$$

$$\exp[(t_1+t_2)\mathbf{v}]p \;=\; \exp(t_1\mathbf{v})\exp(t_2\mathbf{v})p \tag{3.24}$$

whenever defined. Note the distinction between the vector field used as a column vector (v) and as a derivation ($\mathbf{v}$).

The vector field is said to be *complete* if I_p coincides with R. Thus the flow is defined on all of $R\times M$.

Further justification for the exponential notation comes from the action of a vector field on functions. Let v be a vector field on M and $f : M \to R$ a smooth function. The value of f along the flow (along an integral curve of v passing through p) is given in local coordinates by $f(\exp(t\mathbf{v})x)$. Then the rate of change of f can be computed

$$\begin{aligned}\tfrac{d}{dt} f(\exp(t\mathbf{v})x) &= \tfrac{\partial f(\exp(t\mathbf{v})x)}{\partial x}\tfrac{d\exp(t\mathbf{v})x}{dt} = \tfrac{\partial f(\exp(t\mathbf{v})x)}{\partial x}\mathbf{v}(\exp(t\mathbf{v})x)\\ &= \sum_{i=1}^{m} v_i(\exp(t\mathbf{v})x)\tfrac{\partial}{\partial x_i} f(\exp(t\mathbf{v})x) = \mathbf{v}(f)(\exp(t\mathbf{v})x)\end{aligned} \tag{3.25}$$

where $v = \{v_1(x),\ldots,v_m(x)\}$ is also in local coordinates. Similarly,

$$\frac{d^2}{dt^2} f(\exp(t\mathbf{v})x) \;=\; \mathbf{v}^2(f)(\exp(t\mathbf{v})x) \tag{3.26}$$

where $\mathbf{v}^2 = \mathbf{v}(\mathbf{v}(f))$, and so on. Thus, the Taylor series about $t = 0$ is

$$f(\exp(t\mathbf{v})x) \;=\; f(x) + t\,\mathbf{v}(f)(x) + \frac{t^2}{2}\mathbf{v}^2(f)(x) + \cdots = \sum_{k=0}^{\infty} \frac{t^k}{k!}\mathbf{v}^k(f)(x) \tag{3.27}$$

A similar formula is valid for vector valued functions $F : M \to R^n$. Let us interpret the action of $\mathbf{v}$ on F component-wise, that is $\mathbf{v}(F) = (\mathbf{v}(F_1), \ldots, \mathbf{v}(Fn))^T$. Then we have

$$F(\exp(t\mathbf{v})x) \;=\; F(x) + t\,\mathbf{v}(F)(x) + \frac{t^2}{2}\mathbf{v}^2(F)(x) + \cdots = \sum_{k=0}^{\infty} \frac{t^k}{k!}\mathbf{v}^k(F)(x) \tag{3.28}$$

An important operation is the or *Lie derivative* of a map $F : M \to R^n$ with respect to a vector field v on M.

Definition 3.23. *Let $v(x)$ denote a vector field on M and $F(x)$ a mapping $F : M \to R^n$, both in local coordinates. Then the* Lie derivative *of F with respect to v of order $0, \ldots, k$ is*

$$L_v^0(F) = F, \;\; L_v^k(F) = \frac{\partial L_v^{k-1}(F)}{\partial x} v \tag{3.29}$$

Using this notation we can write

$$\mathbf{v}^k(F)(x) \;= Ł_v^k(F)(x) \tag{3.30}$$

so that

$$F(\exp(t\mathbf{v})x) \;= \sum_{k=0}^{\infty} \frac{t^k}{k!} L_v^k(F)(x) \tag{3.31}$$

In particular, suppose F is the coordinate map from M to R^m, $F(x) = x$, so that $F(\exp(t\mathbf{v})x) = \exp(t\mathbf{v})x$ and we have

$$\exp(t\mathbf{v})x \;=\; x + t\,\mathbf{v}(x)(x) + \frac{t^2}{2}\mathbf{v}^2(x)(x) + \cdots = \sum_{k=0}^{\infty} \frac{t^k}{k!}\mathbf{v}^k(x)(x) \;= \sum_{k=0}^{\infty} \frac{t^k}{k!} L_v^k(x)(x) \tag{3.32}$$

The Taylor expansion is identical to that of the classical exponential.

3.3.5 Lie Bracket

The Lie bracket is a binary operation on vector fields that is essential in the subsequent discussion.

Definition 3.24. *If v, w are differentiable vector fields on M, then their* Lie bracket $[v,w]$ *is the unique vector field defined in local coordinates by the formula*

$$[v,w] = \frac{\partial w}{\partial x}v - \frac{\partial v}{\partial x}w$$

In terms of the derivation viewpoint, the Lie bracket is the unique vector field satisfying

$$[\mathbf{v},\mathbf{w}](f) = \mathbf{v}(\mathbf{w}(f)) - \mathbf{w}(\mathbf{v}(f)) \tag{3.33}$$

for all smooth functions $f : M \to R$. In local coordinates we can easily derive the formula

$$[\mathbf{v},\mathbf{w}] = \sum_{i=1}^{m} \{\mathbf{v}(w_i) - \mathbf{w}(v_i)\}\frac{\partial}{\partial x_i} = \sum_{i=1}^{m}\sum_{j=1}^{m}\left\{ v_j \frac{\partial w_i}{\partial x_j} - w_i \frac{\partial v_i}{\partial x_j} \right\}\frac{\partial}{\partial x_i} \tag{3.34}$$

which is precisely the definition we have adopted.

The Lie bracket can be given useful geometric interpretations. First, let us consider the Lie bracket as a directional derivative. We will compute the rate of change of a vector field w as seen by an observer moving with the flow $\Psi(x,t)$ generated by a second vector field v.

Proposition 3.25. *Suppose v, w are smooth vector fields on M and $\Psi(x,t)$ is the flow generated by v. Then*

$$\left.\frac{dw(\Psi(x,t))}{dt}\right|_{t=0} = [v,w]|_x$$

Proof: We need to compare $w(\Psi(x,t))$ with $w(x)$ as $t \to 0$. Since these two vectors exist in different tangent spaces ($TM_{\Psi(x,t)}$ and TM_x, respectively) we need to 'pull back' $w(\Psi(x,t))$ to the tangent space TM_x. This is easily done using the differential map. Thus,

$$\begin{aligned}
\left.\frac{dw(\Psi(x,t))}{dt}\right|_{t=0} &= \lim_{t\to 0}\left[\frac{\Psi_x(x,-t)w(\Psi(x,t)) - w(x)}{t}\right] \\
&= \lim_{t\to 0}\left[\frac{(I - v_x(x)t)(w(x) + w_x(x)v(x)t) - w(x)}{t}\right] \\
&= w_x(x)v(x) - v_x(x)w(x) \\
&= [v,w]|_x
\end{aligned}$$

■

Now, let us consider the Lie bracket as a commutator of flows. Beginning at point x in M follow the flow generated by v for an infinitesimal time which we take as $\sqrt{\varepsilon}$ for convenience. This takes us to a point $y = \exp(\sqrt{\varepsilon}\, v)x$. Then follow $\mathbf{w}$ for the same length of time, then $-\mathbf{v}$, then $-\mathbf{w}$. This brings us to a point ψ given by (see Figure (3.7)):

$$\psi(\varepsilon,x) = e^{-\sqrt{\varepsilon}\mathbf{w}} e^{-\sqrt{\varepsilon}\mathbf{v}} e^{\sqrt{\varepsilon}\mathbf{w}} e^{\sqrt{\varepsilon}\mathbf{v}} x \tag{3.35}$$

Proposition 3.26. *Let* **v** *and* **w** *be smooth vector fields on M. Then* $\psi(\varepsilon,x)$*, as given by (3.35), with x fixed defines a continuous path in M. Moreover,*

$$\frac{d}{d\varepsilon}\psi(0^+,x) = [v,w]\big|_x$$

Proof: Our proof follows [89]. Let us write $y = e^{\sqrt{\varepsilon}\mathbf{v}}x$, $z = e^{\sqrt{\varepsilon}\mathbf{w}}y$, $u = e^{-\sqrt{\varepsilon}\mathbf{v}}$, $\psi = e^{-\sqrt{\varepsilon}\mathbf{w}}u$. Now, for any vector field **v** we can use the Taylor series representation for the flow function, i.e.

$$e^{t\mathbf{v}}x = x + v(x)t + \tfrac{1}{2}v_x(x)v(x)t^2 + O(t^3)$$

Applying this successively to ψ, we obtain

$$\begin{aligned}
\psi &= u - w(u)\sqrt{\varepsilon} + \tfrac{1}{2}w_x(u)w(u)\varepsilon + O(\varepsilon^{3/2}) \\
&= z - \{w(z)+v(z)\}\sqrt{\varepsilon} + \left\{\tfrac{1}{2}w_x(z)w(z) + v_x(z)w(z) + \tfrac{1}{2}v_x(z)v(z)\right\}\varepsilon \\
&\qquad + O(\varepsilon^{3/2}) \\
&= y - v(y)\sqrt{\varepsilon} + \left\{v_x(y)w(y) - w_x(y)v(y) + \tfrac{1}{2}v_x(y)v(y)\right\}\varepsilon + O(\varepsilon^{3/2}) \\
&= x + \{v_x(x)w(x) - w_x(x)v(x)\}\varepsilon + O(\varepsilon^{3/2})
\end{aligned}$$

Differentiating with respect to ε we get the desired result:

$$\left.\frac{d\psi}{d\varepsilon}\right|_{\varepsilon=0} = v_x(x)w(x) - w_x(x)v(x)$$

■

As we will see in later chapters, this theorem has important implications for the control of certain types of nonlinear systems.

We say that the vector fields v,w (or their flows) *commute* if

$$\psi(\varepsilon,x) = x = e^{-\sqrt{\varepsilon}w}e^{-\sqrt{\varepsilon}v}e^{\sqrt{\varepsilon}w}e^{\sqrt{\varepsilon}v}x \tag{3.36}$$

for all $\varepsilon, v \in R$ and $x \in M$ such that both sides are defined. The two vector fields commute if and only if $[v,w] = 0$. See Figure (3.7).

We can define higher order Lie Bracket operations. For notational convenience we define the *ad* operator.

Definition 3.27. *If* v,w *are* C^k *vector fields on M we define the* k^{th}*-order iterated Lie bracket or* ad *operation:*

$$ad_v^0(w) = w, \quad ad_v^k(w) = [v, ad_v^{k-1}(w)] \tag{3.37}$$

The following identity will prove useful.

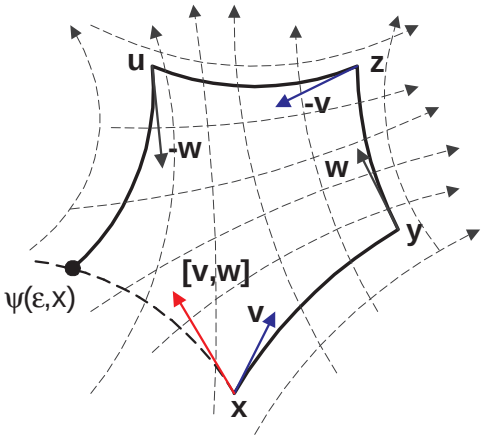

Fig. 3.7: The commutation properties of the Lie bracket are illustrated in this diagram.

Lemma 3.28. *Suppose h is a smooth scalar valued function on a manifold M and f, g are smooth vector fields on M. Then*

$$L_{[f,g]}h = L_f L_g h - L_g L_f h$$

Proof: Compute, in local coordinates x

$$L_f L_g h = \frac{\partial (L_g h)}{\partial x} f$$

and

$$\frac{\partial L_g h}{\partial x} = \frac{\partial}{\partial x}\left(\frac{\partial h}{\partial x} g\right) = \left(g^T \frac{\partial^2 h}{\partial x^2} + \frac{\partial h}{\partial x}\frac{\partial g}{\partial x}\right)$$

Consequently

$$L_f L_g h = g^T \frac{\partial^2 h}{\partial x^2} f + \frac{\partial h}{\partial x}\frac{\partial g}{\partial x} f$$

Similarly,

$$L_g L_f h = f^T \frac{\partial^2 h}{\partial x^2} g + \frac{\partial h}{\partial x}\frac{\partial f}{\partial x} g$$

Since $\partial^2 h / \partial x^2$ is symmetric, we obtain

$$L_f L_g h - L_g L_f h = \frac{\partial h}{\partial x}\left(\frac{\partial g}{\partial x} f - \frac{\partial f}{\partial x} g\right) = \frac{\partial h}{\partial x}[f,g] = L_{[f,g]}h$$

This is the desired result. ■

3.3.6 Covector Fields

Like vector fields, covector fields play an important role in our subsequent discussion.

Definition 3.29. *A* covector field *or* one-form ω*, on a smooth manifold M is a mapping that assigns to each point $p \in M$ a tangent covector $\omega(p)$ in T_p^*M.*

With any smooth function $\lambda : M \to R$ one can associate a covector field $d\lambda$. On the other hand it is not every covector field can be expressed as the differential of a scalar function.

Definition 3.30. *A covector field Ω on the manifold M is said to be* exact *if there exists a smooth, real vaued function $\lambda : M \to R$ such that $\omega = d\lambda$.*

Recall that the Lie bracket can be interpreted as a directional derivative ((3.25)). We can define a directional derivative for covector fields as well. Suppose ω is a smooth covector field and v a smooth vector field on a manifold M. As usual denote the flow generated by v, eminating from $x \in M$ at $t = 0$ by $\Psi(x,t)$. We wish to compute

$$\left.\frac{d\omega(\Psi(x,t))}{dt}\right|_{t=0} \tag{3.38}$$

Proposition 3.31. *Suppose v is a smooth vector field and ω a smooth covector field on M. For each $x \in M$ the derivative exists and in local coordinates is given by*

$$\left.\frac{d\omega(\Psi(x,t))}{dt}\right|_{t=0} = \left[\frac{\partial \omega^T}{\partial x} f\right]^T + \omega \frac{\partial f}{\partial x}$$

Proof: Again, we need to pull back $\omega(\Psi(x,t))$ from $T^*_{\Psi(x,t)}M$ to $T^*_x M$ and compute

$$\left.\frac{d\omega(\Psi(x,t))}{dt}\right|_{t=0} = \lim_{t\to 0}\left[\frac{\delta\Psi(x,t)\,\omega(\Psi(x,t)) - \omega(x)}{t}\right]$$

Now, for small t the pull back is approximated by

$$\delta\Psi(x,t)\,\omega(\Psi(x,t)) \approx \left(\omega(x) + \left[\frac{\partial \omega(x)^T}{\partial x} v(x) t\right]^T\right)(I + v_x(x)t)$$

so that

$$\left.\frac{d\omega(\Psi(x,t))}{dt}\right|_{t=0} = \lim_{t\to 0}\frac{1}{t}\left\{\left[\frac{\partial \omega(x)^T}{\partial x} v(x) t\right]^T + \omega(x) v_x(x) t + O(t^2)\right\}$$

The result follows. ■

Thus, we give the following definition.

Definition 3.32. *Let f be a smooth vector field and ω a smooth covector field on M. The* Lie derivative *of ω along f is the unique covector field denoted $L_f\omega$ and defined in local coordinates at the point $x \in M$ by*

$$L_f\omega(x) = \left[\frac{\partial \omega^T}{\partial x} f\right]^T + \omega\frac{\partial f}{\partial x}$$

Remark 3.33 (Lie Derivative of a Differential Form). Suppose $h(x)$ is a scalar function and let the covector field ω be defined by

$$\omega = dh(x) = \begin{pmatrix} \frac{\partial h(x)}{\partial x_1} & \cdots & \frac{\partial h(x)}{\partial x_n} \end{pmatrix}$$

Using the formula in Definition (3.32) it is straightforward to compute

$$L_f(dh) = f^T(x)\frac{\partial^2 h(x)}{\partial x^2} + \frac{\partial h(x)}{\partial x}\frac{\partial f(x)}{\partial x}$$

On the other hand, recall that the Lie derivative of the scalar function $h(x)$ with respect to a vector field f is

$$L_f h = \frac{\partial h(x)}{\partial x} f(x)$$

We can differentiate to compute

$$d(L_f h) = f^T(x)\frac{\partial^2 h(x)}{\partial x^2} + \frac{\partial h(x)}{\partial x}\frac{\partial f(x)}{\partial x}$$

Hence, we see that

$$d(L_f h) = L_f(dh)$$

3.4 Distributions and the Frobenius Theorem

3.4.1 Distributions

Let $v_1, \ldots, v_r$ denote a set of r vector fields on a manifold M of dimension m. $\Delta(p) = \text{span}\{v_1(p), \ldots, v_r(p)\}$ is a subspace of $TM_p \sim R^m$.

Definition 3.34. *A* smooth distribution *Δ on M is a map which assigns to each point $p \in M$, a subspace of the tangent space to M at p, $\Delta(p) \subset TM_p$ such that Δ_p is the span of a set of smooth vector fields $v_1, \ldots, v_r$ evaluated at p. We write $\Delta = \text{span}\{v_1, \ldots, v_r\}$. A distribution Δ has* dimension $\dim \text{span}\{v_1(p), \ldots, v_r(p)\}$ *at p. It is* nonsingular (or regular) at point *$p \in M$ if there is a neighborhood of p in M on which the dimension of Δ is constant. Otherwise, the point p is a* singular point *of Δ.*

In general the *basis* vector fields $\{v_1,\ldots,v_r\}$ are not unique. If v is a vector field on M we say that v belongs to a given distribution Δ on M if $v(p)\in\Delta(p),\forall p\in M$. We write $v\in\Delta$. Suppose $U\subseteq M$ is an open set and Δ is of constant dimension r on U. For a smooth vector field $v\in\Delta=\text{span}\{v_1,\ldots,v_r\}$ on U, it follows that there is a set of smooth coefficients, $c_1,\ldots,c_r$ such that

$$v(p)=\sum_{i=1}^{r}c_i(p)v_i(p),\ \forall p\in U \tag{3.39}$$

The notion of an integral curve of a single vector field can be generalized to that of an integral manifold of a set of vector fields or its corresponding distribution.

Definition 3.35. *An* integral submanifold *of a distribution $\Delta=\text{span}\{v_1,\ldots,v_r\}$ is a submanifold $N\subset M$ such that $TN_p=\Delta(p)$ for each $p\in N$. The distribution Δ or the set of vector fields $\{v_1,\ldots,v_r\}$ is said to be (completely) integrable if through every point $p\in M$ there passes an integral manifold.*

Suppose N is an integral submanifold of $\Delta=\text{span}\{v_1,\ldots,v_r\}$ on M. Then

$$TM_p\supset\Delta=TN_p \tag{3.40}$$

and $\dim(TN_p)=\dim(N)$ at each $p\in N$. But

$$\dim\Delta(p)=\dim\text{span}\{v_1(p),..,v_r(p)\}$$

may vary as p varies throughout M. Thus, not all integral manifolds need be of the same dimension. Moreover, there may be a manifold N of smaller dimension than Δ that is tangent to it in the sense that Δ contains a subset of smooth vector fields that span TN_p at each point $p\in N$. This is the basis for a weaker notion of integral manifolds and integrability that is sometimes employed. For this reason the integral manifolds of the above definition are sometimes called *maximal* integral submanifolds and the terminology completely integrable requires the existence of maximal integral manifolds.

Definition 3.36. *A system of smooth vector fields $\{v_1,\ldots,v_r\}$ or the distribution $\Delta=\text{span}\{v_1,\ldots,v_r\}$ on M is said to be* in involution *or* involutive *if there exist smooth real valued functions $c_k^{ij}(p)$, $p\in M$ and $i,j,k=1,\ldots,r$ such that for each i,j*

$$[v_i,v_j]\ =\ \sum_{k=1}^{m}c_k^{ij}v_k$$

The concept of an involutive distribution is key to many important results. The following Lemma provides a result that will prove extremely useful in applications.

Lemma 3.37. *Suppose $\Delta = \{v_1(x), \ldots, v_k(x)\}$ is a smooth, nonsingular and involutive distribution of dimension k on a neighborhood U of x_0 in R^n. Then there exists a smooth integral manifold of Δ, of dimension k, passing through the point x_0. Morover, the manifold is parametrically characterized, locally around x_0, by the mapping:*

$$\phi(s) = \phi_1^{s_1} \circ \phi_2^{s_2} \circ \cdots \circ \phi_k^{s_k}(x_0)$$

where $\phi_i^t(x) = \psi_i(x,t)$ is the flow generated by the vector field $v_i(x)$ and '$\circ$' denotes composition with respect to x.

Proof: According to Definition (3.4) we need to show that there exists a neighborhood V of the origin in R^n such that

(i) $\phi(s)$ is a smooth one-to-one map on V

(ii) $\phi(s)$ satisfies the maximal rank condition for each $s \in V$

(iii) the manifold $\phi(V)$ is an integral manifold of Δ, i.e., each $\partial\phi(x)/\partial s_i \in \Delta(x)$, $i = 1, \ldots, k$.

Notice that the mapping is well defined on a neighborhood of the origin of R^k because each flow function $\phi_i^t(x0)$ is defined for sufficiently small t. Now, use the chain rule to compute

$$\begin{aligned}\frac{\partial\phi}{\partial s_i} &= \frac{\partial\phi_1^{s_1}}{\partial x}\cdots\frac{\partial\phi_{i-1}^{s_{i-1}}}{\partial x}\frac{\partial}{\partial s_i}\left(\phi_i^{s_i}\circ\cdots\circ\phi_k^{s_k}(x_0)\right)\\ &= \frac{\partial\phi_1^{s_1}}{\partial x}\cdots\frac{\partial\phi_{i-1}^{s_{i-1}}}{\partial x}v_i\left(\phi_i^{s_i}\circ\cdots\circ\phi_k^{s_k}(x_0)\right)\end{aligned}$$

In particular, at $s = 0$ we have $\phi_i^0 \circ \cdots \circ \phi_k^0(x_0) = x_0$, for each i, including $\phi(0) = x_0$, so that

$$\frac{\partial\phi(0)}{\partial s_i} = v_i(x_0)$$

Since the tangent vectors $v_i(x0)$, $i = 1, \ldots, k$ are independent, the mapping ϕ has rank k at $s = 0$. This establishes (i).

Notice that the point $x_i = \phi_i^{s_i} \circ \cdots \phi_n^{s_n}(x_0)$ reached by propogating forward from x_0 can also be reached by propogating backward from x, i.e., $x_i = \phi_{i-1}^{-s_{i-1}} \circ \cdots \phi_1^{-s_1}(x)$ so that

$$\frac{\partial\phi}{\partial s_i}(x) = \left(\phi_1^{s_1}\right)_* \cdots \left(\phi_{i-1}^{s_{i-1}}\right)_* v_i\left(\phi_{i-1}^{-s_{i-1}} \circ \cdots \phi_1^{-s_1}(x)\right)$$

where $x = \phi(s)$. In view of the fact that vectors $\partial\phi(0)/\partial s_i$ are linearly independent, for sufficiently small s, so are the vectors $\partial\phi(x)/\partial s_i$. What remains to be shown is that each $\partial\phi(x)/\partial s_i \in \Delta(x)$, $i = 1, \ldots, k$. This calculation is given in [7, p27]. ■

Example 3.38 (Parametric from Implicit Manifold). One useful application of Lemma (3.37) is the development of a parametic representation of a manifold from an

implicit representation. Consider the mapping $F : R^k \to R^n$, $k < n$ and suppose $\operatorname{rank} \partial F / \partial x = k$ on the set

$$M = \{x \in R^n \,|F(x) = 0\}$$

Then M is a regular manifold of dimension $n-k$. It follows that

$$\Delta(x) = \ker \frac{\partial F(x)}{\partial x}$$

is a nonsingular, involutive distribution of dimension $n-k$. M is an integral manifold of Δ. Let $v_1(x), \ldots, v_{n-k}(x)$ be a set of basis vector fields for Δ and suppose $x_0 \in M$. Now, let $\phi_i^{s_i}(x)$ denote the flow corresponding to the vector field $v_i(x)$. The a parametric representation of the M is the map $\phi : R^{n-k} \to R^n$ given by $\phi(s) = \phi_1^{s_1} \circ \cdots \phi_{n-k}^{s_{n-k}}(x_0)$.

To compute the parametric $\phi(s)$ given $F(x)$ requires the following procedure. The calculations involve four steps:

(i) compute the Jacobian DF,

(ii) generate a smooth basis set for $\ker DF$,

(iii) compute the flow functions (a local parameterization can be based on the exponential map),

(iv) form the composition.

These steps have been implemented in the *ProPac* function:

```
ParametricManifold[f,x,x0,n].
```

The following illustration shows that the calculations – even though local, because of the use of the exponential map – capture interesting characteristics of the surface.

```
In[9]:= F = {x3^3 + x2 * x3 + x1};

In[10]:= Surf = ParametricManifold[F, {x1, x2, x3}, {0, 0, 0}, 3]

2 vector fields computed.

2 flow functions computed.
Out[10]= {{-k1^3 - k1  k2, k2, k1}, {k1, k2}}

In[11]:= ParametricPlot3D[Surf[[1]][[{1, 2, 3}]], {k1, -1.5, 1.5}, {k2, -2, 2},
           PlotPoints -> {25, 25},
           BoxRatios -> {1, 1, 0.3},
           AxesEdge -> {None, None, None},
           ViewPoint -> {0.25, -1, 0.5},
           Boxed -> False]
```

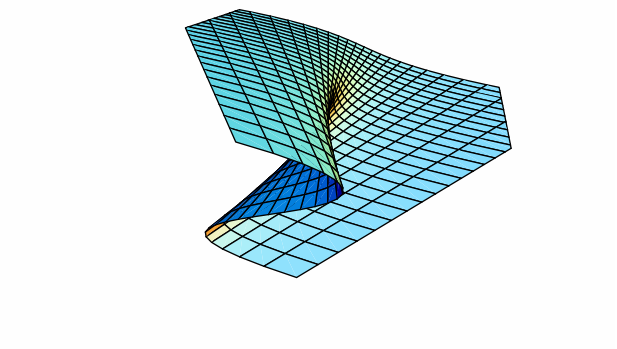

We are now in a position to state the key result of this section. One formulation of the original Frobenius theorem is as follows.

Proposition 3.39. *Let* $\{v_1,\ldots,v_r\}$ *be a nonsingular set of vector fields with*

$$\dim \operatorname{span}\{v_1,\ldots,v_r\} = k$$

on M*. Then the set of vector fields or the distribution* $\Delta = \operatorname{span}\{v_1,\ldots,v_r\}$ *is integrable with all integral manifolds of dimension* k *if and only if it is involutive.*

Proof: Sufficiency is established by Lemma (3.37). Necessity is proved as follows. Suppose x_0 is a point on an integral manifold M of Δ. Then there exists a neigborhood U of x_0 and a mapping $F : R^n \to R^{n-k}$ such that, around x_0, M is defined by

$$M = \{x \in U \,|F(x) = 0\,\}$$

Since M is an integral manifold, by definition we have

$$\frac{\partial F}{\partial x} v_i = 0, \quad i = 1,\ldots,k$$

or equivalently,

$$L_{v_i} F_j(x) = 0, \quad i = 1,\ldots,k,\ j = 1,\ldots,n-k,\ x \in U$$

Now, compute the Lie derivative of F_j along the vector field $[v_j, v_i]$.

$$L_{[v_j,v_i]} F_j(x) = L_{v_j} L_{v_i} F_j(x) - L_{v_i} L_{v_j} F_j(x) = 0$$

Thus, we have

$$\frac{\partial F}{\partial x} [v_i, v_j]\,(x) = 0$$

But the ker $\partial F / \partial x$ is spanned by the vectors $v_1(x), \ldots, v_k(x)$. Thus, we conclude that $[v_j, v_i] \in \Delta$ for $i, j = 1, \ldots, k$ so that Δ is involutive. ■

These integral manifolds allow a partition of M into submanifolds of dimension k. The set of all integral manifolds is called a *foliation* of the manifold M, and the integral manifolds are the *leaves* of the foliation.

A stronger version of this theorem is due to Hermann.

Proposition 3.40. *Let $\Delta = \text{span}\{v_1, \ldots, v_r\}$ be smooth distribution on M. Then the system is integrable if and only if it is in involution.*

Proof: See [39] ■

This theorem provides necessary and sufficient conditions for integrability. Once again, the manifold M is filled with integral submanifolds. However, the integral submanifolds need not be of the same dimension. A more complete discussion of the Frobenius theorem and its implications can be found in [1] or [107].

Example 3.41 (Foliation of a Singular Distribution). An example of an integrable, but singular, distribution is the following. Let $M = R^3$ and consider the distribution $\Delta = \text{span}\{v, w\}$ with

$$v = \begin{bmatrix} -y \\ x \\ 0 \end{bmatrix}, w = \begin{bmatrix} 2zx \\ 2yz \\ z^2 + 1 - x^2 - y^2 \end{bmatrix}$$

A simple calculation shows that $[v, w] \equiv 0$ so that the distribution Δ is completely integrable. However, the distribution is singular because $\dim \Delta = 2$ everywhere except

1. on the z-axis ($x = 0, y = 0$)
2. on the circle $x^2 + y^2 = 1, z = 0$

where $\dim \Delta = 1$. The z-axis and the circle are one-dimensional integral manifolds. All others are the tori:

$$T_c = \left\{ (x, y, z) \in R^3 \,\middle|\, (x^2 + y^2)^{-1/2}(x^2 + y^2 + z^2 + 1) = c > 2 \right\}$$

Set $r^2 = x^2 + y^2$ to obtain a representation of the torus in polar coordinates:

$$\left(r - \frac{c}{2}\right)^2 + z^2 = \left(\frac{c}{2}\right)^2 - 1$$

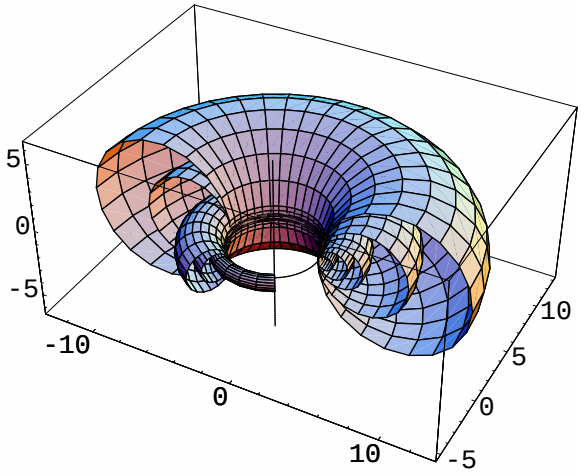

3.4.2 Coordinate System from a set of Vector Fields

We will encounter situations in which we would like to know whether n given vector fields, $\{v_1,\ldots,v_n\}$ defined on an n-dimensional manifold N can be used to establish local coordinates on N.

Theorem 3.42. *Given a set of smooth vector fields $\{v_1,\ldots,v_n\}$ on the n-dimensional manifold N, there exist local coordinates x around $p \in N$, with*

$$\frac{\partial}{\partial x_i} = v_i$$

if and only if

(i) $\dim \operatorname{span}\{v_1(p),\ldots,v_n(p)\} = n$, *and*

(ii) $[v_i, v_j] = 0, \quad 1 \le i, j \le n$

Remark 3.43. Note that since the Lie bracket is antisymmetric, the test (ii) need only be applied for $1 \le i \le n$, $i \le l \le n$.

Proof: For sufficiency follow Warner's [107] version of the Frobenius Theorem.

To prove necessity, assume there is a local coordinate system defined by a chart $\{U, \varphi\}$ consisting of a coordinate map $\varphi : U \to V$ where V is a neighborhood of 0

in R^n, U is a neighborhood of p in N and $\varphi(p) = 0$. Then there are n independent induced coordinate directions given by the vector fields

$$\frac{\partial}{\partial x_i} = v_i = \frac{\partial \varphi^{-1}}{\partial x_i}$$

thereby establishing (i). Now consider a two dimensional slice U_{ij} in U defined by

$$U_{ij} = \{p \in U \,|\varphi_k(p) = c_k,\ k \in \{1,\ldots,n\}\backslash\{i,j\}\}$$

where the c_k's are arbitrary constants, sufficiently small so that $U_{ij} \neq \emptyset$. Take two arbitrarily close points $a, b \in U_{ij}$ with local coordinates $x^a = \varphi(a)$, $x^b = \varphi(b)$. Then, the coordinates of a and b are related by

$$x^b = e^{\mathbf{v}_j(x_j^b - x_j^a)} e^{\mathbf{v}_i(x_i^b - x_i^a)} x^a$$

or going the other way

$$x^a = e^{\mathbf{v}_j(x_j^a - x_j^b)} e^{\mathbf{v}_i(x_i^a - x_i^b)} x^b$$

In other words, the flows generated by the vector fields v_i, v_j, commute. In the limit $x^a \to x^b$ this implies that $[v_i, v_j] = 0$. ■

3.4.3 Codistributions

We may work with dual objects to vector fields and distributions. A *covector field* w on M assigns to each point $p \in M$ an element $w(p) \in T^*M_p$. A *codistribution* Ω on M is a mapping which assigns a subspace $\Omega(p)$ of T^*M_p to each point $p \in M$. As with distributions we write $\Omega = \text{span}\{w_1, \ldots, w_r\}$. Distributions are sometimes associated with special codistributions. As an example, for each $p \in M$, the *annihilator* of the distribution $\Delta(p)$ is the set of all covectors which annihilate vectors in $\Delta(p)$

$$\Delta^\perp(p) := \{w \in T^*M_p \,|w(v) = 0,\ \forall v \in \Delta(p)\} \tag{3.41}$$

It is sometimes more descriptive to denote the annhilator of Δ by $\text{ann}\,\Delta$ as an alternative to $\Delta^\perp$. Conversely, given a codistribution Ω, we define its *kernel* , a distribution $\Omega^\perp$

$$\Omega^\perp(p) := \{v \in TM_p \,|v(w) = 0,\ \forall w \in \Omega(p)\} \tag{3.42}$$

Sometimes we write $\ker\Omega$ as an alternative to $\Omega^\perp$. It is not difficult to verify that the if p is a regular point of a smooth distribution Δ, then it is a regular point of the codistribution $\Delta^\perp$. Moreover, there is a neighborhood U of p such that $\Delta^\perp$ restricted to U is a smooth codistribution.

Remark 3.44 (Computing with Distributions & Codistributions). The comments above are consistent with the association of a distribution with a matrix whose columns are

its basis vector fields and the association of a codistribution with a matrix whose rows are its covector fields. Then it is possible to do formal pointwise geometric calculations (like projections) with distributions and codistributions using standard constructions from linear algebra. Some elemetary relationships between distributions and codistributions will prove particuarly useful in later calculations. For example, $[\Delta_1 \cap \Delta_2]^\perp = \Delta_1^\perp + \Delta_2^\perp$ provides a convenient way to compute the intersection of two distributions.

Now, suppose $\Delta = \text{span}\{v_1, \ldots, v_r\}$ is a smooth, involutive, and nonsingular distribution of dimension k on a neighborhood U of $p \in M$. The k-dimensional integral surfaces of Δ can be characterized on U by $m-k$ functions $\lambda_1(x) = c_1, \ldots, \lambda_{m-k}(x) = c_{m-k}$. Moreover, for each $x \in U$, the differentials $d\lambda_1, \ldots, d\lambda_{m-k}$ must must be orthogonal to Δ or equivalently, the codistribution $\Omega = \Delta^\perp$ is spanned by the exact covectors $d\lambda_1, \ldots, d\lambda_{m-k}$. These observations lead to another version of the classical Frobenius theorem.

Proposition 3.45. *Suppose $\Delta = \text{span}\{v_1, \ldots, v_r\}$ is a smooth, involutive, and nonsingular distribution of dimension k on a neighborhood U of $p \in M$. Then there exist a set of functions $\lambda_1(x), \ldots, \lambda_{m-k}(x)$ on U that satify the first order partial differential equations*

$$\begin{bmatrix} \frac{\partial \lambda_1}{\partial x} \\ \vdots \\ \frac{\partial \lambda_{m-k}}{\partial x} \end{bmatrix} \begin{bmatrix} v_1 & \cdots & v_k \end{bmatrix} = 0$$

The ideas embodied in the Frobenius theorem will prove to be fundamental to the study of nonlinear control systems. The integral surfaces implied by the theorem set up a natural coordinate system that will be used below to study controllability and observability. For the moment, however, consider the following problem of finding a coordinate system 'matched' to a given distribution. Suppose $\Delta = \text{span}\{v_1, \ldots, v_r\}$ is a smooth, nonsingular, involutive distribution of dimension k on some neighborhood U of a point x_0 in an m-dimensional manifold M. Assume that the distribution is characterized by a set of local coordinates, x. Then there are k-dimensional integral surfaces that form a foliation of U. Now, we wish to choose local coordinates in U, k of which locate points within these surfaces and the remaining $m-k$ coordinates identify the surface.

We can characterize the integral surfaces in two ways. First, adjoin to the given k vector fields an additional $m-k$ vector fields $v_{k+1}, \ldots, v_m$ such that

$$\text{span}\{v_1, \ldots, v_m\} = R^m \tag{3.43}$$

Let $\psi_i(t,x) = \psi_i^t(x)$ denote the flow generated by the vector field v_i. Then the composition

$$\Psi(z_1, \ldots, z_m) = \psi_1^{z_1} \circ \psi_2^{z_2} \circ \cdots \circ \psi_m^{z_m}(x_0) \tag{3.44}$$

defines a coordinate transformation $x = \Psi(z)$. The new coordinates are the flow lines associated with the m vector fields. In fact, $\Psi(z)|_{z_{k+1}=0,\ldots,z_m=0}$ is a parametric repesentation of the integral surface passing through the point x_0. Other leaves of the foliation are obtained by setting $z_{k+1} = c_{k+1}, \ldots, z_m = c_m$ where $c_{k+1}, \ldots, c_m$ are constants. Thus, the integral surfaces are naturally identified in these new coordinates.

Another characterization of the integral surfaces can be obtained by identifying the functions $\lambda_1, \ldots, \lambda_{n-k}$ of Theorem (3.45). Let $\Phi(x)$ denote the inverse coordinate transformation, i.e., $z = \Psi^{-1}(x) = \Phi(x)$. Then

$$\lambda_1(x) = \Phi_{k+1}(x), \ldots, \lambda_{m-k}(x) = \Phi_m(x) \tag{3.45}$$

Note that

$$\lambda_1(x) = c_1, \ldots, \lambda_{m-k}(x) = c_{m-k} \tag{3.46}$$

provide implicit representations of the integral surfaces. Choosing the constants $c_1 = 0, \ldots, c_{m-k} = 0$ produces the surface passing through x_0.

Example 3.46. Consider the following example from Isidori ([46], Example 1.4.3). The given distribution

$$\Delta = \text{span}\{v_1, v_2\}$$

is involutive. We add the vector field v_3 :

$$v_1 = \begin{bmatrix} 2x_3 \\ -1 \\ 0 \end{bmatrix},\ v_2 = \begin{bmatrix} -x_1 \\ -2x_2 \\ x_3 \end{bmatrix},\ v_3 = \begin{bmatrix} 1 \\ 0 \\ 0 \end{bmatrix}$$

and compute a new coordinate system as described in the previous paragraphs.

```
In[12]:= v1 = {2 x3, -1, 0}; v2 = {-x1, -2x2, x3}; v3 = {1, 0, 0};
```

First, let us check involutivity.

```
In[13]:= Involutive[{v1, v2}, {x1, x2, x3}]
Out[13]= True
```

Now, check to insure that v_3 as specified does indeed complete the set.

```
In[14]:= Span[{v1, v2, v3}]
Out[14]= {{1, 0, 0}, {0, 1, 0}, {0, 0, 1}}
```

The *Mathematica* function `DSolve` to compute the flows. To do so, we need to convert the vector fields to ordinary differential equations in the form that *Mathematica* requires. The *ProPac* function `MakeODEs` does this.

```
In[15]:= Eqnf1 = MakeODEs[{x1, x2, x3}, v1, t]

         Eqnf2 = MakeODEs[{x1, x2, x3}, v2, t]

         Eqnf3 = MakeODEs[{x1, x2, x3}, v3, t]
```

```
Out[15]= BoxData({-2  x3[t] + x1'[t] == 0, 1 + x2'[t] == 0, x3'[t] == 0})
Out[15]= BoxData({x1[t] + x1'[t] == 0, 2  x2[t] + x2'[t] == 0, -x3[t] + x3'[t] == 0})
Out[15]= BoxData({-1 + x1'[t] == 0, x2'[t] == 0, x3'[t] == 0})
```

```
In[16]:= sols1 = DSolve[Join[Eqnf1, {x1[0] == y1, x2[0] == y2, x3[0] == y3}],
           {x1[t], x2[t], x3[t]}, t];
         sols2 = DSolve[Join[Eqnf2, {x1[0] == y1, x2[0] == y2, x3[0] == y3}],
           {x1[t], x2[t], x3[t]}, t];
         sols3 = DSolve[Join[Eqnf3, {x1[0] == y1, x2[0] == y2, x3[0] == y3}],
           {x1[t], x2[t], x3[t]}, t];
```

```
In[17]:= psi1 = {x1[t], x2[t], x3[t]} /. sols1[[1]];
         psi2 = {x1[t], x2[t], x3[t]} /. sols2[[1]];
         psi3 = {x1[t], x2[t], x3[t]} /. sols3[[1]];
```

The transformation is obtained via Equation (3.44) using the *ProPac* function `FlowCompositon`.

```
In[18]:= Psi = FlowComposition[{psi3, psi2, psi1}, t, {y1, y2, y3},
           {0, 0, 1}, {z3, z2, z1}, ∞]
Out[18]= {2  e^z2  z1 + e^-z2  z3, -z1, e^z2}
```

The *Mathematica* functon `Solve` is used to obtain the inverse transformaton.

```
In[19]:= Trans = Inner[Equal, {x1, x2, x3}, Psi, List]
Out[19]= {x1 == 2  e^z2  z1 + e^-z2  z3, x2 == -z1, x3 == e^z2}
```

```
In[20]:= InvTrans = Solve[Trans, {z1, z2, z3}]
Out[20]= {{z3 → x3  (x1 + 2  x2  x3), z1 → -x2, z2 → Log[x3]}}
```

The λ functions of Theorem (3.45) are obtained using Equation (3.45).

```
In[21]:= λ = z3 /. InvTrans
Out[21]= {x3  (x1 + 2  x2  x3)}
```

We easily confirm the conclusion of Theorem (3.45).

```
In[22]:= Jacob[λ, {x1, x2, x3}]
Out[22]= {{x3, 2  x3^2, x1 + 4  x2  x3}}
```

```
In[23]:= Simplify[Jacob[λ, {x1, x2, x3}].Transpose[{v1, v2}]]
Out[23]= {{0, 0}}
```

3.4.4 Invariant Distributions

The importance of invariant subspaces in linear control theory is well known. For example, controllability, observability and modal subspaces all have a distinctive place in linear systems analysis. A corresponding role in nonlinear control theory is played by invariant distributions.

Definition 3.47. *A distribution $\Delta = \text{span}\{v_1, \ldots, v_r\}$ on M is invariant with respect to a vector field f on M if the Lie bracket $[f, v_i]$, for each $i = 1, \ldots, r$ is a vector field of Δ.*

We will use the notation $[f, \Delta] = \text{span}\{[f, v_i], i = 1, \ldots, r\}$ so that Δ is invariant with respect to f may be stated $[f, \Delta] \subset \Delta$. Observe that in general

$$\Delta + [f, \Delta] \;=\; \Delta + \text{span}\{[f, v_i],\ i = 1, .., r\ \} \;=\; \text{span}\{v_1, .., v_r, [f, v_1], .., [f, v_r]\}$$

Example 3.48 (Invariant Linear Subspaces). It is easily demonstrated that the notion of an invariant distribution is a natural generalization of the concept of an invariant linear subspace. Consider a subspace $V = \text{span}\{v_1, \ldots, v_r\}$ of R^n, where $v_i \in R^n$, $i = 1, \ldots, r$, that is invariant under the linear mapping A, i.e., $AV \subset V$. Define a distribution on R^n

$$\Delta_V(x) = \text{span}\{v_1, \ldots, v_r\}$$

and a vector field

$$f_A(x) = Ax$$

at each $x \in R^n$. We will prove that Δ_V is invariant under the vector field f_A. To do so,we need only show that $[f_A, v_i] \in \Delta_V$ for $i = 1, \ldots, r$. Compute

$$[f_A, v_i] = \frac{\partial v_i}{\partial x} f_A - \frac{\partial f_A}{\partial x} v_i = -Av_i$$

By assumption Av_i is a vector of $V = \text{span}\{v_1, \ldots, v_r\}$.

The notion of invariance applies in the obvious way to codistributions as well.

Definition 3.49. *A codistribution $\Omega = \text{span}\{\omega_1, \ldots, \omega_r\}$ on M is invariant with respect to a vector field f on M if the Lie derivative $L_f \omega_i$ is a covector field of Ω.*

We will use the notation $L_f \Omega = \text{span}\{L_f \omega_i, i = 1, \ldots, r\}$ so that Ω is invariant with respect to f may be written $L_f \Omega \subset \Omega$.

3.4.5 Transformation of Vector Fields

When a distribution Δ is integrable, invariance with respect to a vector field f takes on special significance. If N is an integral manifold of Δ, then the integral curve of f emanating from $p \in N$ remains in N. Using this fact, it is possible to construct a coordinate transformation that puts the vector field in a useful (block) triangular form. Such transformations will be employed to investigate controllability and observability of nonlinear systems as well as to establish feedback linearizaton methods for control system design. The main idea is established in the following lemma.

Lemma 3.50. *Let Δ be a be an involutive distribution of constant dimension d on an open subset U of R^n and suppose that Δ is invariant under a vector field f. Then at each point $x_0 \in U$ there exists a neighborhood U_0 of x_0 in U and a coordinate transformation $z = \Phi(x)$, defined on U_0, in which the vector field f is of the form*

$$\bar{f}(z) = \begin{bmatrix} f_1(z_1, \dots z_d, z_{d+1}, \dots, z_n) \\ \cdots \\ f_d(z_1, \dots z_d, z_{d+1}, \dots, z_n) \\ f_{d+1}(z_{d+1}, \dots, z_n) \\ \cdots \\ f_n(z_{d+1}, \dots, z_n) \end{bmatrix}$$

Proof: Δ is integrable because it is of constant dimension d and involutive. Thus, at each point x_0 there is a neighborhood U_0 of x_0 such that an integral manifold of Δ passes through each point $x \in U_0$. This implies that there exists a transformation of coordinates $z = \Phi(x)$, defined on U_0, with the property that

$$\text{span}\{d\Phi_{d+1}, \dots, d\Phi_n\} = \Delta^\perp$$

i.e., the first d coordinates, are in the integral manifolds and the remaining $n-d$ are orthogonal to the integral manifolds.

Let $\bar{f}(z)$ denote the representation of f in the new coordinates. Define a family of vector fields that define bases for the tangent spaces TM_z

$$\tau^i(z) = \begin{bmatrix} \tau_1^i \\ \vdots \\ \tau_n^i \end{bmatrix}, \ \tau_k^i = \begin{cases} 0 & k \neq i \\ 1 & k = i \end{cases}$$

Then

$$[\bar{f}, \tau^i] = -\frac{\partial \bar{f}}{\partial z}\tau^i = \frac{\partial \bar{f}}{\partial z_i}$$

Moreover, for $1 \leq i \leq d$, the vector field $\tau^i \in \Delta$. In fact, these vector fields form a basis for Δ. By construction, in the new coordinates every vector field of Δ has the property that the last $n-d$ coordinates vanish. Since Δ is invariant with respect to f,

we have $[\bar{f}, \tau^i] \in \Delta$, so that its last $n-d$ components vanish in the new coordinates. Thus,

$$\frac{\partial \bar{f}_k}{\partial z_i} = 0$$

for all $d+1 \leq k \leq n$ and $1 \leq i \leq d$. ■

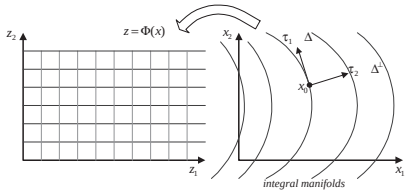

Fig. 3.8: The transformation establishes new coordinates, d coordinates in the d-dimensional integral manifolds and $n-d$ orthogonal to them.

The transformation of Lemma (3.50) is depicted in Figure (3.8) This result implies that under the stated conditions on $f(x)$, the dynamical system

$$\dot{x} = f(x)$$

can be locally represented by the triangular decomposition

$$\dot{z}_1 = f_1(z_1, z_2)$$

$$\dot{z}_2 = f_2(z_2)$$

Let $c \in U_0$ and notice that the set $S_c := \{x \in U_0 | \, z_2(x) = z_2(c)\}$ is a 'slice' (submanifold) of the neighborhood U_0 of dimension d passing through the point $c \in U_0$. Because of the triangular decomposition it is clear that the flow $f(x)$ carries slices into slices. This follows from the observation that all trajectories starting in S_c terminate in $S_{e^{\varepsilon \mathfrak{f}_c}}$ after ε time units. If $z_2(c)$ satisfies $f_2(z_2(c)) = 0$, i.e., $z_2(c)$ is an equilibrium point of the second equation, then S_c is invariant with respect to the flow in the sense that any trajectory beginning in S_c remains therein at least until it leaves the neighborhood U_0.

Example 3.51. Here is another example taken from Isidori ([46], Example 1.6.4). The distribution $\Delta = \text{span}\{v_1, v_2\}$ on R^4 with

$$v_1 = \begin{bmatrix} 1 \\ 0 \\ 0 \\ x_2 \end{bmatrix}, \quad v_2 = \begin{bmatrix} 0 \\ 1 \\ 0 \\ x_1 \end{bmatrix}$$

is easily shown to be involutive and invariant with repect to the vector field

$$f = \begin{bmatrix} x_2 \\ x_3 \\ x_3 x_4 - x_1 x_2 x_3 \\ \sin x_3 + x_2^2 + x_1 x_3 \end{bmatrix}$$

```
In[24]:= v1 = {1,0,0,x2}; v2 = {0,1,0,x1};
         f = {x2, x3, x3  x4 - x1  x2  x3, Sin[x3] + x2^2 + x1  x3};

In[25]:= LieBracket[f, v1, {x1, x2, x3, x4}]
Out[25]= {0, 0, 0, 0}

In[26]:= LieBracket[f, v2, {x1, x2, x3, x4}]
Out[26]= {-1, 0, 0, -x2}
```

Now, to obtain the new coordinate system we augment the basis fields of Δ with v_3, v_4:

```
In[27]:= v3 = {0,0,1,0}; v4 = {0,0,0,1};
```

and confirm that the expanded set does span R^4.

```
In[28]:= Span[{v1, v2, v3, v4}]
Out[28]= {{1,0,0,0}, {0,1,0,0}, {0,0,1,0}, {0,0,0,1}}
```

The *ProPac* function `TriangularDecomposition` implements the procedure illustrated in Example (3.46) to obtain the required transformation and its inverse and applies it to the vector field f.

```
In[29]:= TriangularDecomposition[f, {v1, v2, v3, v4}, {x1, x2, x3, x4},
           {0, 0, 0, 0}, ∞]
Out[29]= {{z1, z2, z3, z1  z2 + z4}, {x1, x2, x3, -x1  x2 + x4},
           {z2, z3, z3  z4, Sin[z3]}}
```

Note that as required the last two elements of the transformed field only depend on z_3, z_4.

3.4.6 Involutive Closure

In this section we describe two algorithms for computing distributions of fundamental importance to the subsequent discussion. We provide a description of them and summarize their essential properties. A more complete discussion can be found in [46].

When working with distributions, a fundamental problem is to find the 'smallest' distribution with the following properties:

1. it is nonsingular

2. it contains a given distribution Δ,
3. it is involutive,
4. it is invariant with respect to a given set of vector fields, $\tau_1, \ldots, \tau_q$.

First, let us establish the concept of a smallest distribution.

Definition 3.52. *Suppose $\mathscr{D}$ is a set of distributions on U. Then the* smallest *or* minimal *element in $\mathscr{D}$, if it exists, is the member of $\mathscr{D}$ that is contained in every other member. The* largest *or* maximal *element, if it exists, is the member that contains every other member.*

The following Lemma is given by Isidori [46].

Lemma 3.53. *Let Δ be a given smooth distribution and $\tau_1, \ldots, \tau_q$ a given set of smooth vector fields. The family of all distributions that are invariant with respect to $\tau_1, \ldots, \tau_q$ and contains Δ contains a minimal element and it is smooth.*

This distribution is denoted $\langle \tau_1, \ldots, \tau_q \mid \Delta \rangle$. An algorithm for finding will now be described. It proceeds by defining a nondecreasing set of distributions:

Algorithm 3.54

$$\begin{aligned} \Delta_0 &= \Delta \\ \Delta_k &= \Delta_{k-1} + \textstyle\sum_{i=1}^{q} [\tau_i, \Delta_{k-1}] \end{aligned} \tag{3.47}$$

The essential properties of the sequence of distribution so generated are given by the following Lemma.

Lemma 3.55. *The distributions Δ_k generated by Algorithm (3.54) are such that*

$$\Delta_k \subset \langle \tau_1, \ldots, \tau_q \big| \Delta \rangle$$

for all k. If there exists an integer k^* such that $\Delta_{k^*} = \Delta_{k^*+1}$, then

$$\Delta_{k^*} = \langle \tau_1, \ldots, \tau_q \mid \Delta \rangle$$

Thus, Algorithm (3.54) produces a distribution that is invariant with respect to the given vector fields. Now, we give conditions under which it is also involutive.

Lemma 3.56. *Suppose Δ is spanned by a subset of the vector fields $\tau_1, \ldots, \tau_q$ and that $\Delta_{k^*} = \langle \tau_1, \ldots, \tau_q \mid \Delta \rangle$ is nonsingular on U. Then $\langle \tau_1, \ldots, \tau_q \mid \Delta \rangle$ is involutive on U.*

Definition 3.57. *The involutive closure of a given distribution Δ is the smallest involutive distribution containing Δ.*

It is obvious how Algorithm (3.54) can be used to compute the involutive closure of a given distribution.

The dual computation of finding the 'largest' distribution with the following properties is also important:

1. it is nonsingular
2. it is contained within a given distribuion Δ,
3. it is involutive,
4. it is invariant with respect to a given set of vector fields, $\tau_1, \ldots, \tau_q$.

The existence of a distribution with these properties implies the existence of a codistribution (namely, its annihilator) with the following properties:

1. it is nonsingular
2. it contains the given codistribution $\Delta^\perp$,
3. it is spanned locally around each $x \in U$ by a set of exact covector fields,
4. it is invariant with respect to a given set of vector fields, $\tau_1, \ldots, \tau_q$.

Thus, we seek the 'smallest' codistribution with these properties.

Lemma 3.58. *Let Ω be a given smooth codistribution and $\tau_1, \ldots, \tau_q$ a given set of smooth vector fields. The family of all codistributions that are invariant with respect to $\tau_1, \ldots, \tau_q$ and contains Ω contains a minimal element and it is smooth.*

This codistribution is denoted $\langle \tau_1, \ldots, \tau_q \mid \Omega \rangle$. An algorithm for finding it is:

Algorithm 3.59

$$\begin{aligned} \Omega_0 &= \Omega \\ \Omega_k &= \Omega_{k-1} + \textstyle\sum_{i=1}^{q} L_{\tau_i} \Omega_{k-1} \end{aligned} \tag{3.48}$$

Lemma 3.60. *The codistributions Ω_k generated by Algorithm (3.59) are such that*

$$\Omega_k \subset \langle \tau_1, \ldots, \tau_q \big| \Omega \rangle$$

for all k. If there exists an integer k^* such that $\Omega_{k^*} = \Omega_{k^*+1}$, then

$$\Omega_{k^*} = \langle \tau_1, \ldots, \tau_q \mid \Omega \rangle .$$

Lemma 3.61. *Suppose Ω is spanned by a set $d\lambda_1, \ldots, d\lambda_s$ of exact covector fields and that $\langle \tau_1, \ldots, \tau_q \mid \Omega \rangle$ is nonsingular. Then $\langle \tau_1, \ldots, \tau_q \big| \Omega \rangle^\perp$ is involutive.*

These two algorithms have been implemented in the *ProPac* functons

1. `SmallestInvariantDistribution`, and
2. `LargestInvariantDistribution`.

Examples of their use will be deferred until Chapter 6.

3.5 Lie Groups and Algebras

The concepts of a linear vector space and its linear subspaces is central to the study of linear systems. As we have suggested, the appropriate generalization of the geometric structure of these objects is achieved by introducing manifolds, tangent spaces and distributions (and their integral submanifolds). However, linear vector spaces also have an important algebraic structure. By introducing an algebraic structure to manifolds we will make the transition: Manifolds $\rightarrow$ Lie groups and distributions $\rightarrow$ Lie (sub)algebras.

Lie groups and Lie algebras play an important role in mechanics and nonlinear control. In the following paragraphs we give a brief summary of the relevant concepts. Our goal here is simply to introduce essential terminology and notation and to provide some elementary examples. The interested reader should consult the many excellent references for more details.

Definition 3.62. *A group is a set G with a group operation (called multiplication) m: $G \times G \rightarrow G$, $m = g \cdot h$ for $g,h \in G$, having the following properties:*

1. *if $g,h \in G$, then $m = g \cdot h \in G$*
2. *associativity: if $g,h,k \in G$*

$$g \cdot (h \cdot k) = (g \cdot h) \cdot k$$

3. *identity element. There is an element $e \in G$ such that*

$$e \cdot g = g = g \cdot e \quad \forall g \in G$$

4. *inverse. For each $g \in G$ there is an inverse denoted g^{-1} with the property*

$$g \cdot g^{-1} = e = g^{-1} \cdot g$$

Example 3.63 (Groups).

1. $G = Z$, the set of integers with scalar addition the group operation:

$$e = 0, g^{-1} = -g, \forall g \in Z$$

2. $G = R$, the real numbers with scalar addition the group operation.
3. $G = R^+$, the positive real numbers with ordinary scalar multiplication as the group operation.
4. $G = GL(n,Q)$, the set of invertible $n \times n$ matrices with rational numbers for elements and matrix multiplication the group operation.
5. $G = GL(n,R)$, as above but the elements are real numbers.

Definition 3.64. *An r-parameter Lie group is a group G which is also an r-dimensional smooth manifold such that both the group operation, $m : G \times G \to G, m(g,h) = g \cdot h$ for $g,h \in G$, and the inversion, $i : G \to G, i(g) = g^{-1}, g \in G$, are smooth mappings between manifolds.*

Example 3.65 (Lie Groups).

1. $G = R$ with scalar addition as the group operation is a 1-parameter Lie group.
2. $GL(n,R)$ of invertible matrices with matrix multiplication the group operation is an n^2-parameter Lie group.
3. Let $G = R^r$ with vector addition the group operation. This is an r-parameter Lie group.
4. The set of nonzero complex numbers C^* form a two parameter Lie group under (complex) multiplication.
5. The unit circle $S^1 \subset C^*$ with multiplication induced from C^* is a one parameter Lie group. This is another characterization of $SO(2)$, the group of rotations in the plane.
6. The product $G \times H$ of two Lie groups is a Lie group with the product manifold structure and the direct product group structure, i.e., $(g_1,h_1) \cdot (g_2,h_2) = (g_1 \cdot g_2, h_1 \cdot h_2), g_i \in G, h_i \in H$.
7. Let K be the product manifold $Gl(nR) \times R^n$ and impose a group structure on K by defining group multiplication via $(A,v) \cdot (B,w) = (AB, v+w), A,B \in Gl(n,R)$ and $v,w \in R^n$. Then K is an n^2+n parameter Lie group. In fact K is the *group of affine motions of* R^n. If we identify the element (A,v) of K with the transformation $x \to Ax+v$ on R^n, then multiplication in K is the composition of affine motions.

Mappings between groups that preserve the algebraic structure of groups are of central importance:

Definition 3.66. *A map beteween Lie groups G and H, $\phi : G \to H$, is a (Lie group) homomorphism if ϕ is smooth and $\phi(a \cdot b) = \phi(a) \cdot \phi(b)$ for all $a,b \in G$. If, in addition, ϕ is a diffeomorphism, it is called an isomorphism.*

Lie groups which are isomorphic (connected by an isomorphism) are considered to be equivalent. Thus, for example, the multiplicative Lie group R^+ and the additive Lie group R are isomorphic and therefore equivalent. The isomorphism is $\phi(t) = e^t, t \in R$. Up to an isomorphism there are only two connected one-parameter Lie groups, R and $SO(2)$. Recall that N is a submanifold of M if there exists a parameter space $\bar{N}$ and a smooth one to one map $\phi : \bar{N} \to M$ such that $N = \phi(\bar{N}) \subset M$. Similarly, we can define Lie subgroups by requiring that the map ϕ respect the group operation.

Definition 3.67. *A Lie subgroup H of a Lie group G is a submanifold of G defined by $H = \phi(\bar{H}) \subset G$ in which the parameter space $\bar{H}$ is itself a Lie group and ϕ is a Lie group homomorphism.*

Example 3.68. If ω is any real number, the submanifold

$$H = \{ (t, \omega t) \mod 2\pi | \ t \in R\} \subset T^2$$

is a one parameter subgroup of the toroidal group $SO(2) \times SO(2)$. If ω is rational then H is isomorphic to the circle group $SO(2)$ and is closed, regular subgroup. If ω is irrational, then H is isomorphic to the Lie group R and is dense in the torus T^4. This Lie subgroup is not a regular submanifold of T^4.

The example illustrates that a Lie subgroup H of a Lie group G need not be a regular submanifold of G and hence a Lie subgroup need not be a Lie group in and of itself. However, the following is true.

Proposition 3.69. *If G is a Lie group, then the Lie subgroup $H = \phi(\bar{H})$ is a regular submanifold of G, and hence it is itself a Lie group, if and only if H is closed as a subset of G.*

Proof: (Warner [107]) ■

Thus, rather than prove that H is a regular submanifold of G, it is sufficient to show that H is a closed subset of G in order to assure that H is a regular Lie subgroup, i.e., a Lie group in its own right (Olver [89]). If G is a Lie group there is a set of special vector fields on G which form a finite dimensional vector space called the Lie algebra of G.

Definition 3.70. *Let G be a Lie group. For any $g \in G$, left and right translation (or multiplication) by g are, respectively, the diffeomorphisms $R_g : G \to G$ and $L_g : G \to G$ defined by*

$$R_g(h) = h \cdot g$$
$$L_g(h) = g \cdot h$$

R_g is a diffeomorphism with inverse $R_{g^{-1}} = (R_g)^{-1}$. Note that

$$R_{g^{-1}}(R_g(h)) = R_g(h)\cdot g^{-1} = h\cdot g\cdot g^{-1} = h$$

Similarly, $L_{g^{-1}} = (L_g)^{-1}$.

Definition 3.71. *A vector field v on G is called right-invariant if*

$$dR_g(v(h)) = v(R_g(h)) = v(h\cdot g)$$

for all $g,h \in G$. It is left invariant if

$$dL_g(v(h)) = v(L_g(h)) = v(g\cdot h)$$

If v,w are right (left) invariant vector fields then so is $av+bw$ where a,b are real numbers. Thus, the set of right (left) invariant vector fields forms a vector space. If v,w are right (left) invariant vector fields on G, then so is their Lie bracket $[v,w]$.

$$dR_g([v,w]) = [v,w]\cdot g = [v\cdot g, w\cdot g] = [dR_g(v), dR_g(w)] = [v,w]$$

Example 3.72 (Right and left invariant vector fields). Here are some examples of right and left invariant vector fields.

1. $G = R$. There is one right (or left) invariant vector field (up to a constant multiplier), $v = 1$ ($\mathbf{v} = \partial/\partial x$). To see this note that $R_y(x) = x+y$, for $x,y \in R$. Thus, the differential map is

   $$dR_y(v) = [\partial R_y(x)/\partial x]\, v = v,\ v \in TR_x$$

   so that right invariance requires $v(x) = v(x+y)$ for all $x,y \in R$,which implies $v(x) =$ constant. Similarly, $L_y(x) = y+x$ implies $dL_y(v) = v,\ v \in TR_x$ so we arrive at the same conclusion.

2. $G = R^+$ (the positive real numbers with ordinary scalar multiplication as the group operation). In this case right and left translation are $R_y(x) = xy$ and $L_y(x) = yx$, for $x,y \in R^+$. The corrsponding differential maps are $dR_y(v) = yv = dL_y(v)$ with $y \in R^+$ and $v \in TR_x^+$. Thus, right or left invariance requires that $yv(x) = v(yx)$ for all $x,y \in R^+$. The general solution to this relation is $v(x) = ax$, $a \in R$. Thus, the unique (up to scalar multiplication) right or left invariant vector field on R^+ is the linear vector field $v = x$.

3. $G = SO(2)$. The unique right or left invariant vector field is easily verified to be $v(\theta) = 1$ ($\mathbf{v} = \partial/\partial\theta$).

Lemma 3.73. *The set of right (left) invariant vector fields of a group G is isomorphic to the tangent space to G at its identity element e, TG_e.*

Proof: First we show that any right invariant vector field on G is determined by its value at the identity element e and then that any tangent vector to G at e determines a right invariant vector field. Any right invariant vector field $v(g)$ on G satisfies

$dR_g(v(h)) = v(R_g(h))$ for all $g,h \in G$. Since $R_g(e) = g$ for each $g \in G$, we set $h = e$ and obtain

$$v(g) = dR_g(v(e))$$

Conversely, any tangent vector to G at e determines a right invariant vector field by this same formula as we now show. First note that

$$dR_g\left(v(h)\right) = dR_g\left(dR_h\left(v(e)\right)\right) = d\left(R_g \circ R_h\right) v(e)$$

Since $R_g \cdot R_h(k) = k \cdot h \cdot g$ for any $k \in G$, this leads to

$$dR_g(v(h)) = dR_{h \cdot g}(v(e))$$

By assumption $v(h \cdot g) = dR_{h \cdot g}(v(e))$, so that we reach the conclusion that

$$dR_g(v(h)) = v(R_g(h))$$

Consequently, $v(g) = dR_g(v(e))$ is a right invariant vector field. A similar computation establishes the result for left invariant vector fields. ■

Definition 3.74. *The Lie algebra of a Lie group G, denoted* $\mathbf{g}$ *is the vector space of all left (or right) invariant vector fields on G.*

Since each left or right invariant vector field on G is uniquely associated with a vector tangent to G at e, we can identify the Lie algebra $\mathbf{g}$ of G with the tangent space to G at e, $\mathbf{g} \cong TG_e$. This implies that $\mathbf{g}$ is a vector space of the same dimension as the underlying Lie group. Moreover, as is convenient, we will view the Lie algebra of a Lie group either as the space of left or right invariant vector fields or as the tangent space to the group at the identity element.

As was done in the above proof, we will find it useful, from time to time, to contruct left and right invariant vector fields on a group G from an element of its Lie algebra $\mathbf{g}$ – viewed as the tangent space to G at the identity. This is accomplished using the formulas $v(g) = dL_g(\beta)$ or $v(g) = dR_g(\beta)$, $\beta \in \mathbf{g}$, respectively. We emphasize that in this application the differential maps take elements in $\mathbf{g} \cong TG_e \to TG_g$. In local coordinates the Jacobian is evaluated at the identity e.

Example 3.75 (Euclidean Space). Suppose $G = R^n$ with vector addition the group operation. Then $L_g : R^n \to R^n$ is given by $R_g(x) = g + x$ with $x, g \in R^n$. The differential map $dL_g : TR^n_x \to TR^n_{x+g}$ is the identity (for all x and in particular for the identity element $x = 0$), i.e.,

$$\frac{\partial L_g}{\partial x} = I \Rightarrow \tilde{v} = v,\ v \in TR^n_x,\ \tilde{v} \in TR^n_{g+x}$$

Any left invariant vector field $v(x)$ must satisfy $dL_g(v(x)) = v(g + x)$ for all x and g, which in this case reduces to $v(x) = v(g + x)$ for all $x, g \in R^n$. Thus, every left invariant vector field is constant in the direction of g for arbitrary g. Thus, the set of left invariant vector fields, and, hence, the Lie algebra of R^n, is the set of constant vector fields.

Example 3.76 (Rotation Group and its Lie Algebra). Let $SO(3)$ denote the group of rotations of three-dimensional euclidean space. $SO(3)$ represents the configuraton space of a rigid body free to rotate about a fixed point. An element, which we denote by L is a rotation matrix (a real 3×3 matrix with $L^TL = I$). A motion of the rigid body corresponds to a path $L(t)$ in the group. The velocity $\dot{L}(t)$ is a tangent vector to the group at the point $L(t) \in SO(3)$. Recall that left and right translation on $SO(3)$ are the functions $L_A(L) = AL$ and $R_A(L) = LA$, $\forall A, L \in SO(3)$. We can easily compute the differential maps associated with these functions. Consider left translation and suppose $g(t)$ is a path in $SO(3)$ passing through the point L at $t = 0$. Its image under left translation by A is $\bar{g}(t) = Ag(t)$, so that $\tilde{g}(t) = A\dot{g}(t)$. $dL_A : TSO(3)_L \to TSO(3)_{AL}$ is $dL_A(L) = AL$. Similarly, $dR_A(L) = LA$.

We can translate the velocity vector to the group identity element by left or right translation, thereby identifying two different elements in the Lie algebra $\mathbf{so}(3)$:

$$\omega_b = dL_{L^T}\dot{L} = L^T\dot{L},\ \omega_s = dR_{L^T}\dot{L} = \dot{L}L^T$$

Since, $L^TL = I$ implies $\dot{L}^TL + L^T\dot{L} = 0$, ω_b and ω_s are skew-symmetric matrices. Moreover, as we will see in the next chapter, ω_b is simply the angular velocity (as observed) in the body and ω_s is the angular velocity (as observed) in space.

The definition of a Lie algebra need not be based on the a priori reference to an underlying Lie group. In general

Definition 3.77. *A Lie algebra is a vector space* $\mathbf{g}$ *together with a bilinear operation*

$$[\cdot,\cdot] : \mathbf{g}\times\mathbf{g} \to \mathbf{g}$$

called the Lie bracket for $\mathbf{g}$*, satisfying the following axioms*

1. *bilinearity*
$$[av_1 + bv_2, w] = a[v_1, w] + b[v_2, w]$$
$$[v, aw_1 + bw_2] = a[v, w_1] + b[v, w_2]$$
for $a, b \in R$ *and* $v, v_1, v_2, w, w_1, w_2 \in \mathbf{g}$.
2. *skew-symmetry*
$$[v, w] = -[w, v]$$
3. *Jacobi identity*
$$[u,[v,w]] + [w,[u,v]] + [v,[w,u]] = 0$$
for all $u, v, w \in \mathbf{g}$.

Notice that in our definition of a Lie algebra $\mathbf{g}$ of a Lie group G, the required bilinear operation occurs naturally and is, in fact, the ordinary Lie bracket of vector fields. The Lie algebra $\mathbf{g}$ of the Lie group G consists of the left invariant vector fields on

G. But it has been shown that the Lie bracket of two left invariant vector fields is a left invariant vector field so that the ordinary Lie bracket of vector fields provides a mapping $[\cdot,\cdot] : \mathbf{g} \times \mathbf{g} \to \mathbf{g}$. Moreover, it satisfies the required properties 1), 2) and 3) of the above definition.

Example 3.78 (Lie algebras).

1. The vector space of smooth vector fields on a manifold M forms a Lie algebra under the Lie bracket operation on vector fields.
2. The vector space $\mathbf{gl}(n,R)$ of all $n \times n$ real matrices forms a Lie algebra if we define $[A,B] = AB - BA$.
3. R^3 with the vector cross product as the Lie bracket is a Lie algebra.

Definition 3.79. *A Lie subalgebra* $\mathbf{h}$ *of a Lie algebra* $\mathbf{g}$ *is a (vector) subspace of* $\mathbf{g}$ *which is closed under the Lie bracket, i.e.,* $[v,w] \in \mathbf{h}$ *whenever* $v,w \in \mathbf{h}$.

If H is a Lie subgroup of a Lie group G, any left invariant vector field on H can be extended to a left invariant vector field on G (set $v(g) = dL_g(v(e))$, $g \in G$ and where $v(e) \in TH_e \subset TG_e$ defines the left invariant vector field on H). In this way the Lie algebra $\mathbf{h}$ of H is realized as a subalgebra of $\mathbf{g}$.

Proposition 3.80. *Let G be a Lie group with Lie algebra $\mathbf{g}$. If $H \subset G$ is a Lie subgroup, its Lie algebra $\mathbf{h}$ is a subalgebra of $\mathbf{g}$. Conversely, if $\mathbf{h}$ is any s-dimensional subalgebra of $\mathbf{g}$, there is a unique , connected subgroup H of G with Lie subalgebra $\mathbf{h}$.*

Proof: We outline the basic idea of the proof. If H is a Lie subgroup with of the Lie group G, then there is a common identity element e and TH_e is a subspace of TG_e. Consequently, $\mathbf{h}$ is a subalgebra of $\mathbf{g}$. To prove the converse, note that any basis of $\mathbf{h}$, say $\{v_1,\ldots,v_s\}$, defines a distribution on G. Since $\mathbf{h}$ is a subalgebra, each

$$[v_i,v_j] \in \mathbf{h} \Rightarrow [v_i,v_j] \in \text{span}\{v_1,\ldots,v_s\}$$

and therefore $\mathbf{h}$ defines an involutive distribution on G. Moreover, at each point $g \in G$, $\{v_1,\ldots,v_s\}$ is a linearly independent set of tangent vectors. Thus, the Frobenius theorem implies that there is an s-dimensional integral submanifold of this distribution passing through every point $g \in G$ and through the identity element e in particular. This is the Lie subgroup H corresponding to $\mathbf{h}$. It remains only to verify that the manifold so defined is indeed a group. ■

Example 3.81 (Lie subalgebras).

1. Recall that $Gl(n,R) = Gl(n)$ is the set of invertible $n \times n$ matrices with real elements and that it is a group under matrix multiplication. In fact it is a Lie group of dimension n^2 The Lie algebra of $Gl(n)$ is denoted $\mathbf{gl}(n)$. Let H be a subgroup of $Gl(n)$. We wish to characterize its Lie algebra $\mathbf{h}$ which a subalgebra of $\mathbf{gl}(n)$. We can find $h \cong TH_e$ by looking at the one dimensional subgroups which are contained in H. That is, suppose $a \in \mathbf{gl}(n) \cong TG_e$ so that a is a (right invariant) vector field on G and the maximal integral manifold of a passing through e is $\{e^{\varepsilon a},\ \varepsilon \in R\}$. Thus,

$$\mathbf{h} = \{\, a \in \mathbf{gl}(n) |\ e^{\varepsilon a} \in H\ \forall \varepsilon \in R\}$$

2. Recall the group of orthogonal matrices $O(n) = \left\{ X \in Gl(n) | X^T X = I \right\}$. This group is a subgroup of $Gl(n)$ with $\dim O(n) = n(n-1)/2$. Since $\mathbf{gl}(n) \cong TG_e$ we may view the elements of $\mathbf{gl}(n)$ as $n \times n$ matrices and its Lie bracket is then matrix commutation. Let the matrix $A \in \mathbf{gl}(n)$, then $A \in \mathbf{h}$ if and only if

$$\left(e^{\varepsilon A}\right)^T \left(e^{\varepsilon A}\right) = I$$

   and this is satisfied if and only if $A^T + A = 0$, i.e., A is antisymmetric.

3. Another subgroup of $Gl(n)$ is the special orthogonal group

$$SO(n) = \{\, X \in Gl(n) | \det X = 1\}$$

   This Lie group is also of dimension $n(n-1)/2$. It is one of the components of $O(n)$. In fact, it is the connected component of the identity. The Lie algebra of $SO(n)$ is the same as the Lie algebra of $O(n)$ (they have the same tangent space at e): $\mathbf{so}(n) =$ real skew symmetric $n \times n$ matrices

Remark 3.82 (Properties of Lie algebras). In the following paragraphs, we briefly summarize some useful terminology and elementary properties associated with Lie algebras.

1. An algebra is the *direct sum* of two algebras $\mathbf{a} + \mathbf{b}$ if $\mathbf{g} = \mathbf{a} + \mathbf{b}$ is a vector space and $[\mathbf{a}, \mathbf{b}] = 0$. We then write $\mathbf{g} = \mathbf{a} \oplus \mathbf{b}$. It is the *semi-direct* sum if $[\mathbf{a}, \mathbf{b}] \subset \mathbf{a}$, i.e., if $[w, v] \in \mathbf{a}$ whenever $w \in \mathbf{a}$, $v \in \mathbf{b}$. We then write $\mathbf{g} = \mathbf{a} \oplus_s \mathbf{b}$.

2. A subalgebra $\mathbf{h}$ is an *ideal* of $\mathbf{g}$ if $[\mathbf{h}, \mathbf{g}] \subset \mathbf{h}$. If $\mathbf{g} = \mathbf{a} \oplus_s \mathbf{b}$, then $\mathbf{a}$ is an ideal of $\mathbf{g}$. If $\mathbf{g} = \mathbf{a}_1 \oplus a_2 \oplus \cdots \oplus \mathbf{a}_n$, then each $\mathbf{a}_i$ is an ideal of $\mathbf{g}$.

3. If H is a subgroup of G, we define the following equivalence relation. For $a, b \in G$,

$$a \equiv b (\bmod H), \quad if\ a^{-1} b \in H$$

   The equivalence classes under this relation are called the *left cosets* of H and are denoted aH. Similarly, if we define the relation

$$a \equiv b (\bmod H), \quad if\ ab^{-1} \in H$$

The equivalence classes under this relation are called the *right cosets* of H and are denoted Ha. H is *normal* if $aH = Ha$ for all $a \in G$.

4. If H is normal, the cosets of H form a group with group operation

$$(aH) \cdot (bH) = a \cdot bH$$

This group is called the *quotient group* and is denoted G/H. Consider the example in Figure (3.9).

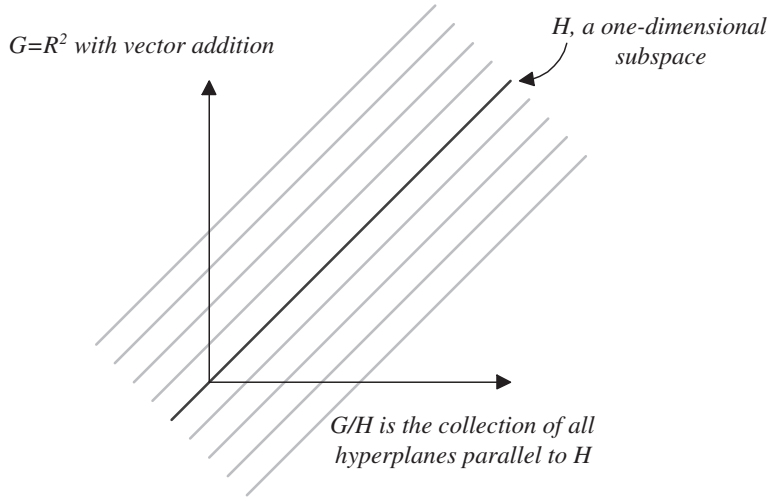

Fig. 3.9: The quotient group associated with the group $G = R^2$ and its subgroup H, a linear subspace of R^2, is the collection of all translations of H.

5. Suppose $\mathbf{h}$ is a subalgebra of $\mathbf{g}$. For any $w \in \mathbf{g}$, define the equivalence class of w in $\mathbf{g}$ by the relation

$$w \equiv v(\bmod h), \quad w - v \in \mathbf{h}$$

The equivalence class of w so defined is denoted $w + \mathbf{h}$. These equivalence classes form a Lie algebra if $\mathbf{h}$ is an ideal of $\mathbf{g}$. We can define a Lie bracket on the classes

$$[w + \mathbf{h}, v + \mathbf{h}] := [w, v] + \mathbf{h}$$

The set of equivalence classes now forms a new algebra called the *quotient algebra* , denoted $\mathbf{g}/\mathbf{h}$.

3.6 Introduction to Differential Forms

In this section we give a brief overview of differential forms. Differential forms will prove to be a useful conceptual and computational tool in geometric control theory. More details can be found in many texts including [89]. The implementation in *ProPac* of the computations described here follows that of Bonanos [13].

3.6.1 Differential Forms

Let M be a smooth manifold and TM_x the tangent space at $x \in M$. A differential k-form is a linear antisymmetric function

$$\omega : \underbrace{TM_x \times \cdots \times TM_x}_{k \text{ copies}} = TM_x^k \to R$$

Thus, we have

1. linearity

$$\omega(v_1,..,\lambda_1 v_i + \lambda_2 \hat{v}_i,..,v_k) \;=\; \lambda_1 \omega(v_1,..,v_i,..,v_k) \;+\; \lambda_2 \omega(v_1,..,\hat{v}_i,..,v_k)$$

   for each $1 \le i \le k$ and $\lambda_1, \lambda_2 \in R$ and

2. antisymmetry

$$\omega(v_{i_1},\ldots,v_{i_k}) = (-1)^{\nu}\omega(v_1,\ldots,v_k)$$

   where

$$\nu = \begin{cases} 0, \textit{ even permutation} \\ 1, \textit{ odd permutation} \end{cases}$$

1-forms

If $(x_1,\ldots,x_n)$ are local coordinates, then TM_x has basis $\{\partial/\partial x_1,\ldots,\partial/\partial x_n\}$. The cotangent space has a dual basis usually denoted $\{dx_1,\ldots,dx_m\}$, with $\langle dx_i, \partial/\partial x_j \rangle = \delta_{ij}$. A differential 1-form is an element in the dual space, i.e., it is a covector field, and has the local coordinate representation

$$\omega = h_1(x)dx_1 + \cdots + h_n(x)dx_n$$

For any vector field $v = \sum \xi_i(x)\partial/\partial x_i$ we have, by definition,

$$\omega(v) = \sum_{i=1}^{n} h_i(x)\xi_i(x) = \langle \omega, v \rangle$$

Note that a real valued function $f(x)$ has associated with it the differential

$$df = \sum_{i=1}^{n} \frac{\partial f}{\partial x_i} dx_i$$

which is itself a 1-form. Thus, it operates on elements of TM_x, and we can write

$$d\ f(v) = v(f)$$

The following notation is equivalent

$$\mathrm{d}f(v) = \langle \mathrm{d}f, v \rangle = L_v(f)$$

3.6.2 The Exterior or Wedge Product

Let $\omega_1, \ldots, \omega_k$ be a collection of 1-forms. We can construct a differential k-form $\omega_1 \wedge \omega_2 \wedge \ldots \wedge \omega_k$ via the formula

$$\omega_1 \wedge \ldots \wedge \omega_k(v_1, \ldots, v_k) = \det[\omega_i(v_j)] \tag{3.49}$$

This is the *wedge product* (or *exterior product*). The wedge product is multilinear and antisymmetric.

1. linearity

$$\omega_1 \wedge \cdots \wedge \left(\alpha \omega_i^{\alpha} + \beta \omega_i^{\beta}\right) \wedge \cdots \wedge \omega_k = \alpha \omega_1 \wedge \cdots \wedge \omega_i^{\alpha} \wedge \cdots \wedge \omega + \beta \omega_1 \wedge \cdots \wedge \omega_i^{\beta} \wedge \cdots \wedge \omega$$

2. asymmetry

$$\omega_{i_1} \wedge \cdots \wedge \omega_{i_k} = (-1)^{\nu} \omega_1 \wedge \cdots \wedge \omega_k$$

where, again

$$\nu = \begin{cases} 0, \textit{ even permutation} \\ 1, \textit{ odd permutation} \end{cases}$$

Every differential k-form may be written

$$\omega^k = \sum_{i_1 < \cdots < i_k} a_{i_1 \cdots i_k}(x) \mathrm{d}x_{i_1} \wedge \cdots \wedge \mathrm{d}x_{i_k}$$

For any smooth k-form on M we can define a $k+1$-form called its differential or exterior derivative. Its differential or exterior derivative is

$$\mathrm{d}\omega^k = \sum_{i_1 < \cdots < i_k} \mathrm{d}a_{i_1 \cdots i_k}(x) \mathrm{d}x_{i_1} \wedge \cdots \wedge \mathrm{d}x_{i_k} = \sum_{i_1 < \cdots < i_k, j} \frac{\partial a_{i_1 \cdots i_k}(x)}{\partial x_j} \mathrm{d}x_{i_1} \wedge \cdots \wedge \mathrm{d}x_{i_k}$$

Example 3.83 (Wedge Product Examples). Let us consider some basic calculations with one and two forms.

1. In the case of a 1-form $\omega = \sum a_i(x)\mathrm{d}x_i$, we have the differential

$$\mathrm{d}\omega = \sum\nolimits_i \mathrm{d}a_i \wedge \mathrm{d}x_i = \sum\nolimits_{i,j} \frac{\partial a_i}{\partial x_j}\mathrm{d}x_j \wedge \mathrm{d}x_i$$

2. Let $v = \sum v_i(x)\partial\big/\partial x_i$, $w = \sum w_i(x)\partial\big/\partial x_i$ be smooth vector fields and consider $\mathrm{d}x_i$ as a 1-form so that

   a) $\mathrm{d}x_i(v) = v_i, \quad \mathrm{d}x_i(w) = w_i$

   b) $\mathrm{d}x_i \wedge \mathrm{d}x_j(v,w) = \begin{vmatrix} \mathrm{d}x_i(v) & \mathrm{d}x_i(w) \\ \mathrm{d}x_j(v) & \mathrm{d}x_j(w) \end{vmatrix} = v_i w_j - w_i v_j$

   c) $\mathrm{d}x_i \wedge \mathrm{d}x_j(v) = \begin{vmatrix} v_i & \mathrm{d}x_i \\ v_j & \mathrm{d}x_j \end{vmatrix} = v_i \mathrm{d}x_j - v_j \mathrm{d}x_i$

3. Given vector fields as in 2., we can evaluate the 2-form of 1.

$$\mathrm{d}\omega(v,w) = \sum\nolimits_{i,j} \frac{\partial a_i}{\partial x_j}\,(v_i w_j - w_i v_j)$$

3.6.3 The Interior Product or Contraction

Suppose that $\omega(v_1,\ldots,v_k)$ is a differential k-form and v a smooth vector field, then we define a $(k-1)$-form $i_v(\omega)$ called the *interior product* or *contraction*

$$i_v(\omega) = \omega(v, v_1, \ldots, v_{k-1})$$

for every set of vector fields $v_1,\ldots,v_{k-1}$. Notice that the inner product is bilinear (linear in each of its two arguments). Thus, it is sufficient to determine it for basis elements. Recall that the basis elements for k-forms are $dx_{j_1} \wedge \ldots \wedge dx_{j_k}$. Consequently, we compute

$$i_{\partial/\partial x_i}(\mathrm{d}x_{j_1} \wedge \ldots \wedge \mathrm{d}x_{j_k}) = \begin{cases} (-1)^{\kappa-1}\mathrm{d}x_{j_1} \wedge \ldots \wedge \mathrm{d}x_{j_{\kappa-1}} \wedge \mathrm{d}x_{j_{\kappa+1}} \wedge \ldots \wedge \mathrm{d}x_{j_k} & i = j_\kappa \\ 0 & i \neq j_\kappa \ \forall \kappa \end{cases} \tag{3.50}$$

Example 3.84 (Contraction Examples). Here are some elementary calculations (from Olver [89])

1. $i_{\partial/\partial x}(\mathrm{d}x \wedge \mathrm{d}y) = \mathrm{d}y$
2. $i_{\partial/\partial x}(\mathrm{d}z \wedge \mathrm{d}x) = -\mathrm{d}z$
3. $i_{\partial/\partial x}(\mathrm{d}y \wedge \mathrm{d}z) = 0$

4. Consider the 2-form on R^3

$$\omega = \alpha(x,y,z)\mathrm{d}y\wedge\mathrm{d}z+\beta(x,y,z)\mathrm{d}z\wedge\mathrm{d}x+\gamma(x,y,z)\mathrm{d}x\wedge\mathrm{d}y$$

and the vector field

$$v=\xi(x,y,z)\frac{\partial}{\partial x}+\eta(x,y,z)\frac{\partial}{\partial y}+\zeta(x,y,z)\frac{\partial}{\partial z}$$

Then compute

$$\begin{aligned} i_v(\omega) &= i_{\xi\partial/\partial x}(\omega)+i_{\eta\partial/\partial y}(\omega)+i_{\zeta\partial/\partial z}(\omega)\\ &= -\xi\beta\mathrm{d}z+\xi\gamma\mathrm{d}y+\eta\alpha\mathrm{d}z-\eta\gamma\mathrm{d}x-\zeta\alpha\mathrm{d}y+\zeta\beta\mathrm{d}x\\ &= (\zeta\beta-\eta\gamma)\,\mathrm{d}x+(\xi\gamma-\zeta\alpha)\,\mathrm{d}y+(\eta\alpha-\xi\beta)\,\mathrm{d}z \end{aligned}$$

Consider the wedge product of a k-form ω and a p-form θ. The formula (3.50) can be used to prove the following identity:

$$i_v(\omega\wedge\theta)=i_v(\omega)\wedge\theta+(-1)^k\omega\wedge i_v(\theta) \tag{3.51}$$

3.6.4 Lie Derivative of Forms

Proposition 3.85. *Let ω be a differential form and v a vector field on the manifold M. Then*

$$Ł_v(\omega)=\mathrm{d}i_v(\omega)+i_v(\mathrm{d}\omega)$$

Proof: (Olver [89], p64). See also Definition (3.32). ■

3.7 Problems

Problem 3.86. Consider the set of affine vector fields $\mathscr{A}$ of the form $f(x)=Ax+b$, $A\in R^{n\times n}$, $b\in R^n$. Show that $\mathscr{A}$ is closed under the Lie bracket operation, i.e., $[f,g]\in\mathscr{A}$ for all $f,g\in\mathscr{A}$.

Problem 3.87. Determine the smallest distribution that is invariant with respect to the vector fields

$$\tau_1(x)=\begin{bmatrix}1\\x_1\end{bmatrix},\ \tau_2(x)=\begin{bmatrix}x_2\\x_1\end{bmatrix}$$

and contains the distribution $\Delta(x)=\mathrm{span}\{\tau_1(x)\}$, i.e., $\langle\tau_1,\tau_2\,|\Delta\,\rangle$.

4

Bifurcation Analaysis

4.1 Introduction

Part II

Analytical Mechanics

5

Kinematics of Tree Structures

5.1 Introduction

Multibody mechanical systems often assume the structure of a chain or a tree. Even when they do not (i. e., a system containing a closed loop), it is typically convenient to build a model for an underlying tree (by breaking the loop) and then to add the necessary constraints (to re-establish the loop). In this chapter we focus on the kinematics of tree structures. The next chapter will supplement the present discussion to accommodate constraints.

The systems we consider are composed of rigid bodies[1] connected together by joints. Each joint has a set of velocity variables and configuration parameters[2] equal to the number of degrees of freedom of the joint. The set of all joint velocities defines the (quasi-) velocity vector, p, for the system and the set of all joint parameters comprise the system generalized coordinate vector, q. Our main goal is to assemble the key kinematic equation that relates the quasi-velocities to the coordinate velocities:

$$\dot{q} = V(q)p \tag{5.1}$$

In addition, we wish to establish formulas that allow the computation of the position, orientation and/or velocity of reference frames at various locations in the system.

We begin in the next section with an analysis of individual joints. The goal is to characterize the motion of an outboard reference frame with respect to an inboard reference frame. Joints are normally defined in terms of constraints on the relative velocity across the joint. Formulas will be derived that provide a natural parameterization of the joint configuraton and all other kinematic quantities. In Section 3 we turn to the kinematics of chain and tree structures. Various formulas are derived

[1] We do not discus flexible bodies in this book. However, the methods described here apply with some additional constructs that are implemented in *ProPac*. See *ProPac* help for more information.

[2] At least locally.

that allow the complete characterizaton of chain and tree configuration and velocities in terms of individual joint quantities. Computer implementation of the required calculations are also described.

5.2 Kinematics of Joints

A joint constrains the relative motion between two bodies. In this section we develop a mathematical desription of joints that is convenient for assembling multibody dynamical models.

5.2.1 The Geometry of Joints

We designate two rigid bodies and reference frames fixed within them *s* (space) and *b* (body). The configuration space M of relative motion between two unconstrained rigid bodies is the Special Euclidean group $SE(3)$ consisting of all rotations and translations of R^3. $SE(3)$ is the semi–direct product of the rotation group $SO(3)$ with the vector group R^3, [89]. An element in $SE(3)$ may be represented by a matrix

$$X = \begin{bmatrix} L^T & R \\ 0 & 1 \end{bmatrix}, \; L \in SO(3), \; R \in R^3 \tag{5.2}$$

Consider a space reference frame XYZ and a body reference frame xyz. The configuration of the body frame relative to the space frame is X as defined in (5.2). Recall that location of a point at position r in the body has location $\mathbf{R}$ in the space frame with

$$\mathbf{R} = R + L^T r$$

as illustrated in Figure 5.1. The inverse of X is

$$X^{-1} = \begin{bmatrix} L & -R \\ 0 & 1 \end{bmatrix} \tag{5.3}$$

Two successive relative motions X_1 and X_2 combine to yield

$$X = X_2 X_1 = \begin{bmatrix} L_2^T & R_2 \\ 0 & 1 \end{bmatrix} \begin{bmatrix} L_1^T & R_1 \\ 0 & 1 \end{bmatrix} = \begin{bmatrix} L_2^T L_1^T & L_2^T R_1 + R_2 \\ 0 & 1 \end{bmatrix}$$

as illustrated in Figure (5.2).

In general geometric terms, a joint is characterized by a relation on the tangent bundle $TSE(3)$. Such a relation is usually expressed in local coordinates by an equation of the type (see, for example [2,3])

$$f(q, \dot{q}) = 0 \tag{5.4}$$

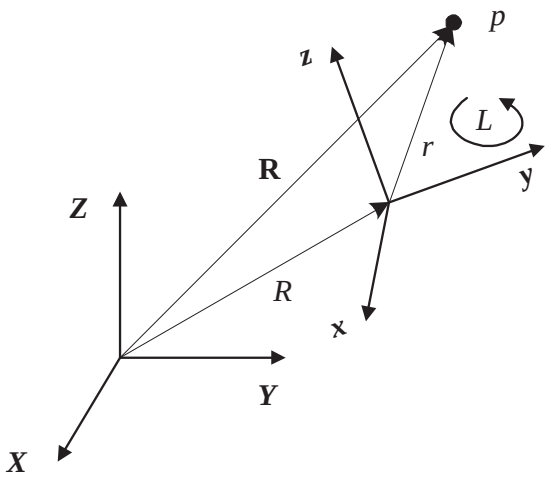

Fig. 5.1: Point p can be represented in either the body frame or space frame.

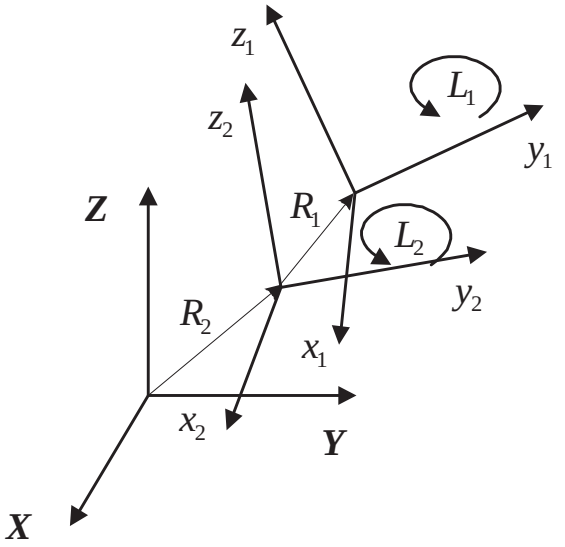

Fig. 5.2: Two successive rigid body motions characterized by configuration matrices X_1, X_2 leave the body in configuration $X = X_2X_1$ with respect to the space frame.

where $f : TSE(3) \to R^k$. Natural constraints almost always occur on one of two forms:

$$f(q) = 0 \tag{5.5}$$

in which only the coordinates appear, or

$$F(q)\dot{q} = 0 \tag{5.6}$$

in which the coordinate velocities appear linearly. Equation (5.5) defines a submanifold of $SE(3)$ which identifies admissible configurations. Constraints of this from are called geometric constraints because they restrict the relative geometry of the two bodies. Constraints of the form (5.6) are called kinematic because they restrict the relative velocity of two bodies. The geometric meaning of (5.6) is highlighted by restating it as

$$\dot{q} \in \Delta(q) \tag{5.7}$$

where $\Delta(q)$ is a distribution on $SE(3)$ defined as $\Delta(q) = \mathrm{Ker}\,[F(q)]$. If the constraint is of the form of (5.6), then it is holonomic [2, 3] if the distribution $\Delta(q)$ is integrable. General conditions for integrability of a distribution are well known and given by the Frobenius theorem. Recall, from Chapter 3, that local coordinates on TM constitute the pair (q,v) with q local coordinates on M and v local coordinates on TM_x. Thus, in general, TM is isomorphic to $M \times \mathbf{g}$, where $\mathbf{g}$ denotes the Lie algebra associated with M, it is possible to characterize joint constraints which involve velocities (i.e., (5.6)) by a smooth map $f : SE(3) \times \mathbf{se}(3) \to R^k$ so that the joint is defined by equations of the form:

$$A(q)p = 0, \tag{5.8}$$

where $p \in \mathbf{se}(3)$ and $A(q)$ is a linear operator on $\mathbf{se}(3)$. The geometric meaning of (5.8) is

$$p \in \mathrm{Ker}\,A(q) \tag{5.9}$$

Equation (5.8) is a more general and will prove to be a more convenient characterization of kinematic joints than (5.6).

Let us take $M = SE(3)$ and consider the formal representation of objects belonging to its Lie algebra $\mathbf{g} = se(3)$. We can use either right or left translations on M to define $\mathbf{g}$. We choose left, so that

$$p := X^{-1}\dot{X} = \begin{bmatrix} L & -R \\ 0 & 1 \end{bmatrix} \begin{bmatrix} \dot{L}^T & \dot{R} \\ 0 & 0 \end{bmatrix} = \begin{bmatrix} L\dot{L}^T & L\dot{R} \\ 0 & 0 \end{bmatrix} = \begin{bmatrix} \tilde{\omega}_b & v_b \\ 0 & 0 \end{bmatrix} \tag{5.10}$$

Notice that in (5.10) we use the conventional notation, by which any vector $a \in R^3$ is converted into a skew-symmetric matrix $\tilde{a}(a)$:

$$\tilde{a}(a) = \begin{bmatrix} 0 & -a_3 & a_2 \\ a_3 & 0 & -a_1 \\ -a_2 & a_1 & 0 \end{bmatrix}$$

Thus, we see that $\mathbf{se}(3)$ is isomorphic to R^6 and we can consider an element p of $\mathbf{se}(3)$ to be a pair of objects– body angular velocity and linear velocity–(ω_b, v_b) or, equivalently, $(\tilde{\omega}_b, v_b)$. When doing formal group calculations however, we use the matrix form shown in (5.10).

5.2.2 Simple Kinematic Joints

Kinematic joints are joints that are described by velocity constraints such as (5.6) or (5.8). They are simple if the motion axes are fixed in (at least) one of the bodies– in which case the constraint can be formulated so that A is a constant (independent of the configuration). For lack of a general terminology we call such joints *simple kinematic joints*. We now focus on simple kinematic joints. It is convenient to define a matrix H whose columns form a basis for $\mathrm{Ker}\,A$, [47, 48, 91], so that

$$\mathrm{Ker}\,A = \mathrm{Im}\,H, \quad H \text{ is of full rank } r = \dim \mathrm{Ker}\,A. \tag{5.11}$$

Solutions of (5.8) are of the form

$$p = H\beta,\ \beta \in R^r \tag{5.12}$$

β represents the joint quasi–velocity and r is the number of velocity degrees of freedom. H is called the joint map matrix .

Examples of Joint Map Matrices of Simple Joints - H

$\begin{bmatrix} 0 \\ 0 \\ 1 \\ 0 \\ 0 \\ 0 \end{bmatrix}$	$\begin{bmatrix} 0 & 0 \\ 1 & 0 \\ 0 & 1 \\ 0 & 0 \\ 0 & 0 \\ 0 & 0 \end{bmatrix}$	$\begin{bmatrix} 0 \\ 0 \\ 0 \\ 0 \\ 0 \\ 1 \end{bmatrix}$	$\begin{bmatrix} 0 \\ 0 \\ 1 \\ 0 \\ 0 \\ s \end{bmatrix}$	$\begin{bmatrix} 0 & 0 \\ 0 & 0 \\ 1 & 0 \\ 0 & 0 \\ 0 & 0 \\ 0 & 1 \end{bmatrix}$
$1\,dof$	$2\,dof$	$1\,dof$	$1\,dof$	$2\,dof$
revolute	*universal*	*prismatic*	*screw*	*cylindrical*
$body\,z-axis$	$body\,y,z-axis$	$body\,z-axis$	$body\,z-axis$	$body\,z-axis$

The joint configuration is defined, in general, by the differential equations

$$\dot{X} = Xp \tag{5.13}$$

or, equivalently

$$\dot{L} = -\tilde{\omega}_b L,\ \dot{R} = L^T v_b \tag{5.14}$$

It is easy enough to replace $\tilde{\omega}_b$ and v_b by β using (5.12). Let H be partitioned so that H_1 contains the first 3 rows and H_2 the second three rows of H, then

$$\dot{X} = X \begin{bmatrix} \widetilde{H_1\beta} & H_2\beta \\ 0 & 0 \end{bmatrix} \tag{5.15}$$

or

$$\dot{L} = -(\widetilde{H_1\beta})L,\ \dot{R} = L^T H_2 \beta. \tag{5.16}$$

The joint kinematics are defined by (5.15) or (5.16). Given the quasi–velocities β, (5.15) and (5.16) can be integrated to provide the relative translational position and rotation matrix of the two bodies. However, this representation may not be the most informative and it certainly provides more information than necessary since it locates the relative position in the six dimensional group $SE(3)$ instead of the relevant subgroup. If the constraint is holonomic, precisely r dimensions would suffice. First, we provide a result for single degree of freedom joints.

Proposition 5.1. *Consider a simple single degree of freedom joint with joint map matrix $H = h \in R^6$. Then the joint configuration matrix can be parameterized by a parameter $\varepsilon \in R$ in the form:*

$$X(\varepsilon) = \begin{bmatrix} L^T(\varepsilon) & R(\varepsilon) \\ 0 & 1 \end{bmatrix} \tag{5.17}$$

with

$$L(\varepsilon) = e^{-\tilde{h}_1 \varepsilon},\ R(\varepsilon) = \int_0^{\varepsilon} e^{-\tilde{h}_1 \sigma} h_2 d\sigma \tag{5.18}$$

Proof: [60]. Consider a general one degree of freedom joint in which H is composed of the single column h. Then the distribution $\Delta(X)$ on $SE(3)$ consists of the single vector field

$$\begin{bmatrix} L^T \tilde{h}_1 & L^T h_2 \\ 0 & 0 \end{bmatrix}$$

This is an integrable distribution and we seek the integral manifold which passes through the point

$$X_0 = \begin{bmatrix} I & 0 \\ 0 & 1 \end{bmatrix}$$

The one dimensional manifold we seek can be characterized (at least locally) by a map $\xi : R \to SE(3)$. Let $\varepsilon \in R$ be the parameter. Then we seek a solution to the differential equation

$$\frac{d\xi}{d\varepsilon} = \begin{bmatrix} L^T \tilde{h}_1 & L^T h_2 \\ 0 & 0 \end{bmatrix},\ \xi(0) = X_0 \tag{5.19}$$

or equivalently

$$\frac{dL}{d\varepsilon} = -\tilde{h}_1 L,\ L(0) = I \tag{5.20}$$

and

$$\frac{dR}{d\varepsilon} = L^T h_2,\ R(0) = 0 \tag{5.21}$$

so that the conclusion follows. ■

Note that if H is composed of several columns, say r columns, then we can consider this joint as a sequence of r single column joints and compute $X_i(\varepsilon_i)$ for each joint. Thus, we have

Corollary 5.2. *Consider a simple joint with r degrees of freedom and joint map matrix $H = [h_1 \dots h_r] \in R^{6\times r}$, then there is a parameter vector $\varepsilon \in R^r$ and the joint configuration matrix can be expressed in the form*

$$X(\varepsilon) = X_r(\varepsilon_r)\dots X_2(\varepsilon_2)X_1(\varepsilon_1) \tag{5.22}$$

where each $X_i(\varepsilon_i)$ is of the form of Proposition (5.1) with $h = h_i$.

We conclude that any simple kinematic joint is holonomic and, in fact, we have explicitly computed a local representation of its configuration manifold. Now, any motion results in a velocity $\dot{X} = Xp$. We wish to characterize this relation (locally) in terms of the rate of change of the joint parameters. In other words, we seek to relate $\dot{\varepsilon}$ and β. The following proposition does that.

Proposition 5.3. *Consider a simple joint with joint map matrix H, and suppose the joint is parameterized according to Proposition (5.1) and Corollary (5.2). Then the joint kinematic equation is*

$$\dot{\varepsilon} = V(\varepsilon)\beta \tag{5.23}$$

where $V(\varepsilon)$ is defined by the following algorithm:

1. *For $j = 1,..r$ define and*

$$U_j^T(\varepsilon_j,..,\varepsilon_1) = L_j^T(\varepsilon_j)U_{j-1}^T(\varepsilon_{j-1},..,\varepsilon_1),\ U_0^T = I \tag{5.24}$$

$$\Gamma_j(\varepsilon_j,..,\varepsilon_1) = L_j^T(\varepsilon_j)\Gamma_{j-1}(\varepsilon_{j-1},..,\varepsilon_1) + R_j,\ \Gamma_0 = 0 \tag{5.25}$$

2. *Define $B(\varepsilon)$*

$$B(\varepsilon) := \begin{bmatrix} b_{11} & \cdots & b_{1r} \\ b_{21} & \cdots & b_{2r} \end{bmatrix} \tag{5.26}$$

$$\tilde{b}_{1i} := U_{i-1}\tilde{h}_{i1}U_{i-1}^T \tag{5.27}$$

$$b_{2i} := U_{i-1}\tilde{h}_{i1}\Gamma_{i-1} + U_{i-1}h_{i2} \tag{5.28}$$

3. *Define $V(\varepsilon)$*

$$V(\varepsilon) := B^*(\varepsilon)H,\ B^*(\varepsilon) \text{ denotes a left inverse of } B(\varepsilon) \tag{5.29}$$

Proof: [60]. Any motion results in a velocity $\dot{X} = X\,p$ which implies

$$\dot{X} = \sum \frac{\partial X}{\partial \varepsilon_i}\dot{\varepsilon}_i = X(\varepsilon)p$$

Now, we directly compute

$$\sum_{i=1}^{r} \frac{\partial X}{\partial \varepsilon_i}\dot{\varepsilon}_i = \sum_{i=1}^{r} \left\{ X_r(\varepsilon_r)\cdots X_{i+1}(\varepsilon_{i+1}) \frac{dX_i}{d\varepsilon_i} X_{i-1}(\varepsilon_{i-1})\cdots X_1(\varepsilon_1)\dot{\varepsilon}_i \right\}$$

and premultiplying by X^{-1} we obtain

$$\sum_{i=1}^{r} \left\{ [X_{i-1}(\varepsilon_{i-1})\cdots X_1(\varepsilon_1)]^{-1} X_i^{-1}(\varepsilon_i) \frac{dX_i}{d\varepsilon_i} X_{i-1}(\varepsilon_{i-1})\cdots X_1(\varepsilon_1)\dot{\varepsilon}_i \right\} = p \qquad (5.30)$$

Notice that

$$X_i^{-1}(\varepsilon_i)\frac{dX_i}{d\varepsilon_i} = \begin{bmatrix} \tilde{h}_{i1} & h_{i2} \\ 0 & 0 \end{bmatrix}$$

Also, define $W_j(\varepsilon_j,\ldots,\varepsilon_1)$, $j = 1,..,r$ by the recursion

$$W_j(\varepsilon_j,\ldots,\varepsilon_1) := X_j(\varepsilon_j)W_{j-1}(\varepsilon_{j-1},\ldots,\varepsilon_1) \qquad (5.31)$$

$$W_1(\varepsilon_1) = X_1(\varepsilon_1) \qquad (5.32)$$

so that (5.30) can be written

$$\sum_{i=1}^{r} W_{i-1}^{-1} \begin{bmatrix} \tilde{h}_{i1} & h_{i2} \\ 0 & 0 \end{bmatrix} W_{i-1}\dot{\varepsilon}_i = p \qquad (5.33)$$

We can easily determine, from (5.31), (5.32), that W_j is of the form

$$W_j = \begin{bmatrix} U_j^T(\varepsilon_j,\ldots,\varepsilon_1) & \Gamma_j(\varepsilon_j,\ldots,\varepsilon_1) \\ 0 & 1 \end{bmatrix}$$

with

$$U_j^T(\varepsilon_j,\ldots,\varepsilon_1) = L_j^T(\varepsilon_j)U_{j-1}^T(\varepsilon_{j-1},\ldots,\varepsilon_1),\ U_0^T = I$$

$$\Gamma_j(\varepsilon_j,\ldots,\varepsilon_1) = L_j^T(\varepsilon_j)\Gamma_{j-1}(\varepsilon_{j-1},\ldots,\varepsilon_1),\ \Gamma_0 = 0$$

Thus, (5.33) reduces to

$$\sum_{i=1}^{r} \begin{bmatrix} U_{i-1}\tilde{h}_{i1}U_{i-1}^T & U_{i-1}\tilde{h}_{i1}\Gamma_{i-1} + U_{i-1}h_{i2} \\ 0 & 0 \end{bmatrix} \dot{\varepsilon}_i = p = \begin{bmatrix} \tilde{H_1\beta} & H_2\beta \\ 0 & 0 \end{bmatrix} \qquad (5.34)$$

Each expression of the form $U_{i-1}\tilde{h}_{i1}U_{i-1}^T$ is an antisymmetric matrix so we can define $b_{1i} \in R^3$ such that

$$\tilde{b}_{1i} = U_{i-1}\tilde{h}_{i1}U_{i-1}^T$$

We also define

$$b_{2I} = U_{i-1}\tilde{h}_{i1}\Gamma_{i-1} + U_{i-1}h_{i2}$$

Then (5.34) can be written

$$B(\varepsilon)\dot{\varepsilon} = H\beta,\ B(\varepsilon) = \begin{bmatrix} b_{11} & \cdots & b_{1r} \\ b_{21} & \cdots & b_{2r} \end{bmatrix}$$

Let B^* denote the left inverse of B-which exists on a neighborhood of $\varepsilon = 0$ because $B(0) = H$ is of full rank. Then

$$\dot{\varepsilon} = B^*(\varepsilon)H\beta = V(\varepsilon)\beta,\ V(\varepsilon) := B^*(\varepsilon)H$$

■

5.2.3 Compound Kinematic Joints

Not all joints are simple kinematic joints. But in many cases it is possible to define the action of a joint in terms of a sequence of simple kinematic joints. We call such joints *compound kinematic joints*. In general, a compound joint is defined as a joint which can be characterized as the relative motion of a sequence of p reference frames such that relative motion between two successive frames is defined by a simple kinematic joint. Then each of the p simple joints is characterized by a joint map matrix H_i with r_i columns, a quasi–velocity vector, β_i, of dimension r_i, a parameter vector, ε_i, of dimension r_i, and a kinematic matrix $\Gamma_i(\varepsilon_i)$. Thus if we define $\varepsilon := [\varepsilon_1 \dots \varepsilon_p]$ and $\beta := [\beta_1 \dots \beta_p]$ we have the joint kinematics defined by

$$\dot{\varepsilon} = diag\,[\Gamma_1(\varepsilon_1), \dots, \Gamma_p(\varepsilon_p)] \tag{5.35}$$

and, assuming the frames are indexed from the outermost, the overall joint configuration matrix is

$$X(\varepsilon) = X_p(\varepsilon_p) \cdots X_2(\varepsilon_2)X_1(\varepsilon_1) \tag{5.36}$$

Equations (5.35) and (5.36) provide the kinematic equations for compound joints. Figure (5.2) may be thought of as depicting a 2-frame compound joint.

Remark 5.4. In view of equation (5.36), a p-frame compound joint with joint map matrices H_i, $i = 1, \dots, p$, yields the same configuration manifold parameterization as a simple joint with joint map matrix $H = [H_1 \cdots H_p]$.

As we will see below, the overall joint map matrix is also required in order to assemble the dynamical equations for multibody systems. The required constructions are provided in the following proposition.

Proposition 5.5. *Consider a compound joint composed of p simple joints with joint map matrices* $H_i = [h_1^1 \cdots h_i^{r_i}] \in R^{6\times r_i}$, $i = 1, \dots, p$. *Suppose* $\varepsilon := [\varepsilon_1 \dots \varepsilon_p]$ *and*

$\beta = [\beta_1 \cdots \beta_p]$ are the corresponding simple joint parameters and quasi–velocities. Then the composite joint map matrix $H(\varepsilon) \in R^{6\times(r_1+\cdots+r_p)}$ is given by the following construction:

$$H(\varepsilon) := \begin{bmatrix} h_{11} & \cdots & h_{1r} \\ h_{21} & \cdots & h_{2r} \end{bmatrix} \tag{5.37}$$

where

$$\begin{aligned} \tilde{h}_{j1} &:= U_{i-1}\tilde{h}^j_{i1}U^T_{i-1} \\ h_{j2} &:= U_{i-1}\tilde{h}^j_{i1}\Gamma_{i-1} + U_{i-1}h^j_{i2} \text{ for } i = 1,..,p, \quad j = 1,..,r_i \end{aligned} \tag{5.38}$$

$$U^T_i(\varepsilon_i,..,\varepsilon_1) = L^T_i(\varepsilon_i)U^T_{i-1}(\varepsilon_{i-1},..,\varepsilon_1), \quad U^T_0 = I \tag{5.39}$$

$$\Gamma_i(\varepsilon_i,..,\varepsilon_1) = L^T_i(\varepsilon_i)\Gamma_{i-1}(\varepsilon_{i-1},..,\varepsilon_1) + R_i, \quad \Gamma_0 = 0 \tag{5.40}$$

Proof: [4][60]. The overall joint velocity is

$$\dot{X} = \sum_{i=1}^{p}\sum_{j=1}^{r_i}\frac{\partial X}{\partial \varepsilon^j_i}\dot{\varepsilon}^j_i = X(\varepsilon)p \tag{5.41}$$

Notice that for each fixed $i > 2$,

$$\sum_{j=1}^{r_i}\frac{\partial X}{\partial \varepsilon^j_i}\dot{\varepsilon}^j_i = X_p(\varepsilon_p)\cdots X_{i+1}(\varepsilon_{i+1})\left\{\sum_{j=1}^{r_i}\frac{\partial X}{\partial \varepsilon^j_i}\dot{\varepsilon}^j_i\right\}X_{i-1}(\varepsilon_{i-1})\cdots X_1(\varepsilon_1) \tag{5.42}$$

But, as computed above for simple joints,

$$\sum_{j=1}^{r_i}\frac{\partial X}{\partial \varepsilon^j_i}\dot{\varepsilon}^j_i = X_i(\varepsilon_i)\begin{bmatrix} \tilde{h_{i1}\beta_i} & h_{i2}\beta \\ 0 & 0 \end{bmatrix} \tag{5.43}$$

Thus we have

$$\begin{aligned} \dot{X} &= X(\varepsilon)p \\ &= \begin{bmatrix} h_{11}\beta_1 & h_{12}\beta_1 \\ 0 & 0 \end{bmatrix} \\ &\quad + \sum_{i=2}^{p} X_p(\varepsilon_p)\cdots X_i(\varepsilon_i)\begin{bmatrix} \tilde{h_{i1}\beta_i} & h_{i2}\beta_i \\ 0 & 0 \end{bmatrix}X_{i-1}(\varepsilon_{i-1})\cdots X_1(\varepsilon_1) \end{aligned} \tag{5.44}$$

or, premultiplying through by $X(\varepsilon)$,

$$\begin{aligned} &\begin{bmatrix} \tilde{h_{11}\beta_1} & h_{12}\beta_1 \\ 0 & 0 \end{bmatrix} + \\ &\sum_{i=2}^{p}[X_{i-1}(\varepsilon_{i-1})\cdots X_1(\varepsilon_1)]^{-1}\begin{bmatrix} \tilde{h_{i1}\beta_i} & h_{i2}\beta_i \\ 0 & 0 \end{bmatrix}X_{i-1}(\varepsilon_{i-1})\cdots X_1(\varepsilon_1) \\ &\quad = p = \begin{bmatrix} \tilde{\omega}_b & v_b \\ 0 & 0 \end{bmatrix} \end{aligned} \tag{5.45}$$

This important relationship gives the body rates across the compound joint in terms of the joint quasi-velocities. Now, we can also write

$$\begin{bmatrix} h_{i2}\tilde{\beta}_i & h_{i1}\beta_i \\ 0 & 0 \end{bmatrix} = \sum_{j=1}^{r_i} \begin{bmatrix} \tilde{h}_{i1}^j & h_{i2}^j \\ 0 & 0 \end{bmatrix} \tag{5.46}$$

So that (5.45) can be written in the form

$$p = H(\varepsilon)\beta$$

where $H(\varepsilon)$ is constructed as stated. ■

Note that these equations differ from those of Proposition (5.3) only in that each ε_i is a vector of dimension r_i rather than a scalar.

5.2.4 Joint Computations

The computations described above have been implemented in *ProPac*. The function `Joints` computes all of the required joint quantities. Recall that simple joints are characterized by the number of degrees of freedom, r, an r-vector of joint quasi-velocities, p, and a $6 \times r$ joint map matrix, H. Across the joint, the relative velocity vector is Hp. Moreover, H is a constant (independent of the joint configuration) and the columns represent the joint action axes in the outboard frame (by convention). A compound joint is equivalent to a sequence of simple joints. Thus, it is necessary to define a set of numbers that represent the degrees of freedom associated with each intermediate frame and a corresponding set of (constant) joint map matrices. When defining a joint in *ProPac*, it is necessary to also assign names for both the joint quasi-velocities and joint configuration variables.

A k-frame compound joint with n degrees of freedom is defined by the data structure:

$$\{r, H, q, p\}$$

where

$r = k-$ vector whose elements define the number of degrees of freedom for each simple joint, with $n = r_1 + \cdots + r_k$.

$H = [H_1 \ldots H_k]$ a matrix composed of the k joint map matrices of the simple joints.

$q = n-$ vector of joint coordinate names.

$p = n-$ vector of joint quasi-velocity names.

Example 5.6 (2 dof simple and compound joints). Here is a sample computation that illustrates the difference between simple and compound joints:

```
In[30]:= (* spherical joint - a simple 2-dof revolute joint *)
         r1={2};H1={{1,0},{0,0},{0,1},{0,0},{0,0},{0,0}};
         q1={a1x,a1z};p1={w1x,w1z};
         (* universal joint - a compound 2-dof revolute joint *)
         r2={1,1};H2={{1,0},{0,0},{0,1},{0,0},{0,0},{0,0}};
         q2={a2x,a2z};p2={w2x,w2z};
         JointLst={{r1,H1,q1,p1},{r2,H2,q2,p2}};
         {V,X,H}=Joints[JointLst];
```

The results are given below.

Spherical Joint:

$$V = \begin{pmatrix} 1 & 0 \\ 0 & \cos a_{1x} \end{pmatrix}$$

$$X = \begin{pmatrix} \cos a_{1z} & -\cos a_{1x}\sin a_{1z} & \sin a_{1x}\sin a_{1z} & 0 \\ \sin a_{1z} & \cos a_{1x}\cos a_{1z} & -\cos a_{1z}\sin a_{1x} & 0 \\ 0 & \sin a_{1x} & \cos a_{1x} & 0 \\ 0 & 0 & 0 & 1 \end{pmatrix}$$

$$H = \begin{pmatrix} 1 & 0 \\ 0 & 0 \\ 0 & 1 \\ 0 & 0 \\ 0 & 0 \\ 0 & 0 \end{pmatrix}$$

Universal Joint:

$$V = \begin{pmatrix} 1 & 0 \\ 0 & 1 \end{pmatrix}$$

$$X = \begin{pmatrix} \cos a_{2z} & -\cos a_{2x}\sin a_{2z} & \sin a_{2x}\sin a_{2z} & 0 \\ \sin a_{2z} & \cos a_{2x}\cos a_{2z} & -\cos a_{2z}\sin a_{2x} & 0 \\ 0 & \sin a_{2x} & \cos a_{2x} & 0 \\ 0 & 0 & 0 & 1 \end{pmatrix}$$

$$H = \begin{pmatrix} 1 & 0 \\ 0 & \sin a_{2x} \\ 0 & \cos a_{2x} \\ 0 & 0 \\ 0 & 0 \\ 0 & 0 \end{pmatrix}$$

Example 5.7 (3 dof Universal Joint).

A widely used example of a compound joint is the 3 degree of freedom universal joint. Such a joint is illustrated in Figure (5.3). This joint is composed of three elements and requires three frames to describe the composite motion. The relative motion between each of them involves one degree of freedom. In our terminology

$$H = \begin{bmatrix} 1 & 0 & 0 \\ 0 & 1 & 0 \\ 0 & 0 & 1 \\ 0 & 0 & 0 \\ 0 & 0 & 0 \\ 0 & 0 & 0 \end{bmatrix}$$

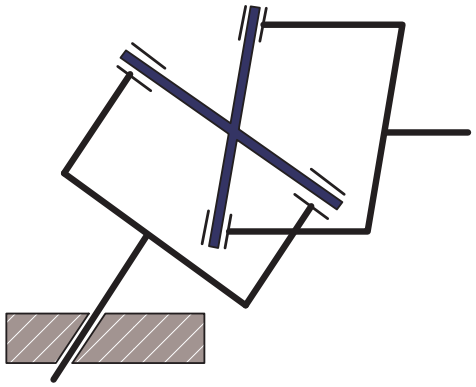

Fig. 5.3: Diagram of a 3 dof universal joint. Note that the joint itself is composed of three bodies in addition to the fixed reference body.

```
In[31]:= H = Join[IdentityMatrix[3], DiagonalMatrix[{0, 0, 0}]];
         r = {1, 1, 1};
         q = {t1, t2, t3};
         p = {w1, w2, w3};
         JointLst = {{r, H, q, p}};
         {V, X, H} = Joints[JointLst];
```

The results of this calculation are:

$$H = \begin{bmatrix} 1 & 0 & -\sin t2 \\ 0 & \cos t1 & \cos t2 \sin t1 \\ 0 & -\sin t1 & \cos t1 \cos t2 \\ 0 & 0 & 0 \\ 0 & 0 & 0 \\ 0 & 0 & 0 \end{bmatrix}$$

$$X =$$

$$\begin{bmatrix} \cos t2\cos t3 & \cos t3\sin t1\sin t2-\cos t1\sin t3 & \cos t1\cos t3\sin t2+\sin t1\sin t3 & 0 \\ \cos t2\sin t3 & \cos t1\cos t3+\sin t1\sin t2\sin t3 & -\cos t3\sin t1+\cos t1\sin t2\sin t3 & 0 \\ -\sin t2 & \cos t2\sin t1 & \cos t1\cos t2 & 0 \\ 0 & 0 & 0 & 1 \end{bmatrix}$$

$$V = \begin{bmatrix} 1 & 0 & 0 \\ 0 & 1 & 0 \\ 0 & 0 & 1 \end{bmatrix}$$

5.2.5 Remarks on Configuration Coordinates

The joint quasi–velocities are naturally defined by the action of the joint. Joint configuration coordinates, however, are defined by the kinematic relation (5.23). While these equations formally define the coordinates (by defining $\dot{\varepsilon}$), they also provide a physical interpretation. Before examining some examples, note that $V(\varepsilon)$ itself follows directly from the joint definition. Therefore to the extent that there is some freedom in specifying the joint parameters (the vector r and the matrix H), the user sets up the physical meaning of the coordinates ε. To see how this works, consider a general six degree of freedom joint (unconstrained 6 dof relative motion) defined by:

```
In[32]:= H = IdentityMatrix[6];
         r = {6};
         q = {ax, ay, az, x, y, z};
         p = {wx, wy, wz, ux, uy, uz};
```

Consider this joint as depicting the relative motion of a body with respect to a space frame. The velocity transformation matrix V is:

$$V = diag(V_1, V_2)$$

$$V_1 = \begin{bmatrix} 1 & \sin ax\tan ay & \cos ax\tan ay \\ 0 & \cos ax & -\sin ax \\ 0 & \sec ay\sin ax & \cos ax\sec ay \end{bmatrix}$$

$$V_2 =$$

$$\begin{bmatrix} \cos ay\cos az & \cos az\sin ax\sin ay-\cos ax\sin az & \cos ax\cos az\sin ay+\sin ax\sin az \\ \cos ay\sin az & \cos ax\cos az+\sin ax\sin ay\sin az & -\cos az\sin ax+\cos ax\sin ay\sin az \\ -\sin ay & \cos ay\sin ax & \cos ax\cos ay \end{bmatrix}$$

Inspection and comparison with standard results (e.g., [31]) reveals that the coordinates ax, ay, az are Euler angles in the 3–2–1 convention, and the coordinates x, y, z define the position of the body frame relative to the space frame, as represented in the space frame. In other words, the quasi–velocity vector (ux, uy, uz) corresponds to the body linear velocity in the body frame whereas the coordinate velocity $(\dot{x}, \dot{y}, \dot{z})$ represent the same body linear velocity in the space frame. By interchanging the first three columns of H, the resultant angle parameters again turn out to be Euler parameters, but in different conventions. If the columns in H corresponding to angles and linear displacements are interchanged, then the representation of the linear velocity and displacement will switch from space to body frame (or vice–versa).

5.3 Remarks on Rotation of Rigid Bodies

5.3.1 Introduction

The orientation of a rigid body has been described as an element in the special orthogonal group $SO(3)$. Rotational motion of a rigid body is thus conceived as a trajectory in the manifold associated with $SO(3)$. In Chapter 3, elements in $SO(3)$ were associated with a rotation matrix L – a 3×3 real matrix that satisfies $L^T L = I$. $SO(3)$ is a 3-dimensional group. Consequently, a local parametrization involving three parameters, such as Euler angles, is commonly used to represent rigid body orientation. Such local parameterizations may be inadequate because they do not lead to global descriptions of all possible trajectories of rotational motion.

One example of this problem can be seen as follows. Consider an Euler angle description involving successive rotations ψ, θ, and ϕ about the body axes z, y, and x, respectively. Then the coordinate derivatives are related to the body angular velocity by the differential equations:

$$\frac{d}{dt}\begin{bmatrix}\phi\\ \theta\\ \psi\end{bmatrix} = \begin{bmatrix}1 & \sin\phi\tan\theta & \cos\phi\tan\theta\\ 0 & \cos\phi & -\sin\phi\\ 0 & \sin\phi\sec\theta & \cos\phi\sec\theta\end{bmatrix}\begin{bmatrix}\omega_x\\ \omega_y\\ \omega_z\end{bmatrix} \tag{5.47}$$

Thus, the coordinate velocity vector belongs to the span of the columns of the kinematic matrix

$$\frac{d}{dt}\begin{bmatrix}\phi\\ \theta\\ \psi\end{bmatrix} \in \text{span}\left\{\begin{bmatrix}1\\0\\0\end{bmatrix}, \begin{bmatrix}\sin\phi\tan\theta\\ \cos\phi\\ \sin\phi\sec\theta\end{bmatrix}, \begin{bmatrix}\cos\phi\tan\theta\\ -\sin\phi\\ \cos\phi\sec\theta\end{bmatrix}\right\}$$

It is not difficult to verify that

$$\lim_{\theta\to\pm\pi/2}\text{span}\left\{\begin{bmatrix}1\\0\\0\end{bmatrix}, \begin{bmatrix}\sin\phi\tan\theta\\ \cos\phi\\ \sin\phi\sec\theta\end{bmatrix}, \begin{bmatrix}\cos\phi\tan\theta\\ -\sin\phi\\ \cos\phi\sec\theta\end{bmatrix}\right\} = \text{span}\left\{\begin{bmatrix}1\\0\\0\end{bmatrix}, \begin{bmatrix}1\\0\\1\end{bmatrix}\right\}$$

This implies that at $\theta = \pm\pi/2$ the motion is restricted by the model (5.47) to two degrees of freedom. Clearly, this is not representative of a rigid body free to rotate in space. The singularity is similar to 'gimbal lock' in a mechanical gyroscope. In a gyroscope the platform does not move with global rotational freedom. The mechanical suspension binds the platform to the inertial frame with a compound three-degree-of-freedom joint with coordinates equivalent to Euler angles. Gimbal lock occurs when the roll axis lies in the plane of the pitch and yaw axes.

One alternative parameterization of $SO(3)$ that avoids the singularity noted above is the 4-parameter *quaternion* introduced by Hamilton in 1843 [31]. The quaternion has been applied successfully in engineering mechanics and will be considered in the following sections.

5.3.2 Preliminary Observations

The control of rigid body orientation is important in

5.3.3 The Quaternion

A quaternion is a four tuple of real numbers $q = (q_0, q_1, q_2, q_3)$. It is convenient to envision a quaternion as composed of two parts, a scalar q_0 and vector $\mathbf{q} = (q_1, q_2, q_3)$. The following operations are defined:

- Addition (and subtraction)

$$q + p = (q_0 + p_0, q_1 + p_1, q_2 + p_2, q_3 + p_3)$$

- Norm

$$\|q\|^2 = q_0^2 + q_1^2 + q_2^2 + q_3^2$$

- Multiplication

$$q \circ p = (q_0 p_0 - \mathbf{q} \cdot \mathbf{p}, q_0 \mathbf{p} + p_0 \mathbf{q} + \mathbf{q} \times \mathbf{p})$$

  or, equivalently,

$$q \circ p = \begin{pmatrix} q_0 & -\mathbf{q}^T \\ \mathbf{q} & q_0 I_3 + \tilde{\mathbf{q}} \end{pmatrix} \begin{pmatrix} p_0 \\ \mathbf{p} \end{pmatrix}$$

- Conjugate

$$(q_0, \mathbf{q})^* = (q_0, -\mathbf{q})$$

- Inverse

$$q^{-1} = q^* / \|q\|$$

- Division

$$q_1/q_2 = q_1 q_2^{-1}$$

The matrix

$$Q = \begin{pmatrix} q_0 & -\mathbf{q}^T \\ \mathbf{q} & q_0 I_3 + \tilde{\mathbf{q}} \end{pmatrix}$$

is called the *quaternion matrix*. Note that

$$p \circ q = \begin{pmatrix} q_0 & -\mathbf{q}^T \\ \mathbf{q} & q_0 I_3 - \tilde{\mathbf{q}} \end{pmatrix} \begin{pmatrix} p_0 \\ \mathbf{p} \end{pmatrix} = Q^* \begin{pmatrix} p_0 \\ \mathbf{p} \end{pmatrix}$$

If $\|q\| = 1$, then q is a *unit quaternion*. If q is a unit quaternion, then $q^{-1} = q^*$. Unit quaternions form a group with multiplication as the group operation. In particular,

- If q, p are unit quaternions, then $q \circ p$ and $p \circ q$ are unit quaternions,
- If q is a unit quaternion, then q^{-1} is a unit quaternion,
- There is a unit quaternion $e = (1, \mathbf{0})$ that is an identity element; i.e., for any unit quaternion q, $eq = qe = q$.

If q is a unit quaternion we can always write q in the form $q = (\cos\theta, \mathbf{u}\sin\theta)$ where $\mathbf{u}$ is a unit vector.

Unit quaternions provide a convenient way to represent rigid body rotations. A quaternion q with $q_0 = 0$ is called a *pure quaternion*. Now consider a generic vector $\mathbf{r}$ fixed in a rotating reference frame. We can associate it with a pure quaternion $r = (0, \mathbf{r})$. Let q be a unit quaternion and consider the transformation of quaternion r to quaternion s defined by

$$s = q \circ r \circ q^{-1} = q \circ r \circ q^*$$

which is equivalent to

$$s = \begin{pmatrix} q_0 & \mathbf{q}^T \\ -\mathbf{q} & q_0 I_3 + \tilde{\mathbf{q}} \end{pmatrix} \begin{pmatrix} q_0 & -\mathbf{q}^T \\ \mathbf{q} & q_0 I_3 + \tilde{\mathbf{q}} \end{pmatrix} \begin{pmatrix} 0 \\ \mathbf{r} \end{pmatrix}$$

This product can be expanded to find

$$s_0 = 0 \tag{5.48}$$

$$\mathbf{s} = \begin{pmatrix} q_0^2 + q_1^2 - q_2^2 - q_3^2 & 2q_1q_2 - 2q_0q_3 & 2q_0q_2 + 2q_1q_3 \\ 2q_1q_2 + 2q_0q_3 & q_0^2 - q_1^2 + q_2^2 - q_3^2 & -2q_1q_2 + 2q_0q_3 \\ -2q_0q_2 + 2q_1q_3 & 2q_0q_1 + 2q_2q_3 & q_0^2 - q_1^2 - q_2^2 + q_3^2 \end{pmatrix} \mathbf{r} \tag{5.49}$$

We wish to show that the action of the quaternion q on a vector, as defined by (5.49), is a rotation. To do this it is convenient to convenient to use the vector calculus equivalent to (5.49)

$$\mathbf{s} = \left(q_0^2 - \mathbf{q}\cdot\mathbf{q}\right)\mathbf{r} + 2q_0\mathbf{q}\times\mathbf{r} + 2\left(\mathbf{q}\cdot\mathbf{r}\right)\mathbf{q} \tag{5.50}$$

which is easily derived using the definition of quaternion product along with the identity $(\mathbf{a}\times\mathbf{b})\times\mathbf{c} = (\mathbf{a}\cdot\mathbf{c})\,\mathbf{b} - (\mathbf{a}\cdot\mathbf{b})\,\mathbf{c}$. Now, if we replace q by $q = (\cos\theta, \mathbf{u}\sin\theta\,)$, we obtain

$$\mathbf{s} = \cos 2\phi\,\mathbf{r} + (1-\cos 2\phi)\,\phi\,(\mathbf{u}\cdot\mathbf{r})\,\mathbf{u} + \sin 2\phi\,\mathbf{u}\times\mathbf{r} \tag{5.51}$$

Recall that a finite rotation can always be represented by a unit vector, $\mathbf{u}$, that defines the axis of rotation and the angle of rotation, θ. We wish to investigate the rotation of a vector $\mathbf{r}$ within a specified frame. define an alternative frame with one axis aligned with the rotation unit vector $\mathbf{u}$ and the other two axes aligned with orthogonal unit vectors $\mathbf{v}$ and $\mathbf{w}$ that both lie in the plane orthogonal to $\mathbf{u}$. Suppose further, that $\mathbf{v}$ lies in the plane defined by $\mathbf{u}$ and $\mathbf{r}$ so that $\mathbf{r}$ can be expressed $\mathbf{r} = r_0\mathbf{u} + r_1\mathbf{v}$. The rotated vector $\mathbf{s}$ is then

$$\mathbf{s} = r_0\mathbf{u} + r_1\mathbf{v}\cos\theta + r_1\mathbf{w}\sin\theta$$

Of course, $r_1\mathbf{v} = \mathbf{r} - (\mathbf{r}\cdot\mathbf{u})\,\mathbf{u}$ and $\mathbf{w} = \mathbf{u}\times\mathbf{v}$. So,

$$\mathbf{s} = \cos\theta\,\mathbf{r} + (1-\cos\theta)\,(\mathbf{r}\cdot\mathbf{u})\,\mathbf{u} + \sin\theta\,\mathbf{u}\times\mathbf{r} \tag{5.52}$$

Comparing (5.51) and (5.52) we see that $q = (\cos\theta/2, \mathbf{u}\sin\theta/2)$ corresponds to a rotation of amount θ about the unit vector $\mathbf{u}$.

5.3.4 Quaternion Representation of a Rotating Frame

Consider a rigid body free to rotate in space. Suppose that a point, fixed in the body, is represented by vector $\mathbf{r}$ defined in a body fixed frame. Then $\mathbf{s}$ can be considered its representation in a space fixed frame. The rotation matrix identified in (5.49) transforms $\mathbf{r}$ from body fixed coordinates to space coordinates. By convention the matrix transforming space coordinates to body coordinates is designated L, so we have

$$L^T(q) = \begin{pmatrix} q_0^2+q_1^2-q_2^2-q_3^2 & 2q_1q_2-2q_0q_3 & 2q_0q_2+2q_1q_3 \\ 2q_1q_2+2q_0q_3 & q_0^2-q_1^2+q_2^2-q_3^2 & -2q_1q_2+2q_0q_3 \\ -2q_0q_2+2q_1q_3 & 2q_0q_1+2q_2q_3 & q_0^2-q_1^2-q_2^2+q_3^2 \end{pmatrix} \tag{5.53}$$

Specifically, if $\mathbf{r}$ is a vector represented in the coordinates of the rotated body frame, and $\mathbf{s}$ its coordinates in the fixed space frame, then

$$\mathbf{r} = L(q)\,\mathbf{s}, \quad \mathbf{s} = L^T(q)\,\mathbf{r}$$

We wish to relate the body angular velocity to the rate of change Euler parameters. We begin with time differentiation of the expression $s = q\circ r\circ q^*$

$$\dot{s} = \dot{q}\circ r\circ q^* + q\circ r\circ\dot{q}^*$$

Now substituting $r = q^*\circ s\circ q$

$$\dot{s} = \dot{q} \circ q^* \circ s + s \circ q \circ \dot{q}^*$$

Since q is a unit quaternion, the time rate of change of its norm is zero. This fact allows us to easily establish that the scalar parts of $\dot{q} \circ q^*$ and $q \circ \dot{q}^*$ are both zero. Furthermore, if $\dot{q} \circ q^* = (0, \mathbf{w})$, then $q \circ \dot{q}^* = (0, -\mathbf{w})$. It follows that the vectorial part of $\dot{s}$ is $\dot{\mathbf{s}} = 2\mathbf{w} \times \mathbf{s}$. From this we identify $\boldsymbol{\Omega} = 2\mathbf{w}$, where $\boldsymbol{\Omega}$ is the angular velocity of the body in space coordinates. Thus,

$$\dot{q} = \frac{1}{2} Q^* \begin{pmatrix} 0 \\ \boldsymbol{\Omega} \end{pmatrix}$$

or

$$\frac{d}{dt} \begin{bmatrix} q_0 \\ \mathbf{q} \end{bmatrix} = \frac{1}{2} \begin{pmatrix} q_0 & -\mathbf{q}^T \\ \mathbf{q} & q_0 I_3 - \tilde{\mathbf{q}} \end{pmatrix} \begin{bmatrix} 0 \\ \boldsymbol{\Omega} \end{bmatrix} = \frac{1}{2} \begin{pmatrix} -\mathbf{q}^T \\ q_0 I_3 - \tilde{\mathbf{q}} \end{pmatrix} \boldsymbol{\Omega} \tag{5.54}$$

It is generally more convenient to write these equations using angular velocity in body coordinates

$$\frac{d}{dt} \begin{bmatrix} q_0 \\ \mathbf{q} \end{bmatrix} = \frac{1}{2} Q \begin{bmatrix} 0 \\ \boldsymbol{\omega} \end{bmatrix} = \frac{1}{2} \begin{pmatrix} -\mathbf{q}^T \\ q_0 I_3 + \tilde{\mathbf{q}} \end{pmatrix} \boldsymbol{\omega} \tag{5.55}$$

where $\boldsymbol{\omega}$ is the body angular velocity in body coordinates. Expanding, with $\boldsymbol{\omega} = (\omega_x, \omega_y, \omega_z)$

$$\frac{d}{dt} \begin{bmatrix} q_0 \\ q_1 \\ q_2 \\ q_3 \end{bmatrix} = \frac{1}{2} \begin{bmatrix} -q_1 & -q_2 & -q_3 \\ q_0 & -q_3 & q_2 \\ q_3 & q_0 & -q_1 \\ -q_2 & q_1 & q_0 \end{bmatrix} \begin{bmatrix} \omega_x \\ \omega_y \\ \omega_z \end{bmatrix} \tag{5.56}$$

Exact integration of these equations for any specified $\boldsymbol{\omega}(t)$ and initial condition $q(0)$ of unit length produce a solution $q(t)$ with $\|q(t)\| = 1$ for all t. However, imperfect integration requires a correction. One common remedy for digital computation is to implement

$$\frac{d}{dt} \begin{bmatrix} q_0 \\ q_1 \\ q_2 \\ q_3 \end{bmatrix} = \frac{1}{2} \begin{bmatrix} q_1 & q_2 & q_3 \\ q_0 & -q_3 & q_2 \\ q_3 & q_0 & -q_1 \\ -q_2 & q_1 & q_0 \end{bmatrix} \begin{bmatrix} \omega_x \\ \omega_y \\ \omega_z \end{bmatrix} + \kappa\lambda \begin{bmatrix} q_0 \\ q_1 \\ q_2 \\ q_3 \end{bmatrix} \tag{5.57}$$

where $\lambda = \left(1 - q_0^2 - q_1^2 - q_2^2 - q_3^2\right)$ and the parameter κ is chosen so that $\kappa h \leq 1$ and h is the step size.

5.3.5 Euler Angles from Quaternion

It is frequently desirable to determine the Euler angles from the quaternion. For Euler angles in the 3-2-1 or *zyx* convention, the rotation matrix, from body to space coordinates, is

$$L(\phi, \theta, \psi) = \begin{pmatrix} \cos\theta\cos\psi & \cos\theta\sin\psi & -\sin\theta \\ \sin\phi\sin\theta\cos\psi - \cos\phi\sin\psi & \sin\phi\sin\theta\sin\psi + \cos\phi\cos\psi & \sin\phi\cos\theta \\ \cos\phi\sin\theta\cos\psi + \sin\phi\sin\psi & \cos\phi\sin\theta\sin\psi - \sin\phi\cos\psi & \cos\phi\cos\theta \end{pmatrix} \tag{5.58}$$

The corresponding rotation matrix in terms of quaternions is

$$L(q) = \begin{pmatrix} q_0^2+q_1^2-q_2^2-q_3^2 & 2(q_1q_2+q_0q_3) & 2(q_1q_3-q_0q_2) \\ 2(q_2q_1-q_0q_3) & q_0^2-q_1^2+q_2^2-q_3^2 & 2(q_2q_3+q_0q_1) \\ 2(q_1q_3+q_0q_2) & 2(q_3q_2-q_0q_1) & q_0^2-q_1^2-q_2^2+q_3^2 \end{pmatrix} \tag{5.59}$$

Note that both of these matrices convert vector in body fixed coordinates to space coordinates. Equation (5.59) is obtained by inverting (equivalently, transposing) the matrix in (5.53).

Now, compare elements of (5.58) and (5.59) to obtained the following

$$\phi = \tan^{-1}\frac{2(q_2q_3+q_0q_1)}{q_0^2-q_1^2-q_2^2+q_3^2} \tag{5.60}$$

$$\theta = \sin^{-1}2(q_0q_2-q_1q_3) \tag{5.61}$$

$$\psi = \tan^{-1}\frac{2(q_2q_1+q_0q_3)}{q_0^2+q_1^2-q_2^2-q_3^2} \tag{5.62}$$

For example, comparing elements (1,3) in (5.58) and (5.59) leads directly to (5.61). Dividing (2,3) by (3,3) in (5.58) and (5.59), respectively, and comparing the result leads to (5.60). Similarly, dividing element (1,2) by (1,1) leads to (5.61).

5.3.6 Quaternion from Euler Angles

It is convenient and sometimes necessary to be able solve for the quaternion parameters given a the Euler angles. For instance when integrating equation (5.57), the initial attitude is often specified in Euler angles which need to be converted to quaternion parameters.

Comparing (5.58) and (5.59) we obtain the following four equations

$$\begin{gathered} \tan\theta\left(q_0^2-q_1^2-q_2^2+q_3^2\right) = 2(q_2q_3+q_0q_1) \\ \sin\theta = 2(q_0q_2-q_1q_3) \\ \tan\psi\left(q_0^2+q_1^2-q_2^2-q_3^2\right) = 2(q_2q_1+q_0q_3) \\ q_0^2+q_1^2+q_2^2+q_3^2 = 1 \end{gathered} \tag{5.63}$$

It is easily verified that these equations are satisfied by

$$\begin{aligned} q_0 &= \cos\tfrac{1}{2}\psi\cos\tfrac{1}{2}\theta\cos\tfrac{1}{2}\phi + \sin\tfrac{1}{2}\psi\sin\tfrac{1}{2}\theta\sin\tfrac{1}{2}\phi \\ q_1 &= \cos\tfrac{1}{2}\psi\cos\tfrac{1}{2}\theta\sin\tfrac{1}{2}\phi - \sin\tfrac{1}{2}\psi\sin\tfrac{1}{2}\theta\cos\tfrac{1}{2}\phi \\ q_2 &= \cos\tfrac{1}{2}\psi\sin\tfrac{1}{2}\theta\cos\tfrac{1}{2}\phi + \sin\tfrac{1}{2}\psi\cos\tfrac{1}{2}\theta\sin\tfrac{1}{2}\phi \\ q_3 &= -\cos\tfrac{1}{2}\psi\sin\tfrac{1}{2}\theta\sin\tfrac{1}{2}\phi + \sin\tfrac{1}{2}\psi\cos\tfrac{1}{2}\theta\cos\tfrac{1}{2}\phi \end{aligned} \tag{5.64}$$

5.4 Chain and Tree Configurations

In general a multibody system can be viewed in terms of an underlying tree structure upon which is imposed additional algebraic and/or differential constraints. In this section we describe the data structures used to define multibody tree structures. In later sections we show how to compute velocities and configuration coordinates of reference frames at arbitrary locations in the tree. A tree can be defined in terms of a set of chains, each beginning at the root body.

Representation of Chain & Tree Structures

ProPac provides tools to build models for mechanical systems that have an underlying tree topology. Chain structures are a special case. Systems with closed loops are accommodated by adding constraints to the underlying tree. A tree consisting of n bodies also contains n joints. Every system contains a base reference frame that is designated body '0'. Otherwise, bodies and joints can be numbered arbitrarily. Joint data and body data are organized into lists by the analyst, i.e.:

```
JointList={JointData_1,...,BodyData_n}
BodyList={BodyData_1,...,BodyData_n}
```

The structure of the individual data objects will be described below. Joints and bodies are implicitly numbered by their position in the data lists. Each body contains a unique 'inboard' node, corresponding to (the outboard side of) a joint through which the body connects to an inner branch of the tree, or to the root (body 0). See Figures (5.4) and (5.5). Each body may also contain 'outboard' nodes. The outboard nodes are distinguished body locations that may be associated with a joint location (the inboard side of the joint), a sensor location, a point of application of an external force or any other feature of interest. Since one joint connects the tree to the root (the root node may be considered an outboard node of body 0), there must be at least $n-1$ outboard nodes among the n bodies corresponding to the remaining $n-1$ joints. These are the n 'outboard joint nodes'. The outboard joint nodes must be numbered 1 through n and must correspond to the associated joint number. The specific association of numbers to joints is not essential but by convention the root node is normally assigned the number 1. The remaining outboard notes can be numbered arbitrarily. The inboard nodes need not be assigned numbers.

In summary there are two important book-keeping principles:

- joints and bodies are numbered according to their position in the data lists,
- outboard joint nodes must be numbered consistently with their repective joints.

A tree is composed of a set of defining chains. For instance consider a tree composed of the following sequences of bodies:

```
0,1,2,4      0,1,2,3,5      0,1,2,3,6
```

All defining chains of any tree will start with body 0, so we need not list it. However, the body sequences alone do not adequately define a tree. For instance bodies 5 and 6 both connect to body 3, but they will do so through different joints. This information can be provided by defining each chain as an ordered list of pairs - each pair consisting of a body and its inboard joint: inboard joint, body. For example, consider the following three chains:

```
{{1,1},{2,2},{5,4}}     {{1,1},{2,2},{3,3},{4,5}}
        {{1,1},{2,2},{3,3},{6,6}}
```

Chain 1 consists of bodies 1, 2, and 4. Body 1 connects to the reference (Body 0) at Joint 1, Body 2 connects to Body 1 at Joint 2, and Body 4 connects to Body 2 at Joint 5. The data also indicates that body 5 connects to body 3 at joint 4 (in the second chain), and body 6 connects to body 3 at joint 6 (third chain). Recall that each joint is uniquely associated with an outboard node of a particular body. A tree is defined by the data structure:

```
Tree = {list of chains}
Chain = ordered list of pairs {inboard joint, body}
      =  {{first inboard joint, first body},...,
                  {last inboard joint, last body}}
```

Reference Frames

It is assumed that there is a single inertially fixed reference frame whose origin is the inboard side of the root joint. Each body has a primary reference frame, fixed in the body with origin at the inboard node. Body data is defined in this frame. As appropriate, there may be other body fixed frames as well with origins at outboard node locations. Normally, the axes of these frames are parallel to the primary frame when the body is undeformed. For the system as a whole, there is a 'reference configuration' corresponding to the nominal joint configurations (associated with zero joint motion parameters) and undeformed bodies. In the reference configuration all reference frames (body and space) are alligned. The analyst sets up the reference configuration when choosing body frame orientations for joint and body data definitions. It is recommended that the analyst begin by defining a physically meaningful reference configuration from which data definitions will logically follow.

Rigid Body Data Structure

A rigid body is defined by its mass, inertia matrix and the location of distinguished points or nodes where joints or sensors may be located. We assume the following:

1. There is a distinguished point that corresponds to the inboard joint of the body. The body frame has its origin located there.
2. The center of mass and all other points of interest (nodes) including outboard joint locations are defined in the body frame.
3. The inertia matrix is defined in the body frame and it is the inertia matrix about the center of mass.

The data for a rigid body is organized in a list as follows. A rigid body with k outboard nodes is defined by the data structure:

```
{com,{out1,..,outk},m,Inertia}
```

where

```
com is the center of mass location,
outi = {node number, location} for the ith outboard node,
m is the mass, and
Inertia is the inertia tensor (about the center of mass).
```

5.4.1 Configuration Relations

Consider a serial chain composed of $K+1$ rigid bodies connected by joints as illustrated in Figure (5.4). The bodies are numbered 0 through K, with 0 denoting the base or reference body, which may represent any convenient inertial reference frame. The kth joint connects body $k-1$ at the point C_{k-1} with body k at the point O_k.

Let F^k denote a reference frame fixed in body k with origin at O_k. r^k_{co} denotes the vector from O_k to C_k in F^k and r^k denotes the vector from O_k to O_{k+1} in F^k. We will use a coordinate specific notation in which vectors represented in F^k (or its tangent space) will be identified with a superscript "k". Coordinate free relations carry no superscript. Sometimes it is convenient to employ a frame fixed in body k and aligned with F^k but with origin at some point P_k other than O_k. We use the designation $F^k_{P_k}$. Let r^k_{po} denote the vector from O_k to P_k in F^k. Then the parallel translation of F^k to $F^k_{P_k}$ results in the configuraton matrix

$$X_{k,P_k} = \begin{bmatrix} I & r_{po} \\ 0 & 1 \end{bmatrix}$$

The kth joint has n_k, $1 \leq n_k \leq 6$ degrees of freedom which can be characterized by n_k coordinates $q(k)$ and, correspondingly, n_k quasi-velocities $\beta(k)$ and a configuration matrix $X_k(q(k))$. We wish to compute the Euclidean configuraton matrix for a reference frame fixed in the last body with origin at the terminal node of the chain, designated P_K. For example, this would be node 5 in Figure (5.4). We obtain the

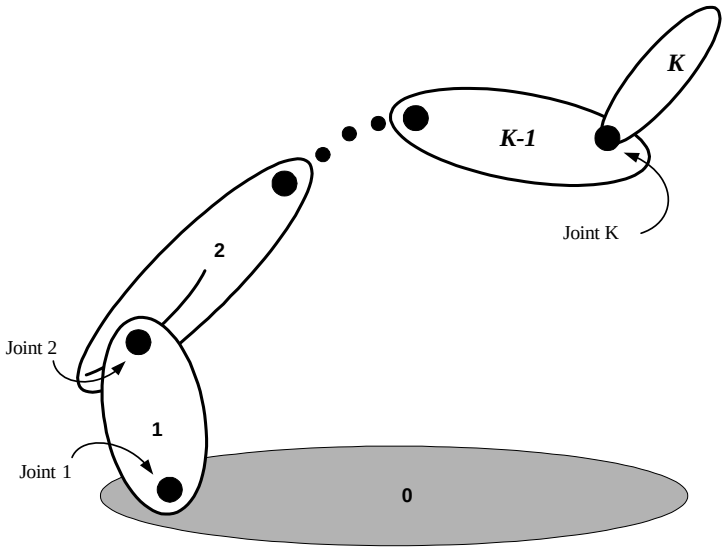

Fig. 5.4: A serial chain composed of $K+1$ rigid bodies numbered 0 through K and K joints numbered 1 through K.

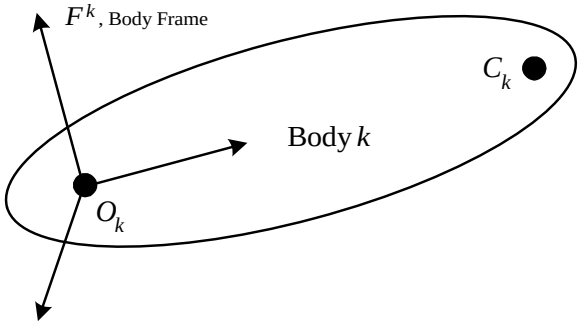

Fig. 5.5: On an arbitrary k^{th} link the inboard and outboard joint hinge points are designated O_k and C_k. The body fixed reference frame has its origin at O_k.

configuration relative to the space frame by successive motions: action of joint 1 $\rightarrow$ translation to $C_1 \rightarrow \cdots \rightarrow$ action of joint K $\rightarrow$ translation to P_K:

$$X_{P_K} = X_{K,P} X_K \ldots X_{2,C_2} X_2 X_{1,C_1} X_1 \tag{5.65}$$

Equation (5.65) can be modified to compute the relative configuration between body fixed frames at any two nodes in a chain or tree. To accommodate trees in this calculation requires a simple procedure to find a chain connecting the two nodes.

5.4.2 Velocity Relations in Chains

Once again consider a chain composed of $K+1$ bodies as illustrated in Figure (5.4). Rodriguez et al [6-8] define the spatial velocity at point C of any body-fixed reference frame with origin at point C as $V_c = [\omega, v_c]$ where v_c is the velocity of point C and ω is the angular velocity of the body. Let O be another point in the same body and let r_{co} denote the location of C in the body frame with origin at O. Then the spatial velocity at point C is related to that at O by the relation

$$V_c \;=\; \phi(r_{co})V_o \tag{5.66}$$

where

$$\phi(r_{co}) = \begin{bmatrix} I & 0 \\ -\tilde{r}_{co} & I \end{bmatrix},$$

and its adjoint

$$\phi^*(r_{co}) = \begin{bmatrix} I & \tilde{r}_{co} \\ 0 & I \end{bmatrix} \tag{5.67}$$

Joint k has a joint map matrix $H(k) \in R^{6\times n_k}$ so that

$$V_o(k) - V_c(k-1) = H(k)\beta(k) \tag{5.68}$$

Thus, sequential application of (5.66) and (5.68) leads to the following recursive velocity relation that we write in coordinate specific notation

$$V^i(k) = \phi(r^i_{co}(k-1))V^i(k-1) + H^i(k)\beta^i(k) \tag{5.69}$$

where the superscript i denotes the reference frame. Let us assume that $H(k)$ and $\beta(k)$ are specified in the frame F^k and $V(k-1)$ has been computed in the frame F^{k-1} . Then it is convenient to compute $V(k)$ in the kth frame

$$V^k(k) = diag(L_{k-1,k}, L_{k-1,k})\phi(r^{k-1}_{co}(k-1))V^{k-1}(k-1) + H^k(k)\beta^k(k) \tag{5.70}$$

If $V^0(0)$ is given, then equation (5.70) allows us to compute recursively, for $k = 1,..,K$, the linear velocity of the origin of F^k and the angular velocity of F^k, both represented in the coordinates of F^k. In what follows we take $V^0(0) = 0$. Abusing notation somewhat, it is convenient to define

$$\phi(k,k-1) \;=\; diag(L_{k-1,k}, L_{k-1,k})\phi(r^{k-1}_{co}(k-1)) \tag{5.71}$$

so that (5.70) can be written

$$V^k(k) = \phi(k,k-1)V^{k-1}(k-1) + H^k(k)\beta^k(k),\;\; k \;=\; 1,\; \ldots\;,\; K,\;\; V^0(0) = 0 \tag{5.72}$$

Equations (5.66) and (5.72) allow a sequential computation of velocities at any point along a chain. Notice that ϕ and H depend on joint configuration parameters so that the joint configuration and velocity variables are needed to perform the computation.

Remark 5.8. We want to clarify the recursive velocity formula (5.72). The spatial velocity, V_{O_k}, at the k^{th} joint outboard node, O_k, can be computed in terms of the velocity $V_{O_{k-1}}$ and the joint configuration $X(k)$. The setup is shown in Figure 5.6. Let us write $X(k)$ in the usual form

$$X(k) = \begin{bmatrix} L^T(k) & R(k) \\ 0 & 1 \end{bmatrix}$$

Now, we proceed as follows. First compute the velocity at the point C_{k-1}:

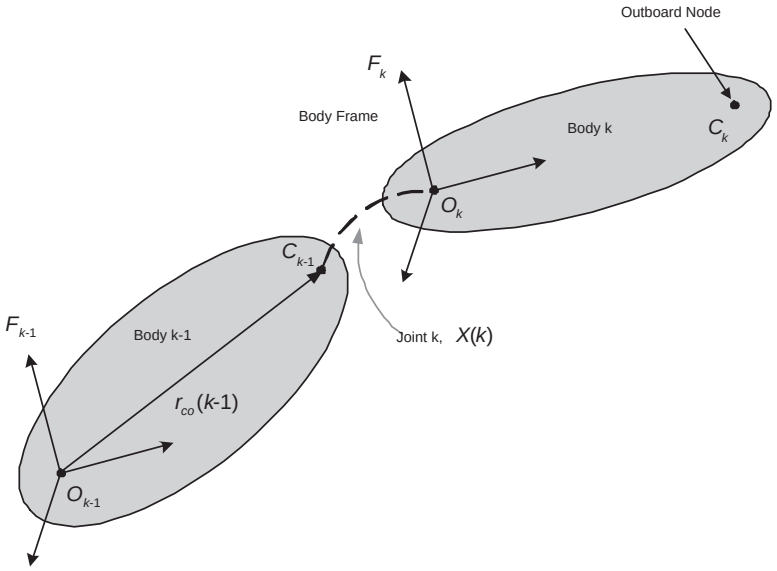

Fig. 5.6: Two links in a chain provide the basis for a single recursive step.

$$V_{C_{k-1}} = \phi(r_{co}(k-1)) V_{O_{k-1}}, \quad \phi(r) = \begin{bmatrix} I & 0 \\ -\tilde{r} & I \end{bmatrix}$$

Next obtain the velocity across the joint in two parts, compute the velocity at O_k' before the joint action

$$V_{O_k'} = \phi(R(k)) V_{C_{k-1}}$$

and then add the joint action. If we assume that the action is defined in the k^{th} body frame then we need to represent $V_{O_k'}$ in that frame before adding $H\beta$. Thus, we obtain

$$V_{O_k} = \text{diag}(L(k), L(k)) \phi(R(k)) \phi(r_{co}(k-1)) V_{O_{k-1}} + H(k)\beta(k)$$

Suppose we define $V(k) := V_{O_k}$ and

$$\phi(k,k-1) := \mathrm{diag}(L(k), L(k))\,\phi(R(k))\,\phi(r_{co}(k-1))$$

Then, we have the recursive velocity relation

$$V(k) = \phi(k,k-1)V(k-1) + H(k)\beta(k)$$

5.4.3 Configuration and Velocity Computations

In addition to the function `Joints` described above, there are other kinematic computations implemented in *ProPac*. We will describe and illustrate three of them: `EndEffector`, `RelativeConfiguration` and `NodeVelocity`.

`EndEffector[BodyList,X]` returns the Euclidean configuration matrix of a frame in the last body of a chain, with origin at the outboard joint location. `BodyList` is list of body data in nonstandard chain form, X is a corresponding list of joint Euler configuration matrices. `EndEffector` can also be used in the form `EndEffector[ChainList,TerminalNode,BodyList,X]` where `BodyList` is the standard body data structure. `ChainList` identifies the system subchain that terminates with `TerminalNode`. `EndEffector` can also be used in the form `EndEffector[TerminalNode,TreeList,BodyList,X]` in the event that the appropriate chain has not been identified. This last form is probably the most useful.

`RelativeConfiguration[Node1,Node2,TreeList,BodyList,X,q]` returns the configuration matrix for a body fixed frame at node `Node2` as seen by an observer in a body fixed frame at node `Node1`. Note that each node is defined in a specific body and the frame is fixed in the body in which the node is defined.

`NodeVelocity[ChainList,TerminalNode,BodyList,X,H,p]` returns the velocity at `TerminalNode`, where the body data, `BodyList`, the joint data `X` and `H`, and the quasivelocity names `p` corresponds to the chain defined by `ChainList`. The velocity is a six element vector defined in the body fixed frame. This function is used by `GeneralizedForce` that will be described later. The following syntax may also be used, similarly to the function `EndEffector`:

`NodeVelocity[ChainList,TerminalNode,BodyList,X,H,q,p]`,

and

`NodeVelocity[TerminalNode,TreeList,BodyList,X,H,q,p]`.

Example 5.9 (5 dof Robot Arm). The functions described above will be illustrated with an example of a 5 dof robot arm as shown in Figure (5.7).

First define the joint data:

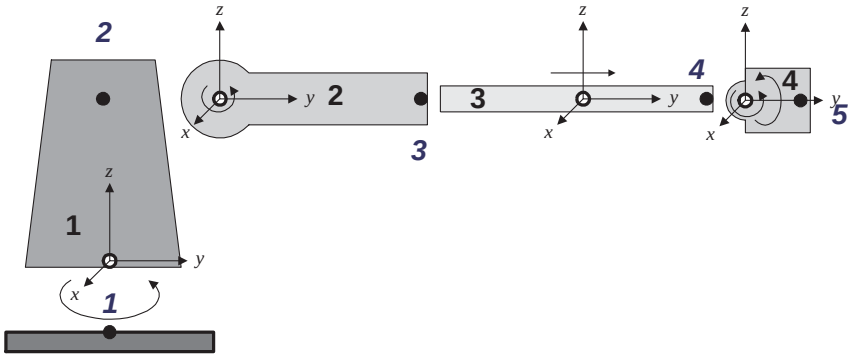

Fig. 5.7: A 5 dof robot arm is illustrated. The body fixed reference frames located at the inboard joint nodes are illustrated. Note that in the reference configuration the reference frames are alligned.

```
In[33]:= r1 = {1}; H1 = {{0}, {0}, {1}, {0}, {0}, {0}};
         q1 = {theta1}; p1 = {w1};
         r2 = {1}; H2 = Transpose[{{1, 0, 0, 0, 0, 0}}];
         q2 = {theta2}; p2 = {w2};
         r3 = {1}; H3 = Transpose[{{0, 0, 0, 0, 1, 0}}];
         q3 = {y}; p3 = {v};
         r4 = {2}; H4 = Transpose[{{0, 1, 0, 0, 0, 0}, {1, 0, 0, 0, 0, 0}}];
         q4 = {theta3, theta4}; p4 = {w3, w4};
         JointList = {{r1, H1, q1, p1}, {r2, H2, q2, p2}, {r3, H3, q3, p3}, {r4, H4, q4, p4}};
```

Define body data:

```
In[34]:= com1 = {0, 0, l1/2}; mass1 = m1; out1 = {2, {0, 0, l1}};
         Inertia1 = DiagonalMatrix[{J1x, J1x, J1z}];
         com2 = {0, l2/2, 0}; mass2 = m2; out2 = {3, {0, l2, 0}};
         Inertia2 = DiagonalMatrix[{J2x, 0, J2x}];
         com3 = {0, l3/2, 0}; mass3 = m3; out3 = {4, {0, l3, 0}};
         Inertia3 = DiagonalMatrix[{J3x, 0, J3z}];
         com4 = {0, l4/2, 0}; mass4 = m4; out4 = {5, {0, 0, l4}};
         Inertia4 = DiagonalMatrix[{J4x, J4y, J4z}];

         BodyList = {{com1, {out1}, mass1, Inertia1}, {com2, {out2}, mass2, Inertia2},
         {com3, {out3}, mass3, Inertia3}, {com4, {out4}, mass4, Inertia4}};
```

and the interconnection structure

```
In[35]:= TreeList={{{1,1},{2,2},{3,3},{4,4}}};
```

The joint parameters are computed with the command:

```
In[36]:= {V, X, H} = Joints[JointList];
```

The joint velocity transformation matrices can be displayed as follows.

```
In[37]:= V[[1]]//MatrixForm
Out[37]= (1)

In[38]:= V[[2]]//MatrixForm
Out[38]= (1)

In[39]:= V[[3]]//MatrixForm
Out[39]= (1)

In[40]:= V[[4]]//MatrixForm
Out[40]= (1   0
          0 Cos[theta3])
```

Using the function `EndEffector` the configuration of a frame fixed at node 4 can be computed.

```
In[41]:= TerminalNode = 4;

         XE = EndEffector[TerminalNode, TreeList, BodyList, X];

In[42]:= XE[[{1, 2, 3}, 4]]//MatrixForm
Out[42]= (-l2 Cos[theta2] Sin[theta1] - l3 Cos[theta2] Sin[theta1] - y Cos[theta2] Sin[theta1]
          l2 Cos[theta1] Cos[theta2] + l3 Cos[theta1] Cos[theta2] + y Cos[theta1] Cos[theta2]
                                  l1 + l2 Sin[theta2] + l3 Sin[theta2] + y Sin[theta2])

In[43]:= XE[[{1, 2, 3}, {1, 2, 3}]]//MatrixForm
Out[43]= (Cos[theta1]  -Cos[theta2] Sin[theta1]   Sin[theta1] Sin[theta2]
          Sin[theta1]   Cos[theta1] Cos[theta2]  -Cos[theta1] Sin[theta2]
                   0              Sin[theta2]              Cos[theta2])
```

As another example, we can compute the relative configuration of a frame at node 4 as seen by an oberver in a frame at node 2. We use the function `RelativeConfiguration`.

```
In[44]:= Node1 = 2; Node2 = 4; q = Flatten[{q1, q2, q3, q4}];

         RelativeConfiguration[Node1, Node2, TreeList, BodyList, X, q]//MatrixForm
Out[44]= (1  0              0              0
          0  Cos[theta2]   -Sin[theta2]   (l2 + l3 + y) Cos[theta2]
          0  Sin[theta2]    Cos[theta2]   (l2 + l3 + y) Sin[theta2]
          0  0              0              1)
```

The configuration of a frame at node 4 relative to node 3 is a pure translation:

```
In[45]:= RelativeConfiguration[3, 4, TreeList, BodyList, X, q]//MatrixForm
```

```
Out[45]= 1 0 0  0
         0 1 0  y
         0 0 1 l3
         0 0 0  1
```

Finally, we compute the spatial velocity of a frame fixed in body 3 at node 4.

```
In[46]:= p = Flatten[{p1, p2, p3, p4}];

         TerminalNode = 4;

         NodeVelocity[TerminalNode, TreeList, BodyList, X, H, q, p] // MatrixForm

Out[46]=          w2
          w1 Sin[theta2]
          w1 Cos[theta2]
         -w1 (l2 + l3 + y) Cos[theta2]
                   v
          w2 (l2 + l3 + y)
```

5.5 Problems

Problem 5.10 (Reconnaissance robot). The reconnaissance robot shown in Figure (5.8) moves on a flat surface. The vehicle has three degrees of freedom, its linear coordinates x, y and its angular orientation θ. The radar system also has three degrees of freedom. It can move vertically, z, and rotate in both azimuth and elevation, ϕ, ψ, relative to the vehicle. Suppose the radar system is pointing at a target, the vehicle and radar configuration are known as well as the range to target. Compute the target coordinates in a space fixed frame.

Problem 5.11 (Overhead crane). The overhead crane shown in Figure (5.9) is used to move and position heavy loads in the $x-z$ plane. The cart moves in one (x) linear direction on rails, the arm connects to the cart via a revolute joint (angle ϕ from downward z direction) and the cable length L is variable. Assume that the cable is always in tension and treat the payload as a point mass. The arm cable joint can be treated as a two degree of freedom compound joint consisting of rotation and extension (to model cable playout). Determine the spatial coordinates of the payload in terms of the four joint parameters.

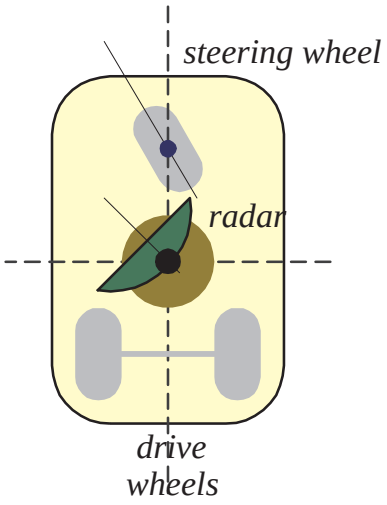

Fig. 5.8: A reconnaissance vehicle carrying a range-finding radar system.

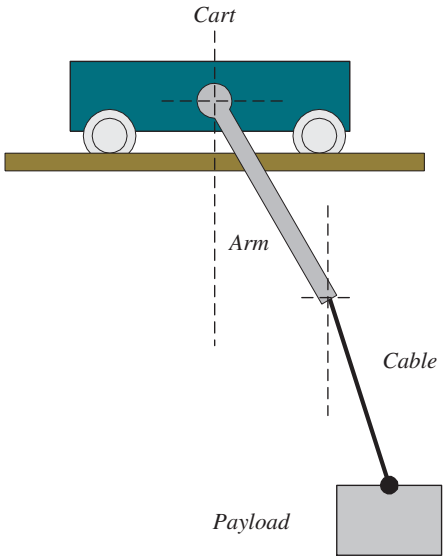

Fig. 5.9: An overhead crane used for moving and positioning heavy loads.

6

Dynamics

6.1 Introduction

The purpose of this chapter is to describe symbolic computing tools for assembling and manipulating control system design models for constrained multibody mechanical systems. The methods introduced in [60] for chains and trees are summarized and extended to constrained systems. New computing tools that support the analysis of constrained systems are described and illustrated.

The derivation of the explicit dynamical equations of motion for mechanical systems of even moderate complexity is difficult and time consuming.[1] Consequently, there has been a growing interest in automated derivation using computers [60, 73, 18, 11]. Much of this work has focused on chain and tree structures that characterize important robotic and vehicular systems. Many systems, however, are not tree structures; they involve closed loops or other forms of algebraic and/or differential constraints imposed on top of an underlying tree. Typical examples would be a grasping robotic hand or a vehicle with rolling wheels. The additional complexity of such systems magnifies the utility of computer assembly of the governing equations.

Our discussion is based on *Poincaré's equations* [2, 19, 20] also referred to as *Lagrange's equations in quasi-coordinates*[85, 86] or *pseudo-coordinates* [27], and the *Euler-Poincaré's equations* in [83]. Poincaré's equations preserve the underlying theoretical structure and elegance of the Lagrange formulation, but they are often more natural and can be substantially simpler than Lagrange's equations. Furthermore, their assembly can be much easier to automate making them a practical choice for modeling 'industrial strength' systems. Perhaps most importantly, in the words of [86]: "The main advantage... is the unification of the form of the ordinary Lagrange equations, the equations of motion of nonholonomic systems, and also equations such as Euler's dynamical equations of motion of a rigid body with a fixed point."

[1] Note that modeling and simulation software such as ADAMS and DADS do not produce explicit nonlinear equations of motion required for control system analysis and design.

The dynamical equations will be generated in the form

$$M(q)\dot{p} + C(p,q)p + F(p,q) = Q \tag{6.1}$$

where p is a vector of quasi-velocities, q is the generalized coordinate vector, Q is a vector of externally applied generalized forces and the functions $M(q)$, $C(p,q)$ and $F(p,q)$ are the parameters of the system. The assembly of Q, $M(q)$, $C(p,q)$ and $F(p,q)$ is the main topic of this chapter. In combination with the kinematic equations describe in the previous chapter

$$\dot{q} = V(q)p \tag{6.2}$$

these equations provide a consistent closed set of equations.

In Section 2 we develop Poincaré's formulation of Lagrange's equations and in Section 3 we apply it to general chain and tree structures. Then we consider constrained systems in Section 4 in which we treat both holonomic and nonholonomic differential constraints as well as configuraton constraints. We describe symbolic computing tools and give examples along the way. Finally, in Section 5, we describe numerical simulation.

6.2 Poincaré's Equations

It is well known that in some cases it is easier to formulate the equations of motion in terms of velocity variables that can not be expressed as the time derivatives of any corresponding configuration coordinates. Such velocities are called quasi-velocities and are often associated with so-called quasi-coordinates. Quasi-velocities are meaningful physical quantities. The angular velocity of a rigid body is a prime example. Quasi-coordinates are not meaningful physical quantities. They make sense only in terms of infinitesimal motions. The notion of quasi-velocities and quasi-coordinates leads to a generalization of Lagrange's equations which is applicable to systems with nonholonomic as well as holonomic constraints. Such generalizations were produced at the turn of the century and are associated with the names of Poincare, Appell, Maggi, Hamel, Gibbs and Boltzman (see, for example, Arnold et al [2] and Niemark and Fufaev [86], Gantmacher [27]).

6.2.1 Preliminaries

Consider a holonomically constrained system whose possible configurations correspond to the points of a smooth manifold M of dimension m called the *configuration manifold*. Local coordinates on M can be used to define the system configuration. They are called *generalized coordinates*. Any motion of the system over a time interval $[t_1, t_2]$ traces a path in M characterized in local coordinates by a map

$q(t) : [t_1,t_2] \mapsto M$. At any point $q \in M$ the *generalized velocity* $\dot{q}$ belongs to the *tangent space* to M at q denoted by T_qM. The state space for the dynamical system is the $2m$ dimensional manifold $TM = \bigcup_{q\in M} T_qM$, called the *tangent bundle*.

A *virtual displacement* of the system at a configuration $q \in M$ is an infinitesimal displacement δq that takes the system to an admissible configuration $q' \in M, q' = q + \delta q$. Clearly, δq is a virtual displacement if and only if it is infinitesimal and satisfies $\delta q \in T_qM$. If a system in configuration q is acted upon by a *generalized force, Q*, then the *virtual work* performed by the force under a virtual displacement δq is $\delta W = Q^T \delta q$.

Let M be the m-dimensional configuration manifold for a Lagrangian system and suppose $v_1, \ldots, v_m$ constitute a system of m linearly independent vector fields on M. Then each commutator or Lie bracket can be expressed

$$[v_i, v_j] = \sum_{k=1}^{m} c_{ij}^k(q) v_k \tag{6.3}$$

Indeed, the coefficients are easily computed in local coordinates.[2] Define

$$V := [v_1\ v_2\ \cdots v_m],\ \ U = \begin{bmatrix} u_1 \\ u_2 \\ \vdots \\ u_m \end{bmatrix} := V^{-1},\ \chi_{ij} = [c_{ij}^1\ c_{ij}^2\ \ldots c_{ij}^m]^t. \tag{6.4}$$

Then (6.3) yields

$$\chi_{ij} = U[v_i, v_j] \quad \text{or} \quad c_{ij}^k = u_k[v_i, v_j]. \tag{6.5}$$

Suppose $q(t) : [t_1,t_2] \mapsto M$ is a smooth path, then $\dot{q}(t)$ denotes the tangent vector to the path at the point $q(t) \in M$. Thus, we can always express $\dot{q}(t)$ as a linear combination of the tangent vectors $v_i, i = 1, \ldots, m$:

$$\dot{q} = \sum_{i=1}^{m} v_i(q) p$$

or:

$$\dot{q} = V(q) p \tag{6.6}$$

where

$$p = U(q)\dot{q} \tag{6.7}$$

The variables p are called *quasi-velocities*. Since these quantities are "velocities" we might try to associate them with a set of coordinates π, in the sense that $\dot{\pi} = p$. This is not always possible because in view of (6.7) we must have

$$\delta\pi = U(q) dq$$

but, in fact, the right hand side (of each $\delta\pi_i$) may not be an exact differential.

[2] In local coordinates, vector fields on a manifold of dimension m may be thought of as column vectors of length m and covector fields as row vectors of length m. We will use this device often to do calculations.

6.2.2 Poincaré's Form of Lagrange's Equations

First, let us review some elementary variational constructions that will be used in the drivation of Poincaré's eqauations. If $f : M \mapsto R$ is a smooth function, then $v_i(f)$ is the derivative of f in the direction of the vector field v_i. The rate of change of f along the path is given by

$$\dot{f} = \frac{\partial f}{\partial q}\dot{q} = \sum_{i=1}^{m} v_i(f)p_i \tag{6.8}$$

where the variables p_i are the quasi–velocities defined above.

Once again, consider the smooth path and suppose the end points are q_1, and q_2, i.e., $q(t_1) = q_1, q(t_2) = q_2$. A variation of $q(t)$ is a smooth map $q(\varepsilon,t) : (-\varepsilon_0,\varepsilon_0) \times [t_1,t_2] \to M$ such that $q(0,t) = q(t)$. For every variation, we can define

$$w(t) = \frac{\partial q}{\partial \varepsilon}(0,t) \tag{6.9}$$

$w(t)$ may be thought of as a vector field defined on M along $q(t)$. Conversely, let $w(t)$ be any smooth vector field defined on M along $q(t)$ with $w(t_1) = 0$ and $w(t_2) = 0$. For any such vector field, there is a variation such that (6.9) is satisfied. The implication of this is that we can define variations of $q(t)$ in the form

$$q(\varepsilon,t) = q(t) + \varepsilon w(t). \tag{6.10}$$

It is always possible to write the Lagrangian in terms of q and p. Set $\tilde{L}(p,q) = L(\dot{q},q)$. In terms of $\tilde{L}$ Lagrange's equations are attainable in the form given by the following lemma.

Proposition 6.1. *Hamilton's principle leads to the equations of motion in terms of the coordinates q, p*

$$\frac{d}{dt}\frac{\partial \tilde{L}}{\partial p_k} - \sum_{i;j=1}^{m} c^i_{jk}\frac{\partial \tilde{L}}{\partial p_i}p_j - v_k(\tilde{L}) = Q^t v_k, \quad k = 1,\ldots,m \tag{6.11}$$

or, in local coordinates,

$$\frac{d}{dt}\frac{\partial \tilde{L}}{\partial p} - \sum_{j=1}^{m} p_j \frac{\partial \tilde{L}}{\partial p} U \mathrm{X}_j - \frac{\partial \tilde{L}}{\partial q}V = Q^t V \tag{6.12}$$

where $V = [v_1\ v_2 \cdots v_m]$ and $\mathrm{X}_j = [[v_j,v_1][v_j,v_2]\cdots[v_j,v_m]]$.

Proof: (following Arnold et al [5]). Let $q(\varepsilon,t)$ be a variation of the path $q(t)$. Then we can set

$$\frac{\partial f(q(\varepsilon,t))}{\partial t} = \sum_i v_i(f)p_i \tag{6.13}$$

$$\frac{\partial f(q(\varepsilon,t))}{\partial \varepsilon} = \sum_j v_j(f) w_j \tag{6.14}$$

Among other things, this associates with each fixed t along the path $q(t)$, a virtual displacement $\delta q = \sum_k v_k w_k = Vw$. Differentiating (6.13) with respect to ε and using the fact that differentiation with respect to q and ε commute we obtain:

$$\frac{\partial^2 f(q(\varepsilon,t))}{\partial \varepsilon \partial t} = \sum_i v_i(\frac{\partial f}{\partial \varepsilon}) p_i + v_i(f)\frac{\partial p_i}{\partial \varepsilon} = \sum_{i,j} v_i(v_j(f)) w_j p_i + \sum_i v_i(f)\frac{\partial p_i}{\partial \varepsilon}$$

Similarly, differentiating (6.14) with respect to t results in

$$\frac{\partial^2 f(q(\varepsilon,t))}{\partial t \partial \varepsilon} = \sum_{j,i} v_j(v_i(f)) p_i w_j + \sum_j v_j(f)\frac{\partial w_j}{\partial t}$$

Equating these expressions, we obtain

$$\sum_i v_i(f)\frac{\partial p_i}{\partial \varepsilon} = \sum_{j,i} (v_j(v_i(f)) - v_i(v_j(f)) p_i w_j + \sum_j v_j(f)\frac{\partial w_j}{\partial t}$$

$$\sum_i v_i(f)\frac{\partial p_i}{\partial \varepsilon} = \sum_{j,i} [v_i, v_j](f) p_i w_j + \sum_j v_j(f)\frac{\partial w_j}{\partial t}$$

$$\sum_i v_i(f)\frac{\partial p_i}{\partial \varepsilon} = \sum_{j,i}\sum_k c_{ij}^k v_k(f) p_i w_j + \sum_j v_j(f)\frac{\partial w_j}{\partial t}$$

Now, renaming some summation indices

$$\sum_k v_k(f)\frac{\partial p_k}{\partial \varepsilon} = \sum_k v_k(f)\sum_{j,i} c_{ij}^k p_i w_j + \sum_k v_k(f)\frac{\partial w_k}{\partial t}$$

In view of the fact that this relation must hold for any f and any variation $q(\varepsilon,t)$, we have:

$$\frac{\partial p_k}{\partial \varepsilon} = \sum_{j,i} c_{ij}^k p_i w_j + \frac{\partial w_k}{\partial t}$$

We can use this formula to calculate the variation of the action integral

$$\delta \int_{t_1}^{t_2} \tilde{L}(p,q)dt = \lim_{\varepsilon\to 0}\frac{d}{d\varepsilon}\int_{t_1}^{t_2} \tilde{L}(p(\varepsilon,t),q(\varepsilon,t))dt$$

$$\begin{aligned}\frac{d}{d\varepsilon}\int_{t_1}^{t_2}\tilde{L}(p(\varepsilon,t),q(\varepsilon,t))dt &= \int_{t_1}^{t_2}\left\{\tilde{L}_p\frac{\partial p}{\partial\varepsilon}+\tilde{L}_q\frac{\partial q}{\partial\varepsilon}\right\}dt\\ &= \int_{t_1}^{t_2}\left\{\sum_k\tilde{L}_{p_k}\left(\sum_{j,i}c_{ij}^k p_i w_j+\frac{\partial w_k}{\partial t}\right)+\tilde{L}_q\frac{\partial q}{\partial\varepsilon}\right\}dt\end{aligned}$$

Integrating by parts the second term of the integral

$$\delta\int_{t_1}^{t_2}\tilde{L}(p,q)dt=\sum_k\frac{\partial\tilde{L}}{\partial p_k}w_k\Big|_{t_1}^{t_2}+\int_{t_1}^{t_2}\sum_k\left[-\frac{d}{dt}\frac{\partial\tilde{L}}{\partial p_k}+\sum_{i,j}c_{ik}^j\frac{\partial\tilde{L}}{\partial p_j}p_i+v_k(\tilde{L})\right]w_k dt$$

Now, we use the fact that

$$Q^T\delta q=\sum_k Q^T v_k w_k$$

to obtain

$$\begin{aligned}\int_{t_1}^{t_2}\left\{\delta\tilde{L}(p,q)+Q^T\delta q\right\}dt &= \sum_k\frac{\partial\tilde{L}}{\partial p_k}w_k\Big|_{t_1}^{t_2}\\ &+\int_{t_1}^{t_2}\sum_k\left[-\frac{d}{dt}\frac{\partial\tilde{L}}{\partial p_k}+\sum_{i,j}c_{ik}^j\frac{\partial\tilde{L}}{\partial p_j}p_i+v_k(\tilde{L})+Q^T v_k\right]w_k dt\end{aligned}\tag{6.15}$$

Since the variations w_k are independent in the interval $t_1<t<t_2$ and vanish at its end points, we have the desired result. ■

Remark 6.2 (Remarks on Poincaré's Equations). We will make a few general observations about Equations (6.11) and (6.12):

1. These equations are referred to as Poincaré's equations Arnold et al [5], Chetaev [6, 7] and Lagrange's equations in quasi-coordinates by Meirovitch [8] and Neimark and Fufaev [9]. They are related to Caplygin's equations and to the Boltzman-Hamel equations [9] and also to the generalized Lagrange equations of Noble (see Kwatny et al [64]).

2. Poincaré's equation (6.11) or (6.12) along with (6.6) form a closed system of first order differential equations which may be written in the form

$$\dot{q}=V(q)p\tag{6.16}$$

$$\dot{p}^t\frac{\partial^2\tilde{L}}{\partial p^2}+p^tV^t\frac{\partial^2\tilde{L}}{\partial q^t\partial p}-\sum_{j=1}^m p_j\frac{\partial\tilde{L}}{\partial p}U\mathrm{X}_j-\frac{\partial\tilde{L}}{\partial q}V=Q^tV\tag{6.17}$$

3. If M is a Lie group G and $v_i, i=1,\ldots,m$ are independent right-invariant vector fields on G, then c_{ij}^k = constant, i.e., they are independent of q. If, in addition,

$\tilde{L}$ is invariant under right translations on G, then $v_k(\tilde{L}) \equiv 0$ and $\tilde{L}$ depends only on the quasi-velocities p. Thus, the Poincaré equations form a closed system of differential equations on the Lie algebra $\mathbf{g}$ of the Lie group G, i.e., in the quasi-velocities p.

4. Notice that $L(\dot{q},q) = \tilde{L}(U(q)\dot{q},q)$. Thus, Lagrange's equations can be written

$$\frac{d}{dt}\frac{\partial L}{\partial \dot{q}} - \frac{\partial L}{\partial q} = \frac{d}{dt}\left(\frac{\partial \tilde{L}}{\partial p}U(q)\right) - \frac{\partial \tilde{L}}{\partial p}\frac{\partial U(q)\dot{q}}{\partial q} - \frac{\partial \tilde{L}}{\partial q} = Q^t$$

from which we can derive:

$$\frac{d}{dt}\frac{\partial \tilde{L}}{\partial p} - \sum_{j=1}^{m} p_j \frac{\partial \tilde{L}}{\partial p} U \mathrm{X}_j - \frac{\partial \tilde{L}}{\partial q}V = Q^t V$$

Thus, formally, we can derive Poincare's equations from lagrange's equations.

Example 6.3 (Rotating Rigid Body). A classic example of the application of Poincaré's equations is a rigid body with one point **O** fixed in space so that the body is free to rotate about **O**. The configuration of the body at any time t can be associated with the rotation matrix $L(t) \in SO(3)$ which characterizes the relative angular orientation of a body fixed frame with origin at **O** with respect to a space fixed frame with origin also at **O**. The velocity of rotation $\dot{L}(t)$ may be thought of as a tangent vector to the group $SO(3)$ at the point $L(t)$. It is commonplace to translate this vector to the tangent space to the group at the identity, therby associating the velocity with an element of the Lie algebra $\mathbf{so}(3)$. As described in the previous chapter, we do this with left translations so that the skew symmetric matrix $\tilde{\omega}_b = L^{-1}(t)\dot{L}(t)$ represents the angular velocity of the the body in the body frame. Recall that the matrix $\tilde{\omega}_b$ can be associated with the vector ω_b via the relation

$$\tilde{\omega}_b = \begin{bmatrix} 0 & -\omega_{b3} & \omega_{b2} \\ \omega_{b3} & 0 & -\omega_{b1} \\ -\omega_{b2} & \omega_{b1} & 0 \end{bmatrix}$$

The mapping $f : L^{-1}\dot{L} \mapsto \omega$ defines an isomorphism of the Lie algebra $\mathbf{so}(3)$ to R^3.

Notice also that a basis for the tangent space to $SO(3)$ at the identity is

$$A_1 = \begin{bmatrix} 0 & 0 & 0 \\ 0 & 0 & -1 \\ 0 & 1 & 0 \end{bmatrix}, A_2 = \begin{bmatrix} 0 & 0 & 1 \\ 0 & 0 & 0 \\ -1 & 0 & 0 \end{bmatrix}, A_3 = \begin{bmatrix} 0 & -1 & 0 \\ 1 & 0 & 0 \\ 0 & 0 & 0 \end{bmatrix} \tag{6.18}$$

We can regard these as a basis for the Lie algebra $\mathbf{so}(3)$.

If $R(t)$ is the position vector, in the space frame, of a point fixed in the body, then $R(t) = L(t)R(0)$. Thus,

$$V(t) = \dot{R}(t) = \dot{L}(t)R(0) = L(t)\tilde{\omega}(t)R(t) = \omega_s \times R(t) \tag{6.19}$$

where ω_s is the angular velocity vector represented in the space frame. Thus the abstract characterization of the rotational velocity of a rigid body does indeed coincide with the conventional notion of angular velocity. Similarly, if $r(t)$ is the inertial position vector of the body fixed point, represented in the body frame, then $r(t) = L^{-1}(t)R(t)$, and

$$v(t) = L^{-1}(t)V(t) = L^{-1}\omega_s \times R(t) = L^{-1}(t)\omega_s \times L(t)r(t) = \tilde{\omega}_b(t)r(t) = \omega_b(t) \times r(t)$$

which is the body frame equivalent of (6.19).

Suppose that $I_b = \text{diag}(I_1, I_2, I_3)$ is the inertia tensor in principle (orthogonal) body coordinates and suppose e_1, e_2, e_3 denote unit vectors of the principle axes, indexed in the usual way to provide a right hand system: $e_1 \times e_2 = e_3$, $e_2 \times e_3 = e_1$, $e_3 \times e_1 = e_2$. Let v_1, v_2, v_3 denote the preimages of e_1, e_2, e_3 under the isomorphism $f : \mathbf{so}(3) \to R^3$. Then v_1, v_2, v_3 are left-invariant vector fields on $SO(3)$ and they satisfy.[3]

$$[v_1, v_2] = v_3,\ [v_2, v_3] = v_1,\ [v_3, v_1] = v_2 \tag{6.20}$$

Thus, we can define quasi-velocities in terms of these vector fields as in (6.6) and (6.7). Let

$$\omega_b = \omega_{b1}e_1 + \omega_{b2}e_2 + \omega_{b3}e_3 \tag{6.21}$$

so that the kinetic energy can be written

$$T(\omega_b) = \tfrac{1}{2}\left\{I_1\omega_{b1}^2 + I_2\omega_{b2}^2 + I_3\omega_{b3}^2\right\}_j = \tfrac{1}{2}\omega_b^T I_b \omega_b \tag{6.22}$$

The potential energy is zero, so we have $\tilde{L} = T(\omega_b)$. Since $\tilde{L}$ is independent of the coordinates and in the absence of external forces Poincaré's equations reduce to

$$\frac{d}{dt}\frac{\partial \tilde{L}}{\partial \omega_b} - \sum_{j=1}^{3} \omega_{bj}\frac{\partial \tilde{L}}{\partial \omega_b} UX_j = 0 \tag{6.23}$$

Recall that (think local) $X_j = [[v_j, v_1]\ [v_j, v_2]\ [v_j, v_3]]$, from which we compute

$$X_1 = [0\ v_3\ -v_2],\ X_2 = [-v_3\ 0\ v_1],\ X_3 = [v_2\ -v_1\ 0]$$

which can be expressed

$$X_1 = [v_1\ v_2\ v_3]\begin{bmatrix} 0 & 0 & 0 \\ 0 & 0 & -1 \\ 0 & 1 & 0 \end{bmatrix} \tag{6.24}$$

$$X_2 = [v_1\ v_2\ v_3]\begin{bmatrix} 0 & 0 & 1 \\ 0 & 0 & 0 \\ -1 & 0 & 0 \end{bmatrix} \tag{6.25}$$

[3] This can also be verified by computing the commutators of the basis elements (6.18) via AB-BA

$$X_3 = [v_1\ v_2\ v_3] \begin{bmatrix} 0 & -1 & 0 \\ 1 & 0 & 0 \\ 0 & 0 & 0 \end{bmatrix} \tag{6.26}$$

Since $U = [v_1\ v_2\ v_3]^{-1}$ we have

$$\begin{aligned} \sum_{j=1}^{3} \omega_{bj} \tfrac{\partial \tilde{L}}{\partial \omega_b} U X_j = \omega_b^T I_b \Bigg\{ & \omega_{b1} \begin{bmatrix} 0 & 0 & 0 \\ 0 & 0 & -1 \\ 0 & 1 & 0 \end{bmatrix} \\ & + \omega_{b2} \begin{bmatrix} 0 & 0 & 1 \\ 0 & 0 & 0 \\ -1 & 0 & 0 \end{bmatrix} + \omega_{b3} \begin{bmatrix} 0 & -1 & 0 \\ 1 & 0 & 0 \\ 0 & 0 & 0 \end{bmatrix} \Bigg\} \\ = \omega_b^T I_b \tilde{\omega}_b^T & \end{aligned}$$

and finally,

$$I_b \dot{\omega}_b + \tilde{\omega}_b I_b \omega_b = 0 \tag{6.27}$$

These are recognized as Euler's equations.

Example 6.4 (Submerged Rigid Body). Consider a rigid body free to translate and rotate in an fricitionless, incompressible fluid of density ρ and infinite extent. The configuration manifold is the group of rotations and translations of R^3, $SE(3)$. As discussed in the previous chapter, the rigid body configuration may be regarded as the matrix

$$X = \begin{bmatrix} L^T & R \\ 0 & 1 \end{bmatrix}$$

and the corresponding velocity is an element in the corresponding Lie algebra $\mathbf{se}(3)$,

$$p = X^{-1}\dot{X} = \begin{bmatrix} \tilde{\omega}_b & v_b \\ 0 & 0 \end{bmatrix} \leftrightarrow \begin{bmatrix} \omega_b \\ v_b \end{bmatrix}$$

Recall that $SE(3)$ is the product of the rotation group $SO(3)$ and the translation group R^3. Its Lie algebra $\mathbf{se}(3)$ has basis vectors:

$$A_1 = \begin{bmatrix} 0 & 0 & 0 & 0 \\ 0 & 0 & -1 & 0 \\ 0 & 1 & 0 & 0 \\ 0 & 0 & 0 & 0 \end{bmatrix}, A_4 = \begin{bmatrix} 0 & 0 & 0 & 1 \\ 0 & 0 & 0 & 0 \\ 0 & 0 & 0 & 0 \\ 0 & 0 & 0 & 0 \end{bmatrix}$$

$$A_2 = \begin{bmatrix} 0 & 0 & 1 & 0 \\ 0 & 0 & 0 & 0 \\ -1 & 0 & 0 & 0 \\ 0 & 0 & 0 & 0 \end{bmatrix}, A_5 = \begin{bmatrix} 0 & 0 & 0 & 0 \\ 0 & 0 & 0 & 1 \\ 0 & 0 & 0 & 0 \\ 0 & 0 & 0 & 0 \end{bmatrix}$$

$$A_3 = \begin{bmatrix} 0 & -1 & 0 & 0 \\ 1 & 0 & 0 & 0 \\ 0 & 0 & 0 & 0 \\ 0 & 0 & 0 & 0 \end{bmatrix}, A_6 = \begin{bmatrix} 0 & 0 & 0 & 0 \\ 0 & 0 & 0 & 0 \\ 0 & 0 & 0 & 1 \\ 0 & 0 & 0 & 0 \end{bmatrix}$$

Let $v_1, v_2, v_3, v_4, v_5, v_6$ denote the corresponding left-invariant vector fields. Then we easily compute the commutator relations. The nontrivial ones are:

$$[v_1, v_2] = v_3, \quad [v_1, v_3] = -v_2, \quad [v_1, v_5] = v_6, \quad [v_1, v_6] = -v_5, \quad [v_2, v_3] = v_1,$$
$$[v_2, v_4] = -v_6, \quad [v_2, v_6] = v_4, \quad [v_3, v_4] = v_5, \quad [v_3, v_5] = -v_4$$

Thus, we can express each of the X_j in the form

$$X_j = [v_1 v_2 v_3 v_4 v_5 v_6] \Lambda_j = V \Lambda_j$$

where each Λ_j is a 6×6 column 'reordering' matrix. These are

$$\Lambda_1 = \begin{bmatrix} 0 & 0 & 0 & 0 & 0 & 0 \\ 0 & 0 & 0 & 0 & 0 & 0 \\ 0 & 0 & 1 & 0 & 0 & 0 \\ 0 & -1 & 0 & 0 & 0 & 0 \\ 0 & 0 & 0 & 0 & 0 & 1 \\ 0 & 0 & 0 & 0 & -1 & 0 \end{bmatrix}, \Lambda_2 = \begin{bmatrix} 0 & 0 & 0 & 0 & 0 & 0 \\ 0 & 0 & -1 & 0 & 0 & 0 \\ 0 & 0 & 0 & 0 & 0 & 0 \\ 1 & 0 & 0 & 0 & 0 & -1 \\ 0 & 0 & 0 & 0 & 0 & 0 \\ 0 & 0 & 0 & 1 & 0 & 0 \end{bmatrix}$$

$$\Lambda_3 = \begin{bmatrix} 0 & 1 & 0 & 0 & 0 & 0 \\ -1 & 0 & 0 & 0 & 0 & 0 \\ 0 & 0 & 0 & 0 & 0 & 0 \\ 0 & 0 & 0 & 0 & 1 & 0 \\ 0 & 0 & 0 & -1 & 0 & 0 \\ 0 & 0 & 0 & 0 & 0 & 0 \end{bmatrix}, \Lambda_4 = \begin{bmatrix} 0 & 0 & 0 & 0 & 0 & 0 \\ 0 & 0 & 0 & 0 & 0 & -1 \\ 0 & 0 & 0 & 0 & 1 & 0 \\ 0 & 0 & 0 & 0 & 0 & 0 \\ 0 & 0 & 0 & 0 & 0 & 0 \\ 0 & 0 & 0 & 0 & 0 & 0 \end{bmatrix}$$

$$\Lambda_5 = \begin{bmatrix} 0 & 0 & 0 & 0 & 0 & -1 \\ 0 & 0 & 0 & 0 & 0 & 0 \\ 0 & 0 & 0 & 1 & 0 & 0 \\ 0 & 0 & 0 & 0 & 0 & 0 \\ 0 & 0 & 0 & 0 & 0 & 0 \\ 0 & 0 & 0 & 0 & 0 & 0 \end{bmatrix}, \Lambda_6 = \begin{bmatrix} 0 & 0 & 0 & 0 & 1 & 0 \\ 0 & 0 & 0 & -1 & 0 & 0 \\ 0 & 0 & 0 & 0 & 0 & 0 \\ 0 & 0 & 0 & 0 & 0 & 0 \\ 0 & 0 & 0 & 0 & 0 & 0 \\ 0 & 0 & 0 & 0 & 0 & 0 \end{bmatrix}$$

Any motion of an ideal fluid can be characterized by a *velocity potential* ϕ that satisfies the partial differential equation $\nabla^2 \phi = 0$ in the coordinates (x, y, z) of a body fixed frame. The velocity of at any point within the fluid or on the body surface is given by $u = -\nabla \phi$ and the pressure by $P = \rho \phi$. Khirchoff showed that the if the fluid is at rest at infinity ($\nabla \phi = 0$ at infinity), the potential function is a linear function of the rigid body velocity, i.e.,

$$\phi(x, y, z) = a(x, y, z) p$$

the coefficient row vector can be explicitly computed for simple rigid body shapes, such as an elipsoid, or it can be computed via finite element approximaton for shapes of arbitrary complexity.

The kinetic energy of the fluid can be expressed as the integral of the fluid pressure times the normal velocity over the surface of the body. The result is that the fluid kinetic energy is a quadratic function of the body velocity

$$T_f = \tfrac{1}{2} p^T M_f p,\ M_f^T = M_f = \begin{bmatrix} M_{f11} & M_{f12} \\ M_{f12}^T & M_{f22} \end{bmatrix}$$

For convenience, we fix the origin of the body frame at the center of buoyancy and suppose that in this frame the center of mass is located at r_{com}. If the body has mass m_b and inertia matrix J_b (about the center of mass) the the body kinetic energy is

$$T_b = \tfrac{1}{2} p^T M_b p,\ M_b = \begin{bmatrix} m_b I & -m_b \tilde{r}_{com} \\ m_b \tilde{r}_{com} & J_b \end{bmatrix}$$

Thus, we have

$$T(p) = \tfrac{1}{2} p^T M p,\ M = M_f + M_b$$

The system potential energy arises from the gravitational field. If we assume that the body has neutral buoyancy (displace fluid mass is the same as the vehicle mass) and that the center of buoyancy and center of mass coincide, then the potential energy function is identically zero. The Lagrangian, then, is $\tilde{L} = T(p)$. Now, we compute

$$\sum_{j=1}^{6} p_j \frac{\partial \tilde{L}}{\partial p} U X_j = \left(p^T M\right) \sum_{j=1}^{6} p_j \Lambda_j = p^T M \begin{bmatrix} \tilde{\omega}_b^T & \tilde{v}_b^T \\ 0 & \tilde{\omega}_b^T \end{bmatrix}$$

and, finally

$$M \begin{bmatrix} \dot{\omega}_b \\ \dot{v}_b \end{bmatrix} + \begin{bmatrix} \tilde{\omega}_b & \tilde{v}_b \\ 0 & \tilde{\omega}_b \end{bmatrix} M \begin{bmatrix} \omega_b \\ v_b \end{bmatrix} = 0$$

Notice that if we define the momentum

$$\begin{bmatrix} \Pi \\ P \end{bmatrix} = M \begin{bmatrix} \omega_b \\ v_b \end{bmatrix}$$

Then the equations can be expressed (recall, $\tilde{a}b = a \times b$, $a, b \in R^3$)

$$\dot{\Pi} + \omega_b \times \Pi + v_b \times P = 0$$

$$\dot{P} + \omega_b \times P = 0$$

These can be compared with those given by Leonard [72].

6.3 Chain and Tree Configurations

In general a multibody system can be viewed in terms of an underlying tree structure upon which is imposed additional algebraic and/or differential constraints. In this section we describe the assembly of dynamical equations for the tree. In later sections we show how these equations are modified to accommodate any additional constraints. A tree can be defined in terms of a set of chains, each beginning at the root body. We describe in some detail the process of modeling a chain. Extending the process to a tree requires is merely a book keeping process.

6.3.1 Kinetic Energy and Poincaré's Equations

The key issue in developing Lagrange's or Poincaré's equations is the formulation of the kinetic energy function and we focus on that construction. It is necessary to define a spatial inertia tensor. Recall the recursive velocity relation from the previous Chapter.

$$V^k(k) = \phi(k,k-1)V^{k-1}(k-1) + H^k(k)\beta^k(k), \;\; k = 1, \ldots, K, \;\; V^0(0) = 0 \quad (6.28)$$

Consider the kth rigid link and let $I_{cm}(k)$ denote the inertia tensor about the center of mass in coordinates F^k, $m(k)$ denote the mass, and $a(k)$ denote the position vector from the center of mass to an arbitrary point O. The spatial inertia about the center of mass, M_{cm}, and about O, M_o, are

$$M_{cm}(k) = \begin{bmatrix} I_{cm} & 0 \\ 0 & mI \end{bmatrix}$$

$$M_o(k) = \phi^*(a)M_{cm}(k)\phi(a) = \begin{bmatrix} I_o & m\tilde{a} \\ -m\tilde{a} & mI \end{bmatrix} \quad (6.29)$$

where I_o is the inertia tensor about O.

The spatial velocity and spatial inertia matrix and, hence, the kinetic energy function for the entire chain can now be conveniently constructed. Let us define the chain spatial velocity and joint quasi-velocity

$$V = [V^T(1), \ldots, V^T(K)]^T, \;\; \beta = [\beta^T(1), \ldots, \beta^T(k)]^T \quad (6.30)$$

so that we can write

$$V = \Phi\mathscr{H}\beta \quad (6.31)$$

where

$$\Phi = \begin{bmatrix} I & 0 & \ldots & 0 \\ \phi(2,1) & I & \ldots & 0 \\ : & : & : & : \\ \phi(K,1) & \phi(K,2) & \ldots & I \end{bmatrix}$$

$$\mathscr{H} = \begin{bmatrix} H(1) & 0 & \ldots & 0 \\ 0 & H(2) & \ldots & 0 \\ : & : & : & : \\ 0 & 0 & \ldots & H(K) \end{bmatrix} \quad (6.32)$$

$$\phi(i,j) = \phi(i,i-1)\ldots\phi(j+1,j), \;\; i = 2,..,K \;\; \text{and} \;\; j = 1,..,K-1$$

The following result is easily verified.

Proposition 6.5. *The kinetic energy function for the chain consisting of links 1 through K is*

$$K.E._{chain} = \tfrac{1}{2}\beta^T\mathscr{M}\beta \quad (6.33)$$

where the chain inertia matrix is

$$\mathscr{M} = \mathscr{H}^T\Phi^T M\Phi\mathscr{H}, \quad M = diag\{M_o(1), \ldots, M_o(K)\} \quad (6.34)$$

Remark 6.6 (The Structure of Poincaré's Equations). The above definitions and constructions provide the kinetic energy function in the form

$$\tilde{T}(q,p) = (1/2)p^T M(q)p$$

Hence, we reduce Poincaré's Equations to the form:

$$M(q)\dot{p} + C(q,p)p + F(q) = Q_p \tag{6.35}$$

where

$$C(q,p) = -\left[\frac{\partial M(q)p}{\partial q}V(q)\right] + \frac{1}{2}\left[\frac{\partial M(q)p}{\partial q}V(q)\right]^T + \left[\sum_{j=1}^{m} p_j X_j^T\right] V^{-T} \tag{6.36}$$

$$F(q) = V^T(q)\frac{\partial \mathscr{U}(q)}{\partial q^T}, \;\; Q_p = V^T(q)Q \tag{6.37}$$

$\mathscr{U}(q)$ is the potential energy function. Notice that Q_p denotes the generalized forces represented in the p-coordinate frame whereas Q denotes the generalized forces in the $\dot{q}$-coordinate frame (aligned with q).

Remark 6.7 (Remark on Computations). The key point to be noted is that the matrix Φ (and hence the product $\Phi.\mathscr{H}$) can be recursively computed. Thus, we can compute the spatial velocity of any or all of the bodies via (6.30) and the inertia matrix using (6.34). Once this is done, we compute $C(q,p)$, $F(q)$, and Q_p explicitly using equations (6.36) and (6.37), assuming that the potential energy function $P(q)$ and the generalized force vector Q are available. In general, both P and Q are defined in terms of coordinates and velocities (in the case of Q) other than the configuration coordinates q and the quasi–velocities p. Thus, it is necessary to develop any transformations required to obtain P and Q in terms of q and p. We will illustrate this process below. For now, we note that velocity transformations are recursively constructed using relations like (6.28) or (6.31), and coordinate transformations are built up from the usual sequential multiplications of configuration matrices. Assembly of the system gravitational potential energy and end effector position and orientation, needed below, require constructions of this type.

Remark 6.8 (Poincaré vs. Lagrange Equations). Notice that the kinetic energy can be expressed in terms of $\dot{q}$ rather than p,

$$T(q,p) = (1/2)\dot{q}^T \left\{V^{-T}(q)M(q)V(q)^{-1}\right\}\dot{q},$$

and hence we have the essential data to construct Lagrange's equations rather than Poincaré's equations. However, Poincaré's equations may have important advantages. An obvious and practical one is the relative simplicity of the inertia matrix. However, there is an important theoretical consideration as well. Lagrange's equations fundamentally constitute a local representation whenever local coordinates are introduced, whereas Poincaré's equations may still admit a global description of the dynamics. This is easily seen by comparing the Lagrange and Poincaré formulations for the dynamics of a rotating rigid body. We do this below.

Example 6.9 (Double Pendulum). As a simple example we consider the double pendulum.

Define Joint Data

```
In[47]:= r1={1};H1={{1},{0},{0},{0},{0},{0}};
         q1={a1x};p1={w1x};
         r2={1};H2={{1},{0},{0},{0},{0},{0}};
         q2={a2x};p2={w2x};
         JointLst={{r1,H1,q1,p1},{r2,H2,q2,p2}};
```

Define Body Data

```
In[48]:= com1={0,0,-l}; mass1=m; out1={2,{0,0,-l}};
         Inertia1=DiagonalMatrix[{0,0,0}];
         com2={0,0,-l}; mass2=m; out2={3,{0,0,-l}};
         Inertia2=DiagonalMatrix[{0,0,0}];
         BodyLst={{com1,{out1},mass1,Inertia1},{com2,{out2},mass2,Inertia2}};
```

Define Interconnection Structure

```
In[49]:= TreeLst={{{1,1},{2,2}}};
```

Define Potential Energy

In this case only gravity contributes to the potential energy. The only generalized forces are external torques acting at the two joints.

```
In[50]:= g=gc; PE=0; Q={T1,T2};
```

```
In[51]:= {V,X,H,M,Cp,Fp,p,q}=CreateModel[JointLst,BodyLst,TreeLst,g,PE,Q];
```

We can look at some results.

```
In[52]:= V
Out[52]= {{{1}},{{1}}}
```

Recall that V returns as a list of kinematic matrices - one for each joint. Hence in this case we get two 1×1 matrices. This can be assembled into a single block diagonal matrix but it is more efficient to retain the list form.

```
In[53]:= M
Out[53]= {{2 l^2 m+l^2 m Cos[a2x]+
              l Cos[a2x] (l m+l m Cos[a2x])+l^2 m Sin[a2x]^2,l^2 m+l^2 m Cos[a2x]},
           {l^2 m+l^2 m Cos[a2x],l^2 m}}
```

```
In[54]:= Fp//MatrixForm
Out[54]= (-T1-gc l m (-2 Sin[a1x]-Sin[a1x+a2x])
          -T2+gc l m Sin[a1x+a2x])
```

We will return to this example below.

Example 6.10 (Thin Disk). As another example of the application of these functions let us consider a thin disk free to rotate about its center of mass in space without any external or gravitational forces. The single joint defining relative motion between the space frame and the body frame is considered as a simple spherical joint.

```
In[55]:= r1 = {3};
         H1 = Join[IdentityMatrix[3], DiagonalMatrix[{0,0,0}]];
         q = {q1,q2,q3};   p = {w1,w2,w3};
         JointLst = {{r1,H1,q,p}};
         m1 = 5;R1 = 2;I1 =
           DiagonalMatrix[{(1/4)*m1*R1^2,(1/4)*m1*R1^2,(1/2)*m1*R1^2}];
         cm1 = {0,0,0};oc1 = {2,{1,0,0}};
         BodyLst = {{cm1,{oc1},m1,I1}};
         TreeLst = {{{1,1}}};Q = {0,0,0};
         {V,X,H,M,Csys,Fsys,psys,qsys} =
           CreateModel[JointLst,BodyLst,TreeLst,g,0,Q];
```

We summarize the results as follows. The Euclidean configuration matrix $X(q)$ is given in Example (5.6). The kinematic equations are

$$\dot{q} = V(q)p$$

$$V(q) = \begin{bmatrix} 1 & \sin q1 \tan q2 & \cos q1 \tan q2 \\ 0 & \cos q1 & -\sin q1 \\ 0 & \sec q2 \sin q1 & \cos q1 \sec q2 \end{bmatrix},$$

and the dynamic equations

$$M(q)\dot{p} + F(q,p) = 0$$

$$M(q) = \begin{bmatrix} 5 & 0 & 0 \\ 0 & 5 & 0 \\ 0 & 0 & 10 \end{bmatrix}, \quad F(t,w) = C(q,p)p = \begin{bmatrix} 5\,w1\,w2 \\ -5\,w1\,w2 \\ 0 \end{bmatrix}$$

Poincaré's equations are recognizable as Euler's equations.

It is interesting to repeat this calculation with the simple spherical joint replaced by a compound 3 dof universal joint. The only change required in the above *Mathematica* code is to replace the definition of `r1={3}` by `r1={1,1,1}`. As noted above, the parameterization of the configuration of the rigid body is the same as that of the simple joint, i.e., $X(q)$ is unchanged and $V(q) = I_3$. The other relevant results are as follows

$$M(q) =$$

$$\begin{bmatrix} 5 & 0 & -5\sin q2 \\ 0 & 5/2(3-\cos q1) & -5/2\cos q2 \sin 2q1 \\ -5\sin q2 & -5/2\cos q2 \sin 2q1 & 10\cos q1^2 \cos q2^2 + 5\cos q2^2 \sin q1^2 + 5\sin q2 \end{bmatrix}$$

$$
\begin{aligned}
F_1(q,w) &= w3(-5w2\cos 2q1\cos q2 - 5w3\cos q2^2\sin 2q1)/2 + w2(5u3\cos q2 \\
&+ (-5w3\cos 2q1\cos q2 + 5w2\sin 2q1)/2) \\
F_2(q,w) &= 1(-5w3\cos q2/2 + 5w3\cos 2q1\cos q2 - 5w2\sin 2q1) \\
&- 5w2w3\sin 2q1\sin q2/4 \\
&+ (w3(-5w1\cos q2 + 5w2\sin 2q1\sin q2/2 - 5w3\cos q1^2\sin 2q2))/2 \\
F_3(q,w) &= w1(5w2\cos 2q1\cos q2 + 5w3\cos q2^2\sin 2q1) \\
&+ w2(5w1\cos q2 - 5w2\sin 2q1\sin q2/2 + 5w3\cos q1^2\sin 2q2)
\end{aligned}
$$

These equations are, of course, Lagrange's equations – a consequence of the fact that the joint formulation commits us to velocity coordinates alligned with the configuration coordinates. The simplicity of the kinematic matrix is more than offset by the complexity of the dynamical equations. Notice also that the dynamical equations in the previous case are independent of the configuration parameters. They are globally valid equations, whereas the latter are not.

6.3.2 Generalized Force Calculations

Building models not only requires the construction of the kinematic relations and kinetic energy function but it is also necessary to characterize the forces that act on the system. This is normally accomplished through the definition of a potential energy function, a dissipation function and/or the specification of generalized forces. The *ProPac* function `CreateModel` accepts each of these as arguments. Several computational tools are provided in *ProPac* to assist in the development of these quantities.

Potential Energy Constructions

The potential energy function $\mathscr{U}(q)$ is typically used to characterize forces due to gravity and elastic storage elements. The associated generalized force is

$$F(q) = -\frac{\partial \mathscr{U}(q)}{\partial q}$$

or

$$F(q) = -V(q)^T \frac{\partial \mathscr{U}(q)}{\partial q}$$

in the p-frame. Computing the gravitational potential energy for a multibody mechanical system is a straightforward but tedious task, since it is necessary to locate the center of mass for each body in space. For convenience, this calculation is automated in `CreateModel` for a uniform gravitational field acting in the negative z-direction. To use a coordinate system with z-axis pointing downward requires specification of the gravitational constant as $-g$.

The potential energy associated with elastic components can also involve complicated geometry. Two functions in *ProPac* can be helpful in performing these calculations. `SpringPotential` computes the potential energy expression in terms

of the configuration coordinates for a spring connected between two nodes located anywhere in the system. It is assumed that the spring potential energy is known as a function of the spring length.

`LeafPotential` is designed to facilitate computing the potential energy of components (such as tires) that interact elastically with the space frame. The potential energy function is presumed known in terms of the spatial location of a contact node. The potential energy function is computed as a function of the generalized coordinates.

Dissipation Functions

Dissipation functions are generally specified in terms of the configuration coordinates and velocities in the form of the Rayleigh dissipation potential

$$\mathscr{R}(\dot{q},q) = \dot{q}^T A(q)\dot{q} + a^T(q)\dot{q} \tag{6.38}$$

or in the more general more general Lur'e form (see [92])

$$D(q,p) = \sum_i f_i(q)v_i(p) \tag{6.39}$$

where p denotes the quasi-velocities. The generalized force associated with the Rayleigh dissipation function (in the p-frame) is

$$F(p,q) = -V^T(q)\frac{\partial R}{\partial \dot{q}}(V(q)p,q)$$

The generalized force associated with the Lur'e potential is

$$F(p,q) = -\frac{\partial \mathscr{D}(p,q)}{\partial p}$$

The function `CreateModel` accepts Lur'e type dissipation potential as an argument and computes the generalized force. The calculation required for the Rayleigh function is performed by the function `RayleighDissipationForce`.

A *ProPac* function, `DamperPotential`, can be used to construct the dissipation potential associated with a damper connected between two nodes in the system. The function is analogous to `SpringPotential`. It requires that the damper can be characterized in terms of a dissipation function depending on the relative velocity across the damper. Then a Lur'e type potential function is constructed as a function of the system coordinates and quasi-velocities.

Applied Force

One way to construct the generalized force associated with an external force applied at a specific node in the system is to view the node as an energy port. Suppose a force

$F_A \in R^6$, composed of three torques and three forces, acts at a node A in a multibody system. Let V_A denote the spatial velocity at A. Both F_A and V_A are represented in the coordinates of a body fixed frame at node A. The instantaneous power flowing into the system is $\mathscr{P} = F_A^T V_A$. In general, the application of Equations (5.66) and (5.72) of the last chapter, as in the derivation of Equation (6.31), leads to the representation of the spatial velocity at node A in terms of the system coordinates and quasi-velocities. If F_A is defined as a function of system coordinates and quasi-velocities, then $\mathscr{P}$ can be expressed in terms of these variables. Once $\mathscr{P}(p,q)$ is constructed we obtain

$$Q_p = \frac{\partial \mathscr{P}(p,q)}{\partial p} \tag{6.40}$$

To facilitate computing Q_p *ProPac* provides several computational tools. One of these, `GeneralizedForce` , is based on the construction described above. The force F_A is assumed to be given as an expression involving the spatial velocity components of a body fixed frame at the node of force application. The function `GeneralizedForce` then computes the generalized force.

Impact

The Hertz model of impact incorporates a simple characterization of the force interaction between two elastic bodies during the contact phase of a collision. During a collision the two actual colliding bodies deform. However, Hertz introduces a parameter that defines the relative position of two nondeforming virtual bodies (labeled A and B), x (see Figure (6.1)). Then a force (on body A) displacement relationship that applies during the contact phase is introduced:

$$f(x) = -K^{-3/2} x^{3/2}$$

where K is a constant that depends on the material properties and (local) geometry of the colliding bodies:

$$K = \tfrac{4}{3}\left\{ q / \left(Q_1 + Q_2 \sqrt{a+b} \right) \right\}$$

As an example, consider a sphere of radius r colliding with a plane surface. In this case,

$$A = B = 1/2r,\ q = \pi^{1/3},\ Q_1 = (1-\mu_1^2)/E_1\pi,\ Q_2 = (1-\mu_2^2)/E_2\pi$$

where E_i and μ_i denote Young's modulus and Poisson's ratio for the respective bodies.

Notice that the force interaction can be completely characterized by a potential energy function, e.g. for the interaction described above, it has the form:

$$\mathscr{V}(x) = \begin{cases} (2/5)K^{-3/2}x^{5/2} & x > 0 \\ 0 & x \le 0 \end{cases}$$

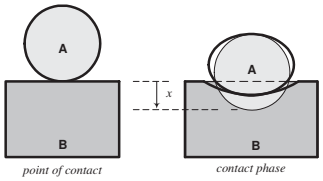

Fig. 6.1: During the contact phase of a collision the two actual bodies deform. The relative position (sometimes called relative approach) of the two bodies is an indicator of the relative location of two (virtual) undeformed bodies.

The interaction force is then recovered by $f(x) = -\partial \mathscr{V} / \partial x$. In summary, a Hertz impact model consists of: a potential function $\mathscr{V}(x) = \pi(x)u(x)$, where π is a differentiable map $\pi : R \to R$ with $\pi(0) = 0$, and an associated force function $f(x) = -\mathscr{V}_x(x) = -\pi_x(x)u(x)$, where $u(x)$ is the unit step function.

Backlash

Suppose that a symmetric backlash element with dead zone parameter ε has a smooth force function $f(x)$ during the contact phase defined by a potential energy function $\mathscr{V}(x)$. Then the backlash mechanism can be characterized by a potential function:

$$\mathscr{V}_b = \mathscr{V}(|x| - \varepsilon) = \pi(|x| - \varepsilon)u(|x| - \varepsilon)$$

so that the backlash force is given by

$$f_b(x) = \begin{cases} f(x-\varepsilon) & x > \varepsilon \\ 0 & -\varepsilon \le x \le \varepsilon \\ -f(-x+\varepsilon) & x < -\varepsilon \end{cases}$$

Working with backlash is facilitated by two functions in *ProPac*

`BacklashPotential`,

and `BacklashForce`.

The former constructs the backlash potential given a Hertz impact potential function and a backlash parameter. The latter returns the associated force. Note that the backlash potential can be included as part of the potential energy function.

Friction

Friction, particularly in joints, is an important factor in many situations. A basic characterization of friction as a static function of contact velocity should include

viscous, coulomb and static (Stribeck) effects. In order to do this efficiently with large scale multibody models we can use a dissipation potential of Lur'e type (6.39).

Suppose the friction depends on a single velocity variable, v, that can ultimately be expressed as a function of the system coordinates and quasi-velocities. Potential functions giving rise to viscous, coulomb and static effects are:

- viscous: $\frac{1}{2}c_v v^2$
- coulomb: $c_c v \operatorname{sgn}(v)$
- static: $\frac{1}{2}c_s v_s \sqrt{\pi} \operatorname{erf}\left({}^{v}/_{v_s}\right) \operatorname{sgn}(v)$

The friction parameters used above are:

c_v, viscous friction coefficient

c_c, coulomb friction coefficient

c_s, static friction coefficient

v_s, Stribeck velocity

The dissipation potential associated with a joint can be assembled with the function `JointFrictionPotential`.

Example 6.11 (Two masses with backlash and friction). Consider the system illustrated in Figure (6.2). The system is composed of two bodies and two joints. Body one translates relative to the space frame and body two translates relative to body one. Thus, the joint definitions are as follows.

```
In[56]:= r1 = {1}; H1 = Transpose[{{0,0,0,1,0,0}}];
         q1 = {x1}; p1 = {v1};
         r2 = {1}; H2 = Transpose[{{0,0,0,1,0,0}}];
         q2 = {x2}; p2 = {v2};
         JointLst = {{r1, H1, q1, p1}, {r2, H2, q2, p2}};
```

Now, we define the body data. The masses can be treated as point masses so we define the inertia matrices to be zero.

```
In[57]:= com1 = {0,0,0}; mass1 = m1; out1 = {2, {0,0,0}};
         Inertia1 = {{0,0,0}, {0,0,0}, {0,0,0}};
         com2 = {0,0,0}; mass2 = m2; out2 = {3, {0,0,0}};
         Inertia2 = {{0,0,0}, {0,0,0}, {0,0,0}};
         BodyLst =
           {{com1, {out1}, mass1, Inertia1}, {com2, {out2}, mass2, Inertia2}};
         TreeLst = {{{1,1}, {2,2}}};
```

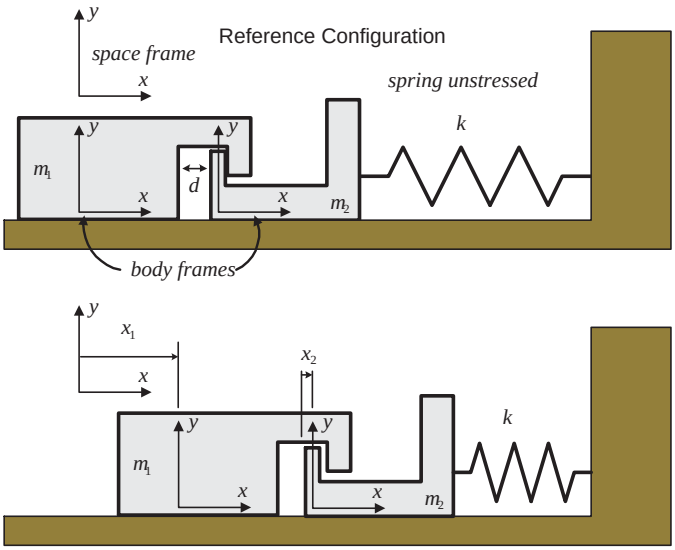

Fig. 6.2: Two masses interact through a 'loose' joint exhibiting backlash.

Bodies one and two interact through a backlash potential function constructued as follows. A simple linear material compliance is assumed. The backlash parameter is $d/2$.

```
In[58]:= PEBack[x_] := (k1 * x^2)/2;
         PE1 = BacklashPotential[PEBack, d/2, x2]
```

$$\texttt{Out[58]=}\ \frac{1}{2}\ \text{k1}\ \left(-\frac{\text{d}}{2}+\texttt{Abs}[\text{x2}]\right)^2\ \texttt{UnitStep}\left[-\frac{\text{d}}{2}+\texttt{Abs}[\text{x2}]\right]$$

The spring is assumed linear so a simple quadratic potential energy function is used.

```
In[59]:= PE2 = (1/2) * k * (x1 + x2)^2;
          PE = PE1 + PE2;
```

The sliding friction of body one is assumed to be significant so a dissipation potential function is constructed.

```
In[60]:= DissPot1 = JointFrictionPotential[v1, cv, cc, cs, vs]
```

$$\texttt{Out[60]=}\ \frac{\text{cv}\ \text{v1}^2}{2}+\text{cc}\ \texttt{Abs}[\text{v1}]+\frac{1}{2}\ (-\text{cc}+\text{cs})\ \sqrt{\pi}\ \text{vs}\ \texttt{Erf}\left[\frac{\text{v1}}{\text{vs}}\right]\ \texttt{Sign}[\text{v1}]$$

Allowing for forces FF_1 and FF_2 to act on bodies one and two, respctively, the model is assembled as follows.

```
In[61]:= Q = {FF1, FF2};
         {JV, JX, JH, MM, Cp, Fp, pp, qq} =
           CreateModel[JointLst, BodyLst, TreeLst, -g, PE, DissPot1, Q];
```

```
Computing Joint Kinematics

Computing joint 1 kinematics

Computing joint 2 kinematics

Computing Potential Functions

Computing Inertia Matrix

Computing Poincare Function
```

Let us examine the F_p function.

```
In[62]:= Fp
Out[62]=
```

$$\{-\text{FF1}+\text{cv}\ \text{v1}+\text{k}\ (\text{x1}+\text{x2})+(-\text{cc}+\text{cs})\ e^{-\frac{\text{v1}^2}{\text{vs}^2}}\ \texttt{Sign}[\text{v1}]+$$
$$\text{cc}\ (-\texttt{UnitStep}[-\text{v1}]+\texttt{UnitStep}[\text{v1}]),-\text{FF2}+\text{k}\ (\text{x1}+\text{x2})+\text{k1}$$
$$\left(-\frac{\text{d}}{2}+\texttt{Abs}[\text{x2}]\right)\ (-\texttt{UnitStep}[-\text{x2}]+\texttt{UnitStep}[\text{x2}])\ \texttt{UnitStep}\left[-\frac{\text{d}}{2}+\texttt{Abs}[\text{x2}]\right]\}$$

The expression is mixed in sign and unit step functions. It may be convert to all sign functions.

```
In[63]:= UnitStep2Sign[Fp]
Out[63]=
```

$$\{-\text{FF1}+\text{cv}\ \text{v1}+\text{k}\ \text{x1}+\text{k}\ \text{x2}+e^{-\frac{\text{v1}^2}{\text{vs}^2}}\ \left(\text{cs}+\text{cc}\ \left(-1+e^{\frac{\text{v1}^2}{\text{vs}^2}}\right)\right)\ \texttt{Sign}[\text{v1}],$$
$$-\text{FF2}+\text{k}\ \text{x1}+\text{k}\ \text{x2}+\frac{\text{k1}\ \text{x2}}{2}-\frac{1}{4}\ \text{d}\ \text{k1}\ \texttt{Sign}[\text{x2}]+\frac{1}{2}\ \text{k1}\ \text{x2}\ \texttt{Sign}\left[-\frac{\text{d}}{2}+\texttt{Abs}[\text{x2}]\right]-$$
$$\frac{1}{4}\ \text{d}\ \text{k1}\ \texttt{Sign}[\text{x2}]\ \texttt{Sign}\left[-\frac{\text{d}}{2}+\texttt{Abs}[\text{x2}]\right]\}$$

Example 6.12 (Automobile directional stability). As a somewhat more complex example we consider building a simplified automobile model often used as a basis for investigating directional stability (Figure 6.3 and Figure 6.4).

For simplicity of the resulting equations, we neglect the rotational energy of each wheel around its axle, that is $I_{yy} << 1$. Also, we will assume that s,t, and δ are sufficiently small that linear approximation in these variables is adequate. None of these assumptions are necessary, by any means, but are useful for expository purposes. For tire cornering force and alignment torque constitutive equations we take:

$$F_{corner} = \kappa\beta, \quad T_{align} = 0$$

These are applied at the tire contact point.

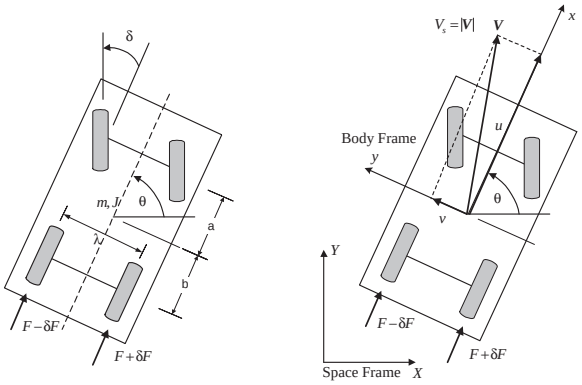

Fig. 6.3: These figures define the dimensions and variables of an automobile that moves in the $X-Y$ plane. The $x-y$ frame denotes a reference frame fixed in the body. κ_f, κ_r are the front and rear tire coefficients, respectively.The system is composed of the vehicle body and its four wheels. The front wheels are used for steering with spindles aligned to provide small amounts of caster and camber.

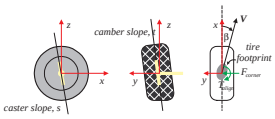

Fig. 6.4: The tire rotation involves a revolute joint with rotation axis defined by the caster and camber angles. Tire cornering force and alignment torque are functions of the sideslip angle.

Joint definitions

There are three joints. The 3 dof main body joint between the space frame and the automobile body and the two front wheel spindles

```
In[64]:= r1 = {3}; q1 = {θ, x, y}; p1 = {ω, vx, vy}; (* main body *)
         H1 = {{0,0,0},{0,0,0},{1,0,0},{0,1,0},{0,0,1},{0,0,0}};
         r2 = {1}; q2 = {delta2}; p2 = {wdel2}; (* right spindle *)
         H2 = Transpose[{{−sr, −tr, 1, 0, 0, 0}}];
         r3 = {1}; q3 = {delta3}; p3 = {wdel3}; (* left spindle *)
         H3 = Transpose[{{−sl, tl, 1, 0, 0, 0}}];
         JointLst = {{r1, H1, q1, p1}, {r2, H2, q2, p2}, {r3, H3, q3, p3}};
```

We compute the joint parameters with

```
In[65]:= {V, X, H} = Joints[JointLst];
```

Body data

The body data includes body inertial properties including center of mass locaton in the body frame and outboard node locations.

```
In[66]:= cm1 = {0,0,0};
         out1 = {{2,{a,-ℓ/2,0}},(* front left tire spindle*)
           {3,{a,ℓ/2,0}},(* front right tire spindle*)
           {4,{-b,-ℓ/2,-R}},(* rear left tire ground contact point *)
           {5,{-b,ℓ/2,-R}}};(* rear right tire ground contact point *)
         I1 = {{Jxx,0,Jxz},{0,Jyy,0},{Jxz,0,Jzz}};
         cm2 = {0,0,0};out2 = {{6,{sr R,tr R,-R}}};
         I2 = DiagonalMatrix[{Ixx,Iyy,Izz}];
         cm3 = {0,0,0};out3 = {{7,{sl R,-tl R,-R}}};
         I3 = DiagonalMatrix[{Ixx,Iyy,Izz}];

In[67]:= BodyLst = {{cm1,out1,m1,I1},{cm2,out2,m2,I2},{cm3,out3,m2,I3}};
         TreeLst = {{{1,1},{2,2}},{{1,1},{3,3}}};
         q = {θ,x,y,delta2,delta3};
         p = {ω,vx,vy,wdel2,wdel3};
```

Notice that the system has a tree structure. The tree is composed of two chains: 1) main body and right tire, 2) main body and left tire.

Tire forces

We need to compute the tire generalized forces. This requires four similar, and somewhat complicated, calculations. To do this we use the function

`GeneralizedForce`.

Furthermore, to reduce computation time (by a factor of ten in this case), we use the function

`KinematicReplacements`.

`GeneralizedForce` computes the generalized force associated with a force applied at any defined node in the system. It is usually the case that the applied force is characterized in the reference frame of the body in which the node is specified. The simplest usage is:

```
GeneralizedForce[TerminalNode,TreeLst,BodyLst,
                                        X,H,q,p,Force,VelNames]
```

`TerminalNode` is the node number at which the force is applied. F is a list of 6 expressions which defines the external torques (first three) and forces (last three) in terms of body velocities (velocities of a body fixed frame at the terminal node). VelNames is a list of (6) names of the velocities used in the expressions F. There must be six names - the first 3 corresponding to the angular velocity and the last 3 to the linear velocity. `KinematicReplacements[V,X,H]` returns {`Vnew,Xnew,Hnew,rules`} where repeated groups of expressions in `V,X,H` are replaced by temporary variables to produce `Vnew,Xnew,Hnew`. The original forms are recovered by applying the rule list "rules". It is often convenient to use the syntax `KinematicReplacements[V,X,H,q]`, which returns {`Vnew,Xnew,Hnew,rules1,rules2`}. In this usage, rules is divided into two sets. The set "rules1" depends on the coordinates q. The set "rules2" do not. rules2 involves expressions that depend only on system parameters. The application of rules1 must occur before using `CreateModel` but rules2 can be applied at any time.

```
In[68]:= {V, X, H, rules1, rules2} = KinematicReplacements[V, X, H, q];
         Force = {0, 0, 0, 0, -kappaf  ArcTan[v6y/v6x], 0}; (* right  front *)
         VelNames = {w6x, w6y, w6z, v6x, v6y, v6z};
         TerminalNode = 6;
         Q1 = GeneralizedForce[
              TerminalNode, TreeLst, BodyLst, X, H, q, p, Force, VelNames];
```

Similar calculations yield the remaining three tire forces. Then we proceed to assemble the model.

```
In[69]:= Q = Q1 + Q2 + Q3 + Q4;
         {V, X, H, Q} = Chop[{V, X, H, Q} /. rules1, 0.001];
         {V, X, H, M, Csys, Fsys, psys, qsys} =
                   CreateModel[JointLst, BodyLst, TreeLst, g, 0, Q, V, X, H];
         {V, X, H, M, Csys, Fsys, psys, qsys} =
                   {V, X, H, M, Csys, Fsys, psys, qsys} /. rules2;
```

For analysis purposes we create a model with the following two features. First, we assume that delta2 and delta3 are inputs rather than coordinates determined by the dynamics. Thus, we eliminate two degrees of freedom. Second, we choose to ignore any steering imperfections and assume delta2 and delta3 are equal and call them both δ.

```
In[70]:= qred = qsys[[{1,2,3}]];
         pred = psys[[{1,2,3}]];
         Mred =
           M[[{1,2,3},{1,2,3}]]/.Inner[Rule,{delta2,delta3},{0,0},List];
         Cred =
           Csys[[{1,2,3},{1,2,3}]]/.Inner[Rule,{delta2,delta3},{0,0},List];
         Fred = Simplify[
             (Fsys[[{1,2,3}]]/.Inner[Rule,{delta2,delta3},{δ,δ},List])
         /.{sl->s,sr->s,tl->t,tr->t,kappaf->κ,kappar->κ}];
         Fred = Truncate[Fred,{s,t},1];
         Vred = V[[{1}]];
```

The results are summarized below.

$$\begin{bmatrix}\dot\theta\\ \dot x\\ \dot y\end{bmatrix} = \begin{bmatrix}1 & 0 & 0\\ 0 & \cos\theta & -\sin\theta\\ 0 & \sin\theta & \cos\theta\end{bmatrix}\begin{bmatrix}\omega\\ v_x\\ v_y\end{bmatrix}$$

$$\begin{bmatrix} J_{zz}+2I_{zz}+2a^2m_2+{m_2\ell^2}/{2} & 0 & 2am_2\\ 0 & m_1+2m_2 & 0\\ 2am_2 & 0 & m+2m_2\end{bmatrix}\begin{bmatrix}\dot\omega\\ \dot v_x\\ \dot v_y\end{bmatrix}$$
$$+\begin{bmatrix}2am_2v_x\omega\\ -(m_1+2m_2)v_y\omega-2am_2\omega^2\\ (m_1+2m_2)v_x\omega\end{bmatrix}+f(\omega,v_x,v_y,\delta,F,\delta F)=0$$

Because of its complexity, we display f only up to second order in v_y,ω:

$$f=\begin{bmatrix}2\kappa(-bv_y+Rsv_y+(a^2+b^2)\omega+a(v_y+2Rs\omega)/v_x\\ 0\\ 2\kappa(2v_y+(a-b+Rs)\omega)/v_x\end{bmatrix}+\begin{bmatrix}0\\2\\0\end{bmatrix}F`$$
$$+\begin{bmatrix}\ell\\0\\0\end{bmatrix}\delta F+\begin{bmatrix}-2(a+Rs)\kappa\\ -2\kappa(v_y+a\omega+Rs\omega)/v_x\\ -2\kappa\end{bmatrix}\delta$$

6.4 Systems with Constraints

The above constructions apply to systems interconnected by simple and compound joints and which have a tree structure. Recall that simple and compound joints as we have defined them impose holonomic constraints on the relative motion between two bodies. We wish to generalize the class of systems to include those with closed loops and nonholonomic differential constraints.

6.4.1 Differential Constraints

Consider a system with m-dimensional configuration manifold M and state space TM. Suppose that additional (differential) constraints are imposed on the motion of the system in the form:

$$F(q)\dot{q} = 0 \tag{6.41}$$

where F is an $r \times m$ matrix of (constant) rank r, or equivalently

$$A(q)p = 0 \tag{6.42}$$

where $A(q) = F(q)V(q)$. We will examine how the imposition of differential constraints affects the equations of motion. Differential constraints may be *adjoined* to the equations of motion via the introduction of Lagrange multipliers or *embedded* which avoids the addition of any auxiliary variables [14]. We consider the latter approach.

Recall that a virtual displacement from an admissible configuration q was required to belong to the tangent space T_qM, that is the space to which velocities $\dot{q}$ naturally belong. When differential constraints such as (6.41) and (6.42) apply, velocities are further constrained to lie in the subspace of $T_qM, \ker F(q)$. Accordingly, virtual displacements are restricted by the same requirement: $F(q)\delta q = 0$.

Proposition 6.13. *Suppose the Lagrangian system of Proposition (6.1) is subject to the constraint $A(q)p = 0$, with* $\dim \ker A(q) = m - r$ *(a constant). Then the dynamical equations of motion are*

$$\dot{q} = V(q)T(q)\hat{p} \tag{6.43}$$

$$\left\{ \dot{p}^t \frac{\partial^2 \tilde{L}}{\partial p^2} + p^t V^t \frac{\partial^2 \tilde{L}}{\partial q^t \partial p} - \sum_{j=1}^{m} p_j \frac{\partial \tilde{L}}{\partial p} U \mathrm{X}_j - \frac{\partial \tilde{L}}{\partial q} V \right\} T(q) = Q^t V T(q) \tag{6.44}$$

$$p = T(q)\hat{p} \tag{6.45}$$

where $T(q)$ is an $m \times (m-r)$ matrix whose columns span $\ker A(q)$.

Proof: The calculations in the proof of Proposition (6.1) that lead to equation (6.15) remain true even when the constraint (6.41) applies. However, in this event, the variation w is not arbitrary. When (6.41) obtains, it is necessary that w satisfy $A(q)w = 0$ (recall that $\delta q = Vw$), so that we can write

$$w = T(q)\alpha \tag{6.46}$$

where the columns of $T(q)$ span $\ker[A(q)]$ and $\alpha \in R^{m-r}$ is arbitrary. Rewrite (6.15) as

$$\int_{t_1}^{t_2} \{\delta\tilde{L}(p,q) + Q^T \delta q\} dt = \sum_k \frac{\partial \tilde{L}}{\partial p_k} T \alpha_k \Big|_{t_1}^{t_2}$$

$$+ \int_{t_1}^{t_2} \sum_k \left[-\frac{d}{dt}\frac{\partial \tilde{L}}{\partial p_k} + \sum_{i,j} c_{ik}^j \frac{\partial \tilde{L}}{\partial p_j} p_i + v_k(\tilde{L}) + Q^T v_k \right] T \alpha_k dt \qquad (6.47)$$

Now, we can invoke the independence of the variations to obtain the dynamical equations

$$\left[\frac{d}{dt}\frac{\partial \tilde{L}}{\partial p_k} - \sum_{i,j=1}^{m} c_{jk}^i \frac{\partial \tilde{L}}{\partial p_i} p_j - v_k(\tilde{L}) - Q^t v_k \right] T(q) = 0 \qquad (6.48)$$

Equation (6.48) is to be solved along with (6.42) and (6.16).

Remark 6.14 (Constrained dynamics).

1. In application, we use (6.45) to replace p after the expression in curly brackets is evaluated. Then (6.43) and (6.44) form a closed system of equations in the dependent variables $(\hat{p}, q) \in R^{2m-r}$.
2. Notice that when the unconstrained dynamical equations are of the form

   $$M(q)\dot{p} + C(q,p)p + F(q) = Q_p$$

   then the constrained dynamics (6.44) are:

   $$\left[T^t(q)M(q)\right]\dot{p} + T^t(q)C(q,p)p + T^t(q)F(q) = T^t(q)Q_p$$

   or

   $$\left[T^t(q)M(q)T(q)\right]\dot{\hat{p}} + T^t(q)\left[C(q,T(q)\hat{p})T(q) + M(q)\frac{\partial T(q)\hat{p}}{\partial q}V(q)\right]\hat{p}$$
   $$+ T^t(q)F(q) = T^t(q)Q_p \qquad (6.49)$$

First, let us examine a simple example.

Example 6.15 (Sleigh on a horizontal plane). Consider a sleigh that moves on a horizontal plane as shown in Figure (6.5). Neimark and Fufaev [86] study the more general problem of a sleigh on an inclined plane (see also Problem (6.24)). The knife edge does not admit sideslip. Thus it imposes a simple differential constraint, $v_y = 0$. First, we formulate the equations of motion without the differential constraint imposed by the knife edge. Define the single (main body) joint:

```
In[71]:= r1 = {3}; q1 = {ϕ, x, y}; p1 = {ω, vx, vy}; (* main body *)
         H1 = {{0,0,0}, {0,0,0}, {1,0,0}, {0,1,0}, {0,0,1}, {0,0,0}};
         JointLst = {{r1, H1, q1, p1}};
```

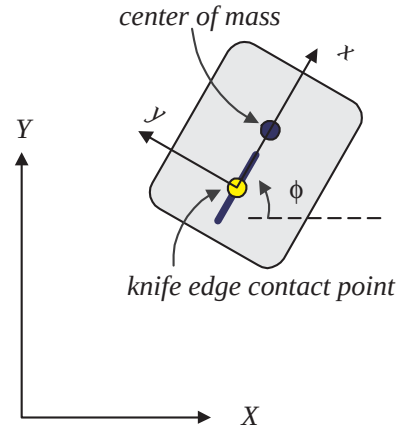

Fig. 6.5: A sleigh on a horizontal plane.

Define the body data:

```
In[72]:= cm1 = {d, 0, 0}; out1 = {{2, {d, 0, 0}}};
         I1 = {{Jxx, 0, Jxz}, {0, Jyy, 0}, {Jxz, 0, Jzz}};

         BodyLst = {{cm1, out1, m1, I1}};
         TreeLst = {{{1, 1}}};
         q = {ϕ, x, y};
         p = {ω, vx, vy};
```

Suppose a drive force F acts along the knife edge axis and a torque T acts about the z-axis. Now, set up the generalized force and obtain the (unconstrained) model:

```
In[73]:= Q = {T, F, 0};
         {V, X, H, M, Csys, Fsys, psys, qsys} =
           CreateModel[JointLst, BodyLst, TreeLst, g, 0, Q];
```

```
*** Dynamics successfully loaded ***
Computing Joint Kinematics
Computing joint 1 kinematics
Computing Potential Functions
Computing Inertia Matrix
Computing Poincare Function
```

Finally, add the constraint.

```
In[74]:= {Mm, Cm, Fm, Vm, Trans, phat} =
           DifferentialConstraints[M, Csys, Fsys, V, {vy}, p, q, {3}];

Vm

Mm

Cm

Fm

In[75]:= Vm
Out[75]= {{1, 0}, {0, Cos[ϕ]}, {0, Sin[ϕ]}}

In[76]:= Mm
Out[76]= {{Jzz + d^2  m1, 0}, {0, m1}}

In[77]:= Cm
Out[77]= {{d  m1  vx, 0}, {−d  m1  ω, 0}}

In[78]:= Fm
Out[78]= {−T, −F}
```

Thus, the dynamical equations of motion are

$$\frac{d}{dt}\begin{bmatrix}\phi\\ x\\ y\end{bmatrix} = \begin{bmatrix}1 & 0\\ 0 & \cos\phi\\ 0 & \sin\phi\end{bmatrix}\begin{bmatrix}\omega\\ v_x\end{bmatrix}$$

$$\begin{bmatrix}J_{zz}+d^2m_1 & 0\\ 0 & m_1\end{bmatrix}\frac{d}{dt}\begin{bmatrix}\omega\\ v_x\end{bmatrix} + \begin{bmatrix}0 & d\,m_1\omega\\ -d\,m_1\omega & 0\end{bmatrix}\begin{bmatrix}\omega\\ v_x\end{bmatrix} + \begin{bmatrix}-T\\ -F\end{bmatrix} = 0$$

Here is another example, only slightly more complicated.

Example 6.16 (Driven Planar Vehicle). Consider the 3-wheeled planar vehicle shown in Figure (6.6). It illustrates the calculations required to assemble a model involving multiple differential constraints. This system is also useful for illustrating basic properties of nonlinear system controllability.

The system is assumed to be composed of a main body with two rear wheels and one front wheel. The front wheel is both the steering and drive wheel. The rear wheels rotate freely about an axle fixed in the body. The assumption of pure rolling imposes a sideslip constraint, but they play no other essential role in the system behavior. Thus, we consider them to have no mass or inertia. The front wheel, on the other hand is assumed to have nontrivial inertia properties and both steering and drive torques are applied to it. It is also assumed to undergo pure rolling.

In summary, the model is composed of two bodies: (1) the main vehicle body including the rear wheels and (2) the and the front wheel. The model has two joints: (1) the main body joint – a three degree of freedom (two displacements and a rotation) joint characterizing the motion of the body in a space fixed frame, and (2) the main

body/front wheel joint – a two degree of freedom (steering column and front axle rotations) joint that characterizes the relative motion of the front wheel relative to the main body.

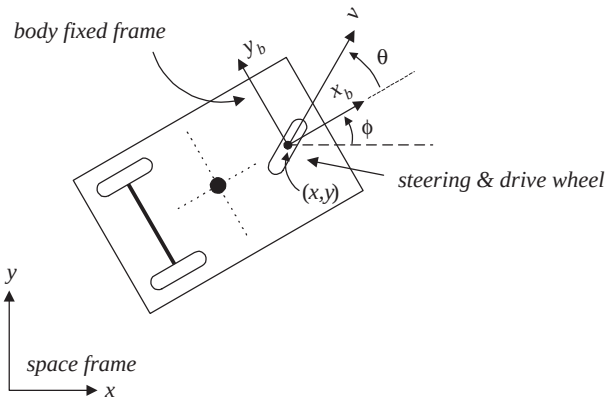

Fig. 6.6: This simple vehicle can be driven around the plane using steering and drive torques, T_s and T_d, respectively, that are applied to the front wheel. The wheelbase is denoted d and the front wheel radius R.

Joint data

```
In[79]:= r1 = {3}; q1 = {ϕ, x, y}; p1 = {ωb, vx, vy};
         H1 = {{0,0,0}, {0,0,0}, {1,0,0}, {0,1,0}, {0,0,1}, {0,0,0}};

In[80]:= r2 = {1,1}; q2 = {θf, θ}; p2 = {ωf, ω};
         H2 = {{0,0}, {1,0}, {0,1}, {0,0}, {0,0}, {0,0}, {0,0}};

In[81]:= JointLst = {{r1, H1, q1, p1}, {r2, H2, q2, p2}};
```

Body data

```
In[82]:= cm1 = {−d/2, 0, 0}; out1 = {{2, {0,0,0}}, {3, {−d, 0, −R}}};
         I1 = {{Jxx, 0, Jxz}, {0, Jyy, 0}, {Jxz, 0, Jzz}};
         cm2 = {0,0,0}; out2 = {{4, {0, RSin[θf], −RCos[θf]}}};
         I2 = DiagonalMatrix[{Ix, J, Ix}];

In[83]:= BodyLst = {{cm1, out1, m1, I1}, {cm2, out2, m2, I2}};
         TreeLst = {{{1,1}, {2,2}}};
         q = Flatten[{q1, q2}]
         p = Flatten[{p1, p2}]
Out[83]= {ϕ, x, y, θf, θ}
Out[83]= {ωb, vx, vy, ωf, ω}
```

Unconstrained Model Assembly

```
In[84]:= Q = {0, 0, 0, Ts, Td};

         {V, X, H, M, Csys, Fsys, psys, qsys} =
           CreateModel[JointLst, BodyLst, TreeLst, g, 0, Q];

Computing Joint Kinematics

Computing joint 1 kinematics

Computing joint 2 kinematics

Computing Potential Functions

Computing Inertia Matrix

Computing Poincare Function
```

Adding Constraints

The rolling assumption implies that the wheel contact point velocity is zero. We compute the velocities for the unconstrained model at each contact point using the function `NodeVelocity`. Because of our assumptions, some components are identically zero but the remaining velocity constraints must be enforced. In the case of the rear wheels we need to enforce a single sideslip constraint (local *y*-direction), and for the front wheel we need to enforce the sideslip and tangential constraints (local *x* and *y*-directions). To do this we use the function `DifferentialConstraints`.

```
In[85]:= Vrear = NodeVelocity[3, TreeLst, BodyLst, X, H, q, p];
         Vfront = NodeVelocity[4, TreeLst, BodyLst, X, H, q, p];
         c1 = Vrear[[5]]
         c2 = FullSimplify[Vfront[[5]] /. {θf → 0}]
         c3 = FullSimplify[Vfront[[4]] /. {θf → 0}]
Out[85]= vy − dωb
Out[85]= vy Cos[θ] − vx Sin[θ]
Out[85]= −Rωf + vx Cos[θ] + vy Sin[θ]

In[86]:= {Mm, Cm, Fm, Vm, Trans, phat} =
         Simplify[DifferentialConstraints[
                 M, Csys, Fsys, V, {c1, c2, c3}, p, q, {1, 2, 3}]];

Vm

Mm

Cm

Fm
```

```
In[87]:= Vm//MatrixForm
```

$$\text{Out[87]}= \begin{pmatrix} \frac{\text{R Sin}[\theta]}{\text{d}} & 0 \\ \text{R Cos}[\theta+\phi] & 0 \\ \text{R Sin}[\theta+\phi] & 0 \\ 1 & 0 \\ 0 & 1 \end{pmatrix}$$

```
In[88]:= q
Out[88]= {ϕ, x, y, θf, θ}

In[89]:= Simplify[Mm]
```

$$\text{Out[89]}= \left\{\left\{\frac{4\,(\text{Ix}+\text{Jzz})\,\text{R}^2+\text{d}^2\,(8\,\text{J}+(5\,\text{m1}+8\,\text{m2})\,\text{R}^2)}{8\,\text{d}^2} - \frac{(4\,\text{Ix}+4\,\text{Jzz}-3\,\text{d}^2\,\text{m1})\,\text{R}^2\,\text{Cos}[2\,\theta]}{8\,\text{d}^2}, \frac{\text{Ix R Sin}[\theta]}{\text{d}}\right\}, \left\{\frac{\text{Ix R Sin}[\theta]}{\text{d}}, \text{Ix}\right\}\right\}$$

```
In[90]:= (Cm.phat + Fm)//MatrixForm
```

$$\text{Out[90]}= \begin{pmatrix} -\text{Ts}+\frac{\left(4\,\text{Ix}+4\,\text{Jzz}-3\,\text{d}^2\,\text{m1}\right)\,\text{R}^2\,\omega\,\omega\text{f}\,\text{Cos}[\theta]\,\text{Sin}[\theta]}{4\,\text{d}^2} \\ -\text{Td}+\frac{\text{Ix R}\,\omega\,\omega\text{f}\,\text{Cos}[\theta]}{\text{d}} \end{pmatrix}$$

Suppose now, that the two control torques can be used to precisely regulate the two remaining quasi-velocities ω, the steering angle rate, and ω_f, the drive wheel angular velocity. Then the problem of moving the vehicle around the plane becomes purely a kinematic one in which these two quasi-velocities can be specified to steer the vehicle along a desired path. Normally, the drive wheel rotation angle is not a coordinate of interest, and since it does not entire into any of the elements of V_m, we can ignore it. Accordingly, eliminating the $\dot{\theta}_f$ equation from the kinematics and reordering the states for convenience we obtain:

```
In[91]:= Vm[[{2,3,1,5}]]//MatrixForm
```

$$\text{Out[91]}= \begin{pmatrix} \text{R Cos}[\theta+\phi] & 0 \\ \text{R Sin}[\theta+\phi] & 0 \\ \frac{\text{R Sin}[\theta]}{\text{d}} & 0 \\ 0 & 1 \end{pmatrix}$$

Now, introduce the drive velocity $v = R\omega_f$ to replace ω_f and take $d = 1$ to obtain the kinematic equations in the final form:

$$\frac{d}{dt}\begin{bmatrix} x \\ y \\ \phi \\ \theta \end{bmatrix} = \begin{bmatrix} \cos(\theta+\phi) & 0 \\ \sin(\theta+\phi) & 0 \\ \sin\theta & 0 \\ 0 & 1 \end{bmatrix}\begin{bmatrix} v \\ \omega \end{bmatrix}$$

We will use this model in the next chapter (Example (7.10)) to illustrate certain important aspects of the controllability of nonlinear systems.

Here is a more complex example.

Example 6.17 (Rolling Disk). As an illustration we take another example from Neimark and Fufaev [9]. Consider a disk that rolls without slipping on the x-y plane (z is up as in Figure (6.7)). Assume that the disk is of mass m and radius R. One approach is to ignore the rolling constraints and formulate the equations of motion for the free disk in space, and then add the required constraints.

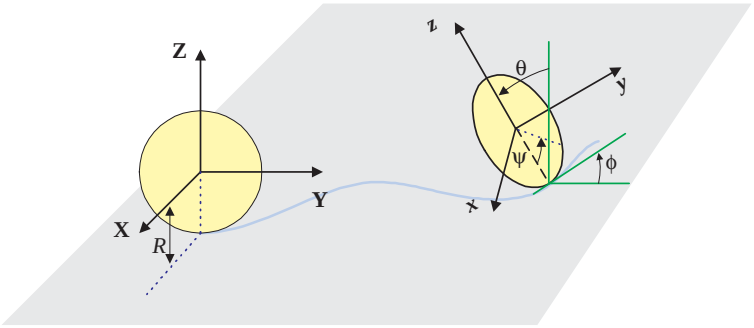

Fig. 6.7: The rolling disk.

A body frame is established with origin at the center of the disk. The six degree of freedom, simple joint is defined by:

```
In[92]:= r={6};
         H=IdentityMatrix[6];
         q={psi,theta,phi,x,y,z};
         p={wx,wy,wz,vx,vy,vz};
         JointList={{r,H,q,p}};
```

In this setup the x, y, z coordinates locate the center of the disk in the space frame and ψ, θ, ϕ are Euler angles in the $z-y-x$ (or 3-2-1) convention. The body data is:

```
In[93]:= Mass=m; CenterOfMass={0,0,0};
         OutboardNode={2,{0,-R*Sin[psi],-R*Cos[psi]}};
         InertiaMatrix=DiagonalMatrix[{J,Iy,Iy}];
         BodyList={{CenterOfMass,{OutboardNode},Mass,InertiaMatrix}};
```

and the remaining data:

```
In[94]:= TreeList={{{1,1}}};
         PE=0; Q={0,0,0,0,0,0};
```

The unconstrained disk model is obtained with

```
In[95]:= {V,X,H,M,Cp,Fp,p,q}=CreateModel[JointList,BodyList,TreeList,g,PE,Q];
```

Now, we formulate the differential constraints. Rolling without slipping implies that the velocity of the disk contact point must be zero. An expression for the (angular and translational) velocity at the outboard node as a function of the configuration variables is easily obtained using the function `EndEffectorVelocity` or `NodeVelocity`.

```
In[96]:= {ChainList}=TreeList;
         VCont=NodeVelocity[ChainList,BodyList,X,H,p]
Out[96]= {wx, wy, wz, vx − R wy Cos[psi] + R wz Sin[psi], vy + R wx Cos[psi],
           vz − R wx Sin[psi]}

In[97]:= {Mm,Cm,Fm,Vm,T,phat}=
         DifferentialConstraints[M,Cp,Fp,V,VCont[[Range[4,6]]],p,q,{4,5,6}];
```

The dynamics are reduced to three dimensions and the original six quasi-velocities are reduced to three, in fact, we have: `phat={wx,wy,wz}`. The set of configuration coordinates is not reduced by the function `DifferentialConstraints`. In general, a set of differential constraints may not admit any such reduction. Such would be the case if the constraints were completely nonholonomic. In the present case, however, the constraints are 'partially' integrable and from basic geometry one can see that $\text{height}_{com} = R(1-\cos\theta)$. Using this relationship, the coordinate z can be eliminated from the equations. Because the translation parameters x, y, z are, in fact, the space coordinates, z is precisely the height of the center of mass. Inspection shows that only Mm and Vm depend on z so we define:

```
In[98]:= {Sols}=Solve[{X[[1]][[3,4]]==R*(Cos[theta]-1)},{z}];
         Mmo=Simplify[Mm/.Sols];
         Vmo=Simplify[Vm[[ {1,2,3,4,5} ]]/.Sols];
```

Now, we assemble the governing equations.

```
In[99]:= Eqns=MakeODEs[phat,q[[{1,2,3,4,5}]],Vmo,Mmo,Cm,Fm,t]
```

Consider the equations of motion as given by the list Eqns. Careful inspection of the equations suggests that representation of the angular velocity in a frame that does not rotate about the body-x axis may simplify them. Thus, we transform the angular velocity coordinates, wy, wz, via the relations:

```
In[100]:= Trans = {wy[t] → Cos[psi[t]] wyy[t] + Sin[psi[t]] wzz[t]
                   wz[t] → −Sin[psi[t]] wyy[t] + Cos[psi[t]] wzz[t]};
```

The transformed equations are obtained with the function `StateTransformation`:

```
In[101]:= StateVars={psi,theta,phi,x,y,wx,wy,wz};
          TrEqns=StateTransformation[Eqns,StateVars,Trans,{wyy,wzz},t]
```

to obtain:

$$\dot{\theta} = w_{yy}$$

$$\dot{\phi} = \sec(\theta) w_{zz}$$

$$\dot{\psi} = w_x + \tan(\theta) w_{zz}$$

$$\dot{x} = R(\sin(\phi) w_x + \cos(\phi)\cos(\theta) w_{yy})$$

$$\dot{y} = -R\cos(\phi) w_x + R\cos(\theta)\sin(\phi) w_{yy}$$

$$\dot{w}_x = \frac{mR^2 w_{yy} w_{zz}}{J + mR^2}$$

$$\dot{w}_{zz} = \frac{w_{yy}(J w_x + I_y \tan(\theta) w_{zz})}{I_y}$$

$$\dot{w}_{yy} = \frac{gmR\sin(\theta) - (J + mR^2) w_x w_{zz} - I_y \tan(\theta) w_{zz}^2}{I_y + mR^2}$$

These equations are obviously equivalent to the disk equations given by Neimark and Fufaev [9].

Another derivation is given by Meirovitch [8]. To compare our equations with his, it is necessary to reduce them to second order form by eliminating the quasi-velocities (thus, we get Lagrange's equations), and to perform a minor transformation of angular coordinates:

```
In[102]:= Rules1=Flatten[Solve[TrEqns[[{1,2,8}]],{wx[t],wyy[t],wzz[t]}]];

In[103]:= Rules2={wx'[t]->D[wx[t]/.Rules1,t],
                  wyy'[t]->D[wyy[t]/.Rules1,t],
                  wzz'[t]->D[wzz[t]/.Rules1,t]};

In[104]:= Rules3={theta[t]->th[t]-Pi/2,
                  theta'[t]->th'[t],
                  theta''[t]->th''[t]};

In[105]:= Rules4={phi[t]->-pi/2+ph[t],
                  phi'[t]->ph'[t],
                  phi''[t]->ph''[t]}

In[106]:= LagEqns=Simplify[TrEqns[[{5,6,7}]]/.Rules1/.Rules2/.Rules3/.Rules4]
```

$$\text{Out[106]= } \Big\{\text{Cos[th[t]]}\,\text{ph}''[t] + \text{psi}''[t] == \frac{(\text{J} + 2\,\text{m}\,\text{R}^2)\,\text{Sin[th[t]]}\,\text{ph}'[t]\,\text{th}'[t]}{\text{J} + \text{m}\,\text{R}^2},$$

$$\frac{(2\,\text{Iy} - \text{J})\,\text{Cos[th[t]]}\,\text{ph}'[t]\,\text{th}'[t] - \text{J}\,\text{psi}'[t]\,\text{th}'[t] + \text{Iy}\,\text{Sin[th[t]]}\,\text{ph}''[t]}{\text{Iy}}$$

$$== 0,$$

$$\text{th}''[t] == \frac{1}{\text{Iy} + \text{m}\,\text{R}^2}(-\text{g}\,\text{m}\,\text{R}\,\text{Cos[th[t]]} + \text{Iy}\,\text{Cos[th[t]]}\,\text{Sin[th[t]]}\,\text{ph}'[t]^2 -$$

$$(\text{J} + \text{m}\,\text{R}^2)\,\text{Sin[th[t]]}\,\text{ph}'[t]\,(\text{Cos[th[t]]}\,\text{ph}'[t] + \text{psi}'[t]))\Big\}$$

These equations are easily confirmed to be equivalent to those given by Meirovitch [8], p. 163.

6.4.2 Holonomy and Integrability

If the distribution $\Delta = \mathrm{Ker}\, F(q)$ is completely integrable (in the sense of Frobenius) then any motion of the constrained system is confined to an integral manifold of a submanifold of M. Thus, the differential constraint (6.41) can be replaced by a configuration constraint of the form

$$f(q) = 0 \tag{6.50}$$

Such differential constraints are called *holonomic*. Of course, an integrable distribution will have an infinity of integral manifolds and the one on which motion takes place is determined by the initial conditions of the system. Since the distribution is nonsingular and of dimension r all of the integral manifolds are of dimension r. Thus, in principle, it is possible to reduce the configuration space by r coordinates. If Δ is not completely integrable, then the constraint is said to be nonholonomic. A nonholonomic constraint may be 'partially integrable.' Recall that the distribution Δ is completely integrable if and only if it is involutive. Suppose this is not the case. Then construct the smallest involutive distribution that contains Δ. Denote this distribution Δ^*. Now let $G(q)$ be a matrix whose columns $\{g_1(q), \ldots, g_{m-r}(q)\}$span $\Delta(q)$. Then (6.41) is satisfied if and only if $q(t)$ satisfies the differential equation:

$$\dot{q} = G(q)v(t) \tag{6.51}$$

where $v(t)$ is arbitrary (except for any conditions necessary to achieve smoothness requirements on $q(t)$). By considering (6.51) to be a control system, we can apply known results on nonlinear system controllability to reach the following conclusion. If Δ^* is nonsingular with dimension $m - r^*$, $0 \leq r^* \leq r$, then there is an $m - r^*$-dimensional integral manifold of Δ^* passing through any point $q_0 \in M$, say S_{q_0}, and all points reachable from q_0 via an admissible motion (one that satisfies (6.41) or, equivalently, (6.51)) belong to S_{q_0}.

Consequently, the differential constraints restrict the motion to an $m - r^*$ dimensional submanifold of the space M. If $r^* = r$, then we have the holonomic case which yields the maximally restricted configuration space. If $r^* = 0$, the configuration space is the entire space M, there is no restriction of the accessible configurations. In this case the constraints are said to be completely nonholonomic.

A standard procedure that can be used to construct Δ^* is described in Chapter 2, Algorithm (3.54). Define

$$\begin{aligned} \Delta_0 &= \Delta \\ \Delta_{k+1} &= \Delta_k + [\Delta, \Delta_k] \end{aligned}$$

and terminate at $k = k^*$ when $\Delta_{k^*+1} = \Delta_{k^*}$. The integer k^* is sometimes referred to as the 'degree of nonholonomy' [12]. It represents the number of Lie bracket operations necessary to achieve integrability by expansion of the distribution.

6.4.3 Configuration Constraints

Suppose that a set of constraints of the form of (6.50) are imposed on a Lagrangian system with configuration manifold M. Assume further that

$$\text{rank}\,[\partial f/\partial q] = r \text{ on } S = \{q \mid f(q) = 0\}$$

Then, S is a regular submanifold of M of dimension $n-r$ and S is the configuration manifold for the constrained system. There are a number of ways to formulate the equations of motion for the constrained system. The two most commonly used are:

- If (6.50) can be solved for r coordinates in terms of the remaining coordinates, then these relations can be used to eliminate r coordinates from the unconstrained equations of motion.
- It is always possible to differentiate (6.50) to obtain

$$J(q)\dot{q} = 0, \quad J(q) := \frac{\partial f}{\partial q} \tag{6.52}$$

Now proceed to use the procedure described above for differential constraints. The resulting equations describe the motion in terms of the original n coordinates but the manifold S can be shown to be an invariant manifold so that if the initial conditions satisfy

$$f(q_0) = 0, \quad J(q_0)\dot{q}_0 = J(q_0)V(q_0)p_0 = 0 \tag{6.53}$$

then the resultant motion evolves in S.

Example 6.18 (Two bar linkage). Consider a planar two bar linkage in which the lower end of bar 1 is constrained by a revolute joint on the y-axis at $y = 0$ and the upper end of bar two slides on the z-axis. The upper end of bar 1 and the lower end of bar 2 are connected by a revolute joint. Figure (6.8) illustrates the system.

```
In[107]:= r1={1};
          H1=Transpose[{{1,0,0,0,0,0}}];
          q1={theta1};p1={omega};

          r2={1};
          H2=Transpose[{{1,0,0,0,0,0}}];
          q2={theta2};p2={omega2};

          JointList={{r1,H1,q1,p1},{r2,H2,q2,p2}};

In[108]:= Mass1=m1; CenterOfMass1={0,0,L1/2};
          OutboardNode1={2,{0,0,L1}};
          InertiaMatrix1=DiagonalMatrix[{m1*L1^2/12,m1*L1^2/12,0}];

          Mass2=m2; CenterOfMass2={0,0,L2/2};
          OutboardNode2={3,{0,0,L2}};
          InertiaMatrix2=DiagonalMatrix[{m2*L2^2/12,m2*L2^2/12,0}];

          BodyList={{CenterOfMass1,{OutboardNode1},Mass1,InertiaMatrix1},

          {CenterOfMass2,{OutboardNode2},Mass2,InertiaMatrix2}};

In[109]:= TreeList={{{1,1},{2,2}}};
          PE=0; Q={0,0};
```

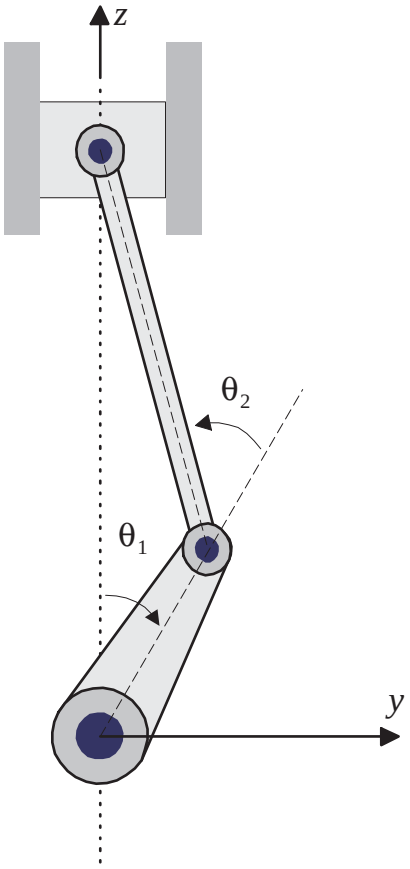

Fig. 6.8: A two bar assembly is illustrative of a closed chain configuration.

```
In[110]:= {V,X,H,M,Cp,Fp,p,q}=CreateModel[JointList,BodyList,TreeList,g,PE,Q];
```

We have the model for the unconstrained tree structure. Now, we formulate the constraint.

```
In[111]:= ChnBodyList={{CenterOfMass1,{0,0,L1},Mass1,InertiaMatrix1},
                       {CenterOfMass2,{0,0,L2},Mass2,InertiaMatrix2}};
In[112]:= EndPos=EndEffector[ChnBodyList,X];
In[113]:= G=EndPos[[{2},4]]
Out[113]= {-L1 Sin[theta1]+
            L2 (-Cos[theta2] Sin[theta1] - Cos[theta1] Sin[theta2])}
```

The relation $G = 0$ is not solvable for either theta1 or theta2 for all values of L1 and L2 - although, as we will describe below, it can be solved for particular values of these parameters. Thus, we will not try to eliminate any configuration coordinate. The constrained dynamics are obtained with:

```
In[114]:= {Mm,Cm,Fm,Vm,phat,qhat}=AlgebraicConstraints[M,Cp,Fp,V,G,p,q]
```

These parameters define the constrained system dynamics. Now, let's consider the special case: L1=L2=L. This is the only situation where G=0 can be solved for either theta1 or theta2, so that either angle can be used to parameterize the system configuration. For simplicity, also set m1=m2=m. Since L1=L2=L it is easy to show that theta2=-2 theta1. Hence we can make this replacement. In this case the system matrices are:

```
In[115]:= {Mm,Cm,Fm,Vm}=Simplify[{Mm,Cm,Fm,Vm}/.{L1->L,L2->L,m1->m,m2->m}]
```

It is convenient to assemble the corresponding differential equations.

```
In[116]:= SpEqns=
          Simplify[MakeODEs[phat,qhat,Vm,Mm,Cm,Fm,t]/.theta2[t]->-2*theta1[t]]
```

The result is:

$$\dot{\theta}_1 = -L\cos\theta_1\, w_1$$

$$\dot{\theta}_2 = 2L\cos\theta_1\, w_1$$

$$(7\cos\theta_1 - 3\cos 3\theta_1)\,\dot{w}_1 = -\frac{12}{L^2} g \sin\theta_1 - L\,(2\sin 2\theta_1 - 3\sin 4\theta_1)\, w_1^2$$

Notice that the last two equations consitute a closed system of two first order differential equations in θ_1 and w_1. Let us define some replacement rules to replace these by a single second order equation in θ_1, i.e., Lagrange's equation.

```
In[117]:= Rules = {w1[t] → D[theta1[t], t]/(-L Cos[theta1[t]]),
                   D[w1[t], t] → D[D[theta1[t], t]/(-L Cos[theta1[t]]), t]}

In[118]:= Simplify[SpEqns[[3]]/.Rules]

Out[118]= 0 == 1/3 L^2 m Cos[theta1[t]] (-6 g Sin[theta1[t]] +
              3 L Sin[2 theta1[t]] theta1'[t]^2 - L (-5 + 3 Cos[2 theta1[t]]) theta1''[t]
```

Simple trigonometric identities can be used to verify that these equations are equivalent to those given by Ginsberg [30], p.275 for this example.

6.5 Systems with Flexible Bodies

6.6 Simulation

The equations developed above can be further manipulated symbolically, for example, they can be put into state variable form or linearized or transformed in other ways

of interest to control systems engineers. However, it sometimes desired to perform numerical computations or simulations with these models. It may be convenient to perform simulations within Mathematica, or it may desirable to employ other standard simulation packages. We will describe and illustrate both approaches.

6.6.1 Computing with *Mathematica*

It is easy to construct a simulation within Mathematica. First, assemble the system parameter matrices as computed above into a system of ordinary differential equations using the *ProPac* function `MakeODEs`. `MakeODEs[p,q,V,M,C,F,t]` builds and returns a list of ordinary differential equations in *Mathematica* syntax. They can be integrated using the built in differential equaton solver `NDSolve`. The process is illustrated with a simple example.

Example 6.19 (Double Pendulum Revisited). Let us revisit Example 6.9. All of the information required to invoke the function `MakeODEs` has been assembled.

```
In[119]:= Equations=MakeODEs[p,q,V,M,Cp,Fp,t];
```

Before numerical computation can proceed it is necessary to replace parameter symbols by numbers and set up initial conditions.

```
In[120]:= DataReplacements={m->1,l->1,gc->1,T1->0,T2->0};
```

```
In[121]:= Equations1=Simplify[Equations/.DataReplacements]
```

$$
\begin{aligned}
\text{Out[121]}= \{ & a1x'[t] == w1x[t], \\
& a2x'[t] == w2x[t], \\
& 2\ \mathrm{Sin}[a1x[t]] + \mathrm{Sin}[a1x[t]+a2x[t]] - 2\ \mathrm{Sin}[a2x[t]]\ w1x[t]\ w2x[t] - \mathrm{Sin}[a2x[t]]\ w2x[t]^2 + \\
& 3\ w1x'[t] + 2\ \mathrm{Cos}[a2x[t]]\ w1x'[t] + w2x'[t] + \mathrm{Cos}[a2x[t]]\ w2x'[t] == 0, \\
& \mathrm{Sin}[a1x[t]+a2x[t]] + \mathrm{Sin}[a2x[t]]\ w1x[t]^2 + (1+\mathrm{Cos}[a2x[t]])\ w1x'[t] + w2x'[t] == \\
& 0\}
\end{aligned}
$$

Set up and join the initial conditions:

```
In[122]:= InitialConditions={w1x[0] == 0, w2x[0] == 0, a1x[0] == .1,
          a2x[0] == .2};
          Equations2=Join[Equations1,InitialConditions];
```

Finally, we are ready to integrate the equations using the *Mathematica* function `NDSolve` and plot the results.

```
In[123]:= sols=NDSolve[Equations2,vars,{t,0,40}];
```

```
In[124]:= Plot[Evaluate[a1x[t]/.sols],{t,0,40},AxesLabel->{t,a1x}]
```

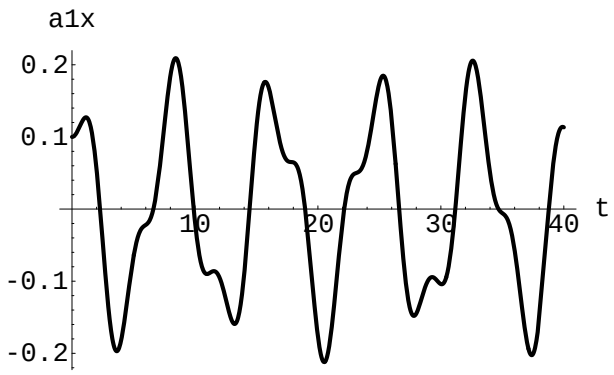

6.6.2 Computing with SIMULINK

It may be desirable to use the system model in an external program. Matlab/SIMULINK is especially popular among control systems engineers. Simulink provides a convenient block diagram environment for building and running simulations. *ProPac* provides functions to create C-Code that compiles as a MEX-File for use as an S-function in SIMULINK. The code is computationally optimized. An S-function may have inputs and outputs so that it can be interconnected with other subsystems within SIMULINK and it can have parameters that can be defined from within SIMULINK. The main tool for building MEX-files is the function `CreateModelMEX`. It has the calling syntax:

```
CreateModelMEX[p,q,Inputs,Outputs,PassedParameters,
        PassedParametersDimensions,V,C,Fp,M,MEXFilename]
```

Example 6.20 (Double Pendulum Revisited). In this example, we define the joint torques as inputs and the (y,z) coordinates of mass 2 as the outputs. Parameters include the two masses, the two lengths and the gravitational constant.

The *ProPac* function `EndEffector` is employed to define the output expressions.

```
In[125]:= ChainLst={{1,1},{2,2}};
          TerminalNode=3;
          Xout=EndEffector[ChainLst,TerminalNode,BodyLst,X];
          yout={Xout[[2,4]],Xout[[3,4]]}
Out[125]= {l Sin[a1x] - l (-Cos[a2x] Sin[a1x] - Cos[a1x] Sin[a2x]),
             -l Cos[a1x] - l (Cos[a1x] Cos[a2x] - Sin[a1x] Sin[a2x])}
```

Now, the data for `CreateModelMEX` is set up and the function is executed.

```
In[126]:= Inputs = Q;
          Outputs = yout;
          MEXFilename = "dbl_{}pend.c";
          paramvec ={m1,l1,m2,l2,gc};
          PassedParams = {"X0","m1","l1","m2","l2","gc"};
          PassedParamsDimensions =
          {{2*Length[p],1},{1,1},{1,1},{1,1},{1,1},{1,1}};
          CreateModelMEX[p,q,Inputs,Outputs,PassedParams,PassedParamsDimensions,
                         V,Cp,Fp,M,MEXFilename];

...Generating Header Code

...Generating Initial Condition Function Code

...Generating State Derivative Function Code

...Collecting all function terms

...Generating temp variable declarations

...Converting Expressions to C form

...Generating Output Function Code

MEX File created with name: dbl_pend.c
```

Detailed information on compiling and using MEX files with Matlab/SIMULINK can be found in the appropriate MATLAB references. CreateModelMEX (and also CreateControllerMEX) assemble C source code that needs to be compiled. During the compilation process the compiled code will be linked with additional code segments and libraries provided with *ProPac* or MATLAB or the compiler. It is necessary that this code be available at the time of compilation. The easiest way to proceed is to perform the compilation from within MATLAB using scripts provided with MATLAB (either cmex with MATLAB 4 or mex with MATLAB 5). This should automatically define the locations of all required MATLAB or compiler code segments. In addition to the file created by *ProPac* (e.g, dbl_pend.c) you will need the files linsolv.c, f2c.h and trigfun.h - all provided with *ProPac*.

One way to compile dbl_pend.c is to place the files dbl_pend.c, linsolv.c, f2c.h and trigfun.h in a common directory, for example C:\DoublePend. Then in the MATLAB command window set the current directory to C:\DoublePend to insure that the four required files are in the search path:

cd C:\DoublePend

then use the command

mex dbl_pend.c linsolv.c

in MATLAB 5, or

!cmex dbl_pend.c linsolv.c

in MATLAB 4.2.

If you have followed the MATLAB installation instructions as appropriate for your compiler this should work fine. Otherwise, you can reinstall MATLAB 5 and follow the instructions (which setsup the appropriate paths in mex), or in MATLAB 4.2 you can edit cmex as described therein.

6.7 Problems

Problem 6.21 (Reconaissance robot, continued). Reconsider the robot of Problem (5.10). Suppose the vehicle has mass m and inertia J_{zz} about the verticle axis, at its center of mass. The radar is mounted at the vehicle center of mass. It has mass m_r and it rotates about its center of mass with body fixed inertias, I_{zz}, and I_{yy}. The drive force T and steering angle δ are inputs to the system. Assume perfect rolling without side slip and derive the equations of the motion for the system.

Problem 6.22 (Overhead crane, continued). Consider the overhead crane of Problem (5.11). Assume the cable is massless and treat the payload as a point mass. Assign inertial parameters and dimensions as required and assemble the equations of motion for this system. Consider the three following controllable inputs to be applied to the system: a drive force, F, applied to the cart, a joint torque, T_a, applied to the revolute upper arm joint, and a cable tension force, T_c.

Problem 6.23 (Synchronous motor). Consider a three phase synchronous motor with the variables and parameters defined in Table (6.1). The load torque T_L is an exogenous disturbance and the voltages v_1, v_2, v_3, v_f are control inputs. The generalized coordinates are $q = [\,\theta \quad q_1 \quad q_2 \quad q_3 \quad q_f\,]$. Define the Blondel transformation matrix

$$B = \sqrt{\tfrac{2}{3}} \begin{bmatrix} \cos\theta & \cos\left(\theta - \frac{2\pi}{3}\right) & \cos\left(\theta + \frac{2\pi}{3}\right) \\ \sin\theta & \sin\left(\theta - \frac{2\pi}{3}\right) & \sin\left(\theta + \frac{2\pi}{3}\right) \\ \frac{1}{\sqrt{2}} & \frac{1}{\sqrt{2}} & \frac{1}{\sqrt{2}} \end{bmatrix}$$

Note that $B^{-1} = B^T$. Define the quasi-velocities, $p^T = [\,\omega \quad i_d \quad i_q \quad i_0 \quad i_f\,]$, via $\dot{q} = V(q)p$, in this case

$$\begin{bmatrix} \dot{\theta} \\ \dot{q}_1 \\ \dot{q}_2 \\ \dot{q}_3 \\ \dot{q}_f \end{bmatrix} = \begin{bmatrix} 1 & 0 & 0 \\ 0 & B^T & 0 \\ 0 & 0 & 1 \end{bmatrix} \begin{bmatrix} \omega \\ i_d \\ i_q \\ i_0 \\ i_f \end{bmatrix}$$

The currents i_d, i_q, i_0 are called the Blondel currents. It is also convenient to define the Blondel voltages v_d, v_q, v_0,

$$\begin{bmatrix} v_d \\ v_q \\ v_0 \end{bmatrix} = B \begin{bmatrix} v_1 \\ v_2 \\ v_3 \end{bmatrix}$$

Symbol	Definition
θ	rotor angle relative inertial reference
ω	motor speed
v_f	field winding voltage
v_i, $i = 1,2,3$	stator winding voltages
i_f	field current
i_i, $i = 1,2,3$	stator winding currents
q_f	field winding charge
q_i, $i = 1,2,3$	stator winding charges
J	rotor inertia
M	inertia matrix in rotor (Blondel) frame
T_L	load torque
$I_{ii} = L_1$, $i = 1,2,3$	stator windings self inductances
$I_{ij} = -L_3$, $i \neq j$, $i = 1,2,3$	stator windings mutual inductances
$I_{ff} = L_4$	field windings self inductances
$I_{f1} = L5\cos\theta$ $I_{f2} = L_5\cos(\theta - 2\pi/3)$ $I_{f3} = L_5\cos(\theta + 2\pi/3)$	field/stator mutual inductances
r	stator winding resistance
r_f	field winding resistance
R	dissipation matrix

Table 6.1: **AC motor nomenclature**

The kinetic energy of the system can be expressed in terms of the quasivelocities, the potential energy is trivial and the generalized force can be obtained from a (Lur'e) potential function, $Q = \partial\mathscr{D}/\partial p$

$$\mathscr{T}(p,q) = \tfrac{1}{2}p^T M p$$

$$\mathscr{U}(q) = 0$$

$$\mathscr{D}(p,q) = \tfrac{1}{2}p^T R p + [-T_L \quad v_d \quad v_q \quad v_0 \quad v_f]\, p$$

$$M = \begin{bmatrix} J & 0 & 0 & 0 & 0 \\ 0 & L_1+L_3 & 0 & 0 & \sqrt{\frac{3}{2}}L_5 \\ 0 & 0 & L_1+L_3 & 0 & 0 \\ 0 & 0 & 0 & L_1-2L_3 & 0 \\ 0 & \sqrt{\frac{3}{2}}L_5 & 0 & 0 & L_4 \end{bmatrix}$$

$$R = \mathrm{diag}\{0,r,r,r,r_f\}$$

Show that Poincaré's equations are

$$\begin{bmatrix} J & 0 & 0 & 0 & 0 \\ 0 & L_1+L_3 & 0 & 0 & \sqrt{\frac{3}{2}}L_5 \\ 0 & 0 & L_1+L_3 & 0 & 0 \\ 0 & 0 & 0 & L_1-2L_3 & 0 \\ 0 & \sqrt{\frac{3}{2}}L_5 & 0 & 0 & L_4 \end{bmatrix} \frac{d}{dt} \begin{bmatrix} \omega \\ i_d \\ i_q \\ i_0 \\ i_f \end{bmatrix}$$

$$= - \begin{bmatrix} 0 & 0 & -i_f\sqrt{\frac{3}{2}}L_5 & 0 & 0 \\ 0 & r & \omega(L_1+L_3) & 0 & 0 \\ i_f\sqrt{\frac{3}{2}}L_5 & -\omega(L_1+L_3) & r & 0 & 0 \\ 0 & 0 & 0 & r & 0 \\ 0 & 0 & 0 & 0 & r_f \end{bmatrix} \begin{bmatrix} \omega \\ i_d \\ i_q \\ i_0 \\ i_f \end{bmatrix} + \begin{bmatrix} -T_L \\ v_d \\ v_q \\ v_0 \\ v_f \end{bmatrix}$$

Problem 6.24 (Sleigh on inclined plane). Consider the problem of a sleigh on an inclined plane as described in [15] and illustrated in Figure (6.9). A single knife edge along the centerline represents the runners. Assume that the center of mass lies along a straight line forward of the knife edge a distance d, the sleigh has mass m and moment of inertia J about the center of mass. The sleigh is constrained by the knife edge so that it can not side slip. Supose that a drive force F acts along the centerline and a turning torque T acts about the z-axis.

(a) Derive the equatons of motion.

(b) Derive an expression for the total energy of the system.

(c) Suppose $d = 0$ so that the center of mass is alligned with the knife edge contact point, $m = 1$, $F = 0$, $T = 0$. Verify that the total energy is constant along trajectories. Consider trajectories that begin with only an angular velocity and derive expressions for $x(t), y(t)$ using the fact that total energy is constant. Plot some typical curves in the (x,y)-plane.

(d) Continue with the assumptions of (c) and suppose $\alpha = 0$ so that the motion takes place on a horizontal plane. Notice that the potential energy term now vanishes. Show that the sleigh moves with constant angular velocity and constant forward speed, i.e., it moves in a circle of constant radius. What is the radius?

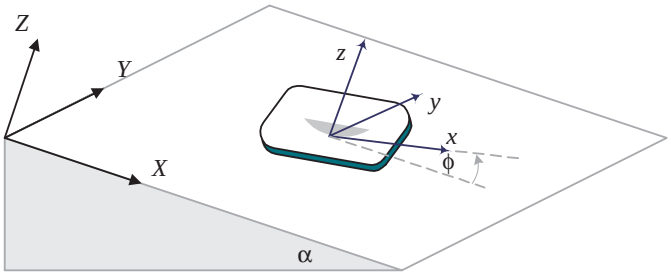

Fig. 6.9: Sleigh on incline.

Part III

Smooth Control Systems

7

Control of Smooth Affine Systems

7.1 Introduction

This chapter is concerned with the analysis and design of controls for nonlinear systems that are linear in control. They take the form:

$$\begin{aligned} \dot{x} &= f(x) + G(x)u \\ y &= h(x) \end{aligned} \tag{7.1}$$

where $x \in R^n$, $y \in R^p$, $u \in R^m$ and f, G and h are smooth functions. Systems of this type are called *smooth, affine systems*. Consistent with the main theme of this book, the discussion to follow emphasizes computations. We will summarize the theoretical concepts that underlie the computations. More complete developments can be found elsewhere, notably, in [46, 87].

In Chapter 3 we discussed some basic tools and computations involving vector fields and distributions. This material is an essential prerequisite for what follows. Section 7.2 of this chapter deals with controllability and Section 7.3 deals with linearization via feedback. Section 7.4 discusses input-output linearization and exact linearization via state feedback. The related topic of dynamic inversion is examined in Section 7.4 and dynamic extension is considered in Section 7.5. In each instance, we summarize the method, describe the relevant computations and give examples.

7.2 Controllability

The notions of reachability and controllability are fundamental to control system design for nonlinear systems just as they are for linear systems. Perhaps more so, because there are important nuances of nonlinear controllability whose counterparts in the linear context are nonexistant or inconsequential. As we will see, these lead to new paradigms for nonlinear control.

Roughly speaking, reachability is the ability to reach any desired terminal state from a given initial state in finite time and controllability is the ability to reach a given terminal state from any initial state in finite time. For linear systems the two properties are equivalent but this may not be the case for nonlinear systems. The controllability of nonlinear systems has many subtleties that will not be explored here. We shall provide only some basic definitions and results. For more information about the controllability of affine systems along the lines of our discussion below see [46, 87].

The notion of controllability to be used herein is provided in the following definition. Readers desiring a deeper motivation for these concepts should consult the pioneering paper [40].

Definition 7.1. *1. The state x_f is U-reachable from x_0 if given a neighborhood U of x_0 containing x_f, there exists a time $t_f > 0$ and a piecewise constant control $u(t)$, $t \in [0,t_f]$ such that if the system (7.1) starts in the state x_0 at time 0, it reaches the state x_f at time t_f along a trajectory that remains entirely in U.*

2. The control system (7.1) is said to be locally reachable from x_0 if for each neighborhood U of x_0 the set of states U-reachable from x_0 contains a neighborhood of x_0. If the reachable set contains merely an open set (not a neigborhood) the system is said to be locally weakly reachable from x_0

3. The control system (7.1) is said to be locally controllable on R^n if it is locally reachable from every initial state $x_0 \in R^n$. It is locally weakly controllable on R^n if it is locally weakly reachable from every initial state $x_0 \in R^n$.

Now, let us define two related distributions (sometimes referred to as *controllability distributions*):

$$\Delta_C = \langle f, g_1 \dots g_m \,|\, \text{span}\{f, g_1, \dots, g_m\} \rangle \tag{7.2}$$

i.e., the smallest involutive distribution containing $\text{span}\{f, g_1 \dots g_m\}$ and invariant with respect to $f, g_1 \dots g_m$, and

$$\Delta_{C_0} = \langle f, g_1 \dots g_m \,|\, \text{span}\{g_1, \dots, g_m\} \rangle \tag{7.3}$$

i.e., the smallest involutive distribution containing $\text{span}\{g_1 \dots g_m\}$ and invariant with respect to $f, g_1 \dots g_m$. These distributions are clearly closely related. The most important relationships are given by the following Lemma from [1].

Lemma 7.2. *The distributions Δ_C and Δ_{C_0} satisfy*

1. $\Delta_{C_0} + \text{span}\{f\} \subseteq \Delta_C$
2. *if x is a regular point of $\Delta_{C_0}(x) + \text{span}\{f(x)\}$, then $\Delta_{C_0}(x) + \text{span}\{f(x)\} = \Delta_C(x)$.*

3. if Δ_{C_0} and $\Delta_{C_0} + \text{span}\{f\}$ are of constant dimension, then $\dim \Delta_C - \dim \Delta_{C_0} \leq 1$.

Proof: see[46], p. 61. ■

When the distribution Δ_C is of constant dimension on a neighborhood of a state x_0 we can construct a local coordinate transformation that reveals the controllability properties of the system. We summarize the main result in the following Lemma.

Lemma 7.3. *Suppose Δ_C and Δ_{C_0} are of constant dimension on some open set U of R^n. Furthermore, suppose that Δ_{C_0} is properly contained in Δ_C, so that* $\dim \Delta_{C_0} = r-1$ *and* $\dim \Delta_C = r$. *Then for each point $x_0 \in U$ there exists a neighborhood U_0 of x_0 and a local coordinate transformation $z = \Phi(x)$ on U_0 such that in the new coordinates the system equations take the form:*

$$\dot{\zeta}_1 = f_1(\zeta_1, \zeta_2) + G_1(\zeta_1, \zeta_2)u$$
$$\dot{\zeta}_2 = f_2(\zeta_2)$$

where $\zeta_1 = (z_1, .., z_{r-1})$, $\zeta_2 = (z_r, .., z_n)$

$$f_2(\zeta_2) = \begin{bmatrix} f_r(\zeta_2) \\ 0 \\ \vdots \\ 0 \end{bmatrix}$$

Moreover, if $\Delta_C = \Delta_{C_0}$ (so that $\dim \Delta_{C_0} = r-1$ *and* $\dim \Delta_C = r-1$*) then the first component of f_2 vanishes so that $\dot{z}_r = 0$.*

Proof: Recall Lemma (3.50). It follows that there exists a local coordinate transformation (matched to Δ_{C_0}) such that each of the vector fields $f, g_1, \ldots, g_m$ have the form

$$\bar{f}(z) = \begin{bmatrix} f_1(z_{r-1}, \ldots z_d, z_r, \ldots, z_n) \\ \cdots \\ f_{r-1}(z_1, \ldots z_{r-1}, z_r, \ldots, z_n) \\ f_r(z_r, \ldots, z_n) \\ \cdots \\ f_n(z_r, \ldots, z_n) \end{bmatrix}$$

Furthermore, since $g_1, \ldots, g_m$ belong to Δ_{C_0}, their last $n-r+1$ coordinates must vanish in the new coordinate system. Now, in view of the fact that Δ_C is of dimension r and contains Δ_{C_0} as well as f, the last $n-r$ components of f must vanish in the new coordinate system. Finally, in the case $\Delta_C = \Delta_{C_0}$, the same arguments lead to the stated conclusion. ■

Remark 7.4. Suppose that $\dim \Delta_C = r$ and consider the controlled motion from any initial state $x_0 \in U$. Trajectories are resticted to the r-dimensional set

$$S_{x_0} = \{x \in U_0 \,|\phi_{r+1}(x) = \phi_{r+1}(x_0), \ldots, \phi_n(x) = \phi_n(x_0)\}$$

by virtue of the fact that the derivatives $\dot{z}_{r+1}, \ldots, \dot{z}_r$ all vanish. Thus a necessary condition for local weak reachability from x_0 is that $\dim \Delta_C = n$.

Remark 7.5. Suppose that $\dim \Delta_C = n$ and $\dim \Delta_{C_0} = n-1$ on U. The controlled motion from an initial state $x_0 \in U$ is again in the set S_{x_0} defined above, with $r = n$. But we can still exploit the last equation which is

$$\dot{z}_r = f_r(z_n)$$

Now, f can not belong to Δ_{C_0} Since Δ_C is strictly larger than Δ_{C_0} (everywhere on U). Thus, f_n can not vanish anywhere on U. Suppose $z_n(t)$ denotes the solution of this differential equation which has the boundary condition $z_n(0) = \phi_n(x_0)$. This relation defines a diffeomorphism

$$\mu : t \mapsto z_n$$

on a time interval $(-\varepsilon, \varepsilon)$ to its image on the z_n axis. Thus, we can take time $t = \mu^{-1}(z_n)$ as the new n^{th} coordinate. In terms of the transformed states $(z-1, \ldots, z_n - 1, t)$, the points reachable from x_0 at precisely time T belong to the set

$$S_{x_0}^T = \left\{x \in U_0 \,\middle|\, \mu^{-1}(\phi_n(x)) = T\right\}$$

It follows that x_0 is on the boundary of the reachable set, it can not be in its interior. Consequently, the set of states reachable from x_0 is not a neighborhood of x_0. It follows that $\dim \Delta_{C_0} = n$ is a necessary condition for local reachability.

Example 7.6. Consider the following example (Isidori [46], Example 1.8.4), involving the system:

$$\dot{x} = f(x) + g(x)u = \begin{bmatrix} x_1 x_3 + x_2 e^{x_2} \\ x_3 \\ x_4 - x_2 x_3 \\ x_3^2 + x_2 x_4 - x_2^2 x_3 \end{bmatrix} + \begin{bmatrix} x_1 \\ 1 \\ 0 \\ x_3 \end{bmatrix} u$$

```
In[127]:= f = {x1  x3 + x2  Exp[x2], x3, x4 - x2  x3, x3^2 + x2  x4 - x2^2  x3};
          g = {x1, 1, 0, x3};
          var = {x1, x2, x3, x4};
          del = Span[{g}]
Out[127]= {{x1, 1, 0, x3}}
```

First, compute the smallest f, g invriant distribution containing span$\{g\}$.

```
In[128]:= Del0 = SmallestInvariantDistribution[{f, g}, del, var]
```

Out[128]= $\{\{1,0,0,0\},\{0,1,0,\text{x3}\}\}$

Now, augment this distribution with two additional vector fields,

In[129]:= $\text{Del} = \textbf{Join}[\text{Del0},\{\{0,0,1,0\},\{0,0,0,1\}\}]$
Out[129]= $\{\{1,0,0,0\},\{0,1,0,\text{x3}\},\{0,0,1,0\},\{0,0,0,1\}\}$

and check that the distribution does span R^4.

In[130]:= $\textbf{Span}[\text{Del}]$
Out[130]= $\{\{1,0,0,0\},\{0,1,0,0\},\{0,0,1,0\},\{0,0,0,1\}\}$

Finally, we generate the transformation and the system equations in the new state variables.

In[131]:= $\textbf{TriangularDecomposition}[\text{f}+\text{g}*\text{u},\text{Del},\text{var},\{0,0,0,0\},\infty]$
Out[131]= $\{\{\text{z1},\text{z2},\text{z3},\text{z2}\ \ \text{z3}+\text{z4}\},\{\text{x1},\text{x2},\text{x3},-\text{x2}\ \ \text{x3}+\text{x4}\},$
$\{\text{u}\ \ \text{z1}+\text{e}^{\text{z2}}\ \ \text{z2}+\text{z1}\ \ \text{z3},\text{u}+\text{z3},\text{z4},0\}\}$

So, we obtain the system in triangular form as anticipated:

$$\dot{z} = \begin{bmatrix} z_1 z_3 + z_2 e^{z_2} \\ z_3 \\ z_4 \\ 0 \end{bmatrix} + \begin{bmatrix} z_1 \\ 1 \\ 0 \\ 0 \end{bmatrix} u$$

Now, we are in a position to establish the main result.

Proposition 7.7. *Suppose Δ_C and Δ_{C_0} are of constant dimension on R^n. Then*

1. *A necessary and sufficient condition for the control system (7.1) to be locally weakly controllable on R^n is that* $\dim \Delta_C(x_0) = n$ *for all* $x_0 \in R^n$.
2. *A necessary and sufficient condition for the control system (7.1) to be locally controllable on R^n is that* $\dim \Delta_{C_0}(x_0) = n$ *for all* $x_0 \in R^n$.

Proof: Only a sketch of the central ideas will be given. The main argument follows [46].

necessity: Necessity is a consequence of the remarks following Lemma (7.3).

sufficiency: We will summarize a constructive proof that the condition $\dim \Delta_C = n$ is sufficient for local weak controllability. To do this we will show that from any point $x_0 \in R^n$ we can construct a piecewise continuous control that steers to an arbitrary point in an open set contained in the slice S_{x_0}. First, let us make several preliminary observations.

(a) Suppose that $\dim \Delta_C = r \leq n$ on a neighborhood U_0 of x_0. All trajectories from x_0 are restricted to the r-dimensional slice S_{x_0}. At any point x we can steer the trajectory in the direction

$$\theta_i(x) = f(x) + g_1(x)u_1^i + \cdots + g_m(x)u_m^i \tag{7.4}$$

where $u_1^i, \ldots u_m^i$ are real numbers. By choosing $k \leq m$ sets of constant controls we can define k vector fields $\theta_i(x)$ of the form (7.4), $i = 1, \ldots, k$. Define the mapping $F : V = (-\varepsilon, \varepsilon)^k \to S_{x_0}$ realized by

$$F(t_1, \ldots, t_k) = \phi_k^{t_k} \circ \cdots \circ \phi_1^{t_1}(x_0) \tag{7.5}$$

where $\phi_i^{t_i}$ is the flow corresponding to the vector field θ_i. Suppose that the differential at $s_i, \ldots, s_k$, $0 < s_i < \varepsilon$ is of rank k, then for ε sufficiently small,

$$M = \left\{ x \in S_{x_0} \,|x = F(t_1, \ldots, t_k),\, t_i \in (s_i, \varepsilon),\, i = 1, \ldots, k \right\}$$

is a regular submanifold of S_{x_0}.

(b) For any $x \in M$, $TM_x \subset \Delta_C(x)$. If $k < r$, it can not be true that for all $x \in M$, $f(x) \in TM_x$ and $g_i(x) \in TM_x$, $i = 1, \ldots, k$. Because if it were true, TM_x would define an involutive distribution containing $f, g_1, \ldots, g_m$ that is smaller than Δ_C, a contradiction. But if it is not true, then it is possible to find an $\bar{x} \in M$ and constants $u_1^{k+1}, \ldots u_m^{k+1}$ such that $\theta_{k+1}(\bar{x}) \notin TM_{\bar{x}}$. In fact, $\bar{x}$ can be found arbitrarily close to x (because ε can be taken arbitrarily small). Let $\bar{x} = F(\bar{s_1}, \ldots, \bar{s_k})$, $\bar{s_i} > s_i$, $i = 1, \ldots, k$. Define the mapping $\bar{F}(t_1, \ldots, t_k, t_{k+1}) = \phi_{k+1}^{t_{k+1}} \circ F(t_1, \ldots, t_k)$. It can be shown that this mapping has rank $k+1$ at the point $(\bar{s_1}, \ldots \bar{s_k}, 0)$ (see [1], p66).

Now, let us turn to the main construction. We can choose constants $u_1^1, \ldots, u_m^1$ to define a vecor field

$$\theta_1 = f + \sum_{i=1}^{m} g_i u_i^1$$

that is not zero at x_0. Define the map

$$F_1 : (0, \varepsilon) \to S_{x_0}$$

$$F_1(t_1) = \phi_1^{t_1}(x_0)$$

and let M^1 be the image of F_1.

Let $\bar{x_1} = F_1(s_1^1)$ be a point of M^1 and θ_2 be a vector field

$$\theta_2 = f + \sum_{i=1}^{m} g_i u_i^2$$

such that $\theta_2(\bar{x_1}) \notin TM_{\bar{x_1}}^1$. Define the mapping

$$F_2 : (s_1^1, \varepsilon) \times (0, \varepsilon) \to S_{x_0}$$

$$F_2(t_1,t_2) = \phi_2^{t_2} \circ \phi_1^{t_1}(x_0)$$

By construction this mapping has rank 2 on its domain. Repeating this procedure, at the k^{th} step we choose a point $\bar{x} = F_{k-1}(s_1^{k-1},\ldots,s_{k-1}^{k-1})$, with $s_i^{k-1} > s_i^{k-2}$ for $i = 1,\ldots,k-2$, $s_{k-1}^{k-1} > 0$, and constants u_i^k such that the vector field $\theta_k \notin TM_{\bar{x}}^{k-1}$. Then construct the map

$$F_k : (s_1^{k-1},\varepsilon) \times \cdots \times (s_{k-1}^{k-1},\varepsilon) \times (0,\varepsilon) \to S_{x_0}$$

$$F_k(t_1,\ldots,t_k) = \phi_k^{t_k} \circ \cdots \circ \phi_1^{t_1}(x_0)$$

The procedure stops with $k = r$.

Notice that any point $x = F_r(t_1,\ldots,t_r)$ in the image of M_r can be reached from x_0 with the piecewise control

$$\begin{array}{ll} u_i(t) = u_i^1 & t \in [0,t_1) \\ u_i(t) = u_i^k & t \in [t_1+\cdots+t_{k-1}, t_1+\cdots+t_k) \end{array}$$

Now, by construction, each mapping F_k parametrically defines regular submanifolds of S_{x_0} of dimension k. Thus, the images under F_r of open sets

$$V_r = (s_1^{r-1},\varepsilon) \times \cdots \times (s_{r-1}^{r-1},\varepsilon) \times (0,\varepsilon)$$

are open sets of S_{x_0} of dimension r. ■

Example 7.8 (Linear system controllability). Let us consider the controllability of a linear system

$$\dot{x} = Ax + Bu,\ x \in R^n,\ u \in R^m$$

by computing the distributions Δ_C and Δ_{C_0} using algorithm (3.54). In this case the relevant vector fields are $f(x) = Ax$ and $g_i(x) = b_i$, $i = 1,\ldots,m$. Notice that

$$[Ax, b_i] = -\frac{\partial Ax}{\partial x} b_i = -Ab_i$$

and

$$[b_j, b_i] = 0,\ [Ax, Ax] = 0$$

To compute Δ_{C_0} begin with $\Delta = \text{span}\{B\}$ and apply the algorithm.

$$\begin{array}{l} \Delta_0 = \text{span}\{B\} \\ \Delta_1 = \text{span}\{B \quad AB\} \\ \quad \vdots \\ \Delta_k = \text{span}\{B \quad AB \quad \cdots \quad A^{k-1}B\} \end{array}$$

In view of the Caley-Hamilton theorem, we may as well stop at $k = n$. Thus, we find that the linear system is locally controllable if and only if

$$\text{rank}[B \quad AB \quad \cdots \quad A^{k-1}B] = n \tag{7.6}$$

To compute Δ_C we begin the process with $\Delta = \text{span}\{Ax, B\}$ to obtain

$$\Delta_C = \text{span}\{\, Ax \quad B \quad AB \quad \cdots \quad A^{n-1}B \,\}$$

If $\text{rank}\Delta_{C_0} = n-1$ it is possible that $\text{rank}\Delta_C = n$ at points other than $x = 0$, so weak local reachability around points $x_0 \neq 0$ is possible. However, controllability still requires (7.6).

ProPac provides functions that construct the distributions Δ_C and Δ_{C_0} and implement the test for controllability. The following example exploits these calculations to illustrate the distinction between local controllability and weak local controllability.

Example 7.9 (Bilinear System Controllability). Consider the following bilinear, scalar input system (Example 7.35 in Vidyasagar [105]):

$$\dot{x} = \begin{bmatrix} 0 & 0 & -14 \\ 0 & 0 & 0 \\ 0 & 0 & -19 \end{bmatrix} x + \begin{bmatrix} 1 & 2 & 4 \\ 0 & 2 & 0 \\ 0 & 0 & 3 \end{bmatrix} xu$$

We use the *ProPac* package to compute the control distributions. First, the distribution

$$\langle f, g_1 \ldots g_m \,|\, f, g_1 \ldots g_m \rangle$$

```
In[132]:= A = {{0,0,-14},{0,0,0},{0,0,-1}};
          B = {{1,2,4},{0,2,0},{0,0,3}};
          x = {x1,x2,x3};
          f = A.x;
          g = B.x;
          ControlDistribution[f,g,x]//MatrixForm
```

$$\text{Out[132]=} \begin{pmatrix} 1 & 0 & 0 \\ 0 & 1 & 0 \\ 0 & 0 & 1 \end{pmatrix}$$

The control distribution has constant dimension 3 (=n) and thus the system is *weakly locally controllable*.

It does not always make sense to rely on the drift term, f, to steer a system from one state to another. So an option to compute the control distribution without the drift term is made available, i.e.,

$$\langle f, g_1 \ldots g_m \,|\, g_1 \ldots g_m \rangle$$

```
In[133]:= ControlDistribution[f,g,x,IncludeDrift->False]//MatrixForm
```

$$\text{Out[133]=} \begin{pmatrix} 1 & 0 & 0 \\ 0 & 2 & x2 \\ 3 & x3 & \end{pmatrix}$$

In this case the generic rank is 2. Thus without accounting for the drift term, the bilinear system is not controllable, i.e., it is not *locally controllable*.

The following example illustrates another important and distinctive aspect of nonlinear system controllability.

Example 7.10 (Parking). A classic problem in control system analysis is the 'parking problem' [106]. The simplified equations of motion of the vehicle to be parked are (see Example (6.16)):

$$\frac{d}{dt}\begin{bmatrix} x \\ y \\ \phi \\ \theta \end{bmatrix} = \begin{bmatrix} \cos(\phi+\theta) & 0 \\ \sin(\phi+\theta) & 0 \\ \sin(\theta) & 0 \\ 0 & 1 \end{bmatrix} \begin{bmatrix} v \\ w \end{bmatrix}$$

where x, y and ϕ represent the planar location and orientation of the center of mass, and θ represents the steering angle. The controls v and w represent the drive velocity and the angular velocity of the steering angle, respectively. The equations represent the kinematics of the vehicle motion. It is assumed that the velocities can be changed instantaneously. There are two control actions defined by the vector fields:

$$\text{drive} = \begin{bmatrix} \cos(\phi+\theta) \\ \sin(\phi+\theta) \\ \sin(\theta) \\ 0 \end{bmatrix}, \quad \text{steer} = \begin{bmatrix} 0 \\ 0 \\ 0 \\ 1 \end{bmatrix}$$

First, let us compute the controllability distribution. Note that since the system is drift free ($f = 0$), $\Delta_C = \Delta_{C_0}$.

```
In[134]:= f = {0,0,0,0};
          G = {{Cos[ϕ + θ], Sin[ϕ + θ], Sin[θ], 0}, {0,0,0,1}};
          var = {x, y, ϕ, θ};
          ControlDistribution[f, Transpose[G], var] // MatrixForm
```

$$\text{Out[134]=} \begin{pmatrix} 1 & 0 & 0 & 0 \\ 0 & 1 & 0 & 0 \\ 0 & 0 & 1 & 0 \\ 0 & 0 & 0 & 1 \end{pmatrix}$$

The control distribution has constant dimension 4 (=n) so that the system is locally controllable. Thus, the vehicle can be moved from any position and orientation to any other position and orientation in finite time. Notice, however, the linearization of the system at any point is not controllable. To better appreciate the information contained in the controllability distibution Δ_C (or Δ_{C_0}) let us consider the details of its construction. Since $f = 0$, we begin with span$\{drive, steer\}$ and expand this distribution by taking Lie brackets of its component vector fields until we achieve a distribution of maximum dimension.

As it turns out we need to add two vector fields to reach the maximum dimension of 4. These are called *wriggle* and *slide*.

```
In[135]:= drive = {Cos[ϕ + θ], Sin[ϕ + θ], Sin[θ], 0};
          steer = {0, 0, 0, 1};
          wriggle = LieBracket[steer, drive, {x, y, ϕ, θ}];
          wriggle//MatrixForm
```

$$\text{Out[135]=}\begin{pmatrix} -\text{Sin}[\theta+\phi] \\ \text{Cos}[\theta+\phi] \\ \text{Cos}[\theta] \\ 0 \end{pmatrix}$$

```
In[136]:= slide = Simplify[LieBracket[wriggle, G[[1]], {x, y, ϕ, θ}]];

          slide//MatrixForm
```

$$\text{Out[136]=}\begin{pmatrix} -\text{Sin}[\phi] \\ \text{Cos}[\phi] \\ 0 \\ 0 \end{pmatrix}$$

These two new control vector fields enable complete configuration control of the vehicle. Experienced drivers will recognize that maneuvering a vehicle in and out of parking a space requires the control action generated by wriggle. The wriggle vector is the Lie bracket of the steer and the drive vector fields. To actually move the vehicle in the direction of this vector field, at least approximately, would require infinitesimal excursions along the steer vector field, then the drive vector field, then the reverse of the steer vector field, then the reverse of the drive vector field. Thus, the name wriggle. Movement along higher order bracket directions (e.g. slide) involves more complicated switching schemes.

The following example shows that, in contrast to linear systems, local controllability does not imply asymptotic stabilizability via simple state feedback control.

Example 7.11 (Sleigh on a horizontal plane, continued). Let us return to the sleigh of Example (6.15). We will first show that the system is locally controllable. To do this, we need to put the equations obtained previously into state space form.

```
In[137]:= f1 = Vm.phat;
          f2 = Inverse[Mm].(−Cm.phat − Fm);
          f = Join[f1, f2]/.{T → 0, F → 0}
```

$$\text{Out[137]=}\left\{\omega, \text{vx}\ \text{Cos}[\phi], \text{vx}\ \text{Sin}[\phi], -\frac{\text{d}\ \text{m1}^2\ \text{vx}\ \omega}{\text{Jzz}\ \text{m1}+\text{d}^2\ \text{m1}^2}, \frac{\text{d}\ \text{m1}\ (\text{Jzz}+\text{d}^2\ \text{m1})\ \omega^2}{\text{Jzz}\ \text{m1}+\text{d}^2\ \text{m1}^2}\right\}$$

```
In[138]:= G = Simplify[Transpose[Map[Coefficient[Join[f1, f2], #]&, {T, F}]]]
```

$$\text{Out[138]=}\left\{\{0,0\},\{0,0\},\{0,0\},\left\{\frac{1}{\text{Jzz}+\text{d}^2\ \text{m1}},0\right\},\left\{0,\frac{1}{\text{m1}}\right\}\right\}$$

```
In[139]:= var = Join[qsys, phat]
```

$$\text{Out[139]=}\ \{\phi, \text{x}, \text{y}, \omega, \text{vx}\}$$

In summary, the state equations are:

$$\frac{d}{dt}\begin{bmatrix}\phi\\ x\\ y\\ \omega\\ v_x\end{bmatrix} = \begin{bmatrix}\omega\\ v_x\cos\phi\\ v_x\sin\phi\\ -\frac{d\,m_1}{J_{zz}+d^2m_1}v_x\omega\\ d\,\omega^2\end{bmatrix} + \begin{bmatrix}0 & 0\\ 0 & 0\\ 0 & 0\\ \frac{1}{J_{zz}+d^2m_1} & 0\\ 0 & \frac{1}{m_1}\end{bmatrix}\begin{bmatrix}T\\ F\end{bmatrix}$$

Now, we can apply the controllability test.

```
In[140]:= Controllability[f, G, var, LocalControllability → True]
Out[140]= True
```

Thus we confirm that the system is locally controllable. We can obtain more details about controllability by computing the controllability distribution Δ_{C_0}. In the following calculation we display intermediate results. That is, beginning with span$\{g_1, g_2\}$, each time the distribution is expanded by addition of a new vector field arising from Lie bracket operations, the new distribution is displayed.

```
In[141]:= ControlDistribution[f, G, var, IntermediateResults → True,
            ControlDrift → False]

Intermediate distribution is:

{{ω, vx Cos[ϕ], vx Sin[ϕ], 0, 0}, {0, 0, 0, 1, 0}, {0, 0, 0, 0, 1}}

Intermediate distribution is:

{{1, 0, 0, 0, 0}, {0, 1, Tan[ϕ], 0, 0}, {0, 0, 0, 1, 0}, {0, 0, 0, 0, 1}}

Intermediate distribution is:

{{1, 0, 0, 0, 0}, {0, 1, 0, 0, 0}, {0, 0, 1, 0, 0}, {0, 0, 0, 1, 0},
 {0, 0, 0, 0, 1}}
Out[141]= {{1, 0, 0, 0, 0}, {0, 1, 0, 0, 0}, {0, 0, 1, 0, 0}, {0, 0, 0, 1, 0},
            {0, 0, 0, 0, 1}}
```

Since the system is locally controllable consider the posibility of asymptotically stabilizing the origin via smooth state feedback. Suppose $u_1(\phi,x,y,\omega,v_x)$ and $u_2(\phi,x,y,\omega,v_x)$ are arbitrary feedback functions that have continuous first derivatives and $u_1(0,0,0,0,0) = u_2(0,0,0,0,0) = 0$. The closed loop dynamics are:

```
In[142]:= fcl = f + G.{u1[ϕ, x, y, ω, vx], u2[ϕ, x, y, ω, vx]};

          fcl//MatrixForm
```

$$\text{Out[142]= } \begin{pmatrix}\omega\\ \text{vx}\,\text{Cos}[\phi]\\ \text{vx}\,\text{Sin}[\phi]\\ -\frac{\text{d}\,\text{m1}^2\,\text{vx}\,\omega}{\text{Jzz}\,\text{m1}+\text{d}^2\,\text{m1}^2} + \frac{u1[\phi,\text{x},\text{y},\omega,\text{vx}]}{\text{Jzz}+\text{d}^2\,\text{m1}}\\ \frac{\text{d}\,\text{m1}\,(\text{Jzz}+\text{d}^2\,\text{m1})\,\omega^2}{\text{Jzz}\,\text{m1}+\text{d}^2\,\text{m1}^2} + \frac{u2[\phi,\text{x},\text{y},\omega,\text{vx}]}{\text{m1}}\end{pmatrix}$$

Equilibria of the closed loop system occur when $f_{cl} = 0$. Clearly, the origin is an equilibrium point. However, it is not an isolated equilibrium point. To see this, observe that $f_{cl} = 0$ if and only if $\omega = 0$, $v_x = 0$, and $u(\phi, x, y, 0, 0) = 0$, i.e., all points (ϕ, x, y) that satisfy the two equations $u(\phi, x, y, 0, 0) = 0$ are equilibrium points. Notice that

$$\text{rank} \begin{bmatrix} \frac{\partial u_1(0)}{\partial \phi} & \frac{\partial u_1(0)}{\partial x} & \frac{\partial u_1(0)}{\partial y} \\ \frac{\partial u_2(0)}{\partial \phi} & \frac{\partial u_2(0)}{\partial x} & \frac{\partial u_2(0)}{\partial y} \end{bmatrix} \leq 2$$

If the rank is 2, the Implicit Function Theorem establishes that there are explicit smooth functions expressing two of the variables, ϕ, x, y, as functions of the third and passing through the origin. Consequently, there is a one dimensional set of equilibrium states in every neighborhood of the origin. If the rank is 1, then there is a two dimensional set and if it is zero, there is a three dimensional set (all values of ϕ, x, y are equilibria).

Thus, the origin is certainly not an isolated equilibrium point. It follows from Lemma (2.16) that the origin can not be asymptotically stable. We conclude that even though the system is locally controllable it can not be asymptotically stabilized via smooth state feedback.

In order to better appreciate the relationship of controllability for nonlinear and linear systems we consider two additional distributions.

$$\Delta_L = \text{span}\{ f, ad_f^k g_i, 1 \leq i \leq m, 0 \leq k \leq n-1 \} \tag{7.7}$$

and

$$\Delta_{L_0} = \text{span}\{ ad_f^k g_i, 1 \leq i \leq m, 0 \leq k \leq n-1 \} \tag{7.8}$$

Note that $\Delta_L \subseteq \Delta_C$ and $\Delta_{L_0} \subseteq \Delta_{C_0}$. What is missing in these distributions, in relation to Δ_C and Δ_{C_0}, are the Lie brackets among the control vector fields, g_i. These new distributions have obvious connections to the Kalman test for controllability of linear systems.

Example 7.12 (Linear system controllability, revisited). For the linear system of Example (7.8) we have $f(x) = Ax$, $G = B$, so it is easy to compute

$$\Delta_C = \Delta_L = \text{span}\left\{ Ax, B, AB, \ldots, A^{n-1}B \right\}$$

$$\Delta_{C_0} = \Delta_{L_0} = \text{span}\left\{ B, AB, \ldots, A^{n-1}B \right\}$$

With linear systems the control vector fields are constant so that the missing Lie brackets contribute nothing to the controllability distributions.

Now, let us state the following obvious results:

Proposition 7.13. *1. A sufficient condition for the control system (1) to be locally weakly reachable around x_0 is that* $\dim \Delta_L(x_0) = n$.

2. A sufficient condition for the control system (1) to be locally weakly controllable on R^n is that $\dim \Delta_L(x_0) = n$ *for all* $x_0 \in R^n$.

The relationships between the various distributions, weak local controllability and local controllability are summarized in the following diagram.

$$\begin{array}{ccccc} \textit{weak local controllability} & \Leftrightarrow & \dim \Delta_C = n & \Leftarrow & \dim \Delta_L = n \\ \Uparrow & & \Uparrow & & \Uparrow \\ \textit{local controllability} & \Leftrightarrow & \dim \Delta_{C_0} = n & \Leftarrow & \dim \Delta_{L_0} = n \end{array}$$

7.3 Input–Output Linearization

When confronted with a nonlinear control design problem, it is reasonable to ask if it is transformable into a linear one. The earliest investigations of this question considered the possibility of using a state transformation to do this. Of course, the set of transformable systems turns out to be quite limited. The idea of using feedback to accomplish linearization is generally attributed to Brockett [17]. As a matter of fact, many practical control system designs already used feedback to accomplish linearization. We will consider a constructive process for linearizing the input-output dynamics of a given nonlinear system using state transformations and feedback. When this is possible, a reasonable approach for controller design is a two level strategy that implements first the linearizing control and then a linear feedback that regulates the linearized system. *ProPac* contains the constructions required to implement this process. We describe the essentials in the following paragraphs.

A system is exactly linearizable or input-state linearizable if the state equations are linearizable by a combination of a state transformation and state feedback. If a system is not exactly feedback linearizable, it may still be linearizable in an input-output sense. In this event, we can find a state transformation and a nonlinear state feedback control such that the input-output behavior is described by a linear dynamical system. However, in this case there remain residual nonlinear dynamics, called the internal dynamics, which are decoupled from the output. Hence the input-output behavior is linear even though the entire state dynamics are not. In this section we consider input-output linearization and in the next section we consider input-state linearization.

7.3.1 SISO Case

First, we consider the single-input single-output case:

$$\begin{aligned} \dot{x} &= f(x) + g(x)u \\ y &= h(x) \end{aligned} \tag{7.9}$$

where $x \in R^n$, $u \in R$ and $y \in R$. Now, let us differentiate $y = h(x)$ with respect to time to obtain

$$\dot{y} = L_f h(x) + L_g h(x) u$$

If $L_g h(x) \neq 0$ we stop, if $L_g h(x) = 0$, we differentiate again to obtain

$$\ddot{y} = L_f^2 h(x) + L_g L_f h(x) u$$

Again, the coefficient of u vanishes or it does not. If not, we continue to differentiate until after r steps we have

$$y^{(r)} = L_f^r h(x) + L_g L_f^{r-1} h(x) u \tag{7.10}$$

with $L_g L_f^{r-1} h(x) \neq 0$ and the process is terminated. Assume that the process does stop in a finite number of steps.

Definition 7.14. *Consider the system (7.9). Let U be a neighborhood of x_0 and suppose there is a finite integer r such that*

$$L_g L_f^k h(x) = 0,\ \forall x \in U,\ k = 0, \ldots, r-2 \ \ L_g L_f^{r-1} h(x_0) \neq 0 \tag{7.11}$$

Then r is the relative degree of (7.9). If the sequence specified in (7.11) does not terminate in finite steps the system relative degree is $r = \infty$.

Example 7.15 (Linear system relative degree). Consider a SISO linear system

$$\dot{x} = Ax + bu$$

$$y = cx$$

We make the associations with (7.9): $f(x) = Ax$, $g(x) = b$ and $h(x) = cx$. It is easy enough to verify that $L_f^k h = cA^k x$ and $L_g L_f^k h = cA^k b$. Thus, the conditions expressed in (7.11) for a system of finite relative degree r is

$$cb = 0,\ cAb = 0, \ldots, cA^{r-2}b = 0,\ cA^{r-1}b \neq 0$$

Define the functions

$$z_i(x) = L_f^{i-1} h(x) \tag{7.12}$$

We intend to show, that these functions define a partial state transformation that reduces the system to an important *normal form* from which a linearizing feedback control is obvious. To do this we need to establish two essential facts. First, if the process terminates in finite steps, it does so with $r \leq n$. Second, the functions $z_i(x)$ are independent. Independence will be considered first. However, we will need the following identity.

Lemma 7.16. *Suppose the system (7.9) has finite relative degree r. Then*

$$L_{ad_f^i g} L_f^k h = \begin{cases} 0 & if\ i+k \leq r-1 \\ (-1)^i L_g L_f^{r-1} h & if\ i+k = r-1 \end{cases} \tag{7.13}$$

Proof: Let us fix k and prove the claim by induction on i. First note that for $i = 0$, the claim (7.13) reduces to the definition of relative degree (7.11). Now, assume that the (7.13) is true for $i = 0, \ldots, p-1$. We will prove that it is true for $i = p$. Recall that $\text{ad}_f^i g = [f,\ ad_f^{i-1} g]$ and compute

$$L_{\text{ad}_f^p g} L_f^k h = L_f L_{\text{ad}_f^{p-1} g} L_f^k h - L_{\text{ad}_f^{p-1} g} L_f L_f^k h$$

In view of the induction hypothesis this reduces to

$$L_{\text{ad}_f^p g} L_f^k h = -L_{\text{ad}_f^{p-1} g} L f L_f^k h = -L_{\text{ad}_f^{p-1} g} L_f^{k+1} h$$

Now, $p+k < r-1$ implies $(p-1)+(k+1) < r-1$ so that by the induction hypothesis

$$L_{\text{ad}_f^p g} L_f^k h = 0,\ p+k < r-1$$

If $p+k = r-1$ the induction hypothesis allows the sequential reduction

$$L_{\text{ad}_f^p g} L_f^k h = -L_{\text{ad}_f^{p-1} g} L_f^{k+1} h = \cdots (-1)^p L_g L_f^{r-1} h$$

■

Lemma 7.17. *Consider the system (7.9) and suppose it has finite relative degree r. Then the covectors $\{dz_1, dz_2, \ldots, dz_r\}$ associated with the functions $z_i(x)$ defined in (7.12) are independent and $r \leq n$.*

Proof: We will show that the only set of constants $a_1, \ldots, a_r$ for which the relation

$$\sum_{i=1}^{r} a_i dz_i(x_0) = 0 \tag{7.14}$$

is satisfied is the trivial set $a_i = 0$ for $i = 1, \ldots, r$. To do this consider the scalar function

$$\alpha(x) = \sum_{i=1}^{r} a_i z_i(x) \tag{7.15}$$

First we show that $a_r = 0$. Suppose that (7.14) is true, which means that $d\alpha(x_0) = 0$. Then

$$L_g \alpha(x_0) = d\alpha(x) \cdot g(x)|_{x=x_0} = 0 \tag{7.16}$$

Now,

$$L_g\alpha(x) = \sum_{i=0}^{r-1} L_g L_f^i h(x) \tag{7.17}$$

But, by assumption $L_g L_f^k h(x) = 0,\ k = 0,\ldots,r-2$, $L_g L_f^{r-1} \neq 0$, so we have

$$L_g\alpha(x) = a_r L_g L_f^{r-1} h(x) \tag{7.18}$$

Thus, we conclude $a_r = 0$, so that

$$\alpha(x) = \sum_{i=1}^{r-1} a_i z_i(x) \tag{7.19}$$

Now, we show that $a_{r-1} = 0$. Note that

$$L_{ad_f g}\alpha(x_0) = 0 \tag{7.20}$$

From the previous lemma, we have

$$L_{ad_f g}\alpha(x) = \sum_{i=0}^{r-2} L_{ad_f g} L_f^i h(x) = -a_{r-1} L_g L_f^{r-1} h(x) \tag{7.21}$$

so that we must have $a_{r-1} = 0$. Continuing in this way, we show that all $a_i = 0$. ■

If $r < n$ we can always complete the mapping $x \mapsto z(x)$ to be a transformation by specifying $n-r$ functions $\xi(x)$ independent of $z(x)$ in the sense that the set of covectors $d\xi_1(x_0),\ldots,d\xi_{n-r}(x_0), dz_1(x_0),\ldots,dz_r(x_0)$ are linearly independent. Then the transformed equations are

$$\dot{\xi} = F(\xi, z, u)$$

$$\dot{z} = Az + b\left[\alpha\left(x(\xi,z)\right) + \rho\left(x(\xi,z)\right)u\right]$$

where

$$A = \begin{bmatrix} 0 & 1 & 0 & & \\ 0 & 0 & 1 & 0 & \\ \vdots & & \ddots & \ddots & \\ & & & \ddots & 1 \\ 0 & & & 0 & 0 \end{bmatrix},\ b = \begin{bmatrix} 0 \\ \vdots \\ \vdots \\ 0 \\ 1 \end{bmatrix}$$

and

$$\alpha(x) = L_f^r h(x),\ \rho(x) = L_g L_f^{r-1} h(x)$$

However, we can actually do more that that. We seek functions $\xi(x)$ with the property that $L_g\xi_i(x) = 0$ around x_0. That is, $d\xi_1(x),\ldots,d\xi_{n-r}(x) \in \mathscr{G}^\perp$, where $\mathscr{G} = \text{span}\{g\}$.

Proposition 7.18. *Suppose the system (7.9) has finite relative degree r at x_0. Then $r \leq n$. Moreover, if $r < n$ it is possible to find $n-r$ functions $\xi_1(x),\ldots,\xi_{n-r}$ such that the mapping*

$$\Phi(x) = \begin{bmatrix} \xi(x) \\ z(x) \end{bmatrix}$$

is a local coordinate transformation on a neighborhood of x_0. *Moreover, it is always possible to choose* $\xi_1(x), \ldots, \xi_{n-r}(x)$ *so that*

$$L_g \xi_i(x) = 0,\ 1 \leq i \leq n-r$$

The transformed equations are

$$\dot{\xi} = F(\xi, z) \tag{7.22}$$

$$\dot{z} = Az + b\left[\alpha\left(x(\xi,z)\right) + \rho\left(x(\xi,z)\right)u\right] \tag{7.23}$$

$$y = cz \tag{7.24}$$

where

$$A = \begin{bmatrix} 0 & 1 & 0 & & \\ 0 & 0 & 1 & 0 & \\ \vdots & & \ddots & \ddots & \\ & & & \ddots & 1 \\ 0 & & & 0 & 0 \end{bmatrix},\ b = \begin{bmatrix} 0 \\ \vdots \\ \vdots \\ 0 \\ 1 \end{bmatrix}$$

$$c = \begin{bmatrix} 1 & 0 & \cdots & \cdots & 0 \end{bmatrix}$$

and

$$\alpha(x) = L_f^r h(x),\ \rho(x) = L_g L_f^{r-1} h(x)$$

Proof: By the definition of relative degree $g(x_0)$ is not zero. Thus, the distribution $\mathcal{G} = \text{span}\{g\}$ is nonsingular around x_0. Since it is one dimensional it is also involutive. Thus, the Frobenius theorem implies the existence of $n-1$ functions $\lambda_1, \ldots, \lambda_{n-1}$ defined on a neighborhood of x_0 such that

$$\text{span}\{d\lambda_1, \ldots, d\lambda_{n-1}\} = \mathcal{G}^{\perp} \tag{7.25}$$

Now, it must be that

$$\dim\left(\mathcal{G}^{\perp} + \text{span}\left\{dh, dL_f h, \ldots, dL_f^{r-1} h\right\}\right) = n$$

at x_0. Otherwise,

$$\mathcal{G}(x_0) \cap \ker\left(\text{span}\left\{dh(x_0), dL_f h(x_0), \ldots, dL_f^{r-1} h(x_0)\right\}\right) \neq \{\} \tag{7.26}$$

In other words, the vector $g(x_0)$ is annihilated by all of the covectors in

$$\text{span}\left\{dh(x_0), dL_f h(x_0), \ldots, dL_f^{r-1} h(x_0)\right\}$$

But this is a contradiction because $\left\langle dL_f^{r-1} h(x_0), g(x_0)\right\rangle = L_g L_f^{r-1} h(x_0)$ is nonzero by assumption. Since $\text{span}\left\{dh, dL_f h, \ldots, dL_f^{r-1} h\right\}$ has dimension r, it follows from

(7.25) and (7.26) that there are $n-r$ covectors in $\mathscr{G}^{\perp}$, say, $d\lambda_1,\ldots,d\lambda_{n-r}$ so that $dh, dL_f h,\ldots,dL_f^{r-1}h, d\lambda_1,\ldots,d\lambda n-r$ are independent at x_0. Furthermore, by construction, we have $L_g\lambda_i(x)=0,\ 1\le i\le n-r$. Finally, the form of the equations follows from the construction of the functions $z(x)$and $\xi(x)$. ■

Remark 7.19. Equations (7.23) and (7.24) are called the *linearizable dynamics* because we can introduce a new control variable v and define $\alpha+\rho u=v$ to reduce (7.23) and (7.24) to the linear system

$$\dot{z}=Az+bv,\ y=cx$$

with input v and output y. Equation (7.22) are called the *internal dynamics* because they are decoupled from the (linearized) input-output dynamics. Moreover, since the linear system is controllable (it is in controllable form) it can be stabilized by an appropriate linear control of the form $v=Kz$. If this is done, then the overall system is stabilized if and only if the system

$$\dot{\xi}=F(\xi,0) \tag{7.27}$$

The system of equations (7.27) are referred to as the *zero dynamics* or *zero output dynamics* of (7.9) because they represent the residual dynamical behavior that can take place under the constraint $y(t)\equiv 0$.

The following is an important property of 'relative degree' is that it is invariant under state transformation and feedback

Lemma 7.20. *Suppose the system (7.9) has finite relative degree r, then r is invariant under state transformation and feedback.*

Proof: Consider a transformation $x\mapsto z$ realized by the mapping $z=\Phi(x)$ and its inverse $x=\Phi^{-1}(z)$. In the new state coordinates the system equations are

$$\begin{aligned}\dot{z}&=d\Phi\left(\Phi^{-1}(z)\right)\left[f\left(\Phi^{-1}(z)\right)+g\left(\Phi^{-1}(z)\right)u\right]\\&=\bar{f}(z)+\bar{g}(z)\end{aligned}$$

and

$$y=h\left(\Phi^{-1}(z)\right)=\bar{h}(z)$$

Now, let us compute $L_{\bar{g}}\bar{h}(z)$:

$$L_{\bar{g}}\bar{h}(z)=\left.\frac{\partial h}{\partial x}\right|_{x=\Phi^{-1}(z)}\frac{\partial\Phi^{-1}}{\partial z}\left.\frac{\partial\Phi}{\partial x}\right|_{x=\Phi^{-1}(z)}g\left(\Phi^{-1}(z)\right)$$

But, the relation

$$x=\Phi^{-1}(\Phi(x))$$

implies

$$I = \frac{\partial \Phi^{-1}}{\partial z}\frac{\partial \Phi}{\partial x}$$

so that we conclude

$$L_{\bar{g}}\bar{h}(z) = L_g h\left(\Phi^{-1}(z)\right)$$

Identical calculations lead to the result

$$L_{\bar{f}}\bar{h}(z) = L_f h\left(\Phi^{-1}(z)\right)$$

and indeed,

$$L_{\bar{g}}L_{\bar{f}}^{k}\bar{h}(z) = L_g L_f^k h\left(\Phi^{-1}(z)\right)$$

Thus, in view of the definition of relative degree we have the result that relative degree is invariant under state coordinate transformations.

Now, let is apply state feedback $u = \kappa(x) + v$ so that the system equations become

$$\dot{x} = f(x) + g(x)\kappa(x) + g(x)u = \bar{f}(x) + g(x)u$$

$$y = h(x)$$

Now compute

$$L_{\bar{f}}h(x) = L_f h(x) + L_{g\kappa}h(x)$$

but notice that

$$L_{g\kappa}h(x) = L_g h(x)\,\kappa(x)$$

So we have

$$L_{\bar{f}}h(x) = L_f h(x) + L_g h(x)\,\kappa(x) = L_f h(x)$$

since $L_g h(x) = 0$. Similarly, we successively compute

$$L_{\bar{f}}^{i}h(x) = L_f^i h(x) + L_g L_f^{i-1}h(x)\,\kappa(x) = L_f^i h(x), \quad 1 \le i \le r-1$$

using the fact that $L_g L_f^{i-1}h(x) = 0, \quad 1 \le i \le r-1$. Thus we have

$$L_g L_{\bar{f}}^{i}h(x) = L_g L_f^i h(x), \quad 1 \le i \le r-1$$

so that $L_g L_{\bar{f}}^{i}h(x) = 0, \quad 1 \le i \le r-2$ and $L_g L_{\bar{f}}^{r}h(x) \neq 0$. Consequently, the system system retains relative degree 'r' under feedback. ■

In the SISO case, the coordinate transformation can always be chosen such that the decoupled (internal) dynamics are independent of the control, [46] Chapter 4.3. This calculation has been implemented in the *ProPac* function `SISONormalFormTrans`.

Example 7.21 (I–O Linearization and normal forms). Consider the following example (example 4.1.5 in Isidori [46]):

$$\begin{bmatrix}\dot{x}_1\\ \dot{x}_2\\ \dot{x}_3\\ \dot{x}_4\end{bmatrix} = \begin{bmatrix}x_1x_2 - x_1^3\\ x_1\\ -x_3\\ x_1^2 + x_2\end{bmatrix} + \begin{bmatrix}0\\ 2+2x_3\\ 1\\ 0\end{bmatrix} u \tag{7.28}$$
$$y = x_4$$

Below we perform the required computations. Notice that a control can be chosen such that the output $y = x_4 = z_1$ is identically equal to zero if and only if $z_1 = 0$ and $z_2 = 0$.

When this obtains, the internal dynamics reduce to the zero (output) dynamics .

```
In[143]:= f29 = {x1  x2 - x1^3, x1, -x3, x1^2 + x2};
          g29 = {0, 2 + 2  x3, 1, 0}; h29 = {x4};
          var29 = {x1, x2, x3, x4}; newvar29 = {z1, z2, z3, z4};
          {T1, T2} = SISONormalFormTrans[f29, g29, h29, var29]
Out[143]= {{x4, x1^2 + x2}, {x1, x2 - 2  x3 - x3^2}}

In[144]:= Trans = Join[T1, T2];
          InvTrans = InverseTransformation[var29, newvar29, Trans];

In[145]:= {Newf, Newg} =
            TransformSystem[f29, g29, var29, newvar29, Trans, InvTrans];
          Newf//MatrixForm
          Newg//MatrixForm
Out[145]= ( z2
            z3 + 2  z2  z3^2 - 4  z3^4
            z3  (z2 - 2  z3^2)
            2 + 2  z2 + z3 - 2  z3^2 + 2  Sqrt[1 + z2 - z3^2 - z4] - 2  z4 )
Out[145]= ( 0
            -2  Sqrt[1 + z2 - z3^2 - z4]
            0
            0 )

In[146]:= ZeroDyn = Inner[Equal, ∂t{z3[t], z4[t]},
              (Newf[[{3, 4}]]/.{z1 → 0, z2 → 0, z3 → z3[t], z4 → z4[t]}), List]//
            MatrixForm
Out[146]= ( z3'[t] == -2  z3[t]^3
            z4'[t] == 2 + z3[t] - 2  z3[t]^2 + 2  Sqrt[1 - z3[t]^2 - z4[t]] - 2  z4[t] )
```

7.3.2 MIMO Case

Consider the square MIMO case as described by Equation (7.1) with $p = m$. Recall that the kth Lie derivative (directional derivative) of the scalar function $\phi(x)$ with respect to the vector field $f(x)$ is denoted $L_f^k(\phi)$. Then by successive differentiation of the elements of the output vector y we arrive at the following definitions.

$$\begin{aligned} r_i &:= \inf\{k | L_{g_j}(L_f^{k-1}(h_i)) \neq 0 \quad \text{for at least one } j\} \\ \alpha_i(x) &:= L_f^{r_i}(h_i), \quad i = 1,..,m \\ \rho_{ij}(x) &:= L_{g_j}(L_f^{r_i-1}(h_i)), \quad i,j = 1,..,m \end{aligned} \tag{7.29}$$

Definition 7.22. *Suppose there exists a set of finite integers $\{r_1,\ldots,r_m\}$ as specified in Equation (7.29) with $\det\{\rho(x_0)\} \neq 0$, then $[r_1,..,r_m]$ is called the vector relative degree at x_0.*

An important result is the MIMO generalization of Lemma (7.17).

Lemma 7.23. *Consider the system (7.1) and suppose it has finite vector relative degree $[r_1,..,r_m]$ at x_0. Let $r = r_1 + .. + r_m$ and define the functions z_i, $i = 1,\ldots,r$,*

$$z(x) = \begin{bmatrix} z^1 \\ \\ \vdots \\ \vdots \\ z^m \end{bmatrix} := \begin{bmatrix} h_1 \\ \vdots \\ L_f^{r_1-1}(h_1) \\ \vdots \\ \vdots \\ h_m \\ \vdots \\ L_f^{r_m-1}(h_m) \end{bmatrix} = \begin{bmatrix} y_1 \\ \vdots \\ y_1^{r_1-1} \\ \vdots \\ \vdots \\ y_m \\ \vdots \\ y_m^{r_m-1} \end{bmatrix} \tag{7.30}$$

where $z^i \in R^{r_i}$. Then the covectors $\{dz_1, dz_2, \ldots, dz_r\}$ are independent and $r \leq n$ on some neighborhood of x_0.

Proof: We need to show that the r n-dimensional row vectors

$$\left\{ dL_f^k h_i(x_0) \,|0 \leq k \leq r_i - 1, 1 \leq i \leq m \right\}$$

are linearly independent. Then it follows imediately that r can not be greater that n.

To establish independence, select real numbers a_{ik}, $0 \leq k \leq r_i - 1$, $1 \leq i \leq m$, such that

$$\sum_{i=1}^{m} \sum_{k=1}^{r_i-1} a_{ik} dL_f^k h_i(x_0) = 0 \tag{7.31}$$

We will show that the only set of such constants is the trivial set. Define

$$a(x) = \sum_{i=1}^{m} \sum_{k=1}^{r_i-1} a_{ik} dL_f^k h_i \tag{7.32}$$

Now, the assumption of finite relative degree implies $L_{g_i} L_f^k h_i(x) = 0$ for $k = \ldots, r_i - 2$. Thus, compute

$$L_{g_j}a = \sum_{i=1}^{m} a_{i,r_i-1} L_{g_j} L_f^{r_i-1} h_i = \sum_{i=1}^{m} a_{i,r_i-1}\rho_{ij} \tag{7.33}$$

Now, using (7.31) we can compute

$$L_{g_j}a(x_0) = da \cdot g_j\big|_{x_0} = 0$$

which implies

$$\left[a_{1,r_{i-1}}, \ldots, a_{m,r_m-1}\right] \rho(x_0) = 0$$

Since $\rho(x_0)$ is nonsingular we conclude that the m numbers $a_{i,r_i-1} = 0$, for $i = 1, \ldots m$. Thus, $a(x)$ reduces to

$$a(x) = \sum_{i=1}^{m} \sum_{k=1}^{r_i-2} a_{ik} dL_f^k h_i \tag{7.34}$$

Now compute $L_{ad_f g}a$ using (7.34) for each j. An identical argument as above leads to the conclusion that $a_{i,r_i-2} = 0$, for $i = 1, \ldots m$ and $a(x)$ reduces to

$$a(x) = \sum_{i=1}^{m} \sum_{k=1}^{r_i-3} a_{ik} dL_f^k h_i \tag{7.35}$$

The argument is repeated to show that all $a_{ij} = 0$. ■

Now, we consider the partial state transformation $x \to z \in R^r$, $r = r_1 + .. + r_m \leq n$ as defined in equation (7.30). It is a straightforward calculation to verify that

$$\begin{aligned} \dot{z} &= Az + E[\alpha(x) + \rho(x)u] \\ y &= Cz \end{aligned} \tag{7.36}$$

where A, E, and C have the special structure:

- A is of the form

$$A = diag(A_1, ..., A_m),\ A_i = \begin{bmatrix} 0 & I_{r_i-1} \\ 0 & 0 \end{bmatrix} \in R^{r_i \times r_i}$$

- the only nonzero rows of E are the m rows $r_1, r_1 + r_2, \ldots, r$ and these form the identity I_m
- the only nonzero columns of C are the m columns $1, r_1 + 1, r_1 + r_2 + 1, \ldots, r - r_m + 1$ and these form the identity I_m

The remaining part of the transformation can be defined by arbitrarily choosing additional independent coordinates. The condition $\det\rho(x_0) \neq 0$ insures the existence of a local (around x_0) change of coordinates $x \to (\xi, z), \xi \in R^{n-r}, z \in R^r$ such that

$$\dot{\xi} = \hat{F}(\xi, z, u) \tag{7.37}$$

$$\dot{z} = Az + E[\alpha(x(\xi,z)) + \rho(x(\xi,z))u] \tag{7.38}$$

It is common to call (7.37) the internal dynamics and (7.38) the linearizable dynamics.

Notice that in view of (7.38), we can apply the control

$$u = \rho^{-1}(x)\{-\alpha(x) + v\} \tag{7.39}$$

and reduce (7.38) to a linear system

$$\begin{aligned} \dot{z} &= Az + Ev \\ y &= Cz \end{aligned} \tag{7.40}$$

This justifies the terminology of linearizable dynamics for (7.38). Notice that when the control (7.39) is applied the internal dynamics (7.37) are decoupled from the output (not necessarily the input, as is the case for SISO systems). It is a simple matter to design a linear stabilizing controller for (7.40) – for example a state feedback law of the form $v = Kz$ that insures $z(t) \to 0$ as $t \to \infty$. Such a control does not necessarily stabilize the complete system (7.37) and (7.38), because we need to account for the decoupled internal dynamics (7.37).

Lemma 7.24. *Suppose that $\rho(x)$ has continuous first derivatives with*

$$\det \rho(x) \neq 0 \text{ on } M_0 = \{x | z(x) = 0\}$$

Then $\partial z(x)/\partial x$ is of maximum rank on the set M_0.

Proof: The result follows directly from Lemma (7.23). ■

The Lemma is extremely important because it relates the invertibility of the decoupling matrix with the geometry of the set M_0. With it, we can obtain several important results, one of which we state here.

Proposition 7.25. *Suppose that $\rho(x)$ has continuous first derivatives with*

$$\det \rho(x) \neq 0 \text{ on } M_0 = \{x | z(x) = 0\}$$

Then M_0 is a regular, $n-r$ dimensional submanifold of R^n and any trajectory segment $x(t), t \in T$, T an open interval of R^1, which satisfies $h(x(t)) = 0$ on T lies entirely in M_0. Moreover, the control that obtains on T is

$$u_0(x) = -\rho^{-1}(x)\alpha(x) \tag{7.41}$$

and every such trajectory segment with boundary condition $x(t_0) = x_0$, $t_0 \in T$ satisfies

$$\dot{x} = f(x) - G(x)\rho^{-1}(x)\alpha(x), \;\; z(x(t_0)) = 0. \tag{7.42}$$

Proof: In view of Lemmas (7.23) and (7.24), it follows from $\det\rho(x) \neq 0$ on M_0 that

1. the covectors $\{dz_1, dz_2, \ldots, dz_r\}$ are independent around every point $x_0 \in M_0$,
2. $\partial z(x)/\partial x$ is of maximum rank on the set $M_0 = \{x | z(x) = 0\}$.

This maximal rank condition insures that M_0 is a well defined regular manifold of dimension $n-r$. From the definition of $z(x)$, it follows that y is identically zero on an open time interval if and only if z is zero on that interval. Thus, it follows from (7.36) that the unique (provided $\det\rho \neq 0$) control which must obtain during any motion constrained by $h(x) = 0$ is (7.41). With this control (7.1) reduces to (7.42). ■

The analysis above leads to the following observations:

- The manifold M_0 is invariant with respect to the dynamics (7.42).
- These equations are equivalent to the output constrained dynamics

$$\begin{aligned} \dot{x} &= f(x) + G(x)u \\ 0 &= h(x) \end{aligned} \tag{7.43}$$

  hence they are called the zero dynamics.
- The proposition defines the zero dynamics in global form. An equivalent local form is

$$\begin{aligned} \dot{\xi} &= F(\xi, 0, 0) \\ F(\xi, z, v) &= \hat{F}(\xi, z, \rho^{-1}(x(\xi, z))\{-\alpha(x(\xi, z)) + v\}) \end{aligned} \tag{7.44}$$

Let us collect these results in the following proposition that justifies the design procedure depicted in Figure (7.1).

Proposition 7.26. *Suppose the conditions of (7.25) hold, and*

1. *$x_0 \in M_0$ is an equilibrium point of (7.1) which implies $x_0 \to (\xi_0, z_0) = (\xi_0, 0)$*
2. *ξ_0 is a stable equilibrium point of the zero dynamics, and*
3. *$v = Kz$ is a stabilizing controller for (7.40).*

Then

$$u = \rho^{-1}(x)\{-\alpha(x) + Kz(x)\} \tag{7.45}$$

is a stabilizing controller for the system (7.1).

Before proceeding with examples, let us consider the computation of the local zero dynamics. One approach is to obtain the internal dynamics by completing the local transformation and then to set $z = 0, v = 0$. We will describe an alternative in which the local zero dynamics are computed directly. Note that the functions $z(x)$ can be computed using (7.30). Once they are obtained, we are in a position to compute the

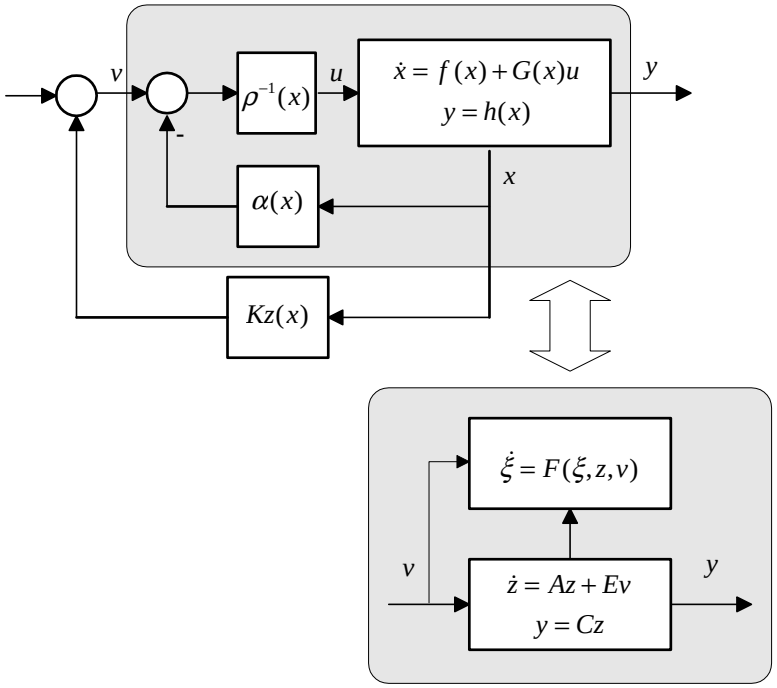

Fig. 7.1: The two level controller design process of Proposition (7.26) is depicted in this diagram.

local form of the zero dynamics near any point $x_0 \in M_0$ in the following way. Without loss of generality assume $x_0 = 0$. Now, split $z(x)$ into its linear and nonlinear parts:

$$z(x) = Ax + N(x), \quad A = \frac{\partial z}{\partial x}(0) \tag{7.46}$$

We assume that $x_0 = 0$ is a regular point (ρ is nonsingular) so that A is of full rank. Let A^* denote a right inverse of A and define K such that its columns span $\ker A$. Define new coordinates v, w so that

$$x = A^* v + Kw \tag{7.47}$$

Then on the zero dynamics manifold, we have

$$v + N(A^* v + Kw) = 0 \tag{7.48}$$

Clearly, the Implicit Function Theorem guarantees the existence of a local solution to (7.48), $v^*(w)$, that is

$$v^*(w) + N(A^* v^*(w) + Kw) = 0 \tag{7.49}$$

on a neighborhood of $w = 0$, and $v^*(0) = 0$. Furthermore, $v^*(w)$ can be efficiently estimated because the mapping

$$v_{i+1} = -N(A^* v_i + Kw) \tag{7.50}$$

is a contraction. In fact, we have the following result.

Proposition 7.27. *Suppose $z(x)$ is smooth, and A is of full rank. Then*

1. *there exists a smooth function $v^*(w) = 0 + O(\|w\|)$,*
2. *if $v_i(w)$ satisfies $\|v^* - v_i\| = O(\|w\|^k)$, then $v_{i+1}(w)$, obtained via (7.50), satisfies $\|v^* - v_{i+1}\| = O(\|w\|^{2k})$.*

Proof: The first conclusion follows directly from the implicit function theorem and the fact that $v^*(w)$ is smooth. To prove the second, first subtract (7.50) from to obtain

$$v^* - v_{i+1} = -N(A^* v^* + Kw) + N(A^* v_i + Kw) \tag{7.51}$$

Now, consider the function $N_x(x) := \partial N(x)/\partial x$. Since N is smooth, with $\partial N(0)/\partial x = 0$, we have $N_x(0) = 0$ and by continuity of the second derivative of N, we conclude that $\partial N_x(x)/\partial x$ is bounded on a neigborhood of $x = 0$. Let L be such a bound on an appropriately defined neighborhood, U, so that the usual arguments based on the Mean Value Theorem provide

$$\|N_x(x) - N_x(y)\| \leq L \|x - y\|, \ \forall x, y \in U \tag{7.52}$$

Thus, we can write

$$N(x) - N(x + \delta x) = N_x(x)\delta x + O(\|\delta x\|^2) \tag{7.53}$$

which in view of (7.52) gives

$$\|N(x) - N(x + \delta x)\| = O(\|\delta x\|^2) \tag{7.54}$$

for $x, y = x + \delta x \in U$. In order to apply this result to (7.51), take $x = A^* v^* + Kw$ and $\delta x = A^*(v^* - v_i)$. Then (7.51) and (7.54) yield

$$\|v^* - v_{i+1}\| = O(\|A^*(v^* - v_i)\|^2) = O(\|w\|^{2k}) \tag{7.55}$$

which is the desired conclusion. ■

Recall the global form of the zero dynamics:

$$\dot{x} = f(x) - G(x)\rho^{-1}(x)\alpha(x) \tag{7.56}$$

which defines the zero dynamics flow everywhere on M_0. Near x_0 we simply project the flow onto the tangent space to M_0 at x_0. K has a left inverse K^* so that

$$\dot{w} = K^* f(x^*(w)) - K^* G(x^*(w))\rho^{-1}(x^*(w))\alpha(x^*(w)) \tag{7.57}$$

$$x^*(w) = A^* v^*(w) + Kw \tag{7.58}$$

ProPac provides the computations necessary to implement the above control design method. The main functions

- `IOLinearize`
- `NormalCoordinates`
- `LocalZeroDynamics`

are illustrated in the following examples.

Example 7.28 (A basic example). Consider the following simple single-input single-output example from [46]:

$$f(x) = \begin{bmatrix} 0 \\ x_1 + x_2^2 \\ x_1 - x_2 \end{bmatrix}, \quad G(x) = \begin{bmatrix} e^{x_2} \\ e^{x_2} \\ 0 \end{bmatrix}, \quad h(x) = x_3$$

Below, we compute the relative degree vector, the decoupling matrix and the feedback linearizing using the function `IOLinearize`. Then to compute the zero dynamics, we obtain the partial state transformation, i.e, $z(x)$ and the control with $v_i(t) = 0, \quad i = 1, \ldots, m$, and finally we compute the local zero dynamics.

```
In[147]:= var2 := {x1, x2, x3}
          f2 := {0, x1 + x2^2, x1 - x2}
          g2 := {Exp[x2], Exp[x2], 0}
          h2 := {x3}

In[148]:= {ρ, α, ro, control} = IOLinearize[f2, g2, h2, var2]

Computing Decoupling Matrix

Computing linearizing/decoupling control

Out[148]= {{{-e^x2 - 2  e^x2  x2}}, {-2  x2  (x1 + x2^2)}, {3}, {(v1 + 2  x2  (x1 + x2^2))/(-e^x2 - 2  e^x2  x2)}}

In[149]:= z = NormalCoordinates[f2, g2, h2, var2, ro];
          u0 = control /. {v1 → 0};
          LocalZeroDynamics[f2, g2, h2, var2, u0, z]

The system is completely linearizable.

There are no zero dynamics.
Out[149]= {}
```

The result should have been anticipated. Since $r = 3 = n$, there are no decoupled dynamics.

Example 7.29 (Zero dynamics of a simple vehicle). Consider a simple wheeled vehicle that moves in the plane as illustrated in the Figure (7.2). The model incorporates two simplifications; $m_2 = 0, s << 1$, so that only first order terms in s are included.

kinematics:

$$\begin{bmatrix} \dot{\theta} \\ \dot{x} \\ \dot{y} \\ \dot{\delta} \end{bmatrix} = \begin{bmatrix} 1 & 0 & 0 & 0 \\ 0 & \cos(\theta) & -\sin(\theta) & 0 \\ 0 & \sin(\theta) & \cos(\theta) & 0 \\ 0 & 0 & 0 & 1 \end{bmatrix} \begin{bmatrix} \omega_\theta \\ v_x \\ v_y \\ \omega_\delta \end{bmatrix}$$

dynamics:

$$\begin{bmatrix} I_{zz}+J_{zz} & 0 & 0 & I_{zz} \\ 0 & m_1 & 0 & 0 \\ 0 & 0 & m_1 & 0 \\ I_{zz} & 0 & 0 & I_{zz} \end{bmatrix} \begin{bmatrix} \dot{\omega}_\theta \\ \dot{v}_x \\ \dot{v}_y \\ \dot{\omega}_\delta \end{bmatrix} + \begin{bmatrix} 0 \\ m_1 v_y \omega_\theta \\ -m_1 v_x \omega_\theta \\ 0 \end{bmatrix} + \begin{bmatrix} f_1 \\ f_2 \\ f_3 \\ f_4 \end{bmatrix} = 0$$

The coordinates x and y locate the center of mass of the main body, and θ its orientation. The front wheels rotate an amount δ about an axis of slope s ($s = 0$, results in a vertical axis), s is assumed small as are the tire inertial parameters. The functions f_i, which include a description of how the steering torque T and the drive force F enter the model, are omitted for the sake of space.

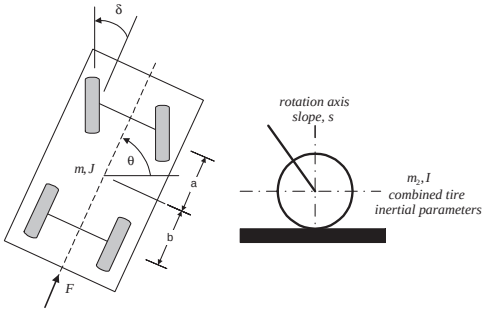

Fig. 7.2: The essential parameters of the example are illustrated in this figure.

Our goal is to consider the problem of steering the vehicle along a path of constant radius, and at constant speed V_d. There are several ways of formulating this problem. One common approach is to replace the constant radius condition by the requirement that the angular velocity ω_θ is a constant, say ω_d. This leads to a constant curvature path of radius, with $R = V_d/\omega_d$.. Thus, we introduce two output relations

$$y_1 = v_x^2 + v_y^2 - V_d^2$$

$$y_2 = \omega_\theta - \omega_d$$

We are interested in the zero dynamics relative to these two outputs and the two controls T, F. Notice that in this formulation it is not necessary to retain the kinematic equations which define the vehicle location and orientation in the plane, i.e., θ, x, y. Thus, the system equations include dynamics and only the last equation of the kinematics.

We will compute the zero dynamics corresponding to V_d =constant, $\omega_d = 0$. The equilibrium point is $(x_1, x_2, x_3, x_4, x_5) = (0, V_d, 0, 0, 0)$, so we compute the local zero dynamics near this point. In order to exhibit a complete example without using excessive space we exhibit results for the case $s = 0$.

```
In[150]:= f27 := {-κ*(a^2*x1 + b^2*x1 + a*x3 -
                 b*x3 - a*x2*x5)/(Jzz*x2),
                 -(m1*x1*x3 - κ*(a*x1 + x3)*x5/x2)/m1,
                 -(-(m1*x1*x2) + κ*(a*x1 - b*x1 + 2*x3 - x2*x5)/x2)/m1,
                 -(κ*(-(a^2*x1) - b^2*x1 - a*x3 + b*x3 +
                 a*x2*x5)/(Jzz*x2)),
                 x4};
          g27 := {{-1/Jzz, 0}, {0, 1/m1}, {0, 0}, {(1/Izz + 1/Jzz), 0}, {0, 0}};
          h27 := {x2^2 + x3^2 - Vd^2, x1 - wd};
          var27 := {x1, x2, x3, x4, x5};

In[151]:= {ρ, α, ro, control} = IOLinearize[f27, g27, h27, var27];
          za = NormalCoordinates[f27, g27, h27, var27, ro]/.{wd -> 0};
          {fa, ga, ha, controlsa, za} =
            {f27, g27, h27, control, za}/.{x2 -> x2 + Vd};
          u0 = controlsa/.{v1 -> 0, v2 -> 0};
          f0 = LocalZeroDynamics[fa, ga, ha, var27, u0, za, 4];
          Simplify[f0]//MatrixForm

Computing Decoupling Matrix

Computing linearizing/decoupling control
```

$$\text{Out[151]=} \quad \begin{pmatrix} \dfrac{\left(\mathrm{b}\ \mathrm{w3}\ \left(2\ \mathrm{Vd}^2 + \mathrm{w3}^2\right) + \mathrm{a}\ \left(2\ \mathrm{Vd}^3\ \mathrm{w1} - 2\ \mathrm{Vd}^2\ \mathrm{w3} - \mathrm{w3}^3\right)\right)\ \kappa}{2\ \mathrm{Izz}\ \mathrm{Vd}^3\ \mathrm{w2}} \\ \dfrac{\left(\mathrm{Vd}^3\ \mathrm{w1} - 2\ \mathrm{Vd}^2\ \mathrm{w3} - \mathrm{w3}^3\right)\ \kappa}{\mathrm{m1}\ \mathrm{Vd}^3} \end{pmatrix}$$

We can test the stability of the equilibrium point, by examining the linearized zero dynamics. The eigenvalues are readily obtained but they are lengthy functions of the parameters. Some insight is obtained, however, by examining the special case, $a = b$, in which case the eigenvalues simplify to those shown where κ is the tire coefficient that determines the cornering force. In this case, the zero dynamics are unstable.

```
In[152]:= Anu = Jacobian[f0, {w1, w2, w3}]/.{w1->0, w2->0, w3->0, b->a+η};
          Eigenvalues[Anu/.{η->0}]
Out[152]= {-Sqrt[a] Sqrt[κ]/Sqrt[Izz], Sqrt[a] Sqrt[κ]/Sqrt[Izz], -2 κ/(m1 Vd)}
```

7.3.3 Exact (Input-State) Linearization

We begin consideration of the exact linearization problem by considering the single input case,

$$\dot{x} = f(x) + g(x)u \tag{7.59}$$

Definition 7.30. *The single input control system (7.59) is locally exactly feedback linearizable around x_0 if there exists a state transformation $z = \phi(x)$ and nonlinear feedback $u = \varphi(x) + \Phi(x)v$, $\Phi(x_0) \neq 0$, all defined on a neighborhood X of $x_0 \in R^n$, that transforms (7.59) into the controllable linear state space system*

$$\dot{z} = Az + bv \tag{7.60}$$

The single input state space exact feedback linearization problem *is is that of finding the transformation and the feedback, if they exist, given the control system (7.59).*

Recall that any linear controllable single input system is similar to the canonical system

$$\dot{z} = \begin{bmatrix} 0 & 1 & 0 & \cdots & 0 \\ 0 & 0 & 1 & \ddots & \vdots \\ \vdots & \vdots & 0 & \ddots & 0 \\ \vdots & \vdots & \vdots & \ddots & 1 \\ 0 & 0 & 0 & \cdots & 0 \end{bmatrix} z + \begin{bmatrix} 0 \\ \vdots \\ \vdots \\ 0 \\ 1 \end{bmatrix} u \tag{7.61}$$

Thus, the exact linearization problem is equivalent to achieving the form (7.61) by state transformation and feedback.

Proposition 7.31. *The single input exact feedback linearization problem is solvable if and only if there exists a function $h(x)$ such the relative degree of the control system*

$$\begin{aligned} \dot{x} &= f(x) + g(x)u \\ y &= h(x) \end{aligned} \tag{7.62}$$

Proof: Sufficiency is obvious in view of the input-output linearization result. To establish necessity, assume the the existence of a state transformation and feedback

control that transforms (7.59) to (7.61). Then take $y = z_1$, so that (7.61) with this output has relative degree n. The corresponding output map, $h(x)$, is $h(x) = \Phi_1^{-1}(x)$. Now since relative degree is invarient under state transformation and feedback, we conclude that (7.59) with output $y = h(x)$ has relative degree n. ■

This theorem implies that $h(x)$ must satisfy the system of partial differential equations

$$L_g L_f^i h(x) = 0, \quad 0 \leq i \leq n-2$$

and the boundary condition

$$L_g L_f^{n-1} h(x_0) \neq 0$$

Using Lemma (7.16) it can be shown that these equations are equivalent to

$$L_{ad_f^i g} h(x) = 0, \quad 0 \leq i \leq n-2 \tag{7.63}$$

$$L_{ad_f^{n-1} g} h(x_0) \neq 0 \tag{7.64}$$

These relations lead to the following result, in which we employ the following notation:

$$\mathscr{G}_i = \operatorname{span}\{\, g(x) \quad \operatorname{ad}_f g(x) \quad \cdots \quad \operatorname{ad}_f^i g(x) \,\} \tag{7.65}$$

Proposition 7.32. *The SISO linear control system (7.62) is exactly feedback linearizable around x_0 if and only if*

1. *the distribution $\mathscr{G}_{n-2}$ is involutive on a neighborhood of x_0.*
2. $\operatorname{rank}\mathscr{G}_{n-1}(x_0) = n$

Proof: Notice that

$$L_{\operatorname{ad}_f^i g} L_f^k h(x) = \left\langle dL_f^k h(x), \operatorname{ad}_f^i g \right\rangle$$

so that Lemma (7.16) leads us to conclude, for a system of relative degree r, the matrix

$$\begin{pmatrix} dh(x_0) \\ dL_f h(x_0) \\ \vdots \\ dL_f^{r-1} h(x_0) \end{pmatrix} \begin{pmatrix} g(x_0) & \operatorname{ad}_f g(x_0) & \cdots & \operatorname{ad}_f^{r-1} g(x_0) \end{pmatrix} =$$

$$\begin{pmatrix} 0 & \cdots & 0 & \left\langle dL_f^{r-1} h(x_0), \operatorname{ad}_f^{r-1} g(x_0) \right\rangle \\ \vdots & & \bullet & * \\ 0 & \bullet & & \vdots \\ \left\langle dL_f^{r-1} h(x_0), g(x_0) \right\rangle & * & \cdots & * \end{pmatrix}$$

has rank r. Thus, if $h(x)$ exists, producing relative degree n, we have necessity of condition (2).

If (2) holds then the distribution $\mathscr{G}_{n-2}(x)$ is nonsingular and of dimension $n-1$ on a neighborhood of x_0. Equations (7.63) can be written in the form

$$dh(x)\begin{pmatrix} g(x) & \mathrm{ad}_f g(x) & \cdots & \mathrm{ad}_f^{n-2} g(x)\end{pmatrix} = 0$$

This implies that the covector field $dh(x)$ is a basis for the codistribution $\mathscr{G}_{n-2}^{\perp}$ (alternatively, ann$\mathscr{G}_{n-2}$). As a consequence, the Frobenius theorem implies that $\mathscr{G}_{n-2}$ is involutive, establishing the necessity of (1).

Conversely, if (2) holds the distribution $\mathscr{G}_{n-2}$ is nonsingular and $n-1$ dimensional around x_0. If (1) also holds, then the Frobenius theorem implies existence of the function $h(x)$ on a neighborhood of x_0 such that $dh(x)$ solves (7.63). Moreover, $dh(x_0)$ spans the one one dimensional linear subspace $\mathscr{G}_{n-2}(x_0)^{\perp}$. Thus, (7.64) is also satisfied because otherwise $dh(x_0)$ would annihilate a set of n linear independent vectors, a contradiction. ■

When a system is exactly linearizable several methods are available for constructing the coordinate transformation and computing the required feedback control. One approach transforms the system into a normal form in which the linearizing control is obvious. We consider a simple example.

Example 7.33 (Feedback linearization). The function

`FeedbackLinearizable`

implements the specified test. Consider the system:

$$\begin{bmatrix}\dot{x}_1\\ \dot{x}_2\\ \dot{x}_3\end{bmatrix} = \begin{bmatrix}\theta x_1^3 + x_2\\ x_3\\ 0\end{bmatrix} + \begin{bmatrix}0\\ 0\\ 1\end{bmatrix} u$$

First check for linearizability

```
In[153]:= f30 = {θ  x1^3 + x2, x3, 0};
          g30 = {0, 0, 1};
          var30 = {x1, x2, x3};
          FeedbackLinearizable[f30, g30, var30]
Out[153]= True
```

From these computations, we see that this system is linearizable. Thus, we can proceed to obtain the exact feedback linearizing state transformation with the function `SIExactFBL`, which implements the feedback linearization algorithm described in [46] Chapter 4.2.

```
In[154]:= Trans = SIExactFBL[f30, g30, var30, True]
Out[154]= {x1, θ  x1^3 + x2, 3  θ  x1^2  (θ  x1^3 + x2) + x3}
```

To obtain the linearizable system in normal form coordinates, we need to first invert the transformation using

```
InverseTransformation
```

and then use

```
TransformSystem
```

to obtain the system representation in the new coordinates. These computations are illustrated below.

```
In[155]:= InvTrans = InverseTransformation[var30, {z1, z2, z3}, Trans];

In[156]:= TransformSystem[f30, g30, var30, {z1, z2, z3}, Trans, InvTrans]
Out[156]= {{z2, z3, 3 θ z1 (2 z2^2 + z1 z3)}, {0, 0, 1}}
```

In these coordinates it is seen that the control:

$$u = -3\theta z_1(2z_2^2 + z_1 z_3) + v$$

reduces the system to

$$\begin{bmatrix} \dot{z}_1 \\ \dot{z}_2 \\ \dot{z}_3 \end{bmatrix} = \begin{bmatrix} z_2 \\ z_3 \\ 0 \end{bmatrix} + \begin{bmatrix} 0 \\ 0 \\ 1 \end{bmatrix} v$$

The control can be obtained as a function of the original state variables by using the transformation equations.

Now, we turn to the MIMO case. Formally, the MIMO exact feedback linearization problem is defined as follows. Consider the system

$$\dot{x} = f(x) + G(x)u \tag{7.66}$$

where $x \in R^n$, $u \in R^m$ and $f(x)$, $G(x)$ are smooth.

Definition 7.34. *Given a control system (7.66), it is said to be exactly feedback linearizable if there exists a coordinate transformation $x = \phi(z)$ on a neighborhood X of the origin of R^n and a feedback control $u = \varphi(x) + \Phi(x)v$, also defined on X with $\Phi(x)$ nonsingular on X such that the transformed system is of the form*

$$\dot{z} = Az + Bv$$

with (A,B) controllable.

To determine if a system is feedback linearizable, we can use the conditions established in the following proposition that generalizes Proposition (6.196) to the MIMO case.

Proposition 7.35. *Suppose the matrix $G(x_0)$ has rank m. Then the system (7.66) is exactly feedback linearizable around x_0 if and only if:*

1. *the distributions*

$$\mathscr{G}_j = \{ad_f^k g_i : \ 0 \le k \le j, 1 \le i \le m\}, \quad 0 \le j \le n-1,$$

   where g_i are the columns of G, have constant dimension near x_0.

2. *the distribution $\mathscr{G}_{n-1}$ has dimension n at x_0,*

3. *for each j, $0 \le j \le n-2$, the distribution $\mathscr{G}_j$ is involutive near x_0.*

Proof: [46], Chapter 5. ■

Notice that $\mathscr{G}_{n-1} = \Delta_{L_0}$ so that local controllability is necessary for exact feedback linearizability.

Example 7.36 (Feedback linearizability).
Another illustration of the function `FeedbackLinearizable` is:

$$\begin{bmatrix} \dot{x}_1 \\ \dot{x}_2 \\ \dot{x}_3 \end{bmatrix} = \begin{bmatrix} 1+x_1+x_3 \\ 1+x_2 \\ -x_3 \end{bmatrix} + \begin{bmatrix} 1+x_1+x_3 & 0 \\ 1+x_2 & 0 \\ 0 & e^{x_3}+x_1x_2 \end{bmatrix} v$$

```
In[157]:= f33 = {1+x1+x3, 1+x2, -x3};
          g33 = {{1+x1+x3, 0}, {1+x2, 0}, {0, Exp[x3]+x1  x2}};
          var33 = {x1, x2, x3};

In[158]:= FeedbackLinearizable[f33, g33, var33]
Out[158]= False
```

We see that the system is not feedback linearizable. This fact is not remarkable, but the way in which linearizability fails is interesting. First, we test controllability and find that the system is controllable.

```
In[159]:= Controllability[f33, g33, var33]
Out[159]= True
```

Actually, we need a stronger version of controllability, i.e., $\text{rank}\Delta_{L_0} = n = 3$. The calculation is

```
In[160]:= Rank[{g1, g2, Ad[f33, g1, var33], Ad[f33, g2, var33],
              Ad[f33, g1, var33, 2], Ad[f33, g2, var33, 2]}]
Out[160]= 3
```

The system satisfies this more restrictive controllability condition. Now, let us test for involutivity of the requisite distributions. There are two of them and one fails.

```
In[161]:= {g1, g2} = Transpose[g33];
          Involutive[{g1, g2}, var33]
```

```
Out[161]= False

In[162]:= Involutive[{g1, g2, Ad[f33, g1, var33], Ad[f33, g2, var33]}, var33]
Out[162]= True
```

7.4 Control via Dynamic Inversion

Control design based on input-output linearization breaks down if the decoupling matrix $\rho(x)$ does not have an inverse. Nevertheless, the basic ideas can be extended to a wider class of systems with some modification. The approach we take is from the vantage point of system invertibility. Given a control system such as (7.1), with initial state fixed, we can define both a right and a left inverse. Roughly speaking, a right inverse generates a control u that will produce a given output y, and a left inverse generates the control that produced an observed output.

Definition 7.37 (Invertible).

1. *The system (7.1) is* invertible *at $x_0 \in R^n$ if whenever $u_1(t)$ and $u_2(t)$ are distinct admissible (real, analytic) controls, $y(\cdot, u_1, x_0) \neq y(\cdot, u_2, x_0)$.*
2. *The system (7.1) is* strongly invertible *at $x_0 \in R^n$ if there exists a neighborhood V of x_0 such that for all $x \in V$ the system is ivertible at x.*
3. *The system (7.1) is* strongly invertible *if it is strongly invertible at x_0 for all $x_0 \in R^n$.*

First, observe that if the system (7.1) is square ($p = m$) and can be input–output linearized as described above, that is if $\det\{\rho(x)\} \neq 0$, then both right and left inverses exist. Notice that the linearized input–output dynamics (7.40) can be written

$$y^{(\mathrm{r})} = v$$

where r is the vector relative degree and

$$y^{(\mathrm{r})} = (y_1^{(r_1)}, \ldots, y_m^{(r_m)})^T$$

Consequently, in view of (7.37), (7.38) and (7.39), the inverse can be explicitly represented:

$$\begin{aligned} \dot{\xi} &= F(\xi, z, y_R^{(\mathrm{r})}) \\ \dot{z} &= Az + Ey_R^{(\mathrm{r})} \\ u &= \rho^{-1}(x(\xi, z))\{-\alpha(x(\xi, z)) + y_R^{(\mathrm{r})}\} \end{aligned} \tag{7.67}$$

The system (7.67) can serve either as a right ($y_R^{(\mathrm{r})}$ is a prescribed reference output) or a left ($y_R^{(\mathrm{r})}$ is an observed output) inverse. As a right inverse, we consider $y_R(t)$

to be prescribed and sufficiently smooth so that all of its derivatives, including the highest order derivatives which drive (7.67) are known, $y_R^{(r)} = \left[y_{R,1}^{(r_1)},..,y_{R,m}^{(r_m)}\right]$. As a left inverse the required smoothness is automatic if $u(t)$ is piecewise continuous. Note that (7.67) is equivalent to:

$$\begin{array}{l} \dot{x} = f(x) + G(x)u \\ u = \rho^{-1}(x)\left\{-\alpha(x) + y_R^{(r)}\right\} \end{array} \quad or \quad \begin{array}{r} \dot{x} = f(x) + G(x)u \\ y_R^{(r)} = \alpha(x) + \rho(x)u \end{array} \tag{7.68}$$

Equations (7.67) and (7.68) represent the same system described in different state coordinates.

Equation (7.67) clearly displays the relationship between input–output linearization and inversion. We have seen above that if the decoupling matrix is nonsingular then a system inverse exists. On the other hand, singularity of the decoupling matrix does not imply that an inverse fails to exist. We seek a more general construction for an inverse with the goal of identifying a larger class of control laws. The basic tool for constructing a right inverse is the *structure algorithm* introduced by Hirshorn [42] and Singh [95]. If the system (7.1) has an inverse, then application of the structure algorithm leads to identification of a finite integer β and matrices $H_\beta(x)$, $C_\beta(x)$, $D_\beta(x)$ such that

$$H_\beta(x)Y_\beta(t) = C_\beta(x) + D_\beta(x)u \tag{7.69}$$

where

$$Y_\beta(t) = [y^{(1)^T}, y^{(2)^T}, .., y^{(\beta)^T}]^T \tag{7.70}$$

and $D_\beta(x)$ is an $p \times m$ matrix with rank $\min(m, p)$. Thus, (7.69) may be thought of as a generalization of the second equation of (7.68). Suppose $p = \min(m, p)$. It follows that $D_\beta(x)$ has a right (matrix) inverse $D_\beta^\dagger(x)$. Consequently, the right system inverse is defined by:

$$\begin{array}{l} \dot{x} = f(x) + G(x)u \\ u = D_\beta^\dagger(x)\left\{-C_\beta(x) + H_\beta(x)Y_\beta(t)\right\} \end{array} \tag{7.71}$$

In this case, given a reference $y_R(t)$, a control $u(t)$ is obtained that will reproduce it when applied to the system (assuming the correct initial state). While $u(t)$ is not unique (if $p < m$), it does the job. On the other hand if $m = \min(m, p)$, then $D_\beta(x)$ has a left (matrix) inverse $D_\beta^\dagger(x)$ and (7.71) defines a left system inverse. In this case an observed $y(t)$ drives the (left) inverse system which produces the unique control that generated $y(t)$. However, there may be different observed outputs that result in the same control.

The following summarizes the Structure algorithm.

Algorithm 7.38 (Structure Algorithm) *Consider the system (7.1).*

1. *Step 1 Compute*

$$\dot{y} = \frac{\partial h}{\partial x}[f + Gu] =: L_f h(x) + L_G h(x)u \tag{7.72}$$

and define $r_1 := \text{rank} L_G h(x)$[1]. *Permute the output components so that the first* r_1 *rows of* $L_G h$ *are independent. Since the last* $p - r_1$ *rows are linearly dependent on the first* r_1 *rows, combinations of the first rows can be used to zero out the last rows. Let* E_1^1 *and* $E_1^2(x)$ *be the permutation and row zeroing matrices. Then define*

$$z_1 = E_1^2(x) E_1^1 \dot{y} \tag{7.73}$$

$$z_1 = E_1^2(x) E_1^1 (L_f h(x) + L_G h(x) u) \tag{7.74}$$

Now, write $z_1 = (\bar{z}_1^T, \hat{z}_1^T)^T$, *with* $\bar{z}_1 \in R^{r_1}$, $\hat{z}_1 \in R^{p-r_1}$. *From the first* r_1 *rows of (7.74)*

$$\bar{z}_1 = \bar{c}_1(x) + \bar{D}_1(x) u, \quad \text{rank} \bar{D}_1 = r_1 \tag{7.75}$$

and from the last $p - r_1$ *rows of*

$$\hat{z}_1 = \hat{c}_1(x) \tag{7.76}$$

Finally, define System 1 *to be*

$$\dot{x} = f(x) + G(x) u$$

$$z_1 = \begin{bmatrix} \bar{z}_1 \\ \hat{z}_1 \end{bmatrix} = c_1(x) + D_1(x) u$$

where

$$c_1(x) = \begin{bmatrix} \bar{c}_1(x) \\ \hat{c}_1(x) \end{bmatrix}, \; D_1(x) = \begin{bmatrix} \bar{D}_1(x) \\ 0 \end{bmatrix}$$

2. *Step 2 Differentiate* $\hat{z}_1$ *to obtain*

$$\dot{\hat{z}}_1 = \frac{\partial \hat{z}_1}{\partial x} [f + Gu]$$

which can be written as

$$\dot{\hat{z}}_1 = L_f \hat{c}_1(x) + L_G \hat{c}_1(x) u$$

Now, consider

$$\begin{bmatrix} \bar{z}_1 \\ \dot{\hat{z}}_1 \end{bmatrix} = \begin{bmatrix} \bar{c}_1(x) \\ L_f \hat{c}_1(x) \end{bmatrix} + D(x) u, \; D(x) := \begin{bmatrix} \bar{D}_1(x) \\ L_G \hat{c}_1(x) \end{bmatrix}$$

Let $r_2 = \text{rank} D$. *Then permute the rows of* D *to make the first* r_2 *rows independent and the zero out the last rows. Let* E_2^1 *and* $E_2^2(x)$ *be the permutation and row zeroing matrices. Define*

$$z_2 = E_2^2(x) E_2^1 \begin{bmatrix} \bar{z}_1 \\ \dot{\hat{z}}_1 \end{bmatrix}$$

and divide z_2 *into* $\bar{z}_2 \in R^{r_2}$ *and* $\hat{z}_2 \in R^{p-r_2}$*:*

[1] By the notation $L_G h$, we mean the matrix whose columns are $L_{g_i} h$.

$$\bar{z}_2 = \bar{c}_2(x) + \bar{D}_2(x)u$$

$$\hat{z}_2 = \hat{c}_2(x)$$

Finally, define System 2 *to be*

$$\dot{x} = f(x) + G(x)u$$

$$z_2 = \begin{bmatrix} \bar{z}_2 \\ \hat{z}_2 \end{bmatrix} = c_2(x) + D_2(x)u$$

$$c_2(x) = \begin{bmatrix} \bar{c}_2(x) \\ \hat{c}_2(x) \end{bmatrix},\ D_2(x) = \begin{bmatrix} \bar{D}_2(x) \\ 0 \end{bmatrix}$$

3. *Step $k+1$ Suppose that in steps 1 through k, the integers $r_1, \ldots, r_k$ and the functions $\bar{z}_1 \in R^{r_1}, \ldots, \bar{z}_k \in R^{r_k}, \hat{z}_k \in Rp - r_k$ have been defined so that we have* System *k:*

$$\dot{x} = f(x) + G(x)u$$

$$z_k = \begin{bmatrix} \bar{z}_k \\ \hat{z}_k \end{bmatrix} = c_k(x) + D_k(x)u$$

with

$$c_k(x) = \begin{bmatrix} \bar{c}_k(x) \\ \hat{c}_k(x) \end{bmatrix},\ D_k(x) = \begin{bmatrix} \bar{D}_k(x) \\ 0 \end{bmatrix}$$

Then differentiate $\hat{z}_k$

$$\dot{\hat{z}}_k = \frac{\partial z_k}{\partial x}[f + Gu] \tag{7.77}$$

which can be rewritten as

$$\dot{\hat{z}}_k = L_f \hat{c}_k(x) + L_G \hat{c}_k(x)u \tag{7.78}$$

Now, consider

$$\begin{bmatrix} \bar{z}_k \\ \dot{\hat{z}}_k \end{bmatrix} = \begin{bmatrix} \bar{c}_k(x) \\ L_f \hat{c}_k(x) \end{bmatrix} + D(x)u,\ D(x) := \begin{bmatrix} \bar{D}_k(x) \\ L_G \hat{c}_k(x) \end{bmatrix}$$

Let $r_{k+1} :=$ rank$D$. Permute the rows of D to make the first r_{k+1} rows independent. Use combinations of these rows to zero out the remaining (dependent) rows. Denote the permutation matrix and row zeroing matrices E^1_{k+1} and $E^2_{k+1}(x)$, respectively. Then define

$$z_{k+1} = E^2_{k+1}(x)E^1_{k+1}\begin{bmatrix} \bar{z}_k \\ \dot{\hat{z}}_k \end{bmatrix} \tag{7.79}$$

Finally, define System $k+1$

$$\dot{x} = f(x) + G(x)u$$

$$z_{k+1} = \begin{bmatrix} \bar{z}_{k+1} \\ \hat{z}_{k+1} \end{bmatrix} = c_{k+1}(x) + D_{k+1}(x)u$$

with

$$c_{k+1}(x) = \begin{bmatrix} \bar{c}_{k+1}(x) \\ \hat{c}_{k+1}(x) \end{bmatrix},\ D_{k+1}(x) = \begin{bmatrix} \bar{D}_{k+1}(x) \\ 0 \end{bmatrix}$$

4. *Stop By construction the integers r_i satisfy $r_1 \leq r_2 \leq \ldots \leq r_k$. Moreover, there is a smallest positive integer k^* such that $r_{k^*} \leq \min(m,p)$ is maximal. If the procedure terminates in finite steps, it does so at step k^* with $r_{k^*} = \min(m,p)$ and an inverse can be constructed (a right inverse if $p = \min(m,p)$ and a left inverse if $m = \min(m,p)$. The* relative order *β is k^* if the procedure terminates in finite steps, otherwise $\beta = \infty$. The number β identifies the highest order derivative required to drive the inverse. Thus, it can not be greater than the number of states, n. Thus, the procedure should not proceed beyond n steps.*

In *ProPac*, the structure algorithm is implemented in the function

`StructureAlgorithm`.

Example 7.39 (Inverse system, output restrictions). This first example is considered in both Hirschorn [7] and Singh [9].

```
In[163]:= x = {x1, x2, x3};
          f = {0, x3, 0}; G = {{x1, 0}, {-x3, 0}, {0, x1}};
          h = {x1, x2};
          {DD, CC, HH, ZZ} = StructureAlgorithm[f, G, h, x, t];

In[164]:= u = Simplify[RightInverse[DD].(-CC + ZZ)];
          (f + G.u)//MatrixForm
```

$$\text{Out[164]=} \begin{pmatrix} y1'[t] \\ x3 - \dfrac{x3\ \ y1'[t]}{x1} \\ \dfrac{-x3\ \ y1'[t]^2 + x1\ \ (x3\ \ y1''[t] + x1\ \ y2''[t])}{x1\ \ (x1 - y1'[t])} \end{pmatrix}$$

It is to be anticipated that a complete discussion of system inverses would include a characterization of the system input and output spaces. In [42], Hirschorn gives sufficient conditions for the existence of an inverse and shows that they do not apply in the case of this example. Modifying the arguments in [42], Singh in [95] derives sufficient conditions for existence of a left system inverse that apply with restrictions imposed on the system output space. These conditions, applied to this example, establish the existence of a left inverse provided $y_1^{(1)} \neq x_1$. Clearly, if our inverse is to be meaningful, this condition must be satisfied.

Example 7.40 (Inverse system). The following example is from Neijmeijer and Van der Schaft [87].

```
In[165]:= x = {x1, x2, x3, x4};
          f = {0, x3, x4, 0}; G = {{1, 0}, {x4, 0}, {0, 0}, {0, 1}};
          h = {x1, x2};
          {DD, CC, HH, ZZ} = StructureAlgorithm[f, G, h, x, t];

In[166]:= u = RightInverse[DD].(-CC + ZZ);
          (f + G.u) // MatrixForm
```

$$\text{Out[166]=}\begin{pmatrix} y1'[t] \\ x3 + x4\ \ y1'[t] \\ x4 \\ \dfrac{-x4 - x4\ \ y1''[t] + y2''[t]}{y1'[t]} \end{pmatrix}$$

7.4.1 Tracking Control

There are a number of ways in which the results of the structure algorithm can be used to construct feedback controllers. It is an important fact that not all of the elements in Y_β actually survive multiplication by $H_\beta(x)$. Let us denote by n_i and N_i the lowest and highest order derivative of y_i appearing in $H_\beta(x)Y_\beta$. Then, we can write

$$H_\beta(x)Y_\beta = \tilde{H}\tilde{y} \tag{7.80}$$

where

$$\tilde{y} = [y_1^{n_1}, .. y_1^{N_1}, .., y_l^{n_l} .., y_l^{N_l}]^T \tag{7.81}$$

so that (7.71) can be written as:

$$\begin{aligned} \dot{x} &= f(x) + G(x)u \\ u &= D_\beta^\dagger(x)\left\{-C_\beta(x) + \tilde{H}(x)\tilde{y}(t)\right\} \end{aligned} \tag{7.82}$$

One approach to tracking control is based on the concept of using the inverse system to compute a feedforward control and then add a perturbation controller based on the tracking error (see Figure (7.3)). For instance if $y_R(t)$ is the reference trajectory, we could implement the control

$$u = D_\beta^\dagger(x)\left\{-C_\beta(x) + \tilde{H}(x)\tilde{y}_R(t) + v(t)\right\} \tag{7.83}$$

where $v(t)$ is the perturbation controller.

One choice for the perturbation controller is [95]:

$$v_i = \gamma_{i0}\int (y_{Ri} - y_i)dt + \sum_{j=0}^{n_i-1} p_{ij}(y_{Ri}^{(j)} - y_i^{(j)}),\ \ i = 1, .., l \tag{7.84}$$

Stability of the closed loop requires that the following polynomials are Hurwitz:

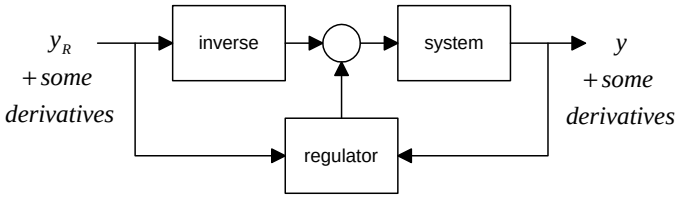

Fig. 7.3: A tracking control concept based on the system right inverse.

$$\sum_{j=0}^{n_i+1} \gamma_{ij} \cdot s^j = 0, \quad i = 1,..,l \tag{7.85}$$

with $\gamma_{ij} = p_{i,j-1}$, $j = 1,..,n_i+1$.

A variant of this controller is given by Singh [96]. Here (7.83) is replaced by

$$u = D_\beta^\dagger(x)\{-C_\beta(x) + M(x)\tilde{y}_0 + N(x)v(t)\} \tag{7.86}$$

where

$$H_\beta(x)Y_\beta = M(x)\tilde{y}_0 + N(x)y^{(n)} \tag{7.87}$$

$$\tilde{y}_0 = [y_1^{(n_1+1)},\ldots,y_1^{(N_1)},\ldots,y_l^{(n_l+1)},\ldots,y_l^{(N_l)}]^T \quad \text{and} \quad y(n) = [y_1^{n_1},\ldots,y_l^{(n_l)}]^T \tag{7.88}$$

and $N(x)$ is an invertible matrix. It is easily verified, by substituting (7.86) and (7.87) into (7.69), that this is a decoupling controller that reduces the input–output equations to

$$y_i^{(n_i)} = v_i, \quad i = 1,\ldots,l \tag{7.89}$$

The perturbation controller is

$$v_i = \gamma_{i,0}\int (y_{Ri} - y_i)dt + \sum_{j=0}^{n_i-1} p_{ij}(y_{Ri}^{(j)} - y_i^{(j)}) + y_{Ri}^{(n_j)}. \tag{7.90}$$

Substituting the perturbation control yields the closed loop error dynamics

$$\varepsilon_i^{(n_i+1)} + \gamma_{i,n_i}\varepsilon_i^{(n_i)} + \gamma_{i,n_i-1}\varepsilon_i^{(n_i-1)} + \ldots + \gamma_{i,0} = 0$$

where $\varepsilon_i := y_i - y_{Ri}$. Implementation of this controller requires measurement of the state x and output derivatives up to $y_i^{(N_i)}$, and knowledge of the reference trajectory and its derivatives up to $y_{Ri}^{(n_i)}$. While output derivatives up to order $y_i^{(n_i-1)}$ are indeed necessary to implement a perfect tracking controller, the higher order derivatives are not. The need to measure or compute the higher order derivatives of the output, specifically $\tilde{y}_0$ can be a serious problem, because they may be noncausal in the sense that computing them may require computing derivatives of the input u. But this can be remedied as follows in the next section.

7.4.2 Dynamic Decoupling Control

Let us rewrite (7.82) in the form

$$u = D_\beta^\dagger(x)\left\{-C_\beta(x) + \tilde{H}_1(x)\tilde{y}_1(t) + \tilde{H}_2(x)y^{(N)}\right\} \tag{7.91}$$

$$\tilde{y}_1 = [y_1^{n_1}, ..y_1^{N_1-1}, .., y_l^{n_l} .., y_l^{N_l-1}]^T \quad \text{and} \quad y^{(N)} = [y_1^{(N_1)}, .., y_l^{(N_l)}]^T \tag{7.92}$$

so that we have pulled out the highest order derivative of y. Now, let $\eta_i \in R^{N_i-n_i}, i = 1,\ldots,l$, set $v = y^{(N)}$ and consider the dynamical systems

$$\dot{\eta}_i = A_i\eta_i + B_i v_i, \;\; i = 1,\ldots,l \tag{7.93}$$

with (A_i, B_i) in Brunovsky canonical form. Notice that $y_i^{(N_i-j)} = \eta_i^j, \; j = 1,\ldots,N_i - n_i$. The control (7.86) can be written

$$u = D_\beta^\dagger(x)\{-C_\beta(x) + \tilde{H}_1(x)\eta + \tilde{H}_2(x)v\}. \tag{7.94}$$

The dynamic compensator defined by (7.93) and (7.94) is a decoupling, input–output linearizing controller. Its application results in the input–output dynamics:

$$y_i^{(N_i)} = v_i, \quad i = 1,\ldots,l \tag{7.95}$$

Thus, we can apply the controller

$$v_i = \gamma_{i,0}\int (y_{Ri} - y_i)dt + \sum_{j=0}^{N_i-1} p_{ij}(y_{Ri}^{(j)} - y_i^{(j)}) + y_{Ri}^{(N_i)}.$$

to obtain the closed loop error dynamics

$$\varepsilon_i^{(N_i+1)} + \gamma_{i,N_i}\varepsilon_i^{(N_i)} + \gamma_{i,N_i-1}\varepsilon_i^{(N_i-1)} + \ldots + \gamma_{i,0} = 0$$

where $\varepsilon_i := y_i - y_{Ri}$.

Implementation of this controller requires measurement of the state x, and either computation or measurement of the output derivatives $y_i, y_i^{(1)}, \ldots, y_i^{(n_i-1)}$, for $i = 1,\ldots,l$. Such an implementation is illustrated in Figure (7.4).

7.5 Dynamic Extension

Another way of dealing with the singularity of the decoupling matrix is a process known as dynamic extension [22, 46]. Dynamic extension entails augmenting the dynamical equations with integrators added at the input channels. The algorithm of Descusse and Moog [22] converges in a finite number of steps if the original

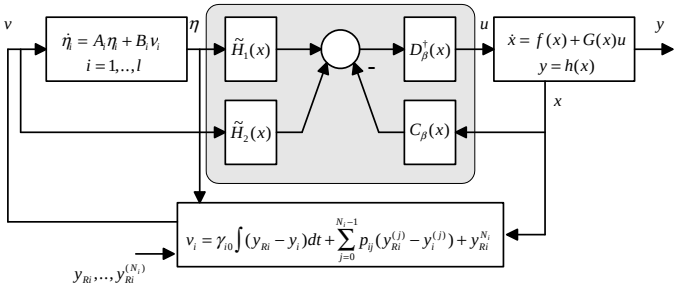

Fig. 7.4: This figure illustrates the implementation of a tracking controller using dynamic decoupling.

system is strongly invertible. It has been implemented in *ProPac* as the function `DynamicExtension`.

To motivate the procedure, consider the simple linear system shown in Figure (7.5):

$$\begin{aligned}\dot{x}_1 &= x_2 + u_1\\ \dot{x}_2 &= u_2\\ \dot{x}_3 &= 2x_2 + u_1\end{aligned}$$

$$\begin{aligned}y_1 &= x_1\\ y_2 &= x_3\end{aligned}$$

Let us try to decouple the system by following the input–output linearization pro-

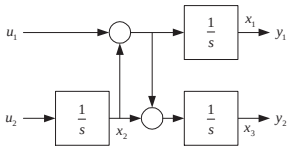

Fig. 7.5: This simple linear system illustrates the delayed appearance of the second control input.

cedure of Section 6.5. To do this, successively differentiate y_1 and y_2 until a control appears,

$$\dot{y}_1 = x_2 + u_1$$

$$\dot{y}_2 = 2x_2 + u_1$$

Thus, we see that

$$\rho = \begin{bmatrix}1 & 0\\ 1 & 0\end{bmatrix}$$

It is singular and the system does not have a well-defined relative degree vector. But the second control has not had an influence because of the premature appearance of u_1 simultaneously in both outputs. Let us delay the appearance of u_1 by placing an integrator before the first input. Thus, the new state equations are

$$\begin{aligned}\dot{x}_1 &= x_2 + u_1\\ \dot{x}_2 &= u_2\\ \dot{x}_3 &= 2x_2 + u_1\\ \dot{u}_1 &= v\end{aligned}$$

Now attempt to decouple the augmented system. Successive differentiation leads to

$$\begin{aligned}\ddot{y}_1 &= u_2 + v\\ \ddot{y}_2 &= 2u_2 + v\end{aligned}$$

So

$$\rho = \begin{bmatrix}1 & 1\\ 2 & 1\end{bmatrix}$$

The augmented system decoupling matrix is nonsingular and the relative degree is well defined $\mathbf{r} = \{2,2\}$. A systematic procedure for attempting to achieve well-defined relative degree by integrator augmentation of the input channels is given in the following Algorithm.

Algorithm 7.41 (Dynamic Extension) *Consider the system (7.1) with $p = m$ (a square system).*

1. *Compute the matrix $\rho(x)$. If* rank$\rho = m$ *Stop!*
2. *if* rank$\rho = s < m$*, perform elementary column operations to make the first s columns independent and the last $m-s$ columns zero. Let E(x) denote the square, nonsingular matrix that does this: $\rho_1(x) = \rho(x)E(x)$.*
3. *Suppose there are q columns (say, $i_1, \ldots, i_q$) each having two or more elements that are not identically zero around x_0. If $q = 0$, Stop! The process fails.*
4. *If $q \neq 0$, define the index set $\alpha = \{i_1, \ldots, i_q\}$ and let $\bar{\alpha}$ denote its complment. Put an integrator in series with the q corresponding controls to obtain a new augmented system*

$$\begin{bmatrix}\dot{x}\\ \dot{u}_\alpha\end{bmatrix} = \begin{bmatrix}f(x) + \sum_{i\in\alpha} g_i(x)u_i\\ 0\end{bmatrix} + \begin{bmatrix}\sum_{i\in\bar{\alpha}} g_i(x)u_i\\ v_\alpha\end{bmatrix}$$

5. *Go to step 1 and repeat the process with the new augmented system.*

Example 7.42 (Dynamic inversion revisited). Let us reconsider Examples (7.39) and (7.40). First, Example (7.39). Recall that `D[f,{x,n}]` is the Mathematica function for the n^{th} partial derivative with respect to x.

```
In[167]:= {fnew, Gnew, hnew, xnew} = DynamicExtension[f, G, h, x];

In[168]:= {ρ, α, r0, u} = IOLinearize[fnew, Gnew, hnew, xnew];
          u = (u/.{v1 -> D[y1[t], {t, r0[[1]]}], v2 -> D[y2[t], {t, r0[[2]]}]});
          Simplify[(fnew + Gnew.u)]//MatrixForm

Computing Decoupling Matrix

Computing linearizing/decoupling control
```

$$\text{Out[168]=}\begin{pmatrix} \text{x1}\ \ \text{z1} \\ \text{x3}-\text{x3}\ \ \text{z1} \\ \dfrac{\text{x1}\ \ \text{x3}\ \ \text{z1}^2-\text{x3}\ \ y1''[\text{t}]-\text{x1}\ \ y2''[\text{t}]}{\text{x1}\ \ (-1+\text{z1})} \\ -\text{z1}^2+\dfrac{y1''[\text{t}]}{\text{x1}} \end{pmatrix}$$

Now, let us turn to the system from Example (7.40). Dynamic extension can also be used to construct the inverse.

```
In[169]:= IOLinearize[f, G, h, x]
          {fnew, Gnew, hnew, xnew} = DynamicExtension[f, G, h, x];

Computing Decoupling Matrix

Decoupling matrix is singular!

Dynamic extension completed

In[170]:= {ρ, α, r0, u} = IOLinearize[fnew, Gnew, hnew, xnew];
          u = (u/.{v1 -> D[y1[t], {t, r0[[1]]}], v2 -> D[y2[t], {t, r0[[2]]}]});
          (fnew + Gnew.u)//MatrixForm

Computing Decoupling Matrix

Computing linearizing/decoupling control
```

$$\text{Out[170]=}\begin{pmatrix} \text{z1} \\ \text{x3}+\text{x4}\ \ \text{z1} \\ \text{x4} \\ -\dfrac{\text{x4}\ \ y1''[\text{t}]}{\text{z1}}+\dfrac{-\text{x4}+y2''[\text{t}]}{\text{z1}} \\ y1''[\text{t}] \end{pmatrix}$$

Example 7.43 (Dynamic extension). Here is another example for which the decoupling matrix is singular and thus feedback linearization can not be employed directly:

$$\begin{bmatrix} \dot{x}_1 \\ \dot{x}_2 \\ \dot{x}_3 \end{bmatrix} = \begin{bmatrix} \cos(x_3) & 0 \\ \sin(x_3) & 0 \\ 0 & 1 \end{bmatrix} \begin{bmatrix} u_1 \\ u_2 \end{bmatrix}$$

$$\begin{bmatrix} y_1 \\ y_2 \end{bmatrix} = \begin{bmatrix} x_1 \\ x_2 \end{bmatrix}$$

```
In[171]:= f12 := {0,0,0};
          g12 := Transpose[{{Cos[x3], Sin[x3], 0}, {0,0,1}}];
          h12 := {x1, x2}; var12 := {x1, x2, x3}
          {fnew, Gnew, hnew, xnew} = DynamicExtension[f12, g12, h12, var12]

Dynamic extension completed
Out[171]= {{z1 Cos[x3], z1 Sin[x3], 0, 0}, {{0,0}, {0,0}, {0,1}, {1,0}},
            {x1, x2}, {x1, x2, x3, z1}}
```

Thus, we find that the extended state vector is (x_1, x_2, x_3, z_1) and f , G and h are modified to:

$$f = \begin{bmatrix} z_1 \cos(x_3) \\ z_1 \sin(x_3) \\ 0 \\ 0 \end{bmatrix}, \quad G = \begin{bmatrix} 0 & 0 \\ 0 & 0 \\ 0 & 1 \\ 1 & 0 \end{bmatrix}, \quad h = \begin{bmatrix} x_1 \\ x_2 \end{bmatrix}$$

The extended system has a nonsingular decoupling matrix.

7.6 Problems

7.6.1 Controllability

Problem 7.44. Check controllability for the system:

$$\begin{aligned} \dot{x}_1 &= u_1 x_3 + u_2 \\ \dot{x}_2 &= u_1 x_1 \\ \dot{x}_3 &= u_1 x_2 \end{aligned}$$

Problem 7.45. Consider the control systems given below. Compute and describe the maximal integral manifolds of the controllability distributions Δ_C and Δ_{C_0}.

(a) the linear system

$$\dot{x} = \begin{bmatrix} 1 & 0 & 0 \\ 0 & -1 & 0 \\ 0 & 0 & 1 \end{bmatrix} x + \begin{bmatrix} 1 \\ 0 \\ 0 \end{bmatrix} u$$

(b) the bilinear system

$$\dot{x} = \begin{bmatrix} 0 & 1 & 0 \\ -1 & 0 & 0 \\ 0 & 0 & 0 \end{bmatrix} x + u \begin{bmatrix} 0 & 0 & 1 \\ 0 & 0 & 0 \\ -1 & 0 & 0 \end{bmatrix} x$$

Problem 7.46. Investigate the controllability properties of the nonlinear system

$$\dot{x} = \begin{bmatrix} x_2 + x_2^2 + x_3^2 \\ x_3 + \sin(x_1 - x_3) \\ x_3^2 \end{bmatrix} + \begin{bmatrix} 1 \\ 0 \\ 1 \end{bmatrix} u$$

Problem 7.47. Consider the (angular) velocity control of a sattelite in space using gas jets. The dynamical equations are:

$$J\dot{\omega} = \omega \times (J\omega) + \tau$$

where ω is the angular velocity, τ is the control torque vector, and $J = \text{Diag}\{J_x, J_y, J_z\}$ is the inertia matrix, all in principal axis body coordinates.

(a) Show that the system is not (locally) controllable if any one actuator is used.

(b) Suppose $J_x > J_y > J_z$. Show that the system is controllable if any two of the actuators are used.

(c) Suppose $J_x = J_y > J_z$. Show that the system is controllable if τ_1 and τ_3 are used or if τ_2 and τ_3, but not controllable if τ_1 and τ_2 are used.

(d) Suppose $J_x = J_y = J_z$. Show that the system is not controllable unless all three actuators are used.

Problem 7.48. A simplied model for the configuration of a vehicle moving in a plane is

$$\begin{bmatrix} \dot{x} \\ \dot{y} \\ \dot{\theta} \end{bmatrix} = \begin{bmatrix} \sin\theta \\ \cos\theta \\ 0 \end{bmatrix} u_1 + \begin{bmatrix} 0 \\ 0 \\ 1 \end{bmatrix} u_2$$

Here x, y denote the planar location of the vehicle and θ denotes its orientation. The model is purely kinematic. It is assumed that the forward velocity u_1 and angular velocity u_2 are control inputs. Show that the system is controllable.

Problem 7.49. A purely kinematic model for the rolling penny is

$$\frac{d}{dt}\begin{bmatrix} \phi \\ \psi \\ x \\ y \end{bmatrix} = \begin{bmatrix} 1 \\ 0 \\ 0 \\ 0 \end{bmatrix} u_1 + \begin{bmatrix} 0 \\ 1 \\ \cos\phi \\ \sin\phi \end{bmatrix} u_2$$

Is it controllable?

Problem 7.50 (Sleigh, continued). Consider the sleigh of Problem (6.24) in Chapter 5 (consider the case $\alpha = 0$).

(a) Show that the sleigh is locally controllable.

(b) Show that the origin is an equilibrium point with controls $, F = 0,\ T = 0$ but that it can not be asymptotically stabilized by any smooth feeback control. Hint: recall Lemma (2.16) of Chapter 2.

7.6.2 Feedback Linearization

Problem 7.51. Consider a linear system characterized by the SISO transfer function

$$G(s) = K\frac{s^m + a_{m-1}s^{m-1} + \cdots + a_0}{s^n + b_{n-1}s^{n-1} + \cdots + b_0},\ n \geq m$$

Determine a state space realization for this system. Show that the definition of relative degree given in Definition (7.14) is consistent with the traditional concept of relative degree in SISO linear systems. Compute the zero dynamics.

Problem 7.52. Consider the simplified vehicle model

(a) Vehicle dynamics:

$$m\ddot{x} = F - \rho\dot{x}^2\mathrm{sgn}(\dot{x}) - d_m$$

(b) Engine:

$$\dot{\xi} = \frac{\xi}{\tau(\dot{x})} + \frac{u}{m\tau(\dot{x})}, \quad F = m\xi$$

m, ρ, d_m are constants, and u is the throttle input. Write these equations in state space form and examine the linearizability of the system from input u to output x. Determine the relative degree and zero dynamics of the system.

Problem 7.53. Find a feedback linearizing and stabilizing control such that the closed loop poles are -1,-2,-3, for the system:

$$\begin{aligned}\dot{x}_1 &= \sin x_2\\ \dot{x}_2 &= \sin x_3\\ \dot{x}_3 &= u\end{aligned}$$

Taylor linearize the system and find a linear perturbation control that places the poles at -1,-2,-3. Compare the two controllers.

Problem 7.54. Consider the bilinear system

$$\dot{x} = \begin{bmatrix}0 & 0 & 3\\ 0 & 0 & 6\\ 0 & 0 & -2\end{bmatrix}x + \begin{bmatrix}1 & 2 & 4\\ 2 & 2 & 0\\ 0 & 0 & 3\end{bmatrix}xu$$

(a) Determine if this system is locally controllable around the origin.

(b) Consider the Taylor linearization of this system and determine if it is controllable.

(c) Determine if the system is exactly feedback linearizable around the origin.

(d) Design an asymptotically stabilizing state feedback controller.

Problem 7.55. (from [2]) Consider the system

$$\begin{aligned} \dot{x} &= f(x) + G(x)u \\ y &= h(x) \end{aligned}$$

with $f(x_0) = 0$. Denote its linearization around $x = x_0,\ u = 0$ by $\dot{\chi} = A\chi + Bu$ with $A = \partial f(x_0)/\partial x$ and $B = G(x_0)$. Suppose the system is exactly feedback linearizable around x_0. Show that the system can be transformed via state transformation and feedback to the linear system $\dot{z} = Az + Bv$ with $A,\ B$ as given above.

Problem 7.56. (from [87]) Consider the Hamiltonian control system

$$\dot{q}_i = \frac{\partial H(q,p)}{\partial p_i},\ \dot{p}_i = -\frac{\partial H(q,p)}{\partial q_i} + u_i$$

where $i = 1, \ldots, n$ and the Hamiltonian is

$$H(q,p) = \tfrac{1}{2} p^T G(q) p + V(q)$$

with $G(q)$ a positive definite matrix for each q and $\partial V(q_0)/\partial q = 0$. Check feedback linearizability about the point $(q_0, 0)$.

Problem 7.57 (Overhead crane, continued). Consider the overhead crane of Problems (5.11) and (6.22).

(a) Design a feedback linearizing control that steers the payload to a specified location, $x = x_d$, $z = z_d$, in the plane with the arm pointing straight down, $\phi = 0$. Use all three control inputs.

(b) Compute the zero dynamics.

(c) Specify numerical values for the parameters and simulate the closed loop behavior.

Problem 7.58. ([99], Example 6.14) Consider the system

$$\begin{aligned} \dot{x}_1 &= x_1^2 x_2 \\ \dot{x}_2 &= 3x_2 + u \end{aligned}$$

(a) Taylor linearize the system at the origin $u = 0, x_1 = 0, x_2 = 0$ and show that the linear system is not controllable. Examine the controllability of the nonlinear system and explain your findings.

(b) Test to see if the system is exactly feedback linearizable. If so, compute the normal form transformation and feedback linearizing control. What's wrong with this picture?

(c) Consider the output $y = -2x_1 - x_2$. Find the input–output linearizing control. Obtain the zero dynamics and evaluate their stability. Can the system be asymptotically stabilized?

Problem 7.59 (Stabilizing Nonminimum Phase Systems). Consider the following system

$$\begin{aligned}\dot{x}_1 &= -x_1^3 x_2^2 + (2 + x_1^2)u \\ \dot{x}_2 &= x_3 \\ \dot{x}_3 &= -x_3^3 + x_2^5 - x_1 x_2\end{aligned}$$

(a) Transform the system to normal form and determine the feedback linearizing control law. Show that the feedback linearized system is

$$\begin{aligned}\dot{z}_1 &= v \\ \dot{z}_2 &= z_3 \\ \dot{z}_3 &= -z_1 z_2 + z_2^5 - z_3^3\end{aligned}$$

where v is the new control.

(b) Determine if the zero dynamics have a stable origin.

(c) Now, stabilize the system using a two-step (backstepping) procedure:

(1) Consider z_1 to be a psuedo-control and use it to stabilize the zero dynamics. Hint: Consider the Lyapunov function (why this function?)

$$V_0 = \tfrac{1}{2} z_3^2 + \tfrac{1}{6} z_2^6$$

for the system

$$\begin{aligned}\dot{z}_2 &= z_3 \\ \dot{z}_3 &= -\mu z_2 + z_2^5 - z_3^3\end{aligned}$$

and pick $\mu = \mu(z_2, z_3)$ to insure stability.

(2) Choose v to stablize the full system using the Lyapunov function

$$V = V_0 + \tfrac{1}{2}\left(z_1 - \mu(z_2, z_3)\right)^2$$

(d) What is the final control, $u(x_1, x_2, x_3)$?

Problem 7.60 (Issues with Decoupling). Consider the system

$$\begin{aligned}\dot{x}_1 &= x_1^3 + x_1 x_2 + (1 + x_2)u \\ \dot{x}_2 &= -x_2 + (1 + 2x_2)^2 x_1 \\ y &= x_1\end{aligned}$$

(a) Put the system in normal form and show that the zero dynamics are globally exponentially stable.

(b) Use a feedback linearizing control law to stablize the linearizable part so that $y \to 0$. Show, by simulation or other means, that if the initial value $z_1(0)$ (the new first state) is large enough, then the trajectory is unbounded. Thus, even though the linearized part and the zero dynamics are both globally exponentially stable, the closed loop system is not globally stable.

Problem 7.61 (Tracking Contol). Consider a SISO system

$$\dot{x} = f(x) + g(x)u, \quad y = h(x)$$

Assume the system has well-defined relative degree r, so that the feedback linearized input-output dynamics are:

$$y^{(r)} = v$$

Suppose $y_R(t)$ is a smooth (continuous derivatives up to $y_R^{(r)}$ will suffice) reference trajectory.

(a) Design a tracking controller based on stabilizing the error dynamics.

(b) Consider the following flexible joint robot:

$$I\ddot{q}_1 + mgl\sin q_1 + k(q_1 - q_2) = 0$$

$$J\ddot{q}_2 - k(q_1 - q_2) = u$$

Take $I = 1$, $mgl = 1$, $J = 1$, $k = 10$. Design a tracking controller so that $q_1(t)$ tracks $y_R(t) = 1 - e^{-t/5}$.

(c) Add friction to the joint

$$I\ddot{q}_1 + mgl\sin q_1 + k(q_1 - q_2) + c(\dot{q}_1 - \dot{q}_2) = 0$$

$$J\ddot{q}_2 - k(q_1 - q_2) - c(\dot{q}_1 - \dot{q}_2) = u$$

Take $c = 0.05$ and repeat the above design.

(d) Apply both controllers to the system with friction and discuss your results.

8

Observability and Observer Design

8.1 Introduction

When nonlinearities are essential, observability and observer design present new complexities and opportunities that are absent in linear problems. Unlike linear systems, a nonlinear system may be observable for some inputs and not so for others. A positive consequence of this is that there are opportunities for state estimation in nonlinear systems even when its linearization is not observable or there is some other pathology associated with observability (see Section 8.2). There are important practical implications because problems like this occur when operating around bifurcation points, such as an aircraft operating near stall, or a power network operating near voltage limits. They also arise in problems involving fault detection and identification. However, to take advantage of these possibilities it is necessary to build observers using new design paradigms, some of which have emerged in recent years.

This Chapter begins with an overview of observability and a summary of nonlinear observer design methods is given in Section 8.2. An observability hierarchy is defined that progresses, in weakening degree, from 'linearly observable' to 'zero-input observable' to satisfaction of the 'observability rank condition' to 'locally observable.' The tools we describe herein apply to all of these cases. A general observable form for nonautonomous nonlinear systems, introduced in[62], as well as a multiple output generalization of the observer form construction given in [37] are discussed in Section 8.4. We also describe in detail the computations required to construct the observable and observer forms. In Section 8.5.1 our implementation of them in *Mathematica* is discussed. Examples that illustrate all of the observability types in our hierarchy follow in Section 8.5.2.

8.2 Observability

Like controllability, observability is a fundamental property of nonlinear control systems just as it is for linear systems. Our treatment will be similar in many ways to the previous discussion of controllability. While observability does not have precisely the dual structure to controllability as it has in linear system theory, there are interesting parallels. Moreover, we will see that nonlinear observability has important nuances that distinguish it from the linear counterpart.

8.2.1 Definitions and Tests

Consider the nonlinear affine system described by Equation (7.1) and rewritten here as

$$\begin{aligned} \dot{x} &= f(x) + \sum_{i=1}^{m} g_i(x)u_i = f_u(x) \\ y &= h(x) \end{aligned} \tag{8.1}$$

where $x \in M$ (a neighborhood of x_0 in R^n), $u \in R^m$, and $y \in R^p$. Assume x_0 is an equilibrium point corresponding to zero input and output, i.e., $f(x_0) = 0$, $h(x_0) = 0$. The functions f, g_i, h are smooth. We write the right hand side of the differential equation as $f_u(x)$ to emphasize the role of u as a parameter of the vector field.

Denote by $y(\cdot; x_0, u)$ the entire output response $y(t; x_0, u)$, $\forall t > 0$ corresponding to the initial state x_0 and control $u(t)$, $\forall t > 0$.

Definition 8.1. *1. Let U be an open set in R^n. Two states $x_1, x_2 \in U$ are said to be U-distinguishable if there exists a control $u(t)$, $\forall t > 0$, whose trajectories from both x_1, x_2 remain in U, such that $y(\cdot; x_1, u) \neq y(\cdot; x_2, u)$. Otherwise they are U-indistinguishable.*

2. *The control system (7.1) is said to be strongly locally observable at $x_0 \in R^n$ if for every neighborhood U of x_0, every state in U other than x_0 is U-distinguishable from x_0. It is said to be locally observable at $x_0 \in R^n$ if there exists a neighborhood W of x_0 such that for every neighborhood U of x_0 contained in W every state in U other than x_0 is U-distinguishable from x_0.*
3. *The control system (7.1) is sad to be strongly locally observable if it is strongly locally observable at x_0 for every $x_0 \in R^n$. It is said to be locally observable if it is locally at observable x_0 for every $x_0 \in R^n$.*

In essence, local observability at x_0 requires only that x_0 be distinguishable from its immediate neighbors. More insight into the distinction between strong local observability and local observability can be found in [40] (where they are termed, respectively, local observability and weak local observability).

We can establish an observability triangular decomposition similar to the controllability decomposition of Lemma (7.3). First, we define the *observability codistribution*

$$\Omega_O = \left\langle f, g_1, \ldots, g_m | \text{ span} \left\{ dh_1, \ldots, dh_p \right\} \right\rangle \tag{8.2}$$

and its kernel

$$\Delta_O = \Omega_O^{\perp} \tag{8.3}$$

This distribution is invariant with respect to $f, g_1, \ldots, g_m$ and it is contained in the kernel of span $\left\{ dh_1, \ldots, dh_p \right\}$. If it is nonsingular, it is also involutive.

Proposition 8.2. *Suppose Δ_O is of constant dimension r on some open set U of R^n.*

(i) Then for each point $x_0 \in U$ there exists a neighborhood U_0 of x_0 and a local coordinate transformation $z = \Phi(x)$ on U_0 such that in the new coordinates the system equations take the form:

$$\dot{\zeta}_1 = f_1(\zeta_1, \zeta_2) + G_1(\zeta_1, \zeta_2)u$$

$$\dot{\zeta}_2 = f_2(\zeta_2) + G_2(\zeta_2)u$$

$$y = h(\zeta_2)$$

where $\zeta_1 = (z_1, \ldots, z_r)$ and $\zeta_2 = (z_{r+1}, \ldots, z_n)$.

(ii) Moreover,

a) any two initial states x_1 and x_2 in U_0 such that

$$\phi_i(x_1) = \phi_i(x_2),\ i = r+1, \ldots, n$$

produce identical output functions for any input that keeps the trajectory in U_0.

b) any initial state $x \in U_0$ that cannot be distinguished from $x_0 \in U_0$ under piecewise constant input functions belongs to the slice

$$S_{x_0} = \{ x \in U_0 |\ \phi_i(x) = \phi_i(x_0),\ i = r+1, \ldots, n \}$$

Proof: For part (i), Again, recall Lemma (3.50) from which it follows that there exists a local coordinate transformation (matched to Δ_O) such that each of the vector fields $f, g_1, \ldots, g_m$ have the form

$$\bar{f}(z) = \begin{bmatrix} f_1(z_r, \ldots z_d, z_{r+1}, \ldots, z_n) \\ \cdots \\ f_r(z_1, \ldots z_r, z_{r+1}, \ldots, z_n) \\ f_{r+1}(z_{r+1}, \ldots, z_n) \\ \cdots \\ f_n(z_{r+1}, \ldots, z_n) \end{bmatrix}$$

In the new coordinates the covector fields $dh_1,\ldots,dh_2$ must belong to $\Omega_O = \Delta_O^{\perp}$, so that

$$\frac{\partial h_i}{\partial z_j} = 0$$

for all $0 \le j \le r$ and $1 \le i \le p$. For part (ii), we provide a sketch of the proof, along the lines of [1]. Consider the following points.

(a) Consider a piecewise constant control function (recall the proof of Proposition (7.7))

$$\begin{array}{ll} u_i(t) = u_i^1 & t \in [0,t_1) \\ u_i(t) = u_i^k & t \in [t_1+\cdots+t_{k-1}, t_1+\cdots+t_k),\ k>1 \end{array}$$

for $i = 1,\ldots,m$, and define the vector field

$$\theta_k = f + \sum_{i=1}^{m} g_i u_i^k$$

Let ϕ_k^t denote its flow. The state reached at time t_k from x_0 at time $t = 0$ is given by the composition

$$x(t_k) = \phi_k^{t_k} \circ \cdots \circ \phi_1^{t_1}(x_0)$$

The output at time t_k is

$$y(t_k) = h(x_{t_k})$$

Accordingly, we may define an output map $Y^{x_0} : (-\varepsilon,\varepsilon)^k \to R^p$

$$Y^{x_0}(t_1,\ldots,t_k) = h \circ \phi_k^{t_k} \circ \cdots \circ \phi_1^{t_1}(x_0)$$

If two arbitrarily close initial states x_1 and x_2 produce identical outputs for any possible piecewise input, we have

$$Y^{x_1}(t_1,\ldots,t_k) = Y^{x_2}(t_1,\ldots,t_k)$$

for all possible $(t_1,\ldots,t_k)$, $t_i \in [0,\varepsilon)$. From this we can verify by direct computation that

$$L_{\theta_1}\ldots L_{\theta_k} h_i(x_1) = L_{\theta_1}\ldots L_{\theta_k} h_i(x_2)$$

(b) Since θ_j, $j = 1,\ldots,k$ depends on the constants $(u_1^j,\ldots,u_m^j)$, and the equality of (a) must hold for all possible choices of $(u_1^j,\ldots,u_m^j) \in R^m$, it can be verified that

$$L_{v_1}\ldots L_{v_k} h_i(x_1) = L_{v_1}\ldots L_{v_k} h_i(x_2)$$

for any set of vector fields, $v_1,\ldots,v_k$ belong to $\{f, g_1,\ldots,g_m\}$.

(c) Recall that the distribution Δ_O is invariant with respect to $f, g_1,\ldots,g_m$ and is contained in the kernel of span $\{dh_1,\ldots,dh_p\}$. Consequently, in view of (b), we can conclude that x_2 belongs to a set that is contained in the maximal integral manifold of Δ_O that passes through x_1, i.e., it belongs to S_{x_1}.

■

An immediate consequence of the above theorem is the following.

Corollary 8.3. *If Ω_O (equivalently, Δ_O) is of constant dimension on some open set U then the system (7.1) is locally observable on U if and only if the observability codistribution Ω_O has dimension n, or equivalently, its kernel Δ_O has dimension* 0.

As a first example of the necessary computations consider the observability of a linear system.

Example 8.4 (Linear System Observability). Let us consider the observability of a linear system

$$\dot{x} = Ax + Bu$$

$$y = Cx$$

We will compute the codistribution Ω_O. To do this, we apply the algorithm (3.59) and the formula for the directional derivative of a covector field as defined in (3.32). For the linear system the necessary vector fields are $f(x) = Ax$ and $g_i(x) = b_i$, $i = 1, \dots m$. Also, $h(x) = Cx$ so that codistribution $dh = \text{span}C$. Notice that for any constant covector field, c_j, using (3.32),

$$L_{Ax}c_j = c_jA, \text{ and } L_{b_i}c_j = 0$$

Thus, compute

$$\Omega_0 = \text{span}\{C\}, \Omega_1 = \text{span}\left\{\begin{array}{c} C \\ CA \end{array}\right\}, \dots, \Omega_k = \text{span}\left\{\begin{array}{c} C \\ CA \\ \vdots \\ CA^{k-1} \end{array}\right\}$$

From the Caley-Hamilton theorem, we may as well stop at $k = n$. Consequently, the observability necessary condition reduces to the familiar

$$\text{rank}\begin{bmatrix} C \\ CA \\ \vdots \\ CA^{n-1} \end{bmatrix} = n$$

The following example illustrates the decomposition claimed in Proposition (8.2).

Example 8.5. We consider a modification of Example (7.6) in which a single output equation is added:

$$y = x_3$$

First, define the system

```
In[172]:= f = {x1  x3 + x2  Exp[x2], x3, x4 - x2  x3, x3^2 + x2  x4 - x2^2  x3};
          g = {x1, 1, 0, x3};
          h = {x3};
          var = {x1, x2, x3, x4};
```

Now, compute the distribution Δ_O:

```
In[173]:= DelO = LargestInvariantDistribution[{f, g}, h, var]
Out[173]= {{0, 1, 0, x3}, {1, 0, 0, 0}}
```

Since Δ_O is not empty, the system is not observable. Proceed to obtain the transformation by appending a set of independent vector fields to Δ_O to obtain a distribution of rank 4.

```
In[174]:= Del = Join[DelO, {{0, 0, 1, 0}, {0, 0, 0, 1}}]
Out[174]= {{0, 1, 0, x3}, {1, 0, 0, 0}, {0, 0, 1, 0}, {0, 0, 0, 1}}
```

Check the rank,

```
In[175]:= Span[Del]
Out[175]= {{1, 0, 0, 0}, {0, 1, 0, 0}, {0, 0, 1, 0}, {0, 0, 0, 1}}
```

and compute the transformed system equations.

```
In[176]:= TriangularDecomposition[f + g * u, h, Del, var, {0, 0, 0, 0},
            ∞]
Out[176]= {{z2, z1, z3, z1  z3 + z4}, {x2, x1, x3, -x2  x3 + x4},
            {u + z3, E^z1  z1 + z2  (u + z3), z4, 0}, {z3}}
```

Thus, the equations are in the anticipated form with $\zeta_1 = (z_1 \quad z_2)$ and $\zeta_2 = (z_3 \quad z_4)$.

$$\dot{z} = \begin{bmatrix} z_3 \\ e^{z_1} z_1 + z_2 z_3 \\ z_4 \\ 0 \end{bmatrix} + \begin{bmatrix} 1 \\ z_2 \\ 0 \\ 0 \end{bmatrix} u$$
$$y = z_3$$

The next example shows that nonlinear system observability does provide some new twists not evident in linear systems.

Example 8.6. This example is from Vidyasagar [4] (Example 65, Section 7.3). Consider the system

$$\begin{bmatrix} \dot{x}_1 \\ \dot{x}_2 \\ \dot{x}_3 \end{bmatrix} = \begin{bmatrix} x_2 \\ x_3 \\ 0 \end{bmatrix} + \begin{bmatrix} 0 \\ x_1 \\ 0 \end{bmatrix} u, \quad y = x_2$$

Based on linear system results it would be anticipated that this system is not observable. However, let us compute $\Omega_O^{\perp}$.

In[2]:=

```
f={x2,x3,0}; g={0,x1,0}; h1=x1;  h2=x2; var={x1,x2,x3};
```

```
In[177]:= f = {x2, x3, 0};
          g = {0, x1, 0};
          h = x2;
          var = {x1, x2, x3};

In[178]:= LargestInvariantDistribution[{f, g}, {h}, var]
Out[178]= {}
```

Thus, we conclude that the system is indeed observable. The reason for this is that the state x_1 can be easily ascertained by observing the response to specified control signals.

The question of observability can be answered directly with the *ProPac* test `Observability`, and the observability codistribution can be obtained with the function `ObservabilityCodistribution`. Here are the calculations with and without the control input.

In[3]:=

```
Observability[f,g,h,var]
```

Out[3]= `True`

```
In[179]:= Observabiity[f, g, h2, var]
Out[179]= True

In[180]:= Observability[f, {{}}, {h2}, var]
Out[180]= False

In[181]:= ObservabilityCodistribution[f, Transpose[{g}], {h2}, var]
Out[181]= {{1, 0, 0}, {0, 1, 0}, {0, 0, 1}}

In[182]:= ObservabilityCodistribution[f, {{}}, {h2}, var]
Out[182]= {{0, 0, 1}, {0, 1, 0}}
```

Similarly to the case of controllability, it is of interest to introduce the codistribution

$$\Omega_L = \operatorname{span}\left\{L_f^k(dh_i),\, 1 \le i \le p,\, 0 \le k \le n-1\right\} \tag{8.4}$$

Clearly, Ω_L is a subdistribution of Ω_O. Thus, a sufficient condition for local observability around x_0 is $\dim \Omega_L(x_0) = n$. Moreover, for a linear system it is easy enough to verify that $\Omega_O = \Omega_L$, so that in a crude sense $\dim \Omega_L(x_0) = n$ establishes an observability that is linear-like. Indeed, what is missing in Ω_L as compared to Ω_O are: 1) the Lie derivatives of the covector fields dh_i with respect to the control input vector fields and 2) the higher order ($> n-1$) Lie derivatives. Thus, if $\dim \Omega_L(x_0) = n$, observability is achieved without the need to exploit the control input.

8.2.2 The Observation Space

Definition 8.7. *Observation Space. The* observation space $\mathscr{O}$ *of system (8.1) is the linear space of functions $M \to R$ over the field R spanned by all functions of the form*

$$L_{v_k} \cdots L_{v_1}(h_i),\ k \geq 0,\ 1 \leq i \leq p,\ v_k, \cdots, v_1 \in \{f, g_1, \ldots, g_m\} \tag{8.5}$$

i.e.,

$$\mathscr{O} = \text{span}_R \left\{ L_{v_k} \ldots L_{v_1}(h_i) \,|\, 1 \leq i \leq p,\ k \geq 0,\ v_1, \ldots, v_k \in \{f, g_1, \ldots g_m\} \right\} \tag{8.6}$$

It is important to emphasize that the observation space consists of all linear combinations of the functions (8.5) with real constant coefficients – viz., 'over the field R'.

Another characterization of the observation space is given by the following result.

Lemma 8.8. *The observation space $\mathscr{O}$ is equivalent to the linear vector space of functions $M \to R$ over the field R*

$$\tilde{\mathscr{O}} = \text{span}_R \left\{ L_{f_{u^k}} \ldots L_{f_{u^1}}(h_i) \,\middle|\, 1 \leq i \leq p,\ k \geq 0,\ u^1, \ldots, u^k \in \{0,1\}^m \right\} \tag{8.7}$$

Proof: Obviously, each vector field f_u, $u \in \{0,1\}^m$, is a linear combination over R of the vector fields $\{f, g_1, \ldots, g_m\}$. We need to show the converse, i.e., that each vector field in $\{f, g_1, \ldots, g_m\}$ is a linear combination of the vector fields in (8.7). To see this first note that f is of the form in (8.7) with $u = 0$. Now, any g_i can be written

$$g_i = (f + g_i) - f$$

We obtain $f_u = f + g_i$ by taking $u_j = 0$ $j \neq i$ and $u_i = 1$. It follows that

$$\text{span}_R \{f, g_1, \ldots g_m\} = \text{span}_R \{f_u \,|\, u \in \{0,1\}^m\} \tag{8.8}$$

For any two vector fields v, w we have

$$L_{v+w} h_i = L_v h_i + L_w h_i$$

This relation can be used repeatedly, along with (8.8) to show that (8.6) and (8.7) are equivalent. For example, suppose $L_v h_i \in \mathscr{O}$ implying that

$$v \in \text{span}_R \{f, g_1, \ldots g_m\}$$

Then, by (8.8), there exists a set of vector fields $\{w_1, \ldots, w_r\}$, with

$$w_i \in \text{span}_R \{f_u \,|\, u \in \{0,1\}^m\}$$

such that

$$v = c_1 w_1 + \cdots + c_r w_r$$

Consequently,

$$L_v h_i = L_{c_1 w_1 + \cdots c_r w_r} h_i = c_1 L_{w_1} h_i + \cdots + c_r L_{w_r} h_i \in \tilde{\mathscr{O}}$$

Similar calculations work the other way and with higher order Lie derivatives. In this way we show that any function in $\mathscr{O}$ is in $\tilde{\mathscr{O}}$ and vice-versa. ■

Observability can be characterized in terms of the observation space.

Lemma 8.9. *An analytic system (8.1) is observable on M if and only if the observation space $\mathscr{O}$ distinguishes the points of M, that is, for any $x_1, x_2 \in M$, $x_1 \neq x_2$, there is a function $\Phi \in \mathscr{O}$ such that $\Phi(x_1) \neq \Phi(x_2)$.*

Proof:

■

An analytic system (8.1) is observable on M if for any $x_1, x_2 \in M$, $x_1 \neq x_2$, there is a function $\Phi \in \mathscr{O}$ such that $\Phi(x_1) \neq \Phi(x_2)$.

Associated with the observation space $\mathscr{O}$ is it's differential $d\mathscr{O}$, the codistribution

$$d\mathscr{O} = \text{span}\,\{d\lambda \,|\, \lambda \in \mathscr{O}\}$$

We can connect $\mathrm{d}\mathscr{O}$ with the observability codistribution Ω_O.

Lemma 8.10. *The kernel of $\mathrm{d}\mathscr{O}$, $\mathrm{d}\mathscr{O}^\perp$, is invariant with respect to the vector fields $\{f, g_1, \ldots, g_m\}$. If $\mathrm{d}\mathscr{O}$ is nonsingular, then it too is invariant with respect to the vector fields $\{f, g_1, \ldots, g_m\}$.*

Proof: To establish the first conclusion, let $\lambda \in \mathscr{O}$ and suppose τ is a vector field in $\mathrm{d}\mathscr{O}^\perp$. Then $\langle \mathrm{d}\lambda, \tau \rangle = 0$ by definition and $\langle \mathrm{d}L_f\lambda, \tau \rangle = 0$ because $L_f\lambda$ also belongs to $\mathrm{d}\mathscr{O}$. Consequently,

$$\langle \mathrm{d}\lambda, [f, \tau] \rangle = L_f \langle \mathrm{d}\lambda, \tau \rangle - \langle \mathrm{d}L_f\lambda, \tau \rangle = 0$$

This means that $[f, \tau]$ annihilates all members of $\lambda \in \mathscr{O}$ so that $[f, \tau]$ is a vector field in $\mathrm{d}\mathscr{O}^\perp$ establishing that $\mathrm{d}\mathscr{O}^\perp$ is invariant with respect to f. Identical calculations establish invariance with respect to $g_1, \ldots, g_m$.

The second conclusion now follows from the fact that if the distribution $\mathrm{d}\mathscr{O}^\perp$ is smooth – i.e., when the codistribution $\mathrm{d}\mathscr{O}$ is nonsingular – then it's annihilator, $\mathrm{d}\mathscr{O}$, is also invariant with respect to the vector fields $f, g_1, \ldots, g_m$. ■

This result leads to the following.

Lemma 8.11. *The differential of the observation space* $\mathrm{d}\mathscr{O}$ *and the observability codistribution are related in the following way*

1. $\mathrm{d}\mathscr{O}^{\perp} \subset \Delta_O$
2. *if* $\mathrm{d}\mathscr{O}$ *is nonsingular, then* $\mathrm{d}\mathscr{O}^{\perp} = \Delta_O$*, equivalently,* $\mathrm{d}\mathscr{O} = \Omega_O$.

Proof: By definiton Δ_O is the largest distribution contained in the kernel of $\mathrm{span}\{\mathrm{d}h_1, \ldots, \mathrm{d}h_p\}$ that is also invariant with respect to $f, g_1, \ldots, g_m$. But $\mathrm{d}\mathscr{O}^{\perp}$ is contained in the kernel of $\mathrm{span}\{\mathrm{d}h_1, \ldots, \mathrm{d}h_p\}$ and it is invariant with respect to $f, g_1, \ldots, g_m$. Consequently, $\mathrm{d}\mathscr{O}^{\perp} \subset \Delta_O$.

By definition Ω_O is the smallest codistribution that contains the covectors $\{\mathrm{d}h_1, \ldots, \mathrm{d}h_p\}$ and is invariant with respect to the vector fields $f, g_1, \ldots, g_m$. But $\mathrm{d}\mathscr{O}$ contains $\{\mathrm{d}h_1, \ldots, \mathrm{d}h_p\}$ and if it is regular, by Lemma (8.10) it is also invariant with respect to the vector fields $f, g_1, \ldots, g_m$. Thus, it must be true that $\Omega_O \subset \mathrm{d}\mathscr{O}$.

Now, it is easy to show that Ω_O contains all of the covectors of $\mathrm{d}\mathscr{O}$. By definition of Ω_O, $\mathrm{d}h_i \in \Omega_O,\ 1 \leq i \leq p$. Since it is invariant with respect to $f, g_1, \ldots, g_m$, we have

$$L_v \mathrm{d}h_i \in \Omega_O,\ 1 \leq i \leq p,\ v \in \{f, g_1, \ldots, g_m\}$$

Recursive application of the invariance property leads to

$$L_{v_k} \ldots L_{v_1} \mathrm{d}h_i \in \Omega_O,\ 1 \leq i \leq p,\ v_1, \ldots, v_k \in \{f, g_1, \ldots, g_m\},\ \forall k \geq 0$$

But these are all of the elements of $\mathrm{d}\mathscr{O}$ so it must be that $\Omega_O = \mathrm{d}\mathscr{O}$. ■

Remark 8.12. Remarks on the Observability Codistributions. The system is locally observable at x_0 if the observability codistribution, Ω_O has rank n at x_0. This is called the *observability rank condition*. If x_0 is a regular point of $\Omega_O(x_0)$, the observability rank condition is necessary as well as sufficient. If the system has zero input, then the observability codistribution reduces to Ω_L.

When $\dim \Omega_O(x_0) = n$ but $\dim \Omega_L(x_0) < n$, the implication is that some states are distinguishable only under the action of control inputs. When this occurs, most control inputs do distinguish the states. There are a few *singular inputs*, notably $u = 0$, that do not. Thus, when $\dim \Omega_L(x_0) = n$ we will use the terminology *observable for zero input at* x_0. It is also possible to test the linearization of (8.1) at x_0 for observability. That is, define

$$A_0 = \frac{\partial f}{\partial x}(x_0),\ C_0 = \frac{\partial h}{\partial x}(x_0)$$

and test the pair (A_0, C_0). If the linearization is observable then we say that it is *linearly observable at* x_0. Linear observability implies zero-input observability. It is easy to prove that a system is linearly observable at x_0 if and only if $\dim \Omega_L(x_0) = n$. Thus, we have the following hierarchy

$$\begin{array}{ccc} \dim \Omega_O(x_0) = n & \Rightarrow & \textit{locally observable} \\ \Uparrow & & \Uparrow \\ \dim \Omega_L(x_0) = n & \Rightarrow & \textit{zero input observable} \\ \Updownarrow & & \Uparrow \\ \dim \begin{bmatrix} C_0 \\ C_0A_0 \\ \vdots \\ C_0A_0^{n-1} \end{bmatrix} = n & \Leftrightarrow & \textit{linearly observable} \end{array}$$

Consider a time interval $[0,T]$, divided into r subintervals of length $t_1, t_2, \ldots, t_r$. Now, define a piecewise constant control input

$$\hat{u} = u^k, \ for\, t \in [t_1 + \cdots + t_{k-1}, t_1 + \cdots + t_k), \ 1 \le k \le r, \ u^k \in R^m$$

Here we have $t_0 = 0$ and $t_1 + \cdots + t_r = T$. Let $y_i(x_0, t_1, \ldots, t_r)$ denote the i^{th} output variable at time T starting at x_0 and under the action of the control $\hat{u}$. The following result gives the joint sensitivity of the output y_i with respect to the times $t_1, \ldots, t_r$ in the limit as $T \to 0$.

Lemma 8.13. *Consider the output y_i of the system (8.1), beginning at the state x_0 and driven over the interval $[0,T]$ by the piecewise continuous control $\hat{u}$. Then*

$$\left. \frac{\partial^r y_i}{\partial t_1 \cdots \partial t_r} \right|_{t_k = 0,\, 1 \le k \le r} = \mathrm{d}L_{f_{u^k}} \ldots L_{f_{u^1}} h_i(x_0)$$

8.3 Local Decompositions

In linear system theory, the *Kalman decomposition* utilizes a set of coordinates that explicitly reveals the controllability/observability structure of a control system. Thus, new state variables are identified such that the system equations are in the form

$$\begin{bmatrix} \dot{z}_1 \\ \dot{z}_2 \\ \dot{z}_3 \\ \dot{z}_4 \end{bmatrix} = \begin{bmatrix} A_{11} & A_{12} & A_{13} & A_{14} \\ 0 & A_{22} & 0 & A_{24} \\ 0 & 0 & A_{33} & A_{34} \\ 0 & 0 & 0 & A_{44} \end{bmatrix} \begin{bmatrix} z_1 \\ z_2 \\ z_3 \\ z_4 \end{bmatrix} + \begin{bmatrix} B_1 \\ B_2 \\ 0 \\ 0 \end{bmatrix} u$$

$$y = \begin{bmatrix} 0 & C_2 & 0 & C_4 \end{bmatrix} \begin{bmatrix} z_1 \\ z_2 \\ z_3 \\ z_4 \end{bmatrix} + Du$$

The coordinates z_1, z_2 correspond to the controllable subspace and the coordinates z_2, z_4 correspond to the observable subspace. A similar decomposition is achievable for affine nonlinear systems.

Proposition 8.14 (Local Decomposition). *Consider the system (7.1). Suppose that the controllability distribution Δ_{C_0} and the observability codistribution Ω_O as well as $\Delta_{C_0} + \Omega_O^{\perp}$ are all of constant dimension on a neigborhood U of $x_0 \in R^n$. Then there exists a local diffeomorphism Ψ on U such that the system equations in the new coordinates are:*

$$\begin{bmatrix} \dot{\zeta}_1 \\ \zeta_2 \\ \zeta_3 \\ \zeta_4 \end{bmatrix} = \begin{bmatrix} f_1(\zeta_1,\zeta_2,\zeta_3,\zeta_4) \\ f_2(\zeta_2,\zeta_4) \\ f_3(\zeta_3,\zeta_4) \\ f_4(\zeta_4) \end{bmatrix} + \begin{bmatrix} G_1(\zeta_1,\zeta_2,\zeta_3,\zeta_4) \\ G_2(\zeta_2,\zeta_4) \\ 0 \\ 0 \end{bmatrix} u$$

$$y = h(\zeta_2,\zeta_4)$$

Moreover, the system restricted to $\zeta_3 = 0, \zeta_4 = 0$ is locally controllable and the system restricted to $\zeta_1 = 0, \zeta_3 = 0$ is locally observable.

Proof: The theorem is proved in [2]. We outline a constructive proof, an implementation of which is described later. It proceeds as follows.

1. Compute the controllability distribution Δ_{C_0}
2. Compute its complement $\Delta_{C_0}^{-}$
3. Compute the observability codistribution Ω_O and its annihilator $\Omega_O^{\perp}$
4. Compute the intersection $\Delta_{C\bar{O}}$ of Δ_{C_0} and $\Omega_O^{\perp}$
5. Compute the complement Δ_{CO} of $\Delta_{C\bar{O}}$ in Δ_{C_0}
6. Compute the intersection $\Delta_{\bar{C}\bar{O}}$ of $\Delta_{C_0}^{-}$ and $\Omega_O^{\perp}$
7. Compute the complement $\Delta_{\bar{C}O}$ of $\Delta_{\bar{C}\bar{O}}$ in $\Delta_{C_0}^{-}$
8. Compute and apply the transformation based on $\Delta = \Delta_{C\bar{O}} + \Delta_{CO} + \Delta_{\bar{C}\bar{O}} + \Delta_{\bar{C}O}$

Of course there are technical arguments required at various stages in the process. ■

Example 8.15. Let us revisit Examples (7.6) and (8.5). In those instances we computed the controllable and observable decompositions. Now, the *ProPac* function `LocalDecomposition` is used to compute the complete local decomposition.

```
In[183]:= f = {x1  x3 + x2  Exp[x2], x3, x4 - x2  x3, x3^2 + x2  x4 - x2^2  x3};
          G = Transpose[{{x1, 1, 0, x3}}];
          h = {x3};
          var = {x1, x2, x3, x4};

In[184]:= LocalDecomposition[f, G, h, var, {u}, ∞]
Out[184]= {{z2, z1, z3, z1  z3 + z4}, {x2, x1, x3, -x2  x3 + x4},
            {z3, E^z1  z1 + z2  z3, z4, 0}, {{1}, {z2}, {0}, {0}}, {z3}}
```

Notice that the equations turn to be exactly those of Example (8.5).

8.4 Observable Form

When (8.1) is locally observable, it is often convenient, as in linear theory, to transform the system to either observable or observer form as a means to gaining insight into the observability structure or even as a first step to observer design. In this and the next section we describe these special forms and the computations needed to obtain them.

8.4.1 Autonomous Systems

We will consider systems of the form

$$\begin{aligned} \dot{x} &= f(x) \\ y &= h(x) \end{aligned} \tag{8.9}$$

where $x \in R^n$, $y \in R^p$. For systems of this type we can easily generalize some important concepts that are well known for linear systems. Among these are the notion of 'observability indices' and the 'observable canonical form' (see, for example, Kailath [49]).

Recall the observability codistribution for the system (8.1)

$$\Omega_O = \left\langle f, g_1, \ldots, g_m \,\middle|\, \text{span}\left\{ \mathrm{d}h_1, \ldots, \mathrm{d}h_p \right\} \right\rangle$$

System (8.1) is locally obervable if it satisifies the observability rank condition $\text{rank}\Omega_O = n$. In the absence of inputs, i.e., system (8.14), we immediately obtain

$$\Omega_O = \Omega_L = \text{span}\left\{ L_f^k \left(\mathrm{d}h_i \right), 1 \le i \le p,\ 0 \le k \le n-1 \right\}$$

Local observability requires that $\text{rank}\Omega_L = n$.

We can get even better results because in general, Ω_L is overspecified by the $n \cdot p$ covectors $L_f^k(\mathrm{d}h_i)$ indicated above. At most, n of these can be independent. By identifying n independent covectors the calculations are simplified and a convenient set of new coordinates is identified. Consider, first, the case of one output, $p = 1$. Let us apply the standard algorithm to compute Ω_O:

$$\begin{aligned} \Omega_0 &= \text{span}\left\{ \mathrm{d}h_1 \right\} \\ \Omega_k &= \Omega_{k-1} + L_f \Omega_{k-1} \end{aligned}$$

Of course, there exists a $k^* \le n-1$, such that $\Omega_{k^*+1} = \Omega_{k^*}$. Thus, the algorithm terminates with

$$\Omega_O = \text{span}\left\{ L_f^k \left(\mathrm{d}h_i \right), 1 \le i \le p,\ 0 \le k \le k^* \right\}$$

If $k^* = n-1$, then new coordinates defined by

$$z_1 = h_1(x),\ z_{i+1} = L_f^i(h_1),\ i = 1,\ldots,n-1$$

lead to equations in the *observable form*

$$\frac{d}{dt}\begin{bmatrix} z_1 \\ \vdots \\ z_{n-1} \\ z_n \end{bmatrix} = \begin{bmatrix} z_2 \\ \vdots \\ z_n \\ \tilde{f}(z_1,\ldots,z_n) \end{bmatrix}$$
$$y = z_1$$

Now, let us turn to the multiple output case. Applying the same procedure as above, for each $i = 1,\ldots,p$ we can generate a chain of independent covectors (one-forms), $\mathrm{d}h_i, L_f(\mathrm{d}h_i),\ldots,L_f^{k_i^*}(\mathrm{d}h_i)$. The tableau shown below illustrates these p chains arranged in columns.

$$\begin{array}{ccccc}
\mathrm{d}h_1 & \mathrm{d}h_2 & \mathrm{d}h_3 & \cdots & \mathrm{d}h_p \\
L_f(\mathrm{d}h_1) & L_f(\mathrm{d}h_2) & L_f(\mathrm{d}h_3) & \cdots & L_f(\mathrm{d}h_p) \\
L_f^2(\mathrm{d}h_1) & L_f^2(\mathrm{d}h_2) & L_f^2(\mathrm{d}h_3) & \cdots & L_f^2(\mathrm{d}h_p) \\
L_f^3(\mathrm{d}h_1) & L_f^3(\mathrm{d}h_2) & L_f^3(\mathrm{d}h_3) & \cdots & L_f^3(\mathrm{d}h_p) \\
\vdots & \vdots & \vdots & & \vdots \\
\vdots & L_f^{k_2^*}(\mathrm{d}h_2) & \vdots & & L_f^{k_p^*}(\mathrm{d}h_p) \\
L_f^{k_1^*}(\mathrm{d}h_1) & 0 & \vdots & & 0 \\
0 & \vdots & L_f^{k_3^*}(\mathrm{d}h_3) & & \vdots \\
\vdots & & \vdots & & \vdots \\
0 & 0 & 0 & \cdots & 0
\end{array}$$

Now, we seek to identify the maximum number, $\kappa = \dim \Omega_L \leq n$, of independent covectors from this set. There are many ways to do this. Two systematic procedures are based on a search by columns or a search by rows. The linear system counterparts are well known, e.g., Kailath. With the column search, we begin with the left-most column and proceed down the column retaining independent covectors and replacing dependent covectors by zero. As we will see below, once a dependent element is found in a column the remainder of the column is also dependent. In the row search we begin with the first row and proceed from left to right accros the row. In this process also, once a dependent element is identified the remainder of the column consists of dependent elements. Let us illustrate these procedures with an example.

Example 8.16. Suppose we consider a system with state space of dimension 6 and three outputs. Then we might generate three chains of row vectors of lengths 4, 6, and 5 as illustrated below. From these we need to select 6 (assuming observability) independent row vectors. We can do this by searching rows as shown on the left or searching columns as shown on the right.

$$\begin{bmatrix} \mathrm{d}h_1 & \mathrm{d}h_2 & \mathrm{d}h_3 \\ L_f(\mathrm{d}h_1) & L_f(\mathrm{d}h_2) & L_f(\mathrm{d}h_3) \\ L_f^2(\mathrm{d}h_1) & L_f^2(\mathrm{d}h_2) & L_f^2(\mathrm{d}h_3) \\ L_f^3(h_1) & L_f^3(h_2) & L_f^3(h_3) \\ 0 & L_f^4(\mathrm{d}h_2) & L_f^4(\mathrm{d}h_3) \\ 0 & L_f^5(\mathrm{d}h_2) & 0 \end{bmatrix}$$

$$\swarrow \qquad \searrow$$

$$\begin{bmatrix} \mathrm{d}h_1 & \mathrm{d}h_2 & \mathrm{d}h_3 \\ L_f(\mathrm{d}h_1) & L_f(\mathrm{d}h_2) & 0 \\ 0 & L_f^2(\mathrm{d}h_2) & \vdots \\ \vdots & 0 & \\ & \vdots & \end{bmatrix} \qquad \begin{bmatrix} \mathrm{d}h_1 & \mathrm{d}h_2 & 0 \\ L_f(\mathrm{d}h_1) & L_f(\mathrm{d}h_2) & 0 \\ L_f^2(\mathrm{d}h_1) & 0 & \vdots \\ L_f^3(\mathrm{d}h_1) & \vdots & \\ 0 & & \\ 0 & & \end{bmatrix}$$

Notice that in the row search we wind up with three chains of lengths $\{\kappa_1,\kappa_2,\kappa_3\} = \{2,3,1\}$. In the column search we obtain $\{\kappa_1,\kappa_2,\kappa_3\} = \{4,2,0\}$. In each case $\kappa_1 + \kappa_2 + \kappa_3 = 6$

Remark 8.17 (Search for Observability indices).

1. In the column search, we retain the entire first column if $k_1^* \leq \kappa$. Then we begin the second column. Should we encounter a dependent element then the remainder of the column is also dependent. Thus, we replace all remaining elements in the column by zero and proceed to the next column. Let us establish this fact. Clearly, the column lengths, κ_i, $i = 1,\ldots,p$ will depend on the ordering of the output maps $h_i(x)$.
2. In the row search, we work across the first row, and then the second and so forth. When we encounter a dependent element we replace it and and all the elements below it by zero. We can also establish that the set of column lengths resulting from a row search are invariant with respect to the ordering of the output maps.
3. Now consider a row search that terminates with indices κ_i, $i = 1,\ldots,p$ and $\kappa_1 + \cdots + \kappa_p = n$, i.e., the system is observable. Consider the coordinate transformation

$$\begin{gathered} z_1 = h_1(x), z_2 = L_f\left(h_1(x)\right), \ldots z_{\kappa_1} = L_f^{\kappa_1 - 1}\left(h_1(x)\right) \\ z_{\kappa_1+1} = h_2(x), \ldots z_{\kappa_1+\kappa_2} = L_f^{\kappa_2 - 1}\left(h_2(x)\right) \\ \vdots \\ z_{\kappa_1+\cdots+\kappa_{p-1}+1} = h_p(x), \ldots z_{\kappa_1+\cdots+\kappa_p} = L_f^{\kappa_p - 1}\left(h_p(x)\right) \end{gathered}$$

4. The equations in the new variables are in the *observable form* with *observability indices* $\kappa_1,\kappa_2,\ldots,\kappa_p$:

$$\frac{d}{dt}\begin{bmatrix} z_1 \\ \vdots \\ z_{\kappa_1-1} \\ z_{\kappa_1} \\ \vdots \\ z_{\kappa_1+\cdots+\kappa_{p-1}+1} \\ \vdots \\ z_{n-1} \\ z_n \end{bmatrix} = \begin{bmatrix} z_2 \\ \vdots \\ z_{\kappa_1} \\ \tilde{f}_1(z) \\ \vdots \\ z_{\kappa_1+\cdots+\kappa_{p-1}+2} \\ \vdots \\ z_n \\ \tilde{f}_p(z) \end{bmatrix}$$

$$\begin{aligned} y_1 &= z_1 \\ y_2 &= z_{\kappa_1+1} \\ &\vdots \\ y_p &= z_{\kappa_1+\cdots+\kappa_{p-1}+1} \end{aligned}$$

8.4.2 Control Sequences

We now turn to the general, nonautonomous case of Eq. 8.1. It is assumed that the system is locally observable, but not necessarily zero input observable. Lemma 8.8 motivates the following definitions. Define a sequence of codistributions

$$\begin{aligned} &\mathscr{E}_0 := \operatorname{span}\{dh\} \\ &\mathscr{E}_k = \mathscr{E}_{k-1} + \operatorname{span}\left\{ dL_{f_{u^k}} \cdots L_{f_{u^1}}(h) \,\middle|\, u^i \in \{0,1\}^m,\ i = 1,\ldots,k \right\} \end{aligned} \tag{8.10}$$

We assume that, 'almost everywhere' on a neighborhood of x_0, (i) the codistributions $\mathscr{E}_k$ are of constant dimension, and (ii) there exists a smallest p^* such that

$$\mathscr{E}_0 \subset \cdots \subset \mathscr{E}_{p^*} = \mathscr{E}_{p^*+1} = d\mathscr{O} \tag{8.11}$$

Let n_k denote the codimension of $\mathscr{E}_{k-1}$ in $\mathscr{E}_k$. Then there exist sets of *control sequences* [37]

$$\begin{aligned} I_1 &= \left\{ (u^{i_1}) \,\middle|\, u^{i_1} \in \{0,1\}^m \right\}, \\ I_2 &= \left\{ (u^{i_1}, u^{i_2}) \,\middle|\, u^{i_1} \in \{0,1\}^m,\ u^{i_2} \in \{0,1\}^m \right\}, \\ &\vdots \end{aligned} \tag{8.12}$$

that satisfy

(a) If $\left(u^{i_1},\ldots,u^{i_j}\right) \in I_j$ then $\left(u^{i_1},\ldots,u^{i_{j-1}}\right) \in I_{j-1}$, for $j \geq 2$.

(b) The one-forms

$$\bigcup_{l=1}^{k} \left\{ dL_{f_{u^l}} \cdots L_{f_{u^1}}(h) \,\middle|\, \left(u^{i_1},\ldots,u^{i_l}\right) \in I_l \right\} \cup \{dh\}$$

span $\mathscr{E}_k$ on a neighborhood of x_0. In the single output case these one-forms actually constitute a basis for $\mathscr{E}_k$ and the cardinal number of I_k is n_k.

We obtain the control sequences, I_k, by direct, sequential construction of the codistributions $\mathscr{E}_k$. See [37] for more details about the single output case and Section 8.5.1 for our algorithm in the multiple output case.

Example 8.18. Consider the 5^{th} order system

$$\dot{x} = \begin{bmatrix} e^{x_1+x_2} - 1 + ux_1^2 \\ -e^{x_1+x_2} + 1 + u\left(e^{x_3-x_2} - e^{-x_1-x_2} - x_1^2\right) \\ -e^{x_1+x_2} + 1 + x_1^3 e^{-x_1-x_3} - ux_1^2 \\ x_5 \\ x_1 \end{bmatrix}, \quad y = \begin{bmatrix} x_1 \\ x_4 \end{bmatrix}$$

This system is locally observable, but it is not observable for all inputs. In particular, it is not observable with $u \equiv 0$. We use the *ProPac* function **ControlSequences** (see Section 8.5.1) to compute

$$\begin{aligned} \mathscr{E}_0 &= \{d[x_1], d[x_4]\} \\ \mathscr{E}_1 &= \{d[x_1], d[x_2], d[x_4], d[x_5]\} \\ \mathscr{E}_2 &= \{d[x_1], d[x_2], d[x_3], d[x_4], d[x_5]\} \end{aligned}$$

and

$$I_1 = \{0\}, \; I_2 = \{0, 1\}$$

Now, direct computation leads to the four one-forms

$$\begin{aligned} \alpha &= d\left[L_{f_{u=0}}(h_1)\right] = e^{x_1+x_2}\left(d[x_1] + d[x_2]\right) \\ \beta &= d\left[L_{f_{u=0}}(h_2)\right] = d[x_5] \\ \gamma &= d\left[L_{f_{u=1}} L_{f_{u=0}}(h_1)\right] = e^{x_1+x_3}\left(d[x_1] + d[x_3]\right) \\ \delta &= d\left[L_{f_{u=1}} L_{f_{u=0}}(h_2)\right] = d[x_1] \end{aligned}$$

and

$$\begin{aligned} \operatorname{span}\{d[x_1], d[x_4], \alpha, \beta\} &= \operatorname{span}\{d[x_1], d[x_2], d[x_4], d[x_5]\} = \mathscr{E}_1 \\ \operatorname{span}\{d[x_1], d[x_4], \alpha, \beta, \gamma, \delta\} &= \operatorname{span}\{d[x_1], d[x_2], d[x_3], d[x_4], d[x_5]\} = \mathscr{E}_2 \end{aligned}$$

8.4.3 Observability Indices

Recall the construction of the control sequences I_k and codistributions $\mathscr{E}_k$ in the previous Section8.4.2. In the subsequent discusion we use the notation

$$L_{f_{I_j}}(h) = L_{f_{u^j}} \ldots L_{f_{u^1}}(h), \quad \left(u^1, \ldots, u^j\right) \in I_j$$

Now, consider the collection of covectors $dL_{f_{I_i}}(h)$ for $i = 0, \ldots, p^*$, which we can arrange in the (block) tableau

$$\begin{matrix} dh_1 & dh_2 & \cdots & dh_p \\ dL_{f_{I_1}}(h_1) & dL_{f_{I_1}}(h_2) & \cdots & dL_{f_{I_1}}(h_p) \\ \vdots & \vdots & \vdots & \vdots \\ dL_{f_{I_{p^*}}}(h_1) & dL_{f_{I_{p^*}}}(h_2) & \cdots & dL_{f_{I_{p^*}}}(h_p) \end{matrix}$$

From this set we seek to identify a maximal set of independent covectors. We can do this by searching down columns or across rows (recall the linear counterpart). For a row search, begin with the first row and work from left to right, then move to the next row. If the outputs are them selves independent, we identify p chains of covectors $dh_i, dL_{f_{l_1}}(h_i), \cdots, dL_{f_{l_{\kappa_i-1}}}(h_i)$ of length κ_i, $i = 1, \ldots, p$. The integers κ_i are the *observability indices*. For an observable system $\kappa_1 + \kappa_2 + \cdots + \kappa_p = n$. For autonomous systems this definition of observability indices is equivalent to that in [28] and [110].

8.4.4 Observable Form

If the system is observable, then we can define new state variables $z \in R^n$ via the transformation $x \to z$.

$$z = \begin{bmatrix} h_1 \\ \vdots \\ L_{f_{l_{\kappa_1-1}}}(h_1) \\ \vdots \\ h_p \\ \vdots \\ L_{f_{l_{\kappa_p-1}}}(h_p) \end{bmatrix} \tag{8.13}$$

If the inverse is continuous and the the transformed equations produce unique solutions we call the transformed equations an *observable form*. This is consistent with the usual terminology for linear systems and autonomous nonlinear systems. In the latter case, the transformed equations are in the form of p chains,

$$\begin{array}{ccc} \dot{z}_1 = z_2 & \cdots & \dot{z}_{\kappa_1+\cdots+\kappa_{p-1}+1} = z_{\kappa_1+\cdots+\kappa_{p-1}+2} \\ \vdots & \cdots & \vdots \\ \dot{z}_{\kappa_1-1} = z_{\kappa_1} & \cdots & \dot{z}_{\kappa_1+\cdots+\kappa_p-1} = z_{\kappa_1+\cdots+\kappa_p} \\ \dot{z}_{\kappa_1} = \varphi_1(z) & \cdots & \dot{z}_{\kappa_1+\cdots+\kappa_p} = \varphi_p(z) \\ y_1 = z_1 & \cdots & y_p = z_{\kappa_1+\cdots+\kappa_{p-1}+1} \end{array}$$

Remark 8.19 (Xia and Zeitz). Note that if

$$\operatorname{rank} \begin{bmatrix} dh_1 \\ \vdots \\ dL_{f_{l_1}}(h_1) \\ \vdots \\ dh_p \\ \vdots \\ dL_{f_{l_{\kappa_i-1}}}(h_p) \end{bmatrix} (x_0) = n$$

the implicit function theorem guarantees the existence of a smooth (local) inverse of the transformation (8.13) so that the transformation is a diffeomorphism. However, an inverse may exist even if the rank condition fails. In this case, the inverse will only be continuous. If the transformed differential equations have unique solutions on a neighborhood of x_0, then this is still a useful transformation. This point is described more fully in Xia and Zeitz [109].

Example 8.20 (Continuation of Example 8.18). Let us return to Example 8.18 and compute the observable form. We find the observability indices to be $3,2$. The transformation to observable form is

$$z_1 = x_1,\, z_2 = -1 + e^{x_1+x_2},\, z_3 = -1 + e^{x_1+x_3},\, z_4 = x_4,\, z_5 = x_5$$

from which the observable form is obtained

$$\frac{d}{dt}\begin{bmatrix} z_1 \\ z_2 \\ z_3 \\ z_4 \\ z_5 \end{bmatrix} = \begin{bmatrix} z_2 + u z_1^2 \\ u z_3 \\ z_1^3 \\ z_5 \\ z_1 \end{bmatrix},\, y = \begin{bmatrix} z_1 \\ z_4 \end{bmatrix}$$

In this example, we see the two-chain structure of the observable form equations. Also, the role of the control input is displayed. We see clearly that the system is not observable if $u \equiv 0$.

8.5 Observer Form

Observer design based on‘ linearization up to output injection’ was introduced in [54] and [10] for the single output case without inputs and extended to the multiple output case in [55]. In this approach the idea is to transform the system (8.1) into the form

$$\dot{z} = Az + \varphi(y),\, y = Cz \tag{8.14}$$

where A,C is an observable pair. When this is done, observer design is very easy. As might be expected, systems that can be transformed into the form (8.14) are rare but it is interesting to note that linear observability of (8.1) is not necessary if we do not insist that the transformation be a diffeomorphism. An extension to the case where (8.1) is not zero-input observable, is given by [34, 35]. This method begins with reduction of (8.1) into the special form (time-varying linear up to output injection):

$$\begin{aligned} \dot{z} &= A(u(t))z + \varphi(y, u(t)) \\ y &= \begin{bmatrix} z_1 & \cdots & z_p \end{bmatrix}^T = Cz \end{aligned} \tag{8.15}$$

In this form it is possible to use linear methods for observer design. Equation (8.15) will be called an *observer form* of which (8.14) is a special case. Not every locally

observable nonlinear system (8.1) has an observer form. The formulation we follow is that of [34, 37, 35]. First, let us introduce some definitions. Consider a set of p vector fields, $X = \{X_1, \ldots, X_p\}$. Sequentially define sets of $p+1$-forms

$$\begin{aligned}
\Omega_1^X &= \text{span}_R \left\{ dL_{f_u}(h_i) \wedge_{j=1}^{p} dh_j \,|\, i = 1, \ldots, p;\ u \in \{0,1\}^m \right\} \\
\Omega_{k+1}^X &= \text{span}_R \left\{ dL_{f_u}(i_X \alpha) \wedge_{j=1}^{p} dh_j \,\middle|\, \alpha \in \Omega_k^X,\ u \in \{0,1\}^m \right\} \\
\Omega^X &= \textstyle\sum_{k \geq 1} \Omega_k^X
\end{aligned}$$

Let $i_f(\omega)$ denote the usual contraction of the form ω with respect to the vector field f. Then we use the notation

$$i_X(\omega) = i_{X_1} \circ \cdots \circ i_{X_p}(\omega)$$

The following proposition, given in [35], generalizes the single output result in [34] to multiple outputs.

Proposition 8.21. *The system (8.1) is transformable into the observer form (8.15) if and only if:*

(1) $dh_1 \wedge \cdots \wedge dh_p(x_0) \neq 0$ *(independent outputs)*

(2) There exists a set of vector fields $X_1, \ldots, X_p$ *that satisfies*

- *(a)* $L_{X_i} h_j = \delta_{ij}$
- *(b)* $\dim \Omega^X = n - p$
- *(c)* $\forall \omega \in \Omega^X,\ d i_X(\omega) = 0$
- *(d)* $i_X(\omega_1) \wedge \cdots \wedge i_X(\omega_{n-p}) \wedge dh_1 \wedge \cdots \wedge dh_p(x_0) \neq 0$ *where* ω_j $j = 1, \ldots, n-p$ *is any basis for* Ω^X.

If these conditions hold, then the transformation is given by

$$\begin{aligned}
z_1 &= h_1(x), \ldots, z_p = h_p(x) \\
dz_{j+p} &= i_X(\omega_j), \quad j = 1, \ldots, n-p
\end{aligned} \tag{8.16}$$

Proof: A sketch of the proof is given in [35]. However, it is useful here to provide a more complete discussion of the sufficiency part in order to clarify the nature of later computations. It is provided in Appendix 8.A. ■

Let us make a few comments about the stated conditions.

Remark 8.22 (Concerning item 2).

1. item (a) implies the p-tuple of vector fields $X = [X_1, \ldots, X_p]$ forms a right inverse of the Jacobian $\partial h / \partial x$. The vector field X_i is aligned with the direction of $y_i = h_i$,

that is, it is orthogonal to the codimension-1 surfaces $h_i(x) = \text{constant}$. As in the single-output case [36] every X_i satisfying the conditions of Proposition 8.21 is a constant vector field in the linearized coordinates, so it takes the form:

$$X_i = \frac{\partial}{\partial z_i} + c^i_{p+1}\frac{\partial}{\partial z_{p+1}} + \cdots + c^i_n \frac{\partial}{\partial z_n},\ i = 1, \ldots, p$$

Furthermore, a linear change of coordinates $\tilde{z} = Tz$ with $\tilde{z}_i = z_i,\ i = 1, \ldots, p$ leaves the equations in TVLOI form and such a transformation can be found so that

$$X_i = \frac{\partial}{\partial \tilde{z}_i}$$

Such X_i satisfy the conditions of Proposition 8.21 for a system in the observer form (8.15), [34, 35].

2. in item (b) Ω^X is considered a vector space over the reals. So $\dim \Omega^X = \dim \text{span}_R\, \Omega^X$, which is not the same as $\dim \text{span}\, \Omega^X$. See item 5 below.

3. item (c) is an integrability condition for each of the 1-forms $i_X(\omega)$. Recall that any 1-form has the representation

$$\omega = \sum a_i(x) dx_i$$

Thus, we have the differential

$$\mathrm{d}\omega = \sum\nolimits_i \mathrm{d}a_i \wedge \mathrm{d}x_i = \sum\nolimits_{i,j} \frac{\partial a_i}{\partial x_j} \mathrm{d}x_j \wedge \mathrm{d}x_i = 0$$

Since $\mathrm{d}x_j \wedge \mathrm{d}x_i = -\mathrm{d}x_i \wedge \mathrm{d}x_j$, this implies that the Jacobian $\partial a \big/ \partial x$ is symmetric so that the 1-form $\mathrm{d}\omega$ is an exact differential.

4. item (d) implies that the n coordinate functions

$$z_1(x) = h_1(x). \ldots, z_p(x) = h_p(x), z_p(x), \ldots, z_n(x)$$

are independent thereby defining a valid coordinate transformation.

5. item (b) and (d) together imply $\dim \text{span} \Omega^X = n - p$. This follows from the fact item (d) requires $i_X(\omega_1) \wedge \cdots \wedge i_X(\omega_{n-p}) \neq 0$ for every basis $\{\omega_1, \ldots, \omega_{n-p}\}$ of Ω^X, i.e., the 1-forms $i_X(\omega_1), \ldots, i_X(\omega_{n-p})$ are independent in the usual sense (field of admissible functions). But this can be true only if the p-forms ω_i are independent. To see this, suppose X is a vector field on R^n and suppose $\omega_1,\ \omega_2$ are p-forms. Define a third p-form that is dependent on ω_1 and ω_2, $\omega_3 = \gamma_1(x)\omega_1 + \gamma_2(x)\omega_2$. Then $i_X(\omega_3) = \gamma_1(x) i_X(\omega_1) + \gamma_2(x) i_X(\omega_2)$. Consequently,

$$\begin{aligned} & i_X(\omega_1) \wedge i_X(\omega_2) \wedge i_X(\omega_3) \\ & \quad = \gamma_1(x) i_X(\omega_1) \wedge i_X(\omega_2) \wedge i_X(\omega_1) + \gamma_2(x) i_X(\omega_1) \wedge i_X(\omega_2) \wedge i_X(\omega_2) \\ & \quad = 0 \end{aligned}$$

This calculation extends to the general case in which there is a dependence among any number of p-forms.

Now, we need to provide a construction for the set of vector fields X. First, obtain a set of vector fields $Y_1,\ldots,Y_p$ that satisfy

$$\begin{bmatrix} dh_1 \\ \vdots \\ dL_{f_{I_1}}(h_1) \\ \vdots \\ dh_p \\ \vdots \\ dL_{f_{I_1}}(h_p) \end{bmatrix} \begin{bmatrix} Y_1 \cdots Y_p \end{bmatrix} = \begin{bmatrix} 0 \cdots 0 \\ \vdots \ddots \vdots \\ 1 \quad 0 \\ 0 \quad \vdots \\ 0 \cdots \vdots \\ \vdots \cdots 0 \\ 0 \cdots 1 \end{bmatrix} \tag{8.17}$$

For any control sequence $u^1,u^2,\ldots$ we can define the set of vector fields

$$Z^i_{u^1\ldots u^{\kappa_i-1}} = \left[f_{u^{\kappa_i-1}},[\cdots[f_{u^1},Y_i]\cdots]\right],\ i=1,\ldots,p$$

Now, identify the subset of control sequences $\mathscr{I}\subseteq I_{p^*}$ that satisfy

$$\det\left[L_{Z^1_{u^1\ldots u^{\kappa_1-1}}}(h)\ \cdots\ L_{Z^p_{u^1\ldots u^{\kappa_p-1}}}(h)\right]\neq 0 \tag{8.18}$$

and use any one of these sequences to obtain

$$\begin{bmatrix} X_1 \cdots X_p \end{bmatrix} = \left[L_{Z^1_{u^1\ldots u^{\kappa_1-1}}}(h)\cdots L_{Z^p_{u^1\ldots u^{\kappa_p-1}}}(h)\right]^{-1}\left[Z^1_{u^1\ldots u^{\kappa_1-1}}\cdots Z^p_{u^1\ldots u^{\kappa_p-1}}\right] \tag{8.19}$$

The following theorem summarizes the key result. It generalizes the single output case proved in [37].

Proposition 8.23. *The system (8.1) is transformable into the observer form (8.15) if and only if:*

1. $\mathscr{I}\neq\emptyset$, *where* $\mathscr{I}\subseteq I_{p^*}$ *satsifies Eq. 8.18*
2. $\forall(u_1,\ldots,u_{p*})\in\mathscr{I},\ dL_{Z_{u^1\ldots u^{\kappa_i-1}}}(h_i)=0,\ i=1,\ldots,p$
3. *The set of vector fields* $X_1,\ldots,X_p$ *is given by Equation (8.19), and the following conditions hold:*
   (a) $\dim\Omega^X=n-p$
   (b) $\forall\omega\in\Omega^X,\ di_X(\omega)=0$
   (c) $i_X(\omega_1)\wedge\cdots\wedge i_X(\omega_{n-p})\wedge dh_1\wedge\cdots\wedge dh_p(x_0)\neq 0$ *where* $\omega_j\ j=1,\ldots,n-p$ *is any basis for* Ω^X.

Proof: *Sufficiency* follows from Proposition 8.23. *Necessity* is proved in Appendix 8.B. ■

8.5.1 Computational Tools

The computations described above and their implementation in a *Mathematica* package were originally reported in [62]. In this section, we wish to summarize the key elements of our implementation.

The package has three primary high level functions:

1. **`ObservabilityIndices`**, computes the observability indices.
2. **`ObservableTransform`**, computes the transformation to observable form.
3. **`LinearizeToOutputInjection`**, computes the transformation to observer form.

These are supported by several utility functions that compute the control sequences, solve the first order partial differential equations of Proposition (8.21), and others. The most important of these are

1. **`ControlSequences`**
2. **`OmegaForms`**
3. **`SpanR`**

Underlying these calculations are basic tools for working with differential forms. We have slightly extended the Exterior Differential Calculus package of [13]. These three new tools have been incorporated into the *ProPac* package described in [61].

A key construction is **`ControlSequences`** which performs the computations outlined in Section 8.4.2. The algorithm proceeds as follows.

Algorithm : **ControlSequences**
Input : f, h, x, u $(\dot{x} = f_u(x), y = h(x))$
Output : list of indices , n_k, list of sets of control sequences, I_k
begin
  $\mathscr{E}_0 = \{dh\}$; $r = \dim \mathscr{E}_0$; $k = 0$;
  while $(\dim \mathscr{E} < n)\&\&(k < n)$ *do*
    $k{+}{+}$
    Set up $\mathscr{E}_k = \left\{ d\left[L_{f_{u^k}} \ldots L_{f_{u^1}}(h) \right] \cup dh \right\}$ with generic control sequence
    $n_k := \dim \mathscr{E}_k - \dim \mathscr{E}_{k-1}$;
    Enumerate all controls $u^k \in \{0,1\}^m$ that do not reduce $\dim \mathscr{E}_k =: \mathscr{U}_k$
    Pick out n_k control sequences of the form
      $s_k = \{s_{k-1}, u^k\}$, $u^k \in \mathscr{U}_k, s_{k-1} \in I_{k-1} =: I_k$
end

Once the control sequences are obtained, it is a simple matter to set up and solve Equations (8.17) and (8.19). Once the vector fields $X_1, \ldots, X_p$ are obtained, we compute Ω^X using the function **`OmegaForms`**.

Algorithm : **OmegaForms**
Input : $f, h, x, u, X_1, \ldots, X_p$
Output : a basis for Ω^X
begin
$\Omega_1^X = \text{span}_R \left\{ dL_{f_u}(h_i) \wedge_{j=1}^{p} dh_j \,\middle|\, \begin{array}{l} i = 1, \ldots, p \\ u \in \{0,1\}^m \end{array} \right\}$;
$\Omega^X = \Omega_1^X$;
$k = 1$;
while $\dim \Omega^X < n - p$ *do*
$k{+}{+}$
$\Omega_k^X = \text{span}_R \left\{ dL_{f_u}(i_X(\alpha)) \wedge_{j=1}^{p} dh_j \,\middle|\, \begin{array}{l} \alpha \in \Omega_{k-1}^X \\ u \in \{0,1\}^m \end{array} \right\}$
$\Omega^X := \Omega^X + \Omega_k^X$
end

The central calculations in the above procedure are the summation in the last step and the construction span_R. The summation is based on item (4) of Remark 8.22. We successively check each $(p+1)$-form $\alpha \in \Omega_k^X$. If $\alpha \in \text{span}\Omega^X$ we drop it, otherwise we join it to the set of $(p+1)$-forms that define Ω^X.

Now, consider the procedure for computing span_R.

Algorithm : **SpanR**
Input : a list of n forms of dimension p, $A = \{\alpha_1, \ldots, \alpha_n\}$
Output : a set of basis forms for $\text{span}_R A$
begin
$Basis = \{\alpha_1\}$ (assuming α_1 is not trivial)
$k = 2$
while $k \leq n$ *do*
$k{+}{+}$
Check if α_k can be expressed as a linear combination, over the reals, of the forms in *Basis*. If not add α_k to *Basis*.
end

The test in the above algorithm is implemented using the *Mathematica* function **Reduce**. Suppose, at the k^{th} step, we have

$$Basis = \{\beta_1, \ldots, \beta_q\}$$

We want to determine if there exists real numbers $k_1, \ldots, k_q$ such that

$$\alpha_k = k_1\beta_1 + \cdots + k_q\beta_q$$

Reduce allows us to seek solutions of this equation with the unknowns $k_1, \ldots, k_q$ restricted to real numbers.

Remark 8.24. Remarks on Computation. The observability properties of nonlinear systems have nuances that have no counterpart in linear theory. One consequence of this is that there are opportunities for state estimation in nonlinear systems even

when its linearization is not observable or there is some other pathology associated with observability (see Section 8.2). There are important practical implications because problems like this occur when operating around bifurcation points and in fault detection and identification. However, to take advantage of these possibilities it is necessary to build observers using new design paradigms, some of which have emerged in recent years. To do so requires development of new computational tools.

Above, we have described symbolic computations for reducing nonlinear smooth affine systems to observable and observer forms, when possible, as the first step in observer design. These tools can be applied to systems that are linearly observable, locally observable with zero input or merely locally observable. Our approach involves computations with differential forms, which experience shows to be extremely efficient.

Our characterization has at its root the computation of sequences of constant controls as formulated in [37]. This idea appears to have its origins in the pioneering work of [40]. Using this construction, we introduce a local observable form for nonautonomous systems that is consistent with prior work and complements the observer form of [35]. Our approach to computing the observer form is based on a muliple-output generalization (Proposition 8.23) of the method proposed in [37].

8.5.2 Examples

Several examples follow that illustrate the computations (these and other examples can be found worked out in the *Mathematica* notebook Examples.nb that can be downloaded from http://www.pages.drexel.edu/ ˜ hgk22/notebook.htm). In each case we compute both the observable and observer forms. First, Example (8.25) is linearly observable (and therefore zero-input observable). Example (8.26) is zero-input observable but not linearly observable. Example (8.27) is locally observable but is not zero input observable and is, therefore, not the linearly observability. Example (8.28) is linearly observable. Example (8.29) is not zero-input observable but satisfies the observablity rank condition.

Example 8.25 (Krener & Respondek example 7.3). Consider the three state, nonautonomous system from [55]

$$\frac{d}{dt}\begin{bmatrix} x_1 \\ x_2 \\ x_3 \end{bmatrix} = \begin{bmatrix} x_2 \\ x_3 + (1+e^{x_1})\,u \\ 3x_1^2x_2^2 + x_1^3x_3 + (1+x_1+x_2)\,u \end{bmatrix}, \quad y = x_1$$

This system is linearly observable. Notice that it is already in observable form. Applying the tools described above, we find that the system transforms to observer form with the transformation

$$z_1 = x_1,\ z_2 = \left(x_1^4 - 4x_2\right)/2,\ z_3 = -x_1^3x_2 + x_3$$

The observer form is

$$\frac{d}{dt}\begin{bmatrix} z_1 \\ z_2 \\ z_3 \end{bmatrix} = \begin{bmatrix} 0 & -1/2 & 0 \\ 0 & 0 & -2 \\ 0 & -\frac{1}{2}u & 0 \end{bmatrix}\begin{bmatrix} z_1 \\ z_2 \\ z_3 \end{bmatrix} + \begin{bmatrix} \frac{1}{4}y^4 \\ -2\left(1+e^y\right)u \\ \left(1+y-(1+e^y)y^3+y^4/4\right)u \end{bmatrix}$$

Example 8.26 (Xia & Zeitz example 2). Now, consider the simple two state, single output, autonomous example from [109]. Although the transformation is smooth, its inverse is only continuous.

$$\frac{d}{dt}\begin{bmatrix} x_1 \\ x_2 \end{bmatrix} = \begin{bmatrix} x_1 \\ x_2 \end{bmatrix}, \; y = x_1^2 + x_2^5$$

The system is observable with index 2, but it is not linearly observable. The transformation to observable form is smooth

$$z_1 = x_1^3 + x_2^5, \; z_2 = 3x_1^3 + 5x_2^5$$

But its inverse ia not

$$x_1 = -\left(-\tfrac{1}{2}\right)^{1/3}(5z_1 - z_2)^{1/3}$$
$$x_2 = -\left(-\tfrac{1}{2}\right)^{1/5}(-3z_1 + z_2)^{1/5}$$

The observable form equations are

$$\frac{d}{dt}\begin{bmatrix} z_1 \\ z_2 \end{bmatrix} = \begin{bmatrix} z_2 \\ -15z_1 + 8z_2 \end{bmatrix}, \; y = z_1$$

The transformation to observer form is

$$z_1 = x_1^3 + x_2^5, \; z_2 = 5x_1^3 + 3x_2^5$$

and its inverse is

$$x_1 = -\left(-\tfrac{1}{2}\right)^{1/3}(-3z_1 + z_2)^{1/3}$$
$$x_2 = -\left(-\tfrac{1}{2}\right)^{1/5}(5z_1 - z_2)^{1/5}$$

The observer form equations are

$$\frac{d}{dt}\begin{bmatrix} z_1 \\ z_2 \end{bmatrix} = \begin{bmatrix} 8z_1 - z_2 \\ 15z_1 \end{bmatrix} = \begin{bmatrix} -z_2 \\ 0 \end{bmatrix} + \begin{bmatrix} 8 \\ 15 \end{bmatrix} y$$

Example 8.27 (Xia & Zeitz example 3). Now consider a nonautonomous example, from [109]. It is not zero-input observable. However, it is observable with observability index 2. As we will see, the observable and observer form are the same. The transformation is smooth, but its inverse is merely continuous.

$$\dot{x}_1 = x_2^3$$
$$\dot{x}_2 = x_2 u$$
$$y = x_1$$

The transformation to observable/observer form is

$$z_1 = x_1,\ z_2 = -x_2^3$$

and its inverse is

$$x_1 = z_1,\ x_2 = -z_2^{1/3}$$

The transformed equations are

$$\begin{aligned}\dot{z}_1 &= -z_2\\ \dot{z}_2 &= 3z_2u\\ y &= z_1\end{aligned}$$

Example 8.28 (Hou and Pugh). This example is from [44]. They propose a method for linearization to output injection for multiple output autonomous systems different from that implemented here. To obtain the observer form we need to reorder the outputs.

$$\frac{d}{dt}\begin{bmatrix}x_1\\x_2\\x_3\end{bmatrix} = \begin{bmatrix}x_2\\x_2x_3\\x_2\end{bmatrix},\ y = \begin{bmatrix}0&1\\1&0\end{bmatrix}\begin{bmatrix}x_1\\x_2\end{bmatrix}$$

The system is observable with indices $2,1$. The transformation to observable form is simply a reordering of states

$$z_1 = x_3,\ z_2 = x_2,\ z_3 = x_1$$

leading to

$$\frac{d}{dt}\begin{bmatrix}z_1\\z_2\\z_3\end{bmatrix} = \begin{bmatrix}z_2\\z_1z_2\\z_2\end{bmatrix}$$

The transformation to observer form is

$$z_1 = x_3,\ z_2 = x_1,\ z_3 = \frac{1}{2}\left(-2x_2 + x_3^2\right)$$

This transformation produces the observer form

$$\frac{d}{dt}\begin{bmatrix}z_1\\z_2\\z_3\end{bmatrix} = \begin{bmatrix}\frac{1}{2}\left(z_1^2 - 2z_3\right)\\ \frac{1}{2}\left(z_1^2 - 2z_3\right)\\ 0\end{bmatrix} = \begin{bmatrix}0&0&-1\\0&0&-1\\0&0&0\end{bmatrix}\begin{bmatrix}z_1\\z_2\\z_3\end{bmatrix} + \frac{z_1^2}{2}\begin{bmatrix}1\\1\\0\end{bmatrix}$$

$$y = \begin{bmatrix}z_1\\z_2\end{bmatrix}$$

Example 8.29 (Continuation of Example 8.18). We return to Example 8.18 and compute the observer form. The transformation to observer form is found to be

$$z_1 = x_1,\ z_2 = x_4,\ z_3 = -e^{x_1+x_2},\ z_4 = -x_5,\ z_5 = e^{x_1+x_3}$$

From this we find the observer form

$$\frac{d}{dt}\begin{bmatrix} z_1 \\ z_2 \\ z_3 \\ z_4 \\ z_5 \end{bmatrix} = \begin{bmatrix} -z_3 - 1 + u z_1^2 \\ -z_4 \\ u(1-z_5) \\ -z_1 \\ z_1^3 \end{bmatrix} = \begin{bmatrix} 0 & 0 & -1 & 0 & 0 \\ 0 & 0 & 0 & 0 & 0 \\ 0 & 0 & 0 & 0 & -u \\ 0 & 0 & 0 & 0 & 0 \\ 0 & 0 & 0 & 0 & 0 \end{bmatrix} \begin{bmatrix} z_1 \\ z_2 \\ z_3 \\ z_4 \\ z_5 \end{bmatrix} + \begin{bmatrix} -1 + y_1^2 u \\ y_2 \\ u \\ -y_1 \\ y_1^3 \end{bmatrix}$$

Remark 8.30. Remarks on Examples.

The above examples are chosen to illustrate a variety of circumstances. The following cases are covered:

1. autonomous and nonautonomous,
2. linearly observable,
3. not linearly observable, but zero-input observable,
4. not zero-input observable, but satisfies the observability rank condition

There are further enhancements that need to be considered. Of course, not all locally observable systems have an observer form. However, the class of systems that do can be expanded if one allows for a transformation of the outputs. This was pointed out in [54]. In the single-output case, necessary conditions for the output transformation where obtained by [9] in the framework employed herein. In the multiple-output case even output reordering helps (see Example 8.28 and [44]).

8.6 Approaches to Nonlinear Observer Design

An observer for the system (8.1) is a dynamical system with inputs $y(\tau), u(\tau),\ 0 \leq \tau \leq t$ and output $\hat{x}(t) \in R^n$ such that $\hat{x}(t)$ is an estimate of $x(t)$ in the sense that $\|x(t) - \hat{x}(t)\| \to 0$ as $t \to \infty$. When (8.1) is linearly observable there are many approaches to observer design. On the other hand, if (8.1) is not linearly observable, options are limited.

8.6.1 Design Based on the Observer Form

If the system 8.1 can be transformed into the observer form of Section 8.5 then observer design is very straightforward. Unfortunately, this property applies to a limited class of systems. The idea is to transform the system into the 'time varying' version of (8.14), specifically the 'observer form' given in (8.15), repeated here.

$$\begin{aligned} \dot{z} &= A(u(t))z + \varphi(y, u(t)) \\ y &= \begin{bmatrix} z_1 & \cdots & z_p \end{bmatrix}^T = Cz \end{aligned}$$

A constructive approach to computing the transformation for single-output systems is given in [37]. Recently, [100] present a different construction that applies to a somewhat larger class of single-output systems in which the matrix A is allowed to depend on both u and y. That is in (8.15) $A(u(t)) \to A(u(t), y(t))$.

For a system in the form of (8.15) a Kalman observer can be used

$$\begin{aligned} \dot{\hat{z}} &= A(u(t))\hat{z} + \varphi(u(t), y(t)) + P(t)C^T(y(t) - C\hat{z}) \\ \dot{P} &= PA^T(u(t)) + A(u(t))P - PC^TCP + Q \end{aligned}$$

This observer converges exponentially provided $u(t)$ is such that the linear time-varying system

$$\dot{z} = A(u(t))z, \quad y = Cz$$

is completely observable [50]. This 'passive approach' relies on the natural occurrence of a suitably rich input.

8.6.2 Local Exponential Observers

Local exponential observers have been studied since the 1970's, e.g., [53, 111, 101], in an attempt to extend linear methods to nonlinear dynamical systems. For the most part, existing methods are limited to linear-like systems, in the sense that they are smooth and zero input observable [1].

Consider the nonlinear system

$$\dot{x} = f(x,u), \;\; y = h(x) \tag{8.20}$$

and suppose the system has an equilibrium point at (x^*, u^*), i.e. $f(x^*, u^*) = 0$. A *local observer* for (8.20) is another dynamical system, driven by inputs $y(t)$ and $u(t)$, that produces an estimate $\hat{x}(t)$ of $x(t)$ such that the error $e(t) = x(t) - \hat{x}(t)$ converges to zero as time tends to infinity:

$$\|x(t) - \hat{x}(t)\| \to 0, \;\; \text{as} \;\; t \to \infty \tag{8.21}$$

provided $x(t)$ remains sufficiently close to x^*.

One approach to observer design mimics the structure of full state observers for linear systems. Namely, the measurement error (or residual) is used to drive a replica of the system so that the observer equations are

$$\dot{\hat{x}} = f(\hat{x}, u) + \kappa(\hat{x}, y - h(\hat{x})) \tag{8.22}$$

The error dynamics can be computed

$$\dot{e} = \dot{x}(t) - \dot{\hat{x}}(t) = f(x,u) - f(x-e,u) + \kappa(x-e, h(x) - h(x-e)) \tag{8.23}$$

[1] Actually, the system is only required to be detectable as defined below.

Let us consider this as a differential equation that defines e, the error response to an exogenous input $x(t)$ (of course, it must be a solution of (8.20)). Notice that $e = 0$ does indeed correspond to an equilibrium point ($\dot{e} = 0$) of (8.23) for arbitrary $x(t)$ provided $\kappa(x,0) = 0$. Hence, the system (8.22) is an observer if $\kappa(\cdot,\cdot)$ can be chosen so that this equilibrium point is asymptotically stable.

Definition 8.31. *Exponential Detectability*

A system is said to be exponentially detectable at (x^*,u^*) if there exists a function $\gamma(\xi,y)$ defined on a neighborhood of $(x^*,y^* = h(x^*)) \in R^{n+q}$ that satisfies

(i) $\gamma(x^*,y^*) = 0$,

(ii) $\gamma(\xi,h(\xi)) = f(\xi,u^*)$,

(iii) the equilibrium point $\xi = x^*$ of $\dot{\xi} = \gamma(\xi,y^*)$ is exponentially stable.

Exponential detectability implies that the system

$$\dot{\hat{x}} = f(\hat{x},u) - f(\hat{x},u^*) + \gamma(\hat{x},y) \tag{8.24}$$

is a local observer. To see this, compute the error dynamics

$$\dot{e} = f(x,u) - f(x-e,u) + f(x-e,u^*) - \gamma(x-e,h(x)) \tag{8.25}$$

and notice that in view of (ii), $e = 0$ is an equilibrium point for all exogenous inputs $x(t),u(t)$. Moreover, exponential stability is assured by (iii)– as can be verified by linearizing (8.25) with respect to e at the equilibrium point $e = 0$.

Conditions (ii) and (iii) generalize the linear case in a natural way. It is easy to see that $\gamma(\xi,y) := A\xi - L(y - C\xi)$ satisfies (ii), and (iii) is satisfied as well provided L is chosen such that $A + LC$ is asymptotically stable. Moreover, the nonlinear observer (8.22) corresponds to the choice $\gamma(\xi,y) := f(\xi,u^*) + \kappa(\xi,y - h(\xi))$ provided $\kappa(\cdot,\cdot)$ can be chosen to provide exponential stability, i.e., to satisfy (iii).

The function `ExponentialObserver` implements the above construction. Its calling syntax is

```
{fhat,xhat,eigs}=
            ExponentialObserver[f,h,x,u,y,x0,u0,delta]
```

Thus, given: the system as defined by equations (8.20), an equilibrium point (x_0,u_0) and a specified decay rate δ the function returns an observer of the form

$$\dot{\hat{x}} = \hat{f}(\hat{x},u,y)$$

The eigenvalues of the linearized observer at the equilibrium point (x_0,u_0) are also returned.

Example 8.32 (An exponential observer). Here is a simple example of an exponential observer.

```
In[185]:= f = {x1^2 + Cos[x2] * x3 - x2, x2 * Cos[x1], Sin[x3] + Cos[x1] + u1};
          h = {x1 + x1 * x2 + x3, x2 + x3^3};

In[186]:= ExponentialObserver[f, h, {x1, x2, x3}, {u1}, {y1, y2}, {0, 0, 0}, {0}, 4]
Out[186]= {{x1hat^2 - x2hat + 27  (-x1hat - x1hat  x2hat - x3hat + y1) +
              5  (-x2hat - x3hat^3 + y2) + x3hat  Cos[x2hat],
            -10  (-x2hat - x3hat^3 + y2) + x2hat  Cos[x1hat],
            u1 - 45  (-x1hat - x1hat  x2hat - x3hat + y1) -
              5  (-x2hat - x3hat^3 + y2) + Cos[x1hat] + Sin[x3hat]},
           {x1hat, x2hat, x3hat}, {-5, -5, -4}}
```

Notice that the observer states are assigned names that are the original state names extended with 'hat.' Alternatively, the designer can specify a symbol upon which state names will be based.

Construction of Exponential Observers

There is considerable literature concerning the design of exponential observers, including Kazantis and Kravaris [3] consider the single output, observable system (7.1). Since the system (8.20) is (zero-input) observable, its linearization

$$\begin{aligned} \delta\dot{x} &= F\delta x \\ \delta y &= H\delta x \end{aligned} \tag{8.26}$$

is also observable. They use Lyapunov's auxiliary theorem to show that an observable linearization implies the existence of an observer for (7.1) with linear dynamics provided the convex hull of the set of eigenvalues of F does not contain the origin of the complex plane[2], i.e. $0 \notin CH\{\lambda_1, \ldots, \lambda_n\}$, where λ_i, $i = 1, \ldots, n$ denote the eigenvalues of F. When this condition is satisfied, the set of eigenvalues is said to belong to the 'Poincaré domain' [8]. Under these conditions, [3] provides a direct construction of such an observer. It is claimed in [3] that this construction, bypassing as it does the requirement of the intermediate form (**??**), is less restrictive than the requirements in [1]. But still, the eigenvalue constraint on F is itself undesirably restrictive. As a matter of fact, there are many systems that satisfy the necessary conditions of [1] but do not satisfy the conditions of [3]. The following is one such example.

[2]Notice that this is equivalent to having all eigenvalues in the open left half plane or all eigenvalues in the open right half plane, i.e. the origin is a source or a sink.

Appendix

8.A Proof of the Sufficiency Part of Proposition 8.21

Sufficiency: Assume that the hypotheses of the proposition hold, and the new coordinates are defined by Equations (8.16). The vector field f_u can be expressed in the new coordinates

$$f_u = \sum_{i=1}^{n} L_{f_u}(z_i) \frac{\partial}{\partial z_i}$$

We wish to determine the components of the vector field $F_u^i = L_{f_u}(z_i)$. Notice that, for $i > p$, we can write

$$dF_u^i \wedge dz_1 \wedge \cdots \wedge dz_p = L_{f_u}(dz_i) \wedge dz_1 \wedge \cdots \wedge dz_p$$

In view of (8.16) this becomes

$$dF_u^i \wedge dz_1 \wedge \cdots \wedge dz_p = L_{f_u}(i_X(\omega_{i-p})) \wedge dz_1 \wedge \cdots \wedge dz_p$$

But, $L_{f_u}(i_X(\omega_{i-p})) \in \Omega^X$. So, we can express $L_{f_u}(i_X(\omega_{i-p}))$ as a linear combination of the $n-p$ basis elements of Ω^X where the real coefficients depend on the parameter u. Thus,

$$dF_u^i \wedge dz_1 \wedge \cdots \wedge dz_p = \sum_{j=1}^{n-p} \alpha_j^i(u)\, \omega_j \wedge dz_1 \wedge \cdots \wedge dz_p$$

One can easily verify the identity $i_X(\omega_j) \wedge dz_1 \wedge \cdots \wedge dz_p = \omega_j$, which, again in view of (8.16), implies that $\omega_j = dz_{j+p} \wedge dz_1 \wedge \cdots \wedge dz_p$, for $j = 1, \ldots, n-p$. Consequently,

$$dF_u^i \wedge dz_1 \wedge \cdots \wedge dz_p = \sum_{j=1}^{n-p} \alpha_j^i(u)\, dz_{j+p} \wedge dz_1 \wedge \cdots \wedge dz_p$$

Then, it must be true that

$$dF_u^i = \sum_{j=1}^{n-p} \alpha_j^i(u)\, dz_{j+p} + \sum_{j=1}^{p} \phi\,(z_1,\ldots,z_p,u) dz_j$$

Note, that it is the integrability requirement that insures that ϕ depends only on the coordinates $z_1,\ldots,z_p$. Integrating, leads to

$$F_u^i = \sum_{j=1}^{n-p} \alpha_j^i(u) z_{j+p} + \varphi\,(z_1,\ldots,z_p,u), \quad i = p+1,\ldots,n$$

For $j = 1,\ldots,p$,

$$dF_u^i \wedge dz_1 \wedge \cdots \wedge dz_p = dL_{f_u}(z_i) \wedge dz_1 \wedge \cdots \wedge dz_p$$

But, in view of Ω_1^X, $dL_{f_u}(z_i) \in \Omega^X$, for $i = 1,\ldots,p$. So, the remainder of the argument proceeds as before.

8.B Proof of the Necessity Part of Proposition 8.23

Here, we provide a sketch of the proof. The overall logic follows the arguments of [37] for the single-output case.

The conditions of the theorem are coordinate free. So if the system (8.1) is transformable to (8.15) we can verify conditions (1), (2), (3) in the z-coordinates. We begin by introducing the 'unobservable' distributions (replaces the unobservable subspace of linear systems)

$$\begin{aligned}
\mathscr{F}_0 &= \{X \,|L_X(h_i) = 0,\, i = 1,\ldots,p\,\} \\
\mathscr{F}_{k+1} &= \mathscr{F}_k \cap \left\{ X \;\middle|\; \begin{array}{c} L_X L_{f_{u^{k+1}}} \cdots L_{f_{u^1}}(h_i) = 0 \\ u^1,\ldots,u^{k+1} \in [0,1]^m \\ i = 1,\ldots,p \end{array} \right\}
\end{aligned}$$

Our observability assumption on $\mathscr{E}_0,\ldots.\mathscr{E}_{p^*}$ implies that

$$\mathscr{F}_0 \supset \cdots \supset \mathscr{F}_{p^*} = \{0\}$$

In z-coordinates, we can compute (following tedious computations as in [37])

$$\begin{aligned}
\mathscr{F}_0 &= \{X \,|CX = 0\,\} \\
\mathscr{F}_{k+1} &= \mathscr{F}_k \cap \left\{ X \;\middle|\; (CA)_{l_{k+1}} X = 0 \right\}
\end{aligned}$$

Accordingly, introduce the sets of constant vector fields

$$\begin{aligned}
F_0 &= \{X \in R^n \,|CX = 0\,\} = \ker C \\
F_{k+1} &= F_k \cap \left\{ X \in R^n \;\middle|\; (CA)_{l_{k+1}} X = 0 \right\}
\end{aligned}$$

Comparing these, [37] point out that the real vector spaces F_k span the distributions $\mathscr{F}_k$. Their Lemma 5 and Claim 7 are easily extended to the multi-output case:

Lemma 8.33. *(i)* $\forall u \in \{0,1\}^m$, $[f_u, \mathscr{F}_{k+1}] \subset \mathscr{F}_k$ *for* $k = 0,\ldots,p^*-1$. *(ii)* $\forall X \in \mathscr{F}_k \backslash \mathscr{F}_{k+1}$, $\exists u \in \{0,1\}^m$ *such that* $[f_u, X] \in \mathscr{F}_{k-1} \backslash \mathscr{F}_k$ *for* $k = 1,\ldots,p^*$.

Proof: (i) Let $X \in \mathscr{F}_{k+1}$. From the definition of the $\mathscr{F}_k$'s we have for every $\left(u^1,\ldots,u^r\right) \in (\{0,1\}^m)^r$ and $1 \le r \le k+1$, $L_X L_{f_{u^r}} \cdots L_{f_{u^1}}(h_i) = 0$, $i = 1,\ldots,p$. Thus,

$$L_{[f_u,X]} L_{f_{u^r}} \cdots L_{f_{u^1}}(h_i) = L_{f_u} L_{f_{u^r}} \cdots L_{f_{u^1}}(h_i) - L_X L_{f_{u^r}} \cdots L_{f_{u^1}}(h_i) = 0$$

so that $[f_u, X] \in \mathscr{F}_k$.

(ii) Assume the contrary, i.e., there exists $X \in \mathscr{F}_k \backslash \mathscr{F}_{k+1}$ such that for every $u \in \{0,1\}^m$, $[f_u, X] \in \mathscr{F}_k$, then using the formula in (i) above, we obtain $L_X L_{f_u} L_{f_{u^k}} \cdots L_{f_{u^1}}(h_i) = 0$, $i = 1,\ldots,p$, for every $u, u^1,\ldots,u^k \in \{0,1\}^m$. But then, $X \in \mathscr{F}_{k+1}$, which contradicts the assumption. ■

On this basis [37] establish the following corresponding result for the F_k.

Lemma 8.34. *(i)* $\forall u \in \{0,1\}^m$, $[f_u, F_{k+1}] \subset F_k$, *for* $k = 1,\ldots,p^*-1$, *(ii)* $\forall X \in F_k \backslash F_{k+1}$, $\exists u \in \{0,1\}^m$ *such that* $[f_u, X] \in F_{k-1} \backslash F_k$ *for* $k = 1,\ldots,p^*-1$.

Proof: For every $X \in F_{k+1}$, $[f_u, X] \in \mathscr{F}_k$, $0 \le k \le p^*-1$ by Lemma 8.33. Now compute

$$[f_u, X] = -\frac{\partial f_u}{\partial z} X = -A(u)X - \frac{\partial \varphi(y,u)}{\partial y} CX = -A(u)X$$

Thus, $[f_u, X]$ is a constant vector field. Hence, $[f_u, X] \in F_k$. This proves (i). Now, suppose $X \in F_k \backslash F_{k-1}$. Again from Lemma 8.33, we have $[f_u, X] \in \mathscr{F}_{k-1} \backslash \mathscr{F}_k$. But the calculation above shows $[f_u, X]$ is a constant vector field, so $[f_u, X] \in F_{k-1} \backslash F_k$, thus establishing (ii). ■

Proof of main result:

Condition (1): By rewriting Equation (8.17) in z-coordinates and in view of the definition of the sets F_k, we can establish $Y_i \in F_{\kappa_i - 2} \backslash F_{\kappa_i - 1}$, for each $i = 1,\ldots,p$.

Lemma 8.34 implies there exists $u^1 \in [0,1]^m$ such that $[f_{u^1}, Y_i] \in F_{\kappa_i - 2} \backslash F_{\kappa_i - 1}$. Successive application of Lemma 8.34 leads to the conclusion $\exists u_1,\ldots,u_{\kappa_i - 1} \in [0,1]^m$ such that

$$\left[f_{u^{\kappa_i - 1}}, [\cdots [f_{u^1}, Y_i] \cdots]\right] \in F_0 \backslash F_1 \tag{8.27}$$

Now we can show that there exists u_{κ_i} such that

$$\left[f_{u_{\kappa_i}}, [\cdots [f_{u_1}, Y] \cdots]\right] \notin F_0 \tag{8.28}$$

To see this, assume the contrary, i.e.,

$$\forall u^{\kappa_i} \in R^m;\ L_{\left[f_{u^{\kappa_i}}, [\cdots [f_{u^1}, Y_i] \cdots]\right]}(h) \notin F_0$$

so that

$$L_{f_{u^{\kappa_i}}} L_{\left[f_{u^{\kappa_i-1}},\left[\cdots\left[f_{u^1},Y_i\right]\cdots\right]\right]}(h) - L_{\left[f_{u^{\kappa_i-1}},\left[\cdots\left[f_{u^1},Y_i\right]\cdots\right]\right]} L_{f_{u^{\kappa_i}}}(h) = 0$$

Now, since

$$\left[f_{u_{\kappa_i-1}},[\cdots[f_{u_1},Y]\cdots]\right] \in F_0$$

it follows that $L_{\left[f_{u^{\kappa_i-1}},\left[\cdots\left[f_{u^1},Y_i\right]\cdots\right]\right]}(h) = 0$ and, hence,

$$\left[f_{u^{\kappa_i-1}},[\cdots[f_{u^1},Y_i]\cdots]\right] \in F_1$$

which contradicts Equation (8.27). Consequently, (8.28) holds.

By construction

$$Z^i_{u^1\cdots u^{\kappa_i-1}} := \left[f_{u_{\kappa_i-1}},[\cdots[f_{u_1},Y_i]\cdots]\right]$$

is a constant vector field in the z-coordinates, i.e.,

$$Z^i_{u^1\cdots u^{\kappa_i-1}} = \sum_{k=1}^{n} d^i_k \frac{\partial}{\partial z_k}$$

for some constants d^i_k. Now compute,

$$C^j Z^i_{u^1\cdots u^{\kappa_i-1}} = C^j \sum_{k=1}^{n} d^i_k \frac{\partial}{\partial z_k} = d^i_j \frac{\partial}{\partial z_j}$$

so that

$$L_{Z^i_{u^1\cdots u^{\kappa_i-1}}}(Cz) = CZ^i_{u^1\cdots u^{\kappa_i-1}} = \begin{bmatrix} d^i_1 \\ \vdots \\ d^i_p \end{bmatrix}$$

It is not difficult to verify that the (constant) vector fields $Z^i_{u^1\cdots u^{\kappa_i-1}}$ are linearly independent. Now, from (8.28), we have for each $i = 1,\ldots,p$

$$\begin{bmatrix} d^i_1 & \cdots & d^i_p & 0 & \cdots & 0 \end{bmatrix}^T \notin \ker C$$

Since $\operatorname{rank} C = p$, we have $\dim \ker C = n - p$ and there are precisely p independent vectors not contained in $\ker C$. It follows that the p-vectors $\begin{bmatrix} d^i_1 & \cdots & d^i_p \end{bmatrix}$, $i = 1,\ldots,p$ are independent. Consequently,

$$\left[L_{Z^1_{u^1\cdots u^{\kappa_1-1}}}(Cz) \cdots L_{Z^p_{u^1\cdots u^{\kappa_p-1}}}(Cz)\right] = \begin{bmatrix} d^1_1 & \cdots & d^p_1 \\ \vdots & \ddots & \vdots \\ d^1_p & \cdots & d^p_p \end{bmatrix}$$

is invertible. This implies $\mathscr{I} \neq \emptyset$.

Condition (2): Since the $Z^i_{u^1\cdots u^{\kappa_i-1}}$ are constant vector fields in the z-coordinates, Condition (2) holds.

Condition (3): In the z-coordinates, compute

$$X_i = \left[L_{Z^1_{u^1 \cdots u^{\kappa_1 - 1}}}(Cz) \cdots L_{Z^p_{u^1 \cdots u^{\kappa_p - 1}}}(Cz) \right]^{-1} Z^i_{u^1 \cdots u^{\kappa_i - 1}} = \frac{\partial}{\partial z_i}$$

which satisfies the conditions of Proposition 8.21 for a system in the form observer form (8.15), see item (1) in Remark 8.22 and [34, 35]. ■

9

Robust and Adaptive Control Systems

9.1 Introduction

Developments in nonlinear geometric control theory have had a substantial impact on the theory and design of robust and adaptive controls for nonlinear systems. We will describe some of the more established approaches and the associated computations. Our primary interest, in this chapter and the next, is the application of feedback linearization methods to uncertain systems.

Any model-based control design method is vulnerable to model errors. This is obviously a concern with feedback linearization techniques since exact cancelation is a basic ingredient of the method. On the other hand, models used for control system design are never infinitely precise. Thus, it is necessary to investigate the impact of model uncertainty on closed loop system performance and to devise methods for insuring adequate performance when a controller is applied to systems that deviate from the design model.

Model uncertainty is generally of two types. *Unmodeled dynamics* refers to dynamics that are neglected because they act on a time scale (typically) much faster than the time scale of interest. *Functional uncertainty* means uncertainty in the functions f, G, h that define the affine differential equation model. The effect of unmodeled dynamics is often analyzed using singular perturbation or averaging methods. While unmodeled dynamics are extremely important, our focus will be on functional uncertainty. Normally, functional uncertainty is characterized by perturbing a nominal (certain) part by an appropriately bounded, but otherwise unspecified function. In some cases the uncertainty is characterized in terms of an uncertain parameter.

Feedback linearization methods typically begin with the transformation of the design model to a normal form. Thus, we begin, in Section 2, with an investigation of the consequences of applying a state transformation derived on the basis of a nominal model to a perturbation of it. When the uncertainties satisfy certain structural conditions, the transformed system assumes a triangular form that can facilitate analysis.

The design of robust stabilizers, i.e., controllers that guarantee closed loop stability for all admissible perturbations of a nominal plant, for systems with matched uncertainties is considered in Section 3 using the method of *Lyapunov redesign*. In Section 4 we consider the design of robust stabilizing controllers for systems with a class of nonmatched uncertainties. The design we describe employs a *backstepping* method. Backstepping will reappear with some variation in our discussion of adaptive control and variable structure control.

We then turn to the case where the uncertainty can be characterized in terms of uncertain parameters. Thus, we describe the design of parameter-adaptive controls. Section 5 introduces a basic adaptive regulator. In general, this controller requires measurement of the system states and some of the transformed states. The need to measure transformed states can be avoided by using the backstepping approach discussed in Section 6. Section 7 describes an adaptive tracking controller based on dynamic inversion. Computational tools are described and illustrated for each method.

9.2 Perturbations of Feedback Linearizable Systems

We will examine perturbations of systems of known relative degree. There are several important applications of such an analysis. For example, a perturbation may arise as an uncertainty applied to a nominal system. Or it may simply be convenient, for a variety of reasons, to divide a system into a nominal system plus a perturbation in order to isolate certain terms. The main point is that under certain constraints on the perturbation, the perturbed system can be transformed into a triangular or near triangular form that can be exploited for purposes of control system design.

9.2.1 SISO Case

We will consider the 'perturbed' SISO system

$$\begin{aligned} \dot{x} &= f(x) + \varphi(x) + [g(x) + \gamma(x)]\,u \\ y &= h(x) \end{aligned} \tag{9.1}$$

where $x \in R^n$, $u \in R$, $y \in R$ and $\varphi(x)$, $\gamma(x)$ represent a perturbation applied to the nominal system (f,g,h). Previously, we discussed the reduction of the nominal system to normal form via a transformation of coordinates. Under certain conditions, the nominal transformation when applied to the perturbed system still produces a useful form of the system equations. The following definitions apply constraints on the structure of the perturbation $\varphi(x)$, along the lines of [81]. Recall

$$\mathscr{G}_i = \operatorname{span}\left\{g, \ldots, \operatorname{ad}_f^i g\right\}, \quad 0 \le i \le n-1$$

Definition 9.1. *Suppose the system (9.1) is of relative degree r. We say that the perturbation, $\varphi(x)$ satisfies:*

1. *the* triangularity condition *if* $\mathrm{ad}_\varphi \mathscr{G}_i \in \mathscr{G}_{i+1}$, $0 \le i \le r-3$
2. *the* strict triangularity condition *if* $\mathrm{ad}_\varphi \mathscr{G}_i \in \mathscr{G}_i$, $0 \le i \le r-2$
3. *the* extended matching condition *if* $\varphi \in \mathscr{G}_1$
4. *the* matching condition *if* $\varphi \in \mathscr{G}_0$

Notice that these conditions are listed from weakest to strongest, i.e.,

$$\textit{matching} \Rightarrow \textit{extended matching} \Rightarrow \textit{strict triangularity} \Rightarrow \textit{triangularity}$$

Consider the following result which perturbs only the drift term.

Proposition 9.2. *Assume*

1. *the nominal system* (f,g,h) *has relative degree r at the* $x_0 \in R^n$.
2. *the perturbed system* $(f+\varphi,g,h)$ *satisfies the* strict triangularity *assumption on a neighborhood of* x_0*:* $\mathrm{ad}_\varphi \mathscr{G}_i \subset \mathscr{G}_i$, $0 \le i \le r-2$.

There exists a local transformation on a neighborhood of x_0 that reduces the perturbed system to

$$\begin{aligned}
&\dot{\xi} = \hat{F}(\xi,z),\ \xi \in R^{n-r}\\
&\dot{z}_1 = z_2 + \phi_1(\xi,z_1)\\
&\dot{z}_2 = z_3 + \phi_2(\xi,z_1,z_2)\\
&\vdots\\
&\dot{z}_r = \alpha(x(\xi,z)) + \phi_r(\xi,z_1,\ldots,z_r) + \rho(x(\xi,z))u
\end{aligned}$$

Proof: The nominal system has relative degree r. Then there exists a transformation $x \mapsto (\xi,z)$, $\xi \in R^{n-r}$, $z_i \in R$ with $z_i(x) = L_f^{i-1}h(x)$, $1 \le i \le r$, that takes the nominal system to

$$\begin{aligned}
&\dot{\xi} = F(\xi,z)\\
&\dot{z}_1 = z_2\\
&\vdots\\
&\dot{z}_r = L_f^r h(x(\xi,z)) + L_g L_f^{r-1} h(x(\xi,z))u
\end{aligned}$$

Now, we apply this transformation to the system (9.1). First compute

$$\begin{aligned}
\dot{\xi} = \left.\tfrac{\partial \xi}{\partial x}\dot{x}\right|_{x\mapsto(\xi,z)} &= L_f\xi(x) + L_\varphi\xi(x) + L_g\xi(x)u\big|_{x\mapsto(\xi,z)}\\
&= F(\xi,z) + L_\varphi\xi(x)\big|_{x\mapsto(\xi,z)}\\
&= \hat{F}(\xi,z)
\end{aligned}$$

Now compute

$$\begin{aligned}
\dot{z}_1 &= \dot{y} = L_f h(x) + L_\varphi h(x) + L_g h(x)u = z_2 + L_\varphi h(x) \\
\dot{z}_2 &= L_f^2 h(x) + L_\varphi L_f h(x) + L_g L_f h(x)u = z_3 + L_\varphi L_f h(x) \\
&\vdots \\
\dot{z}_r &= L_f^r h(x) + L_\varphi L_f^{r-1} h(x) + L_g L_f^{r-1} h(x)u
\end{aligned}$$

Define the function $\phi(\xi, z)$

$$\begin{bmatrix} L_\varphi h(x(\xi,z)) \\ L_\varphi L_f h(x(\xi,z)) \\ \vdots \\ L_\varphi L_f^{r-1} h(x(\xi,z)) \end{bmatrix} = \phi(\xi, z)$$

so that we can write

$$\begin{aligned}
\dot{z}_1 &= z_2 + \phi_1(\xi, z)) \\
\dot{z}_2 &= z_3 + \phi_2(\xi, z) \\
&\vdots \\
\dot{z}_r &= L_f^r h(x) + \phi_r(\xi, z) + L_g L_f^{r-1} h(x)u
\end{aligned}$$

So, we see that under transformation $\varphi(x) \mapsto \phi(\xi, z)$.

It is necessary to establish the triangular dependence of ϕ on $z_1, \ldots, z_r$. We do the required calculations in the transformed – (ξ, z) – coordinates. Under transformation f and g become

$$f(x) \mapsto \hat{f}(\zeta) = \begin{bmatrix} F(\xi,z) \\ z_2 \\ \vdots \\ z_r \\ L_f^r h(x(\xi,z)) \end{bmatrix}, \quad g(x) \mapsto \hat{g}(\zeta) = \begin{bmatrix} 0 \\ \vdots \\ \vdots \\ 0 \\ L_g L_f^{r-1} h(x(\xi,z)) \end{bmatrix}$$

Thus, we see that

$$\mathrm{ad}_f g = \left[\frac{\partial \hat{g}}{\partial \zeta}\right] \hat{f} - \left[\frac{\partial \hat{f}}{\partial \zeta}\right] \hat{g} = \begin{bmatrix} 0 \\ \vdots \\ 0 \\ 0 \\ L_g L_f^r h \end{bmatrix} - \begin{bmatrix} 0 \\ \vdots \\ 0 \\ L_g L_f^{r-1} h \\ L_g L_f^r h \end{bmatrix} = - \begin{bmatrix} 0 \\ \vdots \\ 0 \\ L_g L_f^{r-1} h \\ 0 \end{bmatrix}$$

Similarly, we compute

$$\mathrm{ad}_f^i g = \begin{bmatrix} 0 \\ \vdots \\ 0 \\ (-1)^i L_g L_f^{r-1} h \\ 0 \\ \vdots \\ 0 \end{bmatrix} \leftarrow (n-i), \quad 1 \le i \le r-1$$

Thus, we have

$$\mathscr{G}_i = \mathrm{span}\left\{ \underbrace{\begin{bmatrix} 0 \\ \vdots \\ \vdots \\ \vdots \\ \vdots \\ 0 \\ L_g L_f^{r-1} h \end{bmatrix} \quad \begin{bmatrix} 0 \\ \vdots \\ \vdots \\ \vdots \\ 0 \\ -L_g L_f^{r-1} h \\ 0 \end{bmatrix} \quad \cdots \quad \begin{bmatrix} 0 \\ \vdots \\ 0 \\ (-1)^i L_g L_f^{r-1} h \\ 0 \\ \vdots \\ 0 \end{bmatrix}}_{i \text{ terms}} \right\}$$

Now, consider

$$\mathrm{ad}_\varphi g = \frac{\partial \varphi}{\partial \zeta} g - \frac{\partial g}{\partial \zeta} \varphi = \frac{\partial \varphi}{\partial z_n} L_g L_f^{r-1} h - \begin{bmatrix} 0 \\ \vdots \\ 0 \\ \frac{\partial L_g L_f^{r-1} h}{\partial \zeta} \varphi \end{bmatrix} \in \mathrm{span}\left\{ \begin{bmatrix} 0 \\ \vdots \\ 0 \\ L_g L_f^{r-1} h \end{bmatrix} \right\}$$

This implies

$$\frac{\partial \varphi_1}{\partial z_r} = 0, \ldots, \frac{\partial \varphi_{n-1}}{\partial z_r} = 0$$

Next consider

$$\begin{aligned} \mathrm{ad}_\varphi \mathrm{ad}_f g &= \tfrac{\partial \varphi}{\partial \zeta} \mathrm{ad}_f g - \tfrac{\partial \mathrm{ad}_f g}{\partial \zeta} \varphi \\ &= \tfrac{\partial \varphi}{\partial z_{r-1}} L_g L_f^{r-1} h - \begin{bmatrix} 0 \\ \vdots \\ 0 \\ \frac{\partial L_g L_f^{r-1} h}{\partial \zeta} \varphi \\ 0 \end{bmatrix} \in \mathrm{span}\left\{ \begin{bmatrix} 0 \\ \vdots \\ \vdots \\ 0 \\ L_g L_f^{r-1} h \end{bmatrix} \quad \begin{bmatrix} 0 \\ \vdots \\ 0 \\ L_g L_f^{r-1} h \\ 0 \end{bmatrix} \right\} \end{aligned}$$

This implies

$$\frac{\partial \varphi_1}{\partial z_{r-1}} = 0, \ldots, \frac{\partial \varphi_{n-2}}{\partial z_{r-1}} = 0$$

Continuing in this way, we find

$$\frac{\partial \varphi_1}{\partial z_{r-i}} = 0, \ldots, \frac{\partial \varphi_{n-i-1}}{\partial z_{r-i}} = 0, \quad 0 \le i \le r-2$$

providing the desired result. ■

The above result can be easily generalized to allow perturbations in the control gain of the form $\gamma \in \mathscr{G}_0$. Although restrictive, this class of perturbations is nontheless useful in applications. Notice that for any scalar function or vector field $w(x)$, if $L_g w(x) = 0$ then if the *matching condition*, $\gamma \in \mathscr{G}_0$, is true we have $L_\gamma w(x) = 0$. Thus, in the calculations in the above proof, the only change is in the last of the transformed state equations. In fact, we have for the transformed system:

$$\begin{aligned}
&\dot{\xi} = \hat{F}(\xi, z), \ \xi \in R^{n-r} \\
&\dot{z}_1 = z_2 + \phi_1(\xi, z_1) \\
&\dot{z}_2 = z_3 + \phi_2(\xi, z_1, z_2) \\
&\vdots \\
&\dot{z}_r = \alpha(x(\xi, z)) + \phi_r(\xi, z_1, \ldots, z_r) + [\rho\,(x(\xi, x)) + \hat{\rho}\,(x(\xi, x))]\, u
\end{aligned}$$

where $\hat{\rho}\,(x(\xi, x)) = L_\gamma L_f^{r-1} h\,(x(\xi, x))$.

Similar results obtain for the other conditions of Definition (9.1). The following is a summary:

Suppose the nominal part of the control system (9.1) has local relative degree r. Then the perturbation conditions of Definition (9.1) assure local transformation to triangular forms as follows:

1. the triangularity condition implies

$$\begin{aligned}
&\dot{\xi} = \hat{F}(\xi, z), \ \xi \in R^{n-r} \\
&\dot{z}_i = z_{i+1} + \phi_i(\xi, z_1, \ldots, z_{i+1}), \ 1 \le i \le r-1 \\
&\dot{z}_r = \alpha(x(\xi, z)) + \phi_r(\xi, z_1, \ldots, z_r) + \rho(x(\xi, z))u
\end{aligned} \tag{9.2}$$

2. the strict triangularity condition implies

$$\begin{aligned}
&\dot{\xi} = \hat{F}(\xi, z), \ \xi \in R^{n-r} \\
&\dot{z}_i = z_{i+1} + \phi_i(\xi, z_1, \ldots, z_i), \ 1 \le i \le r-1 \\
&\dot{z}_r = \alpha(x(\xi, z)) + \phi_r(\xi, z_1, \ldots, z_r) + \rho(x(\xi, z))u
\end{aligned} \tag{9.3}$$

3. the extended matching condition implies

$$\begin{aligned}
&\dot{\xi} = \hat{F}(\xi, z), \ \xi \in R^{n-r} \\
&\dot{z}_i = z_{i+1}, \qquad 1 \le i \le r-2 \\
&\dot{z}_{r-1} = z_r + \phi_{r-1}(\xi, z_1, \ldots, z_r) \\
&\dot{z}_r = \alpha(x(\xi, z)) + \phi_r(\xi, z_1, \ldots, z_r) + \rho(x(\xi, z))u
\end{aligned} \tag{9.4}$$

4. the matching condition implies

$$\begin{aligned} &\dot{\xi} = F(\xi, z),\ \xi \in R^{n-r} \\ &\dot{z}_i = z_{i+1}, \qquad 1 \le i \le r-1 \\ &\dot{z}_r = \alpha(x(\xi,z)) + \phi_r(\xi, z_1, \ldots, z_r) + \rho(x(\xi,z))u \end{aligned} \tag{9.5}$$

Example 9.3 (Strict Triangularity). Consider the following system:

```
In[187]:= f = {x2, x3 - x1 -  x2, x4, x1 - x3 - (1/2)x4};
          g = {0, 0, 0, 1};
          h = x1;

In[188]:= DF = {0, -DF1[x1, x2], 0, -DF2[x3, x4]};
```

First, let us show that the uncertainty satisfies the strict triangularity condition. To do this, we compute the relative degree,

```
In[189]:= VectorRelativeOrder[f, g, {h}, {x1, x2, x3, x4}]
Out[189]= {4}
```

and the required distributions $\mathscr{G}_0$, $\mathscr{G}_1$ and $\mathscr{G}_2$:

```
In[190]:= G0 = Span[{g}]
          G1 = Span[{g, Ad[f, g, {x1, x2, x3, x4}, 1]}]
          G2 = Span[Join[G1, {Ad[f, g, {x1, x2, x3, x4}, 2]}]]
Out[190]= {{0, 0, 0, 1}}
Out[190]= {{0, 0, 1, 0}, {0, 0, 0, 1}}
Out[190]= {{0, 1, 0, 0}, {0, 0, 1, 0}, {0, 0, 0, 1}}
```

Now, test the uncertainty

```
In[191]:= Map[Ad[DF, #, {x1, x2, x3, x4}, 1] &, G0]
Out[191]= {{0, 0, 0, DF2^(0,1)[x3, x4]}}

In[192]:= Map[Ad[DF, #, {x1, x2, x3, x4}, 1] &, G1]
Out[192]= {{0, 0, 0, DF2^(0,1)[x3, x4]}, {0, 0, 0, DF2^(1,0)[x3, x4]}}

In[193]:= Map[Ad[DF, #, {x1, x2, x3, x4}, 1] &, G2]
Out[193]= {{0, DF1^(0,1)[x1, x2], 0, 0},
            {0, 0, 0, DF2^(1,0)[x3, x4]}, {0, 0, 0, DF2^(0,1)[x3, x4]}}
```

and notice that the conditions are indeed satisifed. The transformation that places the nominal system is obtained:

```
In[194]:= {T1, T2} = SISONormalFormTrans[f, g, x1, {x1, x2, x3, x4}]
Out[194]= {{x1, x2, -x1 - x2 + x3, x1 - x3 + x4}, {}}
```

Then, its inverse.

```
In[195]:= InvTrans = InverseTransformation[{x1, x2, x3, x4}, {z1, z2, z3, z4}, T1];
"InverseTransformation : "{x1, x2, x3, x4}" = "{z1, z2, z1 + z2 + z3, z2 + z3 + z4}
```

Application of the transformation to the nominal system confirms the reduction to normal form.

```
In[196]:= {fnew, gnew, hnew} = TransformSystem[f, g, h, {x1, x2, x3, x4},
                                {z1, z2, z3, z4}, T1, InvTrans]
Out[196]= {{z2, z3, z4, -z3 - 3/2 (z2 + z3 + z4)}, {0, 0, 0, 1}, z1}
```

Now, apply the transformation to the perturbed system, to obtain:

```
In[197]:= {ff, gg, hh} = TransformSystem[f + DF, g, h, {x1, x2, x3, x4},
                          {z1, z2, z3, z4}, T1, InvTrans];

In[198]:= ff // MatrixForm
```

$$\text{Out[198]=}\begin{pmatrix} z2 \\ z3 - DF1[z1, z2] \\ z4 + DF1[z1, z2] \\ \frac{1}{2}\ (-3\ \ z2 - 5\ \ z3 - 3\ \ z4 - 2\ \ DF2[z1 + z2 + z3, z2 + z3 + z4]) \end{pmatrix}$$

The system is indeed in the strict triangular form anticipated by Proposition (9.2).

The perturbation is readily modified so that the strict triangularity assumption fails.

```
In[199]:= DF = {0, -DF1[x1, x2, x3], 0, -DF2[x4]};

In[200]:= Map[Ad[DF, #, {x1, x2, x3, x4}, 1] &, G0]
Out[200]= {{0, 0, 0, DF2'[x4]}}

In[201]:= Map[Ad[DF, #, {x1, x2, x3, x4}, 1] &, G1]
Out[201]= {{0, DF1^(0,0,1)[x1, x2, x3], 0, 0}, {0, 0, 0, DF2'[x4]}}

In[202]:= {ff, gg, hh} = TransformSystem[f + DF, g, h, {x1, x2, x3, x4},
                          {z1, z2, z3, z4}, T1, InvTrans];

In[203]:= ff // MatrixForm
```

$$\text{Out[203]=}\begin{pmatrix} z2 \\ z3 - DF1[z1, z2, z1 + z2 + z3] \\ z4 + DF1[z1, z2, z1 + z2 + z3] \\ \frac{1}{2}\ (-3\ \ z2 - 5\ \ z3 - 3\ \ z4 - 2\ \ DF2[z2 + z3 + z4]) \end{pmatrix}$$

In this case we do not achieve strict triangular reduction of the perturbed system because $\mathrm{ad}_\varphi \mathscr{G}_1 \notin \mathscr{G}_1$. However, we do have a (non-strict) triangular form since $\mathrm{ad}_\varphi \mathscr{G}_1 \in \mathscr{G}_2$ (as well as $\mathrm{ad}_\varphi \mathscr{G}_0 \in \mathscr{G}_1$).

9.2.2 MIMO Case

We now turn to the multi-input multi-output system with uncertainty in the drift term

$$\begin{aligned} \dot{x} &= f(x) + \varphi(x) + G(x)u \\ y &= h(x) \end{aligned} \tag{9.6}$$

where $x \in R^n$, $u \in R^m$, $y \in R^m$. Define the distributions

$$\mathscr{G}_i = \text{span}\left\{ \text{ad}_f^j g_k \,|\, 0 \le j \le i, 1 \le k \le m \right\}, \quad 0 \le i \le n-2$$

Then Definition (9.1) can be adapted to the MIMO case.

Definition 9.4. *Suppose the system (9.1) is of (vector) relative degree* $\mathbf{r} = \{r_1, \ldots, r_m\}$, *with* $r = r_1 + \cdots + r_2$. *We say that the perturbation satisfies:*

1. *the* triangularity condition *if* $\text{ad}_\varphi \mathscr{G}_i \in \mathscr{G}_{i+1}$, $0 \le i \le r-3$
2. *the* strict triangularity condition *if* $\text{ad}_\varphi \mathscr{G}_i \in \mathscr{G}_i$, $0 \le i \le r-2$
3. *the* extended matching condition *if* $\varphi \in \mathscr{G}_1$
4. *the* matching condition *if* $\varphi \in \mathscr{G}_0$

The following result generalizes Proposition (9.2).

Proposition 9.5. *Suppose the nominal part of the control system (9.6) has vector relative degree* $\{r_1, \ldots, r_m\}$ *at* x_0 *with* $r_1 \ge r_2 \ge \ldots \ge r_m$ *and* $r = r_1 + \ldots + r_m$. *Moreover assume that the strict triangularity condition applies. Then there exists a local transformation of coordinates such that the perturbed equations take the form:*

$$\begin{aligned}
&\dot{\xi} = \hat{F}(\xi, z, u), \quad \xi \in R^{r-1} \\
&\dot{z}_j^i = z_{j+1}^i + \phi_j^i(\xi, z_{r_1-r_i+1}^1, \ldots, z_{r_1-r_i+j}^1, \ldots, z_{r_m-r_i+1}^m, \ldots, z_{r_m-r_i+j}^m), \\
&\qquad 1 \le j \le r_i - 1 \\
&\dot{z}_{r_i}^i = \alpha_i(x(\xi, z)) + \rho_{i\cdot}(x(\xi, z))u + \phi_j^i(\xi, z^1, \ldots, z^m) \\
&\qquad 1 \le i \le m
\end{aligned}$$

on a neighborhood of x_0.

Proof: The proof proceeds precisely as in Proposition (9.2), although the calculations are considerably more tedious. First, as in Proposition (9.2), we compute

$$\dot{\xi} = \frac{\partial \xi}{\partial x}\dot{x} = F(\xi, z, u) + L_\varphi \xi(x)\big|_{x \mapsto (\xi, z)} = \hat{F}(\xi, z, u)$$

Now, compute

$$\begin{aligned}
&\dot{z}_1^i = z_2^i + L_\varphi h_i(x) \\
&\vdots \\
&\dot{z}_{r_i}^i = L_f^{r_i} h_i(x) + L_\varphi L_f^{r_i-1} h_i(x) + \sum_{j=1}^m L_g L_f^{r_i-1} h_i(x) u_j
\end{aligned}$$

and define the functions

$$\phi^i(\xi,z) = \begin{bmatrix} L_\varphi h_i(x(\xi,z)) \\ L_\varphi L_f h_i(x(\xi,z)) \\ \vdots \\ L_\varphi L_f^{r_i-1} h_i(x(\xi,z)) \end{bmatrix}$$

for $i = 1,\ldots,m$. In (ξ,z) coordinates

$$g_k = \begin{bmatrix} 0 \\ L_{g_k} L_f^{r_1-1} h_1 \\ \vdots \\ 0 \\ L_{g_k} L_f^{r_m-1} h_m \end{bmatrix} \begin{matrix} \\ \leftarrow \text{ row } r_1 \\ \vdots \\ \vdots \\ \leftarrow \text{ row } n = r_1 + \cdots + r_m \end{matrix}$$

and

$$\mathrm{ad}_f^j g_k = \begin{bmatrix} 0 \\ L_{g_k} L_f^{r_1-1} h_1 \\ \vdots \\ 0 \\ L_{g_k} L_f^{r_m-1} h_m \\ 0 \end{bmatrix} \begin{matrix} \\ \leftarrow \textit{ row } r_1 - j \\ \vdots \\ \vdots \\ \leftarrow \textit{ row } n-j = r_1 + \cdots + r_m - j \\ \end{matrix} \quad , \quad 1 \le j \le r_1 - 1$$

Notice that

$$\mathscr{G}_1 = \mathrm{span} \left\{ \begin{bmatrix} \vdots \\ 0 \\ 1 \\ 0 \\ \vdots \\ \end{bmatrix}, \begin{bmatrix} \vdots \\ \\ 0 \\ 1 \\ 0 \\ \vdots \end{bmatrix}, \ldots, \begin{bmatrix} \vdots \\ \\ \\ 0 \\ \vdots \\ 0 \\ 1 \end{bmatrix} \right\} \begin{matrix} \\ \leftarrow \text{ row } r_1 \\ \\ \leftarrow \text{ row } r_1 + r_2 \\ \vdots \\ \leftarrow \text{ row } r_1 + \cdots + r_m = r \end{matrix}$$

$$\mathscr{G}_2 = \mathrm{span} \left\{ \begin{bmatrix} \vdots \\ 0 \\ 1 \\ 0 \\ \vdots \\ \end{bmatrix}, \begin{bmatrix} \vdots \\ \\ 0 \\ 1 \\ 0 \\ \vdots \end{bmatrix}, \ldots, \begin{bmatrix} \vdots \\ \\ 0 \\ \vdots \\ 0 \\ 1 \end{bmatrix}, \begin{bmatrix} 0 \\ 1 \\ 0 \\ \vdots \\ \\ \vdots \end{bmatrix}, \begin{bmatrix} \vdots \\ \\ 0 \\ 1 \\ 0 \\ \vdots \end{bmatrix}, \ldots, \begin{bmatrix} \vdots \\ \\ \\ \vdots \\ 0 \\ 1 \\ 0 \end{bmatrix} \right\} \begin{matrix} \\ \leftarrow \text{ row } r_1 - 1 \\ \\ \leftarrow \text{ row } r_1 + r_2 - 1 \\ \vdots \\ \leftarrow \text{ row } r_1 + \cdots + r_m - 1 \end{matrix}$$

and so on.

Now, as in Proposition (9.2), we apply the triangularity assumption to obtain:

$$\frac{\partial \phi_1^i}{\partial z^j_{r_j-k}} = 0, \ldots, \frac{\partial \phi^i_{r_j-k-1}}{\partial z^j_{r_j-k}} = 0, \quad 0 \le k \le r_i - 2, \quad 1 \le i, j \le m$$

These relations establish the conclusion of the theorem. ■

As in the SISO case uncertainty in the control input matrix of the matched type is easily accommodated. Consider a perturbation of the form $G(x) \to G(x) + \Gamma(x)$, $\Gamma(x) = [\gamma_1(x) \cdots \gamma_m(x)]$ and $\gamma_i \in \mathscr{G}_0$ for each $i = 1, \ldots m$. Then the transformed equations are unchanged other than

$$\rho_{ij} = L_{g_j} L_f^{r_i - 1} h_i + L_{\gamma_j} L_f^{r_i - 1} h_i$$

9.3 Lyapunov Redesign for Matched Uncertainty

Very often a control system is designed on the basis of a nominal model. If the uncertainty is confined to a suitably characterized admissible class, it may be possible to augment the nominal control with a robustifying component that insures asymptotic stability for all admissible uncertainties. When this is accomplished using Lyapunov methods the technique is referred to as *Lyapunov redesign* (see, for example, [52], Chapter 5).

Suppose that the multi-input system (9.6) has well defined relative degree with $r = n$ (i.e., the exact state linearizable case) and the uncertainty satisfies the matching condition. Then, it is reducible, by state transformation, to the form

$$\dot{z} = Az + E[\alpha(z) + \Delta(z, u, t) + \rho(z)u] \tag{9.7}$$

A nominal feedback control designed on the basis of the feedback linearization approach is

$$u^*(z) = \rho^{-1}(z)\{-\alpha(z) + Kz\} \tag{9.8}$$

where K is chosen such that $(A + EK)$ is Hurwitz. Thus, the nominal closed loop system is described by the equation

$$\dot{z} = (A + EK)z \tag{9.9}$$

Moreover, it may be associated with a Lyapunov function $V(z) = z^T Pz$, where P satisfies the Lyapunov equation

$$P(A + EK) + (A + EK)^T P = -Q - I, \quad Q = Q^T > 0 \tag{9.10}$$

and $\dot{V} = -z^T Qz - \|z\|^2 < 0$ along trajectories of the closed loop nominal system. In the sequal it will become apparent why it is convenient to require the right hand side of (9.10) to be more negative than $-I$.

The nominal control u^* does provide some protection against plant unertainty. Indeed, along trajectories of (9.7) with $u = u^*$, we have

$$\dot{V} = -z^T Qz - \|z\|^2 + 2z^T PE\Delta \tag{9.11}$$

If the uncertainty has a bound $\|\Delta\| \leq \gamma\|z\|$, with constant $\gamma \geq 0$, then

$$\dot{V} \leq -\left(\lambda_{\min}(Q)+1\right)\|z\|^2 + 2\gamma\|PE\|\,\|z\|^2$$

Thus, stability is assured provided $\gamma < \left(\lambda_{\min}(Q)+1\right)/2\,\|PE\|$.

Now, consider the system with uncertainty and apply a control $u = u^* + \rho^{-1}\mu$, that includes a 'robustifying' component, μ intended to compensate for the uncertainty. Assume that the uncertainty satisfies the condition $\Delta(0,t) = 0$, $\forall t$, and the bounding condition

$$\left\|\Delta\left(z, u^* + \rho^{-1}\mu, t\right)\right\| \leq \sigma(z)\|z\| + k\|\mu\|, \quad 0 \leq k < 1 \tag{9.12}$$

for some known, smooth bounding function $\sigma(z) > 0$. We wish to choose μ so that the closed loop is asymptotically stable for any admissible uncertainty. The actual system closed loop equation is

$$\dot{z} = (A+EK)z + E\left(\mu + \Delta\left(z, u^*(z) + \rho^{-1}\mu, t\right)\right) \tag{9.13}$$

The derivative of $V(x)$ along trajectories of (9.13) is

$$\dot{V} = -z^T Qz - \|z\|^2 + 2z^T PE\left(\mu + \Delta\right) \tag{9.14}$$

Notice that the first two terms arise from the nominal system and the next is due to the uncertainty, Δ, and the control, μ, that is intended to compensate for it. For the time being, write $w^T = z^T PE$ and observe that the design objective is achieved if μ can be chosen such that $-\|z\|^2 + w^T\left(\mu + \Delta\right) \leq 0$.

In view of (9.12)

$$\begin{aligned} w^T\mu + w^T\Delta &\leq w^T\mu + \|w\|\,\|\Delta\| \\ &\leq w^T\mu + \|w\|\left[\sigma(z)\|z\| + k\|\mu\|\right] \end{aligned} \tag{9.15}$$

For now, let us proceed in a fashion that leads to a smooth control. Set $\mu = -w\kappa$, where $\kappa(z) > 0$ is a scalar valued function not yet defined. Then

$$\begin{aligned} -\|z\|^2 + w^T\mu + w^T\Delta &\leq -\|z\|^2 - \|w\|^2\kappa + \|w\|\left[\sigma(z)\|z\| + k\|w\|\,\|\kappa\|\right] \\ &\leq -\|w\|^2\kappa(1-k) + \|w\|\,\sigma(z)\|z\| - \|z\|^2 \end{aligned}$$

Now choose

$$\kappa = \tfrac{1}{4(1-k)}\sigma^2$$

so that

$$\begin{aligned} -\|z\|^2 + w^T\mu + w^T\Delta &\leq -\|w\|^2\tfrac{1}{4}\sigma^2(z) + \|w\|\,\sigma(z)\|z\|\,1\,\|z\|^2 \\ &= -\left(\tfrac{1}{2}\|w\|\,\sigma(z) - \|z\|\right)^2 \end{aligned}$$

Consequently, a robust control is achieved with $\kappa > \frac{1}{4(1-k)}\sigma^2$. In particular, suppose $\sigma_0 > 0$ is a constant and take

$$\mu = -\left(\sigma_0 + \frac{\sigma^2(z)}{4(1-k)}\right) w = -\left(\sigma_0 + \frac{\sigma^2(z)}{4(1-k)}\right) E^T P z \tag{9.16}$$

These calculations establish the following proposition.

Proposition 9.6. *Consider the uncertain system (9.7) and assume it has an isolated equilibrium point at the origin. Suppose that a nominal control u^*, given by (9.8), is associated with the Lyapunov function $V(z) = z^T P z$, where P satisfies (9.10). Then the control $u = u^* + \rho^{-1}\mu$, where*

$$\mu = -\left(\sigma_0 + \frac{\sigma^2(z)}{4(1-k)}\right) E^T P z,\ \sigma_0 > 0 \tag{9.17}$$

globally stabilizes the origin of (9.7) for all uncertainties that satisfy (9.12).

Proof: Taking $V = z^T P z$, direct calculation as above leads to

$$\dot{V} = -z^T Q z - \sigma_0 \left\|E^T P z\right\|^2 - \left(\tfrac{1}{2}\left\|E^T P z\right\| \sigma(z) - \|z\|\right)^2$$

Thus, $\dot{V} < 0$ everywhere except at the origin $z = 0$. ■

Remark 9.7. As an alternative to the smooth control given above, we could proceed, as in [2], to design a discontinuous control. For example, choose

$$\mu = -\frac{\eta(z)}{1-k}\frac{w}{\|w\|}, \quad \eta(z) \geq \sigma(z)\|z\| \tag{9.18}$$

A simple computation verifies that this control achieves $\dot{V} < 0$,

$$\begin{aligned} w^T\mu + w^T\Delta &\leq -\tfrac{\eta(z)}{1-k}\|w\| + \sigma(z)\|z\|\,\|w\| + \tfrac{k\eta(z)}{1-k}\|w\| \\ &\leq -\eta(z) + \sigma(z)\|z\| \end{aligned} \tag{9.19}$$

However, there are subtleties with discontinuous controls and we will consider them fully in the next chapter.

Remark 9.8. The second term in the uncertainty bounding condition (9.12) can be interpreted in the following way. Suppose that both the nominal system

$$\dot{x} = f(x) + G(x)u$$

and the actual (perturbed) system

$$\dot{x} = (f(x) + \varphi(x)) + (G(x) + \mu(x))u$$

are both exactly feedback linearizable. Then, they are respectively reducible to the normal forms

$$\dot{\hat{z}} = A\hat{z} + E\left[\hat{\alpha}(\hat{z}) + \hat{\rho}(\hat{z})u\right]$$

and

$$\dot{z} = Az + E\left[\alpha(z) + \rho(z)u\right]$$

The feedback linearizing control for the nominal system is $u = \hat{\rho}^{-1}\left[-\hat{\alpha} + v\right]$. Using this control, the perturbed system can be expressed

$$\begin{aligned}\dot{z} &= Az + E\left[\alpha + \rho\left(\hat{\rho}^{-1}\left[-\hat{\alpha} + v\right]\right)\right] \\ &= Az + E\left[v + \left(\alpha - \rho\hat{\rho}^{-1}\hat{\alpha} + \rho\hat{\rho}^{-1}v - v\right)\right]\end{aligned}$$

In the nominal case, $\hat{\rho} = \rho$, $\hat{\alpha} = \alpha$, the equation reduces to

$$\dot{z} = Az + Ev$$

As a result, we identify

$$\Delta(z, v) = \alpha - \rho\hat{\rho}^{-1}\hat{\alpha} + \left[\rho\hat{\rho}^{-1} - I\right]v$$

Now choose $v = v^* + \mu$, $v^* = Kz$ so that

$$\Delta(z, v^* + \mu) = \alpha - \rho\hat{\rho}^{-1}\hat{\alpha} + \left[\rho\hat{\rho}^{-1} - I\right]Kz + \left[\rho\hat{\rho}^{-1} - I\right]\mu$$

Thus,

$$\|\Delta(z, v^* + \mu)\| \leq \left\|\alpha - \rho\hat{\rho}^{-1}\hat{\alpha} + \left[\rho\hat{\rho}^{-1} - I\right]Kz\right\| + \left\|\left[\rho\hat{\rho}^{-1} - I\right]\right\| \|\mu\|$$

The requirement $0 \leq k < 1$ implies

$$0 \leq \left\|\left[\rho\hat{\rho}^{-1} - I\right]\right\| < 1$$

Consequently, there is a specific limit on the tolerable variation of the control gain matrix.

Example 9.9 (Linearization with Matched Uncertainty). This simple example illustrates the effectiveness of robust feedback linearization. Consider the system:

$$\begin{bmatrix}\dot{x}_1 \\ \dot{x}_2\end{bmatrix} = \begin{bmatrix}x_2 \\ -0.1x_2 + x_1^3/2\end{bmatrix} + \begin{bmatrix}0 \\ 1\end{bmatrix}\{u + \underbrace{\kappa x_1^3 + au}_{\textit{uncertainty}}\}$$

The parameters $\kappa \in [0, 1]$ and $a \in [-0.1, 0.1]$ are uncertain. We will design a stabilizing feedback control for the nominal system using feedback linearization. Then we will make it robust via Lyapunov redesign and evaluate performance of both controllers when the system is subject to a perturbation.

First, enter the system definition, and design the nominal system.

```
In[204]:= f0 = {x2, -0.1  x2  + x1 + x1^3/2};
          g0 = {0, 1};
          f1 = {0,  kap  x1^3} ;
          g1 = {0, a};
          x = {x1, x2};

In[205]:= alpha0 = -0.1  x2  + x1  + x1^3/2;
          alpha1 = alpha0 + kap  x1^3;
          rho0 = 1;
          rho1 = rho0 + a;
          K = {-1, -2};
          ustar = (1/rho0)  (-alpha0 + K.x);
```

Now, turn to the redesign process.

```
In[206]:= A = {{0, 1}, {-1, -2}}; Q = 2  IdentityMatrix[2];
          P = LyapunovEquation[A, Q];
```

A bound for the uncertainty needs to be established in order to define the robustifying control component, μ, and assemble the control, u.

```
In[207]:= Del1 = Chop[Simplify[alpha1 - (rho1/rho0)  alpha0 + (rho1/rho0 - 1)  K.x]]

          Del2 = (rho1/rho0 - 1);

Out[207]= kap  x1^3 + a  (-2  x1 - x1^3/2 - 1.9  x2)
```

```
In[208]:= AA = Chop[Coefficient[Del1, {x1, x2, x1^3}]];
          sig2 =
            Simplify[(AA[[1]] + AA[[3]]  x1^2)^2 + AA[[2]]^2]/.{a → -0.1, kap → 1};
          μ = -(1 + (sig2/4)(1/(1 - 0.1))  ){0, 1}.P.x;
          u = Simplify[ustar + μ];
Out[208]= -3.02114  x1 - 0.616667  x1^3 - 0.30625  x1^5 - 2.92114  x2 - 0.116667  x1^2  x2 -
            0.30625  x1^4  x2
```

Now, the equations can be assembled and computations performed. First, the redesigned control is applied to the nominal system.

```
In[209]:= ReplacementRules = Inner[Rule, {x1, x2}, {x1[t], x2[t]}, List];
          Eqns = Chop[MakeODEs[{x1, x2}, f0 + f1 + (g0 + g1)  u, t]]/.{a → 0, kap → 0};
          InitialConds = {x1[0] == 1.5, x2[0] == 0};
          VSsols  =  NDSolve[Join[Eqns, InitialConds], {x1[t], x2[t]}, {t, 0, 10},
              AccuracyGoal → 2, PrecisionGoal-> 1, MaxStepSize-> 10/60000,
              MaxSteps → 60000];
```

```
In[210]:= Plot[Evaluate[{x1[t]} /. VSsols],
            {t,0,10},PlotRange->All,AxesLabel->{t,x1}];
          Plot[Evaluate[{x2[t]} /. VSsols],
            {t,0,  10},PlotRange->All,AxesLabel->{t,x2}];
```

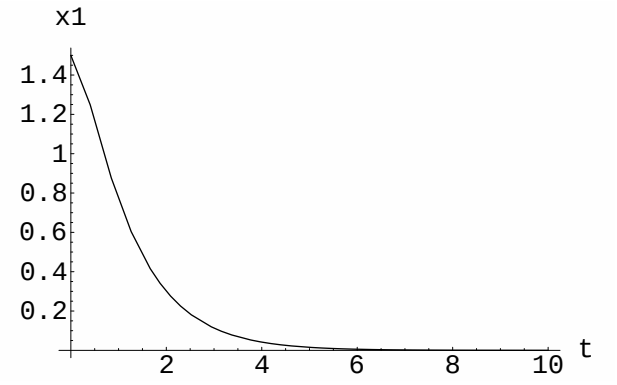

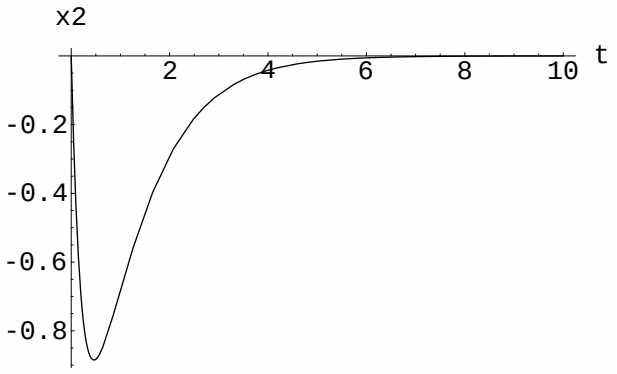

Now apply the control to a perturbed system.

```
In[211]:= Eqns =
            Chop[MakeODEs[{x1,x2},f0+f1+(g0+g1)  u,t]]/.{a->-0.1,kap->1};
          InitialConds = {x1[0]==1.5,x2[0]==0};
          VSsols  =  NDSolve[Join[Eqns,InitialConds],{x1[t],x2[t]},{t,0,10},
              AccuracyGoal->2,PrecisionGoal->1,MaxStepSize->10/60000,
              MaxSteps->60000];
```

```
In[212]:= Plot[Evaluate[{x1[t]} /. VSsols],
            {t,0,10},PlotRange->All,AxesLabel->{t,x1}];
          Plot[Evaluate[{x2[t]} /. VSsols],
            {t,0,  10},PlotRange->All,AxesLabel->{t,x2}];
```

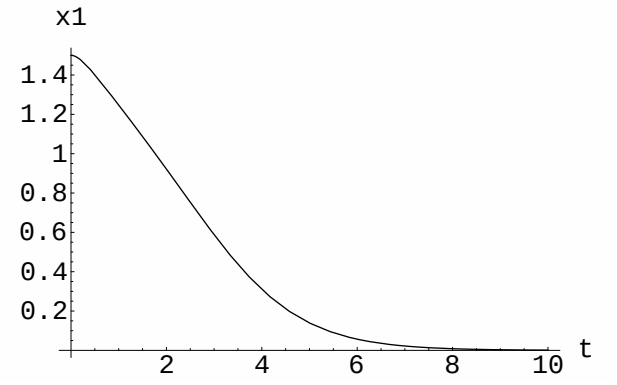

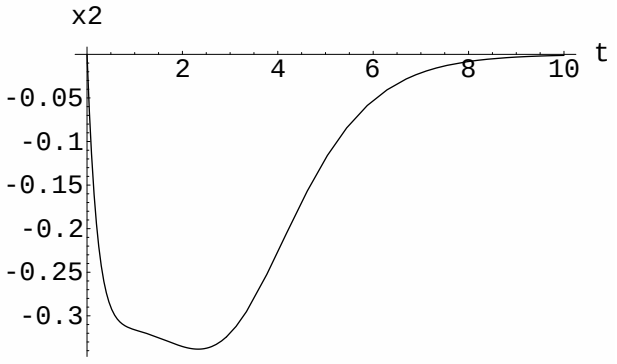

Notice that there is performance degradation but the system remains stable. For comparison, let us apply the nominal control to the perturbed system.

```
In[213]:= Eqns =
            Chop[MakeODEs[{x1, x2}, f0 + f1 + (g0 + g1)  ustar, t]] /. {a → −0.1, kap → 1};
          InitialConds = {x1[0] == 1.5, x2[0] == 0};
          VSsols  =  NDSolve[Join[Eqns, InitialConds], {x1[t], x2[t]}, {t, 0, 1.55},
              AccuracyGoal → 2, PrecisionGoal− > 1, MaxStepSize− > 1.55/60000,
              MaxSteps → 60000];

In[214]:= Plot[Evaluate[{x1[t]}  /.  VSsols],
            {t, 0, 1.5}, PlotRange− > All, AxesLabel → {t, x1}];
          Plot[Evaluate[{x2[t]}  /.  VSsols],
            {t, 0,  1.5}, PlotRange− > All, AxesLabel → {t, x2}];
```

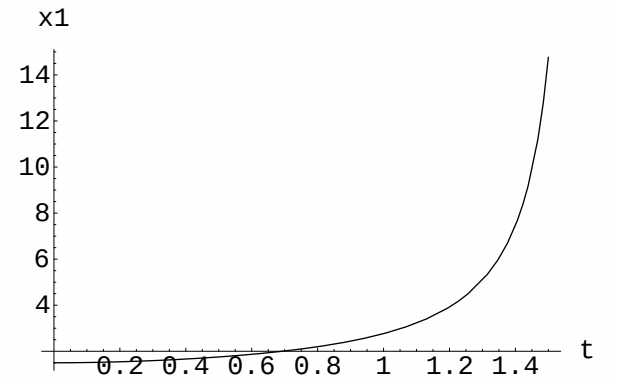

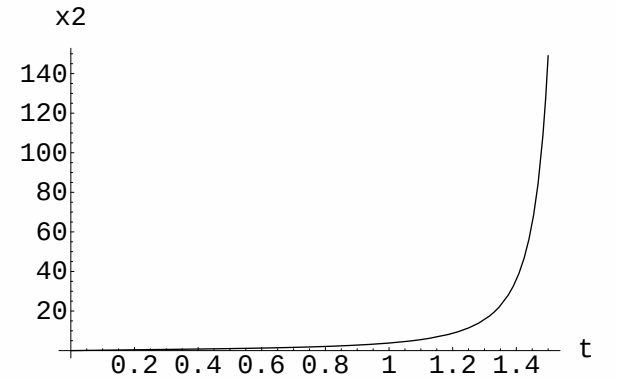

Clearly, the system is unstable – the feedback linearizing control without redesign can not cope with the perturbation.

9.4 Robust Stabilization via Backstepping

When a system involves nonmatched uncertainty, a backstepping procedure might be appropriate. We will describe such an approach to the design of a robust stabilizing controller for SISO systems that satisfy the triangularity conditions. Backstepping will be revisited below for the design of adaptive and variable structure controllers.

Suppose that nominal part (f,g,h) of the system (9.1) has relative degree $r = n$ (alternatively, (f,g) is exactly feedback linearizable) around the origin, and that the strict triangularity condition applies. Moreover, suppose that $\varphi(0,t) = 0$ and $|\varphi(x,t)| \leq \hat{\sigma}(x)\|x\|$ $\forall t$. It follows from Proposition (9.2) that we may as well begin with the triangular form

$$\begin{aligned} \dot{x}_i &= x_{i+1} + \Delta_i(x_1,\ldots,x_i,t), \quad 1 \leq i \leq n-1 \\ \dot{x}_n &= \alpha(x) + \rho(x)u + \Delta_n(x,t) \end{aligned} \tag{9.20}$$

with $\det\rho(x) \neq 0$ at least around the origin, $\Delta(0,t) = 0$ and $|\Delta_i(x,t)| \leq \sigma_i(x)\|x\|$, for some smooth bounding function $\sigma_i(x) \geq 0$. An uncertainty vector $\Delta(x,t)$ that satisifies these two conditions along with the triangular structure exhibited in (9.20) will be called *admissible*. The *robust stabilization problem* is to design a state feedback control such that the origin $x = 0$ is asymptotically stable for every admissible uncertainty.

Now, we design the control sequentially. At each of n steps we design a 'psuedo-control' v_k. At the k^{th} step we consider the system (with $v_0 = 0$)

$$\begin{aligned} \dot{x}_i &= x_{i+1} + \Delta_i(x_1,\ldots,x_i,t), \quad 1 \leq i \leq k-1 \\ \dot{x}_k &= v_k + \Delta_k(x_1,\ldots,x_k,t) \\ y_k &= x_k - v_{k-1}(x_1,\ldots,x_{k-1}) \end{aligned} \tag{9.21}$$

and choose a control v_k to stabilize the input-output behavior (drive $y_k \to 0$ for all initial conditions and all admissible uncertainties). Finally, the actual control u is defined by $u = \rho^{-1}(-\alpha + v_n)$. The process proceeds as follows.

1. $k = 1$ At the first step we have

$$\begin{aligned} \dot{x}_1 &= v_1 + \Delta_1(x_1,t) \\ y_1 &= x_1 \end{aligned} \tag{9.22}$$

Notice that we can write Equation (9.22)

$$\dot{y}_1 = v_1 + y_1\bar{\Delta}_1(y_1,t) := f_1(y_1) \tag{9.23}$$

Now, consider the function

$$V_1 = \tfrac{1}{2}y_1^2$$

and compute it's derivative along trajectories of Equation (9.23).

$$L_{f_1}V_1 = y_1\left(v_1 + \Delta_1(y_1,t)\right)$$

Choose $v_1 = -k_1y_1 - y_1\kappa_1(y_1)$ which yields

$$L_{f_1}V_1 = -k_1y_1^2 - \kappa_1(y_1)y_1^2 + y_1\bar{\Delta_1}$$

Now take $\kappa_1(y_1) > \frac{1}{4}\sigma_1^2(x_1)$ for $x_1 \neq 0$. This insures that

$$\begin{aligned} L_{f_1}V_1 &\leq -(k_1-1)y_1^2 - \left(y_1^2\tfrac{1}{4}\sigma_1^2 + y_1^2\right) \\ &\leq -(k_1-1)y_1^2 - \left(y_1^2\tfrac{1}{4}\sigma_1^2 - \sigma_1y_1^2 + y_1^2\right) \\ &\leq -(k_1-1)y_1^2 - \left(\tfrac{1}{2}\sigma_1\left|y_1\right| - \left|y_1\right|\right)^2 \\ &\leq -(k_1-1)y_1^2 \end{aligned}$$

is negative definite (provided $k_1 > 1$) so that the origin $x_1 = 0$ is asymptotically stable.

2. k=2 Now consider the system

$$\begin{aligned} \dot{x}_1 &= x_2 + \Delta_1(x_1,t) \\ \dot{x}_2 &= v_2 + \Delta_2(x_1,x_2,t) \\ y_2 &= x_2 - v_1(x_1) \end{aligned} \tag{9.24}$$

Consider the coordinate change $(x_1,x_2) \mapsto (y_1,y_2)$ and compute

$$\dot{y}_2 = v_2 + \Delta_2(x_1,x_2,t) - \frac{\partial v_1}{\partial x_1}\left(x_2 + \Delta_1(x_1,t)\right) := v_2 + \bar{\Delta_2}(y_1,y_2,t)$$

The differential equations (9.24) in the new coordinates are

$$\begin{aligned} \dot{y}_1 &= v_1(y_1) + y_2 + \Delta_1(y_1,t) \\ \dot{y}_2 &= v_2 + \Delta_2(y_1,y_2,t) \end{aligned} := f_2(y_1,y_2) \tag{9.25}$$

Notice that the derivative of V_1 along trajectories of Equation (9.25) is

$$L_{f_2}V_1 = y_1(v_1 + y_2 + \bar{\Delta_1}) = L_{f_1}V_1 + y_1y_2$$

Define the function

$$V_2 = V_1 + \tfrac{1}{2}y_2^2$$

and compute

$$\begin{aligned} L_{f_2}V_2 &= L_{f_1}V_1 + y_1y_2 + y_2(v_2 + \bar{\Delta_2}) \\ &= L_{f_1}V_1 + y_2\left(y_1 + v_2 + \bar{\Delta_2}\right) \end{aligned}$$

Now, set $v_2 = -y_1 - k_2y_2 - y_2\kappa_2(y_1,y_2)$ so that

$$\begin{aligned} L_{f_2}V_2 &= L_{f_1}V_1 - k_2y_2^2 - y_2^2\kappa_2(y_1,y_2) + y_2\bar{\Delta}_2 \\ &\le -(k_1-1)y_1^2 - k_2y_2^2 - y_2^2\kappa_2(y_1,y_2) + |y_2|\,\|Y_2\|\,\bar{\sigma}_2(y_1,y_2) \\ &\le -(k_1-2)y_1^2 - (k_2-1)y_2^2 - y_2^2\kappa_2(y_1,y_2) \\ &\qquad + |y_2|\,\|Y_2\|\,\bar{\sigma}_2(y_1,y_2) - \|Y_2\|^2 \\ &\le -(k_1-2)y_1^2 - (k_2-1)y_2^2 - \left(\tfrac{1}{2}|y_2|\,\bar{\sigma}_2(Y_2) - \|Y_2\|\right)^2 \\ &\le -(k_1-2)y_1^2 - (k_2-1)y_2^2 \end{aligned} \tag{9.26}$$

3. $k = 3\ldots n$ We continue in the same fashion. Suppose we have completed i steps ($i = 1,\ldots,n-1$). So, we have already defined the new states $y_1,\ldots,y_i$ and psuedo controls $v_1,\ldots,v_i$ and the functions

$$V_j = V_{j-1} + \tfrac{1}{2}y_j^2, \quad 1 \le j \le i$$

Now, we wish to compute v_{i+1}. Define $y_{i+1} = x_{i+1} - v_i$, and organize the equations

$$\begin{aligned} \dot{y}_j &= v_j(Y_j) + y_{j+1} + \bar{\Delta}(Y_j,t), \quad 1 \le j \le i \\ \dot{y}_{i+1} &= v_{i+1} + \Delta(Y_{i+1},t) \end{aligned} := f_{i+1} \tag{9.27}$$

As above, we have

$$L_{f_{i=1}}V_i = L_{f_i}V_i + y_iy_{i+1}$$

so that

$$L_{f_{i+1}}V_{i+1} = L_{f_i}V_i - y_{i+1}\left(y_i + v_{i+1} + \bar{\Delta}_{i+1}(Y_{i+1},t)\right)$$

Choose $v_{i+1} = -y_i - k_{i+1}y_{i+1} - y_{i+1}\kappa_{i+1}$ and $\kappa_{i+1}(Y_{i+1}) > \frac{1}{4}\bar{\sigma}_{i+1}^2(Y_{i+1})$ to obtain

$$\begin{aligned} L_{f_{i+1}}V_{i+1} &\le -\sum_{j=1}^{i+1}(k_j - (i+2-j))y_j^2 - y_{i+1}^2\kappa_{i+1} \\ &\qquad + |y_{i+1}|\,\|Y_{i+1}\|\,\bar{\sigma}_{i+1}(Y_{i+1}) - \|Y_{i+1}\|^2 \\ &\le -\sum_{j=1}^{i+1}(k_j - (i+2-j))y_j^2 - \left(\tfrac{1}{2}|y_{i+1}|\,\bar{\sigma}_{i+1}(Y_{i+1}) - \|Y_{i+1}\|\right)^2 \\ &\le -\sum_{j=1}^{i+1}(k_j - (i+2-j))y_j^2 \end{aligned} \tag{9.28}$$

These calculations establish the following proposition.

Proposition 9.10 (Smooth Robust Stabilization). *Consider the system (9.1) and suppose*

1. *the nominal system (f,g) is exactly feedback linearizable,*
2. *the strict trangularity condition is true,*
3. *the uncertainty satisfies the conditions: $\varphi(0,t) = 0$ and $|\varphi(x,t)| \le \hat{\sigma}(x)\,\|x\|\ \forall t$.*

Then there exists a smooth state feedback controller such that the origin, $x = 0$, is asymptotically stable for all admissible uncertainties $\varphi(x,t)$.

Proof: Apply the nominal system normal form transformation to the actual uncertain system and follow the construction of Equations (9.20) through (9.28) to obtain

$$L_{f_n} V_n \leq \sum_{j=1}^{n} (k_j - n - 1 + j) y_j^2$$

Notice that we need to choose $k_j > n+1-j$, $j = 1, \ldots, n$. ■

9.5 Adaptive Control of Linearizable Systems

The essential idea is easy to develop. Consider a parameter dependent system reduced to local regular form:

$$\dot{\xi} = F(\xi, z, \vartheta) \tag{9.29}$$

$$\dot{z} = Az + E[\alpha(x, \vartheta) + \rho(x, \vartheta)u] \tag{9.30}$$

$$y = Cz \tag{9.31}$$

Here A, E, C are of the special Brunovsky form as indicated in Section 6.5 and independent of all system parameters. Now, suppose that the control u is different from the ideal decoupling control, $u^* = \rho^{-1}\{-\alpha + v\}$, because it is based on current estimates of the uncertain parameters:

$$u = \rho(x, \hat{\vartheta})^{-1}\{-\alpha(x, \hat{\vartheta}) + v\} \tag{9.32}$$

equivalently,

$$\alpha(x, \hat{\vartheta}) + \rho(x, \hat{\vartheta})u = v$$

Then we can compute

$$\dot{z} = Az + E[\alpha(x, \vartheta) + \rho(x, \vartheta)u] \tag{9.33}$$

$$\dot{z} = Az + E[v + \Delta] \tag{9.34}$$

where

$$\Delta = [\alpha(x, \vartheta) + \rho(x, \vartheta)u] - [\alpha(x, \hat{\vartheta}) + \rho(x, \hat{\vartheta})u] \tag{9.35}$$

Assumption 1:

$\Delta(\xi, z, \hat{\vartheta}, \vartheta, u)$ is linear in the parameter estimation error, i.e.,

$$\Delta(\xi, z, \hat{\vartheta}, \vartheta, u) = \Psi(\xi, z, \hat{\vartheta}, u)(\vartheta - \hat{\vartheta}) \tag{9.36}$$

Thus, we have the

$$\dot{\xi} = F(\xi, z, \vartheta) \tag{9.37}$$

$$\dot{z} = A_c z + E\Psi(\vartheta - \hat{\vartheta}) \tag{9.38}$$

We are in a position to employ the standard Lyapunov argument to derive an update law for the parameter estimate.

Proposition 9.11. *Asymptotic output stabilization, $y \to 0$, is achieved with the parameter estimator*

$$\dot{\hat{\vartheta}} = Q\Psi^T(\xi, z, \hat{v}, u)E^T Pz$$

where P is a symmetric, positive definite solution of

$$(A+EK)^T P + P(A+EK) = -I$$

and Q is any symmetric positive definite matrix.

Proof: Choose a candidate Lyapunov function

$$V = z^T Pz + (\vartheta - \hat{\vartheta})^T Q^{-1}(\vartheta - \hat{\vartheta})$$

Differentiate with respect to time to obtain

$$\begin{aligned}
\dot{V} &= 2z^T P\dot{z} - 2\dot{\hat{\vartheta}}^T Q^{-1}(\vartheta - \hat{\vartheta}) \\
&= 2z^T P(A_c z + E\Psi(\vartheta - \hat{\vartheta})) - 2\dot{\hat{\vartheta}}^T Q^{-1}(\vartheta - \hat{\vartheta}) \\
&= 2z^T PA_c z + 2(z^T PE\Psi - \dot{\hat{\vartheta}}^T Q^{-1})(\vartheta - \hat{\vartheta}) \\
&= z^T(PA_c + A_c^T P)z + 2(z^T PE\Psi - \dot{\hat{\vartheta}}^T Q^{-1})(\vartheta - \hat{\vartheta})
\end{aligned}$$

The assumptions reduce this to

$$\dot{V} = -z^T z$$

■

There are many variants of this basic construction. One model reference adaptive control configuration is illustrated in Figure (9.1). The key point is that the input–output linearizing and decoupling control absorbs all of the parameter dependencies so that only this part of the control law has to be adjusted.

Remark 9.12. The regressor $\Psi(\xi, z, \hat{\vartheta}, u)$ is particularly easy to compute if $\alpha(x, \vartheta)$ and $\rho(x, \vartheta)u$ are linear in the uncertain parameters:

$$\alpha(x, \vartheta) = \alpha_0(x) + \tilde{\alpha}(x)\vartheta$$

$$\rho(x, \vartheta)u = \rho_0(x, u) + \tilde{\rho}(x, u)\vartheta$$

Then

$$\Delta = \{\tilde{\alpha}(x) + \tilde{\rho}(x, u)\}(\vartheta - \hat{\vartheta}),$$

and

$$\Psi = \{\tilde{\alpha}(x) + \tilde{\rho}(x, u)\}$$

In the implementation of the controller illustrated in Figure (9.1), it is necessary to measure or estimate both x and z. Notice that z can not be computed from the normal coordinate relations $z(x, \vartheta)$ because they now depend on the unknown parameter ϑ.

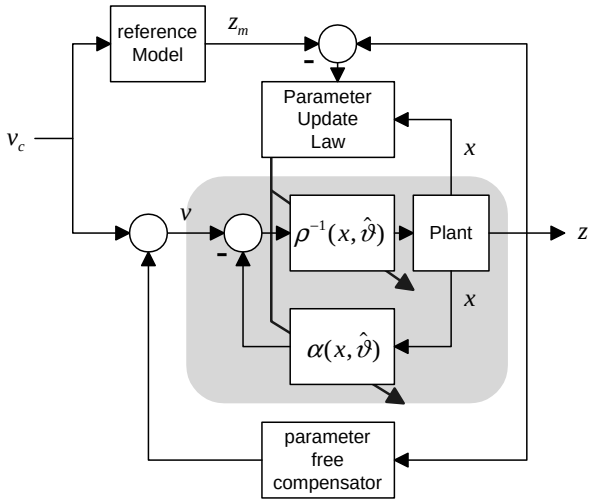

Fig. 9.1: A model reference, adaptive tracking control configuration based on decoupling control.

Example 9.13 (Adaptive Regulator). We will illustrate adaptive regulation using the following example adapted from Isidori [46]:

$$\begin{bmatrix} \dot{x}_1 \\ \dot{x}_2 \\ \dot{x}_3 \end{bmatrix} = \begin{bmatrix} 0 \\ x_1 + x_2^2 \\ \theta x_1 - x_2 \end{bmatrix} + \begin{bmatrix} e^{x_2} \\ e^{x_2} \\ 0 \end{bmatrix} u$$
$$y = x_3$$

We need to specify the desired closed loop pole locations. It is necessary to do this in groups according to the vector relative degree. So we first compute the vector relative degree and then use the function `AdaptiveRegulator`. Here are the computations.

```
In[215]:= var32 := {x1, x2, x3};
          f32 := {0, x1 + x2^2, θ * x1 - x2};
          g32 := {Exp[x2], Exp[x2], 0};
          h32 := {x3};
          ro = VectorRelativeOrder[f32, g32, h32, var32]
Out[215]= {2}

In[216]:= Poles = {{-2, -2}};
          {Parameters, ParameterEstimates, UpdateLaw, Control} =
            AdaptiveRegulator[f32, g32, h32, var32, t, {θ}, {}, Poles]

Computing Decoupling Matrix
```

```
Computing linearizing/decoupling control

Finished Linearizing Control
```
NewParameters $= \{\theta\}$

```
Finished Stabilizing Control

Finished Stabilizing Control

Finished regressor computation

Finished Lyapunov Equation

Finished parameter update law
```

$$\texttt{Out[216]=}\ \Big\{\{\theta\},\{\text{thetahat1}\},\Big\{\frac{125.\ \ \text{AdaptGain1}\ \ \text{e}^{\text{x2}}\ \ \text{z1}\ \ (\text{x1}+\text{x2}^2-4\ \ \text{z1}-4\ \ \text{z2})}{-\text{e}^{\text{x2}}+\text{e}^{\text{x2}}\ \ \text{thetahat1}}+ \frac{156.25\ \ \text{AdaptGain1}\ \ \text{e}^{\text{x2}}\ \ (\text{x1}+\text{x2}^2-4\ \ \text{z1}-4\ \ \text{z2})\ \ \text{z2}}{-\text{e}^{\text{x2}}+\text{e}^{\text{x2}}\ \ \text{thetahat1}}\Big\}, \Big\{\frac{\text{x1}+\text{x2}^2-4\ \ \text{z1}-4\ \ \text{z2}}{-\text{e}^{\text{x2}}+\text{e}^{\text{x2}}\ \ \text{thetahat1}}\Big\}\Big\}$$

While this approach to adaptive control has limitations, it does have its place in applications. See, for example, [8, 7].

We can provide a modest but useful generalization of the above result. Once again, consider a parameter dependent system reduced to local regular form:

$$\begin{aligned}\dot{\xi} &= F(\xi, z, \vartheta)\\ \dot{z} &= Az + E\left[\alpha(x,\vartheta) + \rho(x,\vartheta)\,\phi(u,\vartheta)\right]\\ y &= Cz\end{aligned} \tag{9.39}$$

Here matrices A, E, C are of the special Brunovsky form and independent of all system parameters; $\alpha : R^{n\times p} \to R^m$, $\rho : R^{n\times p} \to R^{m\times m}$ and $\phi : R^{n\times p} \to R^m$ are piecewise smooth in x and continuous in the parameter ϑ; for each admissible ϑ, and the map ϕ has a piecewise smooth inverse $\phi^{-1}(\cdot,\vartheta)$. The inclusion of the map ϕ allows us to treat systems with certain types of control saturation, backlash and similar input nonlinearities (see [6]). If the parameter ϑ is known, it is possible to implement the ideal decoupling control law

$$u^* = \phi^{-1}\left(\rho^{-1}(x,\vartheta)\left(-\alpha(x,\vartheta)+v\right),\vartheta\right)$$

to obtain $\dot{z} = Az + Ev$. If the zero dynamics $\dot{\xi} = F(\xi, 0, \vartheta)$ are stable the control renders the loop stable. On the other hand, if the parameter ϑ is uncertain, then we can implement a control based on estimates of the parameter:

$$u = \phi^{-1}\left(\rho^{-1}\left(\hat{x},\hat{\vartheta}\right)\left(-\alpha\left(\hat{x},\hat{\vartheta}\right)+v\right),\hat{\vartheta}\right) \tag{9.40}$$

equivalently, u satisfies

$$\alpha\left(\hat{x},\hat{\vartheta}\right) + \rho\left(\hat{x},\hat{\vartheta}\right)\phi(u,\hat{\vartheta}) = v$$

In the present case we have

$$\dot{z} = Az + E[v + \Delta]$$

where

$$\Delta = [\alpha(x,\vartheta) + \rho(x,\vartheta)\phi(u,\vartheta)] - \left[\alpha(\hat{x},\hat{\vartheta}) + \rho(\hat{x},\hat{\vartheta})\phi(u,\hat{\vartheta})\right] \tag{9.41}$$

with $x = x(\xi, z, \vartheta)$ and $\hat{x} = x\left(\xi, z, \hat{\vartheta}\right)$. The following basic assumption replaces Assumption 1.

Assumption 2: The control error $\Delta\left(\xi, z, \vartheta, \hat{\vartheta}, u\right)$ has the form

$$\Delta\left(\xi, z, \vartheta, \hat{\vartheta}, u\right) = \Psi\left(\xi, z, \hat{\vartheta}, u\right)\left(\vartheta - \hat{\vartheta}\right) + \varphi_0\left(\xi, z, \vartheta, \hat{\vartheta}, u\right)$$

where φ_0 is a bounded, piecewise smooth function.

Assume, further, that upper and lower bounds, $\vartheta_{i_{\min}}, \vartheta_{i_{\max}}$, respectively, are known for each uncertain parameter ϑ_i. In conjunction with the control (9.40), we implement a parameter update rule:

$$\dot{\hat{\vartheta}} = \Omega\Psi^T\left(\xi, z, \hat{\vartheta}, u\right)E^T P z - \Omega\sigma\left(\hat{\vartheta}\right) \tag{9.42}$$

where $\Omega > 0$ is a (matrix) design parameter, P satisfies the Lyapunov equation

$$(A + EK)^T P + P(A + EK) = -Q, \quad Q > 0 \tag{9.43}$$

and the function $\sigma\left(\hat{\vartheta}\right)$ is defined by

$$\sigma(\hat{\vartheta}) = \left[\sigma_1(\hat{\vartheta}), \ldots, \sigma_p(\hat{\vartheta})\right]^T \tag{9.44}$$

$$\sigma_i\left(\hat{\vartheta}\right) := \begin{cases} \kappa_i & \hat{\vartheta}_i > \vartheta_{i_{\max}} \\ 0 & \vartheta_{i_{\min}} \le \hat{\vartheta}_i \le \vartheta_{i_{\max}} \\ -\kappa_i & \hat{\vartheta}_i < \vartheta_{i_{\min}} \end{cases} \quad \kappa_i > 0, \quad i = 1, \cdots, p \tag{9.45}$$

Remark 9.14 (Implementation). In order to implement the control (9.40) and (9.42), we require direct measurement or estimates of the system state in either the original coordinates x or the normal form coordinates (ξ, z). In many practical cases (ξ, z) are the natural coordinates for measurement. In fact, it is not uncommon with electromechanical systems for the components of z to be a subset of the original states x. In general if the measurements are (ξ, z), then when computing the regressor it is necessary to use the state transformation $\hat{x} = x\left(\xi, z, \hat{\vartheta}\right)$ in ρ and α. On the other hand, if x is the natural measurement and z needs to be computed from the parameter dependent state transformation, then it is necessary to proceed quite differently, i.e. via backstepping as described below.

The closed loop system that obtains when the control (9.40) with update law (9.42) is applied to the system (9.39) enjoys three basic properties:

1. the parameter trajectory $\hat{\vartheta}(t), t > 0$ is bounded,
2. the partial state trajectory $z(t), t > 0$, is bounded and enters a neighborhood of the origin whose size is proportional to the bound on φ_0,
3. under mild additional conditions $z(t), y(t) \to 0$ as $t \to \infty$.

Proposition 9.15 (Bounded states and parameter estimates). *Consider the closed loop system composed of the plant (9.39) and control (9.40)-(9.45). Suppose that Assumption 2 is satisfied. Then the partial state trajectory $z(t), t > 0$ and the parameter estimate $\hat{\vartheta}(t), t > 0$ are bounded. Furthermore, the state trajectory $z(t)$ eventually enters the disk*

$$D = \left\{ z \in R^r \;\middle|\; \left\| Q^{1/2} z - \mathbf{r} \right\|^2 \leq \|\mathbf{r}\|^2 \right\}$$

where $\mathbf{r} = \left(Q^{-1/2} PE\varphi_0 \right)_{\max}$.

Proof: : Choose a candidate Lyapunov function

$$V = z^T P z + (\vartheta - \hat{\vartheta})^T \Omega^{-1} (\vartheta - \hat{\vartheta}) \tag{9.46}$$

and compute

$$\dot{V} = -\left\| Q^{1/2} z - Q^{-1/2} PE\varphi_0 \right\|^2 + \left\| Q^{-1/2} PE\varphi_0 \right\|^2 + 2\left(z^T PE\Psi - \dot{\hat{\vartheta}}^T \Omega^{-1} \right)(\vartheta - \hat{\vartheta}) \tag{9.47}$$

$$\dot{V} = -\left\| Q^{1/2} z - Q^{-1/2} PE\varphi_0 \right\|^2 + \left\| Q^{-1/2} PE\varphi_0 \right\|^2 - \sigma(\hat{\vartheta})(\vartheta - \hat{\vartheta}) \tag{9.48}$$

which is clearly negative provided

$$\left\| Q^{1/2} z - Q^{-1/2} PE\varphi_0 \right\|^2 > \left\| Q^{-1/2} PE\varphi_0 \right\|^2 \tag{9.49}$$

For each fixed φ_0 this condition defines a circular disk in R^r (in the coordinates $Q^{1/2} z$) of radius $\left\| Q^{-1/2} PE\varphi_0 \right\|^2$ and centered at $Q^{-1/2} PE\varphi_0$. Since $\varphi 0$ is bounded there exists a largest disk (of maximum radius) that contains all others. This is the disk D. D lifts to a cylinder in the state space (R^{r+p}). $\dot{V} < 0$ outside of this cylinder. The minimum value of V ($V = 0$) occurs on its boundary. Hence all trajectories must reach a neighborhood of the cylinder in finite time. Since $z(t)$ is continuous for $t > 0$, it is bounded. In view of (9.48) we have

$$\dot{V} \leq \left\| Q^{-1/2} PE\varphi_0 \right\|_{\max}^2 - \sigma(\hat{\vartheta})(\vartheta - \hat{\vartheta}) \tag{9.50}$$

Thus, $\dot{V} < 0$ outside of the rectangular domain

$$\left[\vartheta_{i_{\min}} - \frac{\left\| Q^{-1/2} PE\varphi_0 \right\|_{\max}^2}{\kappa_i}, \vartheta_{i_{\max}} + \frac{\left\| Q^{-1/2} PE\varphi_0 \right\|_{\max}^2}{\kappa_i} \right], \quad i = 1, \ldots, p$$

So that $\hat{\vartheta}(t), t > 0$ is bounded. ■

Notice that we would like to insure that $\hat{\vartheta}(t)$ begins and remains in the parameter cube

$$C_{param} = \left\{ \vartheta \in R^p | \ \vartheta_{i_{\min}} \leq \hat{\vartheta} \leq \vartheta_{i_{\max}}, i = 1, \ldots, p \right\}$$

Since the estimate can always be initialized within the cube, it is desired to insure that trajectories beginning in the cube can not leave it. This is often done by simple projection. However, by choosing each κ_i sufficiently large we can guarantee that the parameter will remain within C_{param} so long as the state trajectory remains within any prespecified bound.

Define the sets

$$S_{ext} = \left\{ (z, \vartheta) \in R^{r+p} \left| \left\| Q^{1/2} z - Q^{-1/2} PE \varphi_0 \right\|^2 > \left\| Q^{-1/2} PE \varphi_0 \right\|^2 \right. \right\}$$

$$S_{int} = \left\{ (z, \vartheta) \in R^{r+p} \left| \left\| Q^{1/2} z - Q^{-1/2} PE \varphi_0 \right\|^2 < \left\| Q^{-1/2} PE \varphi_0 \right\|^2 \right. \right\}$$

Notice that S_{ext} and S_{int} share a common boundary that we denote $\partial S := \partial S_{ext} := \partial S_{int}$. ∂S includes points that satisfy

$$\left\| Q^{1/2} z - Q^{-1/2} PE \varphi_0 \right\|^2 = \left\| Q^{-1/2} PE \varphi_0 \right\|^2$$

as well as points at which φ_0 is undefined. Observe that all points with $z = 0$ belong to ∂S. With this notation we can state the second key result:

Proposition 9.16 (Output convergence). *Suppose Assumption 2 is satisfied and, in addition: (i) the only invariant set of the closed loop system contained in ∂S corresponds to $z = 0$, (ii) all trajectories beginning in S_{int} with initial estimates in C_{param} remain in C_{param} while they are in S_{int}. Then all trajectories of the closed loop system beginning in C_{param} satisfy $z(t) \to 0$ (hence $y(t) \to 0$) as $t \to \infty$.*

Proof: Once again consider the Lyapunov function

$$V = z^T P z + (\vartheta - \hat{\vartheta})^T \Omega^{-1} (\vartheta - \hat{\vartheta})$$

Along closed loop trajectories we have

$$\dot{V} = - \left\| Q^{1/2} z - Q^{-1/2} PE \varphi_0 \right\|^2 + \left\| Q^{-1/2} PE \varphi_0 \right\|^2 - \sigma(\hat{\vartheta})(\vartheta - \hat{\vartheta})$$

Thus, $\dot{V} < 0$ on S_{ext} and $\dot{V} > 0$ along all trajectories in S_{int} that begin in C_{param}. Furthermore, $\inf_{(z,\vartheta) \in S_{ext}} V(z, \vartheta)$ occurs on ∂S so that trajectories beginning in S_{ext} eventually reach ∂S. Similarly, for each fixed $\hat{\vartheta}$, say $\hat{\vartheta} = \hat{\vartheta}^*$, $\sup_{(z,\hat{\vartheta}^*) \in S_{int}} V(z, \hat{\vartheta}^*)$ occurs on ∂S. Consequently, trajectories beginning in S_{int} with initial estimates in C_{param} also reach ∂S. By assumption, the only invariant set in ∂S corresponds to $z = 0$, so all trajectories beginning in C_{param} tend to $z = 0$. ■

Example 9.17 (Example (9.9) Revisited). Let us reconsider the uncertain system of example (9.9). Previously we designed a controller using the Lyapunov redesign approach. For comparison, we now design an adaptive controller. First, the data:

```
In[217]:= f0 = {x2, -0.1  x2  + x1 + x1^3/2}; g0 = {0, 1};
          f1 = {0,  kap  x1^3}  ; (*  0 < kap < 1*)
          g1 = {0, a}; (*  -0.1 < a < 0.1*)
          x = {x1, x2};
          f = f0 + f1; g = g0 + g1; h = {x1};
```

Now, design the adaptive regulator.

```
In[218]:= Poles = {{-1, -2}};
          {Parameters, ParameterEstimates, UpdateLaw, Control} =
            AdaptiveRegulator[f, g, h, x, t, {a, kap}, {0.00002, 0.0005}, Poles];
```

```
Computing Decoupling Matrix

Computing linearizing/decoupling control

Finished Linearizing Control
NewParameters = {a, kap}

Finished Stabilizing Control

Finished regressor computation

Finished Lyapunov Equation

Finished parameter update law
```

We replace occurrences of transformed *z* variables with the measured *x* variables (in this example, the transformation is independent of the uncertain parameters) and add the parameter range limit switch to the update law.

```
In[219]:= u = Control/.{z1 → x1, z2 → x2}

          ULaw = (UpdateLaw/.{z1 → x1, z2 → x2}) -
              Sig[{thetahat1, thetahat2}, {10, 1}, {-0.1, 0}, {0.1, 1}];
```

For a baseline, simulate with perfectly known parameters.

```
In[220]:= Eqns = Chop[MakeODEs[{x1, x2, thetahat1, thetahat2},
                     Join[f + g  u[[1]], ULaw], t]]/.{a → 0, kap → 0};
          InitialConds =
            {x1[0] == 1.5, x2[0] == 0, thetahat1[0] == 0, thetahat2[0] == 0};
          VSsols  =  NDSolve[Join[Eqns, InitialConds], {x1[t], x2[t],
                thetahat1[t], thetahat2[t]}, {t, 0, 10}, AccuracyGoal → 2,
              PrecisionGoal -> 1, MaxStepSize -> 10/60000, MaxSteps → 60000];
```

```
In[221]:= Plot[Evaluate[{x1[t]} /. VSsols],
            {t,0,10},PlotRange->All,AxesLabel->{t,x1}];
          Plot[Evaluate[{x2[t]} /. VSsols],
            {t,0,  10},PlotRange->All,AxesLabel->{t,x2}];
```

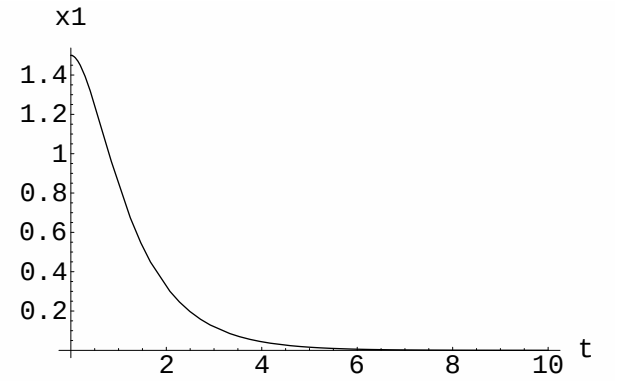

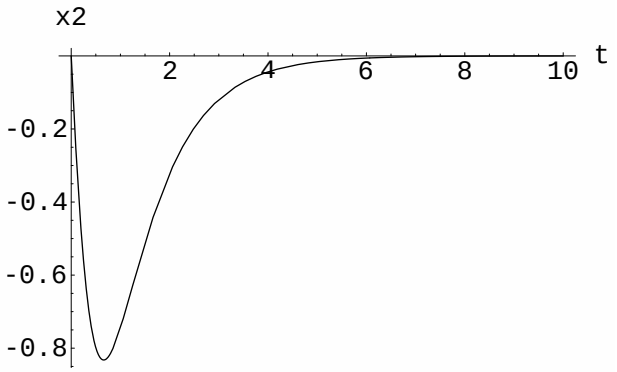

Now, suppose that the parameters are unknown.

```
In[222]:= Eqns = Chop[MakeODEs[{x1, x2, thetahat1, thetahat2},
                Join[f + g u[[1]], ULaw], t]] /. {a → -0.1, kap → 1};
          InitialConds =
            {x1[0] == 1.5, x2[0] == 0, thetahat1[0] == 0, thetahat2[0] == 0};
          VSsols = NDSolve[Join[Eqns, InitialConds], {x1[t], x2[t],
                thetahat1[t], thetahat2[t]}, {t, 0, 10}, AccuracyGoal → 2,
              PrecisionGoal -> 1, MaxStepSize -> 10/60000, MaxSteps → 60000];

In[223]:= Plot[Evaluate[{x1[t]} /. VSsols],
            {t, 0, 10}, PlotRange -> All, AxesLabel → {t, x1}];
          Plot[Evaluate[{x2[t]} /. VSsols],
            {t, 0,  10}, PlotRange -> All, AxesLabel → {t, x2}];
```

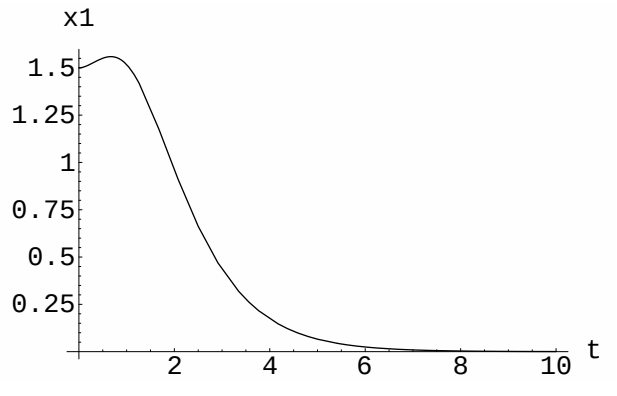

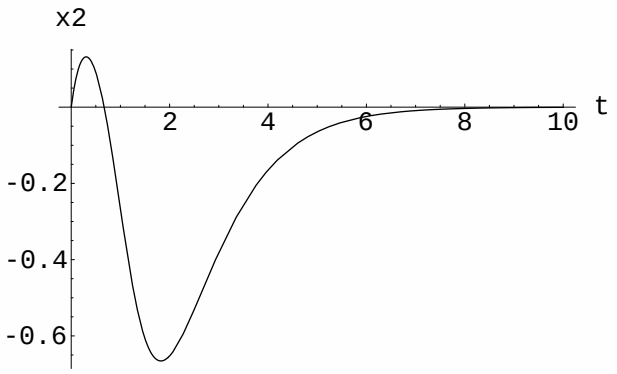

These results should be compared with trajectories in example (9.9).

The following figures illustrate the parameter estimates. Note that there is no guarantee that the estimates will converge to the true parameter values. It is only assured that

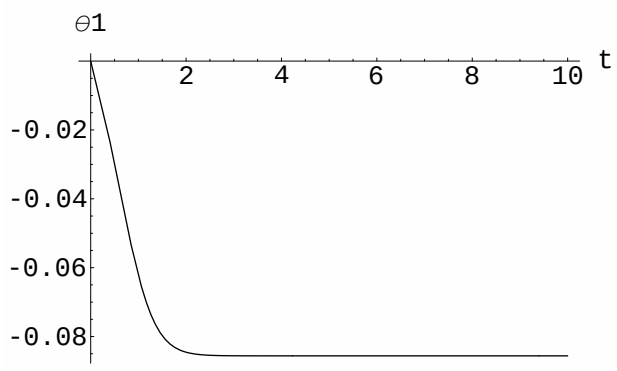

the loop is stable and that the states $z(t)$ converge to zero.

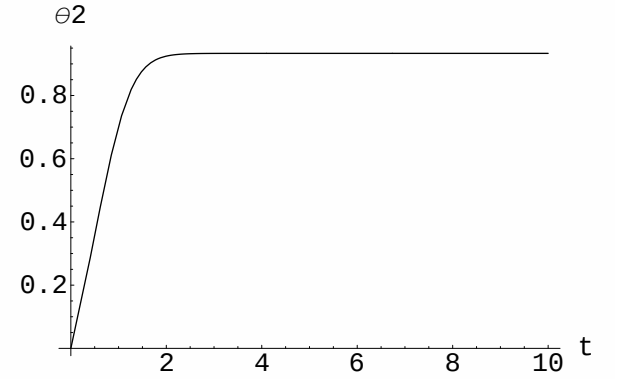

9.6 Adaptive Control via Backstepping

The adaptive control controllers discussed above require access to the full state, *x*, and the transformed partial state, *z*. Also, there is a constraint imposed on the uncertainty structure imposed by equation (9.36) - Assumption 1 - that cannot be validated *a priori*. Another approach to adaptive control design has been described in [51] by Kanellakopolis, Kokotovic and Morse that requires access only to the system state,

x, and characterizes the uncertainty constraint directly in terms of the way in which the parameters appear in the differential equations.

It is assumed that the single-input, feedback linearizable system is of the form

$$\dot{\zeta} = f(\zeta,\theta) + g(\zeta,\theta)u \tag{9.51}$$

where $\zeta \in R^n$ is the state, $u \in R$ is the control, and $\theta \in R^p$ is the uncertain parameter vector. Moreover, f, and g are linear in the parameters:

$$f(\zeta,\theta) = f_0(\zeta) + \sum_{i=1}^{p} \theta_i f_i(\zeta), \quad g(\zeta,\theta) = g_0(\zeta) + \sum_{i=1}^{p} \theta_i g_i(\zeta) \tag{9.52}$$

and $f_i(\zeta), g_i(\zeta), 0 \le i \le p$ are smooth vector fields in a neighborhood of the origin $\zeta = 0$ with $f_i(0) = 0, 0 \le i \le p$ and $g_0(0) \neq 0$. A fundamental assumption is that there exists a parameter-independent diffeomorphism $x = \phi(\zeta)$ that transforms the system into *parametric-pure-feedback form*:

$$\begin{aligned} \dot{x}_i &= x_{i+1} + \theta^T \gamma_i(x_1,\ldots,x_{i+1}), \;\; 1 \le i \le n-1 \\ \dot{x}_n &= \gamma_0(x) + \theta^T \gamma_n(x) + [\beta_0(x) + \theta^T \beta(x)]u \end{aligned} \tag{9.53}$$

with

$$\gamma_i(0) = 0, \;\; 1 \le i \le n \;\text{ and }\; \beta_0(0) \neq 0 \tag{9.54}$$

Necessary and sufficient conditions for such a transformation are given in the following proposition from [51, 56].

Proposition 9.18. *A diffeomorphism $x = \phi(\zeta)$ with $\phi(0) = 0$, transforming (9.51) and (9.52) into (9.53) and (9.54) exists in a neighborhood $B_x \subset U$ of the origin if and only if the following conditions are satisfied in U.*

i) Feedback Linearization Condition: The Distributions

$$\mathscr{G}_i = span\{g_0, ad_{f_0}g_0, \ldots, ad_{f_0}^i\}$$

are involutive and of constant rank $i+1$.

ii) Parametric-Pure-Feedback Condition:

$$g_i \in \mathscr{G}_0$$

$$[X, f_i] \in \mathscr{G}_{j+1}, \forall X \in \mathscr{G}_j, 0 \le j \le n-3, 1 \le i \le p$$

Conditions i) and ii) can be restated in more compact form:

i) $\mathscr{G}_{n-2}$ is involutive, and $\mathscr{G}_{n-1}$ has constant rank n.

ii) $[ad_{f_0}^j g_0, f_i] \in \mathscr{G}_{j+1}, 0 \le j \le n-3, 1 \le i \le p$

A special case of the parametric-pure-feedback form is the so-called *parametric-strict-feedback* form. The system (9.51) and (9.52) is of the parametric-strict-feedback type if it is diffeomorphically equivalent to:

$$\dot{x}_i = x_{i+1} + \theta^T \gamma_i(x_1, \ldots, x_i), \;\; 1 \le i \le n-1$$

$$\dot{x}_n = \gamma_0(x) + \theta^T \gamma_n(x) + \beta_0(x)u \tag{9.55}$$

Necessary and sufficient conditions for the existence of the required diffeomorphism are given by the following proposition [51].

Proposition 9.19. *Suppose there exists a global diffeomorphism, $x = \phi(\zeta)$ with $\phi(0) = 0$, that transforms the (nominal) system*

$$\dot{\zeta} = f_0(\zeta) + g_0(\zeta)u$$

into

$$\dot{x}_i = x_{i+1}, \; 1 \le i \le n-1$$

$$\dot{x}_n = \gamma_0(x) + \beta_0(x)u$$

with $\gamma_0(0) = 0$ and $\beta_0(x) \neq 0, \forall x \in R^n$. Then the system (9.51) and (9.52) is globally diffeomorphically equivalent to (9.55) if and only if the following conditions hold:

(i) $g_i \equiv 0$

(ii) $[X, f_i] \in \mathscr{G}_{j+1}, \forall X \in \mathscr{G}_j, 0 \le j \le n-2, 1 \le i \le p$

The backstepping procedure for adaptive control design is given [51, 56]. We will summarize the constructions for the simpler case of parametric-strict-feedback form in order to explain the basic ideas. More details can be obtained from [51, 56] and their references. Suppose the system has been reduced to parametric-strict-feedback form, (9.55). Then the backstepping procedure sequentially generates:

(i) a (parameter-dependent) state transformation to new coordinates z, $z = z(x, \hat{\theta})$,

(ii) a feedback control law $u = u(x, \hat{\theta})$,

(iii) a parameter update law $\dot{\hat{\theta}} = \tau(x, \hat{\theta})$

When the state transformation and feedback control are applied, the closed loop equations in the z-coordinates have the form

$$\dot{z} = \left[\text{diag}(-c_1, \ldots, -c_n) + \Phi(z, \hat{\theta})\right] z + \Psi(z, \hat{\theta})\tilde{\theta}$$

where $\Phi(z, \hat{\theta})$ is an antisymmetric matrix, i.e., $\Phi^T(z, \hat{\theta}) = -\Phi(z, \hat{\theta})$, and $\tilde{\theta}$ is the parameter estimation error, $\tilde{\theta} = \theta - \hat{\theta}$. Stability can be established via standard Lyapunov arguments. Choose a candidate Lyapunov function in the form

$$V(z,\hat{\theta})+\frac{1}{2}z^T z=\tilde{\theta}^T Q\tilde{\theta},\quad Q^T=Q>0$$

Differentiate and use the closed loop equations to obtain

$$\dot{V}=z^T\left[\text{diag}(-c_1,\ldots,-c_n)+\Phi(z,\hat{\theta})\right]z+\left(z^T\Psi+\dot{\hat{\theta}}^T Q\right)\tilde{\theta}$$

Because of asymmetry, $z^T\Phi(z,\hat{\theta})z=0$, so we can choose the update law

$$\dot{\hat{\theta}}=-Q^{-1}\Psi^T z$$

to obtain

$$\dot{V}=z^T\,\text{diag}(-c_1,\ldots,-c_n)z$$

Provided $c_i>0, i=1,\ldots,n$, this establishes the uniform stability of the equilibrium point $z=0,\hat{\theta}=\theta$, which, corresponds to $x=0$. Moreover, from the LaSalle invariance theorem we can obtain

$$\lim_{t\to\infty}z(t)=0,\lim_{t\to\infty}\dot{z}(t)=0,\lim_{t\to\infty}\dot{\hat{\theta}}=0$$

The update law is implemented in the form

$$\dot{\hat{\theta}}=\tau(x,\hat{\theta})=-Q^{-1}\Psi^T(z(x,\hat{\theta}),\hat{\theta})z(x,\hat{\theta})$$

Remark 9.20. 1. Computations for the parametric-pure-form of the equations are somewhat more complicated but lead to similar results.

2. The controller consists of a feedback law

$$u=\frac{1}{\beta_0(x)}\left[-\gamma_0(x)+\alpha_n(z_1,\ldots,z_n,\hat{\theta})\right]$$

and parameter estimator equations

$$\dot{\hat{\theta}}=\tau_n(z_1,\ldots,z_n,\hat{\theta})$$

where α_n,τ_n are the last of recursively computed sequences as defined in the above references. In actual computation, they are obtained, successively, directly as functions of x (rather than z) which is the way in which the controller is to be implemented. This is easier, and avoids the need to invert the state transformation equations $z=z(x)$.

ProPac implements three functions that assist in the design of backstepping adaptive controllers: `AdaptiveBackstepRegulator`, `PSFFCond`, and `PSFFSolve`. The following example provides an illustration of their use.

Example 9.21 (Backstepping Adaptive Regulator).

Consider the following single input example. First we put the system in parametric strict feedback form using `PSFFSolve`. Then, we design an adaptive regulator. We only display the control and update law.

```
In[224]:= var30 = {x1, x2};
          f30 = {θ  x1^3 + Sin[x2], x2};
          g30 = {0, 1};

In[225]:= PSFFSolve[f30, g30, var30, {θ}]
LinearizingOutputSolutions : {x1}
PSFFTransformationz = T({x1, x2})
z1 = x1
z2 = Sin[x2]
Out[225]= {{x1, Sin[x2]}, {θ  z1^3 + z2, x2  Cos[x2]}, {0, Cos[x2]}}

In[226]:= {control, update, zcoords} = AdaptiveBackstepRegulator[f30, g30,
              var30, {θ}, {{AdGain}}, {c1, c2, c3}];

In[227]:= control
Out[227]= −x1 − c1  c2  x1 − c1  thetahat1  x1^3 − c2  thetahat1  x1^3 −
            3  thetahat1^2  x1^5 − AdGain  x1^7 − AdGain  c1^2  x1^7 −
            4  AdGain  c1  thetahat1  x1^9 −
            3  AdGain  thetahat1^2  x1^11 − x2 − c1  x2 − c2  x2 − 3  thetahat1  x1^2  x2 −
            AdGain  c1  x1^6  x2 − 3  AdGain  thetahat1  x1^8  x2

In[228]:= update
Out[228]= {AdGain  x1^3  (x1 + (c1 + 3  thetahat1  x1^2)  (c1  x1 + thetahat1  x1^3 + x2))}
```

9.7 Adaptive Tracking via Dynamic Inversion

ProPac contains the function `AdaptiveTracking` that produces an adaptive version of the tracking controller defined by (7.86), (7.87) and (7.90) [9]. In this case, the system is assumed to depend on an uncertain parameter vector ϑ. Then the control (7.86) and (7.87) also depends explicitly on ϑ. This control is implemented with an estimate of the parameter and a parameter update law in the form:

$$u = D_\beta^\dagger(x,\vartheta)\left\{-C_\beta(x,\vartheta) + M(x,\vartheta)\tilde{y}_0 + N(x,\vartheta)y^{(n)} + v(t)\right\} \tag{9.56}$$

$$\dot{\hat{\vartheta}} = -\Omega^{-1}W^T R\varepsilon \tag{9.57}$$

where

$$\varepsilon := [e_1,..,e_1^{n_1-1},..,e_l,..,e_l^{n_l-1}]^T \tag{9.58}$$

Computing the Regressor

Recall that application of the exact control (7.86) reduces the input-output dynamics to (7.89). When the 'inexact' control is applied the input-out dynamics can always be expressed in the form

$$y^{(n)} = v + \Delta(x, \vartheta) \tag{9.59}$$

Our goal is to compute $\Delta(x, \vartheta)$. Notice that combining (7.69) and (7.87) and making the parameter dependence explicit, we have

$$N(x, \vartheta) y^{(n)} + M(x, \vartheta)\tilde{y}_0 = C_\beta(x, \vartheta) + D_\beta(x, \vartheta)u \tag{9.60}$$

In view of (9.58), the control satisfies

$$N(x, \hat{\vartheta})v + M(x, \hat{\vartheta})\tilde{y}_0 = C_\beta(x, \hat{\vartheta}) + D_\beta(x, \hat{\vartheta})u \tag{9.61}$$

Now we make the following assumption:

Assumption 3:

The matrices $C_\beta(x, \vartheta), D_\beta(x, \vartheta)$ and $C_\beta(x, \vartheta)$ are linear in the uncertain parameters.

This allows us to write

$$\begin{aligned} C_\beta(x, \vartheta) &= C_{\beta_0}(x) + \tilde{C}_\beta(x)\vartheta \\ D_\beta(x, \vartheta)u &= D_{\beta_0}(x, u) + \tilde{D}_\beta(x, u)\vartheta \\ M(x, \vartheta)\tilde{y}_0 &= M_0(x, \tilde{y}_0) + \tilde{M}(x, \tilde{y}_0)\vartheta \\ N(x, \vartheta)y^{(n)} &= N_0(x, y^{(n)}) + \tilde{N}(x, y^{(n)})\vartheta \end{aligned} \tag{9.62}$$

Subtracting (9.60) from (9.61) and using (9.62) yields

$$\begin{aligned} &N(x, \hat{\vartheta})(v - y^{(n)}) = \\ &\quad \tilde{C}_\beta(x)(\hat{\vartheta} - \vartheta) + \tilde{D}_\beta(x, u)(\hat{\vartheta} - \vartheta) - \tilde{M}(x, \tilde{y}_0)(\hat{\vartheta} - \vartheta) - \tilde{N}(x, y^{(n)})(\hat{\vartheta} - \vartheta) \end{aligned}$$

so that

$$\begin{aligned} \Delta &= -N^{-1}(x, \hat{\vartheta}) \left\{ \tilde{C}_\beta(x) + \tilde{D}_\beta(x, u) - \tilde{M}(x, \tilde{y}_0) - \tilde{N}(x, y^{(n)}) \right\} (\hat{\vartheta} - \vartheta) \\ &= -W(\hat{\vartheta} - \vartheta) \end{aligned} \tag{9.63}$$

The function `AdaptiveTracking` performs two key operations in assembling the regressor W. First it sorts through the matrices C_β, D_β, M and N to identify groups of physical parameters that can be combined to form new parameters that fit the linearity assumption. One of the outputs of `AdaptiveTracking` is a list of these parameter transformation rules. Then the matrices are expanded as in (9.62) in terms of the new parameters so that W can be assembled as in (9.63).

Example 9.22 (Adaptive Tracking Controller). The following example is the same as Example 9.13 (see also [9]). After defining the system equations we define a reference signal, then specify the desired closed loop pole locations and, finally, compute the control. Because of the length of the output, we give only the control and update law.

```
In[229]:= RefSig =
            Table[ToExpression[yd <> ToString[i1] <> [t]], {i1, 1, Length[h32]}];
          Poles = {{-2, -2}};
          {Parameters, ParameterEstimates, UpdateLaw,
          Control, DecoupMatrix, DerivativeOrders} = AdaptiveTracking[
              f32, Transpose[{g32}], h32, var32, t, {θ}, RefSig, {}, Poles];
          Control
```

$$\text{Out[229]=}\ \left\{\frac{x1+x2^2+4\ \ (-x3+yd1[t])+4\ \ (-y1'[t]+yd1'[t])+yd1''[t]}{-e^{x2}+e^{x2}\ \ \text{thetahat1}}\right\}$$

```
In[230]:= UpdateLaw
```

$$\text{Out[230]=}\ \left\{-\frac{1}{-e^{x2}+e^{x2}\ \ \text{thetahat1}}(125.\ \ \text{AdaptGain1}\ \ e^{x2}\ \ (-x3+yd1[t])\ \ (x1+x2^2+4\ \ (-x3+yd1[t])+4\ \ (-y1'[t]+yd1'[t])+yd1''[t]))-\frac{1}{-e^{x2}+e^{x2}\ \ \text{thetahat1}}(156.25\ \ \text{AdaptGain1}\ \ e^{x2}\ \ (-y1'[t]+yd1'[t])\ \ (x1+x2^2+4\ \ (-x3+yd1[t])+4\ \ (-y1'[t]+yd1'[t])+yd1''[t]))\right\}$$

9.8 Problems

Problem 9.23 (DC drive motor). A separately excited dc motor is decscribed by the differential equations

$$J\frac{d\omega}{dt} = -B\omega + Ki_f i_a - T_L$$

$$L_a\frac{di_a}{dt} = -R_a i_a - Ki_f\omega + e_a$$

$$L_f\frac{di_f}{dt} = -R_f i_f + e_f$$

where the variables and parameters are defined in Table (9.1) Consider the control inputs to be the two applied voltages, e_a, e_f. The goal is to regulate speed to a desired value ω_0 and to minimize electrical losses ($R_a i_a^2 + R_f i_f^2$). Thus, we formulate two outputs

$$y_1 = \omega - \omega_0$$

$$y_2 = R_a i_a - R_f i_f$$

Symbol	Definition	Parameter Value
ω	motor speed	
i_a	armature current	
i_f	field current	
e_a	armature applied voltage	
e_f	field applied voltage	
J	motor inertia	$0.1\ kg-m^2$
B	motor damping	$0.01\ Kg-m^2-sec^{-1}$
K	electromechanical transduction	$0.30\ nm/a^2$
T_L	load torque	0 to 15 nm
L_a	armature inductance	1.0 H
L_f	field inductance	10.0 H
R_a	armature resistance	10.0 Ω
R_f	field resistance	50.0 Ω

Table 9.1: **DC motor nomenclature**

(a) Design a feedback linearizing adaptive controller taking the load torque as an uncertain parameter. Assume that ω_0 is a specified constant.

(b) Assume that the load torque, T_L can be measured or accurately estimated, but that the motor friction coefficient is uncertain with $B \in (0, 0.05)$. Design a feedback linearizing adaptive controller. Via simulation compare the adaptive and nonadaptive ($B = 0.01$) performance.

Problem 9.24 (Load with backlash and friction). An inertial load with backlash and friction is illustrated in Figure (9.2). The drive motor angle θ_m is cosidered as the control input to a drive shaft/gear with backlash modeled using the dead zone function:

$$D(\theta) = \begin{cases} \theta - \varepsilon & \theta \geq \varepsilon \\ 0 & |\theta| < \varepsilon \\ \theta + \varepsilon & \theta \leq -\varepsilon \end{cases}$$

The shaft has stiffness K and the load has inertia J and friction $f(\omega) = b\sin\omega$. $d(t)$ is an external disturbance. Thus, the equations of motion are:

$$\dot{\theta} = \omega$$

$$J\dot{\omega} = -f(\omega) + KD(u-\theta) + d(t)$$

(a) Assume $\varepsilon \in [0, 0.5]$ and $b \in [0, 1]$ are uncertain parameters within the given bounds and $d(t) = 0$. Design an adaptive feedback linearizing control. Hint: Take the feedback linearizing and stabilizing control to be of the form

$$\hat{u} = \hat{D}^{-1}\left(-(k_1 - 1)\theta - k_2\omega + \hat{f}(\omega)\right)$$

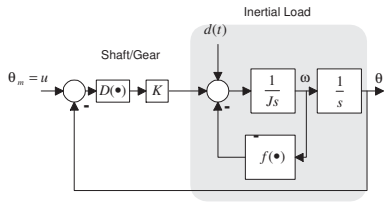

Fig. 9.2: A simplified inertial load with backlash and friction.

(b) Take $J = 1$ and $K = 1$ and compute the closed loop system response.

(c) Can Lyapunov redesign as described in this chapter be used for this problem?

(d) Suppose the disturbance $d(t) = \kappa w(t)$, where $\kappa \in [0,1]$ is an uncertain parameter with known bounds and $w(t) = 1 + 4\sin(2\pi t)$. Repeat (a) and (b).

Part IV

Optimal and Switched Systems

10

Variable Structure Control

10.1 Introduction

Variable structure control systems are switching controllers that exhibit certain desirable robustness properties. Consider a nonlinear dynamical system of the form

$$\dot{x} = f(x,u) \tag{10.1}$$

where $x \in R^n, u \in R^m$ and f is a smooth function of x and u. We will focus on switching control systems in which the control functions u_i are discontinuous across smooth surfaces $s_i(x) = 0$, i.e

$$u_i(x) = \begin{cases} u_i^+(x), & s_i(x) > 0 \\ u_i^-(x), & s_i(x) < 0 \end{cases} \quad i = 1,\ldots,m \tag{10.2}$$

and the control functions u_i^+, u_i^- are smooth functions of x.

The design of switching control systems of the type (10.1), (10.2) often focuses on the deliberate introduction of sliding modes [104][1]. If there exists an open submanifold, M_s, of any intersection of discontinuity surfaces, $s_i(x) = 0$ for $i = 1,\ldots,p \leq m$, such that $s_i\dot{s}_i < 0$ in the neighborhood of almost every point in M_s, then it must be true that a trajectory once entering M_s remains in it until a boundary of M_s is reached. M_s is called a *sliding manifold* and the motion in M_s is called a *sliding mode*. Since the control is not defined on the discontinuity surfaces, the sliding dynamics are not characterized by equations (10.1) and (10.2). However, sliding mode dynamics may often be determined by imposing the constraint $s(x) = 0$ on the motion defined by the differential equation (10.1). Under appropriate circumstances this is sufficient to define an 'effective' control u_{eq}, called the *equivalent control*, which obtains for motion constrained to lie in M_s. If this control is smooth and unique, then the sliding behavior is well defined.

Variable structure control system design entails specification of the switching functions $s_i(x)$ and the control functions $u_i^+(x)$ and $u_i^-(x)$. As we will see, the basis for

design follows from the observations that the sliding mode dynamics depend on the geometry of M_s, that is, on the switching functions $s_i(x)$, and that sliding can be induced on a desired manifold M_s by designing the control functions $u_i^{\pm}(x)$ to guarantee that M_s is attracting. Thus, control system design is a two step process: 1) design of the 'sliding mode' dynamics by the choice of switching surfaces, and 2) design of the 'reaching' dynamics by the specification of the control functions.

10.2 Basic Properties of Discontinuous Systems

Equation (10.1) when combined with control (10.2) is a special case of the general class of discontinuous dynamical systems

$$\dot{x} = F(x,t) \tag{10.3}$$

where for each fixed t, $F(x,t)$ is smooth ($C^k, k > 0$) on R^n except on m codimension-one surfaces (codimension-one regular submanifolds of R^n) defined by $s_i(x) = 0$, $i = 1,\ldots,m$, on which $F(x,t)$ is not defined. Ordinarily, a solution to (10.3) is a curve $x(t) \subset R^n$ that has the property that $dx/dt = F(x(t),t)$ for each $t \in R$. Such a test, however, would be impossible to apply if the prospective solution contains points on the discontinuity surfaces. Since the set of points for which $F(x,t)$ is not defined has measure zero in R^n, one might simply require that the integral curve property be satisfied only where $F(x,t)$ is defined. This is clearly inadequate because segments of trajectories that lie in a discontinuity surface would be entirely arbitrary. Filippov [26] proposed a satisfactory definition of solutions to (10.3):

Definition 10.1. *A curve $x(t) \subset R^n$, $t \in [t_0,t_1], t_1 > t_0$, is said to be a solution of (10.3) on $[t_0,t_1]$ if it is absolutely continuous on $[t_0,t_1]$ and for each $t \in [t_0,t_1]$*

$$\frac{dx(t)}{dt} \in \tilde{F}(x(t),t) := \bigcap_{\delta>0} \text{conv}F(S(\delta,x(t)) - \Lambda(\delta,x(t)),t) \tag{10.4}$$

where $S(\delta,x)$ is the open sphere centered at x and of radius δ, $\Lambda(\delta,x)$ is the subset of measure zero in $S(\delta,x)$ for which F is not defined, and conv$F(U)$ *denotes the convex closure of the set of vectors $\{F(U)\}$.*

Remark 10.2 (Remark on notation). If x is a point in R^n then $S(\delta,x) := \{y \in R^n \mid \|y-x\| < \delta\}$. If U is a set contained in R^n then

$$S(\delta,U) := \bigcup_{x\in U} S(\delta,x)$$

We call $S(\delta,U)$ a δ-vicinity of U.

If x does not lie on a discontinuity surface, then the set $\tilde{F}(x,t) = \{F(x,t)\}$, so that the original differential equation must be satisfied at regular points. However, this definition does help characterize solutions that lie in discontinuity surfaces. Suppose a solution $x(t) \subset R^n$, $t \in [t_0, t_1]$, $t_1 > t_0$, lies entirely in the intersection of some set of p discontinuity surfaces that is a regular embedded submanifold of R^n of dimension $n-p$, which we designate M_s. For each $t^* \in [t_0, t_1]$, $\dot{x}(t^*)$ must belong to the set $\tilde{F}(x(t^*), t^*)$. In addition, $\dot{x}(t^*)$ must lie in the tangent space to M_s at $x(t^*)$, i.e., $\dot{x}(t^*) \in T_{x(t^*)}M_s$. In many important cases, these two conditions uniquely define solutions that contain segments that lie in M_s.

When we of speak of solutions or, equivalently, trajectories of discontinuous systems we shall mean solutions in the sense of Filippov. One important consequence of the definition is an extension of Lyapunov's direct stability analysis to discontinuous systems [59].

Lemma 10.3. *Suppose that $V : R^n \to R$ is a C^1 function. Then:*

1. *the time derivative of $V(x)$ along trajectories of (10.3) satisfies the set inclusion*

$$\dot{V}(x(t)) \in \left\{ \frac{\partial V}{\partial x}\xi \;\middle|\; \xi \in \tilde{F}(x(t),t) \right\} \tag{10.5}$$

2. *if $\dot{V} \leq -\rho < 0$ ($\geq \rho > 0$) at all points in an open set $P \subset R^n$ except on a set $\Lambda \subset P$3 of measure zero where $F(x,t)$ is not defined, then $\dot{V} \leq -\overline{\rho} < 0$ ($\geq \overline{\rho} > 0$), $\overline{\rho} < \rho$, at all points of P.*
3. *if $\dot{V} \leq -\rho \|s(x)\|$, $\rho > 0$, at all points in an open $P \subset R^n$ except on a set $\Lambda \subset P$ of measure zero where $F(x,t)$ is not defined, then $\dot{V} \leq -\rho \|s(x)\|$ at all points of P.*

Proof: The first conclusion (10.5) follows directly from the Filippov definition of a trajectory.

To prove the second, first note that at regular points the inclusion reduces to the usual $\dot{V}(x) = [\partial V/\partial x]F(x,t)$. Consider the negative definite case. The assumption of definiteness implies that $[\partial V/\partial x]F(x,t) \leq -\rho$ at all regular points $x \in P$. Now take any $x^* \in \Lambda$. We need only show that $[\partial V(x^*)/\partial x]\xi \leq -\tilde{\rho}$ for each $\xi \in \tilde{F}(x^*,t)$. Consider a sphere $S(\varepsilon, x^*)$ where $\varepsilon > 0$ is chosen arbitrarily small and so that the sphere is contained in P. By assumption, $[\partial V/\partial x]F(x,t) \leq -\rho$ at all regular points in $S(\varepsilon, x^*)$. Since V is C^1, we can choose ε sufficiently small so that $[\partial V(x^*)/\partial x]\xi \leq -\tilde{\rho} < 0$ for any specified $\tilde{\rho} < \rho$ and all regular x in $S(\varepsilon, x^*)$. By its definition, $\tilde{F}(x^*,t) \subset F(S(\varepsilon, x^*) - \Lambda, t)$. The conclusion follows.

To prove the third conclusion, consider a point x^* in P. By assumption, the condition $\dot{V} \leq -\rho \|s(x)\|$ holds at all regular points. Suppose that x^* is not regular, then the condition holds at almost all points in a sufficiently small neighborhood $S(\varepsilon, x^*)$

of x^*. Now, the smoothness of V 9and s implies the approximations $\partial V(x)/\partial x = \partial V(x^*)/\partial x + O(\varepsilon)$ and $\|s(x)\| = \|s(x^*)\| + O(\varepsilon)$ for all $x \in S(\varepsilon, x^*)$. Thus we have at regular $x \in S(\varepsilon, x^*)$

$$\frac{\partial V(x^*)}{\partial x} F(x,t) \leq -\rho \|s(x^*)\| + O(\varepsilon)$$

Once again, since $\tilde{F}(x^*,t) \subset F(S(\varepsilon,x^*) - \Lambda, t)$, it follows that

$$\frac{\partial V(x^*)}{\partial x} \xi \leq -\rho \|s(x^*)\| + O(\varepsilon), \forall \xi \in \tilde{F}(x^*,t)$$

The conclusion follows in the limit $\varepsilon \to 0$. ■

In applications, $\dot{V}$ is often relatively easy to determine at all points in a given domain other than those on the surfaces of discontinuity. The significance of the lemma is that it makes it unnecessary to actually compute $\tilde{F}(x^*,t)$ in order to determine value of $\dot{V}$ at those points.

Definition 10.4. *Suppose $M_s = \{x \in R^n \mid s(x) = 0\}$ is a regular embedded manifold in R^n and let D_s be an open, connected subset of M_s. D_s is a sliding domain if*

1. *for any $\varepsilon > 0$, there is a $\delta > 0$ such that trajectories of (10.3) which begin in a δ-vicinity of D_s remain in an ε-vicinity of D_s until reaching an ε-vicinity of the boundary of D_s, ∂D_s.*
2. *D_s must not contain any entire trajectories of the 2^m continuous systems defined in the open regions adjacent to M_s and partitioned by the set $M := \bigcup_{i=1,\ldots,m} M_{s_i}$.*

This definition is due to Utkin [104]. By including (2), it is assured that it is the switching mechanism that produces the sliding mode and the possibility of the existence of certain "pathological" sliding domains is excluded.

The definition implies that D_s is invariant with respect to trajectories in the sense of the following rather obvious proposition.

Proposition 10.5. *If D_s is a sliding domain then trajectories of (10.3) which begin in D_s remain in D_s until reaching its boundary, ∂D_s.*

Proof: Since D_s belongs to any δ-vicinity of itself, the definition of a sliding domain implies that trajectories which begin in D_s must remain in every arbitrarily small ε-vicinity of D_s. Hence trajectories beginning in D_s must remain therein until reaching its boundary. ■

Sufficient conditions for the existence of a sliding domain are relatively easy to formulate. One approach is as follows. Define a C^1 scalar function $V : D \subset R^n \to R$ with the following properties

$$V(x) := \begin{cases} = 0 & if\ s(x) = 0 \\ > 0 & otherwise \end{cases} \tag{10.6}$$

Recall that $\dot{V}$ is uniquely defined everywhere but on $M := \bigcup_{i=1,\ldots,m} M_{s_i}$ and on M it is still constrained by the set inclusion of Lemma (10.3). Now the following result can be stated.

Proposition 10.6. *Let V be given by (10.6). Suppose that*

1. *D_s is an open, connected subset of M_s*
2. *D is an open connected subset of R^n which contains D_s*
3. *$\dot{V} \leq -\rho \|s(x)\| < 0$ on $D - M$*

Then D_s is a sliding domain.

Proof: Under the stated assumptions, a trajectory cannot leave D_s at any point $x_0 \in D_s$. This is easily proved by contradiction. Suppose a trajectory $x(t)$ does depart D_s from a point $x_0 \in D_s$ at time t_0. Such a departure implies that there is a time $t_1 > t_0$ and sufficiently small $\varepsilon > 0$, such that the absolutely continuous trajectory segment $x(t)$, $t \in (t_0, t_1)$ is entirely contained in the set $S(\varepsilon, x_0) - M_s$ and along which $\dot{V} > 0$. But in view of Lemma (10.3), the assumptions of the proposition imply that $\dot{V} < 0$ along trajectories at all points in $S(\varepsilon, x_0) - M_s$. This is a contradiction. ■

One distinguishing feature of many variable structure control systems is that trajectories beginning in a vicinity of the sliding surface reach the surface in finite time. This clearly is the case if $\dot{V}$ is bounded below by a negative number. However, such a bound is not necessary as the following proposition illustrates.

Proposition 10.7. *Suppose that the conditions of proposition (10.6) hold and in addition $V(x) = \sigma \|s(x)\|^2$, $\sigma > 0$ on a δ-vicinity of D_s. Then trajectories which reach D_s from a δ-vicinity of D_s do so in finite time.*

Proof: Suppose a trajectory beginning at state x_0 in a δ-vicinity of D_s reaches a point $x_1 \in D_s$. Now, $\|s(x_0)\| \leq \delta$. Since $V(x) = \sigma \|s(x)\|^2$ we have

$$\dot{V} = 2\sigma \|s(x)\| \frac{d\|s(x)\|}{dt} \leq -\rho \|s(x)\|$$

which in view of Lemma (10.3) holds throughout the δ-vicinity of D_s. Thus,

$$\frac{d\|s(x)\|}{dt} \leq -\frac{\rho}{2\sigma}$$

which implies that the trajectory reaches D_s in time not greater than $\delta(2\sigma/\rho)$. ■

10.3 Sliding

In this section we consider the design of sliding surfaces for affine systems of the form

$$\dot{x} = f(x) + G(x)u \tag{10.7}$$

$$y = h(x) \tag{10.8}$$

The procedure begins with the reduction of the given affine system to the *regular form* of

$$\dot{z} = Az + E\left[\alpha(\xi,z) + \rho(\xi,z)u\right] \tag{10.9}$$

$$y = Cz \tag{10.10}$$

as described earlier. Now, we do not feedback linearize as was done in Chapter 6. Instead, we choose a variable structure control law with switching surface, $s(x)$. The variable structure control law is of the form:

$$u_i(x) = \begin{cases} u_i^+(x) & s_i(x) > 0 \\ u_i^-(x) & s_i(x) < 0 \end{cases}$$

Notice that the control is not defined during sliding, i.e., for trajectories completely contained within the surface $s(x) = 0$. We can prove that during sliding the equivalent or effective control is , such that feedback linearized behavior is achieved in the sliding phase (see, [59, 63, 80, 58]).

Proposition 10.8. *Let the switching surface $s(x)$ be such that $s(x) = 0$ if and only if $Kz(x) = 0$ for some specified $K \in R^{m\times r}$ and suppose that*

1. *$\rho(x)$ has continuous first derivatives with $\det\{\rho(x)\} \neq 0$ on $M_0 = \{x|z(x) = 0\}$.*
2. *$\partial s(x)/\partial x$ is of maximum rank on the set $M_s = \{x|s(x) = 0\}$.*

Then M_s is a regular $n-m$ dimensional submanifold of R^n which contains M_0. Moreover, if K is structured so that the m columns numbered $r_1, r_1+r_2, \ldots, r$ compose an identity I_m, then for any trajectory segment $x(t), t \in T$, T an open interval of R, that lies entirely in M_s, the control which obtains on T is

$$u_{eq} = -\rho^{-1}(x)KAz - \rho^{-1}(x)\alpha(x) \tag{10.11}$$

and every such trajectory with boundary condition $x(t_0) = x_0 \in M_s$, $t_0 \in T$ satisfies

$$\dot{x} = f(x) - G(x)\rho^{-1}(x)\left[\alpha(x) + KAz(x)\right], \quad Kz(x(t_0)) = 0 \tag{10.12}$$

Proof: The maximum rank condition insures that M_s is a regular manifold of dimension $n-m$. M_0 is a submanifold of M_s in view of the definition of $s(x)$. Motion

constrained by $s(x(t)) = 0$ must satisfy the sliding condition $\dot{s} = 0$, equivalently, $K\dot{z}(x) = 0$. Direct computation leads to (10.11) and (10.12). ■

In this case observe that the manifold M_s is invariant with respect to the dynamics (10.12). The flow defined by (10.12) on M_s is called the *sliding dynamics* and the control defined by (10.11) is the *equivalent control*. Note that the equivalent control behaves as a linearizing feedback control. The partial state dynamics in sliding is obtained from (10.9) and (10.11):

$$\dot{z} = [I - EK]Az, \quad Kz(t_0) = 0 \tag{10.13}$$

Proposition 10.9. *Suppose the conditions of proposition (10.8) apply. Then M_0 is an invariant manifold of the sliding dynamics (10.12). Moreover, if K is specified as*

$$K = \text{diag}(k_1, \ldots, k_m), \quad k_i = [a_{i1}, \ldots, a_{ir_i-1}, 1] \tag{10.14}$$

where the m ordered sets of coefficients $\{a_{i1}, \ldots, a_{ir_i-1}\}$, $i = 1, \ldots, m$ each constitute a set of coefficients of a Hurwitz polynomial. Then every trajectory of (10.12) not beginning in M_0 approaches M_0 exponentially.

Proof: Notice that (10.13) implies that the only trajectory of (10.12) with boundary condition $z(t_0) = 0$ is $z(t) = 0$ for all t and hence M_0 is an invariant set.

Note that $\text{Im}[E] \oplus \ker[K] = R^r$ so that the motion of (10.13) can be conveniently divided into a motion in $\text{Im}[E]$ and a motion in $\ker[K]$ and the latter has eigenvalues which coincide with the transmission zeros of the triple (K, A, E), Young et al [7]. To prove that trajectories of (10.12) approach M_0 exponentially we need only show that all trajectories of (10.13) in $\ker[K]$ approach the origin asymptotically. Let the matrix N be chosen so that its columns form a basis for $\ker[K]$ and introduce the coordinate vectors $w \in R^{r-m}$ and $v \in R^m$, and write

$$z = Nw + Ev \tag{10.15}$$

The inverse of (10.15) may be written

$$\begin{bmatrix} w \\ v \end{bmatrix} = \begin{bmatrix} M \\ K \end{bmatrix} z \tag{10.16}$$

Direct calculation verifies that (10.13) is replaced by

$$\frac{d}{dt}\begin{bmatrix} w \\ v \end{bmatrix} = \begin{bmatrix} MAN & MAE \\ 0 & 0 \end{bmatrix}\begin{bmatrix} w \\ v \end{bmatrix}, \quad v(0) = 0 \tag{10.17}$$

The result obtains if $\text{Re}\lambda\{MAN\} < 0$. If the matrix K is chosen in accordance with (10.14), then the eigenvalues of MAN are precisely the $r - m$ eigenvalues of the matrices

$$\begin{bmatrix} 0 & 1 & 0 & . & 0 \\ 0 & 0 & 1 & 0 & . \\ . & . & 0 & 1 & 0 \\ . & . & . & . & 1 \\ -a_{i1} & -a_{i2} & . & . & -a_{i(r_i-1)} \end{bmatrix}, \quad i = 1, \ldots, m \tag{10.18}$$

which are lie in the open left half plane by assumption. ■

10.4 Reaching

The second step in VS control system design is the specification of the control functions $u_i^{\pm}$ such that the manifold $s(x) = 0$ contains a stable submanifold which insures that sliding occurs. Thus we seek to choose a control that drives trajectories into $s(x) = 0$, or equivalently, $Kz(x) = 0$. There are many ways of approaching the reaching design problem, [104]. We consider only one. Define a positive definite quadratic form in $\eta = Kz$

$$V(x) = \eta^T Q \eta, \quad Q > 0 \tag{10.19}$$

Consider the set of states that satisfy $\eta(x) = 0$. A subset of this set is attractive if it lies in a region of the state space on which the time rate of change V along trajectories is negative. Upon differentiation we obtain

$$\frac{d}{dt} V = 2\dot{\eta}^T Q \eta = 2\left[KAz + \alpha\right]^T QKz + 2u^T \rho^T QKz \tag{10.20}$$

10.4.1 Bounded Controls

If the controls are bounded, $0 > U_{\min,i} \leq u_i \leq U_{\max,i} > 0$, then, obviously, to minimize the time rate of change of V, we should choose

$$u_i = \begin{cases} U_{\min,i} & s_i(x) > 0 \\ U_{\max,i} & s_i(x) < 0 \end{cases} \quad i = 1, \ldots, m \tag{10.21}$$

$$s(x) = \rho^T(x) QKz(x) \tag{10.22}$$

Clearly, $s(x) = 0 \Leftrightarrow Kz(x) = 0$. Notice that if $U_{\min,i} = -U_{\max,i}$, the control reduces to

$$u_i = -U_{\max,i} \operatorname{sgn}(s_i)$$

In this case it follows that $\dot{V}$ is negative (for $s \neq 0$) provided

$$\left| U_{\max}^T \rho^T QKz \right| > \left| \left[KAz + \alpha\right]^T QKz \right| \tag{10.23}$$

A useful sufficient condition is that

$$|(\rho(x)U_{\max})_i| > |(KAz(x)+\alpha(x))_i| \tag{10.24}$$

Conditions (10.23) or (10.24) may be used to insure that the control bounds are of sufficient magnitude to guarantee sliding and to provide adequate reaching dynamics. This rather simple approach to reaching design is satisfactory when a "bang-bang" control is acceptable.

10.4.2 Unconstrained Controls

Suppose the controls are not constrained to fixed bounds and there exists a continuous bound on the function $\alpha(x)$, i.e.,

$$\|\alpha(x)\| < \sigma_\alpha(x) \tag{10.25}$$

for some continuous function $\sigma_\alpha(x)$. In this case choose u_i and $\sigma(x)$ such that

$$u_i = -\sigma(x)\text{sgn}(s_i(x)), \quad \sigma(x)\|\rho(x)\| > \bar{\sigma}(KA)\|z(x)\| + \sigma_\alpha(x) \tag{10.26}$$

Now, we compute

$$\dot{V} \leq \left(\bar{\sigma}(KA)\|z(x)\| + \sigma_\alpha(x) - \sigma(x)\sum_{i=1}^{m}\{|\text{sgn}(s_i(x))|\}\right)\|QKz(x)\| \tag{10.27}$$

Thus $\dot{V}$ is negative when $s \neq 0$ and the sliding manifold is attractive.

10.4.3 A Variation for Unconstrained Controls

Suppose $\alpha(x)$ and $\rho(x)$ are smooth and known with reasonable certainty. A sometimes useful variation of the controller (10.26) is

$$u(x) = u_0(x) + v(x) \tag{10.28}$$

composed of the smooth part

$$u_0(x) = -\rho^{-1}(x)\alpha(x) \tag{10.29}$$

and discontinuous part

$$v_i = -\sigma(x)\text{sgn}(s_i(x)), \quad \sigma(x)\|\rho(x)\| > \bar{\sigma}(KA)\|z(x)\| \tag{10.30}$$

Notice that the required magnitude of the discontinuous part is reduced. We easily compute from (10.20)

$$\dot{V} \leq \left(\bar{\sigma}(KA)\|z(x)\| - \sigma(x)\sum_{i=1}^{m}\{|\text{sgn}(s_i(x))|\}\right)\|QKz(x)\| \tag{10.31}$$

10.4.4 Closed Loop Stability

$\mathscr{A} \subset M_0$ is a *stable attractor* of the zero dynamics if it is a closed invariant set and if for every neighborhood U of $\mathscr{A}$ in M_0 there is a neighborhood V of $\mathscr{A}$ in M_0 such that every trajectory of (10.13) beginning in V remains in U and tends to $\mathscr{A}$ as $t \to \infty$. The following proposition establishes conditions under which the variable structure controller applied to (10.7) stabilizes $\mathscr{A}$ in R^n.

Proposition 10.10. *Suppose that the conditions of propositions (10.8) and (10.9) apply; $\mathscr{D}$ is an open region in R^n in which (10.23) (or (10.25)) is satisfied; $\mathscr{D}_s = \mathscr{D} \cap M_s$ is nonempty; and $\mathscr{A} \subset M_0$ is a bounded, stable attractor of the zero dynamics which is contained in $\mathscr{D}_s \cap M_0$. Then $\mathscr{A}$ is a stable attractor of the feedback system composed of (10.7) with feedback control law (10.21) (or (10.26), or (10.28)).*

Proof: Since $\mathscr{D}$ is an open region in R^n in which (10.23) is satisfied, a sliding mode exists in $\mathscr{D}_s = \mathscr{D} \cap M_s$ which is nonempty. In fact, $\mathscr{D}_0 = \mathscr{D}_s \cap M_0$ is also nonempty and it contains a bounded, stable attractor $\mathscr{A}$ of the zero dynamics. Proposition (10.9) implies that $\mathscr{A}$ is also a stable attractor of the sliding dynamics (10.12). Thus, for any neighborhood $\tilde{U}$ of $\mathscr{A}$ in M_s there is a neighborhood $\tilde{V}$ of $\mathscr{A}$ in M_s such that trajectories of (10.12) beginning in $\tilde{V}$ remain in $\tilde{U}$ and tend to $\mathscr{A}$ with increasing time. We must show that a similar property applies for neighborhoods of $\mathscr{A}$ in R^n with respect to the dynamics defined by (10.7) and (10.21). Let

$$\kappa_{min} \;=\; \inf_{\mathscr{D}} \{U_{\max}^T \rho^T QKz - [KAz \;+\; \alpha]^T QKz\} \;>\; 0 \tag{10.32}$$

which exists by virtue of (10.23), and

$$\kappa_{max} \;=\; \sup_{\mathscr{D}} \left\{ \left\| f(x) - \textstyle\sum_{i=1}^{m} g_i(x) U_{\max,i} \operatorname{sign}(s_i) \right\|^2 \right\} < \infty \tag{10.33}$$

which exists because f and G are continuous and $\mathscr{D}$ is bounded, and where $\|\bullet\|$ denotes the Euclidean norm. Let $S(r, x_0)$ denote the open sphere in R^n of radius r and centered at x_0 and define the set

$$S(r) := \bigcup_{a \in \mathscr{A}} S(r, a) \tag{10.34}$$

Note that any element of $S(r)$ is at most a distance r from M_s and hence any trajectory starting in $S(r)$ will reach M_s in a finite time not greater than $t_r = r/\sqrt{\kappa_{\min}}$. Thus, any trajectory segment of the of the closed loop system beginning in $S(r)$ and terminating upon reaching M_s is entirely contained in the set $S(R)$ where

$$R = r \left\{ 1 + \sqrt{\frac{\kappa_{\max}}{\kappa_{\min}}} \right\} \tag{10.35}$$

Now, let $\hat{U}$ be any neighborhood of $\mathscr{A}$ in R^n. Define $\tilde{U} = \hat{U} \cap M_s$, so that $\tilde{U}$ is a neighborhood of $\mathscr{A}$ in M_s. Then there exists a neighborhood $\tilde{V}$ of $\mathscr{A}$ in M_s such that

trajectories beginning in $\tilde{V}$ remain in $\tilde{U}$ and tend to $\mathscr{A}$ with increasing time. In view of (10.35), we can always choose r sufficiently small so that $S(R) \cap M_s \subset \tilde{V} \cap \mathscr{D}_s$. Then we identify $\hat{V} = S(r)$. It follows that trajectories of (10.7), (10.21) beginning in $\hat{V}$ remain in $\hat{U}$ and approach $\mathscr{A}$ as $t \to \infty$. ■

Denote $M_h = \{x \mid h(x) = 0\}$ and we assume that M_h is a regular submanifold of R^n of dimension $n-m$. Note that M_0 is a submanifold of both M_h and M_s so that M_0 lies in the intersection of M_h and M_s. The relationships between these manifolds are illustrated in Figure (10.1).

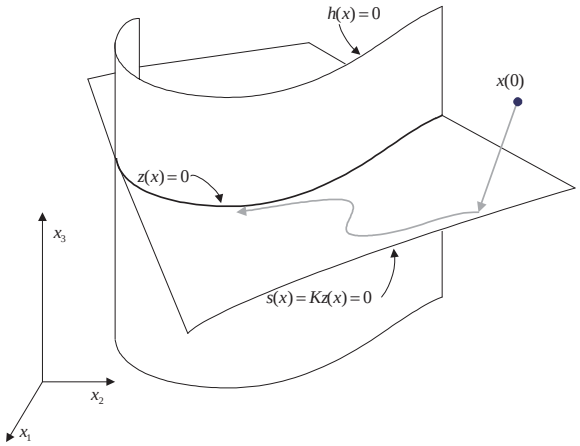

Fig. 10.1: The relationship between the output constraint manifold, the sliding manifold and the zero dynamics manifold is illustrated in a three dimensional state space.

Our results imply that the closed loop system behaves as follows. If the initial state is sufficiently close to $\mathscr{D}_s$, the trajectory will eventually reach $\mathscr{D}_s$ and will thereafter approximate ideal sliding. Ideal sliding is characterized by (10.12) and sliding trajectories which remain in $\mathscr{D}_s$ approach $\mathscr{D}_0$ and eventually $\mathscr{A}$. That $\mathscr{A}$ is a stable attractor of (10.12) is obvious. However, this only implies that trajectories of (10.12) beginning sufficiently close to $\mathscr{A}$ approach $\mathscr{A}$.

10.5 Robustness With Respect to Matched Uncertainties

Variable sructure control systems are especially interesting because they exhibit certain robustness properties with respect to model uncertainty. Suppose we have an uncertain system for which the nominal part (f,G,h) has well defined vector relative degree $\{r_1,\ldots,r_m\}$. Then we can proceed as above to design a variable structure

control system for the nominal system. The key question is; How does this controller perform when applied to the actual system? When the uncertainty is matched and has a known bound it is possible to design the control to insure that the desired sliding manifold is attractive for any actual plant within the admissible class of systems. Moreover, the sliding behavior is identical to that of the nominal system. If the system has matched uncertainty we can take as our starting point the system:

$$\begin{aligned} \dot{\xi} &= F(\xi, z, u) \\ \dot{z} &= Az + E[\alpha(x(\xi, z)) + \Delta(\xi, z, t) + \rho(x(\xi, z))u] \end{aligned} \tag{10.36}$$

where Δ is a function that represents uncertainties and/or disturbances. We assume that $\Delta(\xi, z, t)$ is bounded by a continuous function $\sigma_\Delta(\xi, z) > 0$:

$$\|\Delta(\xi, z, t)\| < \sigma_\Delta(\xi, z), \quad \forall t \tag{10.37}$$

The following proposition establishes the basic robustness result for variable structure controls applied to systems with matched uncertainty.

Proposition 10.11. *Consider a class of* admissible *systems of the form (10.36) satisfying the following conditions*

1. *There is a known and continuous uncertainty bound $\sigma_\Delta(\xi, z) > 0$ such that (10.37) is satisfied.*
2. *There is a continuous bounding function $\sigma_\alpha(x) > 0$ such that*

$$|\alpha(x)| < \sigma_\alpha(x)$$

Then there exists a variable structure controller such that for all admissible systems the switching surface $s(x) = 0$ is a sliding manifold and the sliding behavior is identical to the nominal system sliding behavior.

Furthermore, the control is given by:

$$u_i = -\sigma(x)\mathrm{sgn}(s_i(x)) \tag{10.38}$$

with

$$\sigma(x)\,\|\rho(x)\| > \bar{\sigma}(KA)\,\|z(x)\| + \sigma_\alpha(x) + \sigma_\Delta(x) \tag{10.39}$$

and

$$s(x) = \rho^T(x)QKz(x) \tag{10.40}$$

where K chosen in accordance with Proposition (10.9).

Proof: First, assume that sliding does occur in the surface $s(x) = 0 \Rightarrow Kz(x) = 0 \Rightarrow K\dot{z} = 0$. Then we have u_{eq} defined by

$$KAz + \alpha(x(\xi, z)) + \Delta(\xi, z, t) + \rho(x(\xi, z))u_{eq} = 0$$

and the sliding dynamics reduce, once again, to (10.13). Thus, the actual sliding dynamics are indeed identical to the nominal system sliding dynamics.

Now, we need to show that it is possible to design control functions $u^{\pm}(x)$ such that sliding occurs in $s(x) = 0$ for all admissible systems. The proposition assumes that both α and Δ are bounded by a continuous functions σ_α and σ_Δ. Consider the positive definite quadratic form in $\eta = Kz$

$$V(x) = \eta^T Q \eta$$

A sliding mode exists on a subset of $\eta(x) = 0$, equivalently $s(x) = 0$, that lies in a region of the state space on which the time rate of change V is negative. Upon differentiation we obtain

$$\frac{d}{dt}V = 2\dot{\eta}^T Q\eta = 2\left[KAz + \alpha + \Delta\right]^T QKz + 2u^T \rho^T QKz$$

Now, choose the control u in accordance with Equations (10.38), (10.39) and (10.40) so that

$$\dot{V} \leq \left(\bar{\sigma}(KA)\left\|z(x)\right\| + \sigma_\alpha(x) + \sigma_\Delta(x) - \sigma(x)\sum_{i=1}^{m}\left\{\left|\operatorname{sgn}(s_i(x))\right|\right\} \right) \left\|QKz(x)\right\| \tag{10.41}$$

It follows that $\dot{V}$ is negative wherever it is defined (everywhere but on the sliding manifold), so the sliding manifold is indeed attractive as required. ■

10.6 Chattering Reduction

The state trajectories of ideal sliding motions are continuous functions of time contained entirely within the sliding manifold. These trajectories correspond to the equivalent control $u_{eq}(t)$. However, the actual control signal, $u(t)$ – definable only for nonideal trajectories – is discontinuous as a consequence of the switching mechanism which generates it. Persistent switching is undesirable in most applications. Several techniques have been proposed to reduce or eliminate it. These include: 'regularization' of the switch by replacing it with a continuous approximation; 'extension' of the dynamics by using additional integrators to separate an applied discontinuous pseudo-control from the actual plant inputs; and 'moderation' of the reaching control magnitude as errors become small.

Switch regularization entails replacing the ideal switching function, $\operatorname{sgn}(s(x))$ with a continuous function such as

$$\operatorname{sat}\left(\frac{1}{\varepsilon}s(x)\right) \quad \text{or} \quad \frac{s(x)}{\varepsilon + |s(x)|} \quad \text{or} \quad \tanh\left(\frac{s(x)}{\varepsilon}\right)$$

This intuitive approach is employed by Young and Kwatny [113] and Slotine and Sastry [97, 98] and there are probably historical precedents. Regularization induces

a boundary layer around the switching manifold whose size is $O(\varepsilon)$. The reaching behavior is altered significantly because the approach to the manifold is now exponential and the manifold is not reached in finite time as is the case with ideal switching. On the other hand within the boundary layer the trajectories are $O(\varepsilon)$ approximations to the sliding trajectories as established by Young et al [112] for linear dynamics with linear switching surfaces. Some of those results have been extended to single input–single output nonlinear systems by Marino [80]. Switch regularization for nonlinear systems has been extensively discussed by Slotine and coworkers, e.g., [97, 98]. With nonlinear systems there are subtleties and regularization can result in an unstable system. However, we can state the following result.

Suppose that each ideal switch is replaced by a smooth version of a switch . Specifically, $\text{sgn}(s) \to \tanh(s/\varepsilon)$, $\varepsilon > 0$ so that

$$u_i = -\sigma(x)\text{sgn}(s_i(x)) \to -\sigma(x)\tanh(s_i(x)/\varepsilon)$$

Then $\dot{V}$ is not necessarily negative for $\|s\|$ small. However, for any given $\delta > 0$ there exists a sufficiently small $\varepsilon > 0$ such that $\dot{V} < 0$, for $\|s\| > \delta$ so that all trajectories enter the strip $\|s(x)\| < \delta$. We wish to establish more than that. Namely, we will show that the smoothed control steers the state into a neighborhood of $z = 0$ the size of which shrinks with the design (smoothing) parameter ε.

Proposition 10.12. *Consider the system*

$$\dot{z} = Az + E[\alpha(x(\xi,z)) + \Delta(x(\xi,z),t) + \rho(x(\xi,z))u]$$

Suppose that

1. *there exists a continuous bound on α, $\|\alpha(x)\| < \sigma_\alpha(x)$*
2. *and a continuous bound on Δ, $\|\Delta(x,t)\| < \sigma_\Delta(x), \quad \forall t$*
3. *K is chosen in accordance with Proposition (10.9)*
4. *$u_i = -\sigma(x)\tanh(s_i(x)/\varepsilon)$, where*

$$\sigma(x) > (\bar{\sigma}(KA)\|z(x)\| + \sigma_\alpha(x) + \sigma_\Delta(x))\|QKz(x)\|$$

and $s^*(x) = \rho^T(x)QKz(x)$

Then for any $\delta > 0$ there exists a sufficiently small $\varepsilon > 0$ such that all trajectories enter the ball $\|z\| < \delta$ in finite time.

Proof: Since $KE = I$, we can divide the state space into $\text{Im}E \oplus \ker K$. Thus, we define a transformation (recall the proof of Proposition (10.9):

$$z = [E \quad N]\begin{bmatrix}\zeta_1 \\ \zeta_2\end{bmatrix}$$

where the columns of N span $\ker K$. Notice that we can choose a matrix M such that

$$\begin{bmatrix} K \\ M \end{bmatrix} [E \quad N] = I$$

which implies $K[I-EK]=0$, and $M[I-EK]=M$. In these new coordinates the evolution equations are

$$\begin{bmatrix} \dot{\zeta}_1 \\ \dot{\zeta}_2 \end{bmatrix} = \begin{bmatrix} KAE & KAN \\ MAE & MAN \end{bmatrix} \begin{bmatrix} \zeta_1 \\ \zeta_2 \end{bmatrix} + \begin{bmatrix} I \\ 0 \end{bmatrix} (\alpha(x) + \Delta(x,t) - \rho(x)\sigma(x)\tanh(s^*(x)/\varepsilon))$$

where

$$\tanh(s^*(x)/\varepsilon) = \begin{bmatrix} \tanh(s_1^*(x)/\varepsilon) \\ \vdots \\ \tanh(s_m^*(x)/\varepsilon) \end{bmatrix}$$

In addition, $s = Kz = \zeta_1$. Furthermore, $\mathrm{Re}\lambda(MAN) < 0$ by design ($MAN \sim A_s$). Hence, there exist matrices, $Q_0 \geq 0, R \geq 0$ such that

1. $z^T Q_0 z = 0$ for $z \in \mathrm{Im}E$ and $z^T Q_0 z > 0$ otherwise.
2. $d(z^T Q_0 z)/dt = -z^T R z \leq -\lambda_{\min} \|\zeta 2\|^2$, where $\lambda_{\min}$ is the smallest nonzero eigenvalue of R.

Now, consider the Liapunov function

$$V(z) = z^T Q_0 z + (Kz)^T QKz > 0, \quad \|z\| \neq 0$$

and compute

$$\begin{aligned} \tfrac{d}{dt}V &= 2\dot{z}Q_0 z + 2\dot{s}^T Qs \\ &= 2\{Az + b[\alpha + \Delta + \rho u]\}^T Q_0 z + 2[KAz + \alpha + \Delta]^T QKz + 2u^T \rho^T QKz \end{aligned}$$

$$\frac{d}{dt}V = 2\{Az\}^T Q_0 z + 2[KAz + \alpha + \Delta]^T QKz + 2u^T \rho^T QKz$$

Now, we have

$$\begin{aligned} &[KAz + \alpha + \Delta]^T QKz + u^T \rho^T QKx \leq \\ &\quad (\bar{\sigma}(KA)\|z(x)\| + \sigma_\alpha(x) + \sigma_\Delta(x))\|QKz(x)\| - \sigma(x)\sum_{i=1}^{m} |\tanh(s_i^*(x)/\varepsilon)| \end{aligned}$$

and

$$2\{Az\}^T Q_0 z \leq -\lambda_{\min}\|\zeta_2\|^2$$

so that

$$\frac{d}{dt}V \leq -\lambda_{\min}\|\zeta_2\|^2 + 2\left[\hat{\sigma} - \sigma\sum_{i=1}^{m} |\tanh(s_i^*/\varepsilon)|\right]$$

where

$$\hat{\sigma} = (\bar{\sigma}(KA)\,\|z(x)\| + \sigma_\alpha(x) + \sigma_\Delta(x))\,\|QKz(x)\|$$

Thus, since $\sigma > \hat{\sigma}$ by assumption, for any specified δ there is an ε such that $\dot{V} \leq -c < 0$. Consequently, we have all trajectories entering the strip $\|s\| < \delta(\varepsilon)$ in finite time. In fact, for any given $\delta > 0$ there exists a corresponding sufficiently small $\varepsilon > 0$. Now, since $s = \zeta_1$, it follows that $\|s\| < \delta \Rightarrow \|\zeta_1\| < \delta$. Consequently, from the evolution equations and since *MAN* is asymptotically (exponentially) stable we can conclude that all trajectories enter a ball with radius proportional to δ in finite time. ■

Dynamic extension is another effective approach to control input smoothing, see Emelyanov et al [25]. A sliding mode is said to be of p-th order relative to an output y if the time derivatives $\dot{y}, \ddot{y}, \ldots, y^{(p-1)}$ are continuous in t but y^p is not. The following observation is a straightforward consequence of the regular form proposition: Suppose the system (10.7) and (10.8) is input-output linearizable with vector relative degree $(r_1, \ldots, r_m)$. Then the sliding mode corresponding to the control law (10.22) is of order $p = \min(r_1, \ldots, r_m)$ relative to the output y. We may modify the relative degree by augmenting the system with input dynamics as described. Hence, we can directly control the smoothness of the output vector y.

When parasitic dynamics of sufficiently high order are present a form of persistent switching can arise that is not removed by the above smoothing strategies. This form of switching can be associated with a (series of) bifurcation(s) in the fast dynamics. It is commonly referred to as chattering. Control moderation can be effective in eliminating chattering. Control moderation involves design of the reaching control functions $u_i(x)$ such that the effective gain is reduced when errors are small, i.e., $|u_i(x)| \to$ small as $|e(x)| \to 0$. For example,

$$u_i(x) = |e(x)| \operatorname{sgn}(s_i(x))$$

Control moderation was used by Young and Kwatny [113] and the significance of this approach for chattering reduction in the presence of parasitic dynamics was discussed by Kwatny and Siu [68].

10.7 Computing Tools

We need to be able to reduce the system to normal form, compute an appropriate switching surface, assemble the switching control and insert smoothing and/or moderating functions as desired. Functions to do this are implemented in *ProPac*.

10.7.1 Sliding Surface Computations

There are several methods for determining the sliding surface, $s(x) = Kz(x)$, once the system has been reduced to normal form. We have included a function `SlidingSurface`

that implements two alternatives depending on the arguments provided. The function may be called via

```
{rho,s}=SlidingSurface[f,g,h,x,lam]
```

or

```
s=SlidingSurface[rho,vro,z,lam]
```

In the first case the data provided is the nonlinear system definition f, g, h, x and an m-vector *lam* which contains a list of desired exponential decay rates, one for each input channel. The function returns the decoupling matrix *rho* and the switching surfaces *s* as functions of the state *x*. The matrix *K* is obtained by solving the appropriate Ricatti equation.

The second use of the function assumes that the input-output linearization has already been performed so that the decoupling matrix *rho*, the vector relative degree *vro*, and the normal coordinate (partial) transformation $z(x)$ are known. In this case the dimension of each of the m switching surfaces is known so that it is possible to specify a complete set of eigenvalues for each surface. Thus, *lam* is a list of m-sublists containing the specified eigenvalues, grouped according to the vector relative degree. Only the switching surfaces are returned. In this case *K* is obtained via pole placement.

10.7.2 Switching Control

The function `SwitchingControl[rho,s,bounds,Q,opts]` where *rho* is the decoupling matrix, *s* is the vector of switching surfaces, *bounds* is a list of controller bounds each in the form {lower bound, upper bound}, *Q* is an $m \times m$ positive definite matrix (a design parameter that can be used, for example, to weight switching surfaces, see Utkin [1]), and *opts* are options which allow the inclusion of smoothing and/or moderating functions in the control. The bounds may be functions of the state. The alternative syntax

```
SwitchingControl[alpha,rho,s,bounds,Q,opts]
```

returns the control in the form of (10.28), i.e., it contains a smooth feedback linearizing part plus the discontinuous stabilizing part.

Smoothing functions are specified by a rule of the form

```
SmoothingFunctions[x_]->{function1[x],...,functionm[x]}
```

Where m is the number of controls. Moderating functions are similarly specified by a rule

```
ModeratingFunctions->{function1[z],...,functionm[z]}
```

The smoothing function option replaces the pure switch $\text{sgn}(s)$ by a smooth switch as specified. The moderating function option multiplies the switch by a specified function. We give an example below.

Example 10.13 (Variable structure control). We apply some of the above computations in the single input – single output, third order example shown below. First, we display the moderating ($|x|/(.002+|x|)$) and smoothing ($1-e^{-|x|/0.1}$) functions that will be employed.

In[231]:= **Plot**[**Abs**[x]/(0.002+**Abs**[x]), {x, −3, 3}]

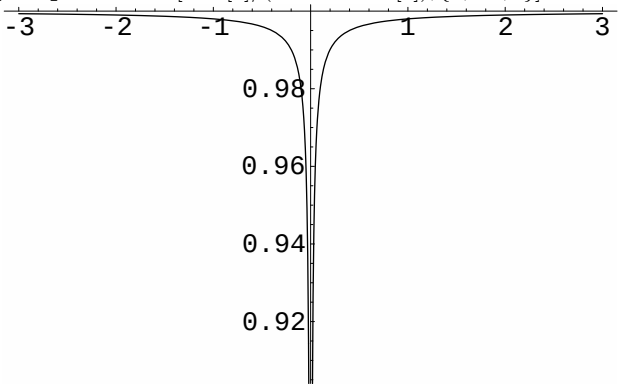

In[232]:= **Plot**[**Sign**[x] (1−Exp[−**Abs**[x/0.1]]), {x, −3, 3}, PlotRange−> All]

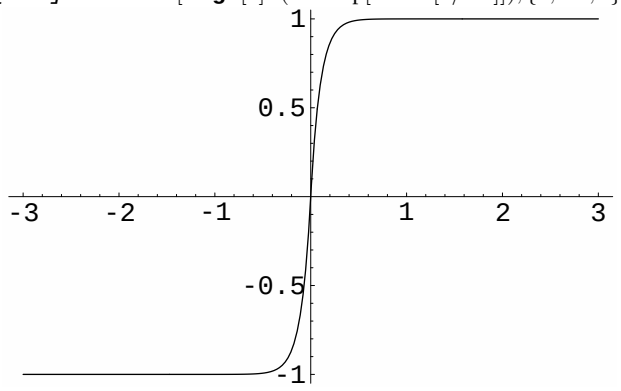

Now we apply input-output linearization. Since the relative degree is 2, there are one-dimensional zero dynamics. They are checked for stability before the control is designed.

```
In[233]:= x = {x1, x2, x3};
          f = {x2, x3, -x1 - x2^2 - Sin[x3]};
          g = {0, 1 + x1^3, 1};
          h = {x1};
          {ρ, α, vro, control} = IOLinearize[f, g, h, {x1, x2, x3}]
```

$$\text{Out[233]= } \left\{\{\{1+x1^3\}\}, \{x3\}, \{2\}, \left\{\frac{v1-x3}{1+x1^3}\right\}\right\}$$

```
In[234]:= z = NormalCoordinates[f, g, h, {x1, x2, x3}, vro];
          u0 = control /. v1 -> 0;
          LocalZeroDynamics[f, g, h, x, u0, z]
```

$$\text{Out[234]= } \left\{-2 \;\; w1 + \frac{w1^3}{6}\right\}$$

Since we have a stable equilibrium point we proceed to design a sliding surface. We have already computed the normal coordinates, so we can specify poles at -2,-3 and compute the sliding surface.

```
In[235]:= s = SlidingSurface[ρ, vro, z, {{-2, -3}}];
          SwitchingControl[ρ, s, {{-1, 1}}, {{1}}]
```

$$\text{Out[235]= } \{-Sign[(1+x1^3) \;\; (6 \;\; x1+5 \;\; x2)]\}$$

Now, we compute the switching control using various combinations of smoothing and moderating functions. The particular functions chosen for this example are shown below in Figure 6. Results can change significantly when other functions are used or when the parameters of the functions are varied. We specify the control bounds as ± 1 and $Q = 1$. The following computation yields the controls.

```
In[236]:= SwitchingControl[ρ, s, {{-1, 1}}, {{1}},
            SmoothingFunctions[xx_] -> {(1 - Exp[-Abs[xx/10]])}]
```

$$\text{Out[236]= } \left\{-Sign[(1+x1^3) \;\; (6 \;\; x1+5 \;\; x2)] + e^{-\frac{1}{10} \;\; Abs\left[\left(1+x1^3\right) \;\; (6 \;\; x1+5 \;\; x2)\right]} \;\; Sign[(1+x1^3) \;\; (6 \;\; x1+5 \;\; x2)]\right\}$$

```
In[237]:= SwitchingControl[ρ, s, {{-1, 1}}, {{1}},
            ModeratingFunctions -> {Abs[z[[1]]]/(0.005 + Abs[z[[1]]])}]
```

$$\text{Out[237]= } \left\{-\frac{Abs[x1] \;\; Sign[(1+x1^3) \;\; (6 \;\; x1+5 \;\; x2)]}{0.005 + Abs[x1]}\right\}$$

10.8 Backstepping Design of VS Controls

We will describe a backstepping procedure for SISO variable structure control system design in the presence of uncertain, possibly nonsmooth, nonlinearities as intro-

duced in [69]. The method differs from the backstepping techniques described in the previous chapter in the following ways: (1) the states are grouped in accordance with the appearance of the uncertainty in the system, and (2) the control designed at each step is a variable structure control. We do not assume that uncertainty enters in every state equation. Thus, the number of steps can be reduced. This is important when nonsmooth uncertainties are present as will be evident in the examples below.

Consider a SISO nonlinear system in the (multi-state backstepping) form:

$$\begin{aligned} x_i^{(n_i)} &= x_{i+1} + \Delta_i(x,t), \quad i = 1,\ldots,p-1 \\ x_p^{(n_p)} &= \alpha(x) + \rho(x)u + \Delta_p(x,t) \\ y &= x_1 \end{aligned} \tag{10.42}$$

We assume that the (possibly nonsmooth) uncertainties $\Delta_i(x,t)$ are bounded by smooth, non-negative functions $\sigma_i(x)$, i.e.,

$$0 \le |\Delta_i(x,t)| \le \sigma_i(x), \quad \forall t \tag{10.43}$$

As noted before, such a model might arise by reduction of a smooth nominal system to regular from and applying the transformation to the (possibly nonsmooth) uncertain system.

The basic idea is very simple. At each of $p-1$ stages we design a 'pseudo-control' v_k, at the k^{th} step (with $v_0 = 0$), using the system

$$\begin{aligned} x_i^{(n_i)} &= v_i + \Delta_i(x,t), \quad i = 1,\ldots,k < p \\ y_k &= x_k - v_{k-1}(x_1,\ldots,x_{k-1}^{n_{k-1}}) \end{aligned}$$

and at the last (p^{th}) stage we design the actual control, u, using the system

$$\begin{aligned} x_i^{(n_i)} &= v_i + \Delta_i(x,t), \quad i = 1,\ldots,p-1 \\ x_p^{(n_p)} &= \alpha(x) + \rho(x)u + \Delta_p(x,t) \\ y_p &= x_p - v_{p-1}(x_1,\ldots,x_{p-1}^{n_{p-1}}) \end{aligned}$$

To design the control v_k we first reduce the k^{th} system to normal form by successive differentiation in the usual way. Thus, we identify the new coordinate $y_k,\ldots,y_k^{(n_k-1)}$ that will replace $x_k,\ldots,x_k^{(n_k-1)}$. The transformed evolution equation is

$$y_k^{(n_k)} = L_{f_k}^{n_k} h_k + L_{g_k} L_{f_k}^{n_k-1} v_k = L_{f_k}^{n_k} h_k + v_k = \alpha_k + v_k \tag{10.44}$$

For analysis purposes it is convenient to carry the equations along in the transformed coordinates as the process proceeds. Doing so explicitly, the k^{th} control is obtained by designing a stabilizing smoothed VS controller for a ('nominal') system in the form:

1. $k = 1$

$$\begin{aligned} x_1^{(n_1)} &= v_1 \\ y_1 &= x_1 \end{aligned} \tag{10.45}$$

2. $k = 2$

$$\begin{aligned} y_1^{(n_1)} &= x_2 \\ x_2^{(n_2)} &= v_2 \\ y_2 &= x_2 - v_1 \end{aligned} \tag{10.46}$$

3. $k = 3, \ldots, p-1$

$$\begin{aligned} y_i^{(n_i)} &= y_{i+1} + \alpha_i + v_i, \quad i = 1, \ldots, k-2 \\ y_{k-1}^{(n_{k-1})} &= \alpha_{k-1} + x_k, \\ x_k^{(n_k)} &= v_k \\ y_k &= x_k - v_{k-1} \end{aligned} \tag{10.47}$$

4. $k = p$

$$\begin{aligned} y_i^{(n_i)} &= y_{i+1} + \alpha_i + v_i, \quad i = 1, \ldots, p-2 \\ y_{p-1}^{(n_{p-1})} &= \alpha_{p-1} + x_p, \\ x_p^{(n_p)} &= \alpha + \rho v_p \\ y_p &= x_p - v_{p-1} \end{aligned} \tag{10.48}$$

Notice that the zero dynamics of the k^{th} system (10.47) are

$$\begin{aligned} y_i^{(n_i)} &= y_{i+1} + \alpha_i + v_i, \quad i = 1, \ldots, k-2 \\ y_{k-1}^{(n_{k-1})} &= \alpha_{k-1} + v_{k-1} \end{aligned} \tag{10.49}$$

Now, we design a VS stabilizing controller, $v_k(y_k, \ldots, k_k^{(n_i)})$ such that $y_k(t) \to 0$ as $t \to \infty$. For each $k < p$ we smooth the controller so that the process can be continued. Working in this way through the p stages, and redefining the states ($x \to y$) at each stage we arrive at the final set of dynamical equations.

$$\begin{aligned} y_i^{(n_i)} &= y_{i+1} + \alpha_i + v_i(y_i, \ldots y_i^{(n_i-1)}) \quad i = 1, \ldots, p-1 \\ y_p^{(n_p)} &= \alpha + \alpha_p + \rho u(y_p, \ldots y_p^{(n_p-1)}) \end{aligned} \tag{10.50}$$

Notice the triangular structure of the transformed nominal system (10.50). It is illustrated in Figure (10.2).

Now, let us define the procedure in detail.

Algorithm 10.14 (Variable Structure Backstepping Algorithm) *The state transformation and control are constructed sequentially as follows:*

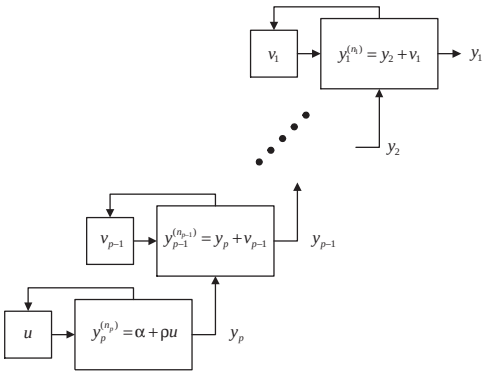

Fig. 10.2: The triangular structure of the closed loop (nominal) dynamics achieved with the multistate backstep control design.

1. $k = 1$ *define the vector fields* $\hat{f}_1$, g_1 *and the scalar function* $\hat{h}_1$*:*

$$\hat{f}_1 = \begin{bmatrix} \dot{x}_1 \\ \vdots \\ x_1^{(n_1-1)} \\ 0 \end{bmatrix}, \quad g_1 = \begin{bmatrix} 0 \\ \vdots \\ 0 \\ 1 \end{bmatrix}$$

$$y_1 = \hat{h}_1(x_1) = x_1$$

Now define the new state variables:

$$\begin{aligned} z_1^1 &= y_1 = \hat{h}_1 \\ z_2^1 &= \dot{y}_1 = L_{\hat{f}_1}\hat{h}_1 \\ &\vdots \\ z_{n_1}^1 &= y_1^{(n_1-1)} = L_{\hat{f}_1}^{n_1-1}\hat{h}_1 \end{aligned}$$

which leads to the state space description

$$\dot{Z}^1 = f_1(Z^1) + g_1 v_1 = \begin{bmatrix} z_2^1 \\ \vdots \\ z_{n_1}^1 \\ L_{\hat{f}_1}^{n_1}\hat{h}_1 \end{bmatrix} + \begin{bmatrix} 0 \\ \vdots \\ 0 \\ 1 \end{bmatrix} v_1$$

$$y_1 = h_1(Z^1) = z_1^1$$

where $Z^1 = \left[z_1^1, \ldots, z_{n_1}^1\right]^T$*. This is the state space equivalent to Equation (10.45). Now, design the smoothed variable structure controller* v_1*.*

2. $k = 2, \ldots, p-1$ *Define* $\hat{f}_k$, g_k, *and* $\hat{h}_k$

$$\hat{f}_k = \begin{bmatrix} f_{k-1}(Z^{k-1}) + g_{k-1} v_{k-2}(z^{k-2}) \\ \dot{x}_k \\ \vdots \\ x_k^{(n_k-1)} \\ 0 \end{bmatrix}, \quad g_k = \begin{bmatrix} 0 \\ \vdots \\ \vdots \\ 0 \\ 1 \end{bmatrix}$$

$$y_k = \hat{h}_k(Z^{k-1}, x_k) = x_k - v_{k-1}(z^{k-1})$$

where

$$Z^{k-1} = \left[\left(Z^{k-2} \right)^T, z_1^{k-1}, \ldots, z_{n_{k-1}}^{k-1} \right]^T$$

Define the next group of new states

$$\begin{aligned} z_1^k &= y_k = \hat{h}_k \\ z_2^k &= \dot{y}_k = L_{\hat{f}_k} \hat{h}_k \\ &\vdots \\ z_{n_k}^k &= y_k^{(n_k-1)} = L_{\hat{f}_k}^{n_k-1} \hat{h}_k \end{aligned}$$

Write the state space equivalent to (10.47).

$$\dot{Z}^k = f_k(Z^k) + g_k v_k = \begin{bmatrix} f_{k-1}(Z^{k-1}) + g_{k-1} v_{k-2}(z^{k-2}) \\ z_2^k \\ \vdots \\ z_{n_k}^k \\ L_{\hat{f}}^{n_k} \hat{h}_k \end{bmatrix} + \begin{bmatrix} 0 \\ \vdots \\ \vdots \\ 0 \\ 1 \end{bmatrix} v_k$$

$$y_k = h_k(Z^k) = z_1^k - v_{k-1}(z^{k-1})$$

and design the smoothed variable structure control v_k.

3. $k = p$ $\hat{f}_p$, g_p, *and* $\hat{h}_p$ *are defined as above for general k. Now introduce the last group of new states*

$$\begin{aligned} z_1^p &= y_p = \hat{h}_p \\ z_2^p &= \dot{y}_p = L_{\hat{f}_p} \hat{h}_p \\ &\vdots \\ z_{n_p}^p &= y_p^{(n_p-1)} = L_{\hat{f}_p}^{n_p-1} \hat{h}_p \end{aligned}$$

to obtain the state space equivalent to (10.48).

$$\dot{Z}^p = f_p(Z^p)+g_p(\alpha+\rho v_p) = \begin{bmatrix} f_{p-1}(Z^{p-1})+g_{p-1}v_{p-2}(z^{p-2}) \\ z_2^p \\ \vdots \\ z_{n_p}^p \\ L_{\hat{f}_p}^{n_p}\hat{h}_p \end{bmatrix} + \begin{bmatrix} 0 \\ \vdots \\ \vdots \\ 0 \\ 1 \end{bmatrix} (\alpha+\rho v_p)$$

$$Z^p = \begin{bmatrix} Z^{p-1} \\ z^p \end{bmatrix} \in R^{n_1+\cdots+n_p}$$

$$y_p = h_p(Z^p) = z_1^p - v_{p-1}(z^{p-1})$$

Finally, design the variable structure controller v_p.

Now we apply this transformation to the actual system (10.42).

Lemma 10.15. *Consider the transformation defined recursively according to Algorithm (10.14). When applied to the actual system (10.42) the transformed evolution equations are*

$$\begin{array}{l} y_i^{(n_i)} = y_{i+1} + \alpha_i + \Delta_i + v_i(y_i, \ldots y_i^{(n_i-1)}) \quad i = 1, \ldots, p-1 \\ y_p^{(n_p)} = \alpha + \alpha_p + \Delta_p + \rho u(y_p, \ldots y_p^{(n_p-1)}) \end{array} \tag{10.51}$$

Proof: Notice that at each stage of Algorithm (10.14), for $k = 1, \ldots, p-1$, n_k new state variables are defined and n_k first order equations are added to the system. The first $n_k - 1$ equations come from the state definitions, i.e. the defining equations

$$\begin{aligned} z_1^k &= y_k = \hat{h}_k \\ z_2^k &= \dot{y}_k = L_{\hat{f}_k}\hat{h}_k \\ &\vdots \\ z_{n_k}^k &= y_k^{(n_k-1)} = L_{\hat{f}_k}^{n_k-1}\hat{h}_k \end{aligned}$$

imply

$$\begin{aligned} \dot{y}_k &= \dot{z}_1^k = z_2^k \\ &\vdots \\ y_k^{(n_k-1)} &= \dot{z}_{n_k-1}^k = z_{n_k}^k \end{aligned}$$

The final equation is obtained by differentiating the last definition and using the evolution equation $x_k^{(n_k)} = v_k$ in the nominal case and $x_k^{(n_k)} = \Delta_k + v_k$ in the actual case, leading to

$$y_k^{(n_k)} = \dot{z}_{n_k}^k = L_{\hat{f}_k}^{n_k}\hat{h}_k + L_{\hat{g}_k}L_{\hat{f}_k}^{n_k-1}\hat{h}_k v_k = L_{\hat{f}_k}^{n_k}\hat{h}_k + v_k$$

in the nominal case, and

$$y_k^{(n_k)} = \dot{z}_{n_k}^k = L_{\hat{f}_k}^{n_k}\hat{h}_k + L_{\hat{g}_k}L_{\hat{f}_k}^{n_k-1}\hat{h}_k(\Delta_k + \nu_k) = L_{\hat{f}_k}^{n_k}\hat{h}_k + \Delta_k + \nu_k$$

in the actual case.

The case $k = p$ is similar except that $\alpha + \rho\nu_p$ is replaced by $\alpha + \Delta_p + \rho\nu_p$. ■

The idea for establishing stability is roughly as follows. A VS controller is designed for system p, (10.50), via methods described above. The system is stable if and only if the zero dynamics,

$$\begin{aligned} y_i^{(n_i)} &= y_{i+1} + \alpha_i + \nu_i(y_i, \ldots y_i^{(n_i-1)}) \quad i = 1, \ldots, p-2 \\ y_{p-1}^{(n_{p-1})} &= \alpha_{p-1} + \nu_{p-1}(y_{p-1}, \ldots y_{p-1}^{(n_{p-1}-1)}) \end{aligned} \tag{10.52}$$

are stable. But, ν_{p-1} is itself a (smoothed) VS control so that (10.52) is stable if its zero dynamics:

$$\begin{aligned} y_i^{(n_i)} &= y_{i+1} + \alpha_i + \nu_i(y_i, \ldots y_i^{(n_i-1)}) \quad i = 1, \ldots, p-3 \\ y_{p-2}^{(n_{p-2})} &= \alpha_{p-2} + \nu_{p-2}(y_{p-2}, \ldots y_{p-2}^{(n_{p-2}-1)}) \end{aligned} \tag{10.53}$$

are stable. The argument proceeds in this way.

Proposition 10.16. *Consider the system (10.42) and suppose the uncertainties Δ_i satisfy the inequality (10.43) with continuous bounding functions ε_i, and α also has a continuous bounding function σ_α. Suppose that a controller is designed via the backstepping procedure of Algorithm (10.14) and each control ν_k, $k = 1, \ldots, p$ is a smoothed variable structure controller designed in accordance with the assumptions of Proposition (10.12). Then for any given $\delta > 0$ there is a sufficiently small smoothing parameter $\varepsilon > 0$ such that all trajectories enter the ball $\|y\| < \delta$.*

Proof: The p-th system

$$y_p^{(n_p)} = \alpha + \alpha_p + \Delta_p + \rho\nu_p(y_p, \ldots y_p^{(n_p-1)}) \tag{10.54}$$

satisfies the conditions of Proposition (10.12) with $z_i = y_p^{(i-1)}$, $i = 1, \ldots, n_p$. Hence, we conclude that y_p (and its $n_p - 1$ derivatives) will be driven, in finite time, into a δ-neighborhood of the origin with a suitably small smoothing parameter. Now, the $p-1$ system is

$$y_{p-1}^{(n_{p-1})} = y_p(t) + \alpha_{p-1} + \Delta_{p-1} + \nu_{p-1}(y_{p-1}, \ldots y_{p-1}^{(n_{p-1}-1)}) \tag{10.55}$$

and $\left|y_p(t)\right| \leq \delta$, $\forall t > t^* < \infty$. Thus, we can incorporate $y_p(t)$ into $\Delta_{p-1}(x,t)$. It follows that (10.55) satisfies the conditions of Proposition (10.12) for $t > t^*$, $z_i = y_{p-1}^{(i-1)}$, $i = 1, \ldots, n_{p-1}$, so that y_{p-1} (and its $n_{p-1} - 1$ derivatives) will be driven, in finite time, into a δ-neighborhood of the origin with a suitably small smoothing parameter. We continue in this way for systems $k = p-2, \ldots, 1$ to establish the conclusion of the theorem. ■

Example 10.17 (Nonsmooth, Uncertain Friction). Consider a simple system with a nonlinear, nonsmooth friction:

$$\begin{aligned}\dot{\theta} &= \omega\\ \dot{\omega} &= -\phi_{fr}(\omega) + \mu\\ \dot{\mu} &= u\end{aligned}$$

with

$$\phi_{fr} = \operatorname{sgn}(\omega)$$

Suppose the friction to be composed of a smooth nominal part and a nonsmooth uncertain part, i.e.,

$$\phi_{fr} = \tanh(\omega/0.02) + \Delta(\omega), \quad \Delta(\omega) = \operatorname{sgn}(\omega) - \tanh(\omega/\varepsilon), \quad \varepsilon > 0$$

Thus, the nominal system is

$$\begin{aligned}\dot{\theta} &= \omega\\ \dot{\omega} &= -\tanh(\omega/0.02) + \mu\\ \dot{\mu} &= u\end{aligned}$$

and the uncertainty is bounded by $\sigma_\Delta = const. > 1$.

Now, we complete step 1 and compute the smoothed variable structure (psuedo-) control, vs1:

```
In[238]:= f1 = {ω, -Tanh[ω/0.02]};
          g1 = {0,1};
          h1 = {θ};
          {rho1,s1} = SlidingSurface[f1,g1,h1,{θ,ω},{2}]

          ctrlbnds = {{-5,5}};
          Q = {{1}};
          vsc1 = SwitchingControl[rho1,s1,ctrlbnds,Q,S
              SmoothingFunctions[x_]->{Tanh[x/0.01]}]
Out[238]= {-5  Tanh[100.  ω+423.607  θ]}
```

In step 2 we compute the actual control vs2. It is designed without smoothing or moderation.

```
In[239]:= f = {ω, -Tanh[ω/0.02]+uu  ,0};
          g = {0,0,1};
          h = {uu-vsc1[[1]]};
          {rho2,s2} = SlidingSurface[f,g,h,{θ,ω,uu},{20}]

          ctrlbnds = {{-5,5}};
          Q = {{1}};
          vsc2 = SwitchingControl[rho2,s2,ctrlbnds,Q]
```

```
Out[239]= {5 Sign[-uu - 5 Tanh[100. ω + 423.607 θ]]}
```

Now, we set up the equations for numerical computation. Notice that the actual plant friction function is taken to be $\mathrm{sgn}(\omega)$ which corresponds to taking $\varepsilon = 0.02$.

```
In[240]:= ReplacementRules =
            Inner[Rule, {θ, ω, uu}, {θ[t], ω[t], uu[t]}, List];

In[241]:= {Surf} = s2 /. ReplacementRules;
          Surf
Out[241]= 5 Tanh[100. ω[t] + 423.607 θ[t]] + uu[t]

In[242]:= {VSControl} = vsc2 /. ReplacementRules;
          VSControl
Out[242]= 5 Sign[-5 Tanh[100. ω[t] + 423.607 θ[t]] - uu[t]]

In[243]:= VSsols =
            NDSolve[{∂t theta[t] == ω[t], ∂t ω[t] == -Sign[ω[t]] + uu[t],
                ∂t uu[t] == VSControl, ω[0] == 0.2, θ[0] == 0, uu[0] == 0},
              {θ[t], ω[t], uu[t]}, {t, 0, 10}, AccuracyGoal → 2,
              PrecisionGoal -> 1, MaxStepSize -> 10/60000, MaxSteps → 60000];
```

Here are some selected results.

```
In[244]:= Plot[Evaluate[{θ[t]} /. VSsols],
            {t, 0, 9}, PlotRange -> All, AxesLabel → {t, θ}];
          Plot[Evaluate[{ω[t]} /. VSsols],
            {t, 0, 9}, PlotRange -> All, AxesLabel → {t, ω}];
          Plot[Evaluate[{VSControl} /. VSsols],
            {t, 0, 9}, PlotRange -> All, AxesLabel → {t, u}];
          ParametricPlot[Evaluate[{θ[t], ω[t]} /. VSsols], {t, 0, 9},
            PlotRange -> All, AxesLabel → {θ, ω}]
```

Here is the output θ as a function of time. Stability is clearly evident.

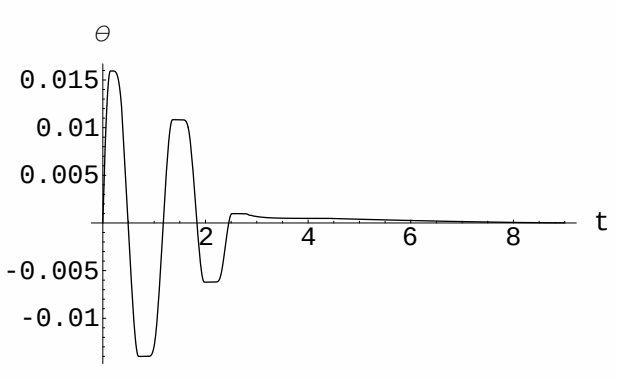

The following plot of angular velocity ω shows the 'stiction' effect of the discontinuous nonlinear friction.

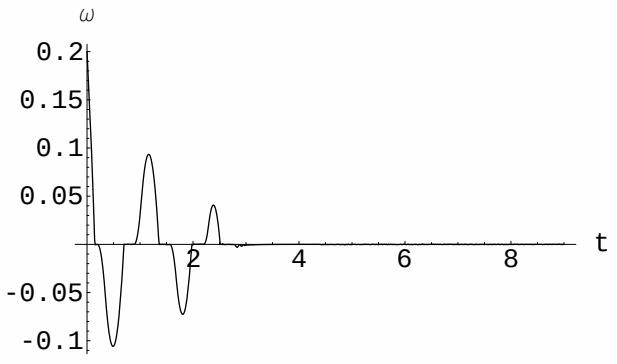

The switching control is shown in the following figure.

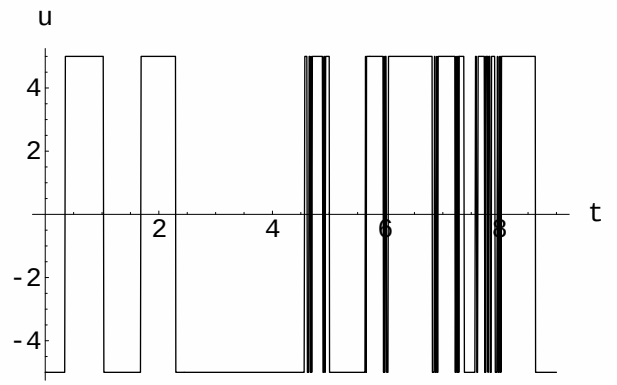

Finally, a phase plot of ω versus θ indicates that *theta* does not go to the origin. Of course, the ultimate error is controlled by choice of smoothing parameter in step 1.

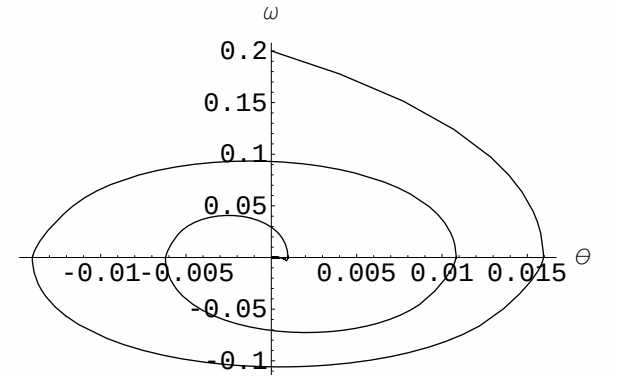

These results clearly illustrate the anticipated properties.

Example 10.18 (Motor-Load System with Nonsmooth friction). Consider a motor-load system illustrated in Figure (10.3) and described by Equation (10.56).

$$\dot{x} = \begin{bmatrix} \omega_1 \\ \theta_2 - \theta_1 - \omega_1/10 \\ \omega_2 \\ \theta_1 - \theta_2 - \omega_2/2 \end{bmatrix} + \begin{bmatrix} 0 \\ -\frac{1}{10}\left(1 + \frac{1}{10}\exp^{-(\omega_1/0.02)^2}\right)\text{sgn}\omega_1 \\ 0 \\ -\frac{1}{10}\text{sgn}\omega_2 \end{bmatrix} + \begin{bmatrix} 0 \\ 0 \\ 0 \\ 1 \end{bmatrix} u \quad (10.56)$$

We begin by reducing the nominal system to normal form.

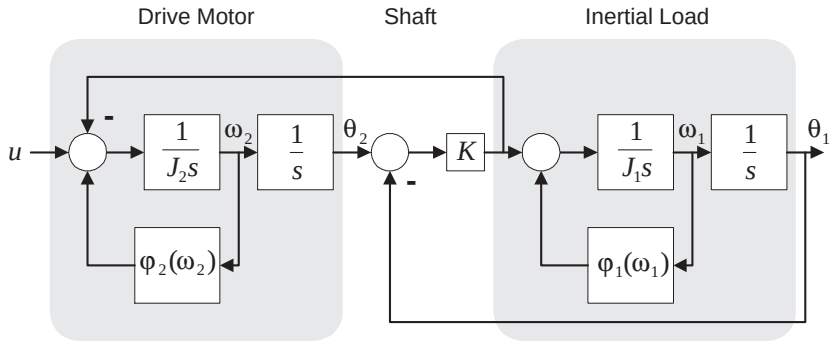

Fig. 10.3: A typical drive system consisting of a motor and an inertial load. The nonlinear friction functions, φ_1 and φ_2 contain uncertain discontinuous components.

```
In[245]:= f =
            {omega1, theta2 - theta1 - omega1/10, omega2, theta1 - theta2 -  omega2/2};
          g = {0, 0, 0, 1};
          h = theta1;

In[246]:= Df = {0, -(1 + Exp[-(omega1/0.02)^2]/10)  Sign[omega1]/10, 0,
              -Sign[omega2]/10};

In[247]:= {T1, T2} =
            Chop[SISONormalFormTrans[f, g, h, {theta1, omega1, theta2, omega2}]];

In[248]:= InvTrans = InverseTransformation[{theta1, omega1, theta2, omega2},
              {x1, x2, x3, x4}, T1];
```

InverseTransformation : $\{\text{theta1}, \text{omega1}, \text{theta2}, \text{omega2}\} = \{\text{x1}, \text{x2}, \frac{1}{10}\ (10\ \ \text{x1} + \text{x2} + 10\ \ \text{x3}),$

$\frac{1}{10}\ (10\ \ \text{x2} + \text{x3} + 10\ \ \text{x4})\}$

The following calculation applies the transformation to the actual (perturbed) system.

```
In[249]:= {fnew, gnew, hnew} = Chop[TransformSystem[f, g, h,
              {theta1, omega1, theta2, omega2}, {x1, x2, x3, x4}, T1, InvTrans]];

In[250]:= {ff, gg, hh} = Chop[TransformSystem[f + Df, g, h,
              {theta1, omega1, theta2, omega2}, {x1, x2, x3, x4}, T1, InvTrans]];

In[251]:= N[ff]
Out[251]= {x2, x3 + 0.01  (-10. - 1.  2.71828^(-2500.  x2^2))  Sign[x2],
            x4 + 0.001  (10. + 2.71828^(-2500.  x2^2))  Sign[x2],
            0.0099  (10. + 2.71828^(-2500.  x2^2))  Sign[x2] +
              0.05  (-12.  x2 - 41.  x3 - 12.  x4 - 2.  Sign[x2 + 0.1  x3 + x4])}
```

Now, the backstepping procedure is applied. Observe the structure of the actual system in normal form. Because uncertainties enter the right hand sides of the second, third and fourth equations, three steps will be required.

1st Step

```
In[252]:= f1 = {x2, 0};
          g1 = {0, 1};
          h1 = {x1};
          {rho1, s1} = SlidingSurface[f1, g1, h1, {x1, x2}, {2}];

In[253]:= ctrlbnds = {{-1, 1}};
          Q = {{1}};
          vsc1 = SwitchingControl[rho1, s1, ctrlbnds, Q,
              SmoothingFunctions[x_] -> {Tanh[x/0.1]}];
```

2nd Step

```
In[254]:= f2 = {x2, x3, 0};
          g2 = {0, 0, 1};
          h2 = {x3 - vsc1[[1]]};
          {rho2, s2} = SlidingSurface[f2, g2, h2, {x1, x2, x3}, {5}];

In[255]:= ctrlbnds = {{-5, 5}};
          Q = {{1}};
          vsc2 = SwitchingControl[rho2, s2, ctrlbnds, Q,
              SmoothingFunctions[x_] -> {Tanh[x/0.1]}];

In[256]:= {T1, T2} = Chop[SISONormalFormTrans[f2, g2, h2, {x1, x2, x3}]];
```

3rd Step

```
In[257]:= f3 = fnew;
          g3 = gnew;
          h3 = Chop[SetAccuracy[{x4 - vsc2[[1]]}, 4], 10^(-4)];
```

It is important to get an estimate of bounds on α in order to set appropriate control bounds.

```
In[258]:= {ρ, α, ro, control} = IOLinearize[f3, g3, h3, {x1, x2, x3, x4}];

In[259]:= Coefficient[Truncate[α[[1]], {x1, x2, x3, x4}, 1], {x1, x2, x3, x4}]
Out[259]= {0, 2117., 498., 49.4}

In[260]:= b = 5 (1 + 10 Abs[x4] + 100 Abs[x3] + 500 Abs[x2]);
```

As it turns out, these bounds are fairly tight. Reducing them significantly rsults in very degraded performance – even of the nominal system.

```
In[261]:= {rho3, s3} = SlidingSurface[f3, g3, h3, {x1, x2, z3, x4}, {20}];

In[262]:= ctrlbnds = {{-b, b}};
          Q = {{1}};
          vsc3 = SwitchingControl[rho3, s3, ctrlbnds, Q,
              SmoothingFunctions[x_] -> {Tanh[x/0.04]}];
```

Simulation of the Actual Plant

```
In[263]:= InitialConds = {x1(0) == 0, x2(0) == 0.2, x3(0) == 0, x4(0) == 0};
          Eqns = MakeODEs[{x1, x2, x3, x4}, ff + ggvsc3[[1]], t];

In[264]:= VSsols = NDSolve[Join[Eqns, InitialConds], {x1(t), x2(t), x3(t), x4(t)}, {t, 0, 4},
          AccuracyGoal -> 2, PrecisionGoal -> 1, MaxStepSize -> 4/60000, MaxSteps -> 60000];

In[265]:= Plot[Evaluate[{x1[t]} /. VSsols],
            {t, 0, 2}, PlotRange -> All, AxesLabel -> {t, θ1}];
          Plot[Evaluate[{x2[t]} /. VSsols],
            {t, 0, 2}, PlotRange -> All, AxesLabel -> {t, ω1}];
          Plot[Evaluate[{x3[t]} /. VSsols],
            {t, 0, 2}, PlotRange -> All, AxesLabel -> {t, x3}];
          Plot[Evaluate[{x4[t]} /. VSsols],
            {t, 0, 2}, PlotRange -> All, AxesLabel -> {t, x4}];
```

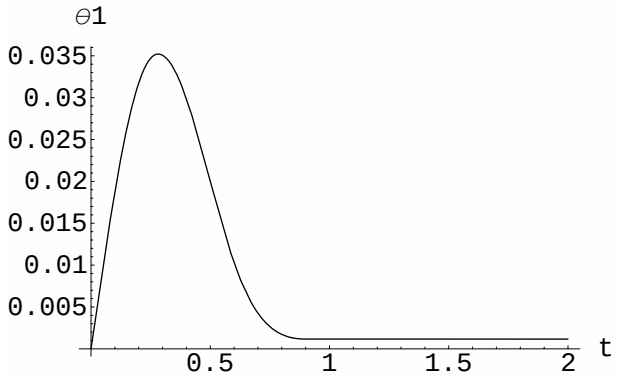

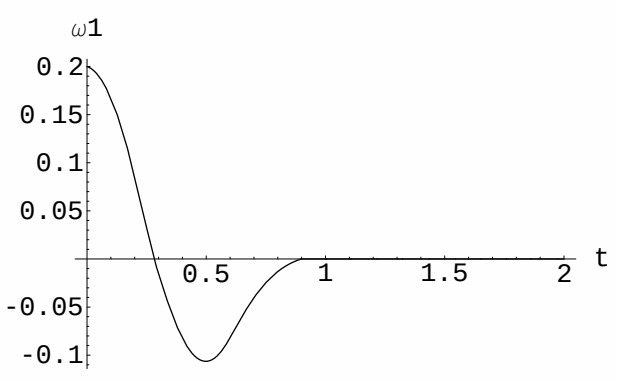
ω1
0.2
0.15
0.1
0.05
-0.05
-0.1
0.5
1
1.5
2
t

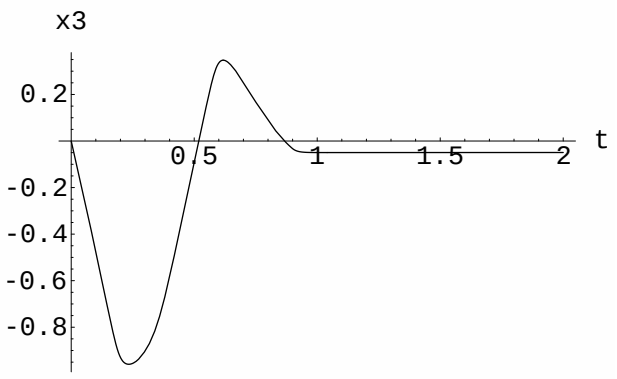
x3
0.2
-0.2
-0.4
-0.6
-0.8
0.5
1
1.5
2
t

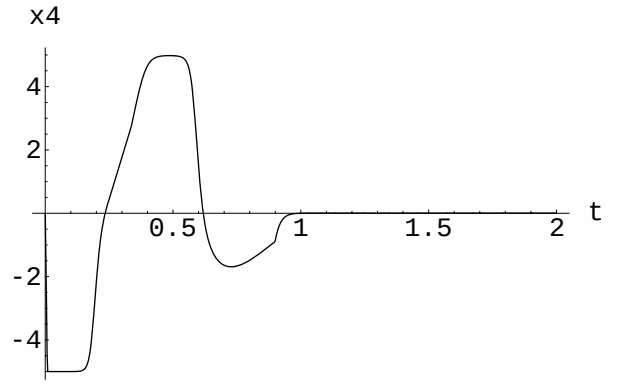
x4
4
2
-2
-4
0.5
1
1.5
2
t

```
In[266]:= Control = vsc3[[1]]/.ReplacementRules;
          Plot[Evaluate[{Control}/.VSsols], {t,0,2}, AxesLabel → {t,u}];
```

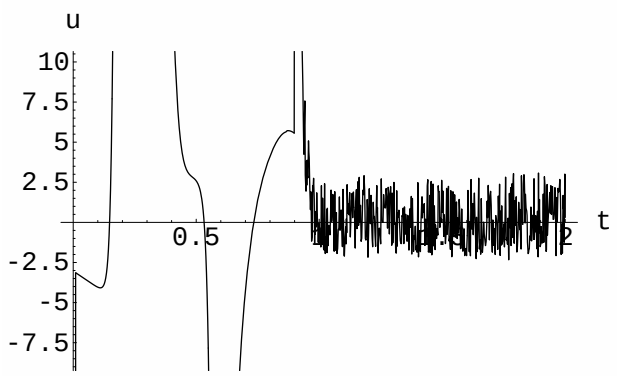

Notice that the position error does not reduce to zero. This is as expected, because of the smoothing of the controllers. By decreasing the smoothing parameter, of course, the error is reduce. On the other hand the (peak) control effort increases. As it is, control effort is quite substantial.

Simulation with Different Initial Conditions

The following computations illustrate response from a different set of initial conditions.

```
In[267]:= InitialConds = {x1[0] == 0.2, x2[0] == 0, x3[0] == 0, x4[0] == 0};

In[268]:= VSsols = NDSolve[Join[Eqns, InitialConds],
              {x1[t], x2[t], x3[t], x4[t]}, {t,0,10}, AccuracyGoal → 2,
              PrecisionGoal− > 1, MaxStepSize− > 10/60000, MaxSteps → 60000];

In[269]:= Plot[Evaluate[{x1[t]} /. VSsols],
            {t,0,4}, PlotRange− > All, AxesLabel → {t, θ1}];
          Plot[Evaluate[{x2[t]} /. VSsols],
            {t,0, 4}, PlotRange− > All, AxesLabel → {t, ω1}];
          Plot[Evaluate[{x3[t]} /. VSsols],
            {t,0, 4}, PlotRange− > All, AxesLabel → {t, x3}];
          Plot[Evaluate[{x4[t]} /. VSsols],
            {t,0, 4}, PlotRange− > All, AxesLabel → {t, x4}];
```

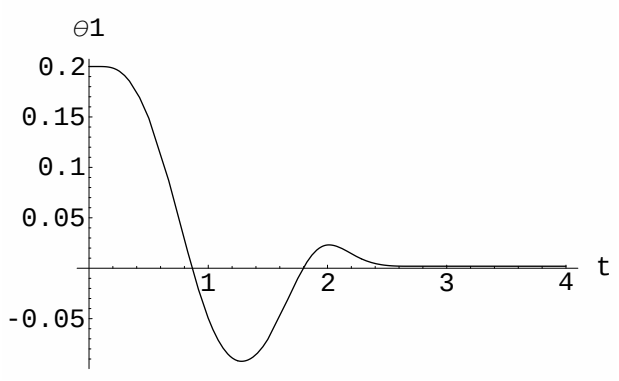
θ1
0.2
0.15
0.1
0.05
-0.05
1
2
3
4
t

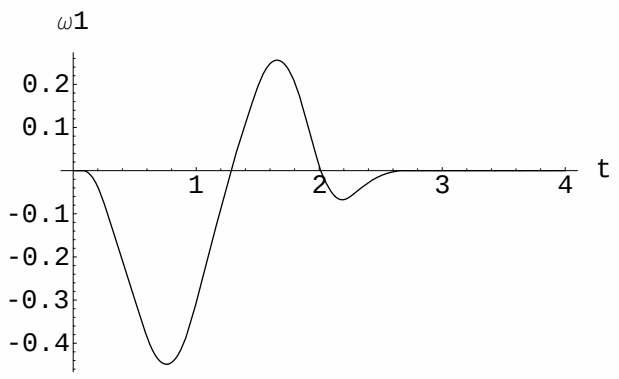
ω1
0.2
0.1
-0.1
-0.2
-0.3
-0.4
1
2
3
4
t

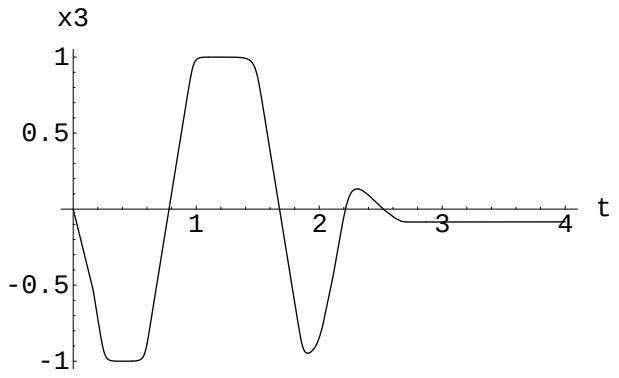
x3
1
0.5
-0.5
-1
1
2
3
4
t

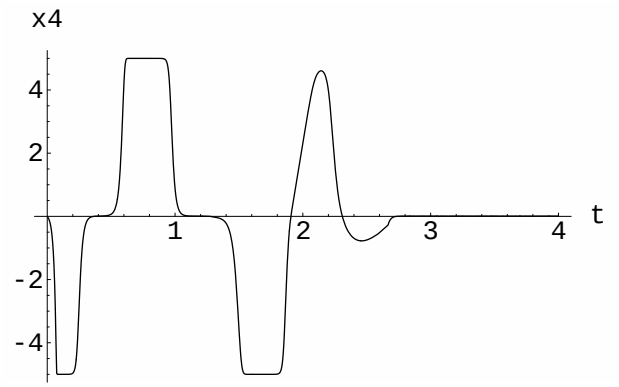

In[270]:= **Plot**[**Evaluate**[{Control}/.VSsols], {t, 0, 4}, AxesLabel → {t, u}];

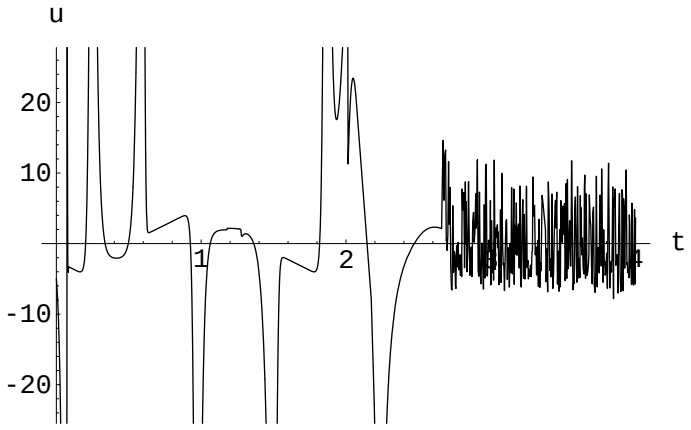

It appears that from these initial conditions the ultimate error is quite small, but it is not zero. Notice also the stiction effects. The control plots give a clear indication of where sliding begins.

10.9 Problems

Problem 10.19. Consider the magnetic suspension system shown in Figure (10.4) Consider the voltage $v(t)$ to be the control input. The attracting force suspending the mass is

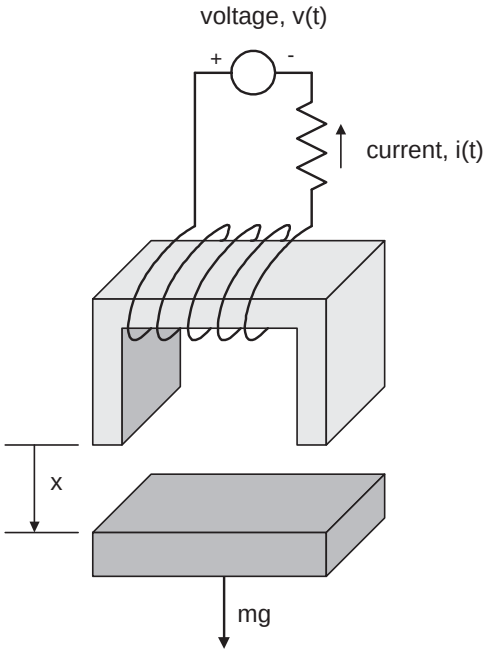

Fig. 10.4: Magnetic suspension system.

$$F = \frac{k_1 i^2}{(x+k_2)^2}$$

Suppose the circuit resistance is R and the combined inductance of the coil and suspended mass is L.

(a) Develop Lagrange's equations for the system.

(b) Design a variable structure control system. Assume all states are available for measurement. Assume that the mass, m, and the constants k_1 and k_2 are uncertain and can vary $\pm 20\%$ from their nominal values.

(c) Develop a simulation of the control system designed in (b).

(d) Assume that only the current and gap width can be measured and incorporate an observer in the control design. Compare the state feedback and observer based designs via simulation.

(e) Design a state feedback adaptive controller and compare its performance with the controller of (b) by simulation.

Problem 10.20. Repeat Problem (9.24) using a variable structure controller.

Problem 10.21. Repeat Problem (9.23) using a variable structure controller.

Problem 10.22 (Synchronous motor, revisited). Consider the synchronous motor described in Problem (6.23) Suppose that the load torque T_L can be measured. Design a variable structure control using the four control variables v_d, v_q, v_0, v_f. Assume that there is a power supply that provides a dc voltage of $\pm V_S$ for the stator and $\pm V_f$ for the field. The outputs to be regulated are defined as follows:

1. Speed regulation. Define

$$y_1 = \dot{\omega} + c(\omega - \omega_0) = (-\sqrt{\tfrac{3}{2}} L_5 i_f i_q - T_L)/J + c(\omega - \omega_0),\ c > 0$$

   where ω_0 is the desired speed.

2. Balanced motor operation. Normally, a 3-phase machine is driven with line voltages v_1, v_2, v_3 that are sinusoids of the same magnitude and frequency and 120 degrees out of phase. Thus, they sum to zero. Some deviation from this balance will be allowed, but to regulate it introduce the new state

$$\chi = \int_0^t v_0 \, dt$$

   (recall, $v_0 = (v_1 + v_2 + v_3)/\sqrt{3}$), and define the output

$$y_2 = \chi$$

3. Constant d-axis current. Define

$$y_3 = i_d - i_{d0}$$

   where i_{d0} is assumed given.

4. Constant field current. Define

$$y_4 = i_f - i_{f0}$$

   where i_{f0} is also given.

Some motivation for choosing this set of regulated output follows from the observation that the electrical torque is $T_E = \sqrt{\frac{3}{2}} L_5 \, i_f i_q$. Thus, we regulate to an equilibrium point in which i_d and i_f assume specified constant values and i_q takes a value that insures $T_E = T_L$. Since the stator current magnitude is $I_s = \sqrt{i_d^2 + i_q^2}$, it is not difficult to show that, in steady-state, $T_E = \sqrt{\frac{3}{2}} L_5 \, i_{f0} I_s \sin\phi$ where ϕ is the usual power angle, i.e., the angle between the stator current and voltage phasers.

Are the zero dynamics stable?

11

Optimal Control

11.1 Introduction

12

Hybrid Control Systems

12.1 Introduction

Many systems undergo reconfiguration or switching during normal and abnormal operations. Such systems can function in different *modes* or *discrete states* in each of which the system may exhibit distinct dynamical behavior. Transitions between modes are defined by logical conditions that can depend on continuous dynamical states or external signals. Such systems are called *hybrid systems* [93] or *Mixed Logical-Dynamical systems* (MLD) [6, 29]. The relevance of such problems to power systems was clearly noted by Dy Liacco in [76, 77, 78]. This chapter is concerned with power systems that operate in this way.

The class of control problems described herein derives from specific applications in power systems, specifically systems that involve operation in highly nonlinear regimes where failure events cause abrupt changes in the controlled system behavior, which, in turn, require a change in control strategy.

All of the applications of interest herein involve both continuous and discrete dynamics and are conveniently conceived as a *hybrid automaton*. Such a model is composed of a description of the discrete transition behavior from one mode to another along with models of continuous dynamic behavior within each mode. The hybrid automaton model has proved to be an important theoretical tool and is a key conceptual device for model building. However, other forms of models, like the MLD, are far more convenient for control system design. The ability to convert from one form of model to another is important.

In the following approach, the transition behavior of a hybrid automaton is modeled by a logical statement (or *specification*). The logical specification can be converted into a set of mixed-integer formulas (IP formulas)[1]. Thus, the transition specification for the automaton is converted into a set of inequalities involving Boolean variables.

[1] a computational tool for this purpose has been constructed in *Mathematica*. This work, described in [66, 67, 65], extends earlier work in this area reported in [108, 75].

Logical constraints other than the transition dynamics can also be added to the specification making this a powerful approach to formulating an optimal control problem. [102] describe a tool for building MLD models that allows the inclusion of Boolean equivalents to logical specifications. So one could use our tool to create those expressions from an arbitrary logical specification.

The IP formulas are used in computing the optimal control strategy. Our approach derives a feedback policy based on finite horizon *dynamic programming* [5]. Dynamic programming has been used extensively in control system design and has recently been explored as a tool for designing hybrid system feedback controls. It's popularity derives from the generality and broad applicability of the *principle of optimality* on which it is based. A drawback of dynamic programming is the *curse of dimensionality* - a term coined by Bellman about 50 years ago, well before the advent of powerful desktop computers.

Branicky et al [16] laid the groundwork for the use of dynamic programming in hybrid systems. They focused on the existence of optimal and near optimal controls, and the establishment of a taxonomy for hybrid systems. In [38], the authors introduced a discrete version of Bellman's inequality to compute a lower bound on the optimal cost function using linear programming. In this way an approximation of the optimal feedback control law is derived. Another innovative work, [79], considers the problem of approximating the value function. They called their procedure value iteration from which a suboptimal solution is found within a user specified distance from the optimal solution. They have applied this *relaxed dynamic programming* approach to design a switched power controller for a DC-DC converter.

The hybrid systems study most closely related to our approach is the one described by Bemporad et al in their recent paper [15]. They consider the optimal control of constrained discrete-time linear hybrid systems with quadratic or linear performance criteria. The associated Hamilton-Jacobi-Bellman equations are solved backwards in time using a multiparametric quadratic (or linear) programming solver. Two cases are considered, one without binary inputs and the other one with binary inputs. In the latter case all possible combinations of binary inputs are enumerated.

In our case we consider nonlinear discrete-time hybrid dynamics with a general convex cost function with primarily binary controls. A central feature of our formulation is that it applies to systems with complex logical constraints, defined either by the transition system or auxiliary considerations. We exploit the fact that the system is highly constrained and most of the constraints are linear in Boolean variables. Thus, we use the *Mathematica* function `Reduce` to determine feasible points from which we identify those of minimum cost by enumeration. `Reduce` is a powerful function that finds feasible solutions by solving equations and inequalties and eliminating quantifiers. The method used depends on the specific structure of the expressions involved.

In Section 12.3 we provide a specific definition of the problems considered herein. Sections 12.4 and 12.5 describe the main concerns of this paper, namely the reduc-

tion of a logical specification for the discrete subsystem to a set of inequalities and the use of this model of a hybrid system to design optimal feedback controllers via dynamic programming. An example is given in Section 12.8.3. The example shows how additional logical constraints - other than the transition behavior - can be incorporated into the control problem.

12.2 Foundations of Discrete Event Systems

12.2.1 Preliminaries

12.2.2 Logical Specification of Transition Dynamics

12.2.3 Observations and Masks

12.2.4 Supervisors

12.2.5 Controllability and Observability

12.2.6 Supervisor Synthesis

12.2.7 Power Network Restoration

12.3 Hybrid Systems

12.3.1 Modeling

The class of hybrid systems to be considered is defined as follows. The system operates in one of m modes denoted $q_1,\ldots,q_m$. We refer to the set of modes $Q=\{q_1,\ldots,q_m\}$ as the discrete state space. The discrete time difference-algebraic equation (DAE) describing operation in mode q_i is

$$\begin{array}{c} x_{k+1}=f_i(x_k,y_k,u_k) \\ 0=g_i(x_k,y_k,u_k) \end{array} \qquad i=1,\ldots,m \tag{12.1}$$

where $x\in X\subseteq R^n$ is the system continuous state, $y\in Y\subseteq R^p$ is the vector of algebraic variables and $u\in U\subseteq R^m$ is the continuous control. Transitions can occur only between certain modes. The set of admissible transitions is $E\subseteq Q\times Q$. It is convenient to view the mode transition system as a graph with elements of the set Q being the nodes and the elements of E being the edges. We assume that transitions are instantaneous and take place at the beginning of a time interval. So, if a system transitions

from mode q_1 to q_2 at time k we would write $q(k) = q_1, q(k^+) = q_2$. We do allow resets. State trajectories are assumed continuous through events, i.e., $x(k) = x(k^+)$, unless a reset is specified.

Transitions are triggered by external *events* and *guards*. We denote the finite set of events Σ. It is convenient to partition the events into two types; those that are controllable (they can be assigned a value by the controller), and those that are not. The latter are exogenous and occur spontaneously. Such an event might correspond to a component failure, or a high level change of operational mode. We will use the symbols s to represent controllable events and p to represent uncontrollable events. Thus, $\Sigma = S \times P$ where $s \in S$ and $p \in P$. A guard is a subset of the continuous state space X that enables a transition. A transition enabled by a guard might represent a protection device. Not all transitions have guards and some transitions might require simultaneous satisfaction of a guard and the occurrence of an event. The guard assignment function is $G : E \to 2^X$.

We consider each discrete state label, $q \in Q$, and each event, $\sigma \in \Sigma$, to be logical variables that take the values True or False. Guards also are specified as logical conditions. In this way the transition system, including guards, can be defined by a logical specification (formula) $\mathscr{L}$.

In summary, a hybrid control system is composed of:

1. Q, discrete space,
2. X, continuous state space,
3. E, set of transitions,
4. Σ, event set,
5. G, guard assignment function,
6. $\mathscr{L}$, logical specification,
7. F, family of controlled vector fields.

Example 12.1 (Three mode system.). Consider the simple three mode hybrid system shown in Figure 12.1. Each mode, q_1, q_2, q_3, is characterized by continuous dynamics $x_{k+1} = f_{q_i}(x_k, u_k), \quad i = 1,2,3.$

Discrete transitions are associated with the events represented by logical variables p, s_1, s_2, s_3, i.e, $\Sigma = \{p, s_1, s_2, s_3\}$. For example, if the system is in mode q_1 and s_1 evaluates to True, then a mode transition occurs in which the mode changes from q_1 to q_2. In this example, we use two different symbols s and p to denote transition variables to underscore the fact that some transitions are controllable and others not so.

In our formulation the transition system behavior is defined by the logical specification:

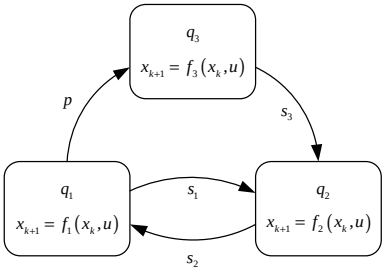

Fig. 12.1: Three mode hybrid system with controllable and uncontrollable events.

$$\begin{aligned}\mathscr{L} = &\mathit{exactly}\left(1, \{q_1(t), q_2(t), q_3(t)\}\right) \wedge \mathit{exactly}\left(1, \{q_1(t^+), q_2(t^+), q_3(t^+)\}\right) \wedge \\ &\left(q_1(t) \wedge s_1 \Rightarrow q_2(t^+)\right) \wedge \left(q_1(t) \wedge p \Rightarrow q_3(t^+)\right) \wedge \left(q_1(t) \wedge \neg(s_1 \vee p) \Rightarrow q_1(t^+)\right) \wedge \\ &\left(q_2(t) \wedge s_2 \Rightarrow q_1(t^+)\right) \wedge \left(q_2(t) \wedge \neg s_2 \Rightarrow q_2(t^+)\right) \wedge \\ &\left(q_3(t) \wedge s_3 \Rightarrow q_2(t^+)\right) \wedge \left(q_3(t) \wedge \neg s_3 \Rightarrow q_3(t^+)\right)\end{aligned} \tag{12.2}$$

Let us dissect this specification. The first line expresses the fact that the system can only be in one discrete state before the transition (at time t) and after the transition (at time t^+). The next line describes all possible transitions from state q_1. Similarly, the last line characterizes all possible transitions from states q_2 and q_3, respectively.

For computational purposes it is useful to associate with each logical variable, say α, a Boolean variable or indicator function, δ_α, such that δ_α assumes the values 1 or 0 corresponding respectively to α being True or False. It is convenient to define the discrete state vector $\delta_q = [\delta_{q_1}, \ldots, \delta_{q_m}]$, the control event vector $\delta_s = [\delta_{s_1}, \ldots, \delta_{s_{m_S}}]$, and the exogenous event vector $\delta_p = [\delta_{p_1}, \ldots, \delta_{p_{m_P}}]$. Precisely one of the elements of δ_q will be unity and all others will be zero.

Notice that with the introduction of the Boolean variables we can replace the set of dynamical equations (12.24) with the single relation

$$\begin{aligned}x(k+1) &= f(x(k), \delta_q(k), u(k)) \\ &= \delta_{q_1} f_{q_1}(x(k), u(k)) + \cdots \\ &\qquad \cdots + \delta_{q_m} f_{q_m}(x(k), u(k)) \\ 0 &= g(x(k), \delta_q(k), u(k)) \\ &= \delta_{q_1} g_{q_1}(x(k), u(k)) + \cdots \\ &\qquad \cdots + \delta_{q_m} g_{q_m}(x(k), u(k))\end{aligned} \tag{12.3}$$

12.3.2 The Control problem

We assume that the system is observed in operation over some finite time horizon T that is divided into N discrete time intervals of equal length. A control policy is a sequence of functions

$$\pi = \left\{ \mu_0 \left(x_0, \delta_{q,0} \right), \ldots, \mu_{N-1} \left(x_{N-1}, \delta_{q,(N-1)} \right) \right\}$$

such that

$$\left[u_k, \delta_{s,k} \right] = \mu_k \left(x_k, \delta_{q,k} \right)$$

Thus, μ_k generates the continuous control u_k and the discrete control $\delta_{s,k}$ that are to be applied at time k, based on the state $\left(x_k, \delta_{q,k} \right)$ observed at time k.

Consider the set of m-tuples $\{0,1\}^m$. Let Δ_m denote the subset of elements $\delta \in \{0,1\}^m$ that satisfy $\delta_1 + \cdots + \delta_m = 1$. Denote by Π the set of sequences of functions $\mu_k : X \times \Delta_m \to U \times \{0,1\}^{m_S}$ that are piecewise continuous on X.

Now, given the initial state $(x_0, \delta_{q,0})$ the problem is to find a policy, $\pi^* \in \Pi$, that minimizes the cost functional

$$J_\pi \left(x_0, \delta_{q,0} \right) = g_N \left(x_N, \delta_{q,N} \right) + \sum_{k=0}^{N-1} g_k \left(x_k, \delta_{q,k}, \mu_k \left(x_k, \delta_{q,k} \right) \right) \tag{12.4}$$

Specifically, the *Optimal Feedback Control Problem* is defined as follows. For each $x_0 \in X, \delta_{q,0} \in \Delta_m$ determine the control policy $\pi^* \in \Pi$ that minimizes the cost (12.26) subject to the constraints (12.24) and the logical specification, $\mathscr{L}$, i.e.,

$$J_{\pi^*} \left(x_0, \delta_{q,0} \right) \leq J_\pi \left(x_0, \delta_{q,0} \right) \quad \forall \pi \in \bar{\Pi} \tag{12.5}$$

where $\bar{\Pi} \subset \Pi$ is the subset of policies that steers (12.24) along trajectories that satisfy $\mathscr{L}$.

Notice that if a receding horizon optimal control is desired, once the optimal policy is determined, we need only implement the state feedback control

$$[u, \delta_s] = \mu_0 \left(x, \delta_q \right) \tag{12.6}$$

12.4 Logical Specification to IP Formulas

The first step in solving the optimal control problem is to transform the logical specification $\mathscr{L}$ into a set of inequalities involving integer (in fact, Boolean) variables and possibly real variables, so-called *IP-formulas*. The idea of formulating optimization problems using logical constraints and then converting them to IP formulas has a long history. This concept was recently used as a means to incorporate qualitative information in process control and monitoring [103], and generally introduced into the study of hybrid systems in [6].

McKinnon, [84], proposed the inclusion of logical constraints in optimization methods. They suggested a sequence of transformations that brings a logical specification into a set of IP-formulas. Li, [75], presents a systematic algorithm for transforming logic formulas into IP formulas. Those methods have been modified and extended in order to obtain simpler and more compact IP formulas with other modifications to enhance their applicability to hybrid systems.

12.4.1 Logical Modeling Language

We use a logical specification to describe the transition behavior of a hybrid automaton. The specification is simply a logical formula. Here we describe the set of formulas, i.e., the language, to be employed. A *propositional variable* is a variable that can assume the values True or False. A *propositional formula* is composed of propositional variables, *logical connectives* (specifically $\wedge, \vee, \Rightarrow, \Leftrightarrow, \neg$), predicates (Boolean-valued functions of propositional variables) and constraints. Specifically, we will use the predicates: atleast(m,S), atmost(m,S), exactly(m,S), and none(S), where $m \geq 1$ is an integer and S is a list of propositional variables or formulas. A constraint is an arithmetic equality or inequality involving integer or real numbers and variables. Constraints evaluate to True (satisfied) or False (not satisfied).

Formulas are defined by the following statements:

1. a propositional variable or a constraint is an atomic formula,
2. an atomic formula is a formula,
3. $F_1 \sim F_2$ is a formula if F_1 and F_2 are formulas and $\sim$ is one of the logical connectives,
4. $\neg F$ is a formula if F is a formula,
5. atleast(m,S), atmost(m,S), exactly(m,S), and none(S) are formulas if S is a list of formulas and $m \geq 1$ is an integer.

12.4.2 Transformation to IP Formulas

Logical formulas are convenient for problem formulation. However, in order to compute efficiently it is often convenient to convert a logical formula into a set of so-called IP-formulas [2], that is, a set of linear equalities or inequalities involving Boolean variables. To do this, we use the transformation procedure defined in [74]. Following [84], the process involves first transforming the original formula into an intermediate form called a Γ-form and then a series of transformations are applied that reduce the Γ-form to a set of IP formulas.

The Γ-form is a logically equivalent normal form that leads to a more compact set of IP formulas than better known normal forms like the CNF (conjunctive normal form) or DNF (disjunctive normal form).

[2] While, generally, computing with IP-formulas is preferred, [43] shows that there are instances when it is an advantage to compute using the original logical constraint.

12.4.3 Implementation

The basic function in our *Mathematica* implementation is `GenIP` which takes as two arguments, the specification and a list of variables, either propositional variables or bounded real or integer variables. The latter are specified in the form $a \leq x \leq b$. `GenIP` performs a series of transformations and simplifications and returns the IP formulas. A typical usage would look like:

$$\texttt{GenIP}[(q1 \oplus q2) \wedge (qq1 \oplus qq2) \wedge ((q1 \wedge (x > 0)) \Rightarrow qq2) \wedge ((q2 \wedge s) \Rightarrow qq1), \{q1, q2, qq1, qq2, s, -2 \leq x \leq 2\}]$$

$$\begin{array}{l}\{1-\delta_{q1}-\delta_{q2} \geq 0, -1+\delta_{q1}+\delta_{q2} \geq 0, 1-\delta_{qq1}-\delta_{qq2} \geq 0,\\ d7-\delta_{q1}+\delta_{qq2} \geq 0, -1+\delta_{qq1}+\delta_{qq2} \geq 0,\\ 1-\delta_{q2}+\delta_{qq1}-\delta_s \geq 0, -2+2d7+x \leq 0, -2 \leq x \leq 2,\\ 0 \leq d7 \leq 1, 0 \leq \delta_{q1} \leq 1, 0 \leq \delta_{q2} \leq 1, 0 \leq \delta_{qq1} \leq 1,\\ 0 \leq \delta_{qq2} \leq 1, 0 \leq \delta_s \leq 1\}\end{array}$$

Notice that propositional variables are replaced by Boolean indicator functions, e.g., q_1 is replaced by δ_{q_1} and new auxiliary variables may be introduced, in this case $d7$.

If all of the guards are linear (set boundaries are composed of linear segments), then the IP formulas are system of linear constraints involving the Boolean variables $\delta_q, \delta_{q^+}, \delta_s, \delta_p$, respectively, the discrete state before transition, the discrete state after transition, the controllable events, the exogenous events. They also involve a set of auxiliary Boolean variables, d, introduced during the transformation process, and the real state variables, x. The general form is [3]

$$E_5\delta_{q^+} + E_6 d \leq E_0 + E_1 x + E_2\delta_q + E_3\delta_s + E_4\delta_p \tag{12.7}$$

where the matrices have appropriate dimensions. As we will see in examples below, with $x, \delta_q, \delta_s, \delta_p$ given, these inequalities typically provide a unique solution for the unknowns δ_{q^+} and d. The system evolution is described by the closed system of equations (12.7) and (12.25).

12.5 Constructing the Optimal Solution

An optimal policy π^* is one that satisfies (12.27). Now we are in a position to apply Bellman's principle of optimality: suppose $\pi^* = \{\mu_1^*, \ldots, \mu_{N-1}^*\}$ is an optimal control policy. Then the sub-policy $\pi_i^* = \{\mu_i^*, \ldots, \mu_{N-1}^*\}$, $1 \leq i \leq N-1$ is optimal with respect to the cost function (12.26).

Let us denote the optimal cost of the trajectory beginning at $x_i, \delta_{q,i}$ as $J_i^*(x_i, \delta_{q,i})$. It follows from the principle of optimality that

[3] Linearity only obtains if the conditions in the specification involving real variables are themselves linear.

$$J^*_{i-1}\left(x_{i-1},\delta_{q,(i-1)}\right)=\min_{\mu_{i-1}}\left\{g_{i-1}\left(x_{i-1},\delta_{q(,i-1)},\mu_{i-1}\right)+J^*_i\left(x_i,\delta_{q,i}\right)\right\} \tag{12.8}$$

Equation (12.8) provides a mechanism for backward recursive solution of the optimization problem. To begin the backward recursion, we need to solve the single stage problem with $i=N$. The end point $x_N,\delta_{q,N}$ is free, so we begin at a general terminal point

$$J^*_{N-1}\left(x_{N-1},\delta_{q,(N-1)}\right)=\min_{\mu_{N-1}}\left\{\begin{array}{r} g_{N-1}\left(x_{N-1},\delta_{q,(N-1)},\mu_{N-1}\right)\\ +g_N\left(f_{N-1},\delta_{q^+,(N-1)}\right)\end{array}\right\} \tag{12.9}$$

Once the pair μ^*_{N-1},J^*_{N-1} is obtained, we compute μ^*_{N-2},J^*_{N-2}. Continuing in this way we obtain

$$J^*_{N-i}\left(x_{N-i},\delta_{q,(N-i)}\right)=\min_{\mu_{N-i}}\left\{\begin{array}{r} g_{N-i}\left(x_{N-i},\delta_{q,(N-i)},\mu_{N-i}\right)\\ +J^*_{N-i+1}\left(f_{N-i},\delta_{q^+,(N-i)}\right)\end{array}\right\} \tag{12.10}$$

for $2\le i\le N$.

We need to solve (12.10) recursively backward, for $i=2,\ldots,N$ after initializing with (12.9). We begin by constructing a discrete grid on the continuous state space. The discrete space is denoted $\bar{X}$. At each iteration the optimal control and the optimal cost are evaluated at discrete points in $Q\times\bar{X}$. To continue with the next stage we need to set up an interpolation function to cover all points in $Q\times X$.

We exploit the fact that the system is highly constrained and almost all of the constraints are linear in Boolean variables. The basic approach is as follows:

1. Before beginning the time iteration:
   a) Separate the inequalities into binary and real sets, binary formulas contain only binary variables, real formulas can contain both binary and real variables.
   b) For each $q\in Q$, obtain all feasible solutions of the binary inequalities; a list of possible solutions of pairs $\left(\delta_{q^+},d\right)$. Our implementation employs the *Mathematica* function `Reduce`.
   c) Define projection $\bar{X}\to\bar{X}_{\mathscr{P}}$ where $\bar{X}_{\mathscr{P}}$ is the subspace of real states actually appearing in the real equations.
   d) For each $x_{\mathscr{P}}\in\bar{X}_{\mathscr{P}}$
      i. pre-screen the binary solutions to eliminate those that do not produce solutions to the real inequalities - typically a very large fraction is dropped
      ii. for every feasible combination of binary variables obtained above, solve the real inequalities for the real variables
   e) Lift real solutions to entire $\bar{X}$.
2. For each i,

a) For each pair $(q,x) \in Q \times \bar{X}$

i. enumerate the values of the cost to go using the feasible sets of binary and real variables

ii. select the minimum

In step 1b above the number of solutions corresponding to each q can be very large because there are numerous redundant solutions associated with nonactive transitions. Thus, we add additional logical constraints that specify the inactive transitions. Step 1c exploits the fact that some real states do not appear in the real formulas. Because a large fraction of the binary solutions do not lead to real solutions, the pre-screening in step 1(d)i is very effective in reducing computing time. Finally, we note that the inequalities are independent of the stage of the dynamic programming recursion. Thus, step 1d, which is by far the most intensive computational element of the optimization is done only once before the recursion step 2a begins.

12.6 Example: Load Shedding

This section provides a simple illustration of the formulation and solution of a power management optimal control problem. For simplicity of exposition load shedding is used as a means for accommodating transmission line faults.

12.6.1 Network and Load Dynamics

A relatively simple system that is known to exhibit interesting voltage stability characteristics is a single generator feeding an aggregated load composed of constant impedance loads and induction motors. The system has been used to study the effect of tap changing transformers and capacitor banks in voltage control, e.g., [88, 90, 4].

Consider the system shown in Figure 12.2. The system consists of a generator, a transmission line, an on-load tap changing transformer (OLTC) and an aggregated load. The generator is characterized by a 'constant voltage behind reactance' model. The generator internal bus voltage E is used to maintain the voltage at bus 2; so long as E remains within the limits imposed by the excitation current limits. The OLTC ordinarily moves in small discrete steps over a narrow range. The load is an aggregate composed of parallel induction motors and constant impedance loads. An induction motor can be characterized as an impedance with slowly varying resistance; consequently, the aggregate load is represented by constant impedance - actually, a slowly varying impedance, where the impedance depends on the aggregate induction motor slip.

The network equations are easily obtained. Suppose δ_1, δ_2 denote the voltage angles at bus 1 and 2. Define the relative angle $\theta_2 = \delta_2 - \delta_1$. The network equations are

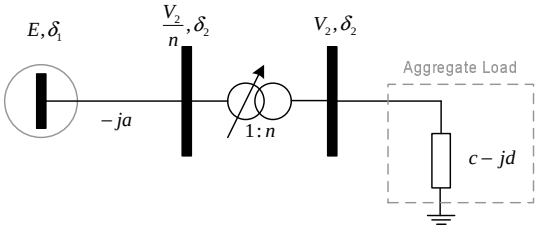

Fig. 12.2: System configuration.

$$I_1 \omega_0 \dot{\omega} = P_g - cV_2^2$$
$$0 = (a/n) EV_2 \sin\theta_2 + cV_2^2$$
$$0 = (a/n) EV_2 \cos\theta_2 + dV_2^2$$

From the last two equations we obtain

$$V_2 = \frac{a/n}{\sqrt{c^2+d^2}} E, \ \theta_2 = \tan^{-1}\frac{c}{d}$$

The power absorbed by the load is

$$P_L = -V_2^2 c, \quad Q_L = V_2^2 d$$

Now, let us turn to the induction motors. An equivalent circuit for an induction motor is shown in Figure 12.3. Here, the parameters R_s, X_s denote the resistance and inductance of the stator, X_m denotes the magnetizing inductance, and R_r, X_r the rotor resistance and inductance. The resistance $R_r(1-s)/s$ represents the motor electrical output power. We will neglect the small stator resistance and inductance. We also assume the approximation of large magnetizing inductance is acceptable.

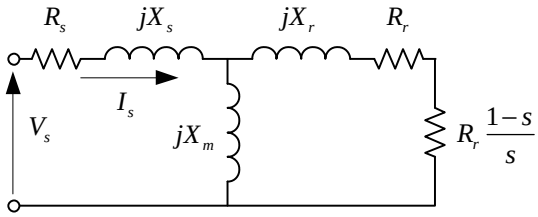

Fig. 12.3: Induction motor equivalent circuit.

Under these conditions obtain the following. The real power delivered to the rotor, P_d, and the power delivered to the shaft, P_e, are

$$P_d = V_s^2 \frac{R_r s}{R_r^2 + s^2 X_r^2} \quad P_e = P_d(1-s)$$

The dynamical equation for the motor (Newton's law) is

$$\dot{\omega}_m = \frac{1}{I_m \omega_0} (P_e - P_m)$$

Introducing the slip, s, $s = (\omega_0 - \omega_m)/\omega_0$, the motor dynamics take the form

$$\dot{s} = \frac{1}{I_m \omega_0^2} (P_m - P_e) = \frac{1}{I_m \omega_0^2} \left(P_m - V_s^2 \frac{R_r s (1-s)}{R_r^2 + s^2 X_r^2} \right)$$

12.6.2 System Operation

In the following, we allow for shedding a fraction, η, of the load. In the present example, we allow three different values of η including zero, so $\eta \in \{0, \eta_1, \eta_2\}$. Consequently, there is normal operation and two prioritized blocks of load that can be dropped in accordance with the transition behavior defined in Figure 12.4. The corresponding logical specification is

$$\begin{aligned}\mathscr{L} = {} & exactly(1, \{q_1(t), q_2(t), q_3(t)\}) \wedge exactly\left(1, \left\{q_1\left(t^+\right), q_2\left(t^+\right), q_3\left(t^+\right)\right\}\right) \wedge \\ & \left(q_1(t) \wedge \neg s_1 \Rightarrow q_2\left(t^+\right)\right) \wedge \left(q_1(t) \wedge s_1 \Rightarrow q_1\left(t^+\right)\right) \wedge \\ & \left(q_2(t) \wedge \neg s_2 \Rightarrow q_3\left(t^+\right)\right) \wedge \left(q_2(t) \wedge s_1 \Rightarrow q_1\left(t^+\right)\right) \wedge \left(q_2(t) \wedge \neg(s_1 \vee \neg s_2) \Rightarrow q_2\left(t^+\right)\right) \wedge \\ & \left(q_3(t) \wedge s_2 \Rightarrow q_2\left(t^+\right)\right) \wedge \left(q_3(t) \wedge \neg s_2 \Rightarrow q_3\left(t^+\right)\right)\end{aligned}$$

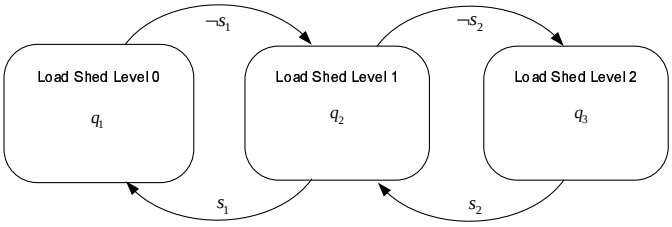

Fig. 12.4: Transition diagram for load shedding optimization.

In the present case, assume the blocks are sized such that

$$q_1 \Rightarrow \eta = 0, \quad q_2 \Rightarrow \eta = 0.4, \quad q_3 \Rightarrow \eta = 0.8$$

Assume also that the OLTC ratio is fixed, i.e., the OLTC is not being used for control, so $n = \text{const}$. If the OLTC is to be employed, the dynamics of tap change must be added.

$$I_1 \omega_0 \dot{\omega} = P_g - c V_2^2 \tag{12.11}$$

$$E = (1 - \eta) \frac{\sqrt{c_0^2 + d_0^2}}{a/n} V_2 \tag{12.12}$$

$$\dot{s} = \frac{(1-\eta)}{I_m \omega_0^2}\left(P_m - V_2^2 \frac{R_r s\,(1-s)}{R_r^2 + s^2 X_r^2}\right) \tag{12.13}$$

$$c = (1-\eta)\,c_0,\; c_0 = \left(\frac{1}{R_L} + \frac{R_r s}{R_r^2 + s^2 X_r^2}\right) \tag{12.14}$$

$$d = (1-\eta)\,d_0,\; d_0 = \left(\frac{X_r s^2}{R_r^2 + s^2 X_r^2}\right) \tag{12.15}$$

Equation (12.11) represents turbine-generator dynamics. Ordinarily, the power input P_g is adjusted to regulate the speed ω which is to be maintained at the value ω_0. Assume that regulation is fast and accurate. It is possible to investigate the impact of frequency variation on system behavior. If it were assumed that frequency variations were small, then the effect on all impedances could be approximated, and this is often done. That has not been included here, so there is no apparent coupling between (12.11) and the remaining equations, consequently it can be dropped. Equation (12.12) represents the network voltage characteristic. The field voltage E is used to control the load bus voltage V_2. It will be assumed that it is desired to maintain $V_2 = 1$. If the exciter dynamics are ignore, then (12.12) allows the determination of the field voltage that yields the desired load bus voltage. However, the field voltage is strictly limited, $0 \leq E \leq 2$. Assume that only the upper limit is a binding constraint. There are two possibilities for satisfying (12.12):

$$V_2 = 1,\; E = \frac{\sqrt{c^2+d^2}}{a/n} \text{ or } E = 2,\; V_2 = 2\frac{a/n}{\sqrt{c^2+d^2}}$$

Equation (12.21) represents the aggregated motor dynamics, and the load admittance is given by the last two equations. The system data is $R_L = 2$, $R_r = 0.25$, $X_r = 0.125$, $a = 1$ (nominal), $I_m \omega_0^2 = 4$.

12.6.3 The Optimal Control Problem Without OLTC, $n = 1$

The problem is formulated as an N step moving horizon optimal control problem, in which the slip dynamics are written in discrete time form. The control variables are $E(k), \eta(k)$. The goal is to keep the load voltage V_2 close to 1, specifically, it is required that $0.95 \leq V_2 \leq 1.05$. Our intent is to use the field voltage, E, to regulate the terminal voltage, V_2 to 1 p.u. Because $0 < E \leq 2$ is constrained, specify that solutions must satisfy

$$(V_2 = 1 \wedge 0 < E < 2) \vee (E = 2)$$

If the field voltage saturates, the only remaining option is to shed some load. We seek an optimal control policy, i.e., a sequence of controls $u(0), \ldots, u(N-1)$, $u(k) = \eta(k)$, that minimizes the cost function

$$J = \sum_{k=0}^{N-1}\left(\|V_2(k) - 1\|^2 + r_1 \|\eta(k)\|^2\right)$$

subject to the system constraints. Some rough assessments of appropriate weighting constants r_1 can be made. Load shedding should be avoided with respect to regulating V_2 unless the V_2 tolerance is violated. Hence it is desired that $r_1 > 0.25^2/0.05^2 = 1/25$.

In summary, the following equations are obtained

1. The slip dynamics in discrete time form (with $s_k = s(t_k), t_k = t_{k-1} + h$)

$$s_{k+1} = f(s_k, V_2, \eta)$$

2. The transition specification in IP form

$$\begin{gathered}
1-\delta_{q_1}-\delta_{q_2}-\delta_{q_3} \geq 0, \quad -1+\delta_{q_1}+\delta_{q_2}+\delta_{q_3} \geq 0 \\
1-\delta_{q_1^+}-\delta_{q_2^+}-\delta_{q_3^+} \geq 0, \quad -1+\delta_{q_1^+}+\delta_{q_2^+}+\delta_{q_3^+} \geq 0 \\
1-\delta_{q_1}+\delta_{q_1^+}-\delta_{s_1} \geq 0, \quad 1-\delta_{q_2}+\delta_{q_1^+}-\delta_{s_1} \geq 0 \\
1-\delta_{q_2}+\delta_{q_2^+}-\delta_{s_2} \geq 0, \quad 1-\delta_{q_3}+\delta_{q_2^+}-\delta_{s_2} \geq 0 \\
-\delta_{q_1}+\delta_{q_2^+}+\delta_{s_1} \geq 0 \\
-\delta_{q_2}+\delta_{q_3^+}+\delta_{s_2} \geq 0, \quad -\delta_{q_3}+\delta_{q_3^+}+\delta_{s_2} \geq 0 \\
0 \leq \delta_{q_1} \leq 1, 0 \leq \delta_{q_2} \leq 1, 0 \leq \delta_{q_3} \leq 1 \\
0 \leq \delta_{q_1^+} \leq 1, 0 \leq \delta_{q_2^+} \leq 1, 0 \leq \delta_{q_3^+} \leq 1 \\
0 \leq \delta_{s_1} \leq 1, 0 \leq \delta_{s_2} \leq 1
\end{gathered}$$

3. The IP formulas for the logical constraint

$$\begin{gathered}
3-d_1-E > 0, \quad 1-d_1+E > 0, \quad -2d_2+E \geq 0 \\
-2d_1+V_2 \geq 0, \quad -2+d_1+V_2 \leq 0 \\
0 \leq d_1, d_2 \leq 1, \quad 0 \leq E, V_2 \leq 2
\end{gathered}$$

4. And the IP formulas for the load shed parameter η

$$\begin{gathered}
-0.4d_4+\eta \geq 0, \quad -0.8d_5+\eta \geq 0, \\
d_3-\delta_{q_1^+} \geq 0, \quad d_4-\delta_{q_2^+} \geq 0, \quad d_5-\delta_{q_3^+} \geq 0 \\
-1+d_3+\eta \leq 0, \quad -1+0.6d_4+\eta \leq 0, \\
-1+0.2d_5+\eta \leq 0 \\
0 \leq d_3 \leq 1, \quad 0 \leq d_4 \leq 1, \quad 0 \leq d_5 \leq 1, \quad 0 \leq \eta \leq 1
\end{gathered}$$

One result is shown in Figure 12.5. It illustrates the optimal load shedding strategy following a line failure represented as a reduction of a. The feedback control is given as a function of the state - the latter composed of the continuous slip and the three discrete states. At each state, the values of the control actions δ_{s_1}, δ_{s_2} are given. The controlled transitions are also indicated.

Suppose immediately post-failure, the system is in mode q_1, with a reduced slip of 0.1, then the system will respond as follows. Given a mechanical power level of 0.7, the equilibrium slip is about 0.47. As slip increases toward its equilibrium value, the first block of load is dropped at about $s = 0.3$ and the second at about $s = 0.4$.

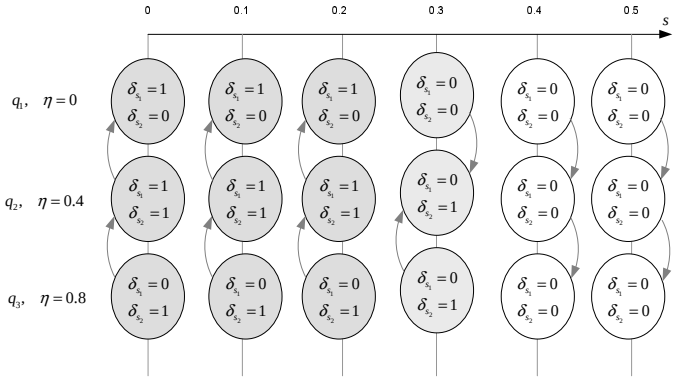

Fig. 12.5: Depiction of the feedback law obtained with $a = 0.25$, $h = 0.5$, and $N = 20$.

12.6.4 Incorporating Time Delays

Sometimes it is desirable to insure that there is a finite time duration between two successive controlled transitions. It is easy to do this by incorporating a time 'residence' requirement within a discrete state. For example, suppose we wish to insure that a load shedding action will not be followed by another until at least a time Δ has passed. This can be accomplished by requiring that after entry into state q_2 the system must remain in q_2 for at least time Δ.

To accomplish this we introduce a resetting 'clock'

$$\tau(k+1) = \tau\left(k^+\right) + h$$

where $\tau(k^+) = 0$ upon entry into q_2 from q_1 or q_3 or $\tau(k^+) = \tau(k)$; and replace the specification $\mathscr{L}$ by

$$\begin{array}{l}
\mathscr{L} = exactly\left(1, \{q_1(t), q_3(t), q_3(t)\}\right) \wedge \\
\quad exactly\left(1, \left\{q_1\left(t^+\right), q_3\left(t^+\right), q_3\left(t^+\right)\right\}\right) \wedge \\
\quad \left(q_1(t) \wedge \neg s_1 \Rightarrow q_2\left(t^+\right) \wedge \tau\left(t^+\right) = 0\right) \wedge \\
\quad \left(q_1(t) \wedge s_1 \Rightarrow q_1\left(t^+\right) \wedge \tau\left(t^+\right) = \tau(t)\right) \wedge \\
\quad \left(q_2(t) \wedge s_1 \wedge \tau(t) > \Delta \Rightarrow q_1\left(t^+\right) \wedge \tau\left(t^+\right) = \tau(t)\right) \wedge \\
\quad \left(q_2(t) \wedge \neg s_2 \wedge \tau(t) > \Delta \Rightarrow q_3\left(t^+\right) \wedge \tau\left(t^+\right) = \tau(t)\right) \wedge \\
\quad \left(\begin{array}{c} q_2(t) \wedge \neg\left((s_1 \wedge \tau(t) > \Delta) \vee (\neg s_2 \wedge \tau(t) > \Delta)\right) \\ \Rightarrow q_2\left(t^+\right) \wedge \tau\left(t^+\right) = \tau(t) \end{array}\right) \wedge \\
\quad \left(q_3(t) \wedge s_2 \Rightarrow q_2\left(t^+\right) \wedge \tau\left(t^+\right) = 0\right) \wedge \\
\quad \left(q_3(t) \wedge \neg s_2 \Rightarrow q_3\left(t^+\right) \tau\left(t^+\right) = \tau(t)\right)
\end{array}$$

The control law now becomes a function of the discrete state, the two components of the continuous state: the slip s, and the clock variable τ. With time delay $\Delta = 1$ the control law is virtually identical to that shown in Figure 12.5 expect that the clock dependence inhibits transitions from q_2 as required.

We will not display the resulting IP formulas, but it is interesting to note that the binary equations involve 24 binary variables 3 of which are the current state. Consequently, there are $2^{21} = 2,097,152$ possible solutions, but actually only 1000 - 2000 prove to be feasible (depending on the current discrete state). From these emerge about 40-80 feasible real solutions. Finally, the associated cost for these few solutions are enumerated and a minimum cost control is chosen.

12.7 Induction Motor Load with UPS

A relatively simple system that is known to exhibit interesting voltage stability characteristics is a single generator feeding an aggregated load composed of constant impedance loads and induction motors [90]. By expanding this system to include a vital load with a UPS, as shown in Figure 12.6, we obtain one of interest to us.

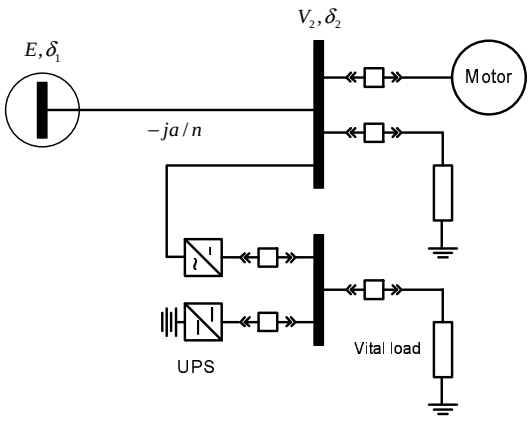

Fig. 12.6: System with vital load and UPS.

The primary means for voltage control is the field voltage. However, in the event of a transmission line fault it may be necessary to shed load in order to avoid a system collapse. This can be accomplished by dropping non-vital load in discrete blocks and, if necessary switching the vital load to battery supply.

Assume that two blocks of non-vital load can be dropped independently by opening circuit breakers. Correspondingly, a load shed parameter is introduced $\eta \in \{0, \eta_1, \eta_2\}$ that denotes the fraction of load dropped.

The battery is connected to the DC load bus through a DC-DC converter. There are three possible UPS operating modes:

1. Battery unconnected.

2. Battery discharging; The battery and vital load are detached from the rest of the network. The battery supplies the load through a voltage controlled DC-DC converter set up to keep the load voltage constant.
3. Battery charging; In this mode the battery is charged through a DC-DC converter operated in current controlled mode – the current is controlled to a specified value.

The overall system transition system is shown in Figure 12.7. It represents operational constraints that are imposed on the system.

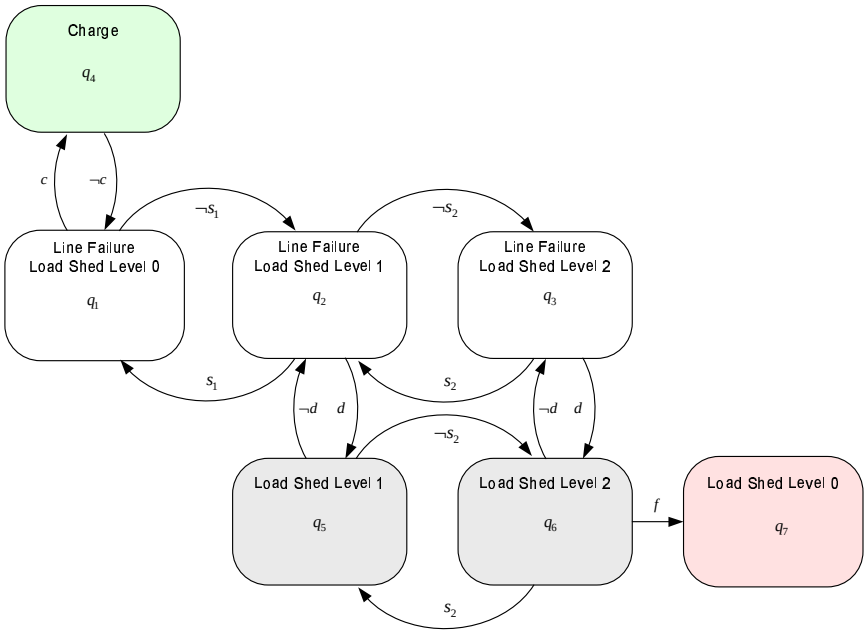

Fig. 12.7: Transition behavior for system with UPS.

12.7.1 Dynamics

Battery disconnected, modes q_1, q_2, q_3

The voltage regulated rectifier controls the voltage on vital load bus.We assume that the rectifier is power factor corrected so that from the AC side of the rectifier, the vital load looks like a constant power load with unity power fact, $P = P_v$, $Q = 0$.

Let δ_1, δ_2 denote the voltage angles at bus 1 and 2. Define the relative angle $\theta_2 = \delta_2 - \delta_1$. The network equations are

$$\begin{aligned} P_v &= a E V_2 \sin\theta_2 - c V_2^2 \\ 0 &= a E V_2 \cos\theta_2 + d V_2^2 \end{aligned} \tag{12.16}$$

Where P_v is the power consumed by the vital load and $c - jd$ is the admittance of the non-vital aggregate load.

The field voltage E is used to control the load bus voltage V_2 to its desired nominal value of 1. If we ignore the exciter dynamics, then (12.16) allows the determination of the field voltage that yields the desired load bus voltage provided the resultant E is within its strict limits, $0 \le E \le 2$. It is always the upper limit that is the binding constraint. This implies two possibilities for satisfying (12.16): either $V_2 = 1$ or $E = 2$. These are:

$$V_2 = 1,\ E = \frac{\sqrt{(c+P_v)^2 + d^2}}{a}, \quad 0 < P_v \tag{12.17}$$

$$\begin{gathered} E = 2, \\ V_2 = \sqrt{\frac{2a^2 - cP_v - \sqrt{4a^4 - 4a^2 cP_v - d^2 P_v^2}}{c^2 + d^2}}, \\ 0 < P_v < 2a^2\left(\sqrt{c^2 + d^2} - c\right) \end{gathered} \tag{12.18}$$

Once the excitation system saturates there is an upper limit to P_v, as seen in (12.18). This is the voltage collapse bifurcation point. Also, these relations are only good for $P_v > 0$. When $P_v = 0$ we have

$$V_2 = \frac{a}{\sqrt{c^2 + d^2}} E \tag{12.19}$$

Equation (12.17) (non-saturated field) does approach the proper limit as $P_v \to 0$, but the Equation (12.18) (saturated field) does not. This is as it should be.

Remark 12.2 (Network Solution). As discussed in Remark 12.5 we can express the network constraints in terms of the logical constraint

$$\mathscr{L}_0 = (V_2 = 1 \Rightarrow E = z_1) \wedge (E = 2 \Rightarrow V_2 = z_2) \tag{12.20}$$

where z_1, z_2 are defined via (12.17), (12.18), and (12.19).

Battery Charging, mode q_4

The battery model is composed of a differential equation describing the battery 'state of charge' σ and an output map that gives the battery terminal voltage v_b as a function of the state of charge.

$$\frac{d}{dt}\sigma = \frac{1}{C}i,\ v_b = f(\sigma),\ 0 \le \sigma \le 1$$

where i is the battery charging current and C is the battery effective capacitance. The DC-DC converter operates in current control mode so the battery is charged with constant current, $i = i_c$. While charging we have:

$$\frac{d\sigma}{dt} = \frac{i_c}{C}$$

Because the AC-DC rectifier maintains constant V_3, from the AC side of the rectifier, charging looks like an additional constant power load, $P_c = V_3 i_c$. The network supplies both the vital load and the power to charge the battery. Thus, the network relation is given by Equations (12.17) and (12.18) with P_v replace by $P_v + P_c$.

Battery Discharging, modes q_5, q_6

The vital loads and battery are separated from the rest of the system and draw no power from the network. Consequently the the relationship between E and V_2 is given by Equation (12.19). The DC-DC converter now maintains constant voltage on bus 3, so that the battery current is $i = -P_v/V_3$ and

$$\frac{d\sigma}{dt} = -\frac{P_v}{CV_3}$$

In the following study we take $C = 0.5$ and $P_v = 10$.

Induction Motors

If we neglect the small stator resistance and inductance and assume a large magnetizing inductance, the equivalent circuit for an induction motor consists of a series rotor resistance and inductance R_r, X_r. Define the slip $s = (\omega_0 - \omega_m)/\omega_0$ and let P_m denote the mechanical load power. Then the motor dynamics take the form

$$\dot{s} = \frac{1}{I_m \omega_0^2}\left(P_m - V_s^2 \frac{R_r s(1-s)}{R_r^2 + s^2 X_r^2}\right) \tag{12.21}$$

Load Shedding

We assume discrete load shedding blocks and define η to represent the fraction of load shed. Thus η can assume a finite number of values $0 \le \eta < 1$. The non-vital load admittances, taking into account the load shedding parameter, are:

$$c = (1-\eta)c_0,\ c_0 = \left(\frac{1}{R_L} + \frac{R_r s}{R_r^2 + s^2 X_r^2}\right) \tag{12.22}$$

$$d = (1-\eta)\, d_0,\ d_0 = \left(\frac{X_r s^2}{R_r^2 + s^2 X_r^2} \right) \tag{12.23}$$

Equation (12.21) represents the aggregated motor dynamics, and the load admittance is given by the last two equations, (12.22), (12.23). The system data is $R_L = 2$, $R_r = 0.25$, $X_r = 0.125$, $a = 1$ (nominal), $I_m \omega_0^2 = 4$.

12.7.2 IP Formulas for UPS System

Four logical constraints need to be converted to IP formulas:

1. the network specification, $\mathscr{L}_0$, Equation (12.20)
2. the transition specification, $\mathscr{L}_1$, of Figure 12.7

(3) the excitation shedding specification

$$\mathscr{L}_2 = (V_2 = 1 \wedge 0 < E < 2) \vee (E = 2)$$

(4) the load shedding specification

$$\mathscr{L}_3 = (q_1^+ \Rightarrow \eta = 0) \wedge (q_2^+ \Rightarrow \eta = 0.4) \wedge (q_3^+ \Rightarrow \eta = 0.8)$$

The corresponding IP formulas are generated automatically. We don't display them here because of space limitations. All of the inequalities derived from $\mathscr{L}_1$ involve only binary variables while some of those derived from $\mathscr{L}_0$, $\mathscr{L}_2$ and $\mathscr{L}_3$ involve both binary and real variables. The latter also contain auxiliary binary variables d_i introduced during the conversion process. All of the inequalities are linear in all variables.

12.7.3 Optimal Control

An optimal control policy is sought that minimizes the cost function

$$J = \sum_{k=0}^{N-1} \left(\begin{array}{c} \|V_2(k) - 1\|^2 + r_0 \|\sigma - 1\|^2 \\ + r_1 \|\eta_L(k)\|^2 \end{array} \right)$$

subject to the system constraints. In the following we take $r_0 = 1, r_1 = 1/25$.

Consider the optimal controller for a line fault that results in a line admittance of $a = 0.375$. This is a severe fault, but one that is manageable. The state space includes the 7 discrete states (modes) and two continuous states induction motor slip, s, indicative of power, and battery state, σ, that represents the fractional battery charge. For computational purposes, the continuous state is discretized $s \in \{.1, .2, .3, .4, .5\}$

and $\sigma \in \{.25, .5, .75 1.0\}$, and the feedback control is computed in terms of these 140 states. In implementation an interpolation function is used for the continuous states.

Figures 12.8, 12.9 and 12.10 illustrate a particular feedback trajectory in which the initial battery state of charge is 0.1 and the initial slip is 0.

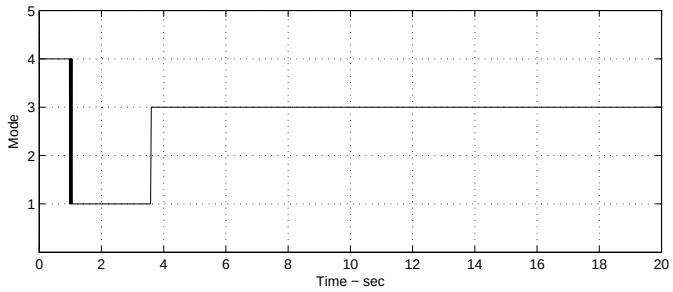

Fig. 12.8: Because of the low battery charge an initial switch into charging mode 4 occurs before load is dropped, modes 2 and 3.

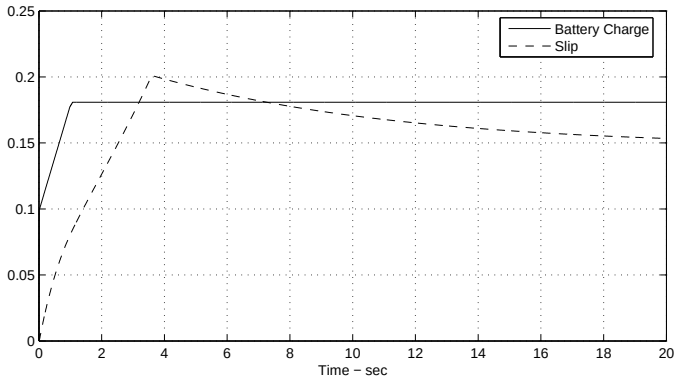

Fig. 12.9: The battery initially charges, but increasing slip, and hence electrical power, eventually requires load shedding.

12.8 Ship Integrated Electric Power System

The number of power supply sources available on a ship power system is determined by the need to supply the maximum anticipated electrical and propulsion load. On a

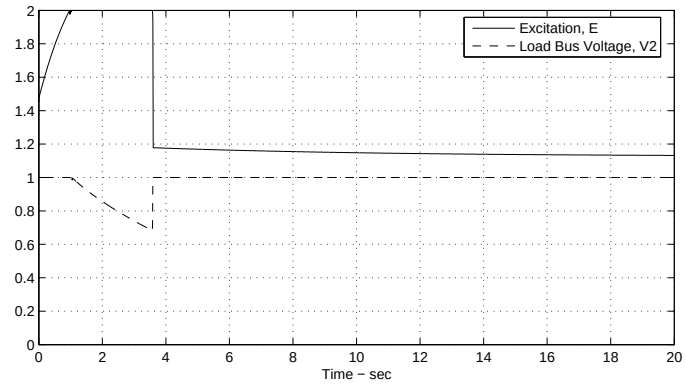

Fig. 12.10: After about 1 second the excitation saturates and load bus voltage drops. Load voltage regulation is re-established following load shedding.

naval ship, operational modes that require high level of online resources persist only for a small fraction of the total time a ship is in service. Consequently, a plan for fuel reduction should focus on the low load, normal operations that dominate the ship's lifetime. A significant reduction of fuel consumption can result from running a small number of turbine-generators during these periods. However, there is a real risk of contingencies that could lead to the need to curtail load. To insure an acceptable level of reliability of power supply it is necessary to maintain sufficient on-line generation and to distribute it appropriately around the network.

In [23], the authors draw an important distinction between *survivability* and *quality of service* (QOS). Survivability addresses prevention of fault propagation and restoration of service under severe damage conditions whereas QOS concerns insuring a reliable supply of power to loads during normal operations, see also [24] and [45]. QOS is an important consideration during normal operations because equipment malfunction is a relativity common occurrence. Not all loads have the same requirements for continuity of power supply. As used in [23], QOS is quantified as the *mean time between service interruptions* where a service interruption is defined as a degraded network condition that lasts longer than a load can tolerate before losing functionality. In [45] loads are divided into four categories that depend on two time parameters associated with the power network. T_1 is the reconfiguration time: the maximum time to reconfigure the network without bringing on additional generators. T_2 is the generator start time: the time to bring on-line the slowest generator. Accordingly, four categories of loads are defined:

1. Uninterruptible loads: cannot tolerate a power loss of duration T_1 .
2. Short term interruptible loads: can tolerate a power loss of duration T_1, but not T_2.

3. Long term interruptible loads: can tolerate a power loss of duration T_2.
4. Exempt loads: loads not considered in evaluating QOS.

Because this QOS metric is intended primarily for DC distribution systems it does not consider power quality measures such as harmonic content, or voltage fluctuations. In fact, it does not consider dynamics at all. In AC systems, however, dynamics are important.

In [70], the authors formulate the fuel optimization problem with QOS constraints, where QOS has a meaning appropriate for AC system power quality. The problem is formulated as follows. Given a time interval, $[0,T]$, over which the ship is to perform a specified mission with corresponding maximum load, ℓ, having a corresponding distribution over the network, determine a commitment, c_ℓ^*, of generation resources that minimizes fuel costs, supplies the load, and also satisfies QOS constraints. In this case the QOS constraints are defined as follows.

Definition 12.3. *Given:*

1. *a set of contingency events,* $\mathscr{R} = \{r_i, i = 1, \cdots, m\}$,
2. *a set of performance variables (e.g., bus voltages, line currents, frequency),* $\mathscr{Y} = \{y_i, i = 1, \cdots, p\}$, *each variable with a corresponding admissible range so that* $Y_{i,\min} \leq y_i(t) \leq Y_{i,\max}$ *and a time duration,* T_i, *for which an out of range value can be tolerated.*

The QOS constraints are satisfied if for every $r \in \mathscr{R}$, *occurring at any time* $t_r \in [0,T]$, *at which time the network is in equilibrium, none of the performance variables* $y_i(t)$ *experience a constraint violation for a duration longer than its corresponding* T_i.

The fuel optimization problem as formulated above is naturally a static optimization problem as meaningful fuel cost savings are obtained when measured over a long period of operation. QOS constraints, on the other hand, involve short term dynamics. They are incorporated by eliminating from consideration any otherwise feasible commitment configuration. This is accomplished by evaluating the response of the given configuration to the specified contingencies. No attempt is made to optimize that response. In [57] that analysis is expanded to allow the temporary use of load shedding and energy storage to avoid violating contingency constraints. The proposed frame-work also allows inclusion of load scheduling as a means of fuel conservation.

In the following discussion, an example based on the ship propulsion system described in Appendix **??** will be employed. The electrical load is assumed constant over the duration of the analysis. Its value varies with the mission and the season and may range from about 2000 KW to 4500 KW.

12.8.1 The Fuel Consumption Model

It is instructive to first consider the operation of the ship in its various configurations in terms of fuel consumption without regard to QOS constraints. The only constraints considered here, are the generation capacity of each of the generators and the electric power flow constraints of the network.

Fuel consumption data was obtained from the Navy's Energy Conservation Program web site http://www.i-encon.com. Based on the DDG 51 CLASS SHIPS data the associated fuel data and fuel curves for both Allison GTGs and GE LM2500 GTMs can be obtained. Curve fits where used to parameterize the data in terms of ship speed, v, in knots. There are three propulsion alignments with distinct fuel curves.

Trail Shaft One GTM engine online and one shaft windmilling.

$$f_{TS} = 117.17 \exp(0.1087\, v)$$

Split Plant One GTM engine online on each shaft.

$$f_{SP} = 181.74 \exp(0.098\, v)$$

Full Power Two GTM engines online on each shaft.

$$f_{FP} = 334.48 \exp(0.082\, v)$$

For the **Allison 501-K34** GTG fuel consumption, the curve was parameterized in KW electric load, L and the number of GTGs, N_{GTG}.

$$f_{GTG} = 0.068L + 97.4 N_{GTG}$$

Figures 12.11 and 12.12 show the fuel consumption at low speed (up to 8 knots) and high speed (above 8 knots), respectively, assuming a constant electric load of 3000 KW. Split plant operation has two GTMs operational, one on each shaft with all electric power supplied by two GTGs, as one would not be sufficient. This is the most fuel costly configuration. Trail shaft operation is somewhat better as only one GTM is operational. Note that one GTM can comfortably produce 22 knots. The HED motoring configuration with 2 GTGs supplying 3000 KW, and 1500 KW (or 2011 HP) for propulsion – so that about 8 knots is achievable – with 500 KW remining. This is the most fuel efficient configuration for low speed operation, see Figure 12.11. The HED generation configuration allows all of the GTGs to be shut down, but this configuration is not as efficient as motoring.

The HED motoring configuration can only be used above 8 knots with 3 GTGs operational, thereby, increasing fuel consumption and raising it to about the same as trail shaft HED generation. With three GTGs and 3000 KW of electrical load, it can

only produce a maximum speed of about 12 knots. Consequently it is omitted from the high speed considerations in Figure 12.12. In the high speed range, trail shaft HED generation is the most fuel efficient operating configuration. Also note that the optimal speed is in the range of 14-15 knots.

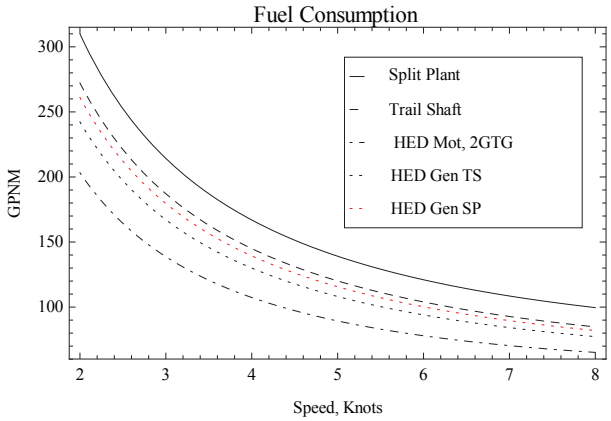

Fig. 12.11: Low speed fuel consumption as a function of speed in various configurations. Electrical load fixed at 3,000 KW.

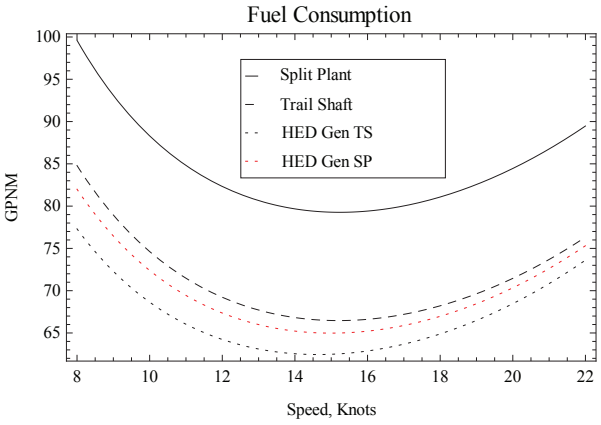

Fig. 12.12: High speed fuel consumption as a function of speed in various configurations. Electrical load fixed at 3,000 KW.

12.8.2 Optimal Response to Contingencies

From Section 12.8.1, it is clear that without consideration of supply reliability the most efficient operational configuration at low speed is trail shaft HED motoring, and at high speed operation it is trail shaft HED generation. The question now turns to how QOS constraints alters this picture. In accordance with Definition 12.3, to answer this it is necessary to evaluate the candidate configuration with respect to all contingency events in $\mathscr{R}$. This requires delineating the admissible corrective actions to each contingency and then evaluating the corresponding response in terms of continuity of supply variables $\mathscr{Y}$.

Example 12.4. Low speed Operation: Loss of Generator. As an example, consider operation of the system described in Appendix **??** at 7 knots, so the trail shaft HED motoring is the most fuel efficient configuration. Suppose one of the specified contingencies is loss of one of the two GTGs. Figure 12.13 illustrates the situation in terms of a state diagram. The normal operating state q_1 consists of two GTGs each producing 2250 KW. The system operating in state q_1 experiences an external event e_1 corresponding to a GTG failure inducing a transition to state q_2. From the failed state it is desired to restore the system back to the HED motoring state with two GTGs and to do so without violating the QOS requirements. To accomplish this the controller should react with a sequence of corrective actions. In this example the actions to be taken include:

1. Start up the spare GTG (it takes 6 minutes to get from shutdown to full power).
2. Temporarily drop non-vital load (1000 KW),
3. Supply power, temporarily from the emergency storage module (ESM)
4. Use the generator crisis capacity (4500 KW for up to 5 minutes).

The discrete states $q_i, i = 2,\ldots,6$ are illustrated along with admissible controllable transitions $s_i, i = 1,\ldots,9$. The contingency triggering event cause the system to transition from q_1 to q_2. There are four controlled events leading to transition from q_2. Any departure from state q_2 initiates startup of GTG 3. Now, it is proposed to select the *best* sequence of controlled transitions aimed at satisfying the QOS constraints. If the best does indeed satisfy the constraints as specified in Definition 12.3, then the same process can be followed for the other contingencies until one fails the test. If all contingencies have an adequate response sequence, the the mode is accepted as a valid operating configuration.

In earlier publications [67] and [65] the authors introduced an approach that uses a nonlinear DAE model to describe the continuous state dynamics. In [57] new concepts were introduced for improving the efficiency of the dynamic programming computations. Logical specifications are used to define the admissible transition behavior of the discrete system, to incorporate saturation of the continuous control, to

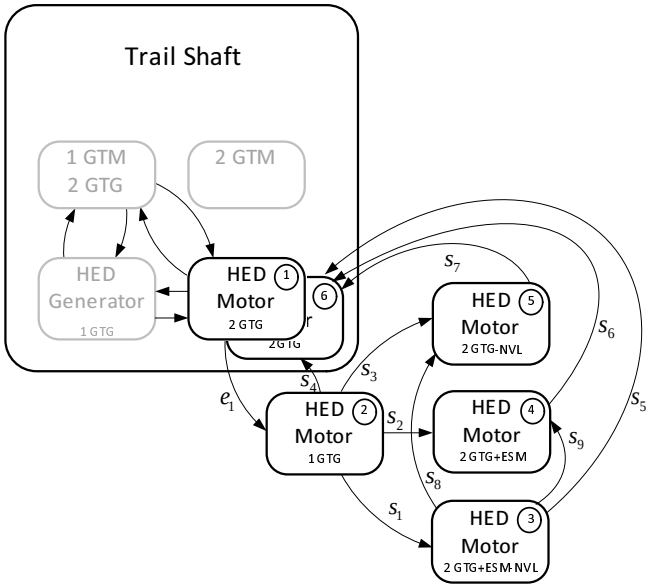

Fig. 12.13: Possible remedial strategies following loss of GTG from trail shaft motoring configuration.

characterize the algebraic constraints of the DAE model, and in the definition of the the cost function. Conversion of the logical specifications to integer formulas using symbolic computation enables the use of mixed-integer dynamic programming to derive an optimal feedback control.

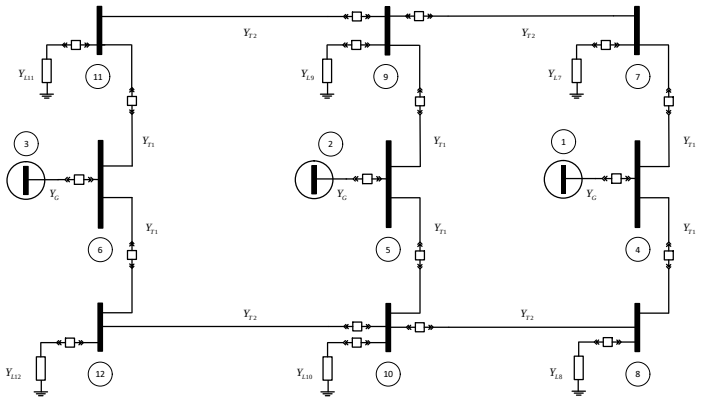

Fig. 12.14: The distribution network 12 bus configuration includes the generator internal buses.

Modeling

The system operates in one of m modes denoted $q_1,\ldots,q_m$. $Q=\{q_1,\ldots,q_m\}$ is the discrete state space. The continuous time differential-algebraic equation (DAE) describing operation in mode q_i is

$$\begin{array}{c}\dot{x}=f_i(x,y,u)\\ 0=g_i(x,y)\end{array}\qquad i=1,\ldots,m \tag{12.24}$$

where $x\in X\subseteq R^n$ is the system continuous state, $y\in Y\subseteq R^p$ is the vector of algebraic variables and $u\in U\subseteq R^l$ is the continuous control. Transitions can occur only between certain modes. The set of admissible transitions is $\mathscr{E}\subseteq Q\times Q$. It is convenient to view the mode transition system as a graph with elements of the set Q being the nodes and the elements of $\mathscr{E}$ being the edges. We assume that transitions are instantaneous. So, if a system transitions from mode q_1 to q_2 at time t we would write $q(t)=q_1, q(t^+)=q_2$. We allow resets. State trajectories are assumed continuous through events, i.e., $x(t)=x(t^+)$, unless a reset is specified.

Transitions are triggered by external *events* and *guards*. Events are designated s and belong to a set Σ. A guard is a subset of the continuous state space X that enables/disables a transition. A transition enabled by a guard might represent a protection device. Not all transitions have guards and some transitions might require simultaneous satisfaction of a guard and the occurrence of an event.

Each discrete state label, $q\in Q$, and each event label, $s\in\mathscr{E}$ is considered to be a logical variable that takes the value True or False. Guards also are specified as logical conditions. In this way the transition system can be defined by a logical specification (formula) $\mathscr{L}$.

For computational purposes it is useful to associate with each logical variable, say α, a binary variable or indicator function, δ_α, such that δ_α assumes the values 1 or 0 corresponding respectively to α being True or False. It is convenient to define the discrete state vector $\delta_q=[\delta_{q_1},\ldots,\delta_{q_m}]$. Precisely one of the elements of δ_q will be unity and all others will be zero.

With the introduction of the binary variables the set of dynamical equations (12.24) can be replaced with the single DAE:

$$\begin{array}{c}\dot{x}=f(x,y,\delta_q,u)=\sum_{i=1}^m \delta_{q_i} f_{q_i}(x,y,u)\\ 0=g(x,y,\delta_q)=\sum_{i=1}^m \delta_{q_i} g_{q_i}(x,y)\end{array} \tag{12.25}$$

Remark 12.5 (Power System DAE Models). Power systems are typically modeled by sets of semi-explicit DAEs as given by (12.24) In any mode q_i the flow defined by (12.24) is constrained to the set $M_i\subset X\times Y$ defined by $0=g_i(x,y)$. Ordinarily, it is assumed that M_i is a regular submanifold of $X\times Y$.

Example 12.6. Loss of Generator, Continued. The dynamical behavior in each of the six discrete states shown in Figure 12.13 will be modeled with reference to the network illustrated in Figure 12.14.Note that the initial state involves two generators corresponding to buses 1 and 2. The spare generator corresponds to bus 3. It is assumed that the bus 2 generator fails. The difference between the initial state q_1 and the final state q_6 in Figure 12.13 is that the replacement generator is on a different bus. In summary, the reduced bus network models for the 6 states are:

State q_1: Generator buses 1 and 2, PQ buses 4,5,6, full load.

State q_2: Generator bus 1, PQ bus 4, full load,

State q_3: Generator buses 1 and 3, PQ buses 4,6, vital load,

State q_4: Generator buses 1 and 3, PQ buses 4,6, ESM, full load,

State q_5: Generator buses 1 and 3, PQ bus 4,6, ESM, vital load

State q_6: Generator buses 1 and 3, PQ bus 4,6, full load.

The Control problem

The system is observed in operation over some finite time horizon T that is divided into N discrete time intervals of equal length. A control policy is a sequence of functions

$$\pi = \left\{ \mu_0 \left(x_0, \delta_{q0} \right), \ldots, \mu_{N-1} \left(x_{N-1}, \delta_{q(N-1)} \right) \right\}$$

such that $[u_k, \delta_{sk}] = \mu_k \left(x_k, \delta_{q_k} \right)$. Thus, μ_k generates the continuous control u_k and the discrete control δ_{sk} that are to be applied at time k, based on the state $\left(x_k, \delta_{qk} \right)$ observed at time k.

Consider the set of m-tuples $\{0,1\}^m$. Let Δ_m denote the subset of elements $\delta \in \{0,1\}^m$ that satisfy $\delta_1 + \cdots + \delta_m = 1$. Denote by Π the set of sequences of functions $\mu_k : X \times \Delta_m \to U \times \{0,1\}^{m_S}$ that are piecewise continuous on X.

The *Optimal Feedback Control Problem* is defined as follows. For each $x_0 \in X, \delta_{q0} \in \Delta_m$ determine the control policy $\pi^* \in \Pi$ that minimizes the cost

$$\begin{array}{l} J_\pi \left(x_0, \delta_{q0} \right) = \\ \quad g_N \left(x_N, \delta_{qN} \right) + \\ \quad \sum_{k=0}^{N-1} g_k \left(x_k, \delta_{qk}, \mu_k \left(x_k, \delta_{qk} \right) \right) \end{array} \tag{12.26}$$

subject to the constraints (12.24) and the logical specification, i.e.,

$$J_{\pi^*} \left(x_0, \delta_{q0} \right) \leq J_\pi \left(x_0, \delta_{q0} \right) \quad \forall \pi \in \Pi \tag{12.27}$$

12.8.3 Example

Consider, again, the loss of generator 2. This event causes the transition from state q_1 to q_2 as indicated in Figure 12.13. The goal now is to determine an optimal response

strategy for this contingency. Departure from q_2 to any of the states $q_3, \ldots, q_6$ initiates startup of the spare generator (GTG3). It is assumed that the generator power increases at a conservative rate of 250 KW/minute. In units of pu per sec,

$$\dot{P}_3 = 1/1200 \tag{12.28}$$

The goal is to steer the system from the initial state $P_3 = 0, q = q_2$ to the terminal state $P_3 = 0.45, q = q_6$. This will take 9 minutes since P_3 must reach 0.45 pu from 0 pu. The fast electrical dynamics will be neglected so that the only dynamics are associated with equation (12.28). Each mode is described by (12.28) and a set of algebraic equations describing the network.

The nine minute interval is divided into nine one-minute segments, and (12.28) is replaced by the discrete time equation

$$P_{3,i+1} = P_{3,i} + 60/1200 \tag{12.29}$$

The goal is to find a sequence of state transitions that steers the system from the initial state $\{0, q_2\}$ to the final state $\{0.45, q_r\}$ such that QOS constraints are met. To do this, an optimal control is sought that minimizes a cost defined to reflect the QOS objectives. In this example, the cost J is

$$J = \sum_{i=4}^{12} |V_i - 1| + \max[0, P_1 - 0.5] + 0.3\,\delta_{ESM} + 0.15\,\delta_{NVL}$$

where δ_{ESM} and δ_{NVL} are binary variables that take the values 0 or 1. $\delta_{ESM} = 1$ denotes the ESM is active and $\delta_{NVL} = 1$ denotes the non-vital load is dropped, whereas in each case, the value zero denotes the opposite. Dynamic programming is used to obtain the switching strategy illustrated in Figure 12.15. The weights assigned to $\delta_{ESM} = 1, \delta_{ESM} = 1$ are selected to reflect a judgement of the relative cost of employing these actions.

Notice that following the failure, the controller immediately switches to configuration q_3 which means that the non-vital load is dropped and the ESM turned on providing 1000 KW of supporting power. It is worth noting that the power provided by GTG1 is $P_1 = 0.494pu$ which is still below the unit's normal rating of 0.5 pu. If no action is taken, GTM1 would provide 0.786 pu power which is just below the unit's five minute crisis capability (0.9 pu). However, the voltage levels are also unacceptably low. After one minute, the optimal strategy switches to q_5, in which the ESM is turned off, but the non-vital loads remain disconnected. The GTG1 power output increases to 0.642 pu. The system remains in this state for four minutes by which time the GTG1 power output has dropped below its normal rating to 0.444 pu. At this point the configuration is switched to q_6, the non-vital load is picked up and the GTG1 power output increase to 0.640 pu. The system remains in this configuration and reaches the target state in four minutes as the GTG1 power output reduces

linearly to its target value. Throughout this trajectory the bus voltages remain within acceptable limits.

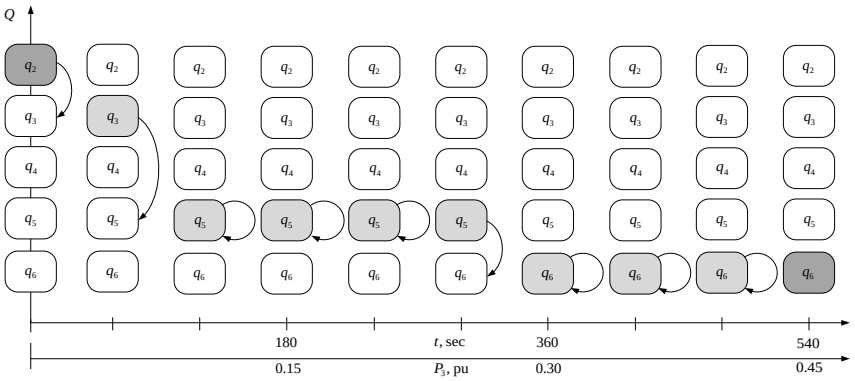

Fig. 12.15: The optimal strategy is shown in terms of the time period and GTG3 power level.

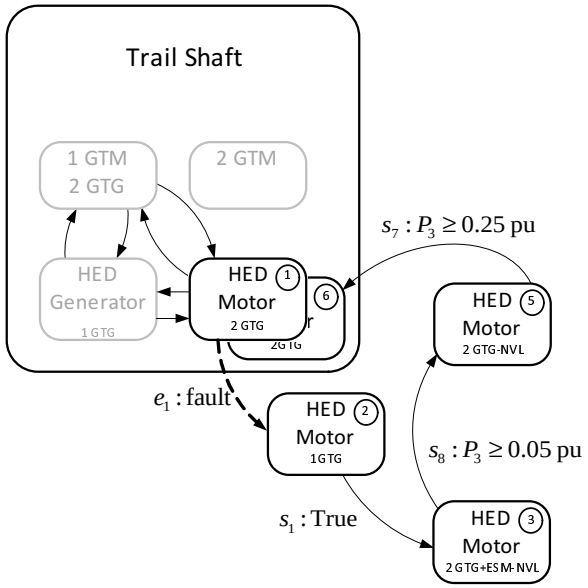

Fig. 12.16: The optimal strategy is shown as a discrete state transition diagram.

In summary, using the engine fuel consumption data, a set of possible operational configurations, and mission specific electric load and ship speed requirements it is

a straightforward matter to compute the most fuel efficient operating configuration. However, when QOS constraints are imposed, the problem is more complicated. In this case, it is necessary to delineate all credible contingencies and eliminate any configuration which violates the QOS constraints for any one of the contingent events. The occurrence of a contingency should trigger a remedial action designed to prevent violation of the QOS constraints. The goal is to design an optimal sequence of available remedial actions. The cost function is constructed from penalties associated with QOS violations which are balanced against costs associated with the using the available remedial actions. With a remediation strategy defined, the response to a contingency can be evaluated to determine if a QOS constraint is violated.

A

ProPac

A.1 Getting Help

The *Mathematica* package *ProPac* is an integral part of this book. *ProPac* contains subpackages for multibody dynamics, linear control, and nonlinear control. Once it is installed, as described in Chapter 1, appropriate packages will be loaded automatically as they are required. However, individual packages can be manually loaded by simply entering GeometricTools, Dynamics, LinearControl, NonlinearControl, or MEXTools as desired. Once a package is loaded, enter ?GeometricTools, ?Dynamics, ?LinearControl, ?NonlinearControl, or ?MEXTools, respectively, to obtain a complete list of available functions. Then enter ?FunctionName to obtain usage information for the function `FunctionName`. After *ProPac* is installed, the *Mathematica* Help index should be rebuilt as described in Chapter 1. When this is done, help will also be available in the Help Browser under Add-ons.

The CD that accompanies this book includes several *Mathematica* notebooks that illustrate the use of *ProPac*. The notebooks, Dynamics.nb and Controls.nb are intended to give an overview of the available functions.

Of course, all standard *Mathematica* functions and packages are available and *ProPac* is compatible with the *Mathematica* package Control Systems Profesional, available from Wolfram Research.

A.2 Quick Reference Tables

The following tables provide a summary of the available functions. They are not all inclusive. A complete list of available functions can be obtained as described in the Section **??**.

Function Name	**Operation**
Bode	produces a Bode plot of the transfer function of a (scalar) continuous time system
RootLocus	generates the root locus plot for a given transfer function
Nyquist	generates the Nyquist plot for a given transfer function
ColorNyquist	generates a color version of the Nyquist plot
PhasePortrait	computes a family of state space trajectories for a vector field on R^2 and returns a list of graphics objects

Table A.1: Graphics Functions

Function Name	**Operation**
ControllablePair	test for controllability
ObservablePair	test for observability
ControllabilityMatrix	returns the controllability matrix
ObservabilityMatrix	returns the observability matrix
PolePlace	state feedback pole placement based on Ackermann's formula with options
DecouplingConrol	state feedback and coordinate transformation that decouples input-output map
RelativeDegree	computes the vector relative degree
LyapunovEquation	computes the solution, P, of $A^T + PA = -Q$
AlgebraicRiccatiEquation	computes the positive solution of the algebraic Riccati equation
LQR, LQE	compute optimal quadratic regulator and estimator parameters

Table A.2: Linear Systems: Time Domain

Function Name	Operation
LeastCommonDenominator	finds the least common denominator of the elements of a proper, rational G(s)
Poles	finds the roots of the least common denominator
LaurentSeries	computes the Laurent series up to specified order
AssociatedHankelMatrix	computes the Hankel matrix associated with Laurent expansion of G(s)
McMillanDegree	computes the degree of the minimal realization of G(s)
RelativeDegree	computes the relative degree of a linear system
ControllableRealization	computes the controllable realization of a transfer function
ObservableRealization	computes the observable realization of a transfer function
KalmanDecomposition	returns a Kalman decomposition of a linear system

Table A.3: Linear Systems: Frequency Domain

Function Name	Operation
LieBracket	computes the Lie bracket of a given pair of vector fields
Ad	computes the iterated Lie bracket of specified order of a pair of vector fields
Involutive	tests a set of vector fields to determine if it is involutive
Span	generates a set of basis vector fields for a given set of vector fields
TriangularDecomposition	computes the transformation that trangularizes a vector field from a given involutive distribution, invariant with respect to the vector field
SmallestInvariantDistribution	Computes the smallest distribution containing a given distribution and invariant with respect to a set of vector fields
LargestInvariantDistribution	Computes the largets distribution contained in the annihilator of an exact codistribution and invariant with respect to a set of vector fields

Table A.4: Geometry Tools

Function Name	**Operation**
Contraction	returns the contraction of a form with a vector field
d	the exterior derivative operator
FormBasis	returns a basis for a given list of forms
FormDegree	returns the degree of a differential form
RankCodistribution	returns the Rank of a codistribution (a list of 1-forms)
Wedge	returns the wedge product of a set of forms

Table A.5: Differential Forms

Function Name	**Operation**
Joints	returns all of the kinematic quantities corresponding to a list of joint definitions
TreeInertia	computes the inertia matrix of a multibody system in a tree structure containing flexible and rigid bodies
EndEffector	returns the Euclidean Configuration Matrix of a body fixed frame at a specified node
NodeVelocity	returns the (6 dim) spatial velocity vector of a body fixed frame at a specified node
GeneralizedForce	computes the generalized force at specified node in terms of generalized coordinates
RelativeConfiguration	computes the relative configuration of body fixed frames at specified nodes
KinematicReplacements	sets up temporary replacement rules for repeated groups of expressions to simplify kinematic quantities

Table A.6: Kinematics

Function Name	Operation
TreeInertia	generates the spatial inertia of a tree structure
LeafPotential	returns the elastic potential energy associated with leaf absolute position in terms of the system generalized coordinates
BacklashPotential	Returns the Hertz impact potential associated with a specified material potential
JointFriction	assembles a dissipation function of Lur'e type for a joint that involves viscous, Coulomb and Stribeck effects
CreateModel	builds the kinematic and dynamic equations for tree structures
DifferentialConstraints	adds differential constraints to a tree configuration
AlgebraicConstraints	adds algebraic constraints to a tree configuration
MakeODEs	assembles differential equations in a form that can be integrated in Mathematica
MakeLagrangeEquations	assembles Lagrange's equations in a form that can be integrated in Mathematica

Table A.7: Dynamics

Function Name	Operation
ControlDistribution	computes the controllability distribution of a nonlinear (affine) system
Controllablity	test for controllability of a nonlinear (affine) system
ObservabilityCodistribution	computes the observability codistribution of a nonlinear (affine) system
Observability	test for observability of a nonlinear (affine) system
LocalDecomposition	computes a transformation that puts a nonlinear (affine) system into Kalman-partitioned form

Table A.8: Nonlinear Controllability and Observability

Function Name	**Operation**
SISONormalFormTrans	Computes the transformation taking an IO linearizable SISO system to its normal form
VectorRelativeOrder	computes the relative degree vector
DecouplingMatrix	computes the decoupling matrix, $\rho(x)$
IOLinearize	computes the linearizing control, $u = \rho^{-1}\{-\alpha(x)+v\}$
NormalCoordinates	computes the partial state transformation, $z(x)$
LocalZeroDynamics	computes the local form of the zero dynamics $F(\xi,0)$, near x_0
DynamicExtension	implements dynamic extension process to produce a nonsingular decoupling matrix when posible
StructureAlgorithm	implements the Hirschorn-Singh structure algorithm for assembling a dynamic inverse

Table A.9: Feedback Linearizing Functions

Function Name	**Operation**
AdaptiveRegulator	generates an adaptive regulator for a class of linearizable systems
AdaptiveBackstepRegulator	computes an adaptive regulator by backstepping for SISO systems in PSFF form
AdaptiveTracking	computes an adaptive tracking controller
PSFFCond	tests a system to determine if it is reducible to PSFF form
PSFFSolve	transforms a system to PSFF form if possible

Table A.10: Adaptive Control

Function Name	**Operation**
LinearizeToOutputInjection	computes a transformation that converts the system to observer form
ObservabilityIndices	returns a list of the observability indices of the system
ObservableForm	computes a transformation that converts the system to observable form

Table A.11: Observer Tools

Function Name	Operation
SlidingSurface	generates the sliding (switching) surface for feedback linearizable nonlinear systems
SwitchingControl	computes the switching functions - allows the inclusion of smoothing and moderating functions

Table A.12: Variable Structure Control

References

1. R. Abraham, J. E. Marsden, and T. Ratiu. *Manifolds, Tensor Analysis, and Applications*. Springer-Verlag, New York, 1988.
2. V. I. Arnold, V. V. Kozlov, and A. I. Neishtadt. *Mathematical Aspects of Classical and Celestial Mechanics*, volume 3 of *Encyclopedia of Mathematical Sciences*. SpringerVerlag, Heidelberg, 1988.
3. D. K. Arrowsmith and C. M. Place. *An Introduction to Dynamical Systems*. Cambridge University Press, Cambridge, 1990.
4. L. Bao, X. Duan, and TY. He. Analysis of voltage collapse mechanisms in state space. *IEE Proceedings - Generation, Transmission and Distribution*, 147(6):395–400, 2000.
5. R.E. Bellman. *Dynamic Programming*. Princeton University Press, Princeton, N. J., 1957.
6. Alberto Bemporad and Manfred Morari. Control of systems integrating logic, dynamics, and constraints. *Automatica*, 35(3):407–427, 1999.
7. W. H. Bennett, H. G. Kwatny, and M.J. Baek. Nonlinear dynamics and control of articulated flexible spacecraft: Application to ssf/mrms. *AIAA Journal on Guidance, Control and Dynamics*, 17(1):38–47, 1994.
8. W. H. Bennett, C. LaVigna, H. G. Kwatny, and G. Blankenship. Nonlinear and adaptive control of flexible space structures. *Transactions ASME, Journal of Dynamic Systems, Measurement and Control*, 115(1):86–94, 1993.
9. G. Besancon. On output transformation for state linearization up to output injection. *IEEE Transactions on Automatic Control*, 44(10):1975–1981, 1999.
10. D. Bestle and M. Zeitz. Canonical form observer design for nonlinear time–variable systems. *International Journal of Control*, 38:419–431, 1983.
11. G. L. Blankenship, R. Ghanadan, H. G. Kwatny, C. LaVigna, and V. Polyakov. Tools for integrated modeling, design, and nonlinear control. *IEEE Control Systems*, 15(2):65–79, April 1995.
12. A. M. Bloch, M. Reyhanoglu, and N. H. McClamroch. Control and stabilization of nonholonomic dynamic systems. *IEEE Transactions on Automatic Control*, 37(11):1746–1757, 1992.
13. S. Bonanos. *Exterior Differential Calculus*. www.mathsource.com/ Content/ Enhancements/ Algebraic/ 0210–935, 2001.
14. William M. Boothby. *An Introduction to Differentiable Manifolds and Riemannian Geometry*. Academic Press, San Diego, 1986.

15. F. Borrelli, M. Baotic, A. Bemporad, and M. Morari. Dynamic programming for constrained optimal control of discrete-time linear hybrid systems. *Automatica*, 41:1709–1721, 2005.
16. M. S. Branicky, V. S. Borkar, and S. K. Mitter. A unified framework for hybrid control: Model and optimal control theory. *IEEE Transactions on Automatic Control*, 43(1):31–45, 1998.
17. R. W. Brockett. Feedback invariants for nonlinear systems. In *IFAC World Congress*, pages 1115–1120, Helsinki, 1978.
18. S. Cetinkunt and B. Ittoop. Computerautomated symbolic modeling of dynamics of robotic manipulators with flexible links. *IEEE Transactions on Robotics and Automation*, 8(1):94–105, 1992.
19. N. G. Chetaev. On the equations of poincar. *PMM (Applied Mathematics and Mechanics)*, (5):253–262, 1941.
20. N. G. Chetaev. *Theoretical Mechanics*. SpringerVerlag, New York, 1989.
21. S.N. Chow and J. K. Hale. *Methods of Bifurcation Theory*. SpringerVerlag, New York, 1982.
22. J. Descusse and C. H. Moog. Decoupling with dynamic compensation for strong invertible affine nonlinear systems. *International Journal of Control*, 42(6):1387–1398, 1985.
23. N. H. Doerry and Jr. J. V. Amy. Implementing quality of service in shipboard power system design. In *IEEE Electric Ship Technology Symposium*, Alexandria, VA, 2011.
24. Norbert H. Doerry. Designing electric power systems for survivability and quality of service. *ASNE Naval Engineers Journal*, 119(2):25 – 34, 2007.
25. S. V. Emelyanov, S. K. Korovin, and L. V. Levantovsky. Higher order sliding modes in control systems. *Journal of Differential Equations*, 29(11):1627–1647, 1998.
26. A. F. Filippov. A differential equation with discontinuous right hand side. *Matemat: Cheskii Sbornik*, 51(1):99–128, 1960.
27. F. Gantmacher. *Lectures in Analytical Mechanics*. Mir, Moscow, english translation edition, 1975.
28. J. P. Gauthier and G. Bornard. Observability for any u(t) of a class of nonlinear systems. *IEEE Transactions on Automatic Control*, 26(4):922–926, 1981.
29. T. Geyer, M. Larsson, and M. Morari. Hybrid emergency voltage control in power systems. In *European Control Conference*, Cambridge, 2003.
30. Jerry H. Ginsberg. *Advanced Engineering Dynamics*. Harper and Row, New York, 1988.
31. Herbert Goldstein. *Classical Mechanics*. AddisonWesley, Reading, 2nd edition, 1980.
32. J. Guckenheimer and P. Holmes. *Nonlinear Oscillations, Dynamical Systems, and Bifurcation of Vector Fields*. Springer–Verlag, New York, 1983.
33. J. K. Hale. *Ordinary Differential Equations*. John Wiley and Sons, New York, 1969.
34. H. Hammouri and J. P. Gauthier. Bilinearization up to output injection. *Systems and Control Letters*, 11:139–149, 1988.
35. H. Hammouri and J. P. Gauthier. Time varying linearization up to output injection. In *28th Conference on Decision and Control*, pages 1038–1039, Tampa, Florida, 1989. IEEE.
36. H. Hammouri and J. P. Gauthier. A global time–varying linearization up to output injection. *SIAM Journal of Control and Optimization*, 30:1295–1310, 1992.
37. H. Hammouri and M. Kinnaert. A new procedure for time–varying linearization up to output injection. *Systems and Control Letters*, 28:151–157, 1996.
38. S. Hedlund and A. Rantzner. Optimal control of hybrid systems. In *Conference on Decision and Control*, pages 3972–3977, Pheonix, AZ, 1999.

39. R. Hermann. Cartan connections and the equivalence problem for geometric structures. *Contributions to Differential Equations*, 3:199–248, 1964.
40. R. Hermann and A. J. Krener. Nonlinear controllability and observability. *IEEE Transactions on Automatic Control*, 22(5):728–740, 1977.
41. M. W. Hirsch. *Differential topology*. Springer–Verlag, New York, 1976.
42. R. M. Hirschorn. Invertibility of multivariable nonlinear control systems. *IEEE Transactions on Automatic Control*, AC-24(6):855–865, 1979.
43. J. Hooker. *Logic–Based Methods for Optimization: Combining Optimization and Constraint Satisfaction*. Wiley–Interscience, 2000.
44. M. Hou and A. C. Pugh. Observer with linear error dynamics for nonlinear multi–output systems. *Systems and Control Letters*, 37:1–9, 1999.
45. IEEE Std 1709-2010. IEEE recommended practice for 1 kv to 35 kv medium voltage dc power systems on ships, 2010.
46. A. Isidori. *Nonlinear Control Systems*. Springer–Verlag, London, 3 edition, 1995.
47. A. Jain. Unified formulation of dynamics for serial rigid multibody systems. *AIAA Jrl. Guidance, Control and Dynamics*, 14(3):531–542, 1991.
48. A. Jain and G. Rodriguez. Recursive flexible multibody system dynamics using spatial operators. *AIAA Journal of Guidance, Control and Dynamics*, 15(6):1453–1466, 1992.
49. Thomas Kailath. *Linear Systems*. Prentice-Hall, NJ, 1980.
50. R. E. Kalman and R. S. Bucy. New results in linear filtering and prediction theory. *ASME Journal of Basic Engineering*, (March):95–108, 1961.
51. I. Kanellakapoulos, P. V. Kokotovic, and A. S. Morse. Systematic design of adaptive controllers for feedback linearizable systems. *IEEE Transactions on Automatic Control*, AC-36(11):1241–1253, 1991.
52. H. K. Khalil. *Nonlinear Systems*. MacMillan, New York, 1992.
53. S. R. Kou, D. L. Elliot, and T. J. Tarn. Exponential observers for nonlinear dynamic systems. *Information and Control*, 29:204–216, 1975.
54. A. J. Krener and A. Isidori. Linearization by output injection and nonlinear observers. *Systems and Control Letters*, 3(June):47–52, 1983.
55. A. J. Krener and W. Respondek. Nonlinear observers with linearizable error dynamics. *SIAM J. Control and Optimization*, 28(2):197–216, 1985.
56. M. Krstic, I. Kanellakopoulos, and P. V. Kokotovic. Adaptive nonlinear control without overparameterization. *Systems and Control Letters*, 19:177–185, 1992.
57. H. Kwatny, G. Bajpai, M. Yasar, and K. Miu. Fuel optimal control with service reliability constraints for ship power systems. In *IFAC World Conference*, volume 19, pages 6386–6391, Capetown, South Africa, 2014.
58. H. G. Kwatny and J. Berg. Drum level regulation at all loads: A study of system dynamics and conventional control structures. In *12th IFAC World Congress*, Sydney, 1993.
59. H. G. Kwatny and J. Berg. Variable structure regulation of power plant drum level. In J. Chow, R. J. Thomas, and P. V. Kokotovic, editors, *Systems and Control Theory for Power Systems*, Institute for Mathematics and its Application, pages 205–234. SpringerVerlag, New York, 1995.
60. H. G. Kwatny and G. L. Blankenship. Symbolic construction of models for multibody dynamics. *IEEE Transactions on Robotics and Automation*, 11(2):271–281, April 1995.
61. H. G. Kwatny and G. L. Blankenship. *Nonlinear Control and Analytical Mechanics: a computational approach*. Control Engineering. Birkhauser, Boston, 2000.
62. H. G. Kwatny and B.-C. Chang. Symbolic computing of nonlinear observable and observer forms. *Applied Mathematics and Computation*, 171:1058–1080, 2005.
63. H. G. Kwatny and H. Kim. Variable structure regulation of partially linearizable dynamics. *Systems & Control Letters*, 15:67–80, 1990.

64. H. G. Kwatny, F. M. Massimo, and L. Y. Bahar. The generalized lagrange equations for nonlinear rlc networks. *IEEE Trans. on Circuits and Systems*, CAS29(4):220–233, 1982.
65. H. G. Kwatny, E. Mensah, D. Niebur, G. Bajpai, and C. Teolis. Logic based design of optimal reconfiguration strategies for ship power systems. In *7th IFAC Symposium on Nonlinear Control Systems*, Pretoria, South Africa, 2007.
66. H. G. Kwatny, E. Mensah, D. Niebur, and C. Teolis. Optimal shipboard power system management via mixed integer dynamic programming. 2005 IEEE Electric Ship Technologies Symposium (IEEE Cat. No. 05EX1110), pages 55–62, Philadelphia, PA, USA, 2005. IEEE.
67. H. G. Kwatny, E. Mensah, D. Niebur, and C. Teolis. Optimal power system management via mixed integer dynamic programming. In *2006 IFAC Symposium on Power plants and Systems*, Kananaskis, Canada, 2006.
68. H. G. Kwatny and T. L. Siu. Chattering in variable structure feedback systems. In *10th IFAC World Congress*, volume 8, pages 334–341, Munich, 1987.
69. H. G. Kwatny, C. Teolis, and M. Mattice. Variable structure control of systems with uncertain friction. *Automatica*, 38(July):1251–1256, 2002.
70. S. Lahiri, K. Miu, H. G. Kwatny, G. Bajpai, A. Beyton, and J. Patel. Fuel optimization under quality of service constraints for shipboard hybrid electric drive. In *4th International Symposium on Resilient Control Systems*, Boise, Idaho, 2011. IEEE.
71. J. LaSalle and S. Lefschetz. *Stability by Liapunovs Direct Method*. Academic Press, New York, 1961.
72. N. E. Leonard. Stability of a bottom-heavy underwater vehicle. *Automatica*, 33(3):331–346, 1997.
73. M. C. Leu and N. Hemati. Automated symbolic derivation of dynamic equations for robotic manipulators. *Journal of Dynamic Systems, Measurement and Control*, 108(September):172–179, 1986.
74. Q. Li, Y. Guo, and T. Ida. Transformation of logical specification into ip–formulas. In *3rd International Mathematica Symposium (IMS '99)*, Hagenburg, Austria, 1999. Computational Mechanics Publications, WIT Press.
75. Q. Li, Y. Guo, and T. Ida. Modelling integer programming with logic: Language and implementation. *IEICE Transactions on Fundamentals of Electronics, Communications and Computer Sciences*, E83–A(8):1673–1680, 2000.
76. T. E. Dy Liacco. The adaptive reliability control system. *IEEE Transactions on Power Apparatus and Systems*, PAS-86(5):517–528, 1967.
77. T. E. Dy Liacco. *Control of Power Systems via the Multi-Level Concept*. PhD thesis, Case Western Reserve, 1968.
78. T. E. Dy Liacco. Processing by logic programming of circuit-breaker and protective-relaying information. *IEEE Transactions on Power Apparatus and Systems*, PAS-82(2):171–175, 1969.
79. Bo Lincoln and Anders Rantzer. Relaxing dynamic programming. 2003.
80. R. Marino. High gain feedback non–linear control systems. *International Joural of Control*, 42(6):1369–1385, 1985.
81. R. Marino and P. Tomei. *Nonlinear Control Design: Geometric, Adaptive and Robust*. Prentice-Hall, Upper Saddle River, 1995.
82. J. E. Marsden and M. McCracken. *The Hopf Bifurcation and its Applications*. Springer–Verlag, New York, 1976.
83. J. E. Marsden and T. Ratiu. *Introduction to Mechanics and Symmetry*, volume 17 of *Texts in Applied Mathematics*. Springer-Verlag, New York, 2nd edition, 1998.

84. K. McKinnon and H. Williams. Constructing integer programming models by the predicate calculus. *Annals of Operations Research*, 21:227–246, 1989.
85. L. Meirovitch. *Methods of Analytical Dynamics*. McGrawHill, Inc., New York, 1970.
86. Ju. I. Neimark and N. A. Fufaev. *Dynamics of Nonholonomic Systems*, volume 33 of *Translations of Mathematical Monographs*. American Mathematical Society, Providence, 1972.
87. H. Nijmeijer and H. J. van der Schaft. *Nonlinear Dynamical Control Systems*. Springer–Verlag, New York, 1990.
88. H. Ohtsuki, A. Yokoyama, and Y. Sekine. Reverse action on-load tap changer in association with voltage collapse. *IEEE Tansactions on Power Systems*, 6(1):300–306, 1991.
89. Peter J. Olver. *Applications of Lie Groups to Differential Equations*. Springer–Verlag, New York, 1986.
90. M. K. Pal. Voltage stability: Analysis needs, modelling requirement, and modelling adequacy. *IEE Proceedings - C*, 140(4):279–286, 1993.
91. G. Rodriguez and K. KreutzDelgado. Spatial operator factorization of the manipulator mass matrix. *IEEE Transactions on Robotics and Automation*, 8(1):65–76, 1992.
92. Reinhardt M. Rosenberg. *Analytical Dynamics of Discrete Systems*. Plenum Press, New York, 1977.
93. A. J. Van der Schaft and H. Schumacher. *An Introduction to Hybrid Dynamical Systems*. Lecture Notes in Control and Information Sciences. Springer-Verlag, London, 2000.
94. K. S. Sibirsky. *Introduction to Topological Dynamics*. Noordhoff International Publishing, Leyden, 1975.
95. S. N. Singh. Decoupling of invertible nonlinear systems with state feedback and precompensation. *IEEE Transactions on Automatic Control*, AC–25(6):1237–1239, 1980.
96. S. N. Singh. A modified algorithm for invertibility in nonlinear systems. *IEEE Transactions on Automatic Control*, 25(6):1237–1239, 1981.
97. J. J. Slotine and S. S. Sastry. Tracking control of non–linear systems using sliding surfaces, with application to robot manipulators. *International Journal of Control*, 38(2):465–492, 1983.
98. J. J. E. Slotine. Sliding controller design for non–linear control systems. *International Journal of Control*, 40(2):421–434, 1984.
99. J. J. E. Slotine and W. Li. *Applied Nonlinear Control*. Prentice Hall, Englewood Cliffs, 1991.
100. I. Souleiman, A. Glumineau, and G. Schreier. Direct transformation of nonlinear systems into state affine miso form for observer design. *IEEE Transactions on Automatic Control*, 48(12):2191–2196, 2003.
101. V. Sundarapandian. Exponential observer design for nonlinear systems with real parametric uncertainty. *Mathematical and Computer Modelling*, 37(177–190), 2003.
102. F. D. Torrisi and A. Bemporad. Hysdel–a tool for generating computational hybrid models for analysis and synthesis problems. *IEEE Transactions on Control Systems Technology*, 12(2):235–249, 2004.
103. M. L. Tyler and M. Morari. Propositional logic in control and monitoring problems. *Automatica*, 35(4):565–582, 1999.
104. V. I. Utkin. *Sliding Modes and Their Application*. MIR, Moscow, 1974 (in Russian) 1978 (in English).
105. M. Vidyasagar. *Nonlinear Systems Analysis*. Prentice Hall, Englewood Cliffs, 2 edition, 1993.
106. C. Von Westenholz. *Differential Forms in Mathematical Physics*. Nort-Holland Publishing Co., New York, 1981.

107. F. W. Warner. *Foundations of Differentiable Manifolds and Lie Groups*. Springer–Verlag, New York, 1983.
108. H. P. Williams. *Model Building in Mathematical Programming*. John Wiley and Sons, 1993.
109. X. Xia and M. Zeitz. On nonlinear continuous observers. *International Journal of Control*, 66(6):943–954, 1997.
110. X. H. Xia and W. B. Gao. Nonlinear observer design by observer linearization. *SIAM Journal of Control and Optimization*, 27:135–142, 1989.
111. Xiao-hua Xia and Wei-bing Gao. On exponentia observers for nonlinear systems. *Systems and Control Letters*, 11:319–325, 1988.
112. K. D. Young, P. V. Kokotovic, and V. I. Utkin. Singular perturbation analysis of high gain feedback systems. *IEEE Transactions on Automatic Control*, AC–22(6):931–938, 1977.
113. K. D. Young and H. G. Kwatny. Variable structure servomechanism and its application to overspeed protection control. *Automatica*, 18(4):385–400, 1982.

Index